I.U.G.G.
INTERNATIONAL ASSOCIATION OF SEISMOLOGY
AND PHYSICS OF THE EARTH'S INTERIOR

EUROPEAN SEISMOLOGICAL COMMISSION

PROCEEDINGS

XXI. GENERAL ASSEMBLY
23 – 27 AUGUST 1988
SOFIA, BULGARIA.

National Palace of Culture
Sofia, 1989

I.U.G.G.

International Association of Seismology and Physics of the Earth's Interior

European Seismological Commission

Activity Reports 1986 - 1988
and
Proccedings of the XXI General Assembly
23 -27 August 1988
Sofia, Bulgaria

CONTENTS

Preface

The XXI. General Assembly 1988 of the European Seismological Commission was organized by the Geophysical Institute of the Bulgarian Academy of Sciences and the National Committee for Geodesy and Geophysics.

All events took place in the new National Congress Centre "L.Zhivkova", located in the central part of Sofia. Beside the oral presentations also poster sessions in the hall between the lecture rooms have been put up and enjoyed great interest among the participants.

The ESC is specially indebted to Prof. L. Christoskov, Director of the Geophysical Institute of B.A.S., chairman of the local organizing committee, and also to the following persons, who contributed so successfully to the organization of the meeting:

From the Geophysical Institute: Alex Anufriev, Irena Asparuhova, Mariana Assatulina, Blagovesta Babachkova, Emil Botev, Ivan Butchvarov, Daniela Deneva, Konstatina Denkova, Rosa Denkova, Borislav Dimitrov, Dimiter Dimitrov, Savka Dineva, Chavdar Dobrev, Nikola Dotzev, Sasho Elenkov, Kostadin Ganev, Rumiana Glavcheva, Dragomir Gospodinov, Ganka Hristova, Vera Ivanova, Vesselina Kalcheva, Yordanka Kamburova, Ivanka Kamenova, Issam Al Khoubbi, Philip Kolev, Sophia Koniarova, Mary Kovacheva, Emil Levy, Emilia Maneva, Valentin Markov, Svetla Maslinkova, Dimiter Mihailov, Vesselin Nikolov, Svetlana Nikolova, Todorinka Pancheva, Ljubomir Petrov, Georgi Popov, Tzvetan Ralchovski, Boyko Ranguelov, Elena Samardjieva, Stella Simeonova, Dimcho Solakov, Edelvais Spassov, Toshko Stoyanov, Margarita Todorova, Raina Yordanova.

From the Earth's Sciences Center: Angel Chankov, Ivan Kabakov

National Committee of Geodesy and Geophysics: Ivan Petkov

From the Company for International Congresses and Meetings: Andrei Medintzev, Todor Mihov, Nina Todorova

From the National Palace of Culture L. Zhivkova: Tamara Razlogova

For Art Design: Mihail Sazdov

On Thursday August 25 a very nice dinner was prepared in the "Lulin" restaurant of the National Congress Centre. During the week and immediately after the meeting a number of interesting excursions in the country and visits to the Institute of Geophysics have been organized.

Thanks to special grants received through our mother organization IASPEI, a number of young scientists could be supported in their efforts to present papers in Sofia. ESC intends to follow up this policy as far as the very limited funds allow.

Beside this, more regional workshops under the auspices of ESC are envisaged.

D. Mayer-Rosa, Secretary general

Meeting of the ESC Bureau
Monday, August 22. 1988, 16-17h

Present: C.Morelli, N.Kondorskaya (for I.Nersesov), P.Burton, D.Mayer-Rosa, L.Christoskov, E.Hurtig (for H.Stiller).

1. Appointment of the Nominating Committee: V. Karnik, H. Korhonen, St. Mueller. Appointment of the Resolutions Committee: P. Burton, D. Mayer-Rosa.

2. New members: Malta applies for membership in the ESC with letter of 15 March 1988 by the Ministry of Education, and appoints Miss P. Farrugia as Titular Member. The ESC Bureau unanimously supports the application and will recommend it to the ESC Council for adoption.

3. The next General assembly: Letters of invitation to host the next meeting have been received from the Instituto Geografico Nacional in Madrid and from the Generalitat de Catalunya in Barcelona.

4. New ESC Statutes have been prepared by a special committee of the Bureau and will be discussed in the Executive Committee and thereafter presented to the Council for adoption.

5. The proceedings of Moscow have been printed recently and the first 100 copies will be distributed during the Sofia meeting. The Bureau is very satisfied with the excellent work done by the colleagues in the Institute of Physics of the Earth in Moscow and specially expresses its thanks to Prof. N. Kondorskaya as the responsible editor.

6. EAEE-ESC memo: A paper worked out by the Secretaries of the European Association for Earthquake Engineering (EAEE) and ESC calls for common future actions, e.g.:
- Better and more efficient cooperation between the two leading European associations in the field of earthquake related investigation is highly desirable and suitable steps should be undertaken.
- Mutual representation in the Executive Committees is recommended. The statutes should be modified accordingly.
- Joint regional workshops are taken into consideration within the next three years in specific fields, such as: Earthquake hazards and risk mitigation, zoning, strong ground motion etc.
- An immediate start of the exchange of proceedings and minutes on general meetings between the officers is agreed.
Signed: J. Studer, Secretary of EAEE and D. Mayer-Rosa, Secretary general of ESC.

Meeting of the ESC Executive Comm. and the Local Organizing Comm.
Monday, Aug. 22. 1988, 17-19h, cont. Friday, Aug. 26, 16-17:30h.

Present: C.Morelli, V.Karnik, N.Kondorskaya, H.Aichele, P.Burton, A.Udias, D.Mayer-Rosa, E.Hjortenberg, L.Christoskov, H.Berckhemer, E.Hurtig, V.Schenk

1. Sofia Meeting 1988:

L. Christoskov presents the printed program and explains the various lecture rooms, offices and services. It is decided to inform all authors of posters to be present at the poster sessions between 13-14h on their specific presentation days.

The following symposia and poster sessions are set up:

S1: Trends in regional seismicity in Europe (V.Karnik, J.Bonnin), oral and poster sessions
S2: Methods of seismic hazard assessment in Europe (V.Schenk, P.Burton, G.Zonno), oral and poster sessions

S3: Comparative studies on crustal and lithospheric structures (C.Morelli, E.Hurtig, L.Vinnik, P.Giese), oral and poster sessions.
S4: Future of observational seismology in Europe (H.Aichele, R.Pearce, D.Seidl, M.Cara)
S5: Calibration of historical earthquakes in Europe and recent developments in intensity interpretation (R.Gutdeutsch, C.Radu, G.Payo, D.Postpischl), oral and poster sessions
S6: Ground motion and rupture mechanism of strong earthquakes (L.Christoskov, A.Udias)
S7: Microseisms and seismic noise in a wide frequency band (E.Hjortenberg, I.Ostrovsky)
S8: Practical problems in earthquake prediction research (H.Berckhemer, I.Nikolaev), oral and poster sessions

Preliminary time schedule for Sofia 1988, August 1988.

Mon. 22:	Morning: arrival. Afternoon: registration, ESC- Exec. committee. Evening: CSEM - Council
Tue. 23:	Morning: opening plenary session, symposia, posters. Afternoon: symposia, posters. Evening: subcommission meetings
Wed. 24:	Morning:symposia, posters. Afternoon: symposia, posters. Evening: subcommission meetings
Thu. 25:	Morning:symposia, posters. Afternoon: symposia, posters. Evening: CSEM-assembly. Commission dinner
Fri. 26:	Morning:symposia, posters. Afternoon: symposia, posters. Evening: ESC-Council, elections
Sat. 27:	Morning:symposia, posters. Afternoon: symposia, posters. Evening: closing plenary session
Sun. 28:	Excursions

2. The activity reports of the subcommission chairmen will be presented in the respective working sessions of the subcommissions. In the opening plenary shorter comments will be included in the general activity report of the ESC President.

3. Resolutions must be delivered to the resolutions committee at least 24 hrs before the closing plenary.

4. Relationship to EAEE: It was agreed, that links to the other leading Association dealing with the effects of earthquakes, the European Association for earthquake Engineering should be strengthened. V.Schenk is appointed as representative into EAEE. D. Mayer-Rosa is appointed as representative into the CSEM council.

5. New Subcommissions: After intensive discussion it was agreed to propose the following new subcommissions:

SC-A: Seismicity (Bureau: Karnik, Papazachos, Schenkova)
SC-B: Data Acquisition, Theory +Interpretation (Bureau: Hurtig, Aichele, Melle)
SC-C: Physics of Earthquake Sources (Bureau: Udias, Trifu, Buforn)
SC-D: Deep Seismic Sounding (Bureau: Morelli, Guterch, Prodehl)
SC-E: Earthquake Prediction Research (Bureau: Berckhemer, Sobolev, Isikara)
SC-F: Engineering Seismology (Bureau: Schenk, Zonno, DeCrook).

6. The new ESC Bylaws and the modifications of the "Internal Rules" for the subcommissions are discussed and decided. As an important point concerning the subcommissions it was stated, that the Chairmen of the subcommissions are free to set up working groups in their respective subcommissions. It was also agreed, that there will be no formal members of the subcommissions.

7. Varia: The agenda for the "Opening Plenary Session" was discussed.
A new working group has been formed within SC-1 (thereafter SC-A): "Volcanoes and Earthquakes", with chairman R. Schick, Stuttgart and secretary: B. Martinelli, Zurich.

Opening Ceremony
Tuesday, August 23. 1988, 11h

Welcome Address by Grigor Stoichkov, Deputy Prime Minister of Bulgaria, President of the Permanent Governmental Commission for Natural Disasters and President of the Organizing Committee:

Ladies and Gentlemen,

For me it is a great honour and pleasure to welcome the participants of the XXI General Assembly of the European Seismological Commission whose host for the first time is the People's Republic of Bulgaria. The meeting of the European seismologists is carried out at a time when the political situation in the world is eased and the confidence among the countries on the old continent and the Mediterranean is increased, which favours the improvement of the research contacts among scientists.

The government of People's Republic of Bulgaria attaches great importance to the problems connected with natural disasters and in particular to the assessment of earthquake hazard. The casualties and material losses caused by earthquakes require profound investigation. Their unfavorable effects do not recognize political borders of the states and include neighbour areas. Because of the great number of small countries in Europe and the Mediterranean, situated in seismic regions, the collaboration among them plays an important role. Such a cooperation is successfully developped and we are pleased with the fact that our country participates in it, too. Bulgaria is ready in future also to make the necessary efforts in the joint activity of the European countries in this field.

I sincerely hope that the work of the XXI General Assembly will be successful and useful and the participating scientists will be able to discuss their experience and results in the different areas of seismology.

Bulgaria is situated in the most seismo-active part on the territory of Europe - the Balkan Region. The consequences of strong earthquakes that have occurred in this country, in the host-town Sofia inclusive, are known since ancient times. The impacts of some earthquakes with sources in neighbouring countries have been strong, too. The casualties and damages caused by the earthquake in Vrancea in 1977 fiiliped our government to render a significant financial assistance and support for the development of the Bulgarian seismology whose 100-year anniversary will be celebrated in 1991. A modern operative centre has been organized which ensures the fast and reliable transmission of information. Seismology is not any more only a scientific matter but it is also a problem of state policy.

Not very long ago in central North Bulgaria a sequence of strong earthquakes occurred, 10 towns and villages were affected, there were damages. The permanent government commission for natural disasters in cooperation with the Bulgarian seismologists carried out very important work on the evaluation of the situation and undertook rescue operations. Lately improved codes and standards for anti-seismic building were introduced.

I wish successful work to the participants in the XXI General Assembly of the European Seismological Commission and I believe that your scientific results will significantly contribute to the decrease of damages and losses during future strong earthquakes.

Thank you.

Welcome Address by Prof. Stoicho Panchev, Corresponding Member and Vice-President of the Bulgarian Academy of Sciences on behalf of the President of the B.A.S.:

Ladies and Gentlemen, Dear Colleagues and Guests,

It is my pleasure to welcome you on behalf of the President of the Bulgarian Academy of Sciences, Academician Blagovest Sendov and the representative body of the Academy.

The activity of your esteemed organization, the European Seismological Commission is very useful and highly valued in this country as well as in the other European and Mediterranean countries, also in the whole world. The earthquakes are natural phenomena which worry people where strong shaking occurs, but also even there where the awful quakes are not felt.

In researchers earthquakes always cause double feelings: during each earthquake one can't help thinking about the consequences, the damages for the economy, the casualties, material and cultural losses. At the same time earthquakes are a unique object for scientists. They help in the investigation and understanding of modern geodynamics, present an opportunity for obtaining invaluable, unique information. The main goal is, before all, to decrease the unfavorable consequences of earthquakes. But we also live on our planet and greatly depend on it, so that in order to ensure our existence the profound knowledge about it is simply obligatory.

It is a matter of fact that the honour to be the host of the present XXI General Assembly is the result of the realized necessity for a wide international collaboration in the field of seismology. The accurate determination of the earthquake parameters requires observations on large areas, based on the effective international cooperation.

One of the prerequisites for you to gather in our capital is the fact that Bulgaria is a strong seismic area. In the past very strong earthquakes with heavy consequences have occurred. Recently the earthquake with the source in Vrancea affected the area of the Balkan countries, including part of our area. In 1986 earthquakes with sources in Bulgaria sensitively damaged a part of central North Bulgaria - chiefly the town of Strazhitza and the towns and villages around. Organized seismological investigations have been carried out in this country since 1891 and soon we shall celebrate the 100-anniversary of the Bulgarian seismology. Bulgaria participates in the activity of ESC since the latter has been founded and according to its possibilities has always actively contributed to carry out a number of scientific investigations in cooperation with many European countries, especially with the Balkan states.I will take the opportunity to mark the most important achievements of our work in the energy classification and the magnitude scales, the long-term prediction and elaboration of the corresponding map with new original methods, the making of a dense seismic network of 14 stations which will continue to develop and the building of a system which collects and processes real time data, etc.

I cannot help mentioning a problem, which affects the users of seismic observations, each citizen and the state as a whole. I have in mind earthquake prediction. It is not by chance that a separate symposium is dedicated to this problem. Undoubtedly this is one of the most serious if not the most difficult problem in modern geosciences. It is clear, this problem requires an increase of efforts, both on behalf of seismologists and on behalf of society in order to guarantee high security by material and technical means of the studies in this field.

I can inform you that in Bulgaria so far only the first attempts are made in this direction, but our intentions are quite serious and far reaching. One of our ideas, to which I would like to draw your attention is: some of the seismically active regions on our area to be turned into an international prediction site.

I would like to greet you once more with a hearty "welcome" and wish you successful work in which we all are so much interested.

Thank you.

Opening plenary session
Tuesday, August 23, 1988, 11:30 -12:30h

1. Welcome Address and General Activity Report of the ESC-President, Prof C. Morelli:

Ladies and Gentlemen, Dear Colleagues,

It is a great honour and pleasure for me to open this XXI General Assembly of Sofia, in these wonderful premises and within this efficient organization, for which I express - also on your behalf - our best thanks to Prof. Christoskov and to all the Organizing Committee. I thank also for their participation the President and General Secretary of IASPEI, Prof. St. Mueller and Dr.R. Adams.

At the beginning of this XXI General Assembly of the ESC, it should be first of all recalled that this year we celebrate the 40th anniversary of ESC. Conceived first in 1948 at the I.U.G.G. General Assembly in Oslo, ESC was born in September 1950 at the Verona meeting. Just 24 people were there as charter members and only few of them are today alive. Among these, Miss C. Lehmann, who celebrated her 100 years on May, 1988. To the telegram sent, she replied: "I feel honoured and I was extremely pleased to receive your kind congratulation for my 100 year birthday on May 13, 1988".

The spirit of the Verona pioneers was really a European one, open to Western and Eastern Europe. From the beginning, we were convinced that specially in Seismology we must work together. This is particularly true in these days, in which a strong effort is done for the improvements on the cooperation between Eastern and Western Europe, not only in science but also in any other field. In our case, everything is facilitated, as well, by the personal relationships and friendship.

At this point, I would like to recall the friends that left us in the last two years: Dr. Heinz Menzel, Professor of Geophysics at the University of Hamburg, died in June 1988. Dr. Michael Fournier D'Albe, first director of the Division of Earth Sciences at UNESCO, died tragically and suddenly last weekend (the audience is asked to rise for a minute of silence).

I will now review in synthesis the activity of our Commission from the last General Assembly in Kiel. The 86-88 period is characterized by rapid improvements in technology and in connected scientific results. They will be properly discussed into details in the meetings of the symposia and subcommission sessions scheduled in the Program. I would like to mention just a few of these results of general interest.

SC-1 (Seismicity of the European Region) Prof. Karnik indicates the principal task in discovering the rules governing the distribution and changes of European earthquake activity in properly defined source regions and the assessment of their earthquake potential. Localization accuracy is improving but magnitude determination, particularly for events of $M < 5$, needs unification at least at the level of the EMSC. Seismotectonic relations remain just vaguely known and much more attention must be paid to them. The last completed regional project was the compilation of a maximum intensity map for Europe (C. Radu).

On-going projects are: - Extension of the uniform European catalogue 1956-1985 (V. Karnik). - Preparation of a volume on large historical earthquakes in Central Europe (R. Gutdeutsch). Two big projects which have been concluded recently: 1. Seismicity map of the Mediterranean area, prepared by CSEM under contract with IOC - UNESCO as an overprint series (10 sheets) to the International Bathymetric Chart of the Mediterranean (IBCM), scale 1:1.000.000.
2. Catalogue of European Earthquakes (2 maps published) and Atlas of European Earthquake Maps (in press) compiled by our past-Secretary I.M. Van Gils under contract with E.C.C., Directorate-General for Science, Research and Development.

Practically, all topics which are under the auspices of SC-1 will be discussed at the traditional fourth symposium on seismicity and seismic risk in September 4-8, 1989 in Bechyne, Czecho-

slovakia. We can expect in 1989 also a meeting of the Working Group on Historical Earthquakes. Finally it can be stated that seismicity studies in Europe continue to concentrate on: - detailed monitoring of microseismicity using local networks, - induced seismicity, - study of time and space variations - estimates of earthquake potential - improvements of comprehensive data bank, - cooperation with teams working on vulnerability and risk.

SC-3 (Physics of Earthquake Sources) An effort has been made to finish the compilation of a Catalogue of focal mechanisms of European earthquakes for shocks with M > 6. The catalogue includes focal mechanisms of 142 earthquakes from 1905 to 1983, derived from 54 references. The catalogue will be published next year. Future joint work of the SC will be established at this General Assembly. There is also a proposal to extend the catalogue to smaller magnitudes.

SC-4 (Microseisms and Seismic Noise) An administrative and a scientific session was held at the XX. ESC General Assembly in Kiel 1986. The papers are published within the proceedings. Members have participated in a study of long period microseisms initiated in 1987 by Prof. Darbyshire. The study will be the subject of a workshop at the 1989 IASPEI meeting. At the IUGG General Assembly in Vancouver 1987, a symposium on Microseisms was held. Its proceedings, together with other papers on microseisms, will be edited by E. Hjortenberg and A. Nikolaev and published as a special issue of Physics of the Earth and Planetary Interiors.

SC-5 (Theory and Interpretation) Prof. Stiller communicates following main activities: 1. XXV Annual Meeting of the European High Pressure Research Group with the international conference High Pressure Geosciences and Material Synthesis (Potsdam GDR 25-27.08.87). 2. Workshop "Seismic Waves in Laterally Inhomogeneous Media" (Liblice, Czechoslovakia, June 1988).

SC-6 (Deep Seismic Sounding) Deep Seismic Sounding (Experimental Seismology) has received a big input by the new technologies in Deep Reflection Seismics (DRS). They include both the equipments (high gain, digital recording, more efficient filtering, tele-transmission, etc.), the recording (narrow trace spacing, multi-sensor traces, 3-D geophones, etc.) and the processing (sophisticated software and hardware). The DRS results integrate and complete DSS ones. Both constrain interpretation of the potential geophysical methods (gravity and magnetics); which permit to extend the seismic results in three dimensions. When all these geophysical methods are applied together with the geological information, we arrive at an integrated interpretation, which permits to obtain the best results possible today. Following are few examples to illustrate the seismogenetic importance of similar well constrained geophysical findings.

Alps: The first geotraverse in the Western Alps was carried out in 1986 by a common profile between the French ECORS and the Italian CROP projects. It is mainly a DRS-DSS profile, integrated with gravity and magnetic data. Preliminary results are: Both geological and geophysical constrains converge to impose a model with two or three lithospheric thrusts. The first major rupture corresponds to the well documented collision of the European and Apulian plates, during upper Cretaceous. It is ascribed to the uptilting of the Apulian plate. The second lithospheric thrust would be underlined into the crust by the reflectors emerging as Penninic Front (PF). The last thrust is the best documented one. It emerges West of the PF, splaying into the Jura thrust and the Belledonne median thrusts, being active during late Tertiary.

These results confirm the assumed nake-like structure of the Western Alps. The appearance of more than one M-discontinuity suggests that overthrust processes in the Alpine region involve the upper mantle. In spite of the long (geological) time elapsed from the main tectonic phases, the tectonic assessment and isostatic balancing is yet in action (as demonstrated by the diffused seismicity in the area). The same is true also for the Eastern Alps, where the very high seismic activity of the Friuli area is connected with a strong vertical gradient in the Moho. That is, mass anomalies in the crust (reflected in the Bouguer gravity anomalies) are seismogenetic, if they have not reached the isostatic equilibrium (sensu lato) or if they are loosing it (by changes on the environmental or physical conditions).

Apennines: As already expected from the strong gravity gradients, big vertical Moho faults were discovered by DSS at the Moho level. The western distensional area, characterized by a thinner crust, ends below the maxima of the Apennines elevations, where compressions characterize the foreland basins. The Moho faulting can be followed all along the Apenninic chain, with a strong correlation with the seismic activity.

The Western Apennines represent an extensional region between the relatively aseismic Tyrrhenian Sea to the west and the Adriatic Sea to the east. In the Southern Apennines, two earthquakes that occurred on 1962 August 21 approximately 50 km NW of the destructive Campania-Basilicata event of 1980 November 23, have been studied in order to investigate their geometry of faulting (Westarray, 1987). Both events involved normal faulting. Preferred focal mechanisms have one nodal plane that strikes NW parallel to the trend of the Apennines, and dips to the NE in a position where motion on the same fault in the geological past has led to subsidence of the hanging wall and to the formation of a sedimentary basin situated to the NE in the hanging wall of the fault. The 1962 events, like that of 1980, occurred at around 10 km depth beneath an intra-Apennine sedimentary basin. A normal fault with the same orientation as the NE dipping nodal plane of the focal mechanisms has been observed on a commercial seismic reflection profile crossing this basin. It is suggested that this is the fault that moved in these events, and that repeated motion on this fault is responsible for the development of the basin and for the subsequent folding of Pliocene sedimentary rocks that outcrop in the area.

The distribution of isoseismals for the events of 1688 and 1494 indicated that these events may have occurred on the same segments of fault as the 1962 and 1980 events respectively. This suggests that the seismicity of the Apennines may be characterized by repeated earthquakes on normal fault segments that are associated with intra-Apennine sedimentary basins. Repetition of earthquakes in these areas suggests that intra-Apennine sedimentary basins should be regarded as areas of high seismic hazard relative to surrounding localities. The similarity of the geometry of faulting of both the 1980 and the 1962 earthquakes to that expected for normal-faulting earthquakes elsewhere, suggests that there are no grounds for invoking any model of crustal deformation that is unique to the Apennines and different from that expected in other areas undergoing crustal extension. In the past, seismic zoning has been carried out in the Apennines by dividing the area up into arbitrary polygonal regions without regard to structural geology. Bearing in mind the observations now discussed, it is however reasonable, to regard intra-Apennine sedimentary basins as areas of high seismic hazard relative to surrounding areas.

Ancona: At higher levels in the sedimentary cover, the effects of the Apennines and Dinarides compressions against the foreland (Adriatic plate) indicate the centripetal vergence of the most recent nappes, which have not jet reached their equilibrium with the environment and are therefore responsible for the very strong seismicity on both sides of the Adriatic sea.

Western Po Plain: From the examples of the integrated geophysical interpretation typical of the Western Po Plain, the centripetal vergence of the Apenninic and Alpine nappes in the recent sedimentary cover, not yet in equilibrium as demonstrated by the seismicity of the area, can be seen. Furthermore, it must be considered that accurate knowledge of seismic velocity distribution within the layers will render possible the preparation of a real structural model. The proper use of seismic networks, which otherwise cannot produce (even when equipped with the best available instruments and operated with the most modern technologies) one of the main parameters needed in seismological investigation: the focal depth, as well as the expected inputs to Seismotectonics.

The European Geotraverse (EGT), which started in 1983 coordinated by the European Science Foundation, represents an unprecedented cooperation programme to study the lithosphere and upper mantle of Europe. In 1986, the Central Segment was completed with a Deep Refraction Profile between Ligurian and Baltic seas. In addition, arcs and fans were performed for a detailed study of the Western Po Plain. The total number of recorded seismograms is 5350. First results will be presented at the ESF Study Centre n.4 in Giessen (Spring 1989).

In 1987, a DSS transversal profile took place in the Ligurian sea. The profile, located along the opening axis of the oceanic crust in the Ligurian sea, had the purpose of better studying this opening in the past and in present, as well as its extension and dynamic implications. Sea operations (26 OBS and shooting) were carried out by ship "Minerva". 30 land mobile stations were operated by I.G. Hamburg and IMGA Trieste and the Ligurian seismic network was conveniently extended to Tuscany, Corsica and Provence.

First results of the EGT-S 1985 big experiment have been presented and discussed in the Nato Workshop in Gradisca (1987/88), followed by the ESF Study Centre n.3 in Gradisca (1988), and continued in Zurich (1988). Having completed most of the experiments on the main ESF line, attention is now shifting towards the Iberian Peninsula, with a major deep seismic sounding campaign taking place during Autumn 1989. The special Iberian Lithosphere Heterogeneity and Anisotropy (ILIHA) project, conceived and coordinated by the EGT Scientific Coordinating Committee, has been granted financial support from EEC.

Finally, it must be mentioned that, with the advent of ultra high-speed computers and global networks offering high-quality digital seismic data, a new process, seismic tomography, has opened exciting avenues for exploring the earth's interior. Data from earthquakes around the world have been analyzed to display velocity variations along ray paths penetrating the Mantle and outer core. Two active research centres operate since few years in this field also within our Commission: the Institute of Earth Sciences, University of Utrecht (Dr. Spaakman) and the I.P.G., Paris (Prof. Hirn). The resulting, very generalized tomographic models depict broad linear regions of relatively low velocity in the upper mantle, roughly corresponding to the great spreading ridges, and areas of higher velocities beneath continents and old ocean basins. Similar zones of contrasting velocity are revealed in the lower mantle and outer core. It is tempting to interpret this velocity distribution as an indication to be expected in convecting systems within the mantle and outer core. This project, coupled with current seismic investigations of the lithosphere, provides potential for a realistic model of a dynamic earth, the beginning perhaps of yet another revolution in earth sciences. Intimately connected with the studies on the lower crust and upper mantle, performed by experimental and observatory seismology, there are two very important projects recently started also in Europe:

The continental deep drilling projects. After the first fundamental results reached, and published in 1987, the super-deep Kola bore-hole has been recovered, deviated and continues the program. A new super-deep bore-hole started in Oberpfalz, F.R. of Germany in autumn 1987, after a very careful geological and geophysical preparation. Results of paramount importance also for seismology are expected. Specially on the nature of seismic discontinuities and the presence of fluids (which are supposed to accumulate most of the energy released by an earthquake).

Laboratory Investigations. Key experiments are performed in different European laboratories for understanding petrophysical and geophysical processes and the state of the material in the earth's interior under high both temperature and pressure conditions. They are essential for a proper interpretation of indirect geophysical methods data, specially seismological ones. The problem is where to find in Europe materials from the lower crust.

A good opportunity in this sense is offered in Calabria, where the outcropping crystalline basement of the Serre Mountains of southern Calabria represents a tilted block of a complete section of continental upper and lower crust. This very favourable and scarce situation allows: 1. to determine the in-situ geophysical properties of lower crustal rocks (P- and S-wave velocities. Poisson-ratio, seismic anisotropy, density, electrical conductivity) in order to calibrate deep exploration sounding and modelling techniques; 2. to investigate the evolution of a tectonically uplifted fossile lower crust and its relationship to the newly formed lower crust in its original position. A joint geophysical common project will start next year between Germany F.R. (Universities of Berlin and Karlsruhe) and Italy (University of Trieste), and can be considered as a key project for lower crustal studies which complements super-deep continental drilling programs for upper and middle crustal levels.

SC-7 (Earthquake Prediction Research) Prof. Berckhemer informs that, in consequence of the ESC Resolution 3 of Kiel, he was invited by the Commission of European Communities and participated in the preparation of the Research Programme 1989-1992 on Climatology and Natural Hazards. This programme will soon be submitted to the European Parliament for approval. ESC Resolution 2 of Kiel recommended the development and the installation of multi-parameter observatories in selected test areas. A major bilateral project, in which German and Turkish scientists are cooperating on earthquake prediction research in a test area, is the western end of the North Anatolian fault zone. Non-seismic parameters considered as possible seismic precursors have also been investigated in the Friuli region for almost ten years now and led to interesting conclusions.

SC-8 (Engineering Seismology) The TERESA Working Group on "Earthquake Hazard Assessment in European Test Areas" organized three very successful workshops in Prague 1987, Milano 1987 and Zurich 1988. Scientists from at least 12 different European countries attended and contributed to the common project. Symposium S 2 in Sofia is the closing meeting of the group and will provide a good overlook on the achieved results. It is intended to continue the work jointly with the corresponding IASPEI groups. The contacts of SC-8 to the "European Association of Earthquake Engineers" have been strengthened and will be even more in future.

In general, the following research projects are endorsed by ESC:
- "Construction of Seismotectonic Maps" initiated by the Working Group on Seismotectonic Maps. (Chairman Dr. N. Pavoni, Zuerich).
- In the frame of the International Heat Flow Commission, a brother commission to ESC in IASPEI, the project "Geothermal Atlas of Europe" has been initiated. In this project some activities of the project "Comprehensive Mapping of the Lithosphere" are included, as well. Prof. Hurtig, Prof. Haenel and Dr. Cermak have put a lot of effort in organizing the cooperation among all European countries on this matter. The ESC and especially the Subcommission Theory and Interpretation is supporting this project.
- The compilation and interpretation of historical seismograms is proceeding well. Prof. Gutdeutsch has invited to another meeting on this matter in Austria in 1987. ESC sponsored this meeting.
- The project "Unification of digital recording" has great importance. SC 2 takes care of this project.

ESC-Sponsorships has been given to the following events:
- TERESA workshop on "Seismic hazard evaluation for European test areas" organized by the Geophysical Institute of the C.A.S., Prague (CSSR) in Prague, 26-30 March 1987.
- Symposium on "Seismicity, Seismotectonics and Engineering Seismology in the Ligurian Area, Italy", organized by the Instituto Geofisico dell'Universit di Genova (Italy) in April 1987.
- Workshop on "Induced Seismicity and Associated Phenomena", organized by the Geophysical Institute of the C.A.S., Prague (CSSR) in Liblice, March 1988.
- Workshop on "Seismic waves in laterally inhomogeneous media", organized by the Geophysical Institute of the C.A.S., Prague (CSSR) in Liblice, June 1988.
- International Symposium on "Geodesy and Geophysics of the Earth", organized in Potsdam by the Zentralinstitut fur Physik der Erde, Academy of Sciences of the GDR, August 1988.

The future of all sciences will depend on the way in which they are able to respond to the social needs. That is, any science is requesting (and obtaining) very much in any type of support from the community. But, what is the fall-out to the community? Benemerits are those, that can foresee the requests and are able to satisfy them. In this sense, I submit your attention to the proposal from our colleague V. Karnik, who with reference to the problem of orientation of ESC activities suggests that "in seismology the work should be focused on prevention and protection problems linked with social and economic aspects, such as prediction of earthquake activity patterns in space and time, physical processes in the focus and in the epicentral area, transfer of results to the users in an applicable form and advancement of seismology in earthquake prone developing countries by increasing the number of well trained seismologists.

In the line suggested fit properly - for aspects typical of the European region - some of the recently proposed new international research projects, like:
-The International Lithosphere Program, which in Eurasia supports "EUROPROBE", a proposal to investigate the European lithosphere by super-deep drilling and deep-seismic sounding. Techniques: Super-deep drill holes: KOLA SG-3, KTB Oberpfalz; Long-range seismic lines with mobile stations: EGT-Kola, Biscaya-KTB-Ugolskov. Goals for the upper crust: Detailed structure and petrology by drillholes; for the lower crust: Detailed seismic structure using conventional lake and drillhole shots with 1-2 to charges every 50-100 km and mobile stations with 2 km spacing; for the lower lithosphere: Deep seismic structure using super-strong charges at 100 km intervals and 10km spacing of mobile stations.
- The "Global Change" Program,
- the program "Man and Biosphere" and the
- "International Decade for Natural Disaster Reduction" (IDNDR) should be mentioned.

This last programme was adopted by the United Nations General Assembly late in 1987 and the Secretary-General of UN has to report within one year on the terms of reference and suggested mechanism for the Decade, which will be held during the 1990's.

Since this project will be one of the major coordinated initiatives interesting Seismology for the next decades, ESC should try to perform - in cooperation with IASPEI - a major effort for an appropriate participation. Suggested projects of interest to IASPEI include the establishment of cooperative programmes for strong motion measurement and analysis, development of new earthquake prediction models, unified risk maps, microzonation, seismic gaps, and the organization of a coordinated international earthquake information service.

Istanbul IASPEI Assembly: The 25th General Assembly of IASPEI will be held in Istambul Aug. 21 - Sep. 1, 1989. Many Symposia and Workshops of big interest will take place during the Assembly and all the IASPEI commissions are expected to have a meeting; so that I hope in a strong participation from ESC members.

Restructuration of ESC: Theoretically, the bulk of the scientific work within ESC should be performed by and within the subcommissions. This is obviously depending from many factors, human ones, the nature of the themes assigned etc. As noticed by some ESC Members, " the present system of subcommissions, e.g. with a fixed membership, is not fully effective because most members attend usually one session and other interested people show up next time". It is therefore suggested " to elect only chairmen of panels and leave to them whom to invite for participation. Some of the chairmen should review or discuss the results at round-table sessions and invite other speakers, if needed. This problem will be brought to the General Assembly, after discussion by the Executive Council.

In such a manner we will try to further improve the efficiency of our Commission, also in consideration of the new important tasks emerging and requesting an adequate consideration. This will permit also to strengthen the mutual understanding, in that " Verona spirit " of cooperation from which ESC started and has so nicely progressed.

Thank you.

2. Obituaries:

Dr. Heinz Menzel,

Professor of Geophysics at the University of Hamburg, died in June 1988, 79 years old. He was born in 1909 in Koenigsberg. After his study time he worked for several years in exploration seismology at PRAKLA. His scientific career began at the University of Hamburg with a thesis on surface waves. In 1957 he obtained the chair of Geophysics at the Bergakademie Clausthal, where he initiated several geophysical working groups such as model seismics, marine seismics and gravity investigations in the Alps. In 1964, back to Hamburg as Professor of Geophysics, he was the first director of the Institute of Physics of the Earth. Under his stimulation marine seismics in Hamburg gained importance. Dr. Menzel was associate member of the Bolivian Academy of Science and was the first chairman of the German FKPE. He certainly belongs to the first generation of outstanding geophysicists after the war. He was equally famous for his warm humour and for the high standard of his lectures. His former students and colleagues will not forget their respected Professor.

ESC Bureau

Dr. Michael Fournier D'Albe

died suddenly at his home in Normandy on 19 August 1988, aged 68. He is known to seismologists for the major contributions he made to our science as the first director of the Earth Science Division of Unesco, but his early training and research were in atmospheric physics. In 1951 he was recruited as part of a three-man team to help the Pakistan Meteorological service initiate work in seismology, geomagnetism and atmospheric physics. After joining Unesco in 1955/56, he gave great impetus to international seismology by arranging for a series of high-level missions to various parts of the world. He helped to establish a seismological centre in South America, the International Institute of Seismology and Earthquake Engineering in Japan and the Balkan Seismological Project. He was involved in the establishment of the International Seismological Centre. Although retired, he was still actively engaged in advising Unesco and UNDRO, particularly on plans for the International Decade of Natural Disaster Reduction. Michael will be sorely missed by us all as a skilled diplomat, a valued colleague and above all as an understanding and helpful friend.

R.D.Adams

3. Call of titular members:

Country	Titular Member old / new	confirm. date	present * = yes	proxy
Albania	E.Sulstarova	26.07.88		Aliaj
Algeria	M.Benhallou			
Austria	J.Drimmel	26.07.88	*	
Belgium	M.DeBecker	20.07.88	*	
Bulgaria	L.Christoskov	08.08.88	*	
Czechoslovakia	J.Vanek	11.05.88	*	
Denmark	J.Hjelme	18.07.88	*	Hjortenberg
Egypt	M.Maamoun			
Finland	H.Korhonen	28.07.88	*	
France	M.Cara		*	
F.R.Germany	H.P.Bonjer	21.09.87	*	
German D.R.	H.Stiller/E.Hurtig	09.06.88	*	
Greece	J.Drakopoulos		*	
Hungary	E.Bisztricsany			
Iceland	R.Stefansson			
Ireland	A.W.B.Jacob	10.08.88		
Israel	A.Shapira	03.08.88	*	Rabinowitz
Italy	C.Morelli	07.07.88	*	
Jordan	Z.El-Isa			
Lebanon	J.Plassard			
Luxembourg	J.Flick		*	Trampert
Malta	P.Farrugia	15.03.88	*	
Morocco	D.Ben Sari			
Monaco	N.Bethoux			
Netherlands	R.Ritsema /de Crook	27.07.88	*	
Norway	S.Mykkelveit		*	
Poland	R.Teisseyre			
Portugal	L.Mendes Victor		*	
Romania	L.Constantinescu	06.02.88	*	Radu
Spain	J.Mezcua		*	
Sweden	O.Kulhanek	24.11.87		
Switzerland	D.Mayer-Rosa	12.10.87	*	
Tunisia	M.Allouche			
Turkey	A.Neclioglu			
United Kingdom	R.Pearce	02.10.87	*	
USSR	I.Nersesov/S.Arefief	20.07.88	*	
Yugoslavia	D.Skoko	12.02.88	*	Lapajne

4. ESC President Prof. C. Morelli declares the XXI. General Assembly of ESC opened.

Activity reports 1986 - 1988 of the Subcommissions

SC 1 Seismicity

Chairman: V. Karnik, Czechoslovakia
Vicechairman: B. Papazachos, Greece
Secretary: Z. Schenkova, Czechoslovakia

Session of SC 1 in Sofia:

WG1 - Standardization of magnitude determination for European earthquakes. As the first step the compilation of methods used by individual stations was recommended using the questionnaire of the IASPEI Commission on Practice. Station reports should contain amplitude data.

WG2 - The continuation of the European catalogue 1901-1955 (V. Karnik) for the years 1956-1985 is under way using the same method of M-determination. The extended homogeneous data base will be used for earthquake statistics.

WG3 - The activity of the WG3 concedes with that of the project on the Earthquake Risk Reduction in the Balkan Region (UNDP RER/88/004 . The outputs in 1984-1990 will be the catalogue 1971-1988 (follow-up of the UNESCO catalogue 1901-1970 and the atlas of isoseismal maps for the same period .

WG5 - Principles for evaluating historical earthquake information in Central Europe have been drafted. The publication of a volume with studies of large historical earthquakes in Central Europe is being organized.

A next meeting of the group is planned on the occasion of the E.S.C. Meeting in Sofia, August 22-27, 1988.

Two new WGs are established, which are:

WG on Statistical Models of Seismicity chaired by Dr. Z. Schenkova Tasks: - Definition of statistical parameters of seismicity and - Development of statistical models fitting various types of spatial and time distributions of earthquake activity.

WG on Aftershock Sequences chaired by S. Arefiev. Tasks: Special field observations incl. strong motion recordings. Interpretation of geometry and seismic regime.

Report on the workshop on Seismotectonic Maps in S. Margherita (Genova), Italy, September 23-25, 1987.(N.Pavoni)

The workshop took place in the frame of a meeting of the E.S.C. Working Group on Seismotectonic Maps. It was organized by Prof. C. Eva and co-workers of the Istituto Geofisico e Geodetico of the University of Genova. The meeting was attended by 39 participants from 11 different countries.

Considering the importance and complexity of seismotectonic studies, as well as the increased demand for reliable seismotectonic maps, the participants of the Workshop make the following recommendations:
- It is desirable that drafts of national seismotectonic maps should be prepared as soon as possible according to the E.S.C. guide-lines (1985). Suggested scales are 1:500 000 and 1:1000 000. It is hoped that the production of these draft maps will provide a basis to further discuss and refine the methods to be used in the preparation of final seismotectonic maps.
- The W. G. should establish contact with the Commission for the Geological Map of the World CGMW and with the European Association of Earthquake Engineers.

- The W. G. should support the ICL project to produce a world map of active faults.

The following problems were identified by the participants as requiring special consideration:
1- Historical Seismicity: Criteria regarding the reliability of historical epicentre locations should be established, and consideration given to alternative ways of representing historical seismicity on seismotectonic maps.
2- Microearthquakes: Further consideration should be given to how micro-earthquake data can best be used in seismotectonic mapping.
3- Strain and stress fields: There should be consideration given as to how regional strain and stress fields can best be represented on seismotectonic maps.
4- Pattern recognition techniques: The possibilities of using pattern recognition techniques for the identification of potentially active areas should be explored.

The participants expressed their thanks to Prof. C. Eva and the Organizing Committee for the excellent organization of the meeting.

SC 2 Data Acquisition and Interpretation

Chairman: H.Aichele, FRG
Vicechairman: J.Hjelme, Denmark
Secretary: W.Melle, GDR

The SC 2 organized the symposium "The Future of observational seismology in Europe" in Sofia, during which 26 scientific papers and several posters were presented and discussed.

At the administrative session of the SC 2 the participants adopted the proposal to join SC 2 (Data acquisition and interpretation) SC 4 (Microseism and Seismic noise) and SC 5 (Theory and Interpretation) forming a new Subcommission C "Data Acquisition, Theory and Interpretation". The ESC-Council decided this new structure and elected resp. approved the nominated officers of the new subcommission: President: Prof. Dr. E. Hurtig (GDR), Vicepresident. Dr. H. Aichele (FRG)Secretary: Prof. Dr. W. Melle (GDR).

Five working groups were formally adopted and the chairpersons nominated:
WG1: Instruments. Chairman: Dr. M. Schmidt (GDR).
WG2: Standardisation and Interpretation. Chairwoman: Prof. Dr. N. Kondorskaya (USSR).
WG3: Data processing and collection. Chairman: Prof. Dr. M. Cara (France)
WG4: Microseism and seismic noise. Chairman: Dr. E. Hjortenberg (Denmark).
WG5: Surface wave tomography for European stations. Chair: Yanovskaya (USSR)
WG6: Complex interpretation of geophysical fields. Chairman: Dr. V. Babuska (CSSR).
WG7: Material properties and rheology of the lithosphere. Chair: Kalinin (USSR)

Furthermore, it was proposed to have a joint WG "Surface wave tomography for European stations" together with SC D "Deep Seismic Sounding". Colleagues who are interested to participate actively in one of the working groups should contact the nominated chairperson or the officers of the subcommission.

Finally a short information was given on the proposal of the IASPEI-working group on seismic and geographical regionalisation to further develop the existing Flinn-Engdahl regionalisation scheme by adding a third tier. The time schedule for this procedure was explained: Proposals may be suggested at the IASPEI-meeting in Istanbul, where this extension of the FER shall be formally adopted. The participants of the administrative meeting suggested that detailed information on this item should be distributed through ESC and/or EMSC.

SC 3 Earthquake Source Physics

Chairman: A.Udias, Spain
Secretary: E.Buforn, Spain

A preliminary version of the "Catalogue of Focal Mechanisms of European Earthquakes", that has been compiled in Madrid, was presented. The Catalogue includes more than 500 focal mechanism solutions for 141 earthquakes of M >6.0 in Europe. The Catalogue will be published early 1989. Some problems regarding the determination of focal mechanisms were discussed. As a consequence of the discussion it was proposed to organize a workshop with the topic of modern concepts and methods in source mechanism studies. The workshop will take place in spring 1990 in Madrid. Invited lecturers and presentation of contributions are envisaged. The workshop will serve as a discussion ground by new methods in focal mechanism determination and their application in Europe.

In order to include young scientists in the subcommission, it was proposed the name of J.C. Trifu for the post of vicechairman. The proposal was accepted with the provision of the notification to the present Vicechairman Dr. I. Krostov.

SC 4 Microseisms and Seismic Noise

Chairman: E.Hjortenberg, Denmark
Vicechairman: V. Tabulevich, USSR
Secretary: C. Eva, Italy

Activity report 1986-1988:

The Subcommission on Microseisms and Seismic Noise held an administrative and a scientific session at the XX. ESC General Assembly in Kiel 1986. The papers are published in the proceedings of the Kiel meeting.

The subcommission has participated in a study of long period microseisms initiated in 1987 by Prof. Darbyshire. The study will be the subject of a workshop at the 1989 IASPEI meeting, but already at the ESC Sofia meeting three of the papers deal with storms selected for this study. They will be presented in the symposium "Microseisms in a wide frequency band".

At the IUGG symposium in Vancouver 1987 a symposium on microseisms was held, its proceedings will, together with other papers on microseisms, be edited by E. Hjortenberg and A. Nikolaev and published as a special section of Physics of the Earth and Planetary Interiors.

The seismic noise is subject of great interest at the Conference of Disarmament in Geneva, because of its influence on detection capability. Results from the Technical Test, GSETT have been published, e.g. by H. Israelson, 1986, E. Hjortenberg, 1987 and in reports and documents from the Group of Scientific Experts in Geneva.

SC 5 Theory and Interpretation

Chairman: H.Stiller, GDR
Vicechairman: J. Behrens (Berlin-W.)
Secretary: S.Frank GDR

Activities in 1986 - 1988:

1. XXV Annual Meeting of the European High Pressure Research Group with the International Conference on High Pressure Geosciences and Material Synthesis (Potsdam GDR 25-27 Aug. 1987).

2. Workshop "Seismic Waves in Laterally Inhomogeneous Media" (Liblice, Czechoslovakia, June 1988).

SC 6 Deep Seismic Sounding

Chairman: C. Morelli, Italy
Vice-Chairman: B. Guterch, Poland
Secretary: C. Prodehl, F.R.G.

The activity report presented in Kiel, 1986, summarized mainly the technological advancements and open problems both in DSS and DRS. The report 1986-88 distributed in Sofia summarizes the main geophysical results obtained in the period. They are mainly obtained from the big experiments on the EGT Southern Segment (1986 and 1987), on the EGT Central Segment (1986) and by the Geotraverses in the Western Alps (ECORS-CROP) and in the Western and Central Alps (NFP-20). following are some preliminary results:

Southern Segment: Due to its complex geologic history the data for the Southern Segment are the most difficult to interpret, but show exciting new results. Both seismic refraction and reflection observations confirm that the Alpine crust is asymmetric with a pronounced intracrustal low-velocity zone. The deepest part of the crust-mantle boundary is found to the Northwest of the Ivrea zone; there the near-vertical Moho reflections disappear in the steeply dipping root zone, but the refraction Moho remains visible.

In the Southern Alps, the Po Basin and the Northern Apennines the data from a dense network of profiles, arcs and fans indicate the presence of two partially overlapping crustal types: in the South the Ligurian (intermediate-type) crust is overriding the Adriatic micro-plate (thickness 40 km) which itself rises to about 20 km depth northwestwards. Additional evidence was presented for incipient differential rifting in the Ligurian Sea which is underlain by a large body of "anomalous mantle" (Pn velocity 7.5 km/s).

The crust of the Corsica-Sardinia block is of Hercynian age and exhibits a bowl shape with a rather undifferentiated internal structure (average P-wave velocity 6.3 - 6.4 km/s). Crustal thickness increases from 20 km at the margins to 33 km beneath the centre of the islands. A thinned crust with thrust tectonics characterizes the Sardinia Channel. The preliminary deep-seismic sounding results in Tunisia show a profound difference in crustal structure from north to south (the transition to the African craton), and from west to east, i.e. to the Pelagian Sea where the basement is deepest.

Central Segment: The Moho depth is 50 km under the central part of the Alps, 26 km under Swabian Jura, 26 km nearly constant further to the north. A characteristic feature of the velocity-depth model north of the Alps is the existence of a low-velocity zone in the middle crust. This zone seems to extend southward underneath the Alps and it evidently vanishes under the North German Lowlands. The central Alpine area is characterized by rather low average crustal velocity of only 6 km/s. In Southern Germany the velocity decreases from 6.2 to 5.5 km/s below depths of about 8 and 11 km and the thickness of this low-velocity zone varies between 3 and 5 km. In the same area a discontinuity with a velocity increase from 6.2 to 6.8 km/s rises from 20 km depth under the Alpine Foreland to 17.0 km depth under the Rhone in the north and merges with the lower boundary of the low-velocity zone under the Rhone. Under the Variscan mountain area north of the Main river the low-velocity zone deepens, becomes thicker (depth range 10 to 17 km) and more pronounced. The velocity decreases from 6.3 to 5.2 km/s. The lower crust between the northern Alpine foreland and the North German Lowlands is characterized by a rather high velocity of about 6.9 km/s.

The proposal of a new working group was discussed and accepted. Title: project of the phase velocity field in Europe. Goal: determination of the phase velocity field of Rayleigh- and Love waves in Europe as precise as possible. Necessary observation material: great number of observed phase- and group velocity curves (10 to 100 s) for traces in Europe. For a precise cal-

culation more then 1000 traces should be known. Proposed program: 1. collect informations about traces observed up to now. 2. report on available traces and recommendation for completion 3. First approximation of the phase velocity field. The collected data, the calculation and the interpretation should be open to anyone. Responsibles: T.B. Yamovskaya (USSR), G. Panza (Italy)

SC 7 Earthquake Prediction Research

Chairman: H.Berckhemer, GDR
Vicechairman: A. Nikolaev, USSR
Secretary; A.M.Isikara, Turkey

Activity Report 1986 - 1988:

As an outcome of the very stimulating session of ESC-SC-7 on August 22 and 23, 1986 at Kiel two resolutions were proposed and later adopted by the ESC Bureau (Ed.: Resolutions No. 2 and 3 on page 16-17 in the Kiel proceedings).

In consequence of Resolution 3, the chairman of SC-7 was invited by the Commission of European Communities and participated in the preparation of the Research Programme 1989-1992 on Climatology and Natural Hazards. The section on seismic hazard comprises the following topics: strong motion measurements, European data centres and information services, multidisciplinary earthquake prediction studies, risk assessment, tsunami hazard, establishment of a task force for scientific missions after a destructive earthquake. This programme will soon be submitted to the European Parliament for approval.

China has shown a keen interest in cooperation with the European Community in earthquake prediction research. A CEC-delegation with the SC-7 chairman as coordinator will be sent to Beijing in September this year to discuss possible topics for joint research.

With regard to Resolution 2 of Kiel it should be remembered that integrated observations were first proposed and partly carried out by Soviet seismologists in Central Asia. Attention should now be drawn to a major bilateral project in which German and Turkish scientists are cooperating on earthquake prediction research in a test area at the western end of the North Anatolian fault zone. A new concept of homogeneous multi-parameter observatories had been developed and employed at 5 stations. The following data are recorded and digitally stored on multi-channel data logger systems: ground tilt, ground water level, ground water temperature, telluric potential, magnetic field, radon emission, soil parameters, atmospheric parameters in addition to seismic ground motion recordings. Some interesting correlations have already been obtained. Non seismic parameters considered as possible seismic precursors have also been investigated in the Friuli region for now almost ten years and led to interesting conclusions. The electro-telluric anomalies studied by the VAN-Group in Greece stimulated other groups to carry out similar investigations. Reports on non seismic parameter observations will also be presented by Romanian and Bulgarian scientists at the Sofia Assembly.

Search for potential places of future earthquakes based on seismicity patterns and statistical analysis in continuing. Research on S-wave polarization for prediction purposes is further carried on by the Edinburgh group.

A summer school on Earthquake Hazard Assessment sponsored by the Commission of the European Communities and the Council of Europe took place under the chairmanship of Prof. Drakopoulos in Athens on May 9 to 16, 1988. It involved lectures on seismic source physics, probability approaches for short term prediction and hazard assessment.

After a rather long time proceedings from the Kiel symposium on earthquake prediction research will soon appear as a special volume of Tectonophysics.

SC 8 Engineering Seismology

Chairman: A. Lopez-Arroyo, Spain
Vicechairman: V. Schenk, Czechoslovakia
Secretary: D. Mayer-Rosa, Switzerland

- WG Macroseismic Scales (N.Shebalin, USSR and G. Gruenthal, GDR)
- WG Near Field Seismology (V.Schenk, CSSR)
- WG Seismic Risk and Design Criteria (P.Burton, U.K.)
- WG Microzonation (from 1988 M. Marcellini, I)

Activity Report 1986-1988.

Seismic hazard: The TERESA Working Group on "Earthquake Hazard Assessment in European Test Areas" organized three very successful workshops in Prague 1987, Milano 1987 and Zurich 1988. In each workshop about 15 scientists from at least 12 different countries contributed to the common project.

The Symposium S2 during the Sofia meeting will give a good overview on the obtained results. It is planned to publish the papers jointly in a special volume. It is intended to continue and broaden the work within a larger corresponding group under IASPEI. The organizers of the workshops gratefully acknowledge the support through IASPEI funds.

Strong ground motion: Research in finding relations between wave motion parameters and macroseismic intensity was going on. Statistical tests of the multidimensional linear regression and one-factor discrimination analysis allows to classify strong motion records with 70% efficiency with respect to the macroseismic intensity (Czechosl: Schenk, Mantlik; USSR: Zhizhin, Tumarkin)

In the processing of strong motion records attention was paid to the following problems:
- Correction and restoration of wave 'acceleration-velocity-displacement' histories (USSR: Greizer; Czechosl.: Schenk, Mantlik)
- Attenuation coefficient assessment (Greece: Drakopoulos, Makropoulos, Tselentis, Theofanopoulos; Czechosl.: Schenk)
- Duration determination of strong ground motion (Czechosl.: Schenk, Mantlik, Kottnauer)

Dependence of strong ground motion parameters on:
- asperities and barriers on the fault plane (Greece: Stavrakakis, Drakopoulos)
- local conditions at a given site (USSR: Stejnberg) and structural severity (Portugal: Duarte, Oliveira, Costa, Vaz)

Modelling of synthetic seismic ground motions (Italy: Panza, Sunadolc; Czechosl.: Zahradnik)
Stochastic prediction of seismic response spectra (Spain: Barbat, Roca)

Close contacts of the SC-8 with the European Association of Earthquake Engineers was established at the 13. Regional Seminar on Earthquake Engineering in Istanbul and was continued with the UNESCO lectures on strong motions and seismic hazard assessment (organized by the Zentralinstitut für Physik der Erde in Potsdam, GDR)

SC session in Sofia:

WG Scientific topics:

Dr. Gruenthal, the chairman of the WG-1 "Macroseismic Scale" discussed the present stage of the work in WG-1. It was decided to publish the last modified version of the MSK-Scale ("MSK-81")in the next ESC Bulletin (Ed.: no.3 mailed in Feb. 89). By this way it will be distributed among the European seismologists and according to the responses and comments the future activity of the WG-1 will be specified.

An activity of the WG-2 "Near-field Seismology" was concerned with numerical processing of strong ground motion records and with finding common correlations between wave motion parameters and macroseismic intensity values. The results were presented on the ECEE Lisbon 1986, the IUGG Vancouver 1987, etc. For future it is believed the multidimensional regression and sensitivity analyses allow us to classify the strong ground motion records with respect to macroseismic intensity and to create a base for "instrumental" description of the macroseismic intensities.

The main discussion of the subcommission meeting was paid to the TERESA Project, which was organized under the plans of the WG-3 "Seismic Risk and Design Criteria". Dr. Zonno delivered a summary report for the test area Sannio-Matese. All participants discussed the future activity in this field and finally was decided that as an important product of the TERESA Project, a summary paper should be published in an international journal. This summary would give details of the methods used by the participants, the problems identified and finally tabulate the results obtained from the different methods when applied to the same test areas, which are (1) Sannio-Matese in S.Italy and (2) the area of Belgium- Netherlands- Germany. One of the problems identified was the inadequacy of fit of single statistical distributions to some regional samples of seismicity which showed anomalous frequency distributions on regional characteristic earthquakes. A growing interest was also noted in time varying on non-stationary approaches to the hazard problem. It was clear that a systematic approach to seismic zoning has not yet emerged.

Further, it was mentioned, that the program of the WG-4 "Microzonation" had not been fully defined, because the chair was open for a long time. Now, Dr. Marcellini has accepted the chairmanship and he is beginning to organize a collaboration under this topic.

Business matters:

The subcommission activity has been considerable during the 1986-88 period and most problems concerned with engineering seismology and its applications were successfully pursued. No changes in the structure of SC 8 were made during this period.However, elections of new officers for the period 1988-90 is necessary because Dr. Lopez-Arroyo (chairman) and Dr. Mayer-Rosa (Secretary) wish to resign. Dr. Lopez-Arroyo, as responsible SC chairman, proposed the following candidates for the SC-8 Bureau: Dr. V. Schenk (chairman), Dr. G. Zonno (Vice-Chairman), Dr. T. de Crook (Secretary). These nominees were unanimously voted for by the assembled SC 8 and they accepted these posts.

A resolution is proposed: Recognizing the success of the TERESA Project, SC8 recommends to constitute a Project "Characteristic Regional Earthquakes and Seismic Hazard (CRASH)".

ESC Council meeting
Friday, August 26. 1988, 18h

1. Election of the Bureau:

The following slate was proposed by the Nominations Committee: President: C. Morelli (Trieste) for re-election, First Vicepresident: P. Burton (Edinburgh) for re-election, Second Vicepresident: L. Christoskov (Sofia), Secretary general: D. Mayer-Rosa (Zurich) for re-election, Assistant Secretary: A. Roca (Barcelona)

After explanation of the rules, the proposed nominees were elected unanimously as a group by show of hands.

2. New Statutes ("ESC Bylaws")

The modified statutes as proposed by the special committee and discussed by the ESC Executive Committee were presented, discussed and voted on in a paragraph by paragraph manner. The same procedure was applied for the "Internal Rules" for the subcommissions. After stating the presence of a quorum, the proposed versions were finally adopted by the Council (text see under 'closing plenary session').

3. Restructuration of the subcommissions:

The following subcommissions have been proposed by the Ecex. Committee and adopted by the Council:

SC-A: Seismicity (Bureau: Karnik, Papazachos, Schenkova)
SC-B: Data Acquisition, Theory +Interpretation (Bureau: Hurtig, Aichele, Melle).
SC-C: Physics of Earthquake Sources (Bureau: Udias, Trifu, Buforn)
SC-D: Deep Seismic Sounding (Bureau: Morelli, Guterch, Prodehl)
SC-E: Earthquake Prediction Research (Bureau: Berckhemer, Sobolev, Isikara)
SC-F: Engineering Seismology (Bureau: Schenk, Zonno, DeCrook)

4. An "ESC advisory body" for the EMSC (CSEM) is formed. It consists of: Romanovicz (France), Mayer-Rosa (Switzerland), Burton (UK), Dost (Netherlands), Sulaco (Bulgaria), Gvishiani (USSR), Ribaric (Yugoslavia), Scarpa (Italy).

5. XXII. Gen. Assembly 1990: At the time of the Council meeting only one invitation of the Servei Geologic de Catalunya (Generalitat de Catalunya) for Barcelona was presented. The ESC Council gratefully accepted this invitation.

6. It was decided, that several business meetings of the ESC are organized at the next IASPEI meeting in Istanbul between 21. Aug. -1.Sept. 1989. All officers are asked to submit needs and ideas for these meetings.

7. Authors of oral- and poster-papers presented in Sofia are invited to publish their work in the proceedings of the Sofia meeting. Prof. Christoskov was successful in finding the necessary funds for the representative printing of the proceedings.

Deadline for submission is Dec. 15, 1988. Rules for preparation of the manuscripts will be distributed to each author. The publication of the symposia is handled by the respective conveners.

Closing plenary session
Saturday, August 27. 1988, 18h

1. After ESC President Morelli opened the Closing Plenary, the Titular Members appointed for 1988-1992 and as given in the list under 'opening plenary session' are announced and confirmed.

2. The new Bureau for 1988-1992 (see under 'Council meeting') is introduced.

3. Malta is adopted as new member country. Seismologists of Malta are welcome to cooperate actively in the scientific and administrative activities of the ESC.

4. European Seismological Commission Bylaws

(adopted by the ESC Council in Sofia 1988)

Article I. Purpose of the Commission

The European Seismological Commission (ESC) promotes seismological studies and projects in Europe, including all countries near the Mediterranean Sea and encompassing the area from the Mid-Atlantic Ridge to the Ural Mountains and from the Arctic Ocean to North Africa.

The ESC was created in 1951 by the International Association of Seismology and Physics of the Earth's Interior (IASPEI) and is a regional commission of IASPEI. Administrative and scientific decisions should be consistent with the general rules and decisions of IASPEI.

Article II. Membership

Each country that adheres to IASPEI and is situated within the region defined in Article I is a member and has the right to nominate a national representative to the ESC, referred to as a "Titular Member". Titular Members should be nominated by the national committees of IASPEI/IUGG. If no candidate is nominated by the national committee, the Bureau may propose a candidate to the appropriate national organization.They are appointed for two successive administrative periods and may be re-appointed thereafter.

Titular Members are responsible for:
a) The votes on behalf of their country;
b) The national reports requested by the ESC;
c) The dissemination of ESC information and announcements on a national basis

In the case of absence from a General Assembly, a Titular Member may delegate his duties to a compatriot present at the General Assembly or to a member of the Bureau.

If a Titular Member fails to fulfil the duties described in Article II of the Bylaws, the ESC Council may approach the national committee to nominate a new member.

Article III. The General Assembly

A General Assembly is the time period from the opening plenary meeting through the closing plenary meeting. Scientific sessions and administrative meetings are scheduled during the General Assembly.

The ESC Council decides the location of the next General Assembly. If no decision is reached by the Council, the choice of a place and date is left to the Bureau. The letters of convocation for a General Assembly shall be sent to all members of the Council at least three months before the date chosen.

An extraordinary General Assembly must be called by the Bureau if requested by the President or by at least one third of all Titular Members.

Article IV. The Council

The ruling body of the ESC is the Council, consisting of the Titular Members, the members of the Bureau and the Executive Committee.

The Council meets at least once during every General Assembly for elections. Before the closing plenary meeting, the Council shall decide on: 1. Date and place for the next General Assembly, based on invitations received; 2. Resolutions forwarded by the Resolutions Committee; 3. Other matters referred to the Council.

All decisions are announced at the closing plenary meeting.

Article V. The Bureau

The administrative body of the ESC is the Bureau, consisting of: the President, the immediate Past-President, two Vice Presidents, the General Secretary and the Assistant Secretary. The Bureau is elected by the Council at each General Assembly.

The President is eligible for re-election once only, the Vice-Presidents twice only and the General Secretary without restriction. The immediate Past-President is a member by right of the Bureau for one administrative period.The Assistant Secretary is responsible for the organization of the next General Assembly and serves for one administrative period.

A country cannot be represented by more than one person in the Bureau.

Article VI. The Executive Committee

The members of the Bureau and the chair-persons of the subcommissions form the Executive Committee. It meets at least once during the General Assembly and at other times if necessary.

It advises the Bureau in the preparation and the coordination of the General Assemblies. In addition it intervenes in any important question at the initiative of the President or of at least one third of its members.

The International Association of Seismology and Physics of the Earth´s Interior (IASPEI), the European-Mediterranean Seismological Centre (EMSC) and the European Association for Earthquake Engineering (EAEE) are represented in the Executive Committee.

The decisions of the Executive Committee must be confirmed or rejected by the Council.

Article VII. The Committees

Resolutions Committee: At the opening plenary meeting of each General Assembly, the president appoints a Resolutions Committee consisting of one member of the Executive Committee and at least two other members. All resolutions presented to the Council for decision must be transmitted in writing to the Resolutions Committee not less than 24 hours before the said meeting. The Resolutions Committee is responsible for wording the resolutions to conform with the terminology of IASPEI and IUGG. The Committee shall post all resolutions and recommendations at least 12 hours before the closing plenary meeting.

Nominating Committee: The president appoints a nominating committee consisting of not more than four members. This committee must be approved by the Executive Committee at the first business meeting of each General Assembly. The Nominating Committee proposes nominees for positions in the Bureau. Members of the Nominating Committee are ineligible for membership in the Bureau.

Other committees: The president may appoint other committees to propose solutions for specific administrative problems.

Article VIII. The Subcommissions

Subcommissions are formed within the ESC for the study of particular scientific problems. Subcommissions can be formed or dissolved by decision of the Council on the recommendation of at least three members of the ESC. Subcommissions are administered by special internal regulations.

Article IX. The Working Groups

Working Groups form part of a subcommission and follow their internal regulations.

Article X. Administrative Period

The administrative period, normally two years, comprises the time interval between the closing plenary meetings of two consecutive General Assemblies.

Article XI. Elections

The Council elects the Bureau, the chair-persons of the Subcommissions and confirms the Titular Members. A country cannot have more than three votes nor can a person have more than one vote by reason of his different offices. Vote by proxy is allowed.

The election of the President, the two Vice-Presidents and the other members of the Bureau is carried out successively. In general, voting is by secret ballot. In cases of a foreseen unanimity, voting may be executed by show of hands.

All decisions by the Council will be made by a simple majority of the eligible votes cast. In case of a tied vote, the President's vote is decisive. For cases other than election of the Bureau, voting by secret ballot is performed only if requested by at least one member.

Article XII. Amendment of Bylaws

Drafts of proposed amendments must be made available to all members of the Council prior to the General Assembly. They must be approved by two thirds of all members of the Council.

If a quorum of two thirds of all members of the Council is not obtained, the same amendments may be approved by two thirds of members present during the next General Assembly.

A Titular Member may cast his vote in written form forwarded by mail.

The bylaws are effective immediately after their adoption by the General Assembly.

Article XIII. Interpretation of the Bylaws

The English text is the guide for the interpretation of the Bylaws. In case of any ambiguity, the statutes of IASPEI will serve as a reference.

Article XIV. Approval of the Bylaws

The text of these Bylaws has been approved by the ESC Council at the General Assembly on 26. August 1988.

Internal Rules for the Subcommissions (adopted in Sofia 1988)

I. Membership and Administration

Everybody interested in the objectives of a subcommission is qualified for membership. Each subcommission is administered by a Bureau consisting of a President, a Vice-President and a Secretary.

II. Obligations

The President of a subcommission is responsible for: 1. The delivery of activity reports of the subcommission to the ESC General Assembly; 2. The announcement of the results and decisions taken by the subcommission to the ESC Bureau; 3. The timely forwarding of resolutions to the Resolutions Committee. The proposed resolutions or recommendations shall concern scientific matters only.

III. Composition

The composition of a subcommission, in particular the establishment and termination of specific Working Groups, is decided by the Bureau of each subcommission.

IV. Dissolution

The dissolution of a subcommission may be pronounced by the ESC in the following cases: 1. On the justified proposition of the President of the subcommission. 2. If the subcommission has not been active during the past two administrative periods.

V. Modifications of the Internal Rules

Internal rules of the subcommissions may be modified by decision of the ESC Council at a General Assembly of ESC.

****

5. The following resolutions are adopted by the General Assembly:

Resolution 1
Recognizing the need to ensure uniformity of earthquake location and catalogues for the determination of seismic hazard and other seismological studies, the General Assembly of the ESC, gathered at Sofia in 1988, recommends that all countries which publish phase readings of local earthquakes are urged also to make available to international agencies estimates of origin coordinates.

Resolution 2
Recognizing the need to remove substantial gaps in the distribution of seismic stations monitoring important earthquake regions in the Mediterranean area, the General Assembly of the ESC, gathered at Sofia in 1988, recommends that those countries in the area such as Malta, Cyprus and others are urged to install new seismological equipment (e.g. Ocean Bottom Seismographs) and to report the readings to international seismological agencies.

Resolution 3
Recognizing the success of the TERESA project in comparative seismic hazard techniques, its contribution to the aims of the IASPEI Subcommission on "Earthquake Hazard", and the need to assist earthquake engineers in their choice of design earthquakes, the General Assembly of the ESC, gathered at Sofia in 1988, recommends: 1. to identify earthquakes which are characteristic of the different seismic zones and seismogenic sources in Europe and 2. to identify the corresponding earthquake strong motion parameters; and resolves, that on the completion of the TERESA project in 1989 these two new objectives constitute the aims of a Project in "Characteristic Regional Earthquakes and Seismic Hazard (CRASH)".

Resolution 4
Recognizing the need for accurate hypocenter determination and uniform seismological practice, the General Assembly of the ESC, gathered at Sofia in 1988, recommends that when possible national bulletins should include estimates of hypocentral accuracy. When available, additional source parameters such as fault plane solutions and seismic moment etc., obtained from local determinations, should also be included.

6. The XXII. General Assembly of ESC in 1990 will be organized by the Servei Geologic de Catalunya (Generalitat de Catalunya) in Barcelona, represented in Sofia by A. Roca, SGC.

7. The ESC President states, that more than 300 participants attended the meetings, 180 papers have been presented. He thanks all speakers and conveners. Finally he closed the XXI general Assembly 1988 in Sofia with warmest thanks to the local organizers.

SEISMIC ENERGY RELEASE AT GLOBAL AND EUROPEAN SCALES, TRENDS IN EARTHQUAKE ACTIVITY

by Vít Kárník
Geophysical Institute, Prague, Czechoslovakia

1. INTRODUCTION

Estimation of trends of earthquake activity in time and space and assessment of earthquake hazard, including the probability of occurrence of medium and large events and of their effects, belong to basic seismological problems. In most earthquake regions the exponentional law of distribution of magnitudes M of earthquakes in relation to their number N holds, i.e.

$$N(M) = \alpha \exp(-\beta M), \qquad (1)$$

or

$$\log N = a - bM.$$

This relationship can provide a mean recurrence period of an event of magnitude M, however, it cannot say much on short- or long-term variation of past or future activity within a particular region. Earthquake data are therefore analysed in detail for a better understanding of the earthquake generating process and results are compared with laboratory experiments.

Simple regularities do not exist in earthquake occurrence and it seems that the same time histories do not repeat. On the other hand the fundamental type of fault movement (or of fracturing) which produces seismic events of different magnitude in a particular region is evidenced by observations, i.e. there should be some regularities in seismic energy release, however, they are not simple.

The behaviour of a source region (fault) can be demonstrated in several ways, e.g. by plotting M, I_o, ΣE, $\Sigma E^{1/2}$, ΣN, M_o or other quantities with time or in space.

In following text mainly the "strain release graphs", i.e. cumulative plots of $E^{1/2}$ with time, are discussed. The original idea of "strain release" stems from H.Benioff, who in his study of aftershocks (1951) introduced the assumption that the deformation during each aftershock is proportional to $E^{1/2}$ (E - seismic energy released by a shock)

$$\Sigma \varepsilon_i = C \Sigma E_i^{1/2}, \qquad (2)$$

where $\Sigma \varepsilon_i$ is the total released strain. It is also assumed that C does not change during the sequence.

V.I.Keilis-Borok (1968) used the quantity $E^{2/3}$ instead of $E^{1/2}$ in studying long sequences of earthquakes because $E^{2/3}$ is roughly proportional to the surface of a rupture. It can be shown that

$$M \sim \frac{2}{3} \log E \sim \log M_o \qquad (3)$$

$$\log E \sim \log L \sim \log S \qquad (4)$$

Thus plotting $E^{1/2}$ or $E^{2/3}$ can roughly describe physical conditions of the earthquake generating process.

The conversion formulae between E and M are used in this

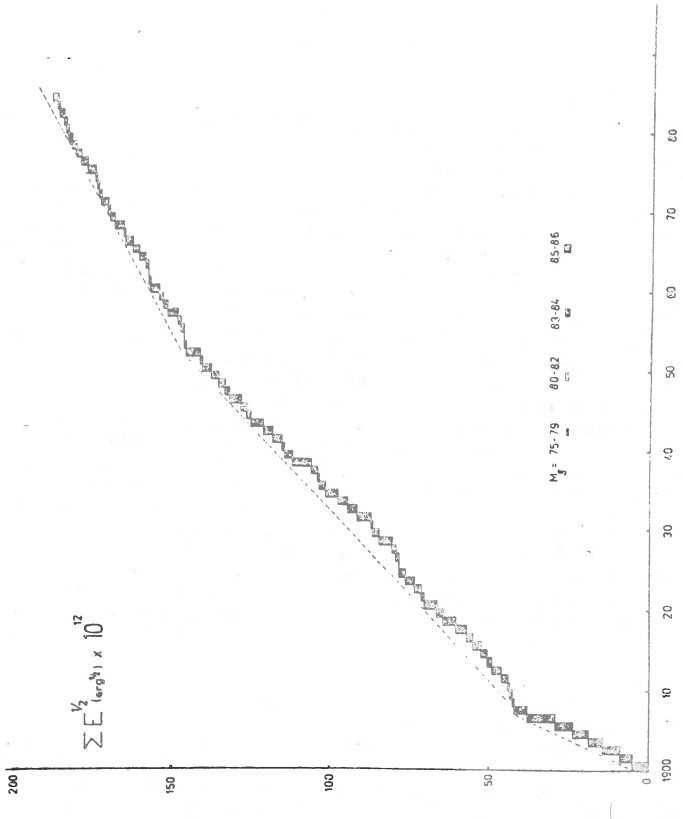

Fig. 1. Global seismic strain release, shallow events.

paper in the form

$$\log E = 11.8 + 1.5\, M_S, \quad \log E = 5.8 + 2.4\, m_B. \qquad (5)$$

2. STRAIN RELEASE CURVES

2.1. The Earth

The global strain release curve in Fig. 1 has been compiled on the basis of the catalogue by K.Abe (1981) which covers the years 1904 to 1980 for large shallow events ($M_S \geq 6.8$) and 1904 to 1974 for intermediate and deep events ($m_B \geq 7$), respectively. The set was completed by data for years 1900 - 1903 and 1981 - 1985 from the catalogues from S.Duda (1965), ISC and NEIS.

New data on global seismic energy release with time have been recently published by H.Kanamori (1983). He used M_W (moment magnitude) of extremely large events for calculating energy and found maxima in intervals 1905 - 1906, 1922 - 1923, 1938 - 1944, the largest one from 1950 to 1965. The pattern is different if M_S is used, the graph of released energy E (Fig. 2) shows that maximum energy was released during short periods 1905 - 1906 and 1910 - 1911 due to several events of $M_S \geq 8$ (shallow) and $M_B \geq 7.5$ (intermediate and deep-focus earthquakes), Kanamori's maximum 1950 - 1965 is not evident. There are other less conspicous maxima recognisable in the graph. The general trend seems to be, according to Fig. 2, a continuous decline in the total amount of released seismic energy with time during the 20th century. The same observation can be made by inspecting the strain release curve ($\Sigma E^{1/2}$), i.e. the decreasing slope of the curve with time. Three intervals of relatively constant strain rate can be identified in the years 1900 - 1907, 1908 - 1950, 1951 - 1985. The trends during the three intervals are: I. - 6×10^{12}, II. - 2.5×10^{12} erg$^{1/2}$, III. - 1.5×10^{12} erg$^{1/2}$. The oscillations of the curve are within: I. - 12.5×10^{12}, II. - 10×10^{12} erg.

The results could be biased by changes in the M determination. The magnitudes at the beginning of the 20th century (1897 - 1906) were calculated from amplitudes recorded by undamped Milne seismographs. Kanamori and Abe (1971) reevaluated the recordings, reduced the original Gutenberg's magnitudes by -0.6 and concluded that the global seismicity peak during 1896-1906 is of "marginal significance". However, even with the corrected and unified data by Abe (1981) the years 1900 - 1907 represent still the most active period (see Fig. 1). The global strain or energy release curves change substantially their trend if moment magnitudes by Kanamori (1983) are used for calculation of E. In that case the slope of the $E^{1/2}$ curve becomes steeper from 1950 to 1966, thereafter it returns to the original strain rate with some decline after 1980 that was not corrected by the large earthquake in Mexico on 19 September 1985. Two more large events within $M = 8.8\pm$ are needed to return the curve to the trend prevailing after 1966.

2.2. European - Mediterranean area

The plot in Fig. 3 demonstrates the long term strain release within the plate boundary between Africa and Eurasia limited by 20° - 52° E and 30° - 50° N, respectively. One curve corresponds to shallow shocks, the other one to shocks deeper than normal ($h \geq 60$km). The shape of the curves is mainly influenced by the largest event, i.e. those of $M > 7$. For shallow shocks the strain rate is relatively constant (2.2×10^{11} erg$^{1/2}$ per year) with oscillations of activity within a limit of 10^{12} erg$^{1/2}$ (i.e.

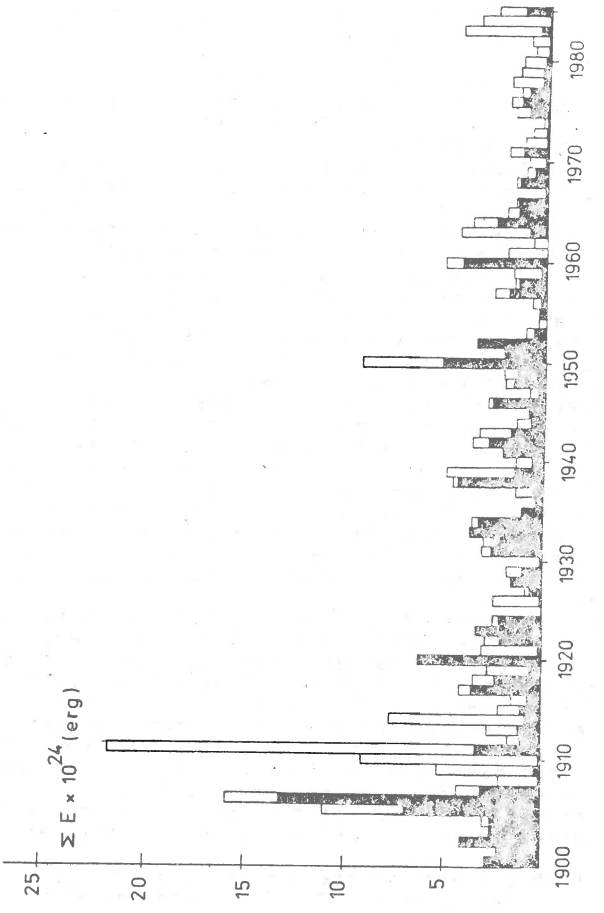

Fig. 2. Global seismic energy release from shallow shocks (full columns) and shocks deeper than normal(empty columns).

10^{24} erg, i.e. $M_{max} \sim 8\frac{1}{4}$). The strain release below the lithosphere (shocks deeper than normal) is different, the rate is smaller, however, it is marked by a sudden release of large amounts of seismic energy in the Hellenic arc in 1925 - 1926, this major episode changes the monotonous character of the curve Subcrustal activity declined after 1955, the only major event was the Vrancea (E. Carpathians) earthquake in 1977.

The oscillatory character of the strain release curve for shallow (lithospheric) shocks is evident and repeats also in most curves compiled for individual earthquake regions. Naturally, there is an influence of delimitation of the regions; their boundaries separate local concentrations of epicentres which are supposed to be linked to a particular active fault under a certain uniform stress field. There is, however, an additional problem: the "preparatory area" of an event of M = 8 would cover theoretically half of the whole Balkan peninsula, i.e. some earthquake region defined for Europe (Kárník 1968) or for the Balkan region (Kárník 1976) may be too small.

The lessons from most strain release curves compiled for earthquake regions in the Mediterranean area (Kárník 1968, Radu 1977) can be summarized as follows: the curves exhibit three phases, the first one of the highest strain release during 1902 - 1906, followed by a decline in activity in 1907 - 1938 and then by the period of alternating maxima but a higher mean rate than in the second phase. Temporary increases in activity alternate with periods of a relative quiescence, their duration depends on the total amount of energy released during the activity maximum.

Time variations of $\Sigma E^{1/2}$ in the European area during the whole period (1901 - 1985) are within 15 x 10^{11} $erg^{1/2}$ (i.e. $M_{max} \sim 8\frac{1}{2}$). It must be realized that most maxima are due to extreme events along the Gibraltar - Azores fault in 1931 (M = = 7.1), 1969 (M = 8.0), 1975 (M = 8). If these events are deleted the trend after 1925 becomes more monotonous with deviations only within 9 x 10^{11} $erg^{1/2}$ until 1985 corresponding to $M \sim 8\frac{1}{4}$. This magnitude is close to the value reached once during the whole observation period in 1930 (E. Anatolia). M = = 8 1/2 $\pm$ can be considered as the upper threshold value that can be attained in the lithosphere of the Mediterranean area (h < 60km).

The high activity at the beginning of the century is caused by several events of M = 7 - 7 1/4 and one of M = 7 3/4 (Kresna, Macedonia, 1904). The latter magnitude is sometimes questioned and some authors give only M = 7 1/2; if this value remained valid then the anomaly in the graph would slightly decrease but the corresponding section would never fit the slope of the later stage.

The $\Sigma E^{1/2}$ curve for h > n is also much smoother after 1926, the oscillations are within 5 x 10^{11} $erg^{1/2}$ whereas prior to 1925 the variations are within 24 x 10^{11} $erg^{1/2}$ (i.e. m_B = 7.3 and 7.9, respectively). The sudden jump is due to four extreme events in the Aegean belt in 1925 - 1927 of the order of m_B = 7 to 7 3/4. Again some authors give lower magnitude estimates, however, never below m = 7 1/4: consequently, the jump would decrease but would still remain.

2.3 Individual European regions

Strain release curves compiled for individual earthquake

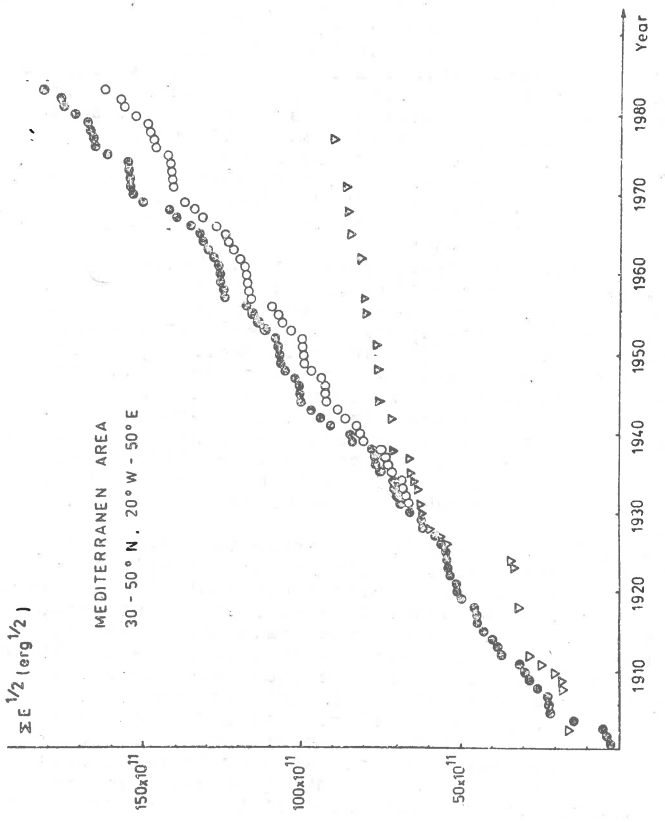

Fig. 3. Seismic strain release in the Mediterranean area, full circles - shallow events, empty circles - without events along the Azores--Gibraltar fault, triangles - events deeper than normal.

regions show different shapes if one scaling of $E^{1/2}$ is used. They seem to be monotonous with a uniform rate of strain release, e.g. in the Pyrenees, the Alps, the Dinarides, and the Caucasus (Kárník 1965, 1968, 1971, Kárník, Radu 1977). This observation is influenced by the scaling of $E^{1/2}$ increments; they are small for regions with medium or low activity ($M < 6\ 3/4$) and the amplitudes of oscillations are smoothed, but always periods of quiescence and activity alternate. In regions of high activity ($M_{max} = 7 - 8$) in the southern part of the Balkan peninsula, in Turkey, along the Gibraltar-Azores fault and in regions of intermediate depth activity the episodic character of activity with periods of maxima and minima is more visible in the graphs (examples Kárník 1965, Kárník, Radu 1977). These observations are confirmed also by plots made for provinces originating by combining several neighbouring regions.

For comparison of development of earthquake activity in time a third category of examples can be considered namely single earthquake sequences and a swarm (see Kárník, Schenková, Schenk 1982). The intervals between maxima as well as the amplitude of oscillation of the curve $E^{1/2}$ vary from region to region. The amplitude of the curve as well as the mean slope are used for classifying the rate and level of activity. The maxima usually encompass not only one but several large events and last several years. The model of alternating maxima and minima and particularly the intervals between them depend on the time window used. Periods of oscillation of activity can be found to be of the order of days, months, years, decades or centuries.

3. COMMENTARY

Judging fro all examples referred to above there is no stationarity in stress accummulation and strain release within an earthquake source region. A seismogenic fault (source region) generates an irregular sequence of active and quiet periods. In some regions two or three such cycles have been observed during the 20th century, however there is no good evidence that next active periods will repeat after identical time intervals. Strain release curves are very helpful in defining the strain release rate, when comparing individual regions and in estimating whether at a certain date the region may be within an active or a quiet stage. One can also estimate the expected M_{max} at a certain moment of the development of the earthquake generating process by checking the distance of the last point of the curve from the upper line limiting the rate.

The curves reflect also the existence of the basic types of earthquake sequences, i.e. main shock + aftershocks, multiple shocks and swarms, foreshocks + main shock + aftershocks, with various minor deviations from these schemes.

In some regions, particularly in larger provinces, the periods of increased activity do not start suddenly, but slowly, with a preparatory stage preceding the relatively short (1 - 2 years) interval of the largest activity; thereafter the activity declines and extends into the period of low activity. Such behaviour is best demonstrated for shallow and intermediate-depth foci along the Hellenic arc, although similar development is indicated by graphs for other regions. The accumulated strain is very seldom released in a single large event but usually in several major events representing the active period. This process is evidently linked to the strenght of the medium, to its fracturing and to the stress rate. It can be correlated with M_{max} and b ($\log N = a - bM$), i.e. regions with extended activity periods

(several years up to fifteen years) have relatively higher b and lower M_{max} ($\leq$ 7 1/4) than regions with a sudden onset of high activity lasting only one or two years (M_{max} = 7 1/2 - 8).

In the Balkan areas the multiple (double) shocks of comparable magnitude are frequent as a particular feature; the second shock follows the first one within hours or several days and both can be considered as a single event.

REFERENCES

Abe K. (1981): Magnitudes of large shallow earthquakes from 1904 to 1980, Phys.Earth Planet.Int. 27, 72-92.

Bath M, Duda S.J. (1979): Some aspects of global seismicity, Tectonophysics, 54, 1-8.

Benioff H. (1955): Seismic evidence of crustal structure and tectonic activity, Geol.Soc.Amer., Spec.Paper 62, 61-73.

Benioff H. (1951): Earthquakes and rock creep, Bull.Seism.Soc.Am., 41, p.31.

Duda S.J. (1965): Secular seismic energy release in the Circum-Pacific belt, Tectonophysics 2(5), 409-452.

Kanamori H., Abe K. (1979): Reevaluation of the turn-of-the-century seismicity peak, Journ.Geophys.Res. 84, No B11, 6131.

Kanamori H. (1983): Global seismicity, Earthquakes; observation, theory and interpretation, LXXXV Corso, Soc.Ital.di Fisica, Bologna, 595-608.

Kárník V. (1965): Magnitude, frequency and energy of earthquakes in the European area, Travaux I Inst.Géophys., No 222, 247-272.

Kárník V. (1968, 1971): Seismicity of the European Area, Parts I, II, Academia, Prague.

Kárník V., Schenková Z., Schenk V. (1981): A note on foreshocks and aftershocks, Proceed. 2nd Symp.on Analysis of Seismicity and on Seismic Hazard, May 18-23, 1981, 78-108.

Kárník V., Radu C. (1977): Time variation of earthquake activity in the Balkan region, Studia geoph.et geod., 21, p.285-293.

Kárník V. (1986): Earthquake catalogue for Europe and the Mediterranean area 1956-1985, manuscript.

Makropulous K.C., Burton P.W. (1983): Seismic risk of Circum-Pacifis earthquakes, I, Strain energy release, PAGEOPH 121, No 2, 247-267.

SPACE AND TIME SEISMICITY PATTERN IN THE VRANCEA REGION

C.Radu, Luminița Ardeleanu

Center of Earth Physics and Seismology, P.O.Box MG-2, Bucharest, Romania

INTRODUCTION

The Vrancea region, the most important Romanian seismic area, situated at the Carpathian arc bend, is defined by the point of coordinates φ=45.7°N and λ=26.6°E. The normal and intermediate depth events of this area define two distinct and parallel zones, orientated N 35° E.

The intermediate depth zone, of 95 km length and 60 km width, is characterized by earthquakes with depth in the range 60 to 200 km and maximum magnitude M_S=7.4.

The aim of this study is to investigate the seismicity pattern in the Vrancea intermediate depth focal region, using the parametrization introduced by Matsumura (1984), and to detect possible time-dependent changes preceding major earthquakes.

METHOD

The parametrization is based on the analysis of point patterns distributed in a two-dimensional space, considering the distribution of distances Δ between the nearest adjacent point pairs (Fig. 1). The horizontal axis represents the time and the vertical axis D refers to the distance of individual hypocenters relative to a reference point.

The interaction between points can be modeled by introducing a Δ-dependence for point density μ. If we take for μ the form given by the relation :

$$\mu = \mu_0 \Delta^{p-2} \qquad (1)$$

the probability density function $f(\Delta)$ will have a general form of the Weibull distribution :

$$f(\Delta) = \pi \mu_0 \Delta^{p-1} \exp(-\pi \mu_0 \Delta^p / p) \qquad (p>0) \qquad (2)$$

The form of μ implies two types of interactions: for $p<2$, μ represents an attractive interaction and for $p>2$, a repulsive interaction. The point patterns resulted under such interactions are characterized as clustered patterns for $p<2$ and regular (periodical in time) patterns for $p>2$. The border value p=2 corresponds to a completely random pattern.

The parameter γ introduced by Matsumura (1984) as an indicator representing the pattern is given by the relation :

$$\gamma = (\bar{\Delta})^2 / \overline{\Delta^2} \qquad (3)$$

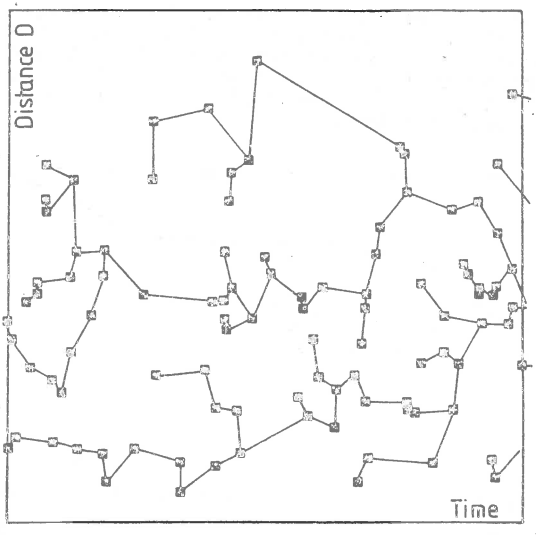

Fig.1 - Example of two dimensional point pattern, distributed at random in a square, for Vrancea intermediate earthquake data.

The Weibull distribution function is formally related to the observed values as in the formulae (4) and (5), where the first and the second moments of the probability density function $f(\Delta)$ of equation (2) equalize the mean and the mean-square of the observed distance Δ, respectively :

$$(p/\pi\mu_0)^{1/p}\ \Gamma(1/p+1) = \overline{\Delta} \qquad (4)$$

$$(p/\pi\mu_0)^{2/p}\ \Gamma(2/p+1) = \overline{\Delta^2} \qquad (5)$$

The relationship between the parameter ν and the parameter p of the Weibull distribution function is presented in Fig.2. The two-dimensional point patterns are classified into three types as regular, random and clustered according to the value of ν.

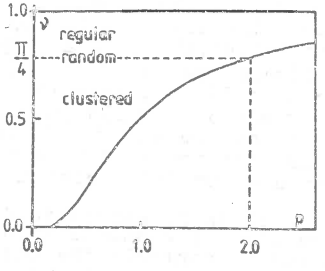

Fig.2 - Relationship between the parameter ν and the parameter p of the Weibull distribution function (after Matsumura, 1984).

The influence of the edge effect due to the enclosure shape was also investigated. The variation of ν for random patterns distributed inside a rectangular enclosure with various length ratio c=b/a is shown in Fig.3. For c-values in the range from o.1 to 5o, deviation of ν from theoretical value $\frac{\pi}{4}$ is small compared with the statistical uncertainty.

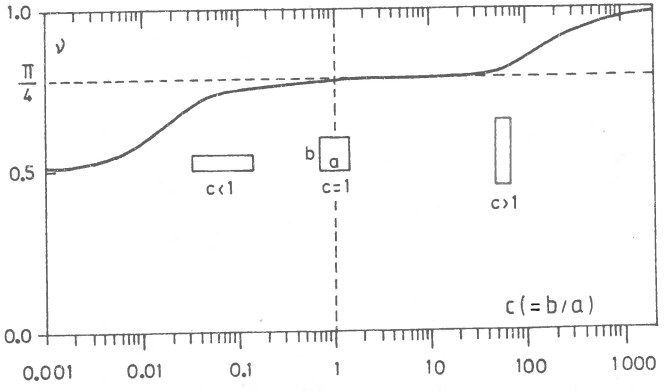

Fig.3 - Variation of parameter ν for various rectangular shape of the enclosure (after Matsumura, 1984).

OBSERVATIONAL DATA

The observational data used in this study refer to 8o4 Vrancea intermediate depth earthquakes ($6o \leq h \leq 2oo$ km) with magnitude $1.9 \leq M_S \leq 7.o$, recorded by the Romanian seismic network, during the last 11 years : June 1977 - May 1988 (Radu et al., 1985 ; Radu, 1988). We note the occurrence of 11 earthquakes with magnitude $M_S \geq 5.o$, the strongest one being the major event of August 3o, 1986 ($M_S=7.o$).

RESULTS

The distance-time distribution of the analysed intermediate earthquakes is shown in Fig.4. The distance D is determined relatively to the reference point situated in the south-western corner of the seismic area ($\varphi = 45.o^{o}N$; $\lambda = 26.o^{o}E$) at 13o km depth.

In order to investigate the seismicity data by the parameter ν the distance-time area is divided into rectangles. Only the events in the distance range $5o \leq D \leq 135$ km, which represent 98.2% of the total number, are considered, the distance width of each rectangle being of 85 km. The moving time window is adjusted so that each rectangle includes 5o data point and the step is of 5 data points.

To compute ν values it is necessary to define a metric spanning the space and time axis. The coordinating coefficient v, which has a dimension of velocity, controls the pattern of connections : a large value of v favors the association of points in the distance direction, while a small value of v favors the associations in the time direction.

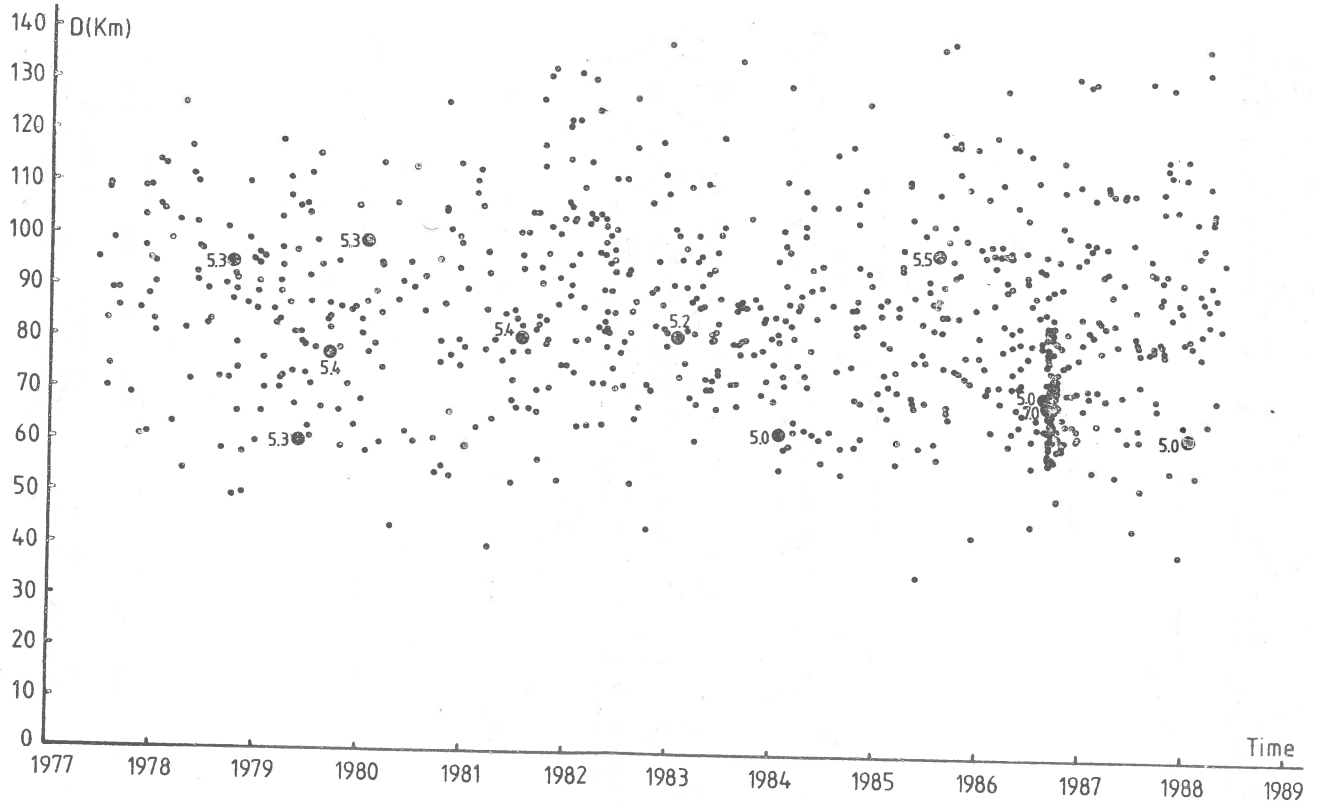

Fig.4 - Distance-time distribution of Vrancea intermediate earthquakes with magnitude $1.9 \leq M_S \leq 7.0$, occurred during the period June 1977-May 1988.

The dependence of γ on the value of v is presented in Fig.5. It shows that γ is rather insensitive to the value selected for v, excepting extreme values for which the edge effect should become proeminent. We selected variable values for v, making the enclosure a square.

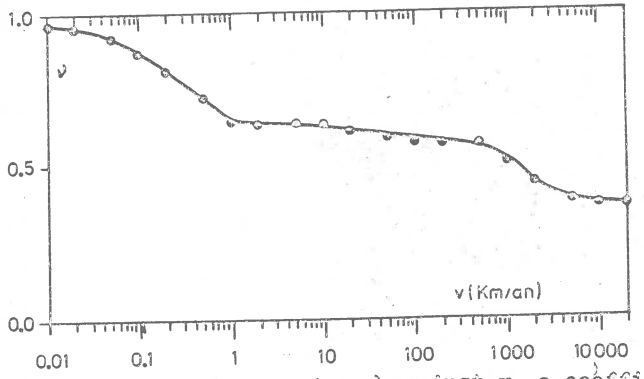

Fig.5 - Variation of parameter γ against v, a coefficient to coordinate distance and time axes (after Matsumura, 1984).

Fig.6 shows the variation of γ versus time. The values of γ parameter are plotted at the end of the time window and the vertical bars mark the earthquakes with magnitude $M_G \geq 5.0$. The horizontal broken line represents the reference value γ_{random}, which was evaluated with a correction, by taking account of nonuniformity of the density on the distance axis (Fig.7), using the relation :

$$\gamma_{random} = (\pi/4)\,\overline{(\sqrt{\mu})^2}\,/\,\overline{\mu} \qquad (6)$$

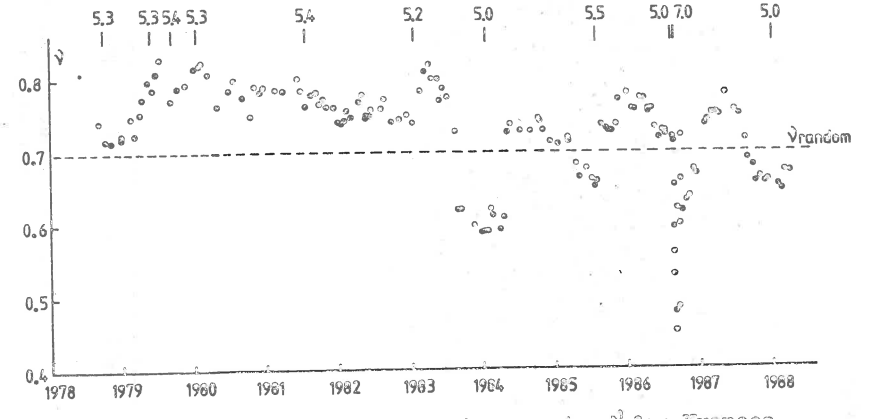

Fig.6 - Temporal variation of parameter γ for Vrancea intermediate earthquakes with magnitude $1.9 \leq M_G \leq 7.0$, occurred during the period June 1977 - May 1988.

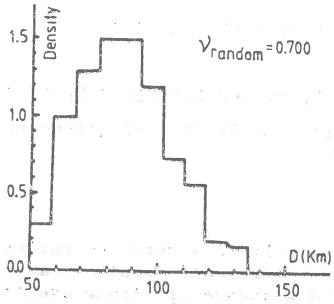

Fig.7 - Distribution of earthquake density (eqs/km.year) on distance axis D.

Considering the variation of ν , the seismicity pattern in the Vrancea intermediate depth focal region can be interpreted as a back ground activity almost random. The significant depression is clearly related to the aftershock sequence of the strong earthquake with M_S=7.o occurred on August 3o, 1986. If aftershocks are removed then the deviations of ν values relative to ν_{random} are < 2o%, deviations comparable with statistical uncertainty.

CONCLUSIONS

The analysis of the results presented above leads to the following remarks :

. The distribution of small and moderate events of Vrancea intermediate depth focal region is almost random. This result is in agreement with the conclusions of Matsumura (1984) and Gardner and Knopoff (1974) that the main sequences are Poissonian, provided that aftershock sequences are removed skillfully.

. The temporal variation of ν parameter does not point out the existence of changes in the seismicity pattern preceding moderate and large earthquakes ($M_S \geq 5.o$) ; also, no significant anomaly was observed before the major event of August 3o, 1986.

REFERENCES

Gardner J.K., Knopoff L. (1974). Is the sequence of earthquakes in Southern California, with aftershocks removed, Poissonian?, Bull.Seism.Soc.Am. 64, 1363-1367.

Matsumura S. (1984). A one-parameter expression of seismicity pattern in space and time, Bull.Seism.Soc.Am. 74, 2559-2576.

Radu C. (1988). Catalogue of Vrancea intermediate depth earthquakes with magnitude $M_D \geq 3.o$ occurred during the period January 1, 1985 - June 3o, 1988. Manuscript, Bucharest, July 15, 1988.

Radu C., Apolozan L., Tenea L. (1985). Catalogue of Vrancea intermediate depth earthquakes with magnitude $M_D \geq 3.o$ occurred during the period June 1, 1977 - December 31, 1984. Internal Report, Theme 3o.81.8/1985, A_3, 16-42, Bucharest, June 25, 1985.

MODEL INVESTIGATIONS OF EARTHQUAKES SPACE DISTRIBUTION

DRAGOMIR GOSPODINOV and LJUDMIL CHRISTOSKOV

Geophysical Institute, Bulgarian Academy of Sciences, Sofia, Bulgaria

1.Introduction

Earthquake clustering, basicly in aftershock series, is the most obvious peculiarity of a space-time sequence of events in a catalog.It is interesting whether it exists for a sequence of strong events only (aftershocks removed), or whether other regularities can be found out in their successive realization.

The aim of this work is to investigate whether a strong earthquakes sequence in a determined seismic zone is one of independent events.First it must be defined what we will mean by independent events.

We assume that a sequence is of independent earthquakes if its characteristics are not essentially influenced by a random reordering of the events in time.Then the sequence characteristics will be determined only by the events space distribution in the zone.

The distance r between the epicenters of all pairs of successive events in a determined magnitude-depth interval is used for characterizing the process of earthquake spatio-temporal realization.

Other authors [4,5,6,7,8,9] have used the distance r to investigate events space distribution but in most cases the accent has been on the geometry of faulting or the aftershocks have not been removed.

Using catalog data, the actual distribution of the distances defined, can be obtained for the real process.And basing on data about the surface epicenter distribution $G(\Delta s)$ only, a model distribution $F(r)$ can be obtained for a sequence of independent events having the same surface distribution.

The data used, is taken from the Balkan Catalog [1], several zones being investigated seperately.For each zone the entire period of 70 years, reflected in the catalog, is considered.The zones have been chosen on the base of seismic zoning, made in [2].Only events under 50 km are dealed and thus we get to two-dimensional investigation.To remove the aftershock we use the seperation of aftershocks made in the catalog itself.

Different model distributions can be developed depending on the surfac epicenter distribution $G(\Delta s)$ in a seismic zone S.

2.Uniform model

Let S is a rectangular zone (fig.1) with dimensions a and b, and $G(\Delta s)$ is an uniform surface distribution.Generating independently points in S with such distribution, the distance distribution between successive points i and i+1 will be of interest.

Here

$$r = \sqrt{(x_{i+1} - x_i)^2 + (y_{i+1} - y_i)^2} \qquad (1)$$

where the coordinates x_{i+1}, x_i, y_{i+1} and y_i are transformed according to a system, connected to the investigated rectangular zone(fig.1).

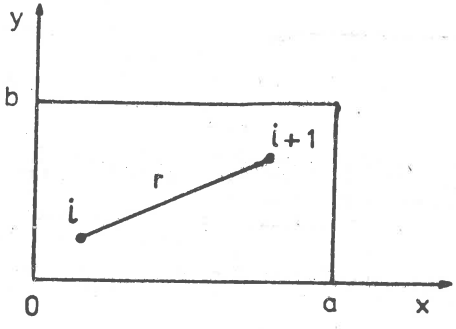

fig. 1

The uniform surface distribution determines uniform distributions of the coordinates x_{i+1}, x_i, y_{i+1}, y_i so they may be considered as independent random values with density functions:

$$f(x_{i+1}) = f(x_i) = \frac{1}{a} \qquad x_{i+1} \in [0,a], x_i \in [0,a]$$

$$= 0 \qquad x_{i+1} \bar{\in} [0,a], x_i \bar{\in} [0,a]$$

$$f(y_{i+1}) = f(y_i) = \frac{1}{b} \qquad y_{i+1} \in [0,b], y_i \in [0,b]$$

$$= 0 \qquad y_{i+1} \bar{\in} [0,b], y_i \bar{\in} [0,b]$$

The distribution law F(r) is searched.The problem is one of the probability theory [3] - knowing the distributions of four independent random values, to find the distribution of a random value, which is function of them.We obtain the solution to be expressed by formula (2), assuming that $a \geq b$.Function graphs of F(r) and density function f(r) are shown on fig.2a.

Formula (2) shows that the random value r has a two parameter distribution.Using it we can calculate the distance distribution between pairs of successively generated independent points, which have an uniform surface distribution in any rectangular zone.So formula (2) gives the model distribution law F(r), which will be used for comparing with the distribution for the actual process.

Formula (2) is applied to zone 1 (fig. 3).Earthquakes in the magnitude range $5.5 \leq M \leq 6.5$ are used to obtain the actual distribution N(r), with aftershocks removed.

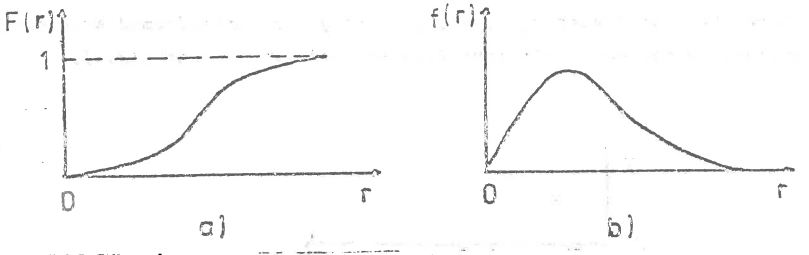

fig. 2

To check whether the epicenter surface distribution $G(\Delta s)$ is uniform, zone 1 is devided into 18 equal cells. The hypothesis $H_0: g(\Delta s)=1/18$ is checked. The results are shown in table 1.

Here $g(\Delta s)$ is the uniform distribution density function, $N_{\Delta s}$ are the numbers of events in the cells and N_{av} is the expected number in a cell for an uniform surface distribution. The table shows that the data on which the statistical test is made do not contradict the hypothesis for a

a) $r \in [0,b]$ (2a)

$$(r)=\frac{\pi r^2}{ab}+\frac{r^4}{2a^2b^2}-\frac{4r^3}{3a^2b}-\frac{4r^3}{3ab^2}$$

b) $r \in [b,a]$ (2b)

$$(r)=\frac{b^2-2r^2}{2a^2}+\frac{r^2}{a^2}+\frac{2(r^3-(r^2-b^2)^{3/2})}{3ab^2}+\frac{2r^2\sqrt{r^2-b^2}-2r^3}{ab^2}-\frac{4b^2}{3a^2}+\frac{\pi r^2}{ab}-$$

$$-\frac{2r^2}{ab}\arcsin\sqrt{\frac{r^2-b^2}{r^2}}-\frac{r^2-b^2}{a^2}$$

b) $r \in [a,\sqrt{a^2+b^2}]$ (2b)

$$(r)=\frac{(r^2-b^2)^2}{2a^2b^2}+\frac{a^2-6r^2}{6b^2}-\frac{b^2+3r^2}{3a^2}-\frac{r^2(r^2-b^2)}{a^2b^2}+\frac{4(r^2-a^2)^{3/2}}{3a^2b}+\frac{2\sqrt{r^2-a^2}}{b}$$

$$-\frac{2(r^2-b^2)^{3/2}}{3ab^2}+\frac{2r^2\sqrt{r^2-b^2}}{ab^2}-\frac{2r^2}{ab}\left(\arcsin\sqrt{\frac{r^2-b^2}{r^2}}-\arcsin\frac{a}{r}\right)$$

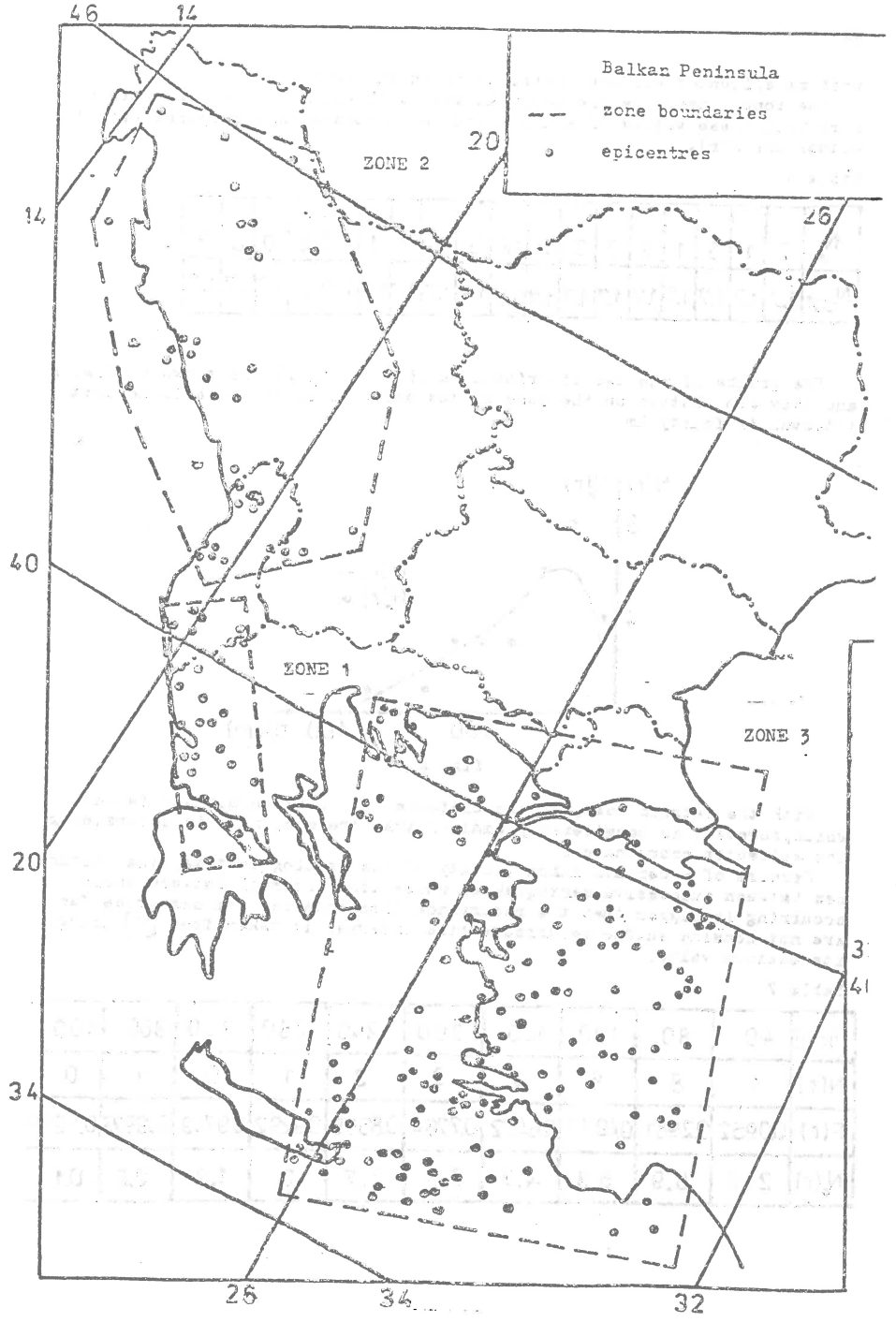
Balkan Peninsula
zone boundaries
epicentres
ZONE 1
ZONE 2
ZONE 3
46
14
20
26
14
40
20
34
26
34
32
3
41

fig. 3

uniform epicenter surface distribution in the zone.

The zone dimensions are a=375 km and b=115 km.The model distribution F(r) with these values of a and b can be calculated and compared with the actual one N(r).

Table 1

$N_{\Delta S}$	2	1	3	1	2	2	3	3	2	3	2	2	1	1	0	0	0	3
$N_{\alpha\beta}$	1.7	1.7	1.7	1.7	1.7	1.7	1.7	1.7	1.7	1.7	1.7	1.7	1.7	1.7	1.7	1.7	1.7	1.7

The graphs of the two distributions N(r) and $N_o(r)$ are shown on fig. 4 and they are plotted on the base of the data, given in table 2.The unit interval is fourty km.

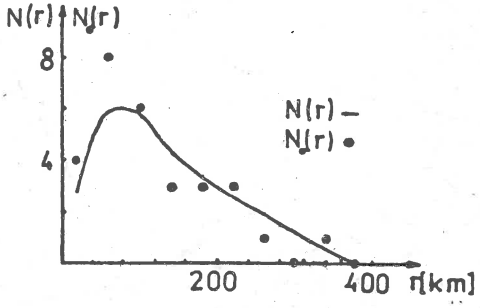

fig. 4

With the metrics used, of the distance r, a certain mistake is made, which,however, is considerably smaller than the one, made in determining the epicenter coordinates.

Because of a certain inhomogeneity of the catalog in time, the distances between successive earthquakes, whose time interval between their occurring is bigger than the recurrence time interval for magnitude M=6, are not considered.The recurrence time interval is taken from [2] using its maximum value.

Table 2

r[km]	40	80	120	160	200	240	280	320	360	400
N(r)	4	8	6	3	3	3	1	0	1	0
F(r)	0.0952	0.2981	0.4977	0.6472	0.7764	0.8599	0.9292	0.9749	0.9973	0.9999
$N_o(r)$	2.8	5.9	5.8	4.3	3.5	2.7	2	1.3	0.6	0.1

$N_o(r)$ are the distance frequencies, calculated using the model distribution $F(r)$. Fig. 4 and Table 2 show that the entries are bigger for the actual distribution than the model one for small distances. If that difference is not random, it may be due to an epicenter migration or to earthquake clustering in the zone. The observed difference was not statistically confirmed.

The model distribution $F(r)$, given by formula (2), was obtained with the requirements for an uniform epicenter distribution $G(\Delta s)$ in a rectangular zone. These requirements are quite strong so a model distribution must be obtained for the case when they are not valid.

3. Empirical model

Let S is a zone of any form(zone 2 and zone 3 on fig.3) and we can not obtain analytically the surface distribution. In that case it can be used without knowing its analytical form. That can be done by randomizing the catalog or by using all distances between any pair of epicenters.

The randomizing algorythm is expressed by:

$$x_i^{rnd} = x_k^{act}$$

where x is a vector of the two epicenter coordinates in the actual (act) or randomized (rnd) catalog 4 .Here k=k(i) is a permutation of the integers $1,2,\ldots,N$, chosen randomly. For any random permutation k=k(i) we obtain a randomized catalog, for which the distances between pairs of successive events will be a random sample of all distances between any pair of events. Then the non-uniform space distribution will be best characterized by the distribution between any pair of epicenters. In both cases - using a randomized catalog or all posiible distances, the regularities (if any exist) in the realization of successive events will be destroyed and we can obtain distance distribution for independent events.

For zone 2 the earthquakes considered, are in the magnitude range $5.5 \leq M \leq 6.5$ and their number is N=40, and for zone 3 the magnitude range is $5 \leq M \leq 6$ and the events number is 234.

For the distance distribution between any pair of events an approximating function fitting well the observed data is:

$$F(r) = 1 - e^{-\pi\lambda r^2} \qquad (3)$$

Then this formula is an empirically obtained model distribution, having in mind that the λ value must be calculated for each zone, and checked whether formula (3) fits well the observations.

The frequencies received, are shown in table 3 and table 4 correspondingly, $N_o(r)$ again being the frequencies received using the model distribution. The graphs of the model $N_o(r)$ and actual $N(r)$ distance distribution for zone 2 and zone 3 are shown on fig.5 and fig.6 correspondingly.

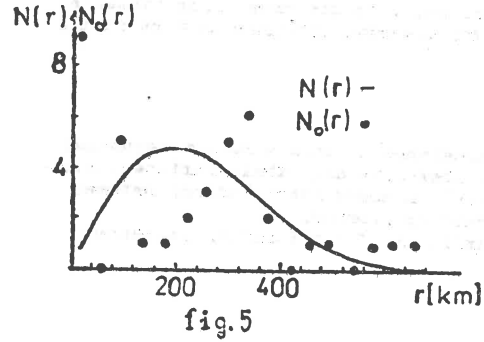

fig.5

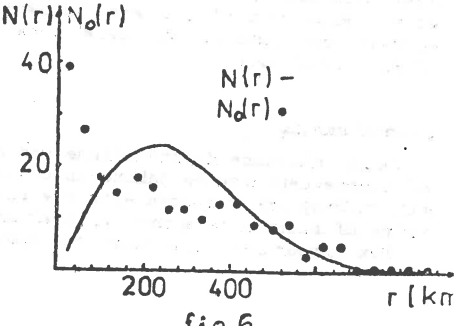

fig.6

It can be seen that again for small distances the distance numbers are bigger for the actual distribution than for the model one.It is an interes ting fact that a second maximum of N(r) can be observed, which is very wel

Table 3

$\lambda = 4.10^{-6}$			
r[km]	N(r)	F (r)	$N_o(r)$
40	9	0.0199	0.8
80	0	0.0772	2.2
120	5	0.1654	3.4
160	1	0.2750	4.3
200	1	0.3949	4.7
240	2	0.5149	4.7
280	3	0.6264	4.3
32	5	0.7237	3.8
360	6	0.8036	3.1
400	2	0.8660	2.4
440	0	0.9121	1.8
480	1	0.9446	1.3
520	1	0.9665	0.9
560	0	0.9805	0.5
600	1	0.9891	0.3
640	1	0.9942	0.2
680	1	0.9970	0.1

Table 4

$\lambda = 3.10^{-6}$			
r[km]	N(r)	F (r)	$N_o(r)$
40	39	0.0150	3.5
80	27	0.0535	10.1
120	17	0.1269	15.8
160	15	0.2143	20.2
200	18	0.3139	2.3
240	16	0.4188	24.2
280	12	0.5222	23.9
320	12	0.6189	22.3
360	10	0.7050	19.9
400	13	0.7785	17
440	13	0.8386	13.9
480	9	0.8859	10.9
520	8	0.9217	8.3
560	9	0.9479	6
600	3	0.9663	4.3
640	5	0.9789	2.9
680	5	0.9872	1.9
720	0	0.9924	1.2
760	0	0.9957	0.7
800	0	0.9976	0.4
840	0	0.9987	0.3
880	0	0.9999	0

expressed for zone 2.It can be suggested that both maximums of N(r) reflect one effect - that of clustering, the first maximum being connected with events in a cluster and the second one with the prevailing distances between the clusters.For these cases the observed differences were statistically confirmed.

4.Conclusions

Model distance distributions are developed in this work for sequences of independent events taking into consideration only their surface distribution.They are compared with the actual distance distributions between pairs of successive events with aftershocks removed.

The comparison shows that the distribution for the actual sequences

differ from the model one, mainly in the small distances range. That may be due to:

- existence of clustering properties of the earthquakes in the investigated zones.
- earthquakes migration in the zones.
- the algorythm of aftershock removing.

Further investigations are necessary to find out the correct interpretation of the observed difference in the distance distributions.

References

1. Catalogue of Earthquakes - Balkan Region, UNDP/UNESCO Survey of the Seismicity of the Balkan Region, UNESCO, Skopje 1974.
2. Karnik V., D. Prochazkova, Discussion of the Magnitude-frequency Relation Using the Balkan Earthquakes, Proceedings of the Seminar on Seismic Zoning Maps, Skopje 27 October - 4 November 1975, Vol. 1.
3. Chistyakov V., Kurs Teorii Veroyatnostei, Moskva, "Nauka", 1987.
4. Prozorov A., A. Dziewonski, A Method of Studying Variations in the Clustering Property of Earthquakes: Application to the Analysis of Global Seismicity, J. Geoph. Res., Vol 87, No. B4, pages 2829-2839, 1982.
5. Kagan Y. and L. Knopoff, 1976 , Statistical Search for Non-random Features of the Seismicity of Strong Earthquakes, Phys. Earth Planet. Interiors, 12, 291-318.
6. Kagan Y. and L. Knopoff, 1980, Spatial Distribution of Earthquakes: the Two-point Correlation Function, Geophys. J. R. Astr. Soc., 62, 303-320.
7. Kagan Y.Y., 1981, Spatial Distribution of Earthquakes: the Three-point Moment Function, Geophys. J. R. Astr. Soc., 67, 697-717.
8. Kagan Y.Y., Spatial Distribution of Earthquakes: the Four-point Moment Function, Geophys. J. R. Astr. Soc., 67, 719-733, 1981.
9. Eneva M., Izsledvaniya Varhu Prostranstvenoto Razpredelenie na Zemetreseniyata - eksperimentalni Danni i Resultati, Balgarsko Geofizichno Spisanie, T. IX No4, 1983.

LONG-TERM STRONG SEISMICITY OF VRANCEA (ROMANIA) REGION

Liviu CONSTANTINESCU

Romanian National Committee for Geodesy and Geophysics, Bucharest, Romania

Vasile I. MÂRZA

Center for Earth Physics and Seismology, Bucharest, Romania

1. *Briefing on seismotectonic setting and salient features of Vrancea seismogenic region (VSR)*

The VSR located at the Romanian Carpathian Arc Bend (CAB) - roughly marked out by the parallels of N45.3° and N46.0°, and by the meridians of E26.0° and E27.0° - is the most outstanding Romanian focal region, and one of the most peculiar seismic zones of the World. For convenience the earthquake (eq) population is divided into two categories , viz., the subcrustal eqs (or intermediate depth eqs) with depths more than or equal to 60 km and crustal eqs with lesser depths.

The subcrustal eqs (seqs) which occur in the VSR are usually called "Romanian eqs" or "Vrancea eqs", their study playing an important rôle in the development of the deep foci concept (Constantinescu, 1978), and moreover they are responsible for the over - whelming seismic energy release budget in the area as compared with crustal eqs.

The most salient features of VSR (Demetrescu & Iacovachi,1944; Purcaru 1979; Marza 1982; Constantinescu & Enescu 1985; Apostol et al. 1985) are as follows:

(i) The outstanding *persistency* of seismic activity, during the whole known period of record (more than a millennium);

(ii)The VSR is rather *isolated* from Alpine-Himalayan seismic belt and especially from the other subcrustal foci;

(iii) The epicenters of the overwhelming majority of quakes are *confined* to an ellipse of roughly 60 kmx40km striking tangential to CAB in N35°E direction, displaying a very *compact* epicentral distribution;

(iv)The activity spans *depths between 0 to 200 km* (with a conven - tional boundary at 60 km separating the subcrustal and crustal domains), the most intense activity being within the depth range 80 to 160 km, and the strongest quakes having the *maximum ob - served magnitude* $M_{GR} \approx 7.5 \div 7.7$ (or equivalently $m_W (= m_B) = 7.4 \div 7.5$);

(v) The hypocenters have a general tendency of gradually descending to NNW;

(vi)The macroseismic effects of Vrancea seqs present a remarkable and quite preferential but stable pattern with maximum attenuation in NW-SE direction and destructive effects in NE-SW di - rection, occasionally up to distances of 300-400 km ;

(vii)The seimic activity at crustal depth (0 to 60km) in VSR, or around it, is very much less significant than the "main" activity at subcrustal depths, but seems to be generally in a genetical connection with this subcrustal activity. There also is no present-day volcanic activity in the region ;

(viii) The strong quakes ($M_{GR} \geq 6.8$) occur with an *outstanding cyclicity* (at least three major events per century) and the aftershock activity is low;

(ix) The great majority of VSR seqs are of *the dip-slip-reverse faulting*, i.e., compressional eqs and their focal mechanism may be separated into two main categories, the first one (containing both strong and weaker seqs) has both nodal planes in a NE-SW direction, while the second category (including only weaker shocks) has both nodal planes in a NW-SE direction.

The seismotectonical models for VSR are mainly hypothesized subduction models using different variants of a paleosubduction or a postsubduction (Roman 1970, Constantinescu et al. 1973; Fuchs et al. 1979; Constantinescu & Enescu 1984, 1985; Oncescu 1984; Apostol et al. 1985) in the collision/convergence area of three or four subplates, at the CAB.

2. *Historical seismicity of VSR over the last 1000 years*

2.1. *Data base and quantification relationships*

The data source used in the present study is the VSR master eq catalog of Constantinescu & Marza (1984), updated with the most recent information. The above VSR master eq catalog is a careful compilation, check-up and (re)interpretation of all historical and instrumental information available to us.

The instrumental magnitude for VSR seqs has been calibrated on the basis of M_{GR} (Gutenberg and Richter, 1965) and not on the basis of M_S or some unspecified $M(=M_u)$ as sometimes was/is asserted. The historical maximum (epicentral) intensities (MM or MSK - 64 scale) were converted into M_{GR} by using a conversion scheme (Table 1) based on a reasonable combination of two magnitude-intensity relationships (Radu 1974 and Purcaru 1975).

Table 1. Maximum intensity (I_{max}) - magnitude (M_{GR}) relationship for VSR seqs

I_{max} (MSK-76)	M_{GR}	$\pm \Delta M$	Source
III 1/2	4.2	0.3	Extrapolation
IV	4.5	0.3	"
IV 1/2	4.7	0.3	"
V	5.0	0.2	Radu (1974)
V 1/2	5.3	0.2	"
VI	5.5	0.2	"
VI 1/2	5.8	0.2	"
VII	6.2	0.2	Purcaru (1975)
VII 1/2	6.5	0.2	"
VIII	6.8	0.2	"
VIII 1/2	7.0	0.2	"
IX	7.3	0.2	"
IX 1/2	7.5	0.2	"
X	7.7	0.2	"
X 1/2	7.9	0.2	Extrapolation

For the present work we have adopted a $M_{GR} = 6.8$ cut-off magnitude, which is usually considered as wide damage threshold value, so altogether we are analysing 37 major/damaging events from 984 (A.D.) to the present time (Annex 1), therefrom resulting a unique data sample.

Recent progresses in eq quantification suggest, as appropriate for seqs, the use of m_B or m_W scale. In this respect a relationship between M_{GR} and m_W (= m_B) was developed (Marza et al. in preparation) for VSR seqs :

$$M_{GR} = (1.58 \pm 0.22)\, m_W - (4.15 \pm 1.48) \qquad (1)$$

$$\left(\sigma = 0.3 \right)$$
$$\left(r = 0.999 \right)$$

Our data base (Annex 1) is definitely complete (for M_{GR}=6.8 threshold) since 1446 to date, and less complete for the previous period, but as it will be discussed later (subsection 3.3) there are retrospective potentialities to infer the lost data.

2.2. Maximum observed and maximum computed magnitude

For this 1000-yr historical record the largest observed eq is "the Great" 1802 October 26 VSR event with a maximum (epicentral) intensity I_{max} = X (MM or MSK-64 scales) which corresponds (cf. Table 1) to a magnitude M_{GR} = 7.7 . Statistical studies based on Gumbel 3rd distribution (Marza et al. 1984, manuscript) resulted in a computed maximum possible magnitude for VSR seqs of M_{GR} = 7.8 to 7.9 which is in agreement with the largest observed eq during a millennium in the area.

3. VSR strong seismicity patterns

Numerous investigators aimed at inferring some salient patterns of the Vrancea seismicity , for example: Popescu (1958), Constantinescu & Enescu (1963, 1985), Enescu & Jianu (1963), Radu (1965), Enescu et al. (1974), Purcaru (1974, 1979), Marza et al. (1977), Marza (1982, 1984), Enescu (1983) etc.

3.1. Periodicity/cyclicity pattern. Decomposition of apparent randomness into periodic components

A first kind of salient regularity in VSR seismicity is its conspicuous periodicity/cyclicity in strong ($M_{GR} \geq 6.8$) subcrustal seismicity. The first definite results were published in 1974 by Enescu and co-workers (1974) and concomitantly and presumably independently by Purcaru (1974). The results were refined later by Purcaru (1979), Marza (1982) or Enescu (1983). The idea which emphasizes our findings is that a superposition of (quasi)periodical series of events yields randomness to total distribution. We pro - ceeded reversely with the observed overall series of VSR seqs, being able to decompose it into three nonrandom components, each component exhibiting *strong periodicity* (Fig.1). Figure 1 is the back-bone of this study, it depicts both overall series of events (Fig.1A) and a decomposition of the previous (which are randomly distributed) series into 3 nonrandom components (Fig. 1B).In the ordinate are ploted the *absolute calendar years of occurrence* vs. *relative years in each century* (the abscissa) for every event (with $M_{GR} \geq 6.8$) occurring in the last millennium. It is to be seen that VSR strong seqs are disposed in three bands of maximum activity, that is, at the beginning (M1), the middle (M2), and the end (M3) of each century. In each band there is a fairly *strong cyclicity* with a mean intersequence time $\Delta t \sim 100$ years. Tables 2 and 3 present a synopsis and respectively a simple statistics of this *remarkable (quasi)periodicity*. It is worth pointing out that the M2 maximum exhibits a full cyclic pattern for almost a millennium

Fig. 1. Overall and decomposed components projections of strong ($M_{GR} \geq 6.8$) Vrancea subcrustal earthquake time series reflecting occurrence regularities(Combined and updated after Purcaru, 1979 and Mârza, 1982)

without exception. Only 2 out of 37 events in the three series are not consistent with the regular in-sequence interval (i.e. 5.4 per cent, indeed a small/negligible proportion). The above regularity allows to predict on a long-term basis the future activity (and in fact the 1977 VSR major event was predictable in this context) and moreover it also allows to retrodict lost events in the past (see subsection 3.3).

It is surprizing and hard to explain why in each band of activity the periodicity is roughly 100 years, i.e. a *secular cycle*, but this is suggested by observation and coincidence with the round figure of 100 years is likely to be a pure random.

3.2. Paired occurrences

Another salient regularity inferred from Fig. 1 is the very often paired occurrence of strong events . For example, during the last 500 years (i.e., during completness period) the following pairs occurred : (1471, 1473), (1543, 1545), (1571, 1590, 1595) , (1620, 1637), (1679, 1681), (1738,1740), (1829, 1838), (1893,1894) and (1977, 1986), that is 9 cases out of 16 cyclic occurrences (namely more than 56%). This *regularity (i.e. paired occurrence)* was used to anticipate also the 1986 VSR major event. As a rule, the paired occurrences happen in M2 and/or M3 activity bands (where the frequency of paired occurrences is roughly 82%).

3.3. Retrodiction potentialities

Several (at least four) events are lost from our data base, indicated (in Fig. 1B) by "?" (question marks), due probably to missing information. Using the fair regularity pattern presented for observed data it is possible to extrapolate backwards in time the periodicity and to find out the likely time spans for some events not yet discovered in the historical data, but focalizing the research on the most promising areas.

3.4. Long-term prediction

It is straigthforward to forecast , on a long-term basis, the next major VSR eqs. They are ploted in Fig. 1B as empty circles , and are to be expected in the following windows:2005 $\pm$ 6 years and 2035 $\pm$ 8 years. The fulfilment probability of the above forcasting is evaluated as rather high(90% or so) based on the strong consistency of the patterns in Fig. 1B.

3.5. A tentative explanation

A crude accountability for this extraordinary cyclic recurrence may emerge from the following features of Vrancea eq process:

(1) *very high space confinement* owing to its physical-mechanical-geometrical properties which do not present great fluctuations
(2) *relative isolation* from other seismic regions, which confers independence in manifestation; and
(3) *quasi-similarity* in the focal mechanism (for strong shocks) which is, probably , due to a constant orientation of the tectonic stress field.

Table 2. Values describing maxima of seismic activity in VSR during historical time (see also the Figure 1)

Activity maxima	*The century*	*M1*	*M2*	*M3*
Individual values of relative occurrence years during each century	X-th			84
	XI-th	?	38	91
	XII-th	7	26	70
	XIII-th	-4	30	(58)
	XIV-th	?	27	?
	XV-th	?	46	71
	XVI-th	16	44*	85*
	XVII-th	5	29*	80*
	XVIII-th	1	39*	90
	XIX-th	2	34*	93*
	XX-th	8	40	81*
Estimated average value of maxima		5±6	35±7	80±10

Note : *) Average value of (relative) year for paired occurrences (doublets)

Table 3. Periodicity/ cyclicity statistics for VSR strong seismicity

Activity maxima	*M1*	*M2*	*M3*
Values of individual intersequence time during each century (secular cycle)	89	88	107
	89	104	79
	96	97	88
	101	119	114
	106	98	95
		85	110
		110	103
		95	88
		106	
Mean value of secular cycles (years)	$(\Delta t)^{M1}_{mean}$ = 96±7	$(\Delta t)^{M2}_{mean}$ = 100±10	$(\Delta t)^{M3}_{mean}$ = 98±12

4. *Other features of VSR seismicity*

4.1. *Preferential macro effects*

The macroseismic fields of VSR strong seqs present an unusual macroseismic pattern, namely a NE to SW orientation and elongation of isoseismal contours, with strong shaking at distant areas, in - duced by preferential radiation and propagation effects.

4.2. *Rupture geometry, directivity and multiplicity*

By extrapolation, recent instrumentally investigated events (i.e., 1940, 1977 and 1986) suggest that the rupture process has a strong directivity and multiplicity

4.3. *Characteristic Vrancea major eq models*

Comparative analysis of major XX century VSR seqs (1908 m_W=6.9; 1940 m_W = 7.4; 1977 m_W = 7.2 ; and 1986 m_W = 7.0) lead (Burlacu et al. 1988) to advance at least two characteristic eq models one of the type of the 1940 event (1986 also pertains to this type) and of the type of 1977 events (1908 also pertains to this type).

4.4. *Predictability of major events*

The research devoted to eq prediction of VSR events brought out promising prospects in this respect. As such we may briefly enumerate :

(i) Seismological precursors (quiescence /gaps, migration/progression, b-value, magnitude shifts etc.)

(ii) Geoscientific precursors (telluric, ionospheric, heat-flow/ underground microtemperature,etc.)

(iii) Abnormal biosystem behaviour, etc.

5. *References*

Apostol A., Arsene Gr. & Marza V.I. (1985) Earthq. Predict. Res. 3 : 105-119.

Burlacu V., Marza V. & Pantea A (1988), E.S.C. Programme and Abstracts, 21st Gen. Ass., Sofia, Bulgaria, August 28-27, 1988, p.36-37.

Constantinescu L (1978) Rev. Roum. Géol. Géophys. Géogr., Géographie 23 : 179-206.

Constantinescu L. & Enescu D. (1963), St. Cerc. Geofiz. 1(2): 239 - 268.

Constantinescu L. & Enescu D. (1984), Rev. Roum. Géol. Géophys. Géogr., Géophysique 28 : 19-32.

Constantinescu L. & Enescu D (1985) The Vrancea earthquakes within their scientific and technological frame-work, Edit. Academiei R.S.R. , Bucharest, 230 pp. (In Romanian with English and Russian abstracts).

Constantinescu L. & Marza V.I. (1984), E.S.C. Abstracts, 19th Gen. Ass. Moscow, October 1-6, 1984, p.176-177.

Constantinescu L., Cornea I. & Lazarescu V (1973), Rev. Roum. Géol. Géophys. Géogr., Géophysique 17 ; 133-143

Demetrescu G. & Iacovachi A. (1942) Persistance et isolement du foyer séismique de la région de Vrancea en Roumanie, Obs. de Bucarest, St. Séismique, 10 pp.

Enescu D. (1983) St. cerc. geol., geofiz., geogr., Geofizică 21 : 24-30.
Enescu D. & Jianu D. (1963) St. cerc. geofiz. 1(2): 277-295.
Enescu D., Marza V.I., & Zamarca I. (1974) Rev. Roum. Géol. Géophys., Géogr., Géophysique 18 : 67-79.
Fuchs K. et al. (1979) Tectonophysics 53 : 225-247.
Gutenberg B. & Richter Ch. F. (1965), Seismicity of the Earth and associated phenomena, Hafner Publ. Co., New York and London, 310 pp.
Marza V. (1982) Ph.D.Thesis, Univ. of Bucharest, Romania , 189 pp. (In Romanian with an English abstract).
Marza V. (1984) E.S.C. Abstracts, 19th Gen. Ass. Moscow, October 1-6, 1984, p. 43-44.
Marza V., Irimescu D., Pantea A. & Anghel M., (1977) C.F.P.S. Report, Theme 30.77.1, Pt.II., Chapt. 8, p. 118-132.
Oncescu M.C. (1984) Ann. Geophysicae 2 : 23-28.
Popescu I.C. (1958) St. cerc.astr.seism. 3 : 165 - 179.
Purcaru G. (1974), Semiannual Tech. Repo. NORSAR, Sci. Rep. No.6-73-74, p.53-55.
Purcaru G. (1975), Proc. of 24th Gen. Ass. E.S.C., Berlin, p.59-64.
Purcaru G. (1979) Phys.Earth Planet Int. 18: 274-287.
Radu C. (1965) St. cerc. geol.geofiz.geogr., Geofizică, 3: 231-289.
Radu C. (1974) Thèse de docteur ès sciences, Univ. L.Pasteur de Strasbourg, 453 pp.
Roman C. (1970) Nature, 228 :1176.

ANNEX 1

MASTER CATALOGUE OF VRANCEA EARTHQUAKES

984-1986

LIVIU CONSTANTINESCU & VASILE I. MARZA

ROMANIAN NATIONAL COMMITTEE FOR GEODESY AND GEOPHYSICS

SEISMOLOGICAL LABORATORY
CENTER FOR EARTH PHYSICS AND SEISMOLOGY
BUCHAREST-ROMANIA

DATA		TIME				LOCATION				MAGNITUDES			MAX.R	S	O	#
YEAR	MO	DA	HR	MN	SC	LAT(N)	LON(E)	DEP	H	MB	GR	ML	INT.C	C		
984						45.7	26.6	150	I		6.8		8 11	FLA	F	1
1038	AUG	15				45.7	26.6	150	I		7.0		8.5 11	FLA	F	2
1091						45.7	26.6	150	I		6.8		8 11	SEC	F	3
1107	FEB	12	03			45.7	26.6	150	I		6.8		8 11	SEC	F	4
1126	AUG	08	00			45.7	26.6	150	I		6.8		8 11	SEC	F	5
1170	APR	01				45.7	26.6	150	I		7.0		8.5 11	SEC	F	6
1196	FEB	13	07			45.7	26.6	150	I		7.3		9 11	SEC	F	7
1230	MAY	10	07			45.7	26.6	150	I		7.1		8.5 11	SEC	F	8
1258	FEB	07	13			45.7	26.6	150	I		6.8		8 11	ATI	F	9
1327						45.7	26.6	150	I		7.0		8 11	SEC	F	10
1446	OCT	10	04			45.7	26.6	150	I		7.3		8.5 11	SEC	F	11
1471	AUG	29	10			45.7	26.6	110	I		7.3		9 11	CBE	F	12
1473	AUG	29				45.7	26.6	150	I		7.0		8.5 11	CBE	F	13
1516	NOV	24	12			45.7	26.6	150	I		7.3		9 11	CBE	E	14
1543						45.7	26.6	150	I		6.8		8 11	CBE	F	15
1545	JUL	19	08	-0	9	45.7	26.6	110	I		6.8		8 11	CBE	E	16
1571	MAY	10				45.7	26.6	150	I		6.8		8 11	FLA	F	17
1590	APR	30				45.7	26.6	100	I		7.0		8.5 11	PO3	F	18
1595	APR	21	10			45.7	26.6	150	I		6.8		8 11	FLA	E	19
1605	DEC	24	15	-1	6	45.7	26.6	150	I		6.8		8 11	CBE	E	20
1620	NOV	08	13	-1	4	45.7	26.6	150	I		7.3		9 11	CBE	E	21
1637	FEB	01	01	-0	2	45.7	26.6	130	I		6.8		8 11	CBE	E	22
1679	AUG	09	01			45.7	26.6	110	I		7.3		9 11	CBE	E	23
1681	AUG	19	00	-0	1	45.7	26.6	150	I		6.8		8 11	CBE	E	24
1701	JUN	12	00	-0	1	45.7	26.6	150	I		6.8		8 11	CBE	E	25
1738	JUN	11	10	-1	1	45.7	26.6	130	I		7.5		9.5 11	CBE	E	26
1740	APR	05	18	-1	9	45.7	26.6	150	I		7.0		8.5 11	CBE	F	27
1790	APR	06	19	29		45.7	26.6	150	I		6.8		8 11	CBE	D	28
1802	OCT	26	10	55		45.7	26.6	150	I		7.7		10 11	CBE	D	29
1829	NOV	26	01	40		45.8	26.6	150	I		7.0		8.5 11	CBE	E	30
1838	JAN	23	18	45		45 7	26.6	150	I		7.3		9 11	CBE	D	31
1893	AUG	17	14	45		45.7	26.6	100	I		6.8		8 11	SEC	D	32
1894	AUG	31	12	20		45.7	26.6	130	I		6.8		8 11	CBE	E	33
1908	OCT	06	21	40		45.5	26.5	125	I		6.8		8 11	CBE	C	34
1940	NOV	10	01	39	07	45.8	26.7	150	I		7.4		9.5 11	CBE	C	35
1977	MAR	04	19	21	54	45.77	26.76	94.1	I	6.4	7.2		9 11	GS	B	36
1986	AUG	30	21	28	35	45.53	26.44	144	I		7.0	7.0	8.5 11	VMI	B	37

END OF CATALOGUE
LEGEND FOLLOWS

37 ITEMS

SOME CONSIDERATIONS ON THE SEISMOTECTONICS OF THE NORTHERN DINARIDES

G.B. Carulli *, R. Nicolich **, A. Rebez *** and D. Slejko ***

* Istituto di Geologia e Paleontologia, Universita' di Trieste, Italy
** Istituto di Geofisica Applicata e Miniere, Universita' di Trieste, Italy
*** Osservatorio Geofisico Sperimentale di Trieste, Italy

ABSTRACT

The region of tectonic contact between the Alps and Dinarides is considered using geological, geophysical and seismological data. Seismotectonic analogies between central Friuli and western Slovenia are identified, and a unique model with a vertical disengagement behind the compression front is proposed. The relation of the eastern Alps and Dinarides to the Pannonian basin is discussed.

INTRODUCTION

The aim of the present work is to investigate the seismotectonic characteristics of the contact between the Alps and Dinarides in order to individuate analogies or differences of seismic behaviour in the context of the geodynamic processes in central Europe. The study area comprises the eastern Alps and the northwestern part of the Dinarides: both systems reflect in shape and geodynamic evolution the effects of the collision between the Adria microplate and Europe. This collision acted at different times creating compressive structures overthrusting the Adria microplate. However, complications arise from the evolution of the Pannonian basin which influenced the tectonic setting of the Internal Dinarides, the eastern Alps and the Carpathian Chain.

GEOLOGICAL OUTLINE

The main geologic units of the investigated area (Fig.1) are:

- the metamorphic basement outcropping in the Southern Alps south of the Insubric Lineament, and more widely in the Austro-Alpine units north of the lineament itself;
- the Paleozoic units of the Austrian Alps and Slovenian Alps with different degrees of metamorphism, and Hercynian non metamorphic and anchimetamorphic sedimentary cover, widely present in the Paleocarnic chain;
- the Mesozoic units of the Southern Alps, of the Dinarides and of the Western Drauzug and Northern Karavanken that consist of rigid Triassic or Cretaceous units of Carbonatic platform, detached and thrusted over plastic, mainly evaporitic layers;
- the mainly Tertiary flysch and molasse, often acting as tectonic lubrificant, and the Tertiary deposits of the Styrian and Pannonian basins;
- the principal Quaternary deposits;
- the Tertiary Periadriatic intrusive masses and the Tertiary lava effusions (Velenje, Gleichenberg hills, etc.).

An important element of the studied area is represented by the northeastern portion of the deformed margin of the Adria microplate, where the crustal Dinarides unit splits off from the eastern Alps. The external margins of the two chains show strong recent tectonic deformation that reaches a maximum in the Friulian piedmont arc (Zanferrari et al., 1982). The geodynamic evolution of the Adria microplate started with its detachment from the

African plate, probably during the middle-upper Triassic (D'Argenio and Horvath, 1984). It collided during the Paleogene against the Dinarides, and during the Neogene against the Alpine chain (Cousin, 1981). In both sectors the tectonic activity during the Quaternary remains evident, with the most notable areas of deformation in the Veneto-Friuli Prealpine arc, in western Slovenia and along the Croatian coast.

In the Southern Alps the main tectonic structures are E-W oriented overthrusts, north-verging in the northern sector between the Gail line and the Fella-Sava line (Castellarin and Vai, 1982), and south-verging in the southern.

The Dinaric area is further characterized by NW-SE overthrusts NE dipping, and by dextral, subvertical faults with directions ranging between NW-SE and NNW-SSE, such as the Idrija, Predjama, Rasa and Divaca lines (Placer, 1981). Buried overthrusts with Dinaric direction can be found also in the northern Friulian plain.

In northern Slovenia the main structures are WNW-SSE orientated and can be considered the eastern prosecution of the Gail line, of the Fella-Sava line and of the Friulian overthrusts. The latter continue eastwards assuming gradually the NE-SW direction (Arsovski, 1976). In the region between Ljubljana and Zagreb the Dinaric style is complicated by ENE-WSW oriented faults (Carulli et al., 1988), indicating the tensional tectonics in the Pannonic domain.

The Pannonian realm subsided in the Neogene and Quaternary, and has been considered as a back arc basin completely surrounded by folded arcs (Horvath and Berckhemer, 1982). It is subdivided into several sub-basins and transitional areas. The most important of these are the inner Dinarides area, marked by two NW-SE elongated depressions (the Sava and Drava throughs), the transitional zone of the eastern Styrian basin, characterizing the boundary of the eastern Alps, and the Vienna basin which developed between the inner and outer Carpathian chains (Royden et al., 1983).

The northward thrusts of both the western Carpathians and the Alps have the European platform as a common foreland; they developed in the Oligo-Miocene starting from late Cretaceous. According to some authors (Gutdeutsch and Aric, 1987) the present tectonic activity in the area must be attributed to the thrusting of the Adria against the European platform which induces a network of strike-slip faults separating a mosaic of blocks in the basement of the western Pannonian area. The induced stresses transmitted by the inherited crustal thicknesses of the mountain chains (Southern Alps, External Dinarides, eastern Alps) are responsible for the actual tectonic movements as well as for the thermal effects (Pannonian basin).

The Alps and Dinarides have their junction in the area between Tolmin, where the principal tectonic orientation changes from Dinaric to Alpine (Carobene e Carulli, 1981), and the canyon of the river Tagliamento (north of Udine), where N-S oriented transcurrent faults play the role of mechanical disengagement (Carulli et al., 1982). This area corresponds to the zone of maximum crustal shortening in the Southern Alps (Castellarin, 1979). Presently, the Friulian Prealpine sector is uplifting, while the plain is gently subsiding; this fact, and the presence in the eastern part of dextral Dinaric lines, such as the Idrija line, can be explained by a model with a NW movement of the Adria plate (Cavallin et al., 1984; Anderson and Jackson, 1987) which compresses the edge of the Southern Alps.

CRUSTAL CHARACTERISTICS

Each of the tectonic units (Alps, Dinarides, Adria and Pannonian basin, Carpathians and European foreland) has its own particular crustal structure and preserves the imprint of its geodynamic history. Significant changes in crustal thicknesses, and probable low velocity layers associated with very high velocity intervals have been found even if more detailed seismic

investigations are required for a more complete outline.

The Alps have been studied by means of several deep seismic soundings (DSS) since the fifties, (e.g. Giese and Prodehl, 1976; Aric et al., 1987; and references in Slejko et al., 1987). A sharp increase in crustal thickness, which causes a Moho depth of more than 50 km in the area included from the Venosta valley to Lienz, has been observed. This flexure or discontinuity in the Moho is documented towards both the south and east, whereas towards the Bavaria region it gradually rises up to a depth of about 30 km (Fig. 2). This trend fits the negative trend of the Bouguer anomalies quite well (see discussion and references in Slejko et al., 1987; Walach and Weber, 1987).

The Adria unit is characterized by a crustal high in the Adriatic Sea-Istria region which is somehow connected to the even more pronounced high of the Lessini-Berici ridge (Verona area). This zone is limited by sharp transitions of the Moho towards the west in the Giudicarie-Adamello system or Trompia valley-Giudicarie Arc (Castellarin and Vai, 1986), towards the north in the front of the Valsugana system, and towards the east in the area of the Schio system. Towards the Apenninic foredeep, the Moho plunges as a monocline to depths ranging from 35 to 40 km. From Istria northwards, the Moho deepens regularly and gains a depth of more than 40 km after a pronounced flexure in front of the Southern Alps (Gemona), and more than 50 km further north in the Venosta valley - Tauern mountains area. A seismic interval with velocity values close to 6.7 km/s has been found in central Friuli at depths of nearly 10 km. According to aeromagnetic interpretations (Cati et al., 1987) this element is linked to structures present near the top of the basement. The aeromagnetic data confirm that the basement is involved along the whole southern Alpine Friulian arc in a complex tectonic setting, and is displaced and overthrust onto the basement of the Adriatic foreland and of its cover (Valsugana and Tagliamento systems, Slejko et al.,1987).

Similar imbrications of the basement have been hypothesised in the Dinaric system (Cati et al., 1987). Hence, the 6.7 km/s basement plays the role of a more rigid crustal block which was formerly wedged into the Dinaric system and then controlled the lateral propagation of 'decollement' surfaces in the Southern Alps, with the appearance of the arc-shaped external front of Plio-Quaternary age.

The Dinaric unit is characterized by a thick crust with a deep trough (thickening from 40 to 45 km) oriented NW-SE and running from Dalmatia-Herzegovina to Tolmin-Idrija. It has been interpreted (Alijnovic et al., 1984) as the root area of crustal SW-verging overthrusts.

The Pannonian basin forms a crustal unit 20-30 km thick (Aric et al., 1976), which includes the inner Carpathians, the easternmost parts of the Alps, and the inner zones of the Dinarides. In Fig. 3a the transition from the Pannonian basin to the European foreland across the Carpathians in the Bratislava area is sketched. The geodynamic evolution of the Pannonian basin strongly conditioned the tectonics of the eastern Alps area. The Pannonian basin-Alps transition is discussed in Aric et al. (1987), and in Walach and Weber (1987) on the basis of DSS profiles and gravity and magnetic data collected across the eastern Alps and Styrian basin. This transition, which develops through a crustal thickening from less than 30 km east of Graz to more than 40 km towards the Tyrol area, was interpreted by Giese (1980) as an example of thrust tectonics where the imbrications of the entire crust and uppermost mantle cause a crustal doubling (Fig. 3b) following the pushing of the internal units (Styrian basin) onto the foreland (eastern Alps).

SEISMICITY

As the earthquake catalogue of the eastern Alps (OGS, 1987) does not cover the whole study region, it was necessary to integrate it with the data

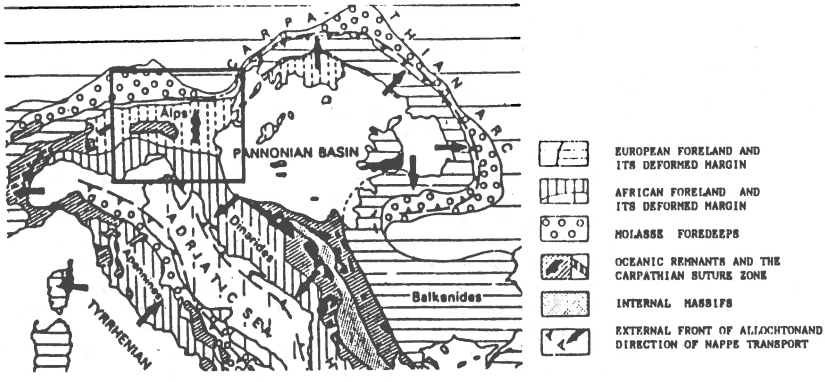

Fig. 1 - The investigated region and the main geotectonic setting of the area (from Horvath and Berckhemer, 1982).

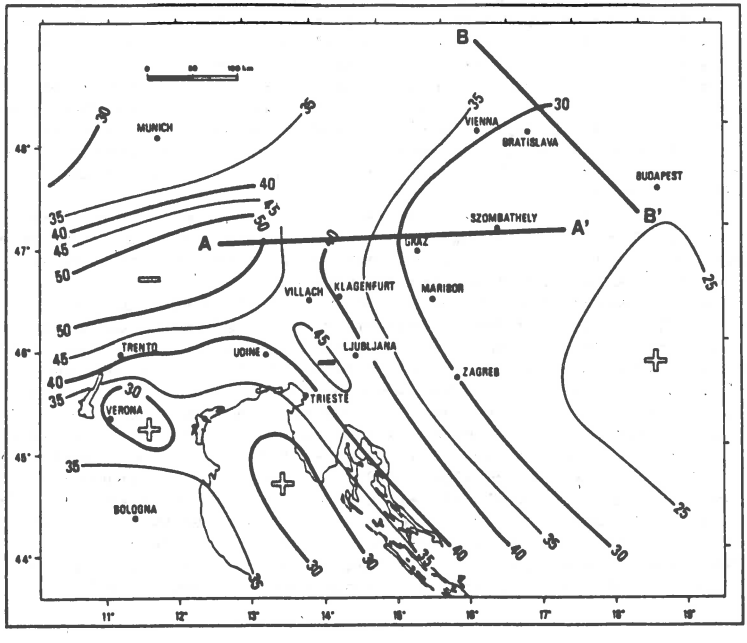

Fig. 2 - Map of the Moho isobathes with the traces of the crustal cross-sections.

taken from the USGS earthquake files. However, the characteristics of relative completeness and homogeneity of the starting catalogue were thus lost, and a filtering of the low intensity (Io≥VI Mercalli-Cancani-Sieberg MCS) events was necessary. The catalogue so obtained contains 924 events since the beginning of the Christian age until 1984 in the region between 45°N, 10°E - 49°N, 18°E. The epicentres of these shocks are reported in Fig. 4, where we can see that they belong to different seismic provinces. The main concentration appears in central Friuli and continues westwards along the Prealpine belt.

In western Yugoslavia the seismicity is concentrated in three parallel narrow bands: the first elongated from Friuli to the Croatian coast, the second from Friuli to Zagreb and the third, between the other two, encompasses the seismicity of Ljubljana.

In this general scheme, the Villach earthquake of 1348 (Io=XI MCS) remains slightly apart, but could belong to an alignment of seismicity from Friuli northeastwards which identifies the western margin of the Pannonian basin.

The seismic activity according to Riznichenko (1959) can be seen in Fig. 4. It was obtained using the data since 1800, and hence some strong historical events were not used in the processing. Its similarities with the epicentre distribution are however, relevant. The main seismic alignments appear more clearly; in particular, the two inner bands in Yugoslavia overlap forming a continuous arc-shaped strip from lake Garda to Croatia. The NE-SW oriented alignment of seismicity is even more evident and separates aseismic regions.

SEISMOTECTONIC CHARACTERISTICS

A correlation has been recognized between the seismically active zones and the abrupt changes in crustal thicknesses (from Adria to the Dinarides, from Adria to the Alps, from the Pannonian basin to the Alps and to the European foreland). The hinterlands are seen as more or less rigid blocks with compression still active at their fronts (Giese et al., 1982). Gutdeutsch and Aric (1987) stress the fact that all the earthquakes occur mainly in the upper crust, and that pressure of the Adria against the European platform induces in the basement of the western Pannonian area a network of strike-slip faults or 'seismic lineaments' separating a mosaic of blocks. Intersections of the lineaments are places of enhanced earthquake risk. Both the source of the seismicity and the thermal effects (Pannonian basin unit) are therefore related to the stress transmitted by distension associated with the different crustal thicknesses in the mountain chains (Southern Alps, Dinarides, eastern Alps).

Interesting additional characteristics are deduced from the analysis of vertical cross-sections with geological and geophysical evidence, and with the present day seismicity (Rebez,1987, Slejko et al., 1987; Carulli et al., 1988). Two transects are here proposed as examples; the first is in Friuli and is N-S oriented; the second, is located in western Slovenia with a NE-SW orientation (see Fig. 4 for the location). The following main characteristics of the seismicity are fairly well individuated.

- The Idrija fault acts as the northeastern boundary of the main seismicity (Fig. 5a) without itself being seismically active, unlike the deep continuation of the Fella-Sava line (Fig. 5b), where the presence of the stations of the Osservatorio Geofisico Sperimentale (OGS) seismometric network guarantees the detection even of low magnitude shocks.
- The horizontal alignment of hypocentres at 20 km depth (Fig. 5a) suggests the presence of an intracrustal detachment plane deeper than that identified in Friuli at the top of the crystalline basement (Siro and Slejko,1982).
- The main concentration of foci seems to be narrower and deeper in Slovenia (Fig. 5a) than in Friuli (Fig. 5b), and could correspond to a subvertical,

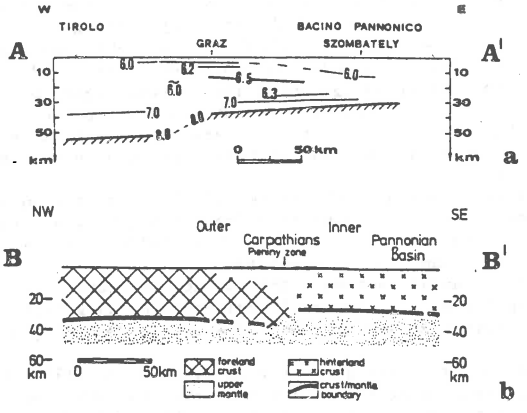

Fig. 3 - Crustal cross-sections of the Pannonian basin (for location see Fig. 2): a) section AA' (from Italian Explosion Seismology Group and Institute of Geophysics, ETH Zurich, 1981); b) section BB' (from Giese et al., 1982)

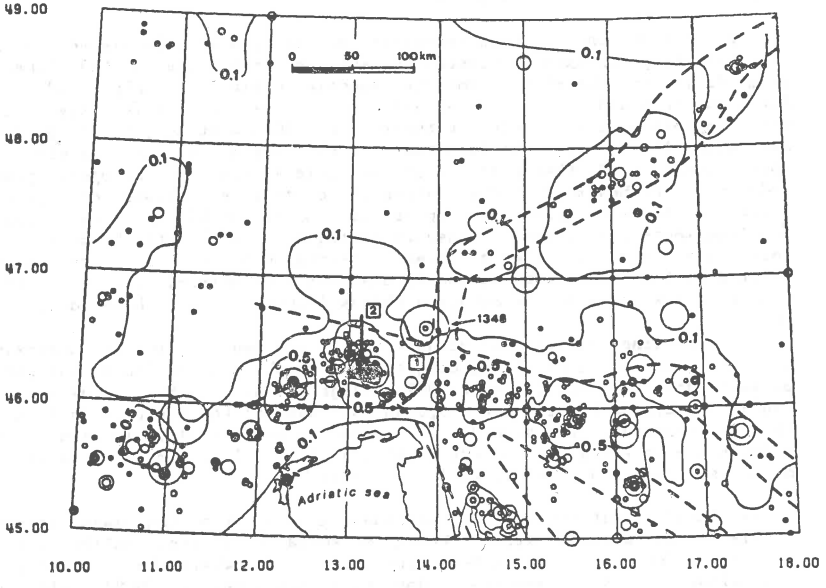

Fig. 4 - Map of the epicentres of the earthquakes with epicentral intensity greater than, or equal to degree VI MCS since the beginning of the Christian age and 1984, seismic activity isolines, traces of the cross-sections presented, and seismic deformational strips according to Gutdeutsch and Aric (1986).

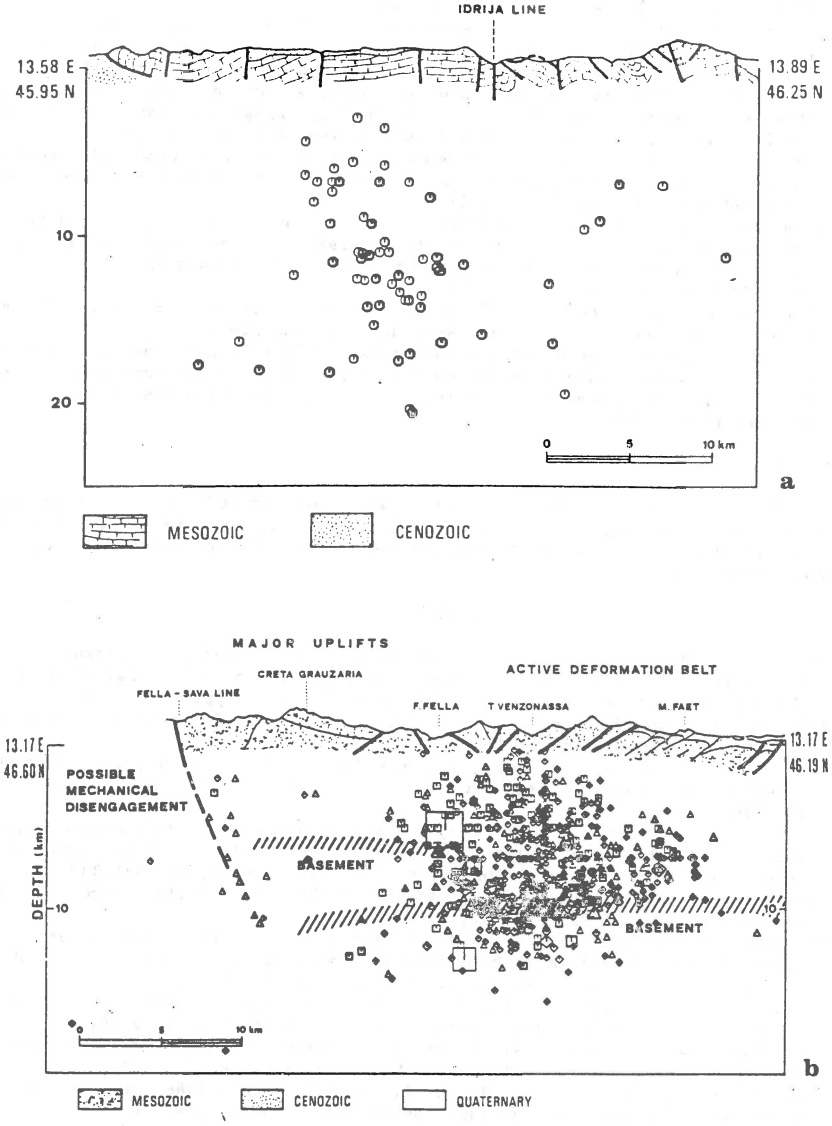

Fig. 5 - Vertical-cross sections (from Carulli et al., 1988; for the location see Fig. 4): a) section 1, 10 km wide across the border between Italy and Yugoslavia with the hypocentres of the earthquakes recorded by the OGS seismometric network in the period 1977-1986. b) section 2, 6km wide in Friuli with the main seismotectonic characteristics.

dipping plane expressing transcurrent activity.
- No superficial, low angle, seismically active dipping plane can be identified, contrary to what has been found in Friuli (Slejko et al.,1987).
- The seismicity is very important in Friuli, where the present uplifting is justified by the crustal thickening or doubling, and a subvertical fault (the Fella-Sava line) acts as a mechanical disengagement that leaves the northernmost part of the Southern Alps inactive (Slejko et al.,1987).
- In the Dinaric sector the seismicity occurs in the band of crustal thickening between the present compressive front of the External Dinarides and a subvertical fault (Idrija line).
- The other two strips of seismicity (Fig. 4) may reflect local structural faults, the presence of the eastern margin of the Southalpine front (Ljubljana area), and the influence of seismic lineaments in the Pannonic basin (Zagreb area: Drava through).
- The seismicity of the Outern Carpathians could be related to left lateral movements between the Pannonian basin and European plate.
- The previously mentioned Villach earthquake could belong to the interaction of the Pannonian basin with the eastern Alps. This is the zone from where the Carpathian alignment starts and is characterized by a distinct increase of crustal thickness.

Acknowledgements

The seismometric network of Friuli is managed by OGS with the financial support of the Regione Autonoma Friuli-Venezia Giulia. Thanks are due to Manuela Sedmach for drawing the figures and to Peter Guidotti for checking the English manuscript.

REFERENCES

Aljinovic, B., Blaskovic, I., Cvijanovic, D., Prelogovic, E., Skoko, D. and Bedarevic, N., 1984. Correlation of geophysical and seismological data in the coastal part of Yugoslavia. Boll. Oceanol. Teor. Appl., 2, 77-90.

Anderson, H. and Jackson, J., 1987. Active tectonics of the Adriatic Region. Geophys. J. R. astr. Soc., 91, 937-983.

Aric, K., Giese, P., Miller, H., Morelli, C., Nicolich, R., 1976. Crustal structure and seismicity at Northern Italy. Boll. Geof. Teor. Appl., 18, 273-278.

Arich, K., Gutdeutsch, R., Klinger, G., and Lenhardt, W., 1987. Seismological studies in the Eastern Alps. In: H.W. Flugel and P. Faupl (Editors), Geodynamics of the Eastern Alps. Franz Deuticke, Vienna, pp. 325-333.

Arsovski, M., 1976. Problemi Neotektonike SFR Jugoslavije. Jugoslovanski geoloski kongres, Ljubljana, 3., 21-36.

Carobene, L. e Carulli, G.B., 1981. Tolmino. In: A. Castellarin (a cura di), Carta tettonica delle Alpi Meridionali alla scala 1:200.000. C.N.R. P.F. Geodinamica pubbl. 441, Tecnoprint, Bologna, pp. 14-18.

Carulli, G.B., Giorgetti, F., Nicolich R. e Slejko D.,1982. Friuli zona sismica: sintesi di dati sismologici, strutturali e geofisici. In: A. Castellarin e G.B. Vai (a cura di): Guida alla geologia del sudalpino centro-orientale. Guida Geol. reg. S.G.I., Bologna, pp. 361-370.

Carulli, G.B., Nicolich, R., Rebez, A. and Slejko, D., 1988. Seismotectonics of the western External Dinarides. Submitted to Tectonophysics.

Castellarin, A., 1979: Il problema di raccorciamenti crostali del Sudalpino. Rend. Soc. Geol. It., 1, 21-23.

Castellarin, A., e Vai, G.B., 1982. Introduzione alla geologia strutturale del Sudalpino centro-orientale. In: A. Castellarin e G.B. Vai (a cura di), Guida alla geologia del Sudalpino centro-orientale, Guida Geol. reg. S.G.I., Tecnoprint, Bologna, pp. 1-22.

Castellarin, A., and Vai G.B., 1986. Southalpine versus Po plain Apenninic

areas. In: F.C. Wezel (Editor), The origin of arcs. Elsevier, Amsterdam, pp. 253-280.

Cati, A., Fichera, R., and Cappelli, V., 1987. Northeastern Italy. Integrated processing of geophysical and geological data. Mem. Soc. Geol. It., 40, (in press).

Cousin, M., 1981. Les rapports Alpes-Dinarides. Les confins de l'Italie et de la Yugoslavie. Soc. Geol. du Nord. publ. 5., 2 vol., S.C.N. Villeneuve d'Ascq.

D'Argenio, B. and Horvath, F., 1984. Some remarks on the deformation history of Adria, from the Mesozoic to the Tertiary. Annales Geophysicae, 2, 143-146.

Giese, P., 1980. Krustenstruktur der Alpen. Berliner geowiss. Abh., (A), 20, 51-64.

Giese, P., Prodhel, C., 1976. Main features of crustal strucrures in the Alps. In: P. Giese, C. Prodhel, and A. Stein (Editors), Explosion Seismology in Central Europe. Springer Verlag, Berlin, pp. 347-375.

Giese, P., Reutter, K.J., Jakobshagen, V., and Nicolich, R., 1982. Explosion seismic crustal studies in the Alpine-Med. Region and their implications to tectonic processes. In: H. Berckemer and K. Hsu (Editors), Alpine-Mediterranean Geodynamics. AGU, Geodyn. Series, vol. 7, pp. 39-73.

Gutdeutsch, R. and Aric, K., 1987. Tectonic block models based on the seismicity in the east Alpine-Carpathian and Pannonian area. In: H.W. Flugel and P. Faupl (Editors), Geodynamics of the Eastern Alps. Franz Deuticke, Vienna, pp. 309-324.

Horvath, F. and Berckhemer, H., 1982. Mediterranean Back Arc Basins. In H. Berckhemer and K. Hsu (Editors), Alpine-Mediterranean Geodynamics. Geodyn. Series, vol. 7, AGU, Washington. D. C., 141-173.

Italian Explosion Seismology Group and Institute of Geophysics, ETH Zurich, 1981. Crust and upper mantle structures in the southern Alps from D.S.S. profiles (1977, 1978) and surface wave dispersion analysis. Boll. Geof. Teor. Appl. 23, 297-330.

Placer, L., 1981. Geoloska zgradba jugozahodne Slovenije. Geologije, 24 (1), 27-60.

OGS, 1987; Earthquake catalogue of the eastern Alps. Computer file. OGS, Trieste.

Rebez, A., 1987; Interrelazone tra aree sismogenetiche al contatto Alpi-Dinaridi. Tesi di laurea, Istituto di Geofisica e Geodesia dell'Universita' di Trieste. Trieste, 225 pp.

Royden, L., Horvath, F. and Rumpler, J., 1983. Evolution of the Pannonian basin system. 1. Tectonics. Tectonics, 2, 63-90.

Siro, L. and Slejko, D., 1982. Space-time evolution of the 1977-1980 seismicity in the Friuli area and its seismotectonic implications. Boll. Geof. Teor. Appl., 24, 67-77.

Slejko, D., Carulli, G.B., Carraro, F., Castaldini, D., Cavallin, A., Doglioni, C., Iliceto, V., Nicolich, R., Rebez, A., Semenza, E., Zanferrari, A. e Zanolla, C., 1987. Modello Sismotettonico dell'Italia nord-orientale. C.N.R. G.N.D.T. Rendiconto 1, Ricci, Trieste, 82 pp..

Walach, G., Weber, F., 1987. Contributions to the relations between the Eastern Alps and the Pannonian Basin in the light of gravimetric and magnetic investigations. In: H.W. Flugel and P. Faupl, (Editors), Geodynamics of the Eastern Alps. Franz Deuticke, Vienna, pp. 345-360.

Zanferrari, A., Bollettinari, G., Carobene, L., Carton, A., Carulli, G.B., Castaldini, D., Cavallin, A., Panizza, M., Pellegrini, G.B., Pianetti, F. e Sauro, U., 1982. Evoluzione neotettonica dell'Italia nord-orientale. Memorie di Scienze Geologiche, 35, 355-376.

VARIATIONS OF SEISMICITY FOR DIFFERENT GEOTHERMAL AREAS

I. A. KIREYEV and N. V. KONDORSKAYA

Institute of Physics of the Earth
Academy of Sciences USSR, Moscow

Abstract. From analysis of seismicity and earthquake sources in the crust with different geothermal conditions it is concluded that within active tectonic belts of continents the strongest shallow earthquakes occur in areas with low heat flow density though background seismicity tends to areas with higher heat flow. Two recent seismic events in Fergana valley (a swarm and an earthquake with aftershocks) within the same tectonic setting are considered. Thermal structure of the crust seems to determine the form of seismic release or creep deformation in the site. This feature is given grounds for use in seismic danger estimation research.

For better understanding of seismicity, its generation and forms of relevance one should pay attention to rheological properties of media embedding earthquake sources. Since temperature is a controlling parameter for strength of rocks we consider seismicity features (such as seismic regime parameters, source parameters of single shocks, clustering, etc.) for different geothermal areas in order to emphasize some relations between seismicity and geothermics. We try to consider the mentioned interrelations in wide scale range: from global to local.

A mere glimpse at the global map of heat flow, volcanoes and seismicity, compiled in WDC-A (Jessop et al., 1976), makes us suggest correlation between heated lithosphere and seismicity: arcs of islands covered by epicenter dots coincide with chains of volcanoes; seismic mid-oceanic ridges and rift zones correspond to the highest heat flow values. On the other hand huge areas of continental and oceanic platforms almost free from epicenters are cooler as heat flow measurements point out. It is a well known fact that heat flow density of continental active belts is almost twice higher than that of continental platforms (Chapman and Pollack, 1975; Smirnov, 1980). The comparison of this fact with characteristic seismic regime parameters is shown in the Table. *b*-parameter can be interpreted as

Table

	heat flow density mW/m^2	M_{max} observed (MLH)	*b*-value	A_{10} seismic activity
continental platforms	30-50	7.7	0.4-0.7	0.-0.01
active tectonic belts	50-100	8.7	0.9+0.3	0.01-1.
references	Chapman, Pollack 1975	authors	authors	Bune, Gorshkov 1980

the fracture factor of media. Notions about high fractureness of media and high seismicity in active tectonic belts are widespread and supported by the authors' data. One can see in the Table and knows from his experience that the greatest shallow continental earthquakes occur in active tectonic belts. Shebalin (1987) and Sadovsky et al. (1987) noticed from general considerations that the largest earthquakes can't and don't occur in heated media. We have shown it earlier (1985) quantatively that there exists a layer in the middle of the crust of basins and orogenic zones in which the strongest earthquakes of the site originate. This layer is bounded by 400°C and 600°C isotherms. Fig. 1 shows compiled data of magnitudes of several strongest observed earthquakes and thickness of the mentioned layer in their epicentre sites. The relation

$$M_{max} < 0.18 * H + 4.2 \qquad (1)$$

seems reasonable to be applied to local seismic danger estimation. The fact that the strongest known earthquakes occurred exclusively in active tectonic belts agrees with the observation that the thermal fields of the latters are not homogeneous but vary abruptly. We suppose that the unity of high velocity deformation (implied by definition of 'active' belts) and of big volumes of passive cool lithosphere within this belts leads to generation of the largest earthquakes. (We call the volume 'cool' if the 600°C isotherm is deeper than the bottom of the crust; this situation corresponds approximately to surface heat flow density < 60 mW/m^2. In such cases the relation (1) is not applicable).

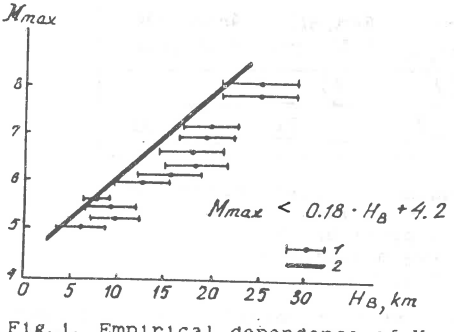

Fig. 1. Empirical dependence of M_{max} on the thickness of layer B.
1 - experimental data with confedence limits, 2 - limiting line.

We have analysed sections of continental lithosphere containing sources of the strongest earthquakes on the USSR territory (Shebalin, 1975), heat flow densities (Smirnov, 1980) for epiceter sites and calculated depths of 400°C and 600°C isotherms (Fig. 2). All these earthquakes except one occurred in areas with low heat flow. This is a good illustration of the supposition that strongest earthquakes 'choose' or 'seek for' cool volumes of lithosphere within active tectonic belts.

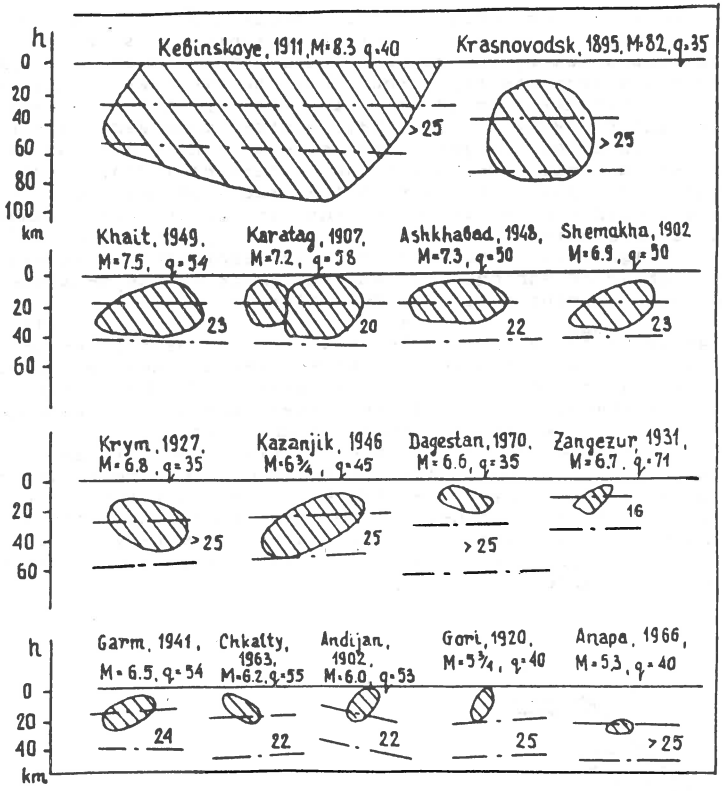

Fig. 2. Scheme of strong earthquake sources (after Shebalin, 1974) and geothermal data. q - heat flow density in mW/m^2; dashed lines designate 400°C (upper) and 600°C (lower) isotherms, numbers between isotherms designate thickness of layer B in Km.

For analysis of seismic process details caused by geothermal conditions two events: the Kairakkum earthquake (13.XI. 1985, MLH=6.0) with aftershocks and the Pap swarm (Jan.-March, 1984, the strongest shock MLH=5.6, 17 Feb.) are investigated. They occurred within the same tectonic setting in Central Asia, that is the contact zone of Fergana basin and Kurama ridge. Both of them are the maximum events observed in their sites for historical time (Kondorskaya, Shebalin, 1982). Fault plane solutions of these events are alike and show SW-NE direction of rupture extention (Zakharova, Chepkunas, 1987), that is almost normal to the direction of the regional tectonic stress axis (Lukk et al., 1987). Using the Joint Hypocetre Determination method (Bruk et al., in press) with combined JB and local travel times we have located the foci of the swarm 41 strongest shocks (M > 4.0) (Fig. 3). More than 150 shocks with M > 3.0 and lots of minor ones occerred in this site. The 400°C and 600°C isotherms are also calculated and shown in Fig. 3. Both of them

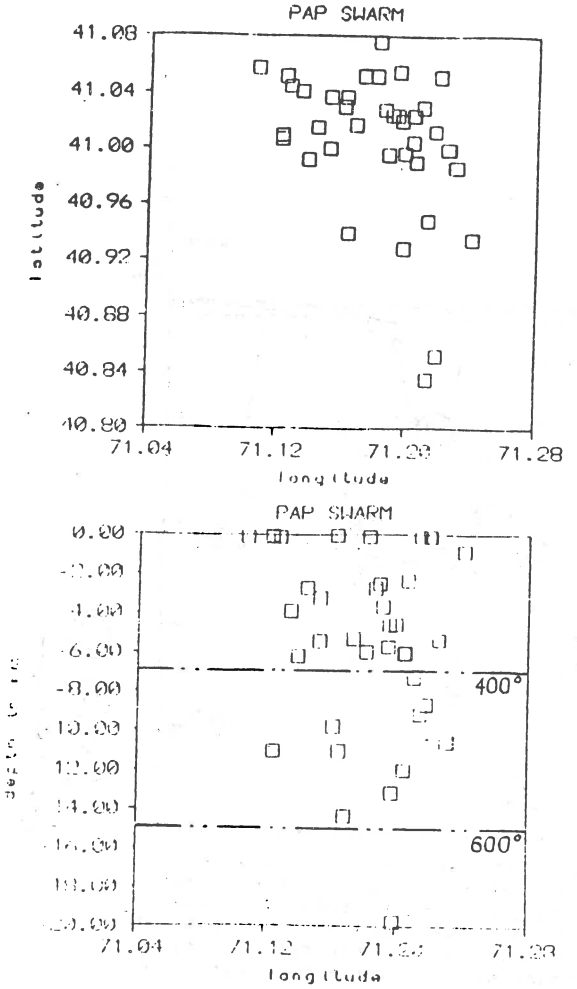

Fig. 3. Pap swarm hypocenters of earthquakes with M >4.0 and isotherms. Heat flow density q > 100 mW/m^2.

lay very close to the day surface due to high heat flow density in the area (q > 100 mW/m^2) (Tal'-Virsky, 1982). The thickness of the layer between the isotherms is 7-9 km and the depth of seismicity is 15 km. Swarm seismicity and clustering are common for this area as well as for the whole north-western margin of Fergana basin. That is why the Kairakkum earthquake looks an exception here: it exceeds all known shocks and has very few and week aftershocks (Amankulov et al., 1988) (Fig. 4). Heat flow density in the epicentral zone is equal to 60-70 mW/m^2 and the layer between 400°C and 600°C isotherms is 12-16 km thick.

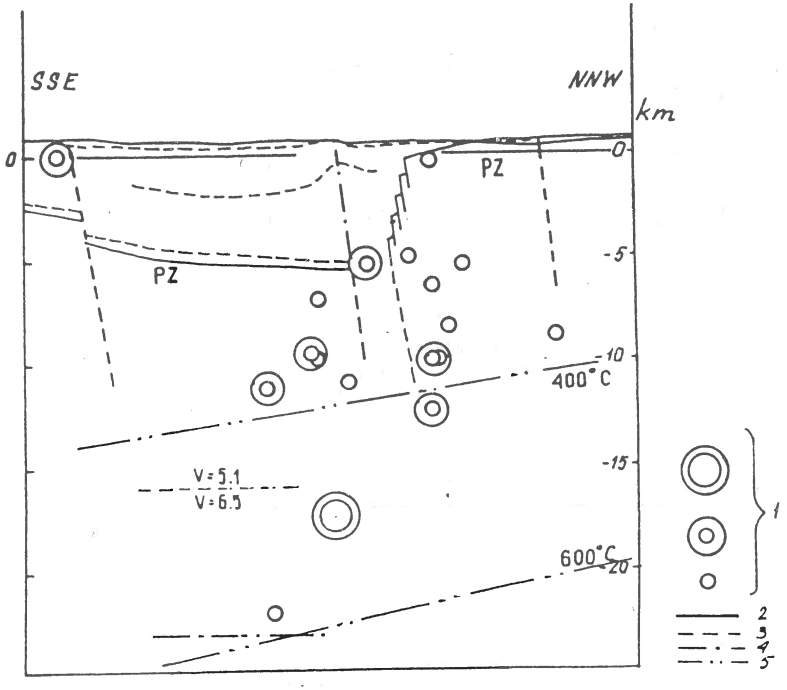

Fig. 4. Kairakkum earthquake (M_{LH}=6.0) and its aftershocks in schematic geological-geophysical cross-section (Amankulov et al., 1988). 1 - earthquakes with M=6.0, 3.0<M<4.5 and M<3.0 respectivly; 2 - geological boundaries; 3 - structural fualts; 4 - seismic boundaries; 5 - isotherms. Heat flow density q=60-70 mW/m^2.

Thus, two seismic situations in common tectonic setting with similar fault-plane solutions at shallow depths under the same regional compression stress displayed quite different stress release patterns: a big swarm and a strong earthquake with a few week aftershocks. Radiated seismic energy in both cases is of the same order. We suppose that the remarkable difference in heat flow density determined different rheology of rocks in these two areas, assuming the rate of regional deformation to be the same at both sites.

On the basis of these results it is possible to conclude that: a) the Kairakkum earthquake occurred in 'cool' volume of the crust within heated active tectonic belt, b) swarm may be considered as a transition form of tectonic deformation between strong earthquake and creep.

REFERENCES

Amankulov T. K., Borisov B. A., Bruk M. G. et al. Kairakkumskoye zemletryaseniye 13 October, 1985. Zemletryaseniya v SSSR v 1985 godu. Moscow, Nauka, 1988, 97-115.

Bruk M. G., Kondorskaya N. V., Lagova N. A. Kaspiyskoye zemletryaseniye 13 March, 1986. Zemletryaseniya v SSSR v 1986 godu. Moscow, Nauka (in press).

Bune V. I. and Gorshkov G. P. (editors). Seismic zoning of the USSR territory. Moscow, Nauka, 1980, 308.

Chapman D. S., Pollack H. W. Global heat flow: a new look. Earth. Plan. Sci. Lett., 1975, v. 28, 23-32.

Jessop A. M., Hobart M. A., Sclater J. G. Heat flow data compilation. World Data Center-A, Boulder, Colorado, USA. Geotherm. Service of Canada, Geotherm. Ser. 5, 1976, 125.

Kireyev I. A., Kondorskaya N. V. et al. In: Modern geodynamics of continental lithosphere. Ed. by Khromovskih V. S. v. 2. Moscow, Nedra (in press).

Kondorskaya N. V., Kireyev I. A. On the estimation of earthquake maximum magnitude based on a joint analysis of seismological and geothermal parameters. In: A. E. Beck (editor), Terrestrial Heat Flow and Thermal Regimes. Tectonophysics, 1985, 121, 79-85.

Kondorskaya N. V. and Shebalin N. V. (editors). New Catalogue of Strong Earthquakes in the USSR from Ancient Times through 1977. U. S. Dept. of Commerce. NOAA. USA, 1982.

Lukk A. A. et al. Mekhanizmy ochagov zemletryaseniy Sredney Azii i Kazahstana. Zemletryaseniya v SSSR v 1984 godu. Moscow, Nauka, 1987, 163-169.

Sadovsky M. A., Pisarenko V. F., Nersesov I. L. Ierarchicheskaya diskretnaya struktura litosfery i seismicheskiy process. In: Sovremennaya tektonicheskaya aktivnost' Zemli i seismichnost'. Moscow, Nauka, 1987, 182-191.

Shebalin N. V. Seismichnost' kak tektonicheskiy process. In: Sovremennaya tektonicheskaya aktivnost' Zemli i seismichnost'. Moscow, Nauka, 1987.

Shebalin N. V. Ochagi sil'nyh zemletryaseniy na territorii SSSR. Moscow, Nauka, 1974, 55.

Smirnov Y. B. Teplovoye polye territorii SSSR. Karta teplovogo potoka territorii SSSR i sopredel'nyh raionov (Scale 1:10,000,000), 1980, 150.

Tal'-Virskiy B. B. Geofizicheskiye polya i tektonika Sredney Azii, Moscow, Nedra, 271.

Zakharova A. I., Chepkunas L. S. Parametry ochagov sil'nyh zemletryaseniy mira. Zemletryaseniya v SSSR v 1984 godu. Moscow, Nauka, 1987, 155-162.

THE SEISMIC ZONES IN THE AEGEAN AND SURROUNDING AREAS

.C.Papazachos, Geophysical Laboratory, University of Thessaloniki,
Mail Box.352-1, GR 54006 Thessaloniki, GREECE

bstract

Seismic and geological data have been used to define the seismic zones and subzones (seismic sources) of the shallow as well as f the intermediate depth earthquakes in the Aegean Sea and the urrounding area. Nineteen (19) shallow seismic zones have been defined and most of these zones have been separated in two or more ubzones and in this way a total number of 36 seismic sources of hallow earthquakes have been defined. The epicenters of the intermediate depth earthquakes in southern Greece define two seismic zones, the external one (zone 1), which corresponds to the slightly ipping branch of the Benioff zone and has a high seismicity with aximum earthquake magnitude equal to about 8.0, and the internal ne, which corresponds to the branch of the Benioff zone which dips ith an angle of 38° and is of low seismicity. The high seismicity f the external branch of the Benioff zone is attributed to the oupling of the eastern Mediterranean lithosphere with the Aegean ithosphere during the subduction of the former lithosphere under he latter.

. Introduction

The solution of several important seismological problems which oncern a certain region such as the seismicity, seismic hazard, earthquake prediction, depends much on the accuracy of separation of his region in smaller subregions which are seismotectonically homogeneous (homogeneous tectonic structure, the same seismicity and ype of faulting, etc). These subregions are usually called **seismic zones** and can be further separated in smaller areas, mainly for geometrical reasons (to have simpler shapes, etc), which are usually called **seismic sources.**

Previous work on seismic zonation in the Aegean and surrounding area has been made by some seismologists (Papazachos 1980, Hatzidimitriou 1984, Hatzidimitriou et al.1985, Papazachos et al. 987). In the present paper,a further attempt is made to improve he definition of seismic zones in this area (34°N-43°N, 18°E-30°E) by the use of a vast number of published seismic data (Papazachos nd Comninakis 1982, Comninakis and Papazachos 1986) and unpublished historical seismic data (Catherine Papazachos 1988, personal ommunication) as well as other geophysical and geological information such as kind of seismic faulting (Papazachos et al.1984), seismicity rates (Papazachos 1980),b values (Hatzidimitriou et al.1985), rientation of isoseismals (Shebalin 1974, Papazachos et al.1982), rends of geological zones (Mountrakis et al.1983),etc.This seismic oning has been done separately for shallow shocks and for intermediate depth earthquakes of this region.

2. Seismic Zones of Shallow Earthquakes

According to the typical definition, shallow earthquakes are those which have a focal depth less than 60Km. However, the shallow earthquakes in the Aegean and surrounding area have usually a focal depth less than 15 Km with the exception of the earthquakes along the convex side of the Hellenic arc, where the seismogenic layer is of the order of 50Km (Karacostas 1988).

Figure (1) shows the **seismic zones** of the shallow earthquakes in the Aegean and surrounding area as well as the epicenters of the earthquakes which have been used to define these zones. Nineteen (19) seimic zones have been defined but most of them have been separated in two or more subzones (e.g.1a,1b,1c)which are considered as **seismic sources**. The total mumber of these seismic sources of shallow earthquakes is 36.

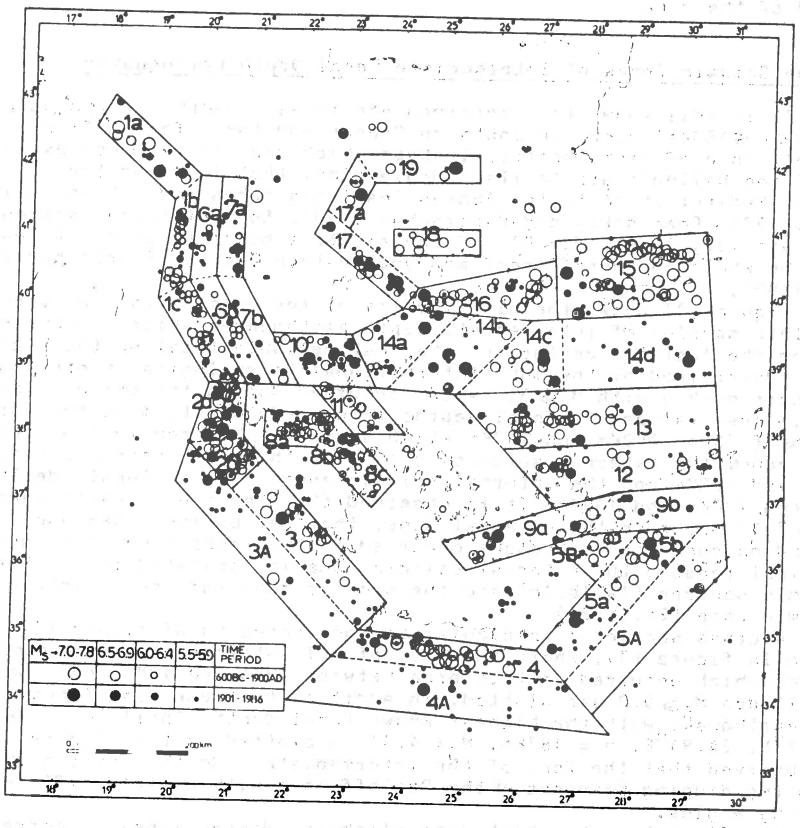

Figure 1. The nineteen (19) seismic zones (1,2,...,19) and the thirty six (36) seismic sources (1a,1b,...,19) of shallow earthquakes in the Aegean and surrounding areas.

The external seismic zones, that is, the zones 1,2,3,4,5,6,are

associated with the compressional stress field along the convex side of the Hellenic arc (Papazachos et al. 1986) and have axes (direction of maximum dimension of each zone) parallel to the external coast of the area and parallel to the strikes of the seismic faults (thrust or strike-slip) associated with the lithospheric convergence. All other seismic zones (internal zones) are dominated by normal faulting (zones 7,8,9,10,11,12,13,14d,17,18,19) or by mixed (normal and strike-slip) faulting (zones 14a,14b,15,16). Most of these zones have axes with an east-west direction but some of them have northwest-southeast (7,8b,8c,11,17) or northeast-southwest(14a, 14b,17a) directions. It seems that in all these internal zones seismic faults (normal or strike-slip) are parallel to the trends (direction of maximum dimension) of the corresponding zones with a very clear exception for zone 17 where seismic faults keep an east - west strike (Papazachos et al. 1984) which is not parallel to the trend of the zone.

3. The Seismic Zones of Intermediate Focal Depth Earthquakes

It is well known that intermediate focal depth earthquakes ($60Km \leq h \leq 180Km$) occur in southern Greece and their foci define a Benioff zone of amphitheatrical shape which dips from the convex side of the Hellenic arc to its concave side, that is, from the eastern Mediterranean to the Aegean Sea (Papazachos and Comninakis 1970, 1971, Comninakis and Papazachos 1980). Some of these earthquakes are very large ($M_S \sim 8$) and constitute a major seismic threat for the whole southern Greece and southestern Turkey (Papazachos et al. 1985).

Figure (2) shows the distribution of the epicenters of three complete samples of intermediate depth earthquakes which occurred during the last two centuries. The most reliable focal depths are those determined by the ISC (International Seismological Center) for the earthquakes with $M_S \geq 5.0$ which occurred during the period 1964-1985. These values of focal depths were used to determine the isodepths of 70Km, 100Km and 160Km which separate the area in two seismic zones: the external seismic zone (1) with focal depths between 70Km and 100Km and the internal seismic zone (2) with focal depths between 100Km and 160Km. It is observed that the big earthquakes ($M_S \geq 7.5$) occur in the external zone, that is, between 70Km and 100 Km and no such big earthquake occurred in the inner zone. For geometrical reasons the external seismic zone is separated in three seismic sources (1a,1b,1c) and the same is done for the internal seismic zone (2a,2b,2c).

A cross section perpedicular to the isodepths of figure (2) is shown in figure (3), where the foci of all intermediate depth earthquakes which occurred in this area between 1964 and 1985 and have magnitudes $M_S \geq 5.0$ are plotted. In addition to these, the focus of the earthquake with the highest known focal depth (April 10, 1976 , $37.31^{o}N$, $24.94^{o}E$, $h = 183Km$, $M_S = 4.3$) is plotted in this figure. It is observed that the foci of the intermediate depth earthquakes form two dipping branches of the Benioff zone with clearly different dipping angles.

The first branch, which dips slightly (dashed line), corresponds to the external seismic zone (1) of figure (2). In this branch, which defines the lower boundary of the seismogenic layer under the inner slope of the sedimentary part of the Hellenic arc, all big intermediate depth earthquakes have been occurred (mamixum magnitude ~ 8.0). This is probably due to the coupling in this zone, of the

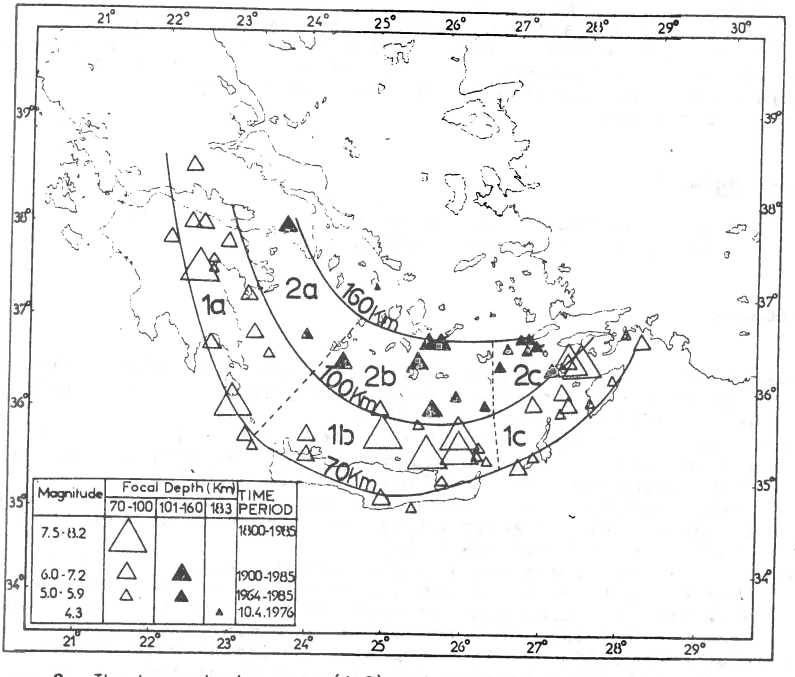

Figure 2. The two seismic zones (1,2) and the six seismic sources (1a,1b,1c, 2a,2b,2c) of intermediate focal depth earthquakes in the southern Aegean area.

eastern Mediterranean lithosphere with the Aegean lithosphere.

The second branch of the Benioff zone dips steeply and corresponds to the internal seismic zone (2) of figure (2). The straight line is the least squares' fit to the data and gives an average dip angle equal to 38° which is in good agreement with previous determinations (Papazachos and Comninakis 1971, Comninakis and Papaza-

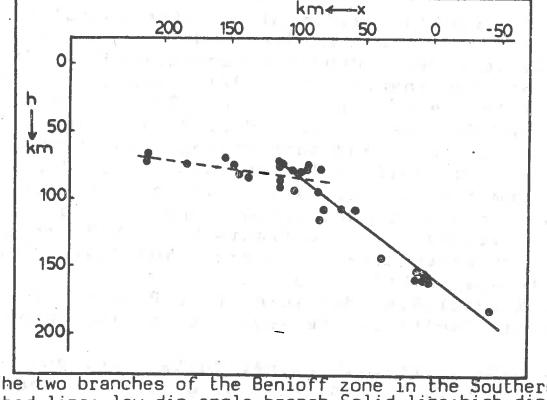

Figure 3. The two branches of the Benioff zone in the Southern Aegean area(Dashed line: low dip angle branch,Solid line:high dip angle branch).

chos 1980). This branch of the Benioff zone dips under the volcanic part of the Hellenic arc and is due to the subduction of the front part of the eastern Mediterranean lithosphere without any coupling with the Aegean lithosphere. This explains the lower seismicity in this internal zone (maximum earthquake magnitude ~7.0) in respect to the external zone.

Acknowledgement

This work has been financially supported by the Ministry of Industry, Energy and Technology (project 87AK 1).

References

Comninakis,P.E. and Papazachos,B.C.,1980. Space and time distribution of the intermediate depth earthquakes in the Hellenic arc. "Tectonophysics", 70, 35-47.

Comninakis,P.E. and Papazachos,B.C.,1986. A catalogue of earthquakes in Greece and surrounding area for the period 1901-1985 . "Publ.Geoph.Lab.,Univ.of Thessaloniki",1,pp.167.

Hatzidimitriou,P.M.,1984. Seismogenic volumes and seismic sources of the Aegean and surrounding area. "Ph.D.Thesis,Univ.Thessaloniki", pp.162 (in Greek).

Hatzidimitriou,P.M.,Papadimitriou,E.E.,Mountrakis,D.M. and Papazachos,B.C., 1985. The seismic parameter b of the frequency - magnitude relation and its association with the geological zones in the area of Greece. "Tectonophysics",120,141-151.

Karacostas,B.G.,1988. Relationship between the seismic activity and geological and geomorphological features of the Aegean and the surrounding areas. "Ph.D.Thesis,Univ.of Thessaloniki",pp. 241 (In Greek).

Mountrakis,D.,Sapountzis,E.,Kilias,A.,Elefteriadis,G. and Christophides,G., 1983. Paleogeographic conditions in the western Pelagonian margin in Greece during the initial rifting of the continental area. "Can.J.Earth.Sci.",20, 1673-1681.

Papazachos,B.C.,1980. Seismicity rates and long term earthquake prediction in the Aegean area. "Quaterniones Geodaesiae",3, 171-190.

Papazachos,B.C. and Comninakis,P.E. ,1970. Geophysical features of the Greek island arc and eastern Mediterranean."Com.Rn. des Seans de la Conference Reunie a Madrid,1969",16,74-75.

Papazachos,B.C. and Comninakis,P.E., 1971. Geophysical and tectonic features of the Aegean arc. "J.Geoph.Res.",76,8517-8533.

Papazachos,B.C. and Comninakis,P.E.,1982. A catalogue of historical earthquakes in Greece and surrounding area, 479B.C.-1900A.D. "Publ. Geoph.Lab.,Univ.of Thessaloniki",6,pp.24.

Papazachos,B.C.,Comninakis,P.E.,Hatzidimitriou,P.M.,Kiriakidis,E.C., Kiratzi,A.A.,Panagiotopoulos,D.G.,Papadimitriou,E.E.,Papaioannou,Ch.A.,Pavlides,S.B. and Tzanis,E.P.,1982. Atlas of isoseismal maps for earthquakes in Greece,1902-1981. "Publ.Geophys. Lab.Univ.Thessaloniki", 4, pp.126.

Papazachos,B.C.,Kiratzi,A.A.,Hatzidimitriou,P.M. and Rocca,A.Ch., 1984. Seismic faults in the Aegean area."Tectonophysics",106, 71-75.

Papazachos,B.C.,Papadimitriou,E.E.,Karacostas,B.G. and Karakaisis , G.F.,1985. Long term prediction of great intermediate depth

earthquakes in Greece. "Proc.12th Regional Seminar on Earthq. Engineering,EAEE-EPPO, Halkidiki-Greece,September 1985",1-12.

Papazachos,B.C.,Kiratzi,A.A.,Hatzidimitriou,P.M. and Karacostas, B. G., 1986. Seismotectonic properties of the Aegean area that restrict valid geodynamic models. "Wegener/Medlas Conference, Athens, May 14-16, 1986", 1-15.

Papazachos,B.C.,Hatzidimitriou,P.M. and Karacostas, B.G.,1987. Seismic fracture zones in the Aegean and surrounding area."Boll. Geof.Teor.Appl.", 113, 75-83.

Shebalin,N.V. (editor), 1974. Atlas of isoseismal maps, part III of the catalogue. "UNESCO, Skopje", pp.275.

A.I.Zakharova, O.E.Starovoit, I.P.Gabsatarova, F.L.Yakovlev
Inst. of Physics of the Earth, Acad. of Sciences U.S.S.R.

SOME PECULIARITIES OF THE NORTH CAUCASUS REGION SEISMICITY

1. Introduction

The North Caucasus region is a large area - about three hundred thousand square kilometers in the south-western part of Russia between the Black and Caspian Seas. This region is geologically located on the border of two great structures - the Skifth plate on the north and Greater Caucasus on the south. Tectonic activity of the Greater Caucasus is expressed by uplifting of the mountainous part of the region and other phenomena - tectonic fault development, seismic activity and post-magmatic mineral water sources.

The analysis of this region seismicity allowed us to separate some peculiarities of it. In this paper we make an attempt to explain them by a blocked structure of the crust (Sadovski et al, 1987).

2. The space distribution of earthquake sources

Strong earthquakes have been known here for a long time. There is a map of epicenters of earthquakes (Fig.1). Strong earthquakes have been known here from the seventeenth century, weak ones - from 1932 up to 1986. One can see that the epicenter distribution is heterogeneous, it is possible to distinguish some epicentral zones: Dagestan, Groznyi, North Osetia, Sochi, Mineral Waters, Anapa, Low Kuban, Upper Kuban. In this map (Fig.1) there are some large territories where earthquake epicenters are missing. In all these zones seismic activity exists during the whole examined period of time. It is possible to distinguish similar area distribution of earthquake epicenters within each zone, for example within the Mineral Waters zone (Fig.1). Detailed observations of seismicity of this zone during the period of 1983 to 1987 have revealed many weak earthquakes with class energy K= 5 - 9. These earthquakes are concentrated along the great tectonic faults. There are some areas where epicenters are missing between these faults.

3. Velocity structures and reccurence graphs of earthquakes

Let us compare two different epicentral zones with sufficient statistics of seismic data - Mineral Waters zone and Groznyi (Fig.2). During the process of hypocenter localization using the computer program Hypo-71 we saw that optimum solutions existed for these zones applying different velocity structures. (Table 1). Both structures have 5 layers with near thickness - 43 and 44 km, but the structure of Mineral Waters zone differs from Groznyi zone in thicness of every layer and in average velocity of P-waves from them (Krasnopevtseva G.V., 1984). Using the usual structure for every zone we get the least travel time deviation, compared with any

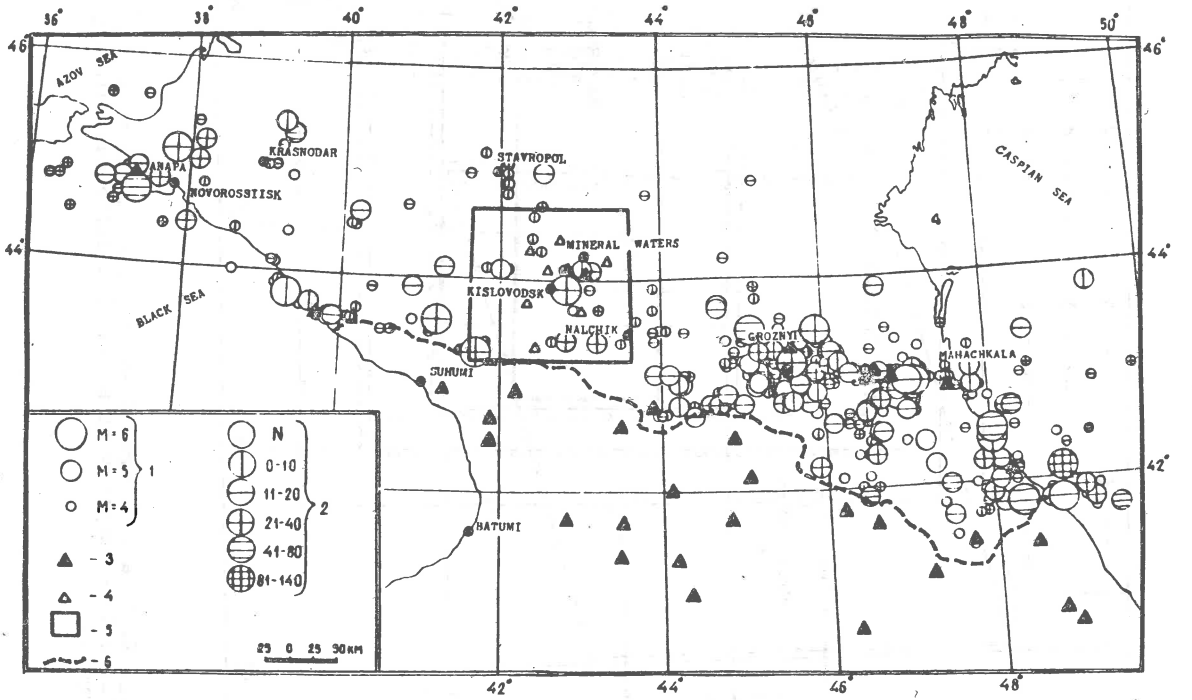

Fig. 1. Epicenter map of North Caucasus: 1 - magnitudes; 2 - depths, km (N - Earth's crust); seismic stations - 3- standard, 4 - field; 5- Caucasus Mineral Waters testground; 6 - Russia's boundary.

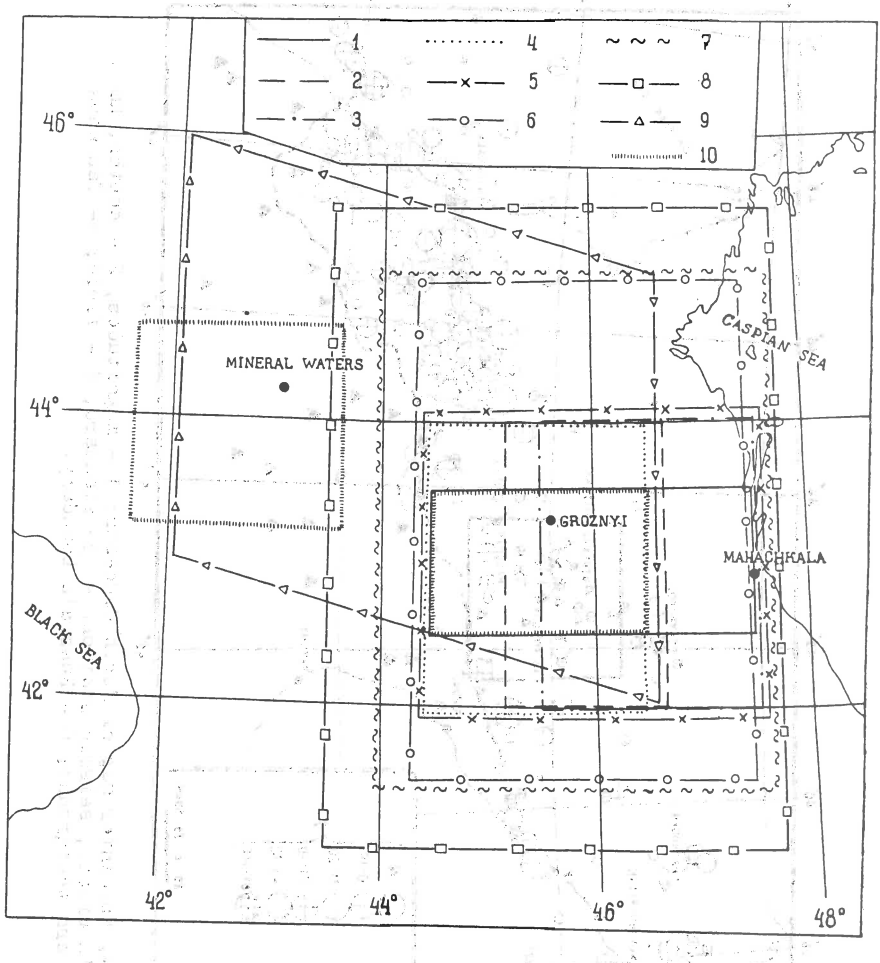

Fig. 2. Area contours (1 -9) for the homogeneous block separation; 10 - boundary of areas with different velocity structures.

VELOCITY STRUCTURES TABLE 1

Mineral Waters zone			Groznyi zone			
Layer	H km	Vp km S^{-1}	Layer	H km	Vp km S^{-1}	Comment
1	0.5	3.2	1	3.3	3.2	
2	15	5.9	2	13	5.3	
3	24	6.0	3	22	6.0	crust
4	29	6.4	4	32	6.5	layers
5	44	7.0	5	43	7.0	
6		8.1	6		8.1	upper mantle

other structure. In Fig.3 the reccurence graphs of earthquakes for Mineral Waters and Groznyi zones are shown. For these graphs calculation of the data on seismic observations for the period of 1975 to 1984 with magnitudes $M \geq 3$ were used. Additionally for Mineral Waters zone detaled observation data for the period of 1983 to 1987 with magnitude $M \geq 1.6$ were used. The graph slopes are different, it means that the reccurence of earthquakes of the same magnitude is different too. For example, earthquakes with magnitude of 4 according to the first graph are repeated every 6 years, but as to the second graph - every year. As the two

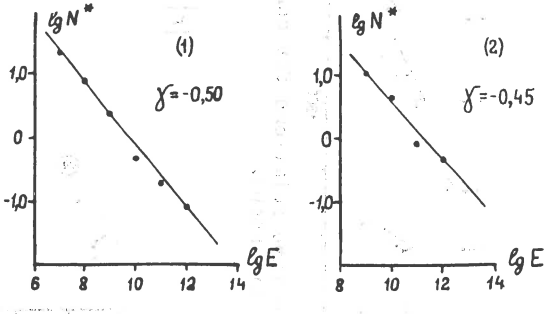

Fig. 3. Energy - frequency relationship for Mineral Waters (1) and Groznyi zones (2)

zones which have been considered here are different in seismic regim parameters ($M_{max}=5.5$, $\gamma=0.50$ in the first zone and $M_{max}=6.5$, $\gamma=0.45$ in the second one) we can suppose that these zones belong to different blocks of the crust.

4. Separation of the homogeneous block area

In Fig.2 different numbers N 1 to 9 denote contour areas around Groznyi zone. For these areas graph of earthquake magnitude - time was constructed. For example, these graphs are shown for contours 2 and 6 in Fig.4 . For these graphs instrumental and macroseismic data were used. The lines drawn round the most strong earthquakes have different inclinations in different time intervals. There is strong inclination during short intervals of

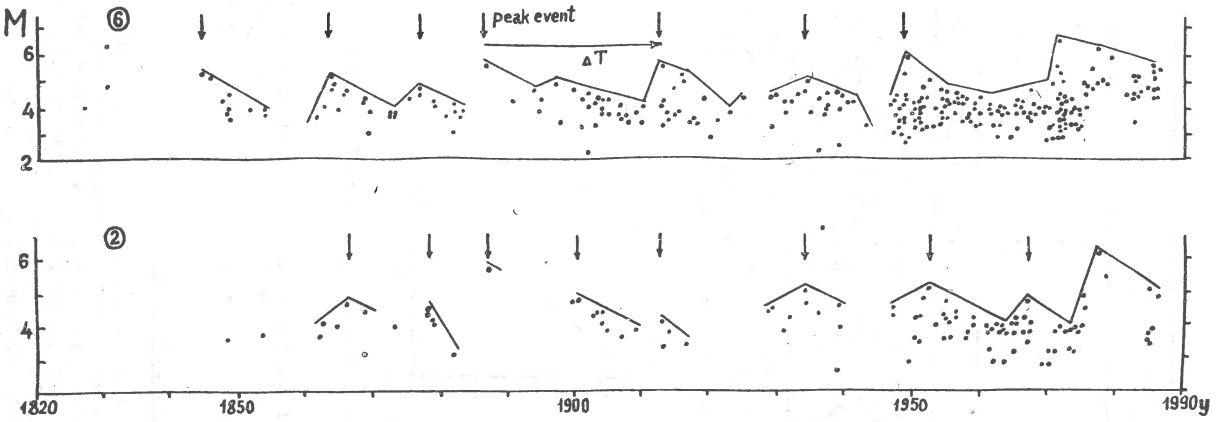

Fig. 4. Magnitude - time relations for contours 2 and 6. The peak events and reccurence interval are shown.

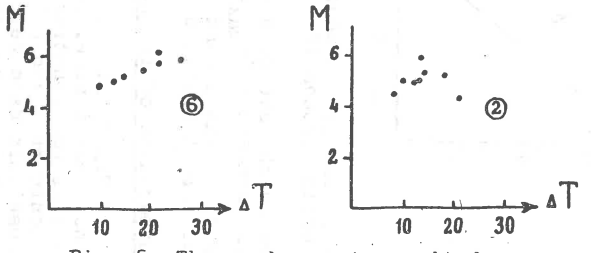

Fig. 5. The peak event magnitude - reccurence interval relation for contour 2 and 6.

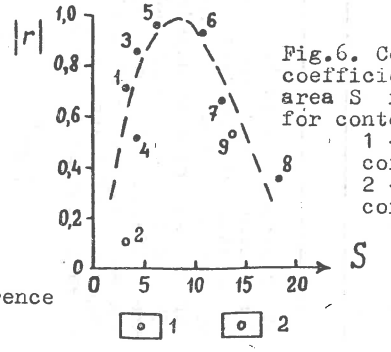

Fig.6. Correlation coefficient r - area S relation for contours NN1-9: 1 - positive correlation; 2 - negative correlation.

magnitude increasing and weak inclination during long intervals of the magnitude decreasing. It is possible to notice short intervals with absence of seismic activity and 6 to 9 peak events on every graph. The time interval ΔT from the first peak event up to the second one is dependent on the first event magnitude M. The M - ΔT dependence for 2, 6 contours are shown in Fig.5 . The correlation coefficients r between M and ΔT are equal to 0.85 - 0.96 for contours MM 3,5,6 and for other contours from -0.45 to 0.66 . The largest value of $r = 0.96$ corresponds to the 5-th contour with Groznyi and Makhachkala seismic zones taken together. The dependence of correlation coefficients - contoured areas is shown in Fig.6 . The optimum value of correlation coefficient corresponds to the area of ~ 9 square degrees ($3° \times 3°$). During decreasing or increasing of this contoured area the value of r only decreases.

This phenomenon can be explained by insufficient number of earthquakes in case of a small area and aggravative influence of seismic blocks around, which have different seismic regimes in case of a large area.

Thus, we can conclude that a homogeneous seismic block has the area of approximately of $3° \times 3°$ and consists of Groznyi and Makhachkala seismic zones.

6. Conclusions

Detailed study of the Northern Caucasus earthquakes in space and time allowed us to see the following peculiarities of its seismicity:

1. The space distribution of strong and weak earthquakes is heterogenic - their sources are formed epicentral zones divided by "empty" areas.
2. These zones differ in earthquake intensities on the earth surface with magnitude - frequency relations, with the level of maximal magnitudes and velocity structures. We think that these zones correspond to different blocks of the Earth's crust.
3. It is possible to separate the optimal dimensions of such homogeneous block using the magnitude - time relation.
4. The methodology considered may be used for the process of seismic zoning.

References

1. Sadovski M.A., Bolhovitinov L.G., Pisarenko V.F., Deformirovanie geophizicheskoj sredy i seismicheskij protses. Moskva, Nauka, 1987.
2. Krasnopevtseva G.V. Glubinnoe stroenie Kavkazskogo seismoactivnogo regiona. Moskva, Nauka, 1984.

RECURRENCE MODELS FOR INTERMEDIATE EARTHQUAKES OF VRANCEA REGION

C. Radu, Victoria Oancea
Center of Earth Physics and Seismology, P.O.Box MG-2,
Bucharest, Romania

INTRODUCTION

The Vrancea intermediate earthquakes are concentrated in a small zone (size 95×60 Km^2), with central coordinates φ = 45.7°N, λ = 26.6°E, at depths of 60 - 200 Km. It was noticed that the large events from this region present a regularity in their occurrence.

It is possible to represent the series of large earthquakes occurring at rather regular intervals by a renewal process, described by a certain distribution w(T) of the time interval T between successive events (Utsu, 1984).

The aim of this paper is to estimate the parameters of different recurrence models for Vrancea intermediate earthquakes and to choose the best suited model for the analysed data. Four distributions (Weibull, lognormal, exponential probability and gamma) were tested on some series of large intermediate events from Vrancea region.

PRESENTATION OF THE MODELS

For the description of strong earthquake recurrence, different models were proposed (Utsu, 1984). In our study, four models for the recurrence of large Vrancea intermediate earthquakes were used and compared: Weibull, lognormal, exponential probability and gamma.

The following functions are used for describing the models:

w(T) = density for the distribution of T;

$\phi(t)$ = probability that the next earthquake will occur at a time later than t;

$\mu(t)\,dt$ = probability that the next earthquake will occur during the time interval (t, t+dt);

$p(\tau/t)$ = conditional probability that the next earthquake will occur during the time interval (t, t+τ),

where: t = time measured from the origin time of the last earthquake, T = the time interval between successive events.

The relations conecting these functions are the following:

$$w(T) = \mu(T)\phi(T) \tag{1}$$

$$\phi(t) = \exp\left\{-\int_0^t \mu(t)\,dt\right\} = \int_t^\infty w(T)\,dT \tag{2}$$

$$p(\tau/t) = 1 - \exp\left\{-\int_t^{t+\tau} \mu(t)\,dt\right\} = 1 - \frac{\phi(t+\tau)}{\phi(t)} \tag{3}$$

For the proposed distributions, the corresponding functions w(T), $\phi(t)$, $\mu(t)$ and $p(\tau/t)$ are described by the following equations:

- Weibull model ($\alpha>0$, $\beta>0$):

$$w(T) = \alpha\beta T^{\beta-1}\exp(-\alpha T^{\beta}) \tag{4}$$

$$\phi(t) = \exp(-\alpha t^{\beta}) \tag{5}$$

$$\mu(t) = \alpha\beta t^{\beta-1} \tag{6}$$

$$p(\tau/t) = 1 - \exp\left\{-\alpha\left[(t+\tau)^{\beta} - t^{\beta}\right]\right\} \tag{7}$$

- Lognormal model ($m > 0$, $\sigma > 0$):

$$w(T) = \frac{1}{\sqrt{2\pi}\,\sigma T}\exp\left[-\frac{(\ln T - m)^2}{2\sigma^2}\right] \tag{8}$$

$$\phi(t) = 1 - \Phi\left(\frac{\ln t - m}{\sigma}\right) \tag{9}$$

$$\mu(t) = \frac{1}{\sqrt{2\pi}\,\sigma t}\exp\left[-\frac{(\ln t - m)^2}{2\sigma^2}\right]\Big/\left[1 - \Phi\left(\frac{\ln t - m}{\sigma}\right)\right] \tag{10}$$

$$p(\tau/t) = 1 - \left[1 - \Phi\left(\frac{\ln(t+\tau) - m}{\sigma}\right)\right]\Big/\left[1 - \Phi\left(\frac{\ln t - m}{\sigma}\right)\right] \tag{11}$$

- Exponential probability model ($a > 0$):

$$w(T) = a\exp\left[\frac{a}{b}\left(1 - e^{bT}\right) + bT\right] \tag{12}$$

$$\phi(t) = \exp\left[\frac{a}{b}\left(1 - e^{bt}\right)\right] \tag{13}$$

$$\mu(t) = a\,e^{bt} \tag{14}$$

$$p(\tau/t) = 1 - \exp\left[\frac{a}{b}e^{bt}\left(1 - e^{b\tau}\right)\right] \tag{15}$$

- Gamma model ($c > 0$, $r > 0$):

$$w(T) = \frac{c}{\Gamma(r)}(cT)^{r-1}e^{-cT} \tag{16}$$

$$\phi(t) = \frac{\Gamma(r,ct)}{\Gamma(r)} \tag{17}$$

$$\mu(t) = \frac{c^r t^{r-1} e^{-ct}}{\Gamma(r,ct)} \tag{18}$$

$$p(\tau/t) = 1 - \frac{\Gamma(r,c(t+\tau))}{\Gamma(r,ct)} \tag{19}$$

where the gamma functions are defined :

$$\Gamma(y) = \int_0^{\infty} e^{-u}\,u^{y-1}\,du \tag{20}$$

$$\Gamma(y,x) = \int_x^{\infty} e^{-u}\,u^{y-1}\,du \tag{21}$$

Referring to the model parameters, we note that for their particular values $\beta = 1$ (for Weibull), $b = 0$ (for exponential probability) and $r = 1$ (for gamma) lead to the Poisson process, which is a special case of these models (considering the occurrence time of the earthquakes as aleatory).

OBSERVATIONAL DATA

For the analysis of the recurrence of strong Vrancea intermediate earthquakes, 11 data sets were used. Table 1 lists the analysed data sets, presenting the time period to which the events belong, their number and the intervals of magnitude and maximum intensity. We note that the pairs of sets I-II and respectively III-IV represent the same two series of earthquakes, the only difference being the presence or absence of the aftershocks following some major earthquakes. Two groups of sets: VI-VII and VIII-XI include earthquakes in the same two domains of magnitude, the difference consisting in the extent of the time period.

In all the data sets, the time between successive events was expressed in years, as time unit.

Table 1 - The analysed data sets

Data set	Time period	N	M interval	I_o interval	Remarks
I	1935-1988	59	5.0-7.4	5.0-9.0	
II	1935-1988	55	5.0-7.4	5.0-9.0	Without aftershocks of November 10, 1940 earthquake
III	1901-1988	33	5.5-7.4	6.0-9.0	
IV	1901-1988	31	5.5-7.4	6.0-9.0	Without aftershocks of May 25, 1912 and November 10, 1940 earthquakes
V	1801-1988	16	6.0-7.5	7.0-9.0	
VI	1601-1988	15	6.4-7.5	7.5-9.0	
VII	1701-1988	10	6.4-7.5	7.5-9.0	
VIII	1401-1988	17	6.8-7.5	8.0-9.0	
IX	1501-1988	15	6.8-7.5	8.0-9.0	
X	1601-1988	11	6.8-7.5	8.0-9.0	
XI	1701-1988	6	6.8-7.5	8.0-9.0	

The magnitude M was computed using the following relation:

$$M = 0.56\ I_o + 2.18 \qquad (22)$$

DATA ANALYSIS

For the estimation of the parameters of the theoretical distributions, two methods were used: the method of moments (MM) and the maximum likelihood method (MLM).

The method of moments (MM), based on the identification between the first empirical moments and the corresponding moments of each theoretical distribution, demands only the mean and the variance computation (the first and the second moments) for the used biparametric models and leads to simple sets of two equations (Radu and Oancea, 1988). For the exponential probability model, this method is not easily applied.

The maximum likelihood method (MLM) is based on the determination of the parameters which assure the maximum of the likelihood function. It is applied for all the proposed models and leads to sets of equations numerically solved (Radu and Oancea, 1988).

The empirical probabilities are also determined:

$$p_e^i = \frac{i}{N+1} \tag{23}$$

where i = 1,..., N counts the events ordered by the decreasing T_i values.

Table 2 includes the values obtained for the parameters of the four proposed models, using the two estimation methods (MM and MLM), for the first data set. The values obtained for the logarithm of the likelihood function (lnL) and the sum of square deviations (SSD), defined as:

$$L = \prod_{i=1}^{N} w(T_i) \tag{24}$$

$$SSD = \sum_{i=1}^{N} [\phi(t_i) - p_e(t_i)]^2 \tag{25}$$

are also included in Table 2. They are used for choosing the best set of parameters for every model (by one of the estimation methods), as corresponding to the maximum of lnL and the minimum of SSD values. We note that for the great majority of the situations, MLM offers the best parameter set.

Table 2 - Model parameters for data set I

Model		Method for parameter estimation	
		MM	MLM
Weibull		1.202	1.207
		0.807	0.789
	lnL	-49.499	-49.458
	SSD	0.078	0.081
Lognormal	m	0.580	1.006
		0.971	1.728
	lnL	-86.549	-56.640
	SSD	0.410	0.611
Exponential probability	a		1.114
	b		4.495×10^{-5}
	lnL		-43.829
	SSD		0.103
Gamma	r	0.717	0.678
	c	0.799	0.756
	lnL	-49.189	-49.120
	SSD	0.519	0.165
Mean interval		0.90 yr	
Standard deviation		1.12 yr	

RESULTS

The occurrence probabilities $\phi(t)$ defined by the formulas (5), (9),(13) and (17) are computed for every model, using the best parameter sets.

The probability curves $1 - \phi(t)$ are plotted for each data set, together with the empirical probabilities $1 - p_e(t)$. Figs. 1 and 2 present the curves $1 - \phi(t)$ obtained for the most convenient theoretical models for the data sets I and VIII. The level of the concordance between the gamma distribution and our data is below the statistical significance level of 95%.

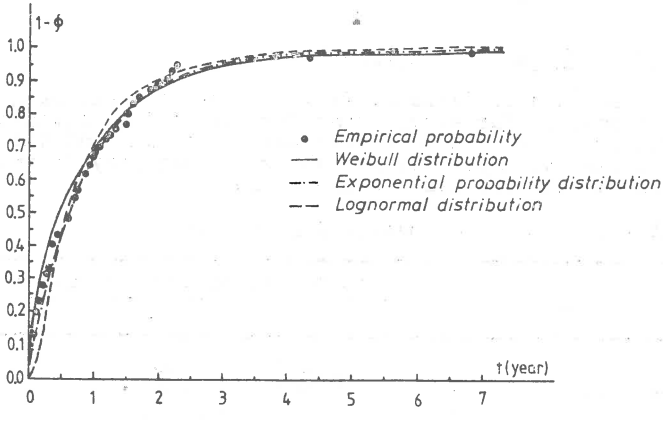

Fig. 1 - The theoretical probability curves $1 - \phi(t)$ and the empirical probabilities $1 - p_e(t)$ for the data set I.

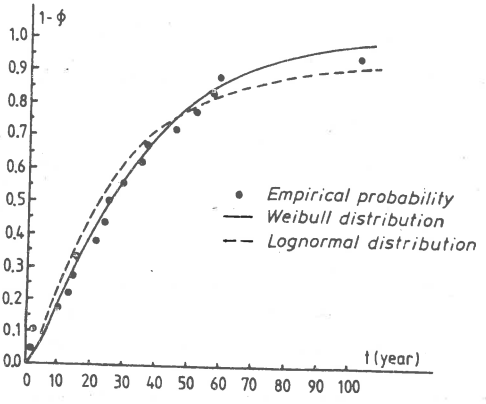

Fig. 2 - The theoretical probability curves $1 - \phi(t)$ and the empirical probabilities $1 - p_e(t)$ for the data set VIII.

By a visual analysis it is difficult to conclude which model offers the best fit for the empirical data. In order to decide on the most adequate model, the values of lnL and SSD are compared for each data set. In addition, for checking the concordance between the empirical data and each theoretical distribution, the Smirnov-Kolmogorov test is applied, for the first four data sets, which include a greater number of T_i values in the corresponding series.

The result obtained taking into account all these criteria, is that the Weibull and the exponential probability models are best suited for the first four data sets (including earthquakes with $M \geq 5.0$ and $M \geq 5.5$) and the Weibull and the lognormal models give best results for the other data sets (including earthquakes with $M \geq 6.0$, $M \geq 6.4$ and $M \geq 6.8$).

Following the formulas (7), (11), (15) and (19), the conditional probabilities $p(\tau/t)$ are computed for the proposed models, for different pairs of t and τ values. Table 3 presents the results obtained for the data set I, using the Weibull model.

Table 3 - The conditional probabilities $p(\tau/t)$ for the data set I, using the Weibull model.

τ \ t	0	20	40	60	80	100 yr
20	0.429	0.498	0.537	0.546	0.560	0.571
40	0.713	0.762	0.785	0.800	0.811	0.820
60	0.804	0.892	0.905	0.914	0.921	0.926
80	0.938	0.952	0.959	0.964	0.967	0.970
100 yr	0.973	0.980	0.983	0.985	0.987	0.988

CONCLUSIONS

The analysis of four theoretical renewal models, applied to different series of large Vrancea intermediate earthquakes, leads to the conclusion that the best suited model for describing the recurrence of the studied events is the Weibull model, followed by the exponential probability model in some cases, or the lognormal model, in other cases.

Taking into account the significance of the β parameter of the Weibull model ($\beta < 1$ - clustering in time, $\beta = 1$ - Poisson process, $\beta > 1$ - intermittent occurrence), we note that the earthquakes with $M \geq 5.0$ and $M \geq 5.5$ present a tendency of clustering, but the events with $M \geq 6.0$ and especially those with $M \geq 6.4$ and $M \geq 6.8$ present a tendency of intermittent occurrence.

REFERENCES

Radu C. and V. Oancea (1988). Recurrence models for Vrancea intermediate earthquakes. Part I. Internal Report, theme 30.86.3/1988, I, A5, 15p. (in Romanian).

Utsu T. (1984). Estimation of parameters for recurrence models of earthquakes. Bull. Earthq. Res. Inst., Univ. of Tokyo, 59, 53-66.

UNKNOWN CATASTROPHIC EARTHQUAKES ON THE EASTERN BLACK SEA COAST: AN EXPERIENCE IN ARCHEOSEISMIC RECONSTRUCTION

A.A.NIKONOV

Institute of Physics of the Earth, Acad. Sci., Moscow 123810, USSR

ABSTRACT

Sings of some destructive seismic events within I, IV, VII,XI and XVIII centuries were revealed using archeoseismic inspections of historical stone monuments of the region under consideration. The new available data make the author to consider the East segment of the Black Sea coast as an area of destructive earthquakes as strong as maximum intensity up to 9 and with possible recurrence interval about 300-700 years.

FORMULATION OF THE PROBLEM IN THE REGIONAL ASPECT

During the last century two highly damaging earthquakes have occured on the Black Sea coast, one in Bulgaria in 1901 (Vatsov, 1903) and the other in the Crimea in 1927 (The Black Sea..,1928). Written records also mention damaging earthquakes of the 2nd or 1st century B.C. and 543 A.D. near Kaliakra Promontory in western Black Sea coast area, as well as that of 63 B.C. on the coast of the Straits of Kerch. There is no evidence on similar seismic events in the eastern Black Sea coast area. The earthquake of 1905, the largest for the 150-yr period, has intensity of VII at most, while its epicentral zone has not been located with a passable reliability (New Catalog..., 1977). The well-known Chkhalti intensity IX, earthquake of 1963 took place in the axial zone of the Greater Caucasian Range and was not associated with the Black Sea Basin structure.

The study of large Black-Sea earthquakes thus raises the question whether the low seismicity and absence of damaging earthquakes in the eastern Black Sea coastal area is indicative of a low earthquake potential of the region or merely reflects our imperfect knowledge of past earthquakes. Many studies in the Caucasus and the map of seismic zoning for the USSR (Map..., 1984) has reflected and fixed the notion of low seismicity in the eastern Black Sea coastal area (intensity VI and VII).

Recently, however, it has been established by studies in a number of areas that periods of instrumental observation as long as 100 or 200 years are still inadequate for reliable inference as to earthquake potential, M_{max}, and recurrence of great earthquake that could provide an estimate of earthquake hazard for a region which would be close to reality. It is true for the Caucasus too (Nikonov, 1987).

For this reason the author have tried to employ an archeoseismic method for reconstruction of earthquakes occured in the past. While written sources are scarce and fragmentary that have relation to the history of the eastern Black Sea coastal area, remain of architectural structures and archeological materials of different epochs are, on the contrary, rather numerous. This is especially true as regards the Colchis, where traces of life and construction activities of many peoples have been preseved (with varying degrees, it is true) for the past 2.500 years.

The methodologies and techniques for identifying past earth-

quakes from ancient architecture and archeological data are presented by the author elsewhere (Nikonov, 1988). We will just mention that the archeoseismic method can detect and identify the traces of great, catastrophic, earthquakes of intensity at least VIII, usually IX.

GENERAL DESCRIPTION OF THE STUDY

A systematic investigation and examination of architectural remains and structural frameworks discovered by means of archeological excavation has been carried out by us within the Colchis. Numerous monuments of stone construction are to be found there beginning from the 5th century B.C. until the late Middle Ages. A careful examination shows traces of past damaging earthquakes on most of them in the shape of collapse and fall of large structures, declinations and departures from the original connections and inclinations of structural elements, deformation and cracking in the walls, floors, foundations. The presence of typical signs of just seismic shock excitation and regular spatial patterns of damage for each monument, frequently independently of ground conditions and the geomorphic position of the monument, allow in most cases a sufficiently reliable identification of the deformation as earthquake-related. The architectural monuments scatterred over the area notably bear traces of damage (collapse) that took place during the same intervals of time (to within a century). Structures in the Colchis show traces of strong seismic excitation in the 1st, 4th, 7th, 11th, and 18th centuries. Naturally enough, the number of monuments bearing the traces of later damage is greater than of earlier ones, the traces themselves being more numerous and better defined. One can note in a number of cases that damages of one and the same time become weaker (or less well-defined) as far as moving away from the seaside.

In order to identify the traces of earthquake excitation(damage) more reliably and to try to outline the epicentral areas of earthquakes detected there, we have used the technique of pinpointing the radiation region on the basis of seismic wave arrival direction. With this end in view, we recorded and systematized, for each monument, the orientations of fall, inclination of structures, architectural elements and objects, cracks and deformations that were produced at that time.

ON THE AZIMUTHAL TECHNIQUE FOR LOCATING EPICENTRAL AREAS

Data on the direction of the main seismic shock or the arrival direction of seismic waves based on the damage and collapse of structures and the sensations reported by the population were used to locate the epicentral area as early as the late 19th - early 20th century by the well-known Russian scientists I.V.Mushketov, M.M.Bronnikov, V.N.Weber and others.

Later, however, as instrumental seismology began to be developed, that technique became nearly obsolete in relation to current seismic events.

As to the analysis of materials for older earthquakes,including those that have left their imprints on past architectural monuments, the use of the above technique for locating epicentral areas remains valid. Indeed, in the absence of other potentialities, the technique turns out to be the only possibility, nearly, and for that reason should by all means be developed. Attempts to

use this technique reported in the scientific literature of this country are rare (Konkov, 1970; Nikonov et al., 1983). A.A.Konkov has called the technique the "azimuthal technique for locating the area of maximum felt intensity". When dealing with relatively recent earthquakes, use is commonly made of reports of witnesses about the direction of rumble and first motion. In application to ancient architectural monuments, we naturally have to restrict ourselves to the tangible traces of earthquake excitation of constructions and structural elements.

The direction of wave arrival can be determined from the dominant direction of fall, inclination, displacement, bulging, throwing away of structural elements or objects, and from the dominant orientation of walls and structures damaged.

One can hardly expect great accuracy in epicentre determining by this technique, but the epicentral area can be outlined. Inaccuracies and discrepancies are possible in determining the arrival directions of seismic waves on the basis of the above evidence owing to: (a) inaccuracies in the determination of arrival direction based on, say, cardinal points rather than on compass points, (b) dominant strike of structures not perpendicularly to the direction of the seismic shock, (c) determination of the direction at different sites for shocks that had taken place at different times and for different waves (P and S) of the same shock, (d) local distortion of arrival directions due to the reflection from local features, relief elements and other local conditions, possibly of wave interference.

Determination of the true direction of shocks in the oscillation plane (along wave propagation or backwards) is also not always reliable.

The difficulties and uncertainties indicated above do not however prevent the technique from being used to determine the dominant and consistent arrival directions based on observations at many sites and at several points of the same site.

The best criterion for the applicability of this technique is to examine it for large earthquakes of the instrumental and pre-instrumental period. A number of fairly consistent determinations of the epicentre (epicentral area) based on macroseismic data and azimuthal determinations of wave propagation were given by A.A. Konkov (1970) and the author (Nikonov and Popova, 1983; Nikonov et al., 1983) for earthquakes of different magnitudes (and within a wide time interval) in Soviet Central Asia.

As to ancient European earthquakes, we refer to the Mor earthquake of 1810 in Hungary in which the epicentral area is clearly outlined by azimuths of waves arriving at different sites. A number of examples could be adduced for the Caucasus.

The examples considered, including cases where independent methods, including instrumental ones, yield consistent determinations of the epicentral area, justify the use of this technique also in archeoseismic research. When consistent results have been obtained, the technique of azimuthal convergence can give the necessary information on the location of epicentral areas of older earthquakes that are not provided with other basic data.

REGIONAL RESULTS IN THE EASTERN BLACK SEA COASTAL AREA

Figures 1 a-d present summaries of factual information on the azimuths of seismic wave propagation determined from the directions of damage in the architectural monuments of the relevant time period.

These data are classified by the distinctness of deformation and by how far the conclusions about arrivals are reliable. Heavy-drawn signs show the more reliable data points and conclusions. It is supposed in all cases that seismic waves went from sea towards land, this being corroborated by a radial propagation of directions from sea towards land areas.

For each century, with damage and collapse discernible in architectural remains, one can clearly distinguish a general consistency in the directions at different sites; this allows one to use their points of intersection for outlining areas that emitted the vibrations (heavy lines denote more reliable data, light ones are for less reliable information). Since there are more monuments survived from the Middle Ages compared with the antiquity, this naturally provides better knowledge of the epicentral areas of later earthquakes. The traces of earthquakes of the 1st and 3-4th centuries A.D. have been specially studied by us in the well-known fragments of Dioscuria and Sebastopolis in the present-day Bay of Sukhumi. The result was to corroborate the fact of catastrophic earthquakes of this time with the sources lying in all probability under the bottom of the Bay.

All the available evidence is thus consistent in indicating the repeated occurence of very large (at least intensity VIII) earthquakes during the past 2.000 years in the shelf of the eastern Black Sea which strongly shook the extensive coastal areas of the Colchis.

The epicentral areas of ancient large earthquakes in the Colchis as recovered by the above technique are located in the eastern Black Sea shelf striking along the coast, that is, in the northwestern direction (Figure 2).

These data lead to the conclusion that the eastern Black Sea coastal area is an area of damaging intensity IX earthquakes with a possible recurrence period of 300-700 years, in spite of the fact that no such events have been recorded there since the early 19th century.

The existing concepts of this area being safe from earthquake hazard as reflected in the map of seismic zoning for the USSR (Map..., 1984) by denoting the eastern coast of the Black Sea as an area of intensity VI and VII at most seem to need revision.

These new possibilities for recovering past earthquakes from archeoseismic data open invaluable perspectives in the identification and refinement of the trends in regional seismicity and the overall earthquake hazard.

REFERENCES

Konkov A.A., 1970. Localization of earthquake pleistoseismic areas by the azimuthal method. - In: Strong earthquakes in Soviet Central Asia and Kazakhstan, I. Dushanbe, "Donish" Publ. House, pp. 152-177 (In Russian).

Map of seismic zoning of the USSR, 1984. Scale: 1:5 mln. With an explanatory text. Moscow, "Nauka" Publ. House (In Russian).

New Catalog of strong earthquakes in the USSR from ancient times through 1977; 1982. World Data Center A from Solid Earth Geophysics, Report SE-3. Ed. by N.V.Kondorskaya and N.V. Shebalin. Boulder, 608 p.

Nikonov A.A., 1987. The strongest historic earthquakes in the Caucasus. - Bolletino di Geofisica Teorica ed Applicata,vol. XXIX, n 116, pp. 333-339.

Nikonov A.A., 1988. On the methodology of archeoseismic research on historical monuments. - In: Proc. of Intern. Symp. on engineering geology of ancient works, monuments and historical sites, vol. 3. Rotterdam, pp. 1315-1320.

Nikonov A.A., Popova E.V., 1983. Garm earthquake of 1941: macroseismics, surface disturbances, source. - In: Problems of engineering seismology, 24. Moscow, "Nauka" Publ. House, pp. 111-129 (In Russian).

Nikonov A.A., Vakov A.V., Veselov I.A., 1983. Seismotectonics and earthquakes of the Pamirs - Tien Shan convergence zone. Moscow, "Nauka" Publ. House, 240 p. (In Russian).

The Black Sea earthquake of 1927 and fates of the Crimea, 1928. Simferopol, 113 p. (In Russian).

Vatsov S., 1903. Earthquakes in Bulgaria. Sofia, 46 p. (In Bulgarian).

CAPTIONS

Figure 1. Epicentral areas of strong past earthquakes on the eastern Black Sea coast: reconstruction based on the directions of seismic effects on architectural and archeological monuments (azimuthal technique) Arrows show arrival directions. Land is shaded. Heavy lines denote more reliable determinations, light ones are for less reliable information. a - III-IV Cent. A.D., b - second half of VII Cent. A.D., c - XI Cent. A.D., d - XVIII Cent. A.D.

Figure 2. General scheme of epicentral areas of strong past earthquakes on the eastern Black Sea coast, reconstructed by archeoseismic method. Heavy lines denote more reliable determinations, light ones are for less reliable information.

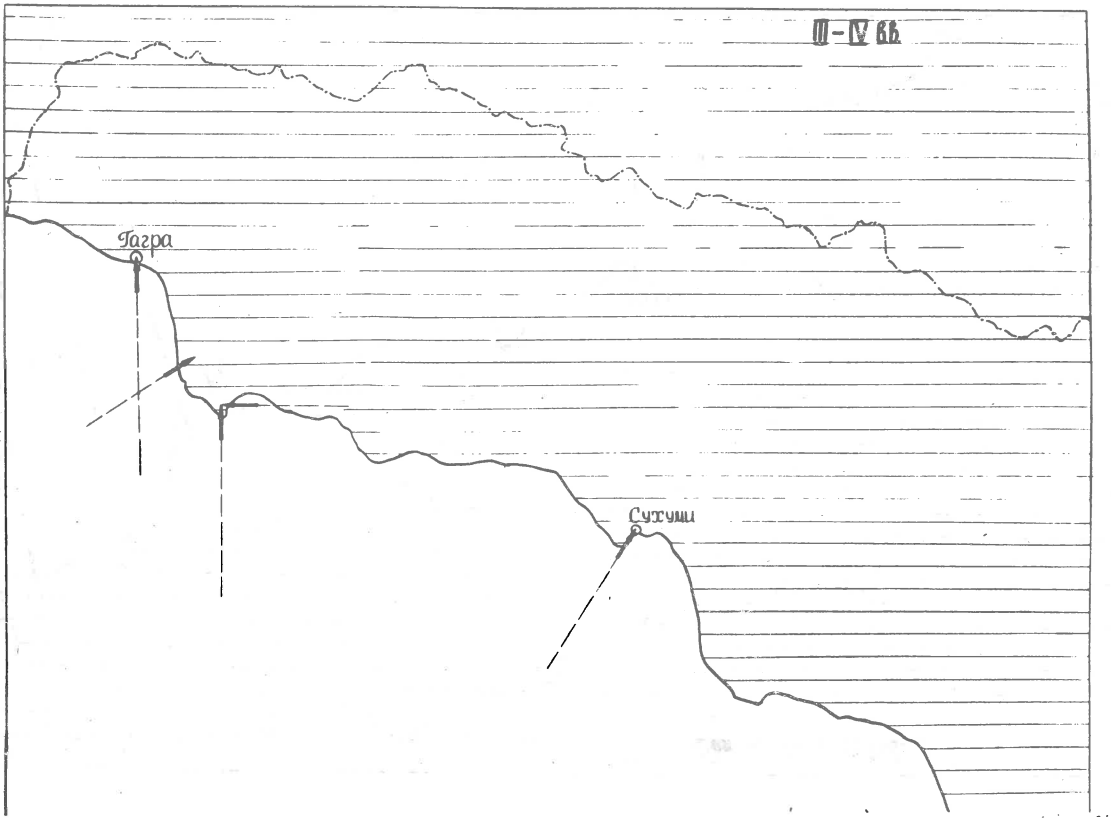
III – IV вв.
Гагра
Сухуми

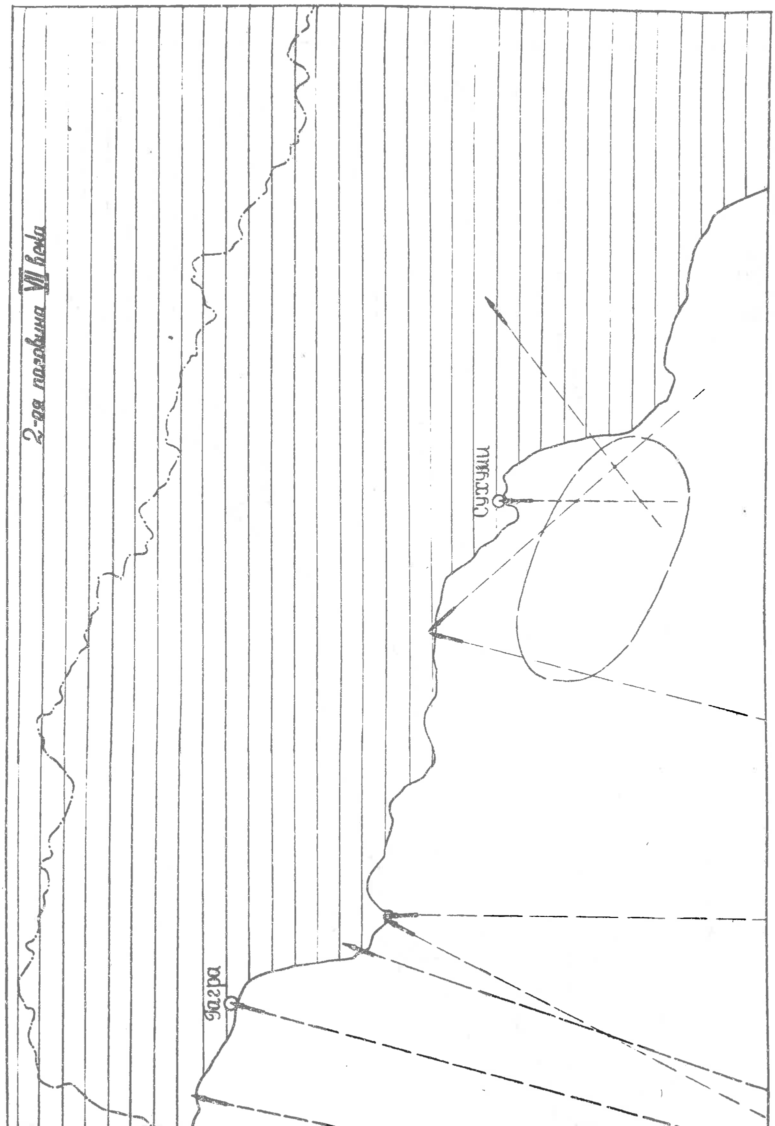
2-ая половина VIII века
Сухуми
Гагра

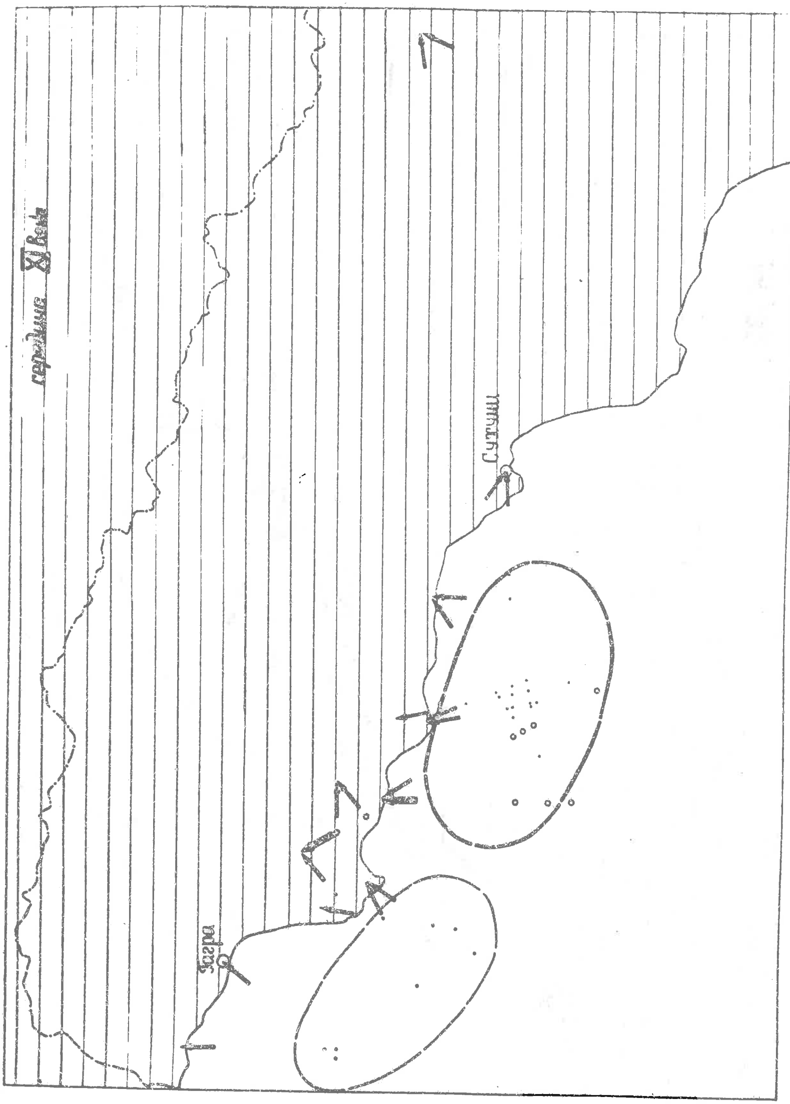
Сутиш
Эсгра

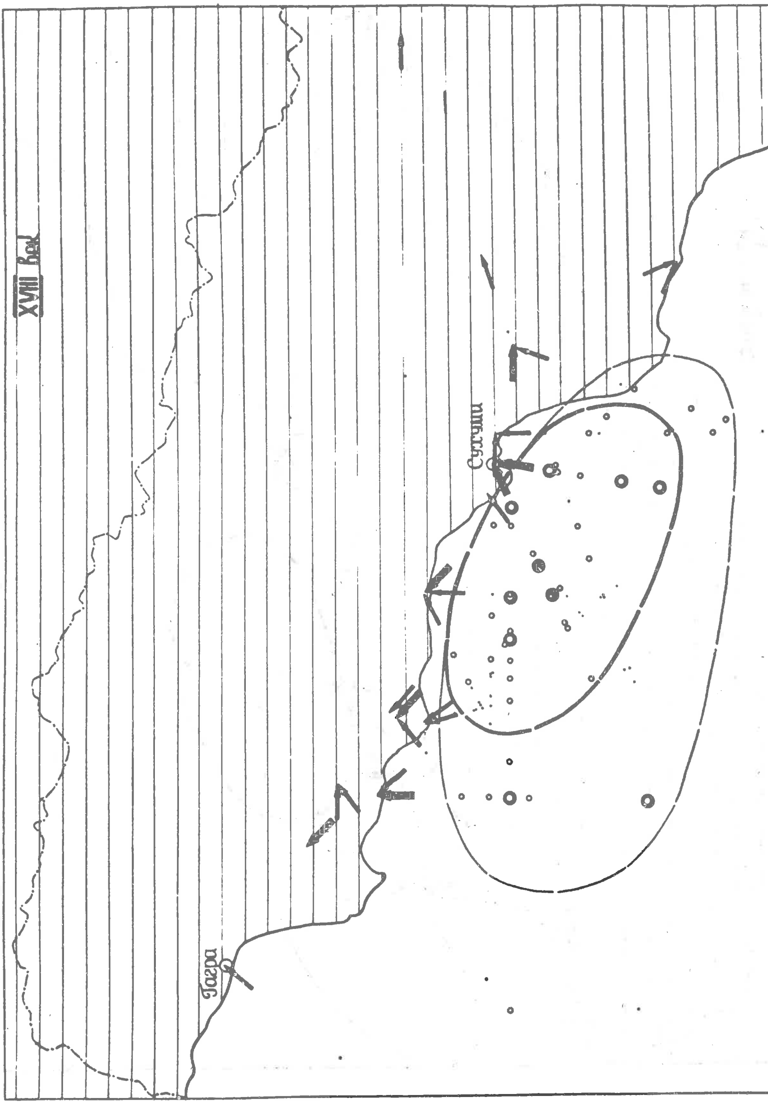
XVIII век
Сухуми
Гагра

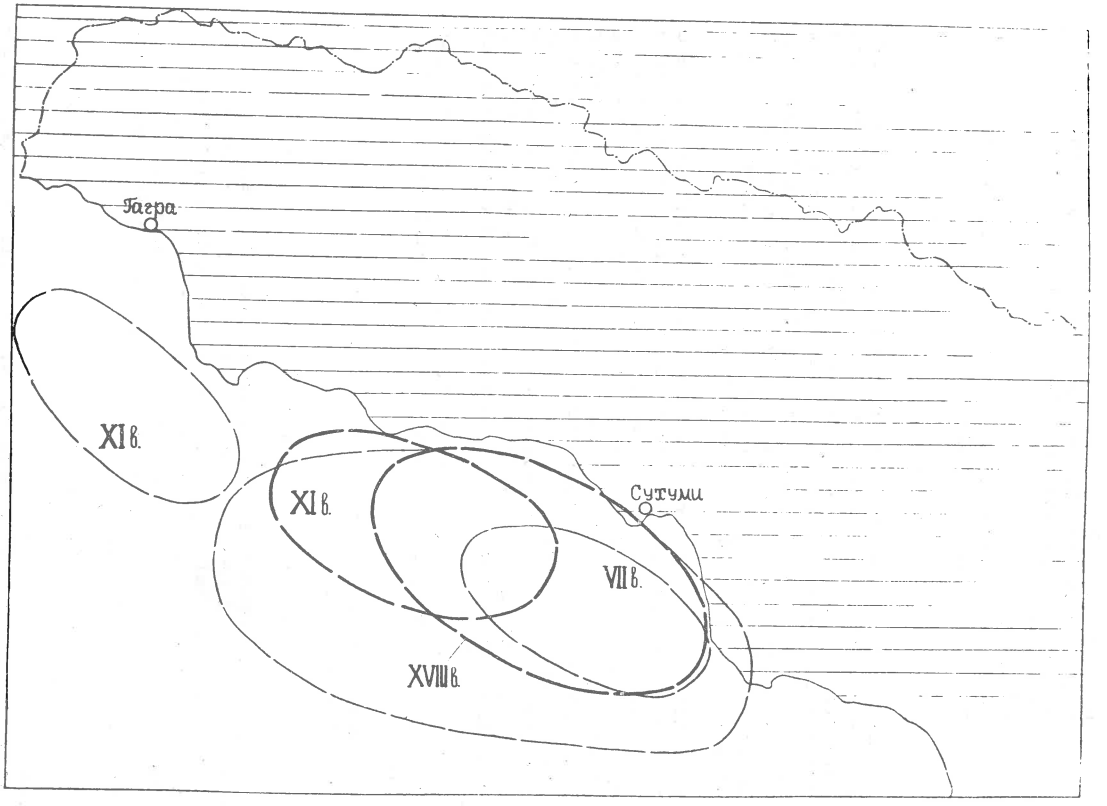
Гагра
XI в.
XI в.
Сухуми
VII в.
XVIII в.

SEISMICITY INVESTIGATION PROBLEM: HYPOCENTER DETERMINATION ACCURACY FOR EARTHQUAKES CLASSIFICATION

BELOBORODOV V. N.
Computer Centre, Sibiria Branch of the Academy of Sciences, Novosibirsk, USSR
BRUK M. G.
KONDORSKAYA N. V.
Institute of Physics of the Earth, Academy of Sciences, Moscow, USSR

ABSTRACT

The present paper consists of the developed joint hypocenter method and the modern statistical method with intensive computer application. The stable station corrections are determined by aftershook monitoring. A matrix of correlations and curves of density distributions of residuals are plotted. Obtained corrections give additional information of the medium, sufficient for adequate description of travel times.

Determination of parameters of earthquake hypocentres and corresponding estimation of its accuracy is an inverse problem and the main question that arises on the way of it solution : whether the adopted model is good for explanation of the data obtained. Simulating the medium in great detail by increasing the number of its parameters leads to a quantitative contradiction: information on the velocity model and on hypocentres which we are eager to extract from the data on arrival times of seismic waves becomes much greater that the data themselves, especially so if the number of earthquakes in the region is low.

Increase in number of parameters certainly leads to less residuals, however, each individual parameter becomes more indeterminate.

Method

Residuals of travel times of seismic waves at i-th station from j-th events is:

$$f_{ij}=(t_{ij}-t_{0j})-T_{ij}=\alpha_i+\varepsilon_{ij} \qquad (1)$$

where t -observed time, t_0 -source time, T -theoretical travel time by a travel time curve or by a model of the medium. The residual f_{ij} consists of two components: the constant α, that is known to give dislocation errors and a random value ε. α is calculated by the JHD method. The correlation of station residuals had been calculated according to the formula:

$$R_{ij}=\sum\xi_{iK}*\xi_{jK}/\left(\sum\xi^2_{iK}*\sum\xi^2_{iK}\right)^{0.5} \qquad (2)$$

Results

We shall present some results of localization two strong earthquakes and their aftershooks at the Caucasus territory: one of them located in the Caspian sea and the other at the most seismic active zone in the Caucasus - Djavachet upland.

Eathquake in the Caspian sea of march 6, 1986.

For this earthquake the joint hypocentre method was used for 117 aftershoks. Stable station corrections α_i for the Jeffreys-Bullen travel time tables are determined. Stability of these station corrections enabled us to construct the whole field of corrections to the J-B tables determined by cubic splining. This field is shown in fig. 1 a, b as isolines (for P and S waves respectively). One can see that configurations of the isolines of station corrections for P and S waves are in good agreement (positive to the south-east from the Caspian sea and negative in the Caucasus area) , though the corrections differ in value.

To decide whether the ε_{ij} are random, we plotted the curves of distribution of residual density $p(\varepsilon)$. These curves for P and S waves are shown in fig. 2(a and b). The curve p(f) obtained without station terms is shown for comparison. The correlation of station residuals is shown in fig. 3 One can see that station residuals are independent for the major part of the stations. This fact alows constructing a confidence ellipce for epicenters. Its main semiaxis is about 10 Km.

We used joint hypocenter determination with different parameters of the master event. The depth varies from 10 to 80 kilometers. The parameters of the master event is recalculated (with the determined station corrections).

For the depth from 16 to 30 km recalculation appeared to lead to the same values. For the depth out of this range discrepancy takes place. This comfirms employment of the modern statistical method with intensive computer application (resembling the butstrep method). In fig. 4 one can see isolines of probability density parameters of hypocenter. Above there is an epicentre corresponding to the hypocenter with maximum density. In stations distribution under consideration depth confidence interval from 16 to 30 km has maximum probability density on the depth about 29 km.

Paravan Eathquake of may 13, 1986.

Similar investigation was conducted with aftershocks of the Paravan earthquake of May 13, 1986. A series of 43 aftershocks was considered. Stable station corrections are shown in fig. 6 as isolines. Curves of distribution of residual density p(f) for P and S waves are given on fig. 2(c and d). The correlation matrix is shown in fig. 5 One can see that just a few stations have significant (more than 0.7) crosscorrelation. The confidence ellipce semiaxis is about 3-4 km.

The depth foci for main earthquake are much more definite than in the case of the Caspian sea. Depth value lyes in the interval from 8 to 10 km.

Thus the results of this investigation show possibility of accuracy estimation in location by aftershook monitoring.

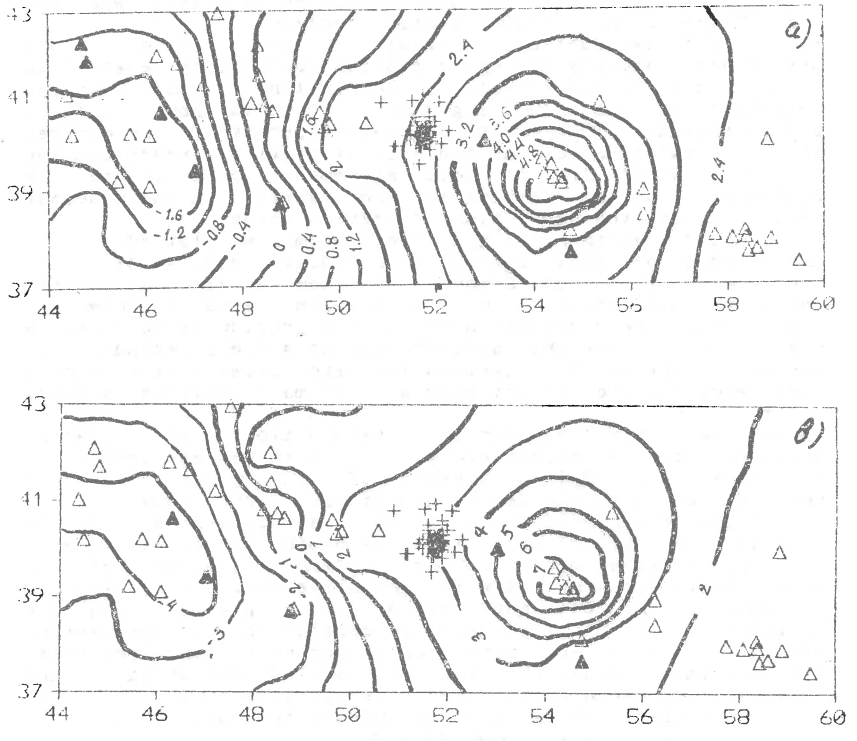

FIG. 1
ISOLINES OF THE STATION CORRECTIONS FOR JEFFREYS-BULLEN TRAVEL-TIME TABLES
(JHD -method , aftershok series of Caspian earthquake)

a - - for P waves b - for S waves

-1.2 - isoline (sec)

△ - station with unstable correction

▲ - station with stable correction

+ - aftershok

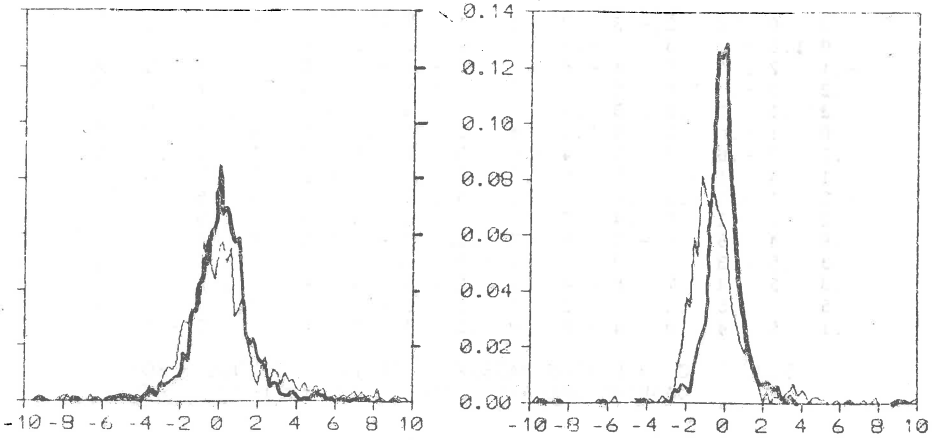

a) P -waves, Caspian aftershocks, march 86

c) P -waves, Paravan aftershocks, may 86

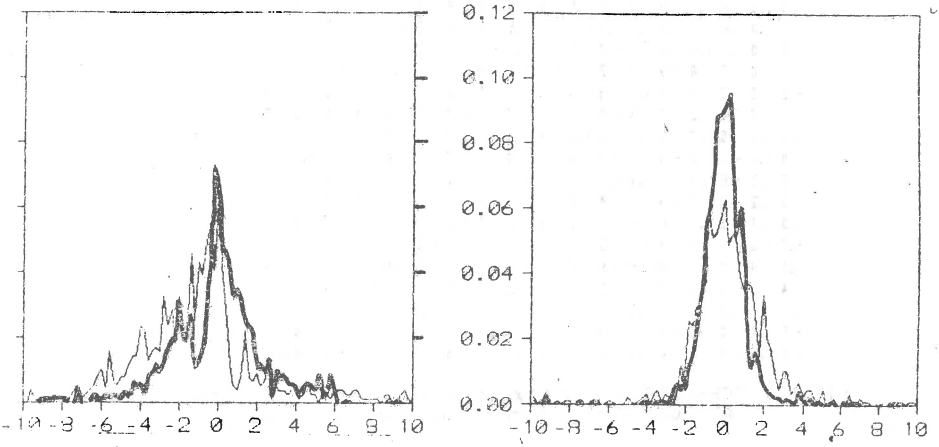

b) S -waves, Caspian Sea

d) S -waves, Paravan

FIG. 2 CURVES OF DISTRIBUTION OF RESIDUAL DENSITY

——— - JHD method, J-B tables (for station terms see fig. 1 and fig. 6)

——— - J-B tables without any station terms

1.0	.0	-.4	-.2	-.3	.0	.2	.1	-.2	-.2	.6	.3	.3	.5	.1
.0	1.0	-.2	.3	.1	-.1	.0	-.4	-.1	-.3	.4	.5	.5	.0	.5
-.4	-.2	1.0	-.0	.1	-.6	-.6	.1	-.2	-.1	-.6	-.3	-.4	-.5	.4
-.2	.3	-.0	1.0	.6	.2	.0	-.1	-.1	.5	.0	.1	-.7	.4	.0
-.3	.1	.1	.6	1.0	.5	.1	.3	.4	.4	-.3	-.0	-.8	-.5	.4
.0	-.1	-.6	.2	.5	1.0	.4	.0	.3	.7	.5	.4	-.4	.3	-.5
.2	.0	-.6	.0	.1	.4	1.0	.0	-.2	.1	.7	-.0	.2	.1	-.0
.1	-.4	.1	-.1	.3	.0	.0	1.0	-.5	.4	-.2	-.0	-.3	-.3	.5
-.2	-.1	-.2	-.1	.4	.3	-.2	-.5	1.0	.0	.8	-.4	-.5	.0	-.7
-.2	-.3	-.1	.5	.4	.7	.1	.4	.0	1.0	-.0	.2	-.5	-.2	-.0
.6	.4	-.6	.0	-.3	.5	.7	-.2	.8	-.0	1.0	.6	.4	.5	-.3
.3	.5	-.3	.1	-.0	.4	-.0	-.0	-.4	.2	.6	1.0	.4	.6	-.2
.3	.5	-.4	-.7	-.8	-.4	.2	-.3	-.5	-.5	.4	.4	1.0	.4	.0
.5	.0	-.5	.4	-.5	.3	.1	-.3	.0	-.2	.5	.6	.4	1.0	-.6
.1	.5	.4	.0	.4	-.5	-.0	.5	-.7	-.0	-.3	-.2	.0	-.6	1.0

FIG. 3 CORRELATION MATRIX OF STATION RESIDUALS FOR CASPIAN SEA AFTERSHOCKS (JHD- METHOD,P-WAVES)

1.0	-.3	-.2	-.3	.2	-.2	.1	-.0	.0	-.2	-.0	-.5	-.2	.1	-.4	-.4	-.5	-.0
-.3	1.0	.0	-.0	.0	.3	-.2	-.5	-.0	-.5	-.2	.4	-.6	.3	.2	.3	.4	.1
-.2	.0	1.0	.4	-.2	.3	-.5	-.5	-.3	-.0	-.0	.6	.2	-.4	.2	.7	.2	-.2
-.3	-.0	.4	1.0	-.8	.0	-.2	-.2	-.0	.4	-.2	.3	.0	-.1	.2	.3	.3	.0
.2	.0	-.2	-.8	1.0	.2	.2	.0	-.3	-.3	-.0	-.0	.0	.2	.1	-.0	-.0	.4
-.2	.3	.3	.0	.2	1.0	-.5	.0	-.3	-.1	-.5	.6	-.0	.0	.7	.3	.2	.6
.1	-.2	-.5	-.2	.2	-.5	1.0	.6	-.2	-.7	-.4	-.3	-.3	.8	-.5	-.8	.5	-.2
-.0	-.5	-.5	-.2	.0	.0	.6	1.0	.4	-.0	-.2	-.2	.0	.5	-.3	-.3	.3	.3
.0	-.0	-.3	-.0	-.3	-.3	-.2	.4	1.0	.4	.6	-.3	.3	-.4	-.1	.0	-.4	.6
-.2	-.5	-.0	.4	-.3	-.1	-.7	-.0	.4	1.0	.3	-.0	.8	-.2	.5	.4	-.3	.5
-.0	-.2	-.0	-.2	-.0	-.5	-.4	-.2	.6	.3	1.0	-.2	.4	-.7	-.0	.3	-.3	-.0
-.5	.4	.6	.3	-.0	.6	-.3	-.2	-.3	-.0	-.2	1.0	.0	.0	.5	.7	.5	.4
-.2	-.6	.2	.0	.0	-.0	-.3	.0	.3	.8	.4	.0	1.0	-.3	.2	.3	-.0	.3
.1	.3	-.4	-.1	.2	.0	.8	.5	-.4	-.2	-.7	.0	-.3	1.0	-.0	-.4	.5	.4
-.4	.2	.2	.2	.1	.7	-.5	-.3	-.1	.5	-.0	.5	.2	-.0	1.0	.4	.1	.5
-.4	.3	.7	.3	-.0	.3	-.8	-.3	.0	.4	.3	.7	.3	-.4	.4	1.0	-.1	-.0
-.5	.4	.2	.3	-.0	.2	.5	.3	-.4	-.3	-.3	.5	-.0	.5	.1	-.1	1.0	-.0
-.0	.1	-.2	.0	.4	.6	-.2	.3	.6	.5	-.0	.4	.3	.4	.5	-.0	-.0	1.0

FIG. 5 CORRELATION MATRIX OF STATION RESIDUALS FOR PARAVAN AFTERSHOCKS (JHD- METHOD,P-WAVES)

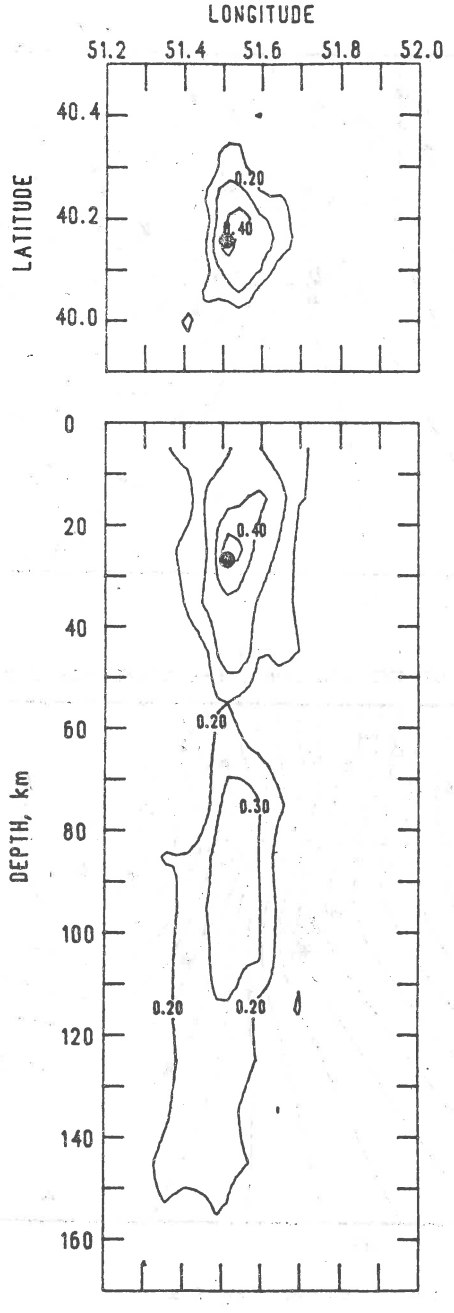

FIG. 4 ISOLINES OF PROBABILITY DENSITY PARAMETERS OF HYPOCENTER CASPIAN EARTHQUAKE OF MARCH 6,1986
(for methode of localization see Belobordov V. N., in press)

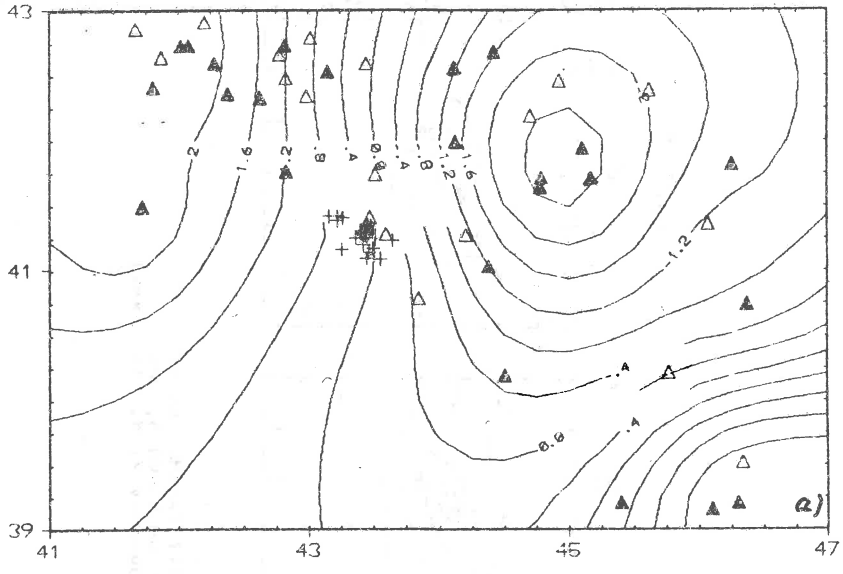

FIG. 6
ISOLINES OF THE STATION CORRECTIONS FOR J-B TABLES

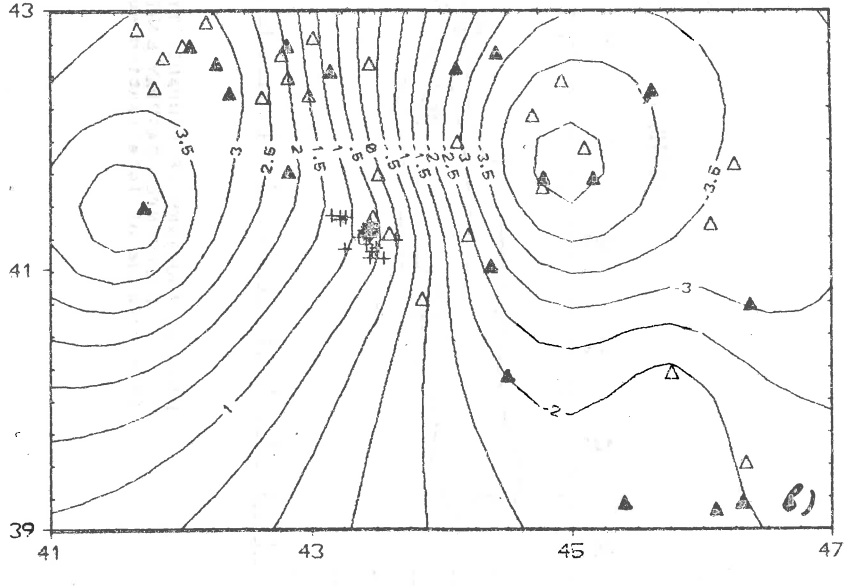

for legend see fig 1

THE PECULIARITIES OF THE SERIES OF NIKAJ-MERTURI (TROPOJA,ALBANIA EARTHQUAKES

Sulstarova E., Muço B.

Seismological Center, Academy of Sciences of PSRA
Tirana, Albania

ABSTRACT

The series of the earthquakes of Nikaj-Merturi, near the basins of Fierza and Koman hydroelectric P/S, iniciated on november 10, 1985 up to august 1986.The nearest station, the one of Bajram Curri (BCI), recorded 17096 shocks having a magnitude up to 4.2

The composite focal mechanism solutions show that there are involved different mechanisms, i.e. the activation of some microfaults bording the rocky microblocks in flisch-limestone contacts.

It is noticed a good correlation between the water levels of Koman and Fierza lakes, the extraordinary aboundant precipitations of that period with the earthquakes frequency of this series. All that is in favour of the hypothesis that the hydrologic factors through the increasing of pore pressure are the first cause that triggered those earthquakes.

REGIONAL SEISMOTECTONICS AND THE SEISMIC HISTORY

The earthquakes included in the epicentral zone of this series occurred sidelong one of the largest dislocation traversing the Albanian territory, i.e. Shkodra-Peja fault,which divides the Albanides into two parts, in the northern and the southern one.

The prevailing geologic formations are limestones and flych from Lower Jurassic to Paleogene, but in the depression of Bajram Curri new deposits are distinguished too [The geological map of PSR of Albania, 1983]. All these formations, situated at the edges of a strong traversal dislocation, are involved in a vigour tectonic history. The microfaults, dividing the rocky microblocks at the borders between flysch, limestones and new deposits are distinguished quite well in these areas. It is a zone of relief contrasts. From the hydrological view point, there are formations of high penetration and water-bearing as limestones are also low penetration and water-bearing as flysch is[The hydrological map of PSR of Albania, 1985].

This zone is situated at the border of two regimes of stresses, i.e. the tensional one of NW-SE direction and compressional of NE-SW direction[Sulstarova E.,1987;Aliaj Sh. et al.1985].

In the past, it wasn't noticed here strong earthquakes [Muço B.,1982](fig.1). The earthquakes felt had been a scarce phenomenon. Such a series as this one the living people of this zone never remind.

The seismological network of the Northern Albania, set up after 1976, includes the seismological stations of Puka(PUK),Kukësi(KKS),Fierza(FRZ),and later Bajram Curri(BCI),Kam-Tropoja(KMA and Peshkopia(PHP), evidenced new data about the seismic activity of the Northern Albania (fig.2). Lots of earthquakes are observed in both sides of Shkodra-Peja dislocation time by time. This acti

vity was intensified more after the filling of Fierza reservoir of the "Drita e Partisë" hydroelecric P/S in 1978. There were some concentrations of microearthquakes in that period which magnitude don't pass M=4.0 [Muço B.,1982].

SEISMICITY PATTERNS

The earthquakes of the series we have called the series of Nikaj-Merturi, occurred from november 10, 1985 up to the end of august 1986. The hypocentres have been determined using two programmes: the standard one used to prepare the seismological bulletin of albanian network [Koçiaj S. et al.,1979] and the programme BAR [Muço B. et al.,1985] with a linear velocity increased by depth, which gives better results especially as regards the focal depth. We have located 1430 hypocenters; F and L errors of 52 percent of them are less than 10km and the error of depth determination is less than 7km. The earthquakes of this series are concentrated mainly in a zone with coordinates: 42.25°-42.35°N and 19.95°-20.05°E, i.e. a zone of 100km^2 (fig.3). The earthquakes generally are at depths bet ween 10-15km. The magnitudes are determined using the standard formula of Richter and for Bajram Curri station a signal duration formula is used for which the respective nomograme is compiled [Muço B.,1982].

By the cumulative number of the seismological events of this series recorded at BCI (fig.4), an interesting picture is obtained. According to the density of seismic events in course of time, we may distinguish 11 different periods presented in (fig. 4). The most intensive period of this series is the one of november 17-23,1985.

The series of Nikaj-Merturi earthquakes is composed mainly by microearthquakes. From 17096 shocks recorded by BCI, 15300 of them are with M<2.0. The energy released by this sequence of earthquakes corresponds to an earthquake with a magnitude equal to 4.9 of Richter scale. This calculation is carried out using the formula recommended by Richter:

$$\log E = 9.9 + 1.9\,M - 0.024\,M^2$$

that in our case give $E = 3.9423 \times 10^{16}$ erg.

Dividing the earthquakes with M≥2.0 into groups of magnitudes with successive difference 0.1 (see tab.1), the coefficient b of the formula $\log N = a - bM$, was determined using a programme which permit to resolve nonlinear equations [Peçi V.et al.,1988]. The variation of this coefficient in time is determined considering cumulatively the shocks of this series. It is remarked that the coefficient b tends towards the value b = 1.05 0.0 while a = 5.5 0.0 The coefficient b was also obtained empirically by the wellknown relation of Utsu:

$$b = 0.4343\ m \,/\, \left(\sum^{m} M - m\,M_{min}\right)$$

gives the value b = 1.13

It must be said that the epicenters of these earthquakes did not trace exactly any tectonic fault. They constitute more a dense swarm and the differences between the first onsets of P and S waves recorded at BCI, varys from 1.2 - 3.0 sec. It is impossible to obtain a single focal mechanism for this zone and for this series of earthquakes. After many attempts we could separate four different patterns with about 650 polarities of first onsets. The composite fault plane solution are used with the emergence angle gived by:

$$i = \tan\left(\left(D - 2Hv/a - H\right) / \left(2D\left(H + v/a\right)\right)\right)$$ [Crosson R;1972]

where D - epicentral distance, H - focal depth, v - the velocity of P -wave and a - the first coefficient at the formula of linear

velocity variation: v = a + b H , ku a=5.3 dhe b=0.03 . As shown in fig.5 the strike-slip of N-NE compression and SW-NW tension prevails.

THE INFLUENCE OF THE HYDROLOGICAL FACTORS ON THE EARTHQUAKES OF THIS SERIES

As it is known the underground waters are the most free component of the Earth's Crust. The role of groundwater in active faults zones is poorly understood and yet is clearly of major importance for the earthquake triggering. At sixty's, in a series articles[HubertM.K,Rubey W.W.,1959] , have been drown the attention to the role of fluid pressure in mechanics of overthrusting faulting. Besides this, the scientists, more and more are turning towards th relations between fluids and earthquakes in different zones of the globe. Such relation may be observed and at the case of Nikaj-Merturi.

This series of earthquakes initiated just when abundant precipitations fell in this zone. During november 1985 the precipitations at Bajram Curri were 654 mm, surpassing in this zone 2.6 times the monthly average of this month, from 1961[the peculiarities of weather for the years 1985,1986]. The gates of HPS of Koman "Enver Hoxha" were closed right in the end of october of that year. The peak earthquakes frequency of this series corresponds well enough to the peak value of the precipitations and to the level of Drini river (fig.6). The precedent studies carried out for these regions have shown that the increase of the waters level of Fierza lake has modified the seismic picture round it, causing many microearthquakes[Muço B.,1982].

Taking into account all mention above and the peculiarities of the earthquakes that have been subject of our study, it must be emphasized that are right the underground waters with their increase of pore pressure triggered, at the beginning, the earthquakes of this series. After this, in this zone characterized by a strong tectonic movements, from the energy accumulated in time, the sizmic process has been developed in his natural way.

REFERENCES

Aliaj Sh.,Muço B.,1985 -"The composite focal mechanism solutions for Northern Albania and tectonic faults responsible for the earthquakes" ; Bul.Shk.Gjeol., Nr.1 (in albanian)

Crosson R.,1972 - "Small earthquakes, structure and tectonic of the Puget Sound region"; Bull.Seism.Soc.of Amer.,vol.62,No;5

The Geological Map of PSR of Albania - Tiranë, 1983

The Hydrogeological Map of PSR of Albania - Tiranë, 1985

Hubert M.K.,Rubey W.W.,1959 - "Role of fluid pressure in mechanics of overthrusting faulting";Bull.of the Geol.Soc.of Amer., vol.70

Koçiaj S.,Zenjo V.,Varfi P.,1979 - "Hypocentral determination of near earthquakes according sizmological albanian network" ; Bul.Shk.të Nat., Nr.4 (in albanian)

Muço B.,1982 - "The seismicity of Drini valley and influence of Fierza lake on it"; Thesis, Seismological Center of Tirana (in albanian)

Muço B.,Minxhozi A.,Kushe R.,1985 - "An algorithm for more precise determination of hypocentres of near earthquakes";Bul.Shk.

të Nat.,Nr.1 (in albanian)

Peçi V.,Minxhozi A.,1988 - "On the determination of coefficient b, in the cumulative distribution according to the magnitudes"; Bul.Shk.Gjeol., Nr.1 (in albanian)

Sulstarova E.,1987 - "The focal mechanism of the earthquakes in Albania and today tectonic stress field"; Bul.Shk.Gjeol. Nr.4 (in albanian)

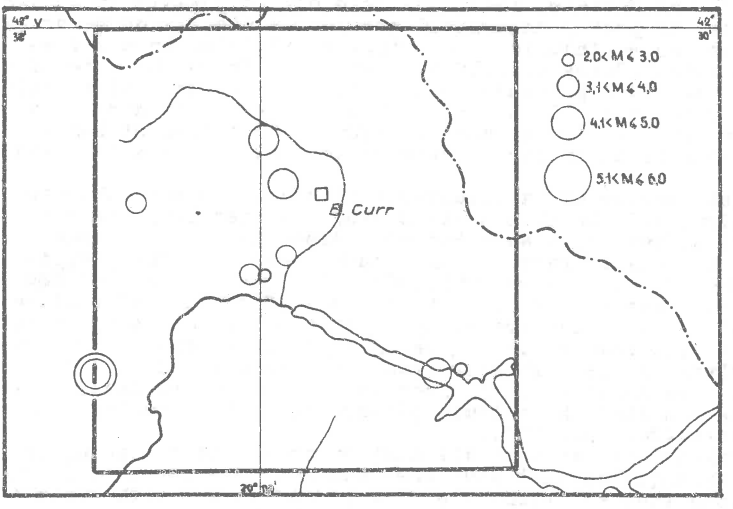

Fig. 1 - The epicenters of Nikaj-Mërturi area, 1900-1975

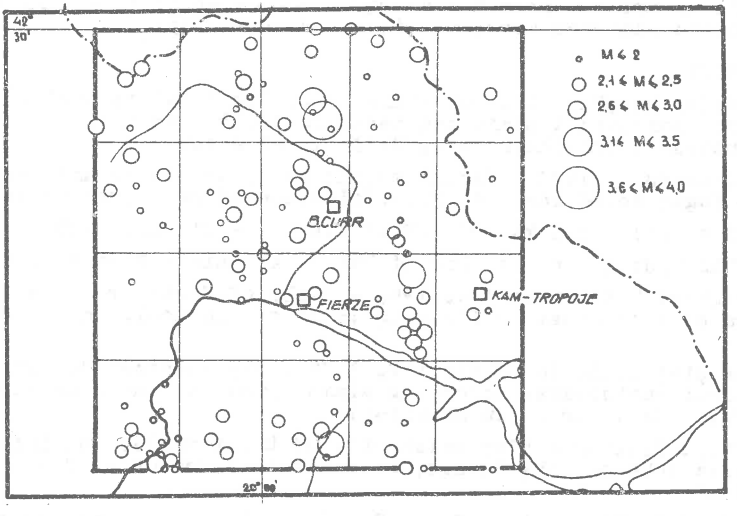

Fig. 2 - The epicenters of Nikaj-Mërturi area, 1976-1985

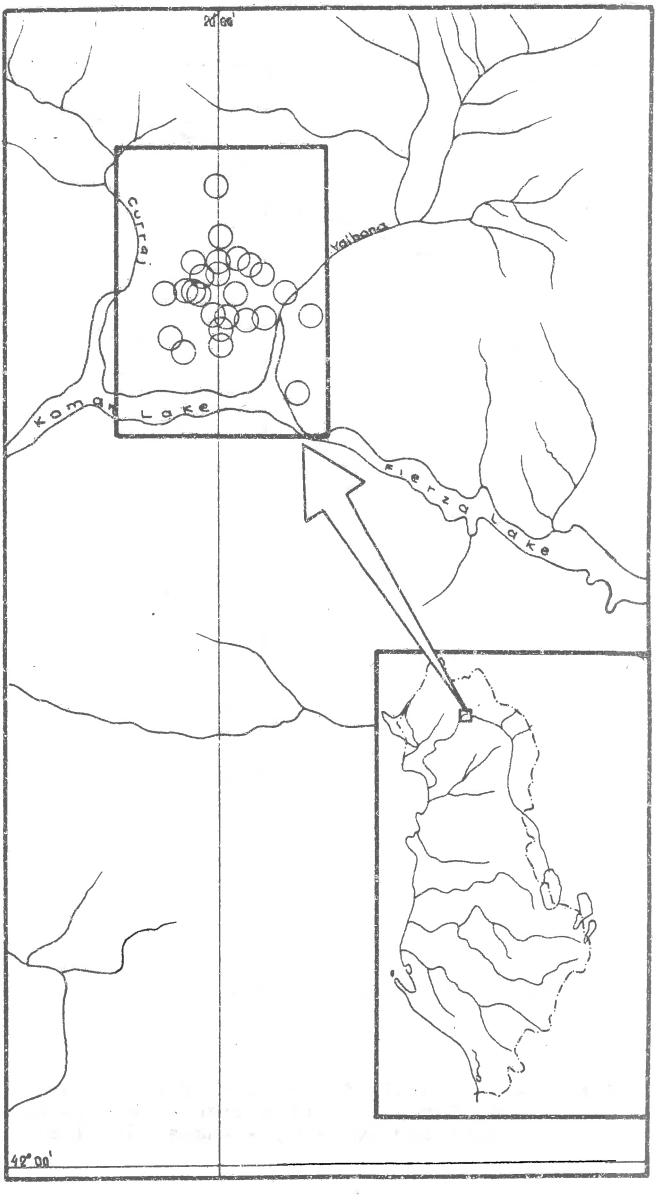

Fig.3 - Nikaĵ-Merturi zone and the epicentres of this series with M ⩾ 3.5

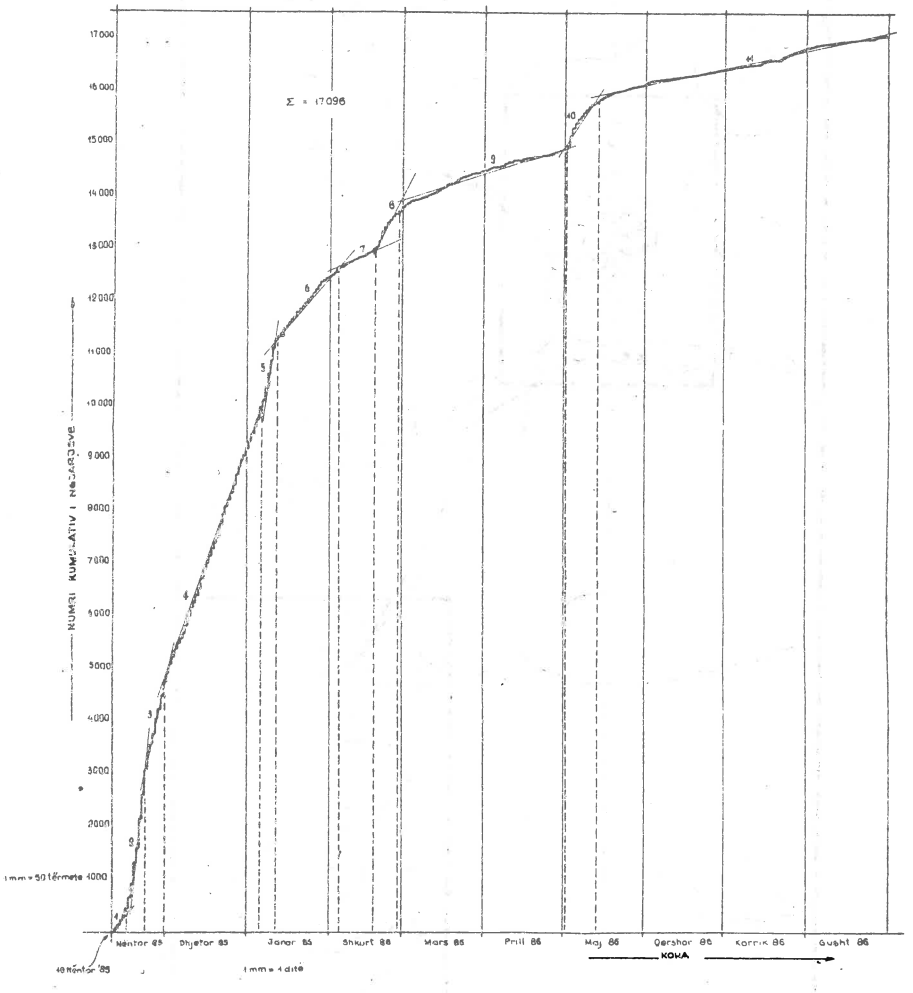

Fig. 4 - The cumulative number of earthquakes in course of time, for the series of Nikaj-Merturi from November 10, 1985 - August 31, 1986

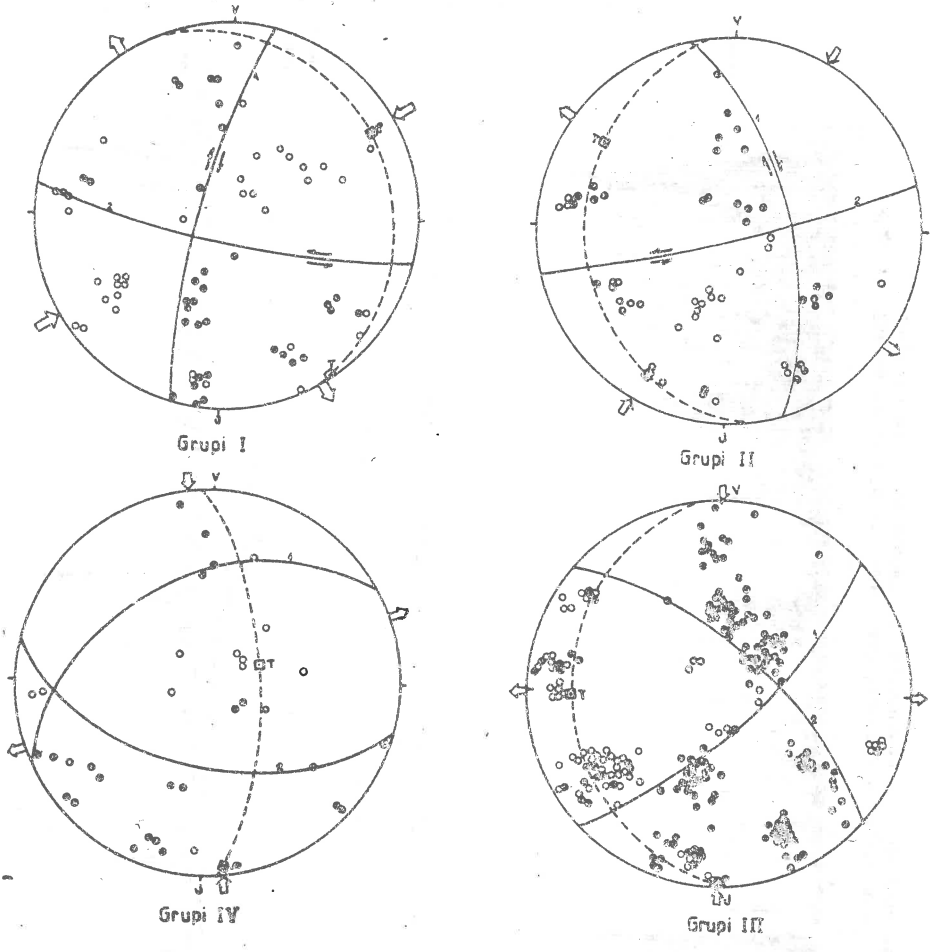

Fig.5 - Equal area azimuthal projection of upper hemisphere of focal sphere for four patterns of earthquakes of this series

Magnitude	<2,0	2,0	2,1	2,2	2,3	2,4	2,5	2,6	2,7	2,8	2,9	3,0	3,1
Number of earthquakes	15300	343	309	279	202	133	134	89	53	60	39	35	18
Magnitude	3,2	3,3	3,4	3,5	3,6	3,7	3,8	3,9	4,0	4,1	4,2	4,3	4,4
Number of earthquakes	24	14	16	11	6	9	8	5	8	0	1	0	0

Tab.1 - The distribution of magnitudes of the Nikaj-Merturi earthquakes

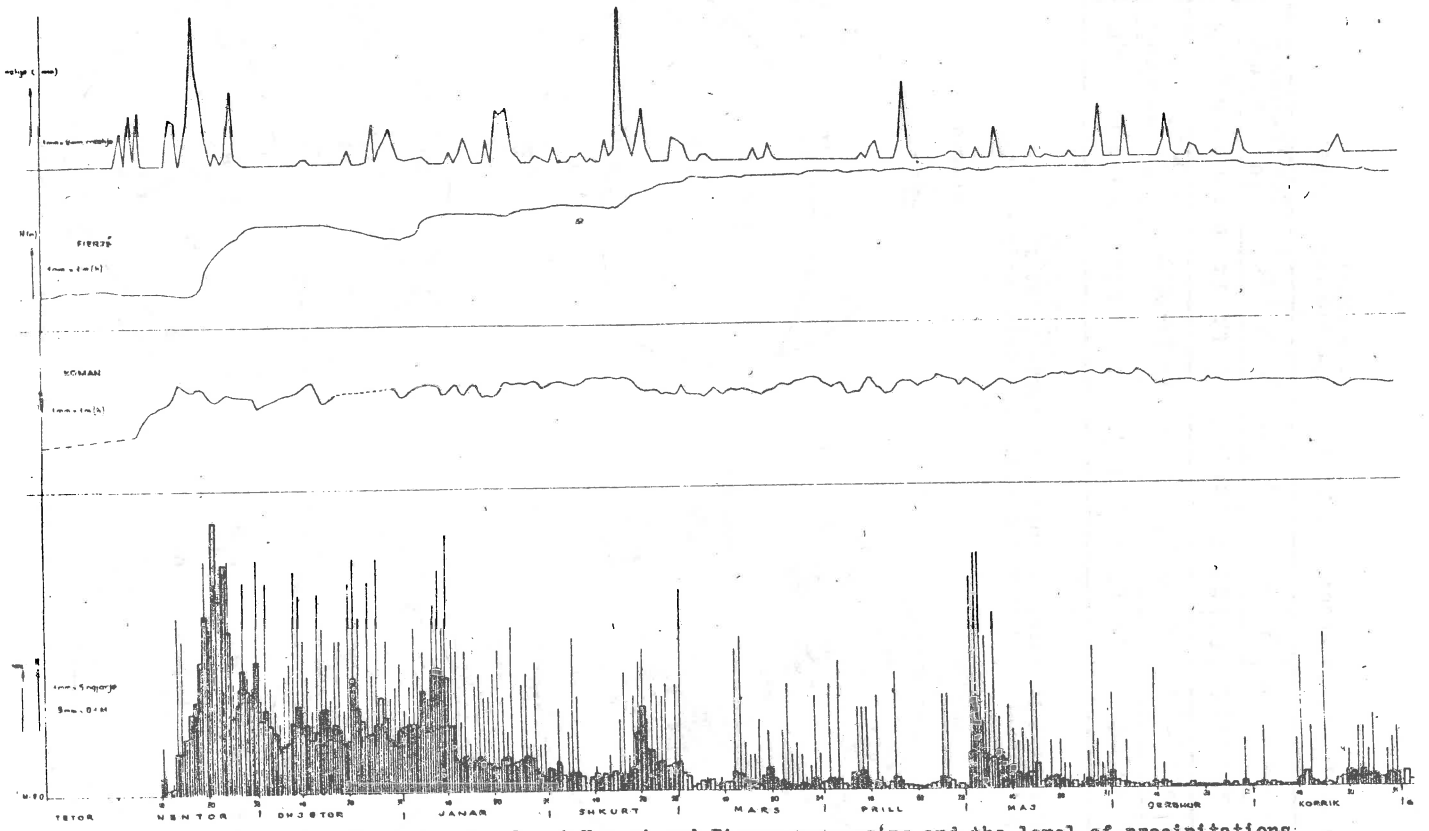

Fig. 6 - The water levels at Komani and Fierza reservoirs and the level of precipitations compared with the number of earthquakes and the peak magnitude per day

THE JANUARY 9, 1988 EARTHQUAKE, TIRANA, ALBANIA

E. Sulstarova, B. Muço, V. Peçi, A. Pitarka
Seismological Center, Tirana, ALBANIA

ABSTRACT

On January 9, 1988, 01:02 (GMT) an earthquake with M=5.4 and Intensity VII degrees MSK-1964 hit Tirana and the villages nearby causing relatively slight damages.

The epicenter of this earthquake is situated in the vicinity of Tirana, the capital city of the PSR of Albania, in the southwestern part of it. Considering the macroseismic data, the depth of its focus is h=5.0 km. In this paper are given the instrumental and macroseismic parameters. During this shock, based on the macroseismic field and the focal mechanism solution, a fault of NW 06° strike-direction and dip direction ENE 48° was activated. This fault is a sinister-strike-slip with a component of normal slide.

This earthquake was recorded by three accelerographs (SMA-1) of our strong motion network and two seismoscops as well. The peak acceleration was recorded by the accelerograph installed in the master station of Tirana (on bedrock-sandstone) -404.8 cm/ /sec^2, on the E-W component.

INSTRUMENTAL DATA OF JANUARY 9, 1988 EARTHQUAKE

The January 9, 1988 earthquake is recorded by all the stations of our seismological network (by the 13 stations of this network), and by the world network too. Using the programme 2 for the determination of hypocenters, the following focus parameters are found processing the seismological data of our network:

H=01:02:45.0, 41°.24 N and 19°.73 E, h = 0 km.

In regard to these data, the epicenter of this earthquake is situated at SW of Tirana.

In all the stations of our seismological network and on most of our seismographs the recordings of the maximal amplitude are cut, so that it made difficult the determination of the magnitude of this earthquake. Only in the station of Leskovik (LSK, SW Albania) has been possible to estimate the magnitude M=5.0. Other foreign stations have reported the following values:

M_{LH} = 5.8 (CLL), 5.4 (KRA);
M_{LV} = 5.8 (NEIS), 5.4 (KRA), 5.3 (VPP);
M_{LG} = 5.4 (SKO);
M = 5.5 (NEIS, PIJ), 5.4 (SUF, UPP), 5.3 (NAO);
M_{AW} = 5.8 (TRI), 5.3 (LOG), 5.1 (ATH);
M_D = 5.6 (FIR, KBA), 5.5 (BDV, PUV, TRI), 5.4 (BRY, TTG, HCY), 5.1 (ATH).

Based on these data the magnitude of January 9, 1988 earthquake id estimated M = 5.4.

The January 9, 1988 earthquake was not preceded by foreshocks but was accompanied with many aftershocks. The seismological station of Tirana recorded, up to January 31, 206 aftershocks, mos of them occurred the first day (196 altogether). The strongest one of this series took place on January 9, 1988, 07:10, and has the following parameters:

H = 07:10:50.3, 41°.20 N and 19°.92 E, M = 3.5.

It was possible to localize the epicenter of only four

aftershocks. The others, being weak enough, are recorded only by the seismological station of Tirana, and consequently is not possible to carry out a study on their distribution in space.

THE SEISMICITY OF THE REGION

The region where January 9, 1988 earthquake occurred is situated is a zone affected by stressed seismic activity. In this region earthquakes occur time by time, some of them had been strong ones. The strongests known are:

The earthquake of May 16, 1860 known as the earthquake of Ura e Bishirit[5], its epicenter is situated at WSW of Tirana: 41°.3 N and 19°.7 E, Io=8 degrees MSK-1964. This earthquake caused heavy damages and destructions in many villages situated at WSW of Tirana.

The earthquake of February 4, 1934: H=09:35:30, 41°.25 N and 19°.6 E, M=5.8, Io=7 degrees MSK-1964. The earthquake caused important damages in many villages at WSW of Tirana (Ndroqi zone).

The earthquake of August 19, 1970: H=02:01:53, 41°.16 N and 19°.75 E, M=5.5, Io=7 degrees MSK-1964. This earthquake caused important damages in many villages at SW of Tirana, slight damages has been noticed in Tirana too.

These three earthquakes and the one of January 9, 1988 are generated by the same fault zone, by Preza one, which takes part in the Ionian-Adriatic seismogenous fault zone that corresponds at SE and NW with Konica-Çorovoda-Rodoni Cape deep fault, which is very active, particularly at its extremities [5].

After 1970, at the vicinity of the focus zone of January 9, 1988 earthquake, our seismological network has recorded many shocks, some of them were with M=4.5 and Io up to 6 degrees.

THE MACROSEISMIC FIELD OF JANUARY 9, 1988 EARTHQUAKE

At the mesoseismal zone of January 9, 1988 earthquake, which includes the city of Tirana and some villages at the western and southwestern part of it, the consequences of this earthquake are investigated and studied by a special group pf the Seismological Center. The way how it is felt throughout the Albanian territory is known by questionnaires.

In Tirana and in the villages near-by are damaged 2083 dwellings houses and other constructions, 287 of which were too heavy damaged (forth degree of damage - according to MSK-1964 scale), 587 of third degree and 1204 of the second one. There were mainly damaged weak objects, old dwelling houses built without the necessary aseismic measures.

In the city of Tirana, at 5-6 story buildings, damages have had the lower floors [4]. Generally the most part of damaged structures had plaster cracks (first degree of damage).

The seismic intensity in the dwelling center, for the mesoseismal zone, was determined by statistical means, while in other places the estimation is qualitative according to MSK-1964 scale. The maximal intensity of the main shock of January 9 at the WSW part of Tirana is evaluated VII degree MSK-1964.

As it is seen by the isoseismal map of this earthquake (fig. 1), compiled for that purpose, the ground motions are felt throughout the territory of the PSR of Albania. They are also felt in Monte Negro and Macedonia.

The isoseismal map is compiled up to the isoseist of the fourth degree. According to this map, the ground motions up to 4 degrees

are felt within a vast territory, including a surface of 49.025 km^2, r = 125 km.

The parameters of the macroseismic field are determined processing this map using a particular programme 6 :

focus depth h = 5.0 0.3 km,
damping intensity coefficient 2.125, and
the average coefficient of the absorption of the energy 0.00556.

The macroseismic magnitude of this earthquake [6] results 5.5, nearly as the instrumental one, while the coordinates of the macroseismic epicenter are 41°.16 N and 19°.48 E.

The general energy propagation direction is NWN-SES, which corresponds with the general extension of the structures of the Albanides. Considering the position of the macroseismic epicenter and the general energy propagation direction, we have reached the conclusion that the January 9, 1988 earthquake is generated by Preza regional fault of NW-SE strike direction.

The isoseist that outlines the mesoseismal zone, i.e. the one of VI ½ degree, undoubtedly is influenced by the local soil conditions.

FOCAL MECHANISM SOLUTION

To carry out the focal mechanism solution of this earthquake the polarities of the first onsets of the longitudinal P waves recorded on 46 seismological stations (of Albanian network, Montenegrin, Macedonian, Greek and Italian ones outlining well enough the focus of this earthquake) are used. The readings of the first onsets are taken out directly from the seismograms sent by the networks mentioned above, except the Italian ones. The National Institute of Geophysics in Rome sent filled questionnaires. The velocity of P waves in the focus of this earthquake, for h = 5 km, used to calculate the incidence angle of P waves, is taken Vp = = 5.0 km/sec. From focal mechanism solution the following parameters results:

the axis of the compressional stresses P = NW 34° dip 40°,
the axis of tensional stresses T = SW 41° dip 16°,
the axis of intermediary stresses, axis B = SE 62° dip 44°.

Based on the superficial distribution of the energy of this earthquake, according to the isoseismal map (fig. 2) the nodal plane of NW 6° strike direction and dip 48° at ENE is accepted as the fault plane, which is a sinister strike-slipe with a component of normal slide, slip angle = - 20°. This direction of the fault plane corresponds with the regional fault of Preza with which is related the focus of the strong earthquake of May 16, 1866, known as the earthquake of Ura e Bishirit. Even the seismological records of Tirana station points out that the greater displacement is observed at NNW-SSE direction.

STRONG MOTION RECORDS

The strong motion of Jenuary 9, 1988 is recorded by the accelerograph (SMA-1) of the seismological station of Tirana, the one of Tirana hotel and by the accelerograph of the seismological station of Laçi (dep. of Kruja, 37 km from the epicenter).

a. THE STRONG MOTION RECORDS OF TIRANA STATION

In the station of Tirana the accelerograph is installed on

Tortonian sandstone. The strong motion data were digitized and processed at the Seismological Center using standart procedures of IEEES[2,3].

Corrected accelerograms are given in(fig. 3). The peak value of the corrected acceleration, computed velocity and displacement of the three components are given in table 1.

Table 1

Comp.	Time sec	Max. Acce. cm/sec^2	Max. velo. cm/sec	Max. disp. cm
EW	4.58	-404.8	-14.3	-1.6
Z	5.08	-69.3	-4.7	-1.6
NS	4.68	106.3	-5.9	-1.3

As it is seen, the maximal horizontal acceleration (-404.8 cm/sec^2) is recorded on the EW component. The peak horizontal acceleration is four times greater than the maximal one of the NS component. These values are not common for moderated earthquakes.

Considering the estimated epicentral distance of Tirana station (only 10 km) and the fault plane direction, we came to the conclusion that the accelerograph was very near the fault, which generated this earthquake. The very high peak value of acceleration on the EW component is explained by this fact.

THE STRONG MOTION RECORDS AT TIRANA HOTEL

The accelerograph (SMA-1) is installed at the top of Tirana hotel (the 15-th floor). The hotel is near the center of the city, approximately 7 km from the epicenter.

The corrected accelerograms are given in(fig. 4). The peak acceleration, velocity and displacement, after the original accelerograms had been corrected, are given in table 2. As it is seen, the highest peak acceleration is recorded on the NS component, different to one in Tirana station.

Besides this, the meximal acceleration on the EW component is not recorded during forced vibrations of the structures, but during free ones.

The differences between the two records, specially those between peak acceleration point out the influence of the local soil conditions, the type and the orientation of the structure towards the position of the epicenter.

Table 2

Comp.	Time sec	Max. acce. cm/ sec^2	Max. velo cm/sec	Max. disp. cm
EW	11.4	-125.9	21.8	6.2
Z	3.4	44.1	-5.6	2.9
NS	4.7	160.1	14.2	-3.3

REFERENCES

1. Koçiaj, S., Zenjo, V., Varfi, P. (1979) - Përcaktimi i hipoqendrave të tërmeteve të afërt sipas vrojtimeve të rrjetit sizmologjik shqiptar, Bul. Shk. Nat., Nr. 4.

2. Naumovski, N., Petrovski, D., Stamatovska, S. (1982) - Processing of strong motion accelerograms, Part II- Computer Programs, IEEES, Publ. 69.

3. Pitarka, A. (1988) - Mbi përpunimin analitik të lëkundjeve të forta të truallit me sistemin e analizës sizmike Sord, Qendra Sizmologjike, Tiranë.

4. Pojani, N., Myslimaj, B., Kondili, J. (1988) - Analiza inxhinierike e dëmeve të shkaktuara nga tërmeti i 9 janarit 1988 në qytetin e Tiranës, Qendra Sizmologjike, Tiranë.

5. Sulstarova, E., Koçiaj, S. (1975) - Katalogu i tërmeteve të Shqipërisë, Qendra Sizmologjike, Tiranë.

6. Sulstarova, E. (1986) - Mekanizmi i vatrave të tërmeteve dhe fusha e sforcimeve tektonike të sotme në Shqipëri, Disertacion për kërkimin e gradës shkencore "doktor i shkencave", Qendra Sizmologjike, Tiranë.

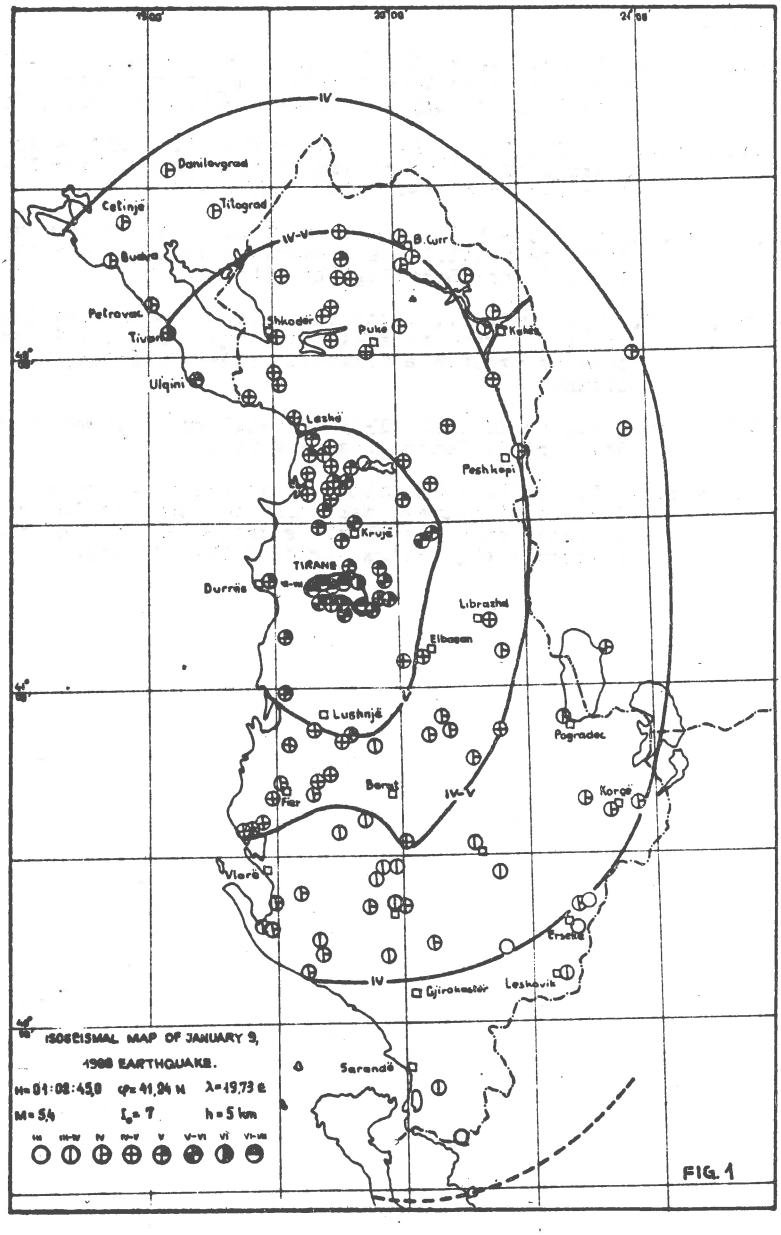
19°00'
20°00'
21°00'
IV
IV-V
Danilovgrad
Cetinje
Tilograd
Budva
B.Curr
Petrovac
Tivar
Shkodër
Puke
Kukës
Ulqini
Lezha
Peshkopi
Kruje
TIRANE
Durrës
Librazhd
Elbasan
Lushnjë
Pogradec
Fier
Berat
Korçë
Vlorë
Ersekë
Gjirokastër
Leskovik
Sarandë
ISOSEISMAL MAP OF JANUARY 9,
1988 EARTHQUAKE.
H=01:08:45,8 φ=41,94 N λ=19,73 E
M=5,4 I0=7 h=5 km
FIG. 1

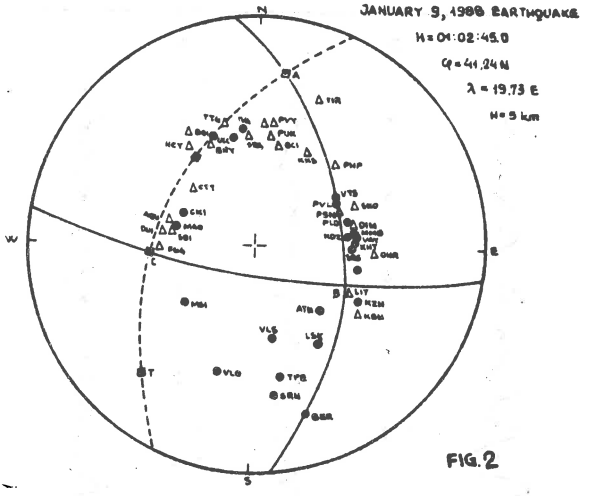

FIG. 2

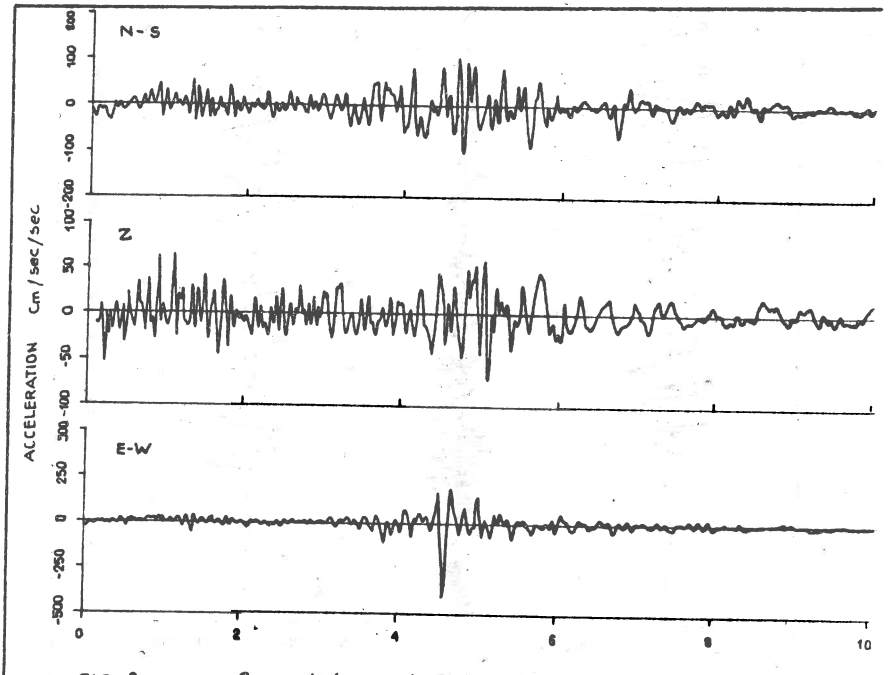

FIG. 3 *Corrected accelerograms recorded at free field conditions (Tirana seismological station)*

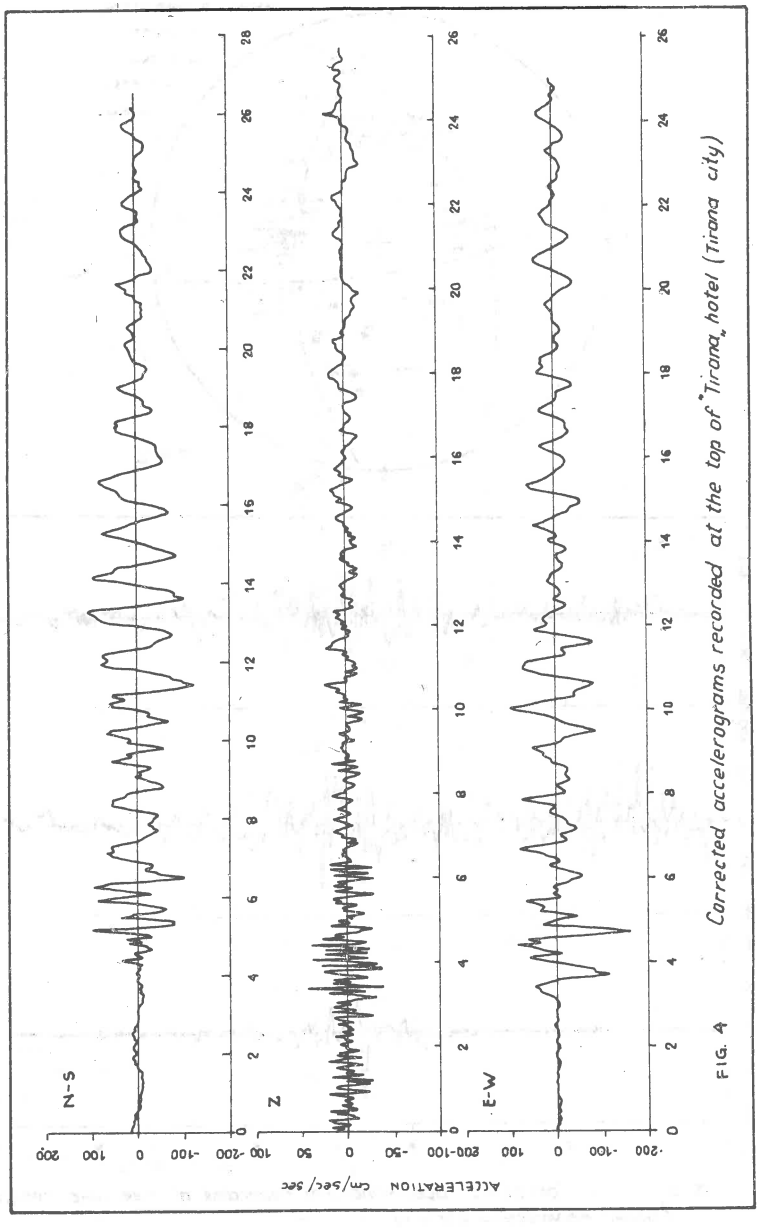

FIG. 4 *Corrected accelerograms recorded at the top of "Tirana" hotel (Tirana city)*

THE STRAJITZA EARTHQUAKE SEQUENCES OF FEBRUARY AND DECEMBER 1986

Oncescu M.C.*, C.-I.Trifu*, C.Hristova+, S.Simeonova+, D.Solakov+

* Center of Earth Physics and Seismology, Bucharest, Romania
\+ Geophysical Institute, BAS, Sofia, Bulgaria

ABSTRACT

The Strajitza seismic sequences of February and December 1986 were investigated using a joint seismic data set from the Bulgarian and Romanian telemetered networks. The JHD method was carried out. The results favour the idea that the occurrence of the two sequences took place at the intersection of two E-W faults (the Pre-Balkan Fault and a secondary one) with an assumed N-S fault.

INTRODUCTION

Two moderate earthquakes of magnitude M_L= 5.1 and M_L= 5.7 occurred in the period of one year (21 February and 7 December 1986) in the Northern Bulgaria in the vicinity of the town of Strajitza.

The seismically activated area is a subzone of Gorna Orjahovitza seismic zone. That zone is situated in the central part of North Bulgaria and is characterized by shallow tectonic earthquakes with a predominating strike-slip component.

According to the long-term prediction the maximum expected magnitude was estimated to be 7.0 (The strongest event in the zone is the 1913 Gorna Orjahovitza earthquake of M_W= 7.0).

DATA

The two seismic sequences of February and December 1986 were recorded by two telemetered seismic networks: the Bulgarian network, consisting of 9 permanent stations plus 3 mobile stations (KRP, PAG, RZN), and the Romanian network, consisting of 14 stations (Figure 1). Thus, a total number of 26 seismic stations surrounding the epicentral area was available, all stations equipped with Teledyne Geotech S13 short period seismometers. Since for accurate location a good azimuthal coverage of stations around the active region is required, it was decided to use only those earthquakes recorded by both network. It means that all earthquakes not recorded by at least one station to the north of the Strajitza region (part of the Romanian telemetered network) have been neglected. In this way, the lowest threshold for common network location was M_L= 2.5. The main tectonic units in the region are presented in Figure 1.

First P and S wave arrival time readings from the common seismic network were used for earthquake locations. The reading error of the arrival times is estimated to be 0.10 - 0.15 s. The identification error of the first P wave arrivals is obviously of this order of magnitude, but for the first S wave arrivals it is larger and more difficult to estimate "a priori". However, since the location method that will be applied contains a simultaneous

determination and use of station corrections, any systematic misindentification will be implicitely absorbed into the station correction.

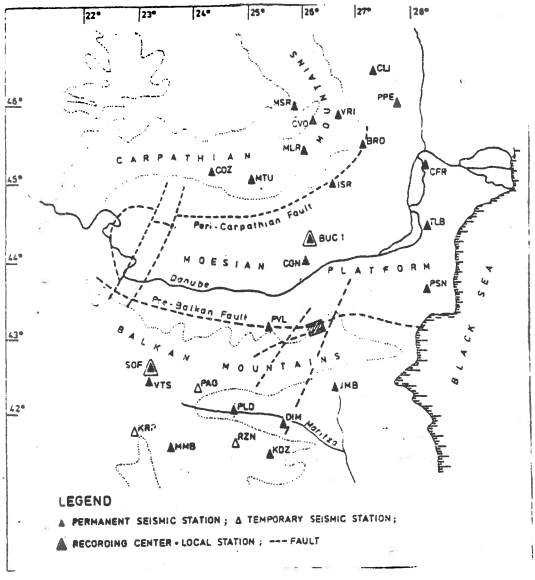

Fig.1
Simplified tectonic map of the Balkan-Carpathian region (compiled after Boncev et al. 1982 and Sandulesku 1984); the joint seismic network is also presented. Hatched area represents epicentral zone.

A number of 9 earthquakes was retained for the study of the February sequence (M_L=3.1-5.4), and 128 earthquakes for the December sequence (M_L=2.5-5.7). The reduced number of the analysed events from February is partly attributed to the accidentally reduced number of Romanian telemetered stations in operating during that winter month, leading to a strong decrease of debection capability of the common network and a corresponding increase of the magnitude threshold.

EARTHQUAKE LOCATION

The Joint Hypocenter Determination (JHD) technique was used as proposed by Frohlich (1979). It was already used by Oncescu and Trifu (1987) to locate the earthquakes belonging to a large seismic sequence occurred on the Peri-Carpathian Fault. The technique consists in the successive determination of hypocentral parameters of each event and station corrections for a large number of earthquakes. It leads to more accurate determination of earthquake locations, as compared to individual ones. Since the seismic stations are spread over a large distance range, and besides, they operate with different magnifications, we expect that different wave phases have been read as first phases for different magnitude values. Thus, the station arrival time corrections could be magnitude dependent. Therefor, the data set was devided in two magnitude clusters (M_L <4.0 and M_L ⩾4.0) and all earthquakes from a certain magnitude range were relocated to-

gether, regardless of the particular seismic sequence they belong to. The M_L magnitude was computed after Lee et al. (1972), using signal duration τ (in seconds) and epicentral distance Δ (in kilometers)

$$M_L = -0.87 + 2 \log \tau + 0.0035 \Delta$$

Several tests were performed in order to choose the velocity model: without sedimentary cover, with a 3 km and with a 5 km thick sediment layer. The most stable depth determinations were obtained for the model given in Table 1. Figures 2 and 3 show the epicentral maps of the two sequences. The foci are mainly very shallow, in the first 10 km of the crust. The statistical errors of spatial coordinates are of the order of 1-2 km. Where no depth error was computed, the depth value was restrained during iterations by the program itself, either to 0.0 km in the case of an "airquake", or to the current value when depth oscillations were detected.

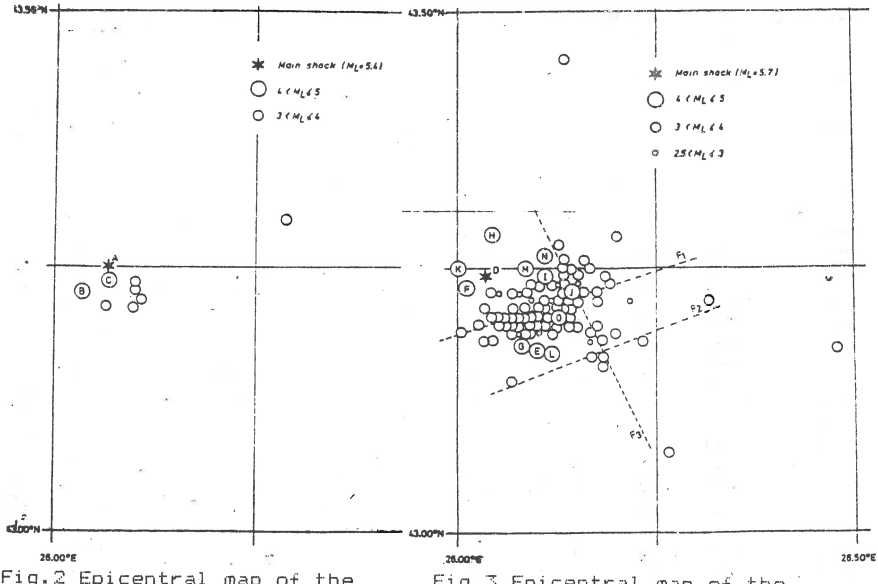

Fig.2 Epicentral map of the February 1986 seismic sequence

Fig.3 Epicentral map of the December 1986 seismic sequence

Events belonging to the second magnitude cluster ($M_L \geq 4.0$) are marked with capital letters.

Usually the gap in azimuth is around 90°, which lead to fairly good results in inversions. In no location the gap is greater than 180°, which means that in all cases the epicenters were within the network.

It is interesting to plot the station corrections listed in Table 2, for events with $M_L \geq 4.0$ versus those for events with $M_L < 4.0$ in order to verify that arrival times corresponding to different

wave branches were indeed read for moderate and small events.

Table 1. P and S wave velocity model adopted in computations.

Layer	Thickness (km)	Depth to top of layer (km)	Vp (km/s)	Vs (km/s)
	3	0	4.50	2.54
	17	3	5.60	3.16
3	20	20	6.77	3.82
4	10	40	7.94	4.49

Table 2. Travel time ($\Delta t_{P,S}$) and magnitude (ΔM_L) station corrections for earthquakes in Strajitza region.

Station	M ⩾ 4.0				M < 4.0				ΔM_L	N M_L
	Δt (s)	Np	Δt (s)	Ns	Δt (s)	Np	Δt (s)	Ns		
BRD	3.85	8	8.90	3	–	0	–	1	0.1	2
BUC1	-0.65	14	-0.84	15	-1.68	2	-1.22	30	0.4	5
CFR	0.22	8	2.76	8	1.19	25	0.32	37	-0.2	39
CGN	0.78	5	1.23	4	1.49	61	2.17	60	0.3	41
CLI	-0.69	6	-0.13	4	–	0	–	0	0.2	3
COZ	-0.19	5	4.03	5	–	1	1.47	3	-0.1	3
CVO	0.25	2	–	0	–	1	–	1	-0.3	2
DIM	0.09	15	0.67	13	-0.67	30	-0.90	42	0.4	17
ISR	0.03	14	2.49	14	-0.17	28	1.10	50	0.0	43
JMB	-0.03	13	0.42	10	0.08	38	0.20	121	0.3	30
KDZ	0.74	14	0.67	13	0.78	54	2.38	87	0.1	50
KRP	-0.42	15	4.47	7	1.82	17	3.17	92	-0.4	20
MLR	0.23	15	4.39	14	1.47	85	2.27	112	-0.3	76
MMB	1.17	15	7.78	3	3.09	34	5.62	78	-0.3	28
MSR	–	1	–	0	–	0	–	0	–	0
MTU	0.07	8	4.51	10	3.25	2	3.70	3	-0.1	9
PAG	0.56	15	0.13	11	1.06	51	2.20	117	0.2	49
PLD	1.64	15	1.23	7	-1.80	37	-3.11	90	0.3	37
PPE	1.03	7	0.72	6	–	0	–	0	-0.2	5
PSN	-0.68	15	-0.81	13	1.06	38	2.01	89	0.1	45
PVL	1.78	12	1.61	8	-2.42	112	-2.13	118	0.0	114
RZN	-0.47	15	1.35	7	0.04	37	0.81	73	-0.1	45
SOF	1.27	8	3.67	8	–	0	–	0	–	0
TLB	0.26	10	1.08	10	-0.79	77	-0.95	97	0.0	85
VRI	1.80	14	0.77	6	1.35	4	7.26	5	-0.2	13
VTS	-0.62	15	1.72	13	0.21	47	1.28	119	-0.3	46

Figure 4 shows a positive correlation for P waves, with a slope of approximately 30° (neglecting stations PLD and PVL). The linear correlation indicates that the station corrections reflect the whole path effects, and the site conditions give only the spread around the linear trend. On the other hand, the fact that the slope is different of 45° indicates that arrival time readings for different wave branches were performed. Moreover, the station corrections for the smaller events are larger than for the stronger ones, suggesting that later phases were identified as first arrivals in the former case (such as Pg instead of Pn). Although the location program interprets all input data as first arrivals, the misinterpretation of P waves for some stations in the case of small events does not bias the final locations: different station corrections were used for small and moderate events. On the contrary, in the case of S waves (Figure 4), the same phase was generally identified in all cases. The difference of about 1s. between the two sets of station corrections is considered to be due to the identification error, a value which seems reasonable for S waves of very shallow earthquakes.

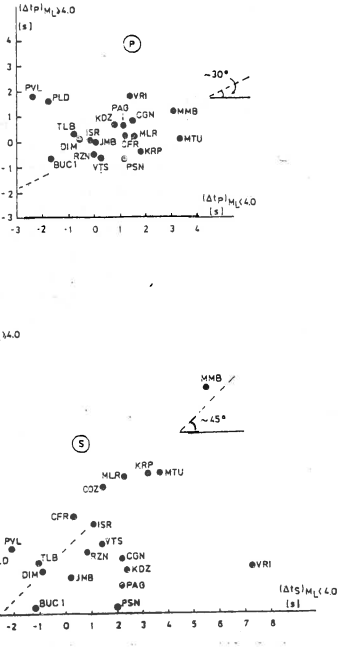

Fig.4
Dependance of P-wave and S-wave travel time station corrections for events with $M_L \geq 4.0$ versus those with $M_L < 4.0$.

The dashed lines in Figure 3, denoted by F_1 and F_2, are suggested by the lineation of epicenters. F_1 and F_2 could be interpreted as a first and second order faults, respectively, as indicated in this region by Boncev et al. (1982) and shown in Figure 1.

One drawback of our procedure is the fact that the two joint locations, corresponding to the two magnitude ranges, are not directly comparable since they were obtained separately. A shift of several kilometers is possible between the two clusters of events. As a tentative, looking at Figure 3 and taking into consideration the orientation of the Pre-Balkan Fault (F_1) in this region, we suggest that all moderate events should be shifted by about 5 km. towards SE relative to their present locations. Figure 5 presents vertical projections of hypocenters of events with $M_L \geq 4.0$ on planes oriented W-E and S-N, both passing through point P of coordinates 43.15°N and 25.90°E. They emphasize that these earthquakes, with the exception of event K (however, with the greatest depth error), generally occurred on a fault plane roughly striking southward and dipping 45° eastward. That makes us to assume the existence of a roughly N-S oriented secondary fault, denoted by F_3 in Figure 4. It follows that the two sequences would have been able to take place at the intersection of F_1 and F_2 faults with F_3, in spite of an insufficient geological evidence of the last one.

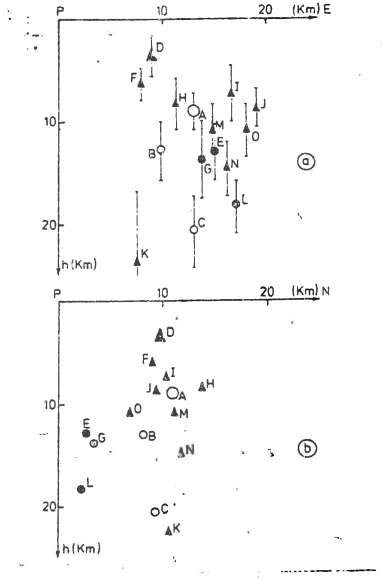

Fig. 5
Projections of $M_L \geq 4.0$ hypocenters on vertical planes oriented a) W-E, and b) S-N. Bars in a) indicate depth standard errors. Open circles denote February sequence; full circles and triangles denote December sequence. Larger symbols correspond to the main shocks.

FINAL REMARKS

The joint use of the Bulgarian and Romanian telemetered seismic networks offered the possibility to include all epicenters within the final network.

The two national networks have their own time-base; if the two clocks at the two Recording Centers in Sofia and Bucharest were

not syncronized at the time of the investigated seismic sequences, the time difference is absorbed in the station corrections obtained with the JHD method, so that the joint network behaves like a single network with a unique time-base. This means that the arrival time errors are due only to reading errors.

The use of travel time station corrections given in Table 2 enables one to individually locate other events from Strajitza region with high accuracy; an inprovement in earthquake locations is expected even if only one national network is used together with the appropriate station corrections. The largest positive station corrections for both P and S waves belong to BRD station, which is known to be situated on 17 km. thick layer of sediments with low velocities (see Oncescu,1984). Magnitude station corrections (to be added to station magnitudes) were also determined for the whole data set consisting of 137 events. An "ad-hoc" inspection shows that stations with high magnifacations (such as CVO,KRP,MLR, MMB and VTS) have large negative corrections,as expected.Of course, different quality factors along the ray path could also contribute to the magnitude correction values.

The joint use of Bulgarian and Romanian seismic data permetted to emphasize the activated faults in the vicinity of the town of Strajitza. If F_1 and F_2 faults (see Figure 1) are suggested by the alignment of epicenters and are supported by tectonic models of the region (Boncev et al.,1982), the F_3 fault is invoked in this study to explain the eastward dipping of hypocenters in Figure 5a. Generally the assumed F_3 fault is oriented N-S and has an average dip of 45°.

The above considerations make us believe that the February sequence occurred at the intersection of the F_1-F_3 faults. While the December sequence took place at the intersection of F_1-F_3 faults and than slightly moved towards the intersection of F_2-F_3 faults.

This study clearly showed that the use of a large amount of data, under appropriate processing methods, can significantly increase the retrieved information,in comparison with single-event studies.

REFERENCES

Boncev Ek., et al.,1982. A method for compilation of seismic zoning prognostic maps for the territory of Bulgaria. Geologica Balcanica,12,3-48

Frohlich C.,1979. An efficient method for joint hypocenter determination for large groups of earthquakes. Computers and Geosciences,5,387-389

Lee W.H.K., et al.,1972. A method of estimating magnitude of local earthquakes from signal duration.USGS Open-File Report,Menlo Park,California,28p.

Oncescu M.C.,1984. Deep structure ofthe Vrancea region,Romania inferred from simultaneous inversion for hypocenters and 3-D velocity structure. Ann. Geophysicae 1,23-28

Oncescu M.C., Trifu C.I.,1987. A large seismic sequence on April 27-29, 1986 in Vrancea foredeep, Romania. St. cerc. geol. geofiz. geogr.,Geofizica,25,88-97

SOME ASPECTS OF EARTHQUAKE HYPOCENTERS DETERMINATION AND SEISMIC NETWORKS ESTIMATION

Dimcho Solakov
Geophysical Institute, BAS, Sofia, Bulgaria

ABSTRACT

Some features of the function minimized at earthquake hypocenters determination have been analyzed. The existence of local minima different from the absolute one has been numerically presented.

An algorithm of absolute minimum determination and a method of seismic networks estimation have been presented.

INTRODUCTION

The hypocenter parameters are determined mainly using Geiger's method (Geiger 1910). The enlarged application of that method after 1960, was ensured by the introduction of computer techniques into seismological practice. After that a lot of algorithms for the hypocenter determination based on Geiger's method have been developed (Bolt 1960, Engdahl and Gunst 1966, Flinn 1960, Epifansky and Kushnir 1983).

AN EXPOSITION OF GEIGER'S METHOD

A set of n observations $t_1, t_2, \ldots, t_n$ with known standard deviations $\sigma_1, \sigma_2, \ldots, \sigma_n$ are given. Let $w_1, w_2, \ldots, w_n$ are arbitrary weights chosen to satisfy the equations: $w_i = \frac{1}{\sigma_i^2}$ $(i=1, \ldots, n)$. The model parameters $x_1, x_2, \ldots x_m$ $(m < n)$ are determined to minimize the following function

$$(1) \qquad \Phi(x_1, x_2, \ldots, x_m) = \sum_{i=1}^{n} w_i (t_i - f_i(x_1, x_2, \ldots, x_m))^2 .$$

where f_i is the theoretical expression for the i-th observation. The minimization is carried out using the non linear Least Square Method (LSM). In our case the function (1) can be written as:

$$(2) \qquad \Phi(\varphi, \lambda, h, T_o) = \sum_{i=1}^{n} w_i (T_i - t(\Delta_i, h) - T_o)^2$$

where (φ, λ, h) are hypocenter coordinates (Geocentric or Cartesian), To - origin time, $t(\Delta, h)$ travel time function, Ti - arrival times, Δ_i - epicentral distances.

Essentially the earthquake location is an inverse problem. The solution of such problems can be divided into two stages:

- Minimization - the process of obtaining minimum. Examples for wrong hypocenter locations based on a small number of observations are given by James et al. (1969). The wrong hypocenter location is due to the existence of more than one local minima of function (2).
- Evaluation - the solution obtained is a random variable due

to the random observation errors, and therefore it should be evaluated.

THEORETICAL CONSIDERATIONS

The objective of this paper is to study the function (2). The problem of uniqueness of the solution will be treated. Only initial P (or S) arrival times will be used in the investigation.

Let us assume an arbitrary wave source with coordinates (a,b,c) To- the beginning of emission, and propagation law t(x,y,z,a,b,c). The time function will be

$$T(x,y,z) = f(x,y,z,a,b,c) + T_o$$

Let $X_1 = (x_1, y_1, z_1)$ and $X_2 = (x_2, y_2, z_2)$ are two arbitrary points, and d is an arbitrary constant, for which the surface:

$$g(x,y,z) = f(X, X_1) - f(X, X_2) - d = 0$$

exists. Thus if the emission begins at time To, at point X_1 the time function on the surface $g(x,y,z) = 0$ will be

$$T_f(x,y,z) = t(X, X_1) - T_o = t(X, X_2) + T_o + d$$

The time function $T_f(x,y,z)$ is the same at point X_2 with emission at a time To+d. So, if the time function only over that surface is known, two solutions for the source determination problem exist. Particularly: for every two points of the Earth, a configuration of arbitrary number of stations exists, for which the hypocenter determination problem could not be unique (two zeros of function (2) exist).

Let's consider the function

$$\Phi^*(\varphi, \lambda, h) = \min_{T_o} \Phi(\varphi, \lambda, h, T_o)$$

It can be easily proved that:

$$\Phi^*(\varphi, \lambda, h) = \sum_{i=1}^{n} (T_i - t(\Delta_i, h) - \sum_{j=1}^{n} (T_j - t(\Delta_j, h))/n)^2$$

(The solution of the equation $\partial\Phi / \partial T_o = 0$ is $\sum_{j=1}^{n} (T_j - t(\Delta_j, h))/n$)

It will be proved that it is possible, the function Φ^* to possess a local maximum at the point with coordinates of the nearest station (φ_1, λ_1) (concerning the epicenter) at a fixed depth equal to zero. The function $\Phi^*(\varphi, \lambda, 0)$ can be written as follows:

$$\Phi^{*}(\varphi,\lambda,h) = \sum_{i=1}^{n}(\delta t_i - f_i(\varphi,\lambda) - \sum_{j=1}^{n}(\delta t_j - f_j(\varphi,\lambda))/n)^2$$

where $\delta t_i = T_i - T_1$, $f_i(\varphi,\lambda) = t(\Delta_i) - t(\Delta_1)$, Δ_i - epicentral distance to the i-th station. In each arbitrary fixed direction with respect to point (φ_1,λ_1), $f(\varphi,\lambda)$ will be a function of Δ_1 only. Thus the equation

$$df_i / d\Delta_1 = dt / d\Delta|_{\Delta_i} \cos\alpha_i - dt/d\Delta|_{\Delta_1}$$

will be satisfied, where α_i depends on the fixed direction and Δ_1. If $x_k(\Delta_1) = \delta t_k - f_i(\Delta_1)$ and $c_k(\Delta_1) = dx_k/d\Delta_1$, then the Taylor's series expansion of $\Phi^*(\Delta_1)$ at the point $\Delta_1 = 0$ is

$$\Phi^{*}(\delta\Delta_1) - \Phi^{*}(0) = 2\sum_{k=1}^{n}(x_k(0) - \sum_{j=1}^{n} x_j(0)/n)c_k(0)\delta\Delta_1 + 0(\delta\Delta_1^2)$$

If $d^2t/d\Delta^2 \geq 0$ /h=0/ is satisfied, then $df_i/d\Delta_1 \leq 0$, $c_i(\Delta_1) \geq 0$. Assuming that

$$x_k(0) - \sum_{i=1}^{n} x_i(0)/n \leq 0 \qquad (3)$$

for $k \neq 1$, and since $c_1(0)=0$, it follows that

$$\Phi^{*}(\delta\Delta_1) \leq \Phi^{*}(0)$$

for sufficiently small $\delta\Delta_1$. It is satisfied for each fixed direction. Thus if inequality (3) is satisfied, Φ^* will have a maximum at point (φ_1,λ_1). An example for such maximum at a constant propagation velocity (5km/s) is given in Figure 1.

NUMERICAL RESULTS

The above considered theoretical points show the possibility of the existence of more than one local minima of the function (2). Usually the coordinates used as a first approximation are either the coordinates of the geometrical center of the network, or these of the first arrival time station. What we are interested in are those local minima which can be obtained by the above mentioned first approximations. The curves $\Phi^*(x,y,0) = \text{const}$ are plotted for a number of configurations of seismic stations and epicenters. The purpose is to trace out the general tendency in the minimized function behaviour. In Figure 2 is shown the behaviour of the function Φ^* at a specific set of stations and an epicenter situated out of it. The local minimum inside the network is also visualized

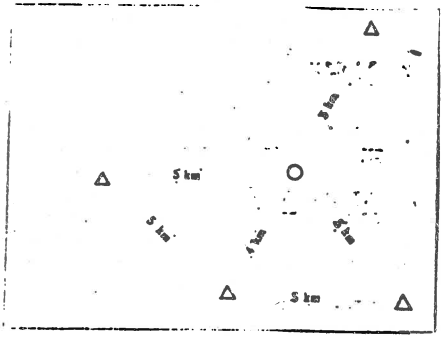

Figure 1. An example of local minimum at the point with the coordinates of the first arrival time station.

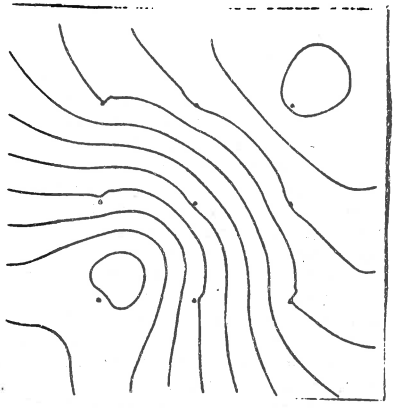

Figure 2. An example of local minimum, different from the absolute one.

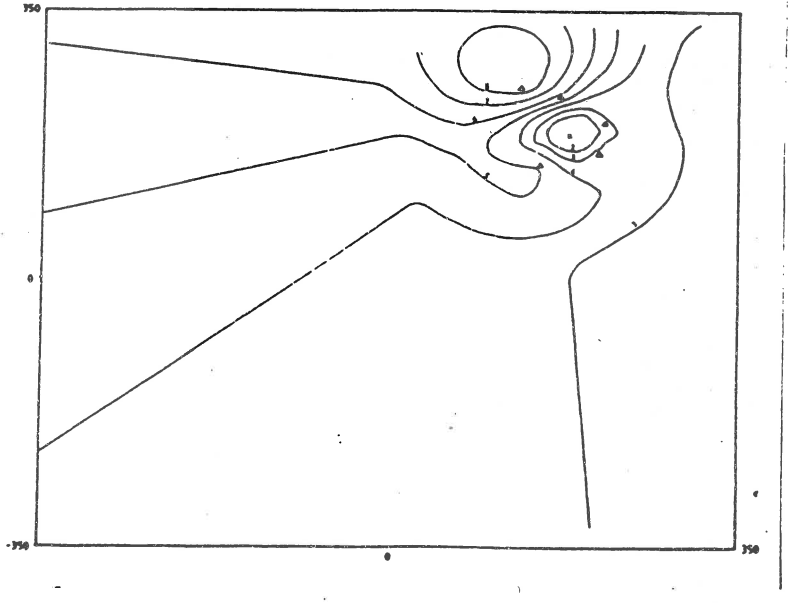

Figure 3. Minimized function behaviour for a fife stations network and epicenter inside it (Δ - station, x - epicenter).

there. The function behaviour for epicenter inside the network (5 stations) is shown in Figure 3. The function decreases in the direction opposite to the epicenter, close to the network. Figure 4 shows the function behaviour in the neighbourhood of the first arrival time station.

The solution obtained by minimization of the function $\Phi(\varphi, \lambda, 0, To)$ has been studied. Random seismic networks have been generated in a square 100x100 km. Theoretical J-B travel times have been calculated for each epicenter in a square 450x550 km , formed by steps of 10 km in x and y directions. For epicenter locations Geiger's method has been applied. As a first approximation the coordinates of the first arrival time stationhave been used. In Figures 5 and 6 are shown two different configurations. When the epicenter is out of the closed curves a wrong solution (local minimum different from the absolute one) is obtained. In many cases the solution obtained is inside the network. Often the local minimum values are around zero. It is essential from a statistical point of view, for in such cases the wrong solution obtained is statistically acceptable.

The same investigations have been performed at a constant propagation velocity. Rather different results have been obtained. It is to be noted that wrong solutions have been obtained only in rare cases. The result is the same when the kind of the first P arrival (Pg,Pb,P) is pointed out and the calculations have been made using the corresponding travel time curves.

Considering that : $X_o = (\varphi_o, \lambda_o, h_o, To_o)$ is a local minimum and $\Phi(\varphi_o, \lambda_o, h_o, To_o) = a_o$, the following algorithm could be used for finding out other local minima.

1. $j=0$
2. $i=0$
3. $To_j = To_j + i\,\delta To$
4. Minimization of $\Phi(\varphi, \lambda, h, To)$ with $To = To_j^i$ restrained.
5. If the minimum obtained is $a_j^i \leq a_j$ - GOTO 7; if not GOTO 6
6. If $i > 1$, as an absolute minimum is accepted X_j ; if not $i=i+1$ GOTO 3
7. Minimization of $\Phi(\varphi, \lambda, h, To)$ with initial iteration $\varphi_j^i, \lambda_j^i, h_j^i, To_j^i$.
   As a result a local minimum $X_{j+1} = (\varphi_{j+1}, \lambda_{j+1}, h_{j+1}, To_{j+1})$ and $\Phi(X_{j+1}) = a_{j+1}$ are obtained.
8. $j=j+1$
9. If $j \leq n$ and $a_j < a_{j-1}$ GOTO 2.
10. X_{j-1} is accepted as an absolute minimum.

It is necessary δTo, 1 and n to be initially involved. This algoritnm was applied to the examples adduced to Figures 5 and 6.

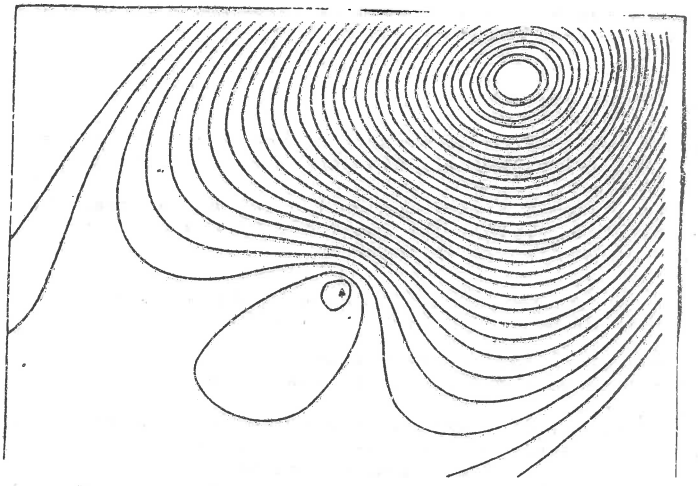

Figure 4. The minimized function behaviour around the first arrival time station

a

b

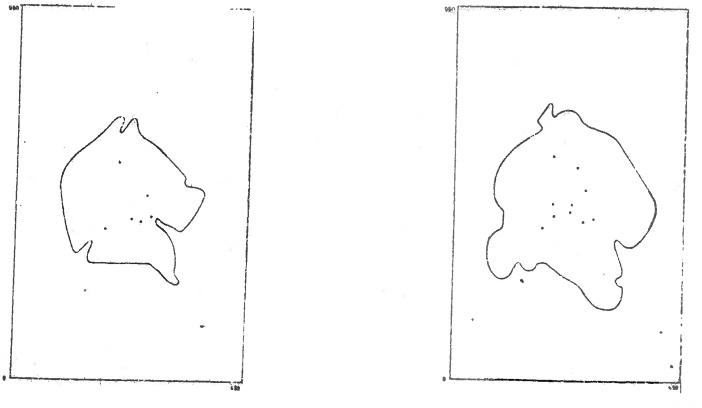

Figure 5. Areas (outside the closed curves) for which a wrong local minimum is reached at arbitrarily chosen network of: a) - six stations, b) - ten stations

In all cases the absolute minimum was reached appling the algorithm at $\delta To = 2s$, $l=5, n=1$.

SEISMIC NETWORK ESTIMATION

A method for estimation of seismic networks will be presented. Let us take a set of n seismic stations with coordinates (x_i, y_i) $i=1, \ldots, n$, travel time function $t(\ ,h)$ and a model hypocenter with coordinates (x,y,h). The equations of the hypocenter location errors can be written as follows:

$$e_i = \frac{\partial t}{\partial \Delta}\frac{\partial \Delta}{\partial x}\Big|_{\Delta_i}\delta x + \frac{\partial t}{\partial \Delta}\frac{\partial \Delta}{\partial y}\Big|_{\Delta_i}\delta y + \frac{\partial t}{\partial h}\Big|_{\Delta_i}\delta h + \delta t$$

where: i - index number of each station
e - observation error of arrival time
$\delta x, \delta y, \delta h, \delta t$ - errors of hypocenter location and origin time

The following assumptions were initially accepted:
- the errors $\delta x, \delta y, \delta h, \delta t$ are small
- e_i are Gaussian distributed with mean value 0, and standard deviation σ_i .

Under these assumptions LSM may be used for an estimation of δx, δy, δh and δt. The joint distribution of δx and δy will be:

$$F(x_0,y_0) = \int_{-\infty}^{x_0}\int_{-\infty}^{y_0} e^{-\frac{1}{2}\left(\frac{x^2}{\sigma_1^2} - \frac{2\rho}{\sigma_1\sigma_2}xy + \frac{y^2}{\sigma_2^2}\right)} \Big/ 2\pi\sigma_1\sigma_2(1-\rho^2)^{1/2}\,dx\,dy$$

where

$$\sigma_1^2 = a_{11}\ ,\quad \sigma_2^2 = a_{22}\ ,\quad \rho = a_{12}/\sigma_1\sigma_2\ ,\quad \|a_{ij}\| = [C^T C]^{-1},$$

$$c_{i*} = \left(\frac{\partial t}{\partial \Delta}\cdot\frac{\partial \Delta}{\partial x}\Big|_{\Delta_i}, \frac{\partial t}{\partial \Delta}\cdot\frac{\partial \Delta}{\partial y}\Big|_{\Delta_i}, \frac{\partial t}{\partial h}\Big|_{\Delta_i}, 1\right)$$

Then the mean value $E(\delta r)$ of $\delta r = (\delta x^2 + \delta y^2)^{1/2}$ will be

$$E(\delta r) = \left[2\pi\sigma_1\sigma_2(1-\rho^2)^{1/2}\right]^{-1}\int_{-\infty}^{\infty}\int_{-\infty}^{\infty}(x^2+y^2)^{1/2}\, e^{-\frac{1}{2}\left(\frac{x^2}{\sigma_1^2} - \frac{2\rho}{\sigma_1\sigma_2}xy + \frac{y^2}{\sigma_2^2}\right)}\,dx\,dy$$

And after transformations it becomes as follows:

$$E(\delta r) = \left(2/\pi\right)^{1/2}\int_0^{\pi/2}(a^2\cos^2\theta + b^2\sin^2\theta)\,d\theta\ ;\quad ab = \sigma_1\sigma_2(1-\rho^2)^{1/2},\ a^2+b^2 = \sigma_1^2+\sigma_2^2$$

The integral

$$\iiint_V E(\delta r)\,dx\,dy\,dh$$

can be used as an estimation of seismic network accuracy if the expected hypocenters are in a volume V. That integral can be treated as a criterion for the best location of new stations.

CONCLUSIONS

1. Let X and Y are two arbitrary points of space,treated as points of emission. A surface exists for which the time field is the same for these two points at properly selected initial times of emission.
2. A configuration of seismic stations and hypocenter exists for which the function (2) has a maximum at the point with the coordinates of the first arrival time station at a fixed depth h=0.
3. As it is shown numerically for different configurations the function (2) has local minima, different from the absolute one.

REFERENCES

Bolt B.,1960, The revision of earthquake epicenters, focal depths and origin times using a high speed computers. Geophys. J., R. Astron. Soc., 3, 433-440

Engdahl E.,R.Gunst.,1966, Use of high speed computers for the preliminary determination of earthquake hypocenters., BSSA, 56, 325-336

Epifanski A.,G.Kushnir.,Opredelenie parametrov ochagov lokalnih zemletresenii v aftomatizirovannoi sisteme prognoza zemletresenii SVK ASPZ, Algoritmi i practika opredelenia parametrov gipocentrov zemletresenii na EVM. Metodicheskie raboti ESSN. M., 1983

Flinn E.,1960, Local earthquake location with an electronic compute BSSA,50, 467-470.

Geiger L.,1910, Herdbestimung bei Erdbeden aus den Ankunftzeiten, K. Gessel, Wiss.Goett.,4,331-349

James D. et al.,1969, On locating local earthquakes using small networks, BSSA,59,1201-1213.

AFTERSHOCK AREA DISTRIBUTION BEHAVIOR IN TIME, SPACE AND ENERGY DOMAIN - THE DECEMBER 1986 STRAZHITZA SEQUENCE

Borislav G. Dimitrov - Geophysical Institute
Chavdar T. Dobrev - Geophysical Institute
Konstantina H. Donkova - Geophysical Institute

Since the aftershock activity of major earthquakes varies in pattern depending on the complex region properties - no law fully explaining the mechanism of aftershock occurence has been established yet. Nevertheless, exploring the space, time and energy distribution of the aftershocks a common expansion pattern for the region could be outlined and, thus, some important conclusions for the mechanical properties of that same region could be provided. As shown by Mogi[1967/8], while in Tokachi-oki region the aftershock pattern of a major event expands widely, the large earthquakes in Alaska and Rat Islands do not cause much extended afterchock area. The former was estimated to be an episodic rupture propagation where single rupture tips interact with some mechanical inhomogenities corresponding to geological features and the latter were interpreted as a relative uniformity in strength indication for the region. Such different cases are considered to be associated with the fault-zone mechanical properties change in space and time. Investigating the seismogenic fault-zone inhomogenities we have examined the spatio-temporal-energetic variations of the aftershock activity caused by the December, 7, 1986 Strazhitsa earthquake. We have followed Mogi's approach as well as an extended state-of-the-art version produced by Tajima and Kanamori [1992].

The Aftershock Series

A sample of 166 events is used starting December 1986 and ending November 1987 with magnitudes $1.8 \leq M \leq 5.6$. All the events occurred in the Gorna Oriahovitza Seismic zone along the line Sevlievo-G. Oriahovitza-Popovo with entire length of about 110 km and width of approximatelly 70-80 km. The most active part of the zone is an extended "band" forming a seismo-lineament where earthquakes with magnitude up to 7.0 could be expected. Shallow earthquakes are typical for the zone - not deeper than 15 km are registered in the sample series. The fault-plane solutions obtained show both normal and reverse faulting with strike to dip component ratio varying from 4 ot 0.2 [Georgiev, Dimitrov, 1987]

The Aftershock Distribution Behavior

First the energy released was estimated as a function of magnitude after Riznitchenko [1976].

(1) $$\log E = 4 + 1.8 \times M$$

The energy domain was divided into 11 classes corresponding to the events number for a proper smoothing as shown by Brooks and Carruthers [1973].

(2) $$Nc = 5 \times \log Ne$$

where Nc is the number of classes and Ne is the number of events. The occurrence frequency of each class is plotted as a bargraph on Fig.1 - it is obvious that the events releasing energy about 10^7 J are most frequent. This fact is considered to be an indication for an existing predominant smaller dimension of the mechanical inhomogenities. Such an opinion is supported by Fig.2 where the spatial occurrence-frequency distribution is shown. In terms of Mogi's and Kanamori's studies mentioned above this widespread aftershock distribution corresponds to a fault zone with decreased strength properties and highly inhomogenions at least laterally. It could be easily seen on Fig.3 that the events radiated most energy are centered in the aftershock area. In order to fully understand and describe the aftershock distribution behavior the so-called "casement" approach was applied involving 4-D graphics by dividing two of the parameters into classes and showing the spatial distribution of each group of events corresponding to any range of the first parameter and the second one respectively. While using a 3-D spatial distribution the time or energy domain was used as fourth dimension. Thus, first Fig.4 was plotted - it shows the aftershocks depths distribution in space and time. A tendency of shallowing the hypocenters in time is clear and the right upper plot shows the entire expansion pattern (as on the following figures). Next we examined the magnitude (Fig.5) and the corresponding energy (Fig.6) classes behavior in space and time. For the former - on Fig.5 it was recognized that events with magnitude 2.0 to 4.0 were dominating after the first period of 133 days - this explained some deficiency of weak events during the same and next periods. That fact was considered to be a kind of an evidence for the existence of fault zone inhomogenities of proper size and strength. Such conclusions are in good correlation with the common geological consideration for the Fore-Balkan structural zone where the presence of longitudinal and diagonal faults determine the segmentary structure of the earth crust. Each individual block includes sedimentary rocks varying along with dimension, facies and thickness thus providing real evidences for the different in nature movements between any two. So-

me further exploration was needed to describe the aftershock hypocenter behavior depending on its magnitude(Fig.7) or corresponding energy(Fig.8). Fig.7 shows deepest events extended wider in space, expecially concernig the lower magnitude class - $M \leq 2.0$. A similar tendency could be seen on Fig.8 which shows also some lack of mid-energy events in the depth interval 10km to 15km. An at-a-glance comparison leads to a conclusion that the stronger the events were the more they tended to cocentrate in space thus supporting Mogi's and Kanamori's studies as well as the "barrier" approach introduced by Das and Aki [1977].

Conclusions

As it had already been mentioned above this study aimed putting the aftershock data under ivestigation into a proper type of distribution behavior in the time, space and energy domain. Strazhitza fault-zone which generated the main shock and the aftershock sequence is found now to be representing an episodic type of rupture propagation - the single ruptures, wide-spread in the zone, are due to that much splitted into individual blocks region as well as to the local mechanical inhomogenities. The result of this study proves almost all of the present geological considerations concernig the Fore-Balkan structure zone. The existence of fault-zone inhomogeneties of a predomining size corresponding to the more frequent magnitude values and their expansion seem to correlate with the real geological fetures.

Acknowledgements

The hypocenter locations and magnitude determinations were promptly provided through NOTSSI - Bulgaria (Seismological Dept., Geophysycal Institute, Bulg. Acad. Of Scinces) by individuals too numerous to be mentioned here. This work was aided by some very useful discussions with Prof. Dr. Ludmil Christoskov.

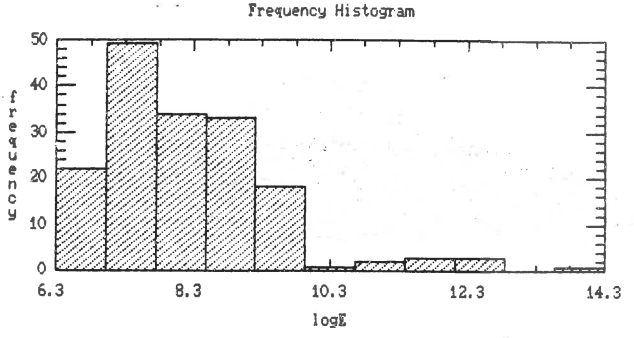
Frequency Histogram
frequency
50
40
30
20
10
0
6.3
8.3
10.3
12.3
14.3
logE

Fig 1

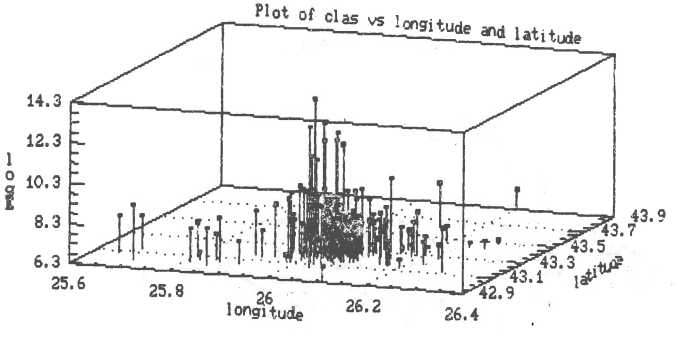
Plot of clas vs longitude and latitude
logE
14.3
12.3
10.3
8.3
6.3
25.6
25.8
26
26.2
26.4
longitude
42.9
43.1
43.3
43.5
43.7
43.9
latitude

Fig. 3

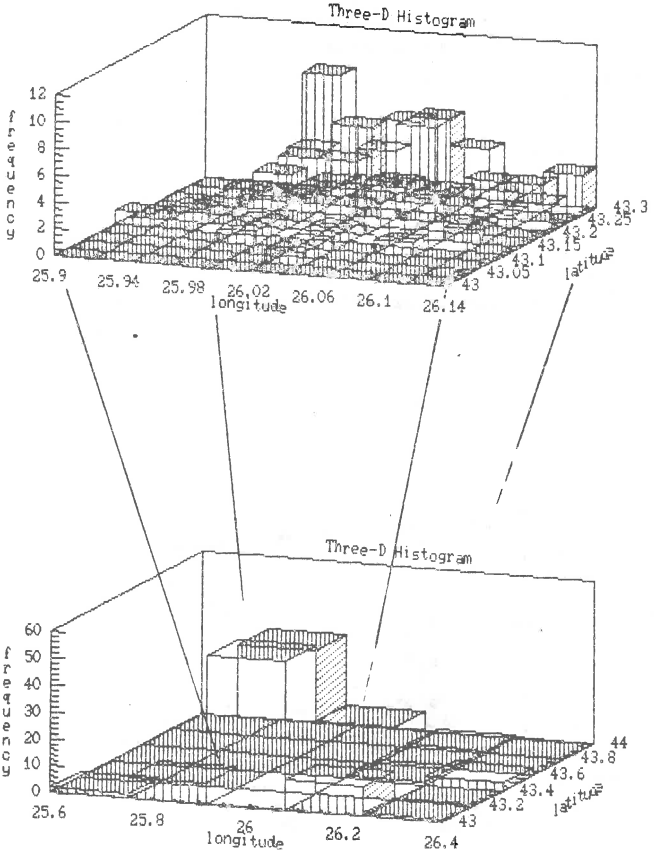
Three-D Histogram
frequency
12
10
8
6
4
2
0
25.9
25.94
25.98
26.02
26.06
26.1
26.14
longitude
43
43.05
43.1
43.15
43.2
43.25
43.3
latitude
Three-D Histogram
frequency
60
50
40
30
20
10
0
25.6
25.8
26
26.2
26.4
longitude
43
43.2
43.4
43.6
43.8
44
latitude

Fig. 2

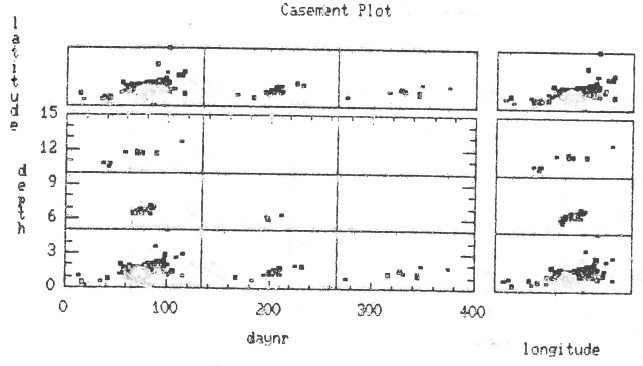
Casement Plot
latitude
depth
15
12
9
6
3
0
0
100
200
300
400
daynr
longitude

Fig. 4

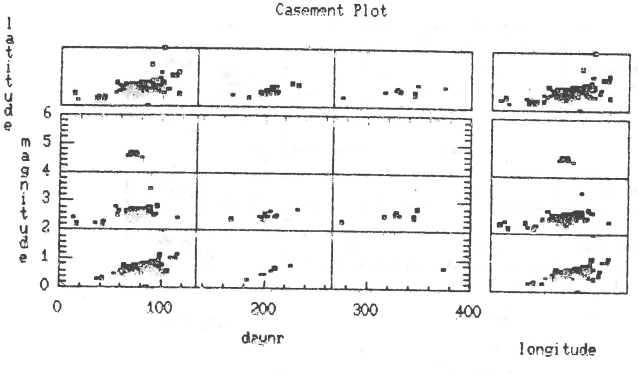
Casement Plot
latitude
magnitude
6
5
4
3
2
1
0
0
100
200
300
400
daynr
longitude

Fig. 5

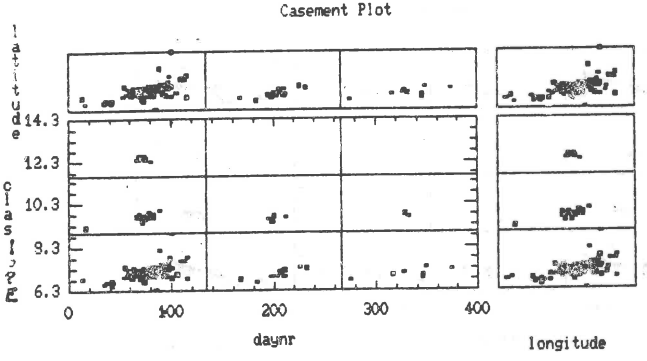
Casement Plot
latitude
classic
14.3
12.3
10.3
8.3
6.3
0
100
200
300
400
daynr
longitude

Fig. 6

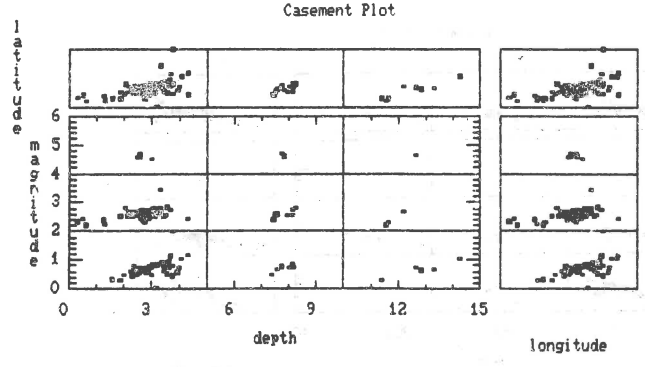
Casement Plot
latitude
magnitude
6
5
4
3
2
1
0
0
3
6
9
12
15
depth
longitude

Fig. 7

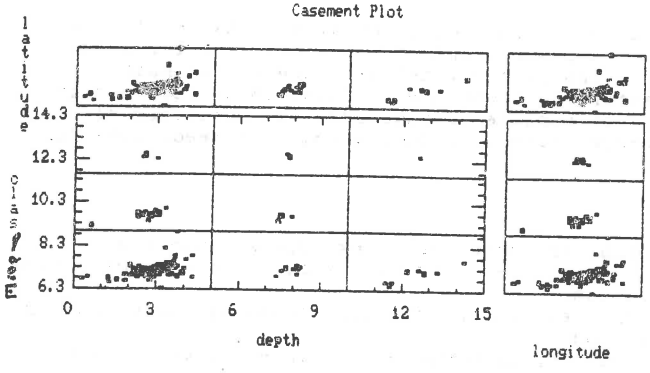
Casement Plot
latitude
14.3
12.3
10.3
8.3
6.3
0
3
6
9
12
15
depth
longitude

Fig 8

ABSTRACT

Some new aspects for investigation of aftershock series are given, using a PC and 4-D graphics\ as a new tool for such a study. Straznitza fault-zone which generateted the main shock and the aftershock sequence is found to be representing an episodic type of rupture propagation. The existence of fault-zone inhomogenities of a dominating size needs some further evidences.

FIGURE CAPTURES

Fig.1. Aftershocks' frequency vs energy class histogram.
Fig.2. Aftershocks' occurence frequency bargraph - twice scaled lateral distribution.
Fig.3. Aftershocks' epicenters and corresponding energy realesed lateral distribution.
Fig.4. Aftershocks' depths distribution in space and time - each pattern shows a lateral distribution for corresponding time and depth intervals. The day number (daynr) and the depth are divided into 3 intervals. The coordinates correspond to Figs.2,3.
Fig.5. Aftershock's magnitude space and time distribution - each pattern shows a lateral epicenter distribution for the corresponding time ("daynr" is the day number) and magnitude intervals for the coordinates observed.
Fig.6. Aftershock's energy space and time distribution - each pattern shows a lateral epicenter distribution for the corresponding time and energy intervals.
Fig.7. Aftershock's hypocenter behavior depending on it's magnitude - each pattern shows a lateral epicenter distribution for the corresponding depth and magnitude intervals.
Fig.8. Aftershocks' space and energy distribution - each lateral pattern corresponds to proper depth and energy intervals.

STUDY OF RECENT SEISMICITY IN THE COASTAL REGION OF CATALONIA

(western Mediterranean area)

T. Susagna[1,2], C. Olivera[1], A. Muñoz[1], A. Roca[1]

[1] Servei Geològic de Catalunya, D.P. i O.P., Generalitat de Catalunya, Diputació,92, 08015 Barcelona.

[2] Observatori Fabra.Reial Acadèmia de Ciències i Arts.Rambla dels Estudis,115, 08002 Barcelona.

Introduction.

The area of this study is the coastal region of Catalonia, which is located at the northeast portion of the Iberian Peninsula (see fig 1).

Although the most seismically active areas of Catalonia are in the Pyrenees, small and moderate (I_o < VIII) earthquakes have occurred also in the coastal region in historical and instrumental times.

Since 1985 a great effort has been made to implement a regional network of short period seismic stations which now allows to study in more detail the seismicity of this region.

Seismic activity.

About 30 isoseismal maps for XX century events showing in-land maximum intensities ranging from IV to VII (MSK) are available. In fig 2 the epicenters of the period 1900-1976 calculated from isoseismal maps[1,2] are shown.Instrumental records have been used to determine the aproximate location for off-shore epicenters.

Local magnitudes of largest events were calculated from ancient seismograms recorded at Fabra Observatory (FBR) since 1907. The greatest M_L value obtained is 5.0.

The number and distribution of stations up to 1976 made not possible to carry out confident instrumental studies.Since 1977 and, furthermore, in the last three years the new seismographic equipment installed on the surrounding area(see fig 3) allows to take on detailed studies yielding to a better knowledge of the seismicity in this region. A map of epicenters in the period 1977-1987 determined from instrumental records[3,4,5,6] is presented in fig 4.

Study of the August 24, 1987 earthquake.

The August 24, 1987 earthquake is the largest event in the region which has been recorded in a relatively large number of stations. A more detailed instrumental study of this earthquake has then been possible; in particular the focal machanism has been obtained; this is the first mechanism calculated for an earthquake in this area. The epicenter of the main shock was located at 40º 56.6'N, 01º 34.0'E off-shore at about 30 km SW to Tarragona.

The main shock was felt in a large number of towns at distances up to 100 km from the epicenter. The Geological Survey of Catalonia and the Fabra Observatory sent macroseismic questionaries andresponses were obtained from 235 locations(see fig 5). The maximum in-land intensity observed is IV (MSK)

Two aftersocks, which were not felt by the population, were recorded. Magnitud M_D has been calculated; the obtained values are 4.2 for the main shock and 2.8 for the largest aftershock occurred on the 20 th of September. To have another estimation of the magnitude of the main shock Wood-Anderson synthetic record has been simulated from digital data obtained at station VAN (65 km W to the epicenter). The maximum amplitude reading on the simulated seismogram (fig 6) yields to a local magnitude M_L = 4.0. P and S wave spectra from the same record is shown in fig 7. The estimated moment is $M_o = 6.10^{20}$ dyn.cm.

The focal mechanism obtained from P wave directions on seismograms is presented in fig 8. Given that the azimutal distribution of stations is insufficient and that the nearest station is at epicentral distance of 60 Km then the focal depth is not very well determined. This fact together with the poor knowledge of the crustal structure in the area yields to a certain unaccuracy in the focal solution. However different crustal models have been used in differents tries to calculate the mechanism and all solutions give a reverse dip-slip movement with a strike-slip component and a N-S pressure axis almost horizontal. The directions of the two focal planes may both be in agreement with the two conjugate fault systems which can be observed in the geological map[7] (fig 1).

Final remarks.

The recent increment on number and quality of seismographic stations has made possible for the first time to calculate the focal mechanisms of an earthquake occured in the coastal region of Catalonia. This mechanism, shown in fig 9 together with other mechanisms computed for earthquakes in neighbouring areas[8,9,10,11,12], is compatible with the focal solutions of the two nearest off-shore events.

It should be emphazised that the calculated focal solutions are indicatives of a pressure regime, solutionns which are in contradiction with the extensional tectonic regime characteristic of the studied area during Neogene times.

The moderate magnitude (M_L 4) of these earthquakes and the complexity of this area do not allow to state a seismotectonic interpretation. However increasing data will hopefully yield in the future to a better knowledge of the dynamics of this western Mediterranean region.

REFERENCES

1 Sanchez-Contador, P. (1988): Sismicidad Catalana 1907-1987 y modelo de Q^{-1} en los Pirineos Orientales. Tesina de especialidad, Escuela Técnica Superior de Ingenieros de Caminos, Canales y Puertos, Univ. Politécnica de Cataluña.

2 Surlñach, E.; Roca, A. (1982): Catálogo de terremotos de Catalunya, Pirineos y zonas adyacentes. En: La Sismicidad de la zona comprendida entre 40ºN-44ºN y 3ºW-5ºE,NE Península Ibérica. Cát. Geofís.,Univ Complutense, Madrid, Publ.190, 9-106.

3 Butlletí de l'Observatori Fabra, 1977-1981, Barcelona.

4 Boletín de sismos próximos , Instituto Geográfico Nacional, 1982-1983, Madrid.

5 Bulletin des seismes proches, Lab. Détect. et Géophys., 1982-1983, Brunyers le Chatel.

6 Butlletí Sismològic de Catalunya, 1984-1987, Barcelona.

7 Anadon, P.; Colombo, F.; Esteban, M.; Marzo, M.; Robles, S.; Santanach, P.; Solé-Sugrañes,Ll.(1979) Evolución tectonoestratigráfica de los Catalánides, Acta Geol. Hisp.,14, 242-270.

8 Gallart, J.; Daignières, M.; Gagnepain-Beyneix, J.; Hirn, A. (1984): Relationship between deep structure and seismicity in the western Pyrenees, Ann. Geophys.,3(2), 239-248.

9 Gallart, J.; Daignières, M.; Gegnepain-Beneix, J.; Hirn, A.; Olivera, C. (1985): Seismostructural Studies in the Pyrenees: Evolution and Recent Results, Pageoph, Vol. 122, 713-724.

10 Nicolas, M.; Santoire, J.P. (1988): A comprehensive study of fault plane solutions for earthquakes in western Europe. Tectonic implication, EGS. Gen. Ass. Bologna.

11 Olivera, C.; Gallart, J.; Goula, X.; Banda, E. (1986): Recent activity and Seismotectonics of the Eastern Pyrenees, Tectonophsics, 129, 367-380.

12 Udias, A.; Espinosa, A.F.; Mezcua, J.; Buforn, E., Vegas, R.; Nishenko, S.P.; Martinez-Solares, J.M.; Lopez-Arroyo, A.(1986): Seismicity and tectonics of the north African-Eurasian plate boundary (Azores-Iberia-Tunisia), U.S. Geological Survey, Open File Report 86-626, Denver.

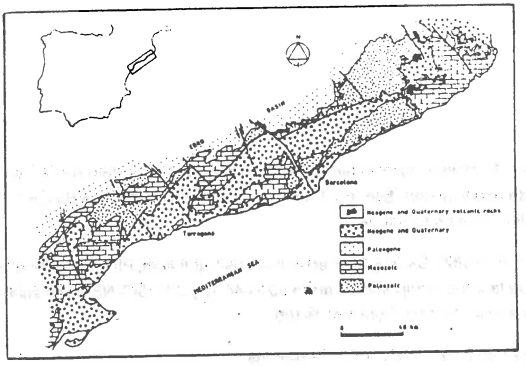

Fig. 1 : Geografical location and Geological sketch of the region of study.

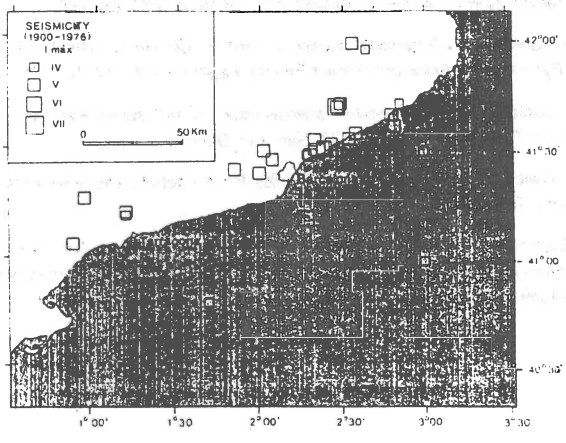

Fig. 2 : Epicenters 1900-1976 of earthquakes for which isoseismals are available.

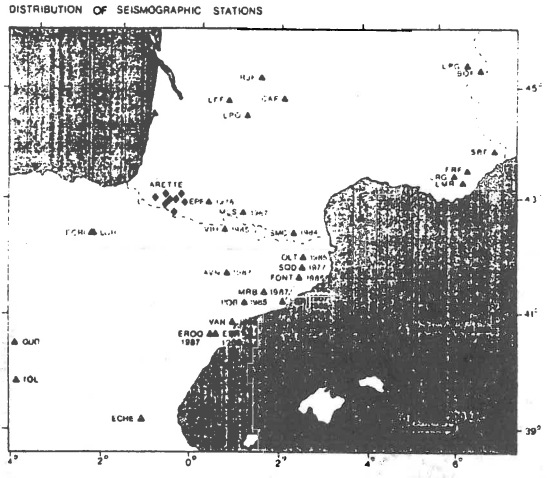

Fig. 3 : Distribution of seismographic stations. For the stations which are closset to the area of study years of installation are indicated.

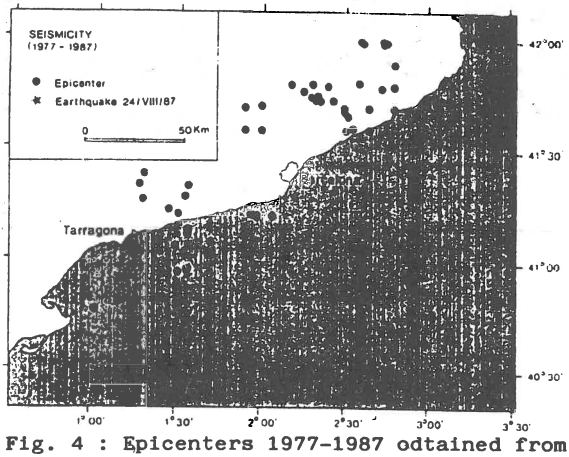

Fig. 4 : Epicenters 1977-1987 odtained from instrumental records.

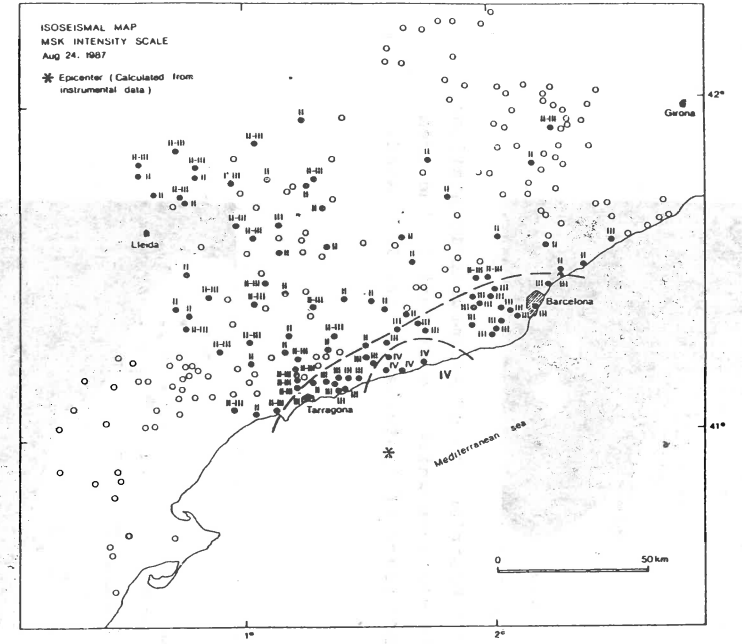

Fig. 5 : Isoseismal map (Aug 24, 1987 earthquake).

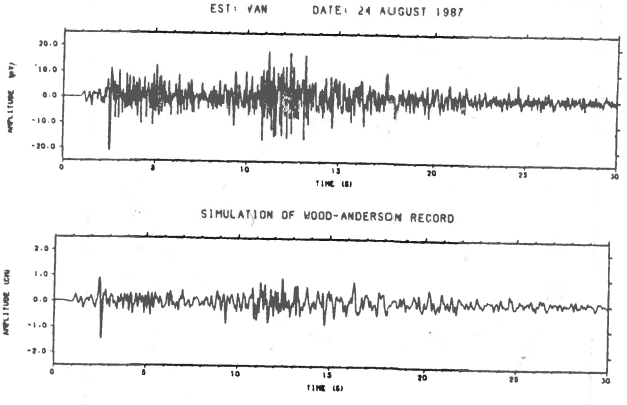

Fig. 6 : Record at digital station VAN (above) and Wood-Anderson simulated seismogram (down)

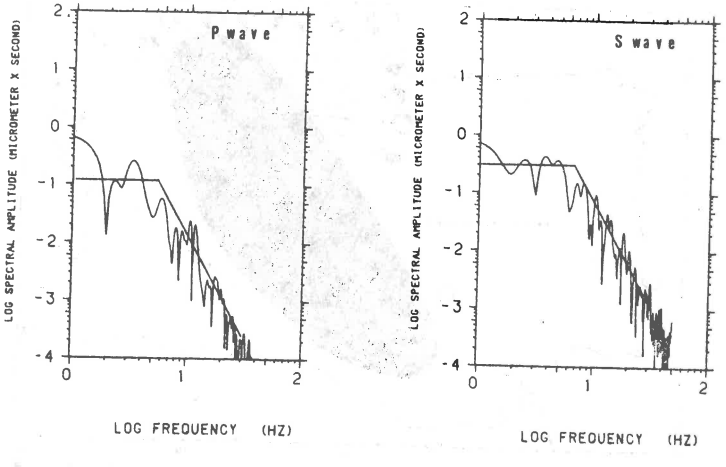

Fig. 7 : P and S wave spectra from digital record at station VAN

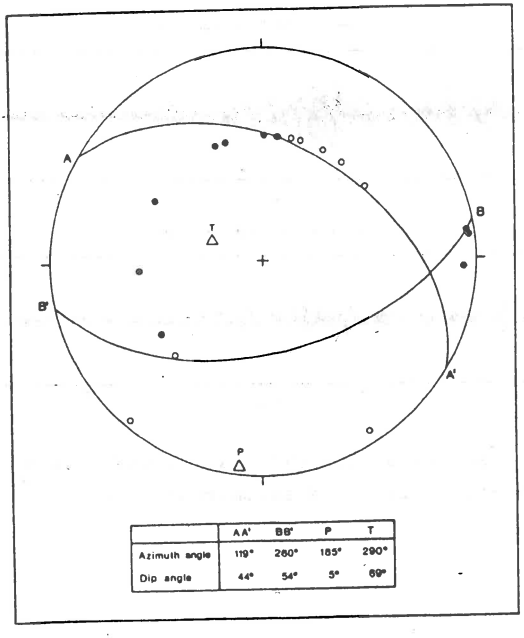

Fig. 8 : Focal mechanism (24.08.87)

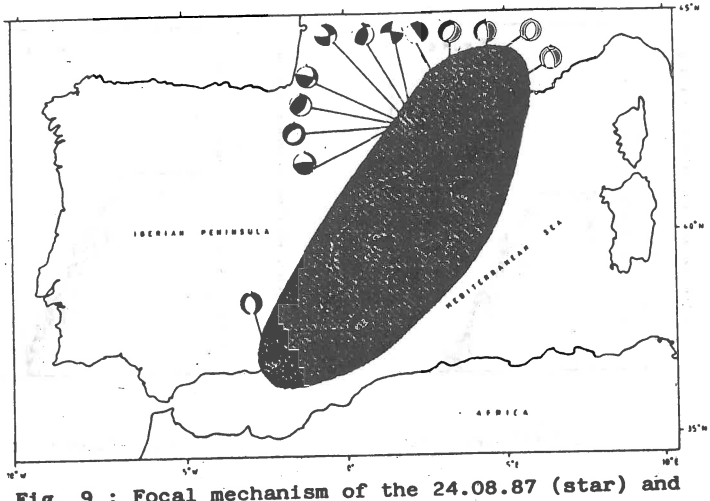

Fig. 9 : Focal mechanism of the 24.08.87 (star) and other solutions (black cercles) in the shading area.

SPECIFIC FEATURES OF AFTERSHOCK SEQUENCE OF EARTHQUAKE OF 15 AUGUST 1985 IN BERHIDA, HUNGARY

M.G.Bruk, N.V.Kondorskaya, E.A.Khrometskaya

Introduction

The earthquake of 15 August 1985 in the region of Berhida at the northern part of the Balaton, Hungary, is one of the strongest earthquakes that have recently occurred at the territory of Hungary. The epicentre of the earthquake was located in a rather active seismic region of the Pannonian basin. This significant event was accompanied by a large series of aftershocks, a part of which was well recorded by the world network of seismic stations.

The present report makes an attemp to locate precisely hypocentre parameters of both the main shock and the aftershocks that are well provided with seismic observations, and to carry out comparison of the aftershock area with the solution of the source mechanism of the main shock obtained on the basis of first onset signs of seismic waves, and with orientation of isolines of the macroseismic field.

Methods

More precise location of hypocentre parameters was performed with the modified joint hypocentre determination method (1).

ISC data were taken as a primary calibration event. Calculations were accomplished in two versions: 1) with the travel time curve calculated by DSS data (2); 2) with the standard Jeffreys-Bullen curve. The solution that resulted in more stable station corrections was considered optimal. Calculations were carried out

with a series of various sets of data. Stability and values of the station corrections obtained in different sets were regarded as criteria for choosing the optimal velocity model. The calculations showed that the most stable corrections are provided by the crust velocity model according to the Jeffreys-Bullen curve.

The material used: first onsets of P and S seismic waves from 60 seismic stations from the ISC Bulletin (3); more precise onsets from a number of seismic stations located near the epicentre were found on the basis of primary origin data - seismograms and station bulletins.

Results

Station corrections to the Jeffreys-Bullen curve on the basis of the aftershock series smoothed with a cubic spline are given in Fig. 1 a,b.

The curves of distribution density of residuals $f_1 = (T_{obs} - T_o) - T_{th} - S_{st}$ are shown in Fig. 2 a,b.

As seen from the diagrams of distribution curves for residuals and from calculation of confidence ellipses of errors with 90% confidence limits, accuracy of determination of basic hypocentre parameters is within the range of 5-10 km. Final estimates of basic epicentre parameters are given in Fig. 3.

Fig. 3 shows epicentres of the main shocks and the aftershocks As can be seen the whole sequence is located within a narrow strip about 10 km wide in the NNE-SSW meridional direction. The main shock is located in the southern part of the sequence.

More precise estimation of the depth of the main earthquake and the aftershocks was performed. The depth of the main earth-

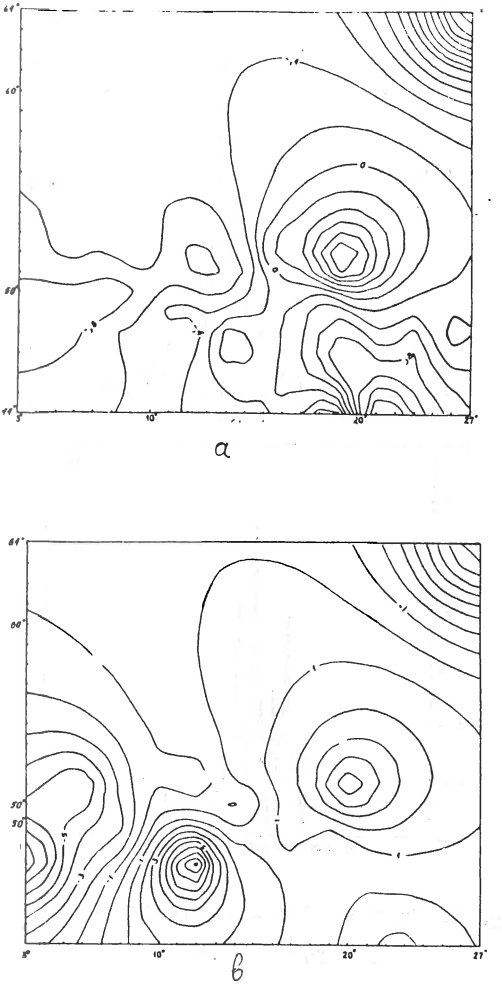

Fig. 1. Station corrections to the Jeffreys-Bullen curve

- isolines, values of the corrections

a - for P waves

b - for S waves

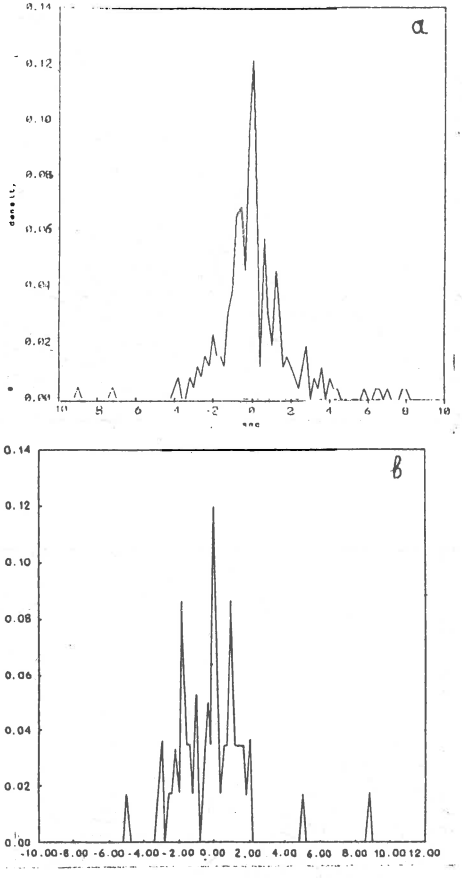

Fig. 2. Curves of distribution density of residuals

a - for P waves

b - for S waves

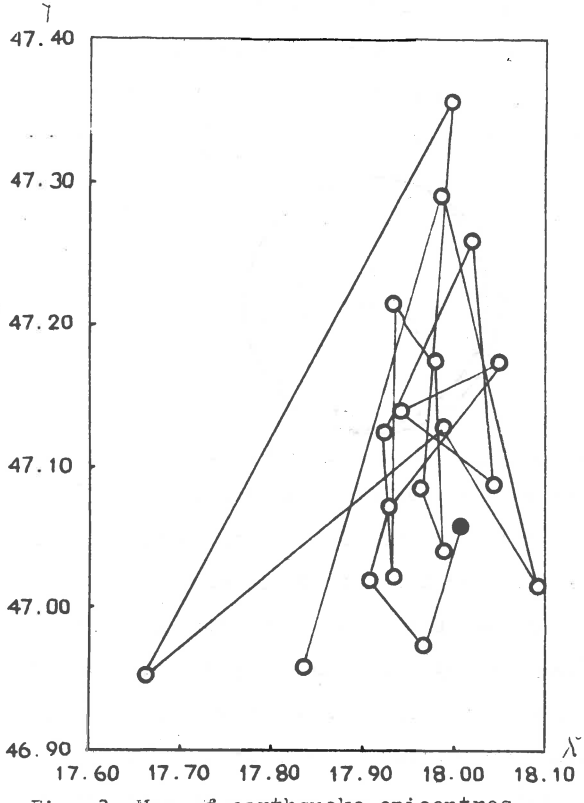

Fig. 3. Map of earthquake epicentres

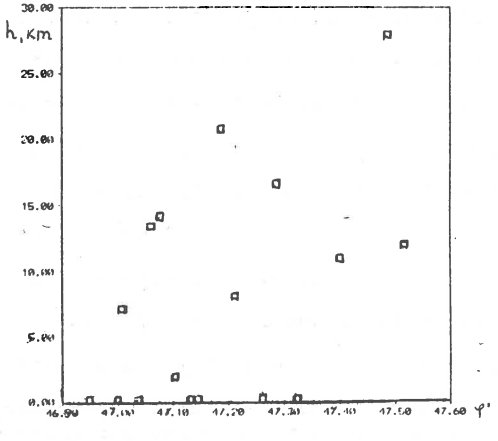

Fig. 4. Aftershock distribution by depth

quake refined with station corrections was stable within the range of 13-17 km. The aftershock depths lie in the range of 0-27 km. Fig. 4 shows a section in the meridional direction. One can see the hypocentres becoming deeper in the SW-NE direction.

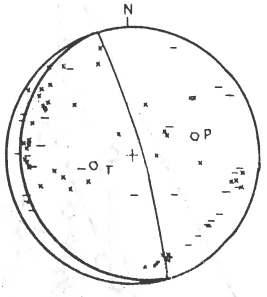

Fig. 5. Source mechanism (according to R.Klima's programme)

Fig. 5 shows the source mechanism. The area of the aftershock sequence gives grounds for the plane of the NNE-SSW direction to be regarded as the acting plane.

Analysis of the macroseismic map for the earthquake of 15 August 1985 compiled by T.Zirosh (Hungary) with additions by V.Brouchek (Czechoslovakia) allowed the following parameters to be obtained: λ°=18.12; φ°=47.10; h_I=20; h_{IM}=18; $\mathcal{I}$=7b.MS Macroseismic data from the map by T.Zirosh* are of rather mosaic character which impedes reliable plotting of isoseists.

Data obtained by V.Brouchek (Czechoslovakia)* at the territory of Slovakia make it possible to say that the isoseists look like isolones drawn along the direction of NNE-SSW. This is in good agreement with the direction of the aftershock sequence of the earthquake of 15 August and zones of active seismic fractures of the Pannonian basin. The aftershock zone of the earthquake of 15 August 1985 within the boundaries of $47^{\circ}.0$-$47^{\circ}.5$ n.l. and $18^{\circ}.0$-$18^{\circ}.5$ e.l. conforms with one of the most active seismic regions (within the same boundaries) at the territory of Hungary.

*) The data were kindly given by T.Zirosh and V.Brouchek

Conclusions

1. The joint hypocentre determination method in the study of the aftershock sequence of the earthquake of 15 August 1985 allowed much more precise estimation of hypocentre parameters; determination of directivity of the source process and the acting plane of the rupture; obtaining good agreement between results of the study and macroseismic data.

2. Resultant fields of station corrections to the Jeffreys-Bullen curve for P and S waves can further be used for more precise redetermination of hypocentre parameters of other earthquakes of the Pannonian region.

References

1. M.V.Kondorskaya, L.B.Slavina, M.G.Bruk. Near earthquake hypocentre determination: the accuracy problem. In press. 1988.
2. Sbornik trudov: Structure of the Earth's crust and the upper mantle of south-eastern Europe. Kiev:Naukova dumka, 1978, P.271.
3. ISC Bulletin, 1985. Newbury, Great Britain.

Some test results of seismometers of the EDS-2 family

Paper presented at ESC General Assembly in Sofia August 1988

STOLJAROV, O.A.; BREDNEV, S.P.; ELTEKOV, A.Y.
Institute for Physics of the Earth of the
Academy of Sciences of USSR, Moscow (IPE, M)

SCHMIDT, M.; BOHL, W.
Central Institute for Physics of the Earth of
the Academy of Sciences of the GDR,
Branch Jena (CIPE, J)

Moscow May 18 to 20, 1988

The EDS-2 family consists of three-compoonent sets of seismometers EDS-2 in different configurations depending on purposes of application

(i) seismometers without feedback with a free period adjustable between 4 s and 12 s especially for using at observatories and under field conditions

(ii) accelerometers by force-balanced feedback with a flat response from d. c. to 15 Hz for application in borehole seismometer systems.

The seismometer itself (mechanical sensor) has been designed as an inclined La COSTE seismometer by the Central Institute for Physics of the Earth of the Academy of Sciences of the GDR, Branch Jena. This principle offers several advantages in carrying out design, production, and adjustment as well as in operating, signal processing and data analysis. In Figure 1 a seismometer component is shown. For using this seismometer without feedback and under field conditions (in a wide temperature range) it was necessary to design a linear displacement transducer for measuring displacements of the seismic mass up to $\pm$ 2,5 mm. This problem was solved by implementing the difference oscillator principle (CIPE Jena). Figure 2 shows the electronic board of this transducer.
The seismometer system (version (i)) has been checked in different manners. Its behaviour against tilting of common baseplate is demonstrated in Figure 3. By using the motor-driven adjustments (zero position and free period) tiltings up to $\leq \pm 0{,}75^{o}$ can be corrected and nullified. The temperature response is shown in the next Figure (Figure 4). It has been proved that the seismometer can be operated in the wide temperature range of - 30 ^{o}C to + 40 ^{o}C without oroblems. The long-term stability is shown in Figure 5 (with permission of D. KRACKE, with CIPE Jena). This has been the last but not least proof for the following statement:
The mechanical sensor offers very good properties to apply it in seismometer systems planned for applications at observatories, in boreholes as well as under field conditiones.
The BODE diagram of a system without feedback is shown in Figure 6. Such a three component system had been installed at Moxa Observatory of CIPE in spring 1984. It has been operated excellently as a broad band seismometer since those time.
To improve linearity and instrumental noise - especially for borehole applications of the seismometer system EDS-2 - the version (ii) has been designed and tested in a very close and fruitful cooperation between CIPE and the Institute for Physics of the Earth, Moscow. Using a capacitive bridge transducer designed by this institute and closing the feedback loop an accelerometer (version (ii)) has been created. The principle of transducer used is shown in Fig. 7. The amplitude transfer characteristic is demonstrated in the next figure (Fig. 8).

Problems of stability has been investigated after occurring of parasitic resonances at about 50 Hz. This parasitic oscillations were caused by an undesired degree of freedom of the

combined leaf spring and torsional wire hinges and the fact that the acceleration is fed back outside of centre of seismic mass due to needs of mechanical construction. They were prevented firstly by frequency band limiting measures in the feedback path and finally by using of a bypass capacitor across the forcer coil. The s-plane of (theoretical) root loci is shown in Figure 9.

Noise measurements were carried out in a vault and in a borehole at a quite seismic observatory of Institute for Physics of the Earth of the Academy of Sciences of the USSR in Kazakhstan at different times (summer, winter). The measurements were carried out by using of at least two seismometers with equal parameters installed with the same orientation (version (i) as well as version (ii)). The results of noise measurements (instrumental noise and seismic noise) have been obtained by digital correlation methods. Some results are drawn in Figure 10 in comparison with the Low Noise Model (LNM) of the earth (used also in IRIS Project). It may be seen that the noise of the versions of the EDS-2 family is equal (at periods of about 100 s) to horizontal noise component of the model and significantly lower at shorter periods than the vertical component of the LNM. Note, that all inclined components are sensitive to horizontal as well as vertical components.

It has been proved evidently by all test results that the properties and parameters of the seismometers of the EDS-2 family planned could be acquired.

The authors have to express gratitude to their colleagues AKIMOV, N.F.; SASONOV, L.S.; PRAVDIN, N.M.; KONSTANTIN, T.M. (IPE, M) and UNTERREITMEIER, E.; KRACKE, D.; RINDT, L.; PFOTENHAUER, P. (CIPE, J) for support and several kinds of help.

Figures

Fig. 1 Mechanical sensor EDS-2, one component

Fig. 2 Displacement transducer (difference oscillator principle), electronic board

Fig. 3 Free period of seismometer as a function of tilting

Fig. 4 Temperature behaviour

Fig. 5 Long-term stability

Fig. 6 Bode diagram (version (i), seismometer without feedback)

Fig. 7 Principle of capacitive bridge transducer

Fig. 8 Amplitude response of version (ii), force balanced accelerometer)

Fig. 9 Root loci of version (ii)

Fig. 10 Results of noise measurements

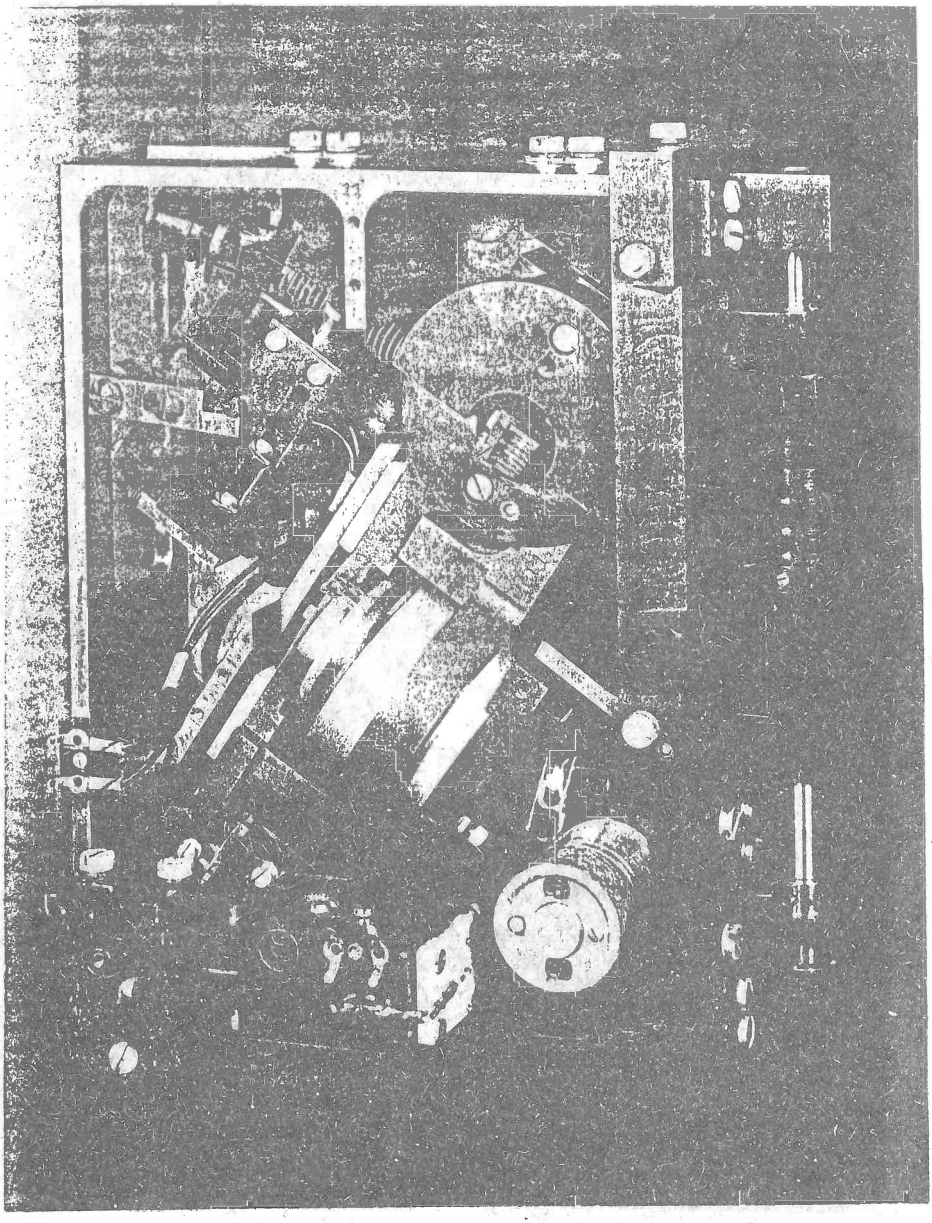

Fig. 1 Mechanical sensor EDS-2, one component

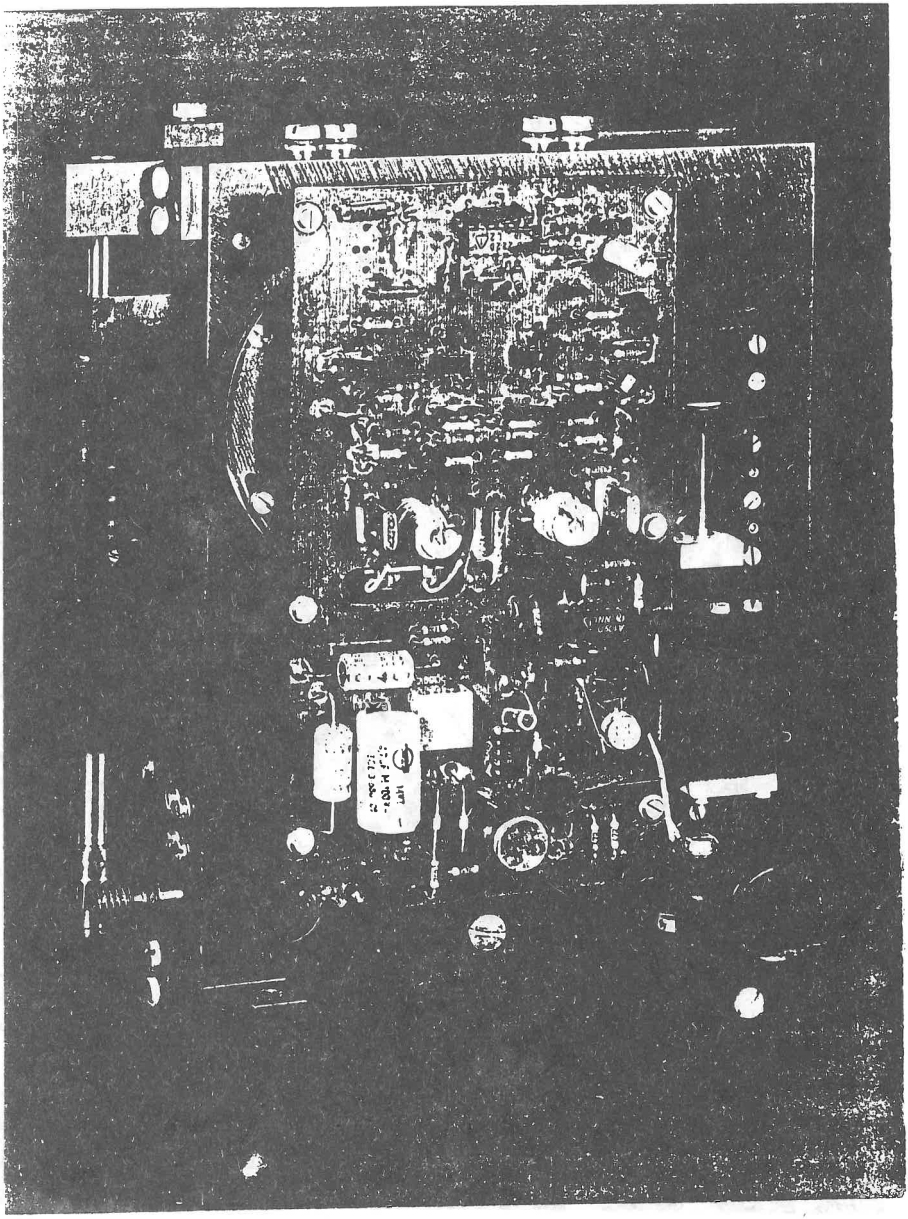

Fig. 2 Displacement transducer (difference oscillator principle), electronic board

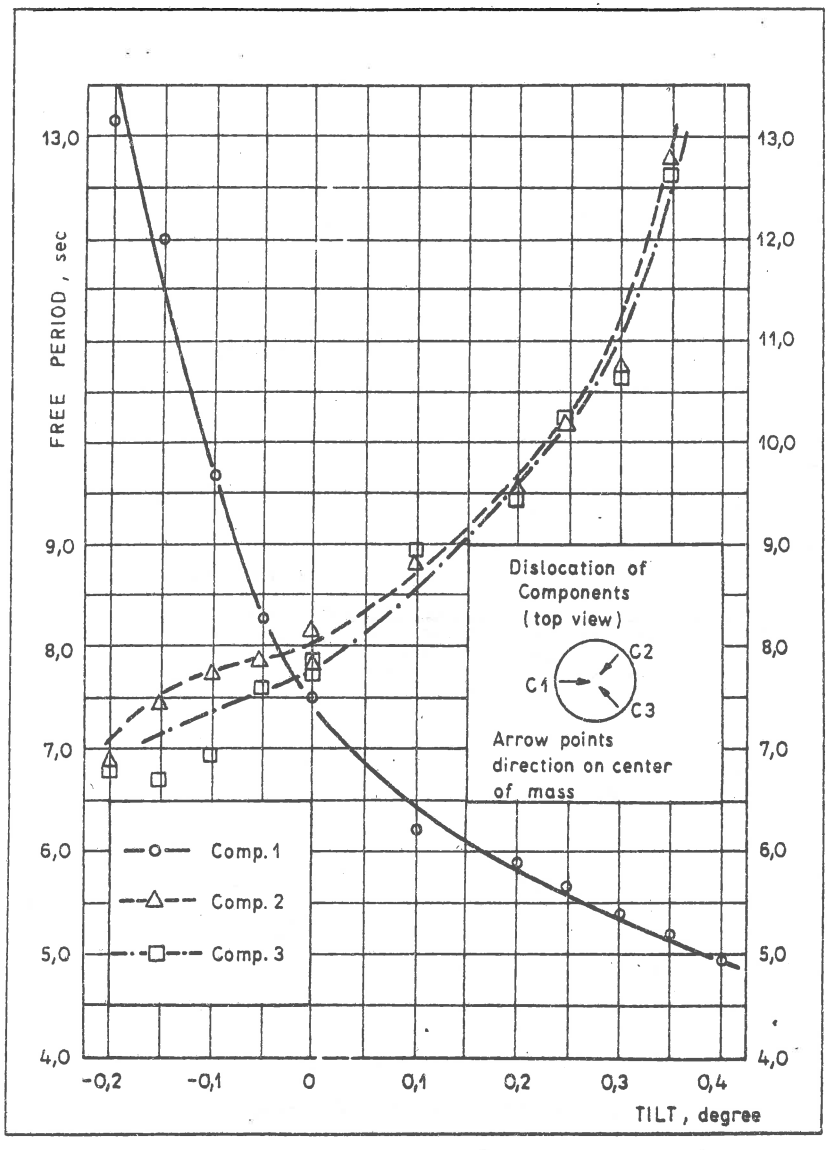

Fig. 3 Free period of seismometer as a function of tilting

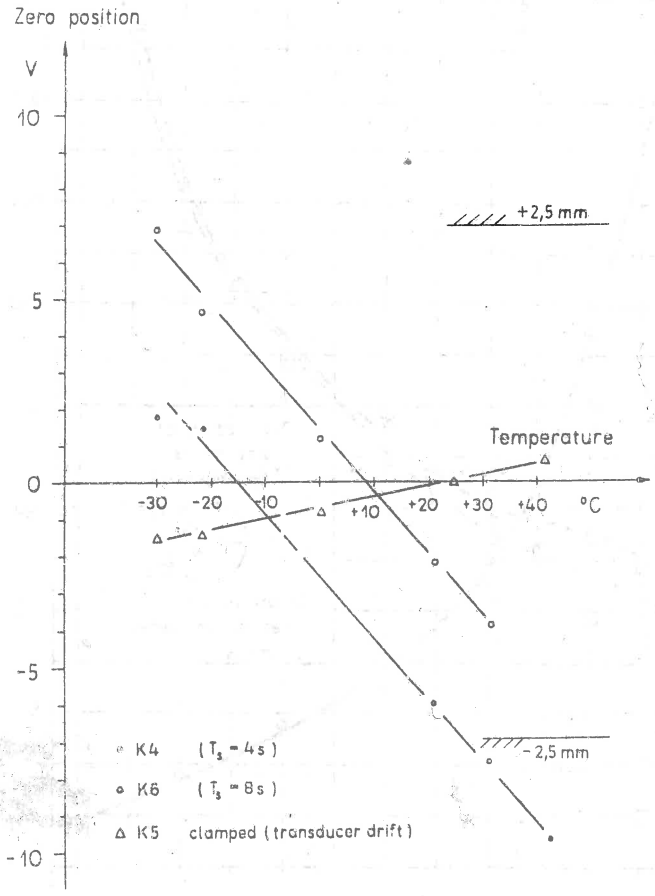

Fig. 4 Temperature behaviour

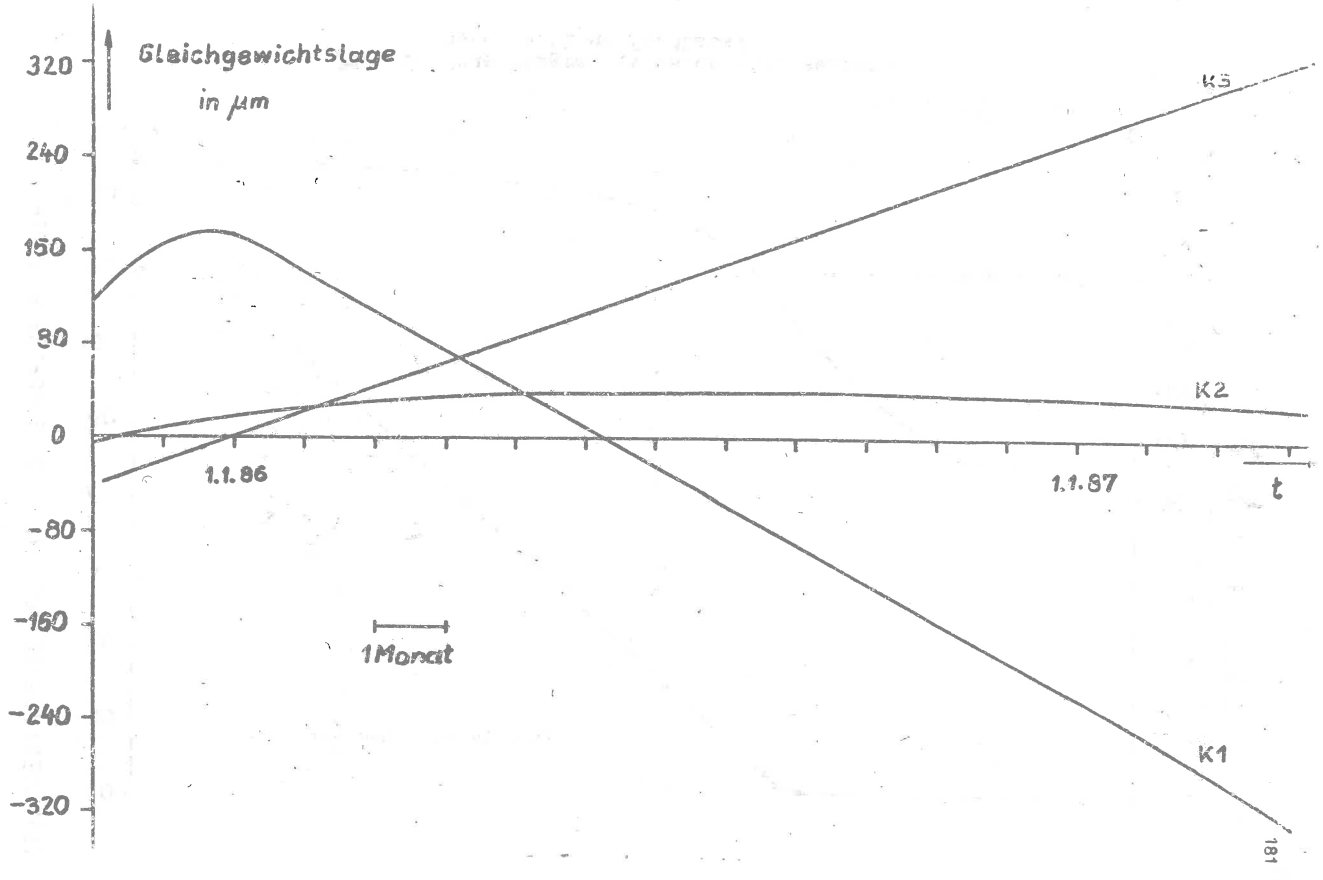
Gleichgewichtslage
in µm
320
240
160
80
0
-80
-160
-240
-320
1.1.86
1.1.87
t
1 Monat
K5
K2
K1
181

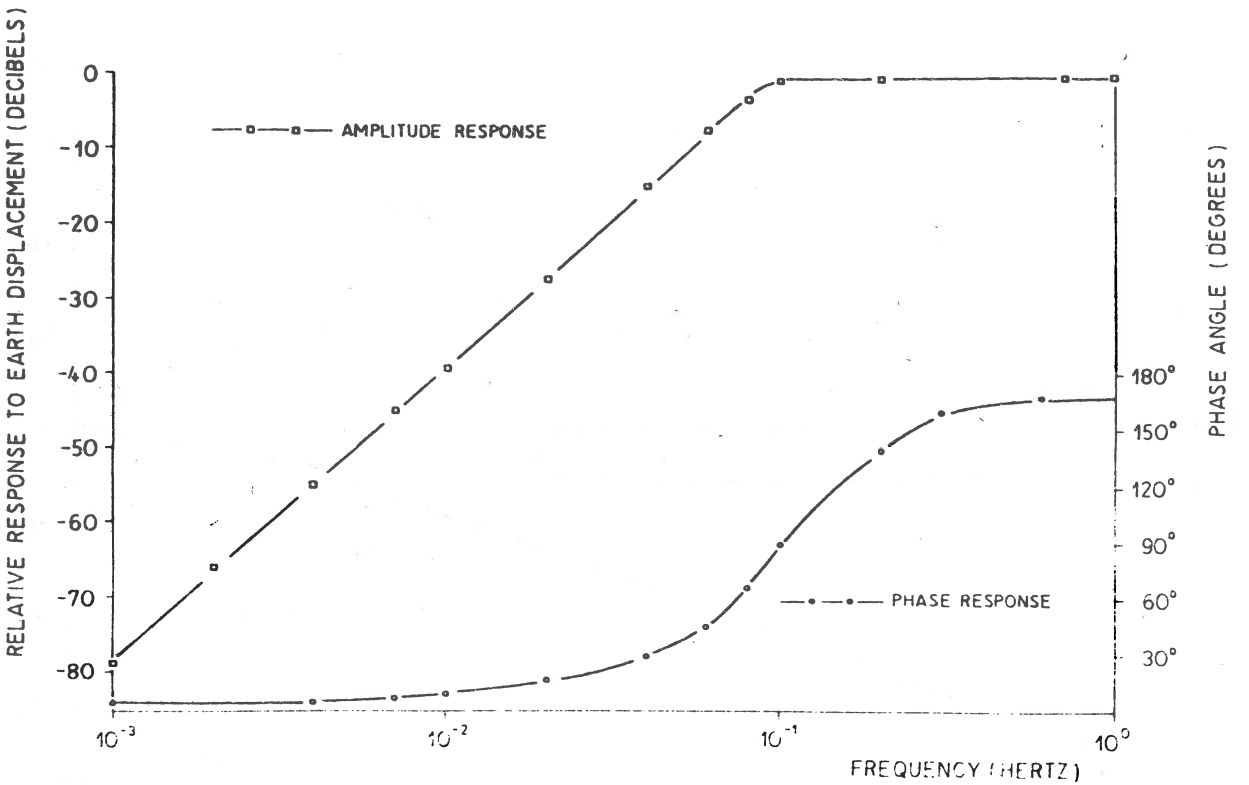

Fig. 6 Bode diagram (version (i), seismometer without feedback)

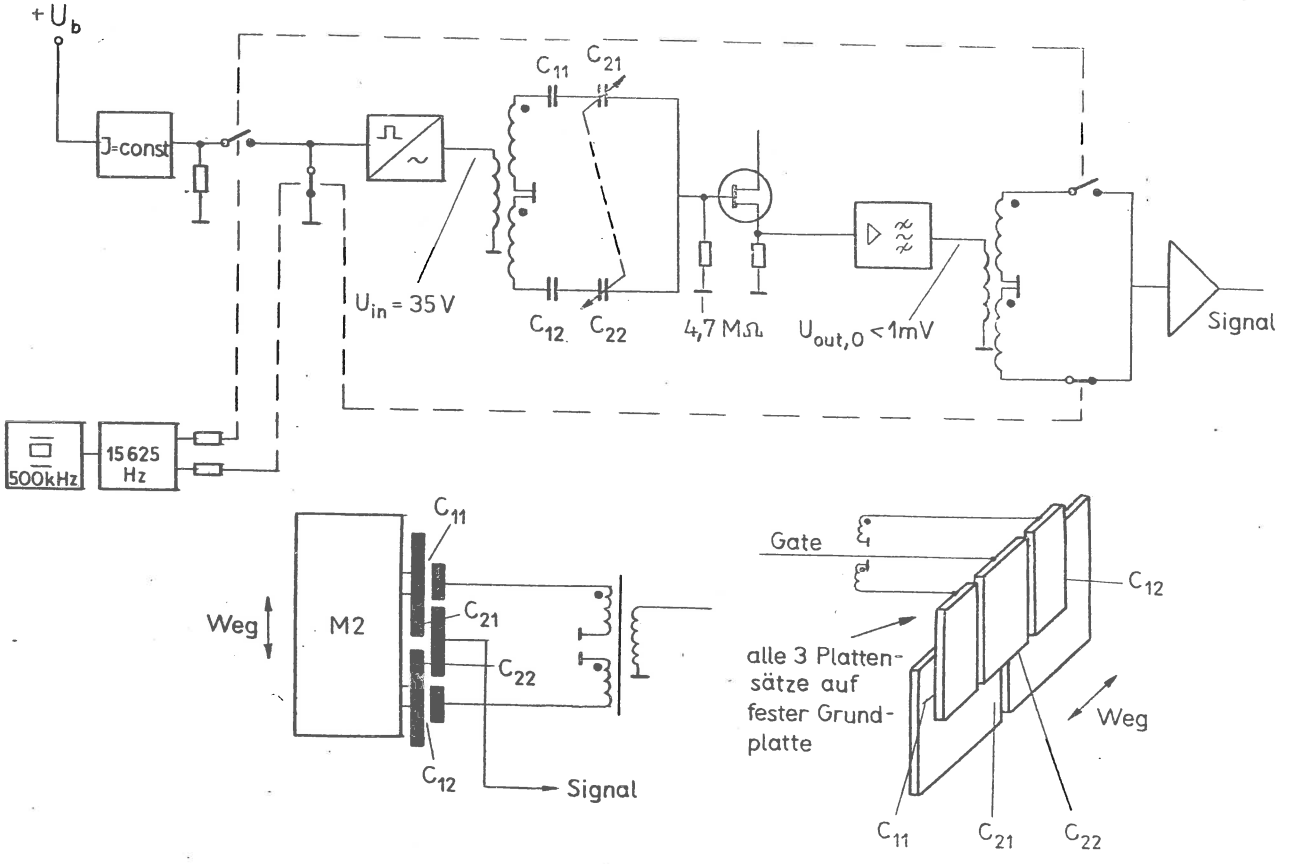

Fig. 7 Principle of capacitive bridge transducer

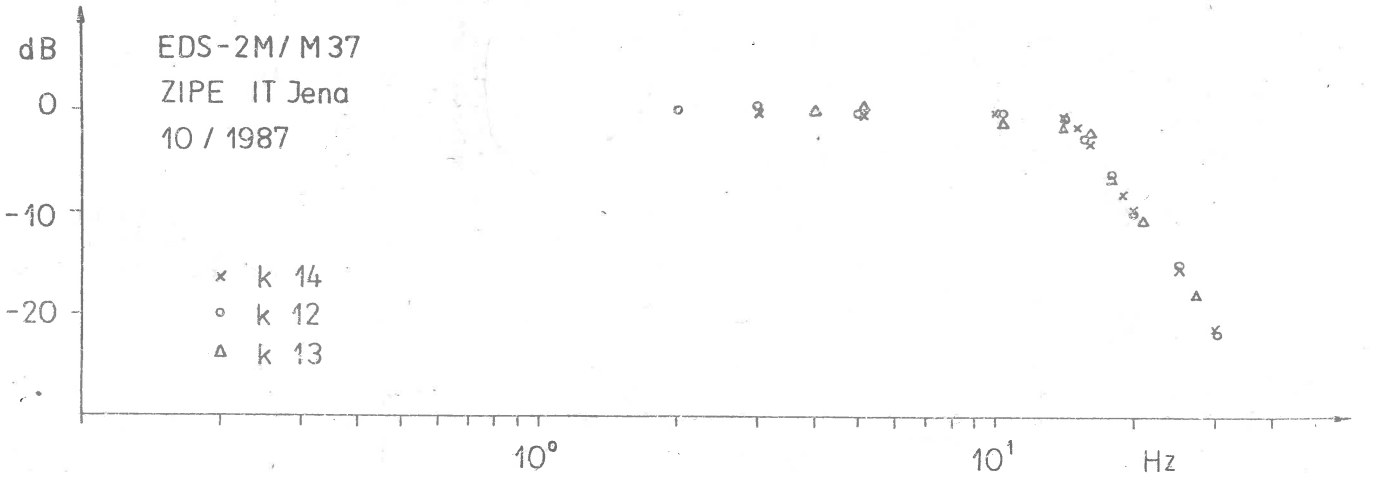

Fig. 8 Amplitude response of version (ii),
(force balanced accelerometer)

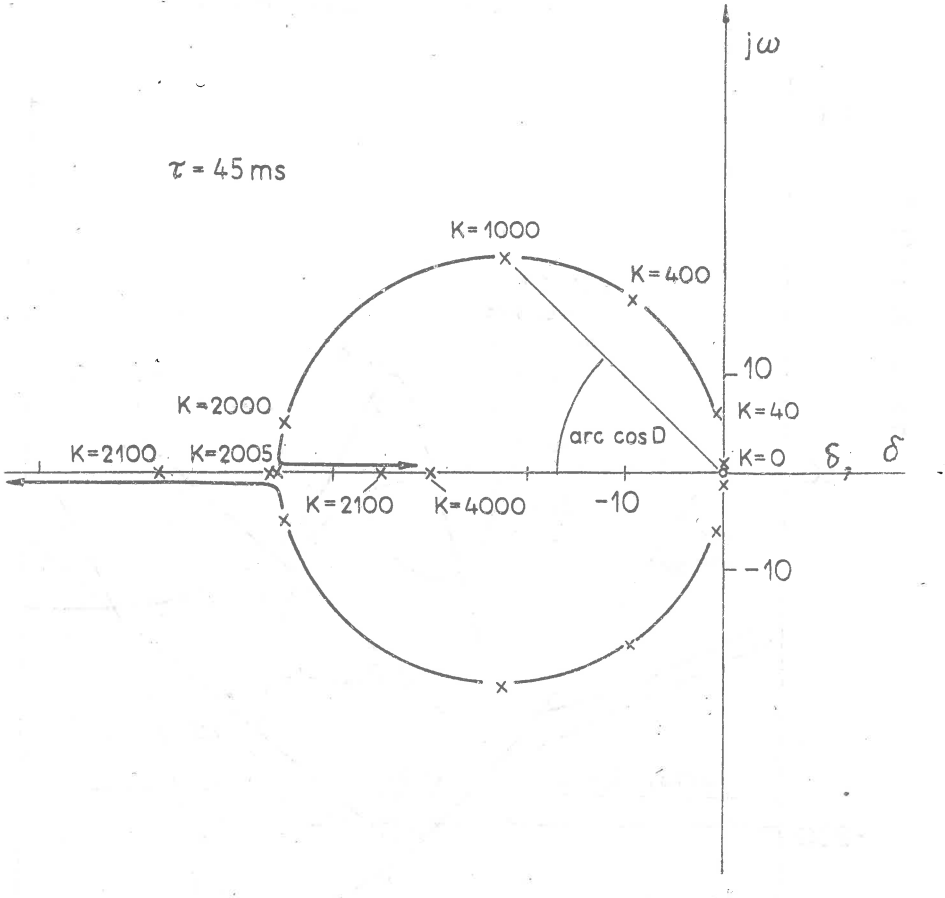

Fig. 9 Root loci of version (ii)

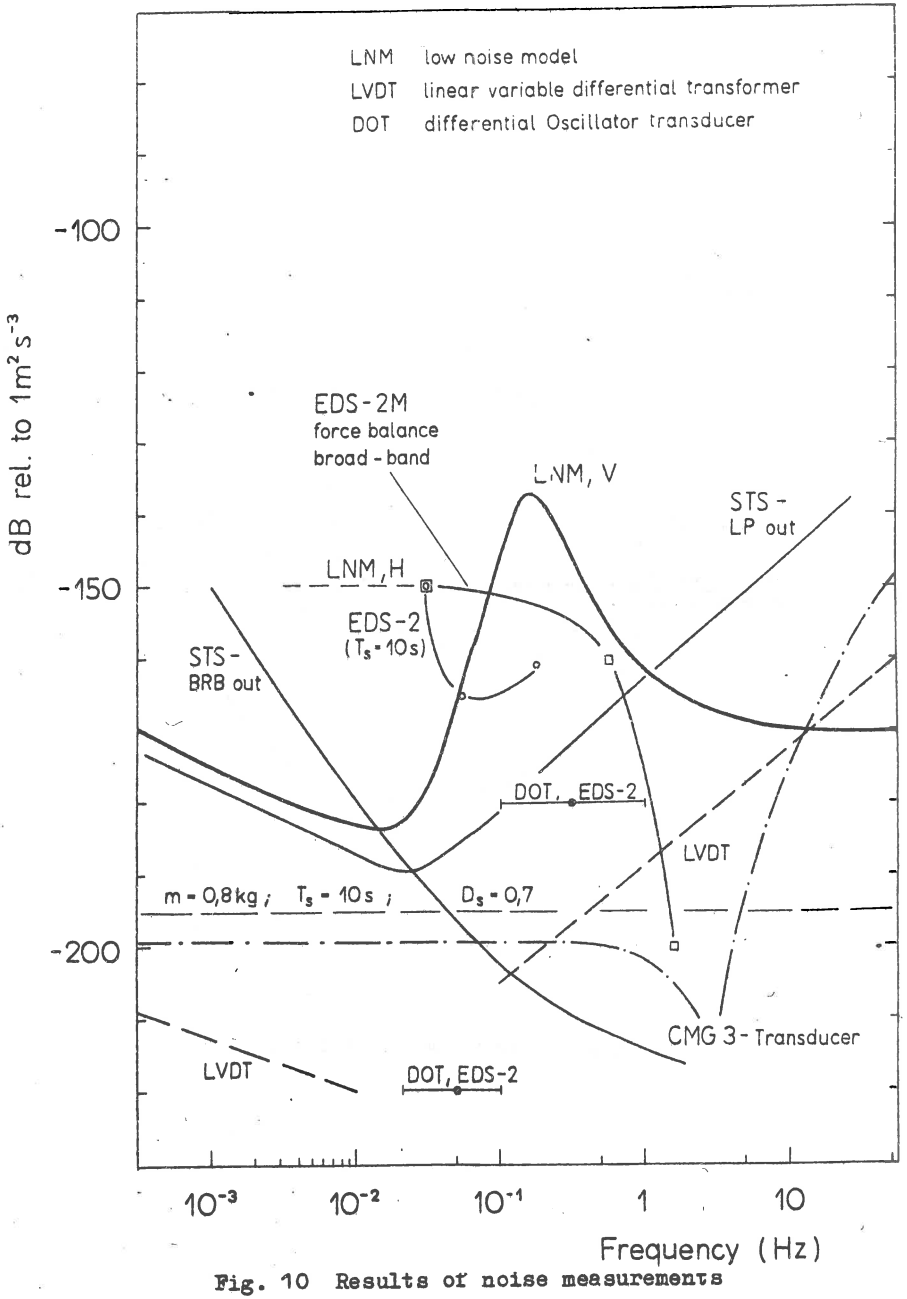

Fig. 10 Results of noise measurements

Microcomputer-controlled data acquisition system for experimental purposes in seismometry

Paper presented at XXI. General Assembly of ESC in Sofia, August 1988

SCHMIDT, Manfred and Karl-Heinz JAECKEL

Central Institute for Physics of the Earth
Branch Jena
Burgweg 11
J e n a
DDR-6900

Jena, July 1988

In order to fulfill some requirements of current seismometry we had so design an autonomous digital seismic data acquisition system for gathering three-component broad-band data using a three-component set of homogeneous seismometers EDS-2. (This seismometer was introduced at XIX. General Assembly in Moscow 1984 [1]; test results of seismometers of this family have been given at the present XXI. General Assembly by STOLJAROV, SCHMIDT et al. [2]). Figure 1 shows the arrangement of a homogeneous three-component seismometer set and the transfer characteristic of the sensors used in the system in comparison with other broad-band characteristics. The digital data acquisition system had to be designed that it is capable of exploiding the good properties of sensors completely:the dynamic range of > 100 dB in the frequency range between 10 mHz and 5 Hz. Additionally, a digital data transfer between the observatory and the branch Jena of the institute via public telefone line over 50 km with 1200 bit/s had to be realized. Following this line and depending on available electronic components a system structure shown in Fig. 2 had to be choosen.
Fig. 3 demonstrates the hardware structure of the "sensor microcomputer", based on the Z80 microprocessor family.

At the beginning of the design procedure only 12 bit ADCs industrially produced were available. A system structure had therefore to be choosen that implements gain ranging procedure. The needs of seismometry (dynamic range, sampling rate of 20 S/s) on one hand and technical limitations of those days on the other hand have led the designers to the following data structure (Fig. 4). In was necessary to handle the data in a packed format in order to fit in the three-component seismic data (floating point with one common exponent for three components) and the real time information in a 1200 baud data stream.
The software implemented in the sensor microcomputer has to fulfill the following task.
- to initialize the memory and peripheral units.
- to read in real time clock.
- to prepare the clock for picking up the measured value.
- to pick up the data of the (three) input channels
- to handle the gain ranging procedure.
- to prepare data to be transmitted, and
- to drive the serial output of data with stops for synchronisation.

The software structure used in the sensor microcomputer is shown in Fig. 5a. Fig. 5b demonstrates the interrupt subroutine with gain ranging procedure. If the signal exceed 50 per cent of full scale the gain will be reduced by one step. In that way off scale samples caused by very large and steep seismic onsets could be avoided practically. (Gathering real seismic data we did not observe out of scale samples so fare.)

The next two figures demonstrate the data acquisition equipment during the installation phase. The rack (Fig. 6, left side) contains power supplies, antialiasing filters and gain ranging amplifiers (three components), CMOS real-time clock, microcomputer and V.24 interface. The computer with screen (right side) is used to receive, display and store

the serial data stream after data remote transfer via public telephone line (Fig. 7).

Figure 8 and 9 show two different cases of monitoring seismic signals on the screen of computer. the generated Z trace digitally lowpass filtered and the digitally highpass filtered trace. The current levels of STA and LTA are monitored by the hight of two bars at the left side beginning of cf this trace (Fig. 8); Fig. 9 demonstrates a three-component display together with the time information and the gain information (exponent).

The gain ranging behaviour of the system is a very important system feature. Problem of long term stability (drift, offset) could be handled with good results in three channels after adjustment. In Fig. 10 this behaviour is shown for one component. Note, that an offset is nearly unvisible between two different gain levels. It is of interest to draw the attention at the different visual impression of quantization steps at different gain levels (rough structure at lowest gain, fine structure at highest gain).

Finally, Fig. 11 demonstrates the computed Z-component (broad-band, highpass filtered) of a weak seismic event. Summarizing, a microcomputer controlled data acquisition system has been designed and tested that is capable of processing seismic signals with a dynamic range of 132 dB, i. e. (0.3 μV) 1.2 μV ... 5 V, theoretically by gain ranging procedure in 6 steps, equivalent to

(±	0.14	nm ... ±	286	nm)
±	0.6	nm ... ±	1.2	μm
±	2.4	nm ... ±	4.9	μm
±	9.6	nm ... ±	19.6	μm
±	38.4	nm ... ±	78	μm
±	154.6	nm ... ±	314	μm

The real dynamic range is frequency-dependent: between 0.1 Hz and 5 Hz a dynamic range of 126 dB and at about 0.01 Hz of approximately 100 ... 110 dB was measured.
The most sensitive range - in parentheses - cannot be used in broad band systems because the microseismic level is under normal conditions to high. A gain reduction by factor 8 (soldered bridge) allows to record larger signals (equivalent up to 2.5 mm).

The data acquisition system have been successfully tested also in connection with other seismometers (TSJ-1).

References:

[1] UNTERREITMEIER, E.; SCHMIDT, M.; KRACKE, D.:
A new portable homogeneous triaxial seismometer: design and performance, test and calibration, direct signal analysis.
Paper, XIX. General Assembly of ESC, Moscow, October 1984

[2] STOLJAROV, O.; SCHMIDT, M. et al.:
Some test results of seismometers of the EDS-2 family.
Paper, XXI. General Assembly of ESC, Sofia, August 1988

Figures

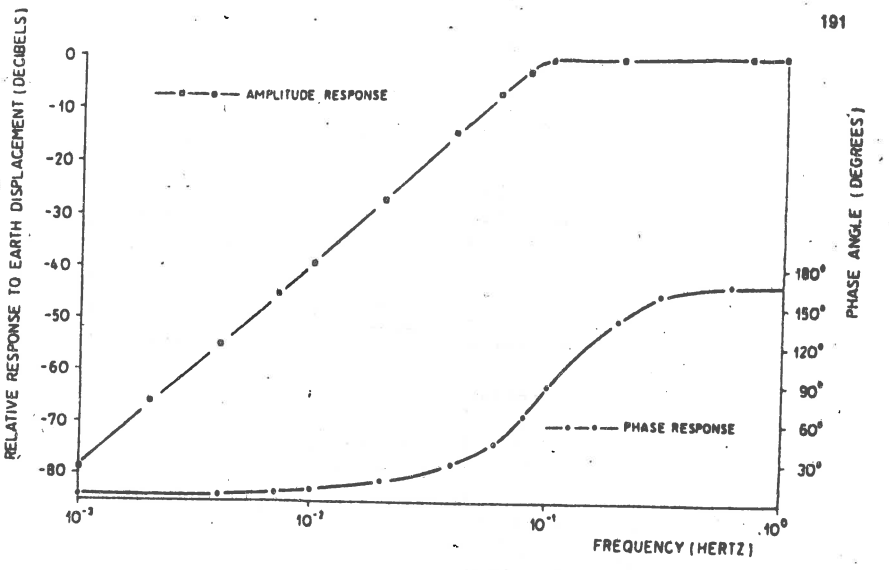
RELATIVE RESPONSE TO EARTH DISPLACEMENT (DECIBELS)
0
-10
-20
-30
-40
-50
-60
-70
-80
AMPLITUDE RESPONSE
PHASE RESPONSE
PHASE ANGLE (DEGREES)
180°
150°
120°
90°
60°
30°
10^{-3}
10^{-2}
10^{-1}
10^{0}
FREQUENCY (HERTZ)

Fig. 1b

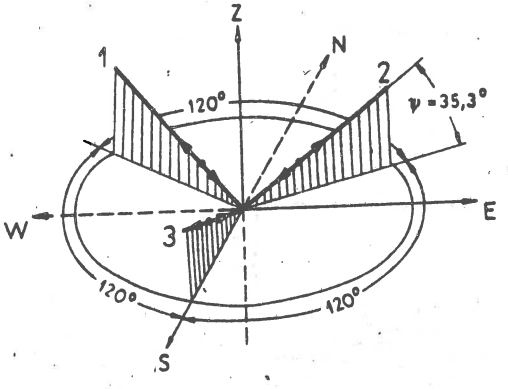
Z
N
1
2
120°
$\psi = 35,3°$
W
E
3
120°
120°
S

Fig. 1a

Errors:

- Amplitude and phase characteristics
- Gain
- Nonlinearities
- Offset

Errors:

- Aliasing
- Nonlinearities
- Offset
- Quantisation noise
- Aperture

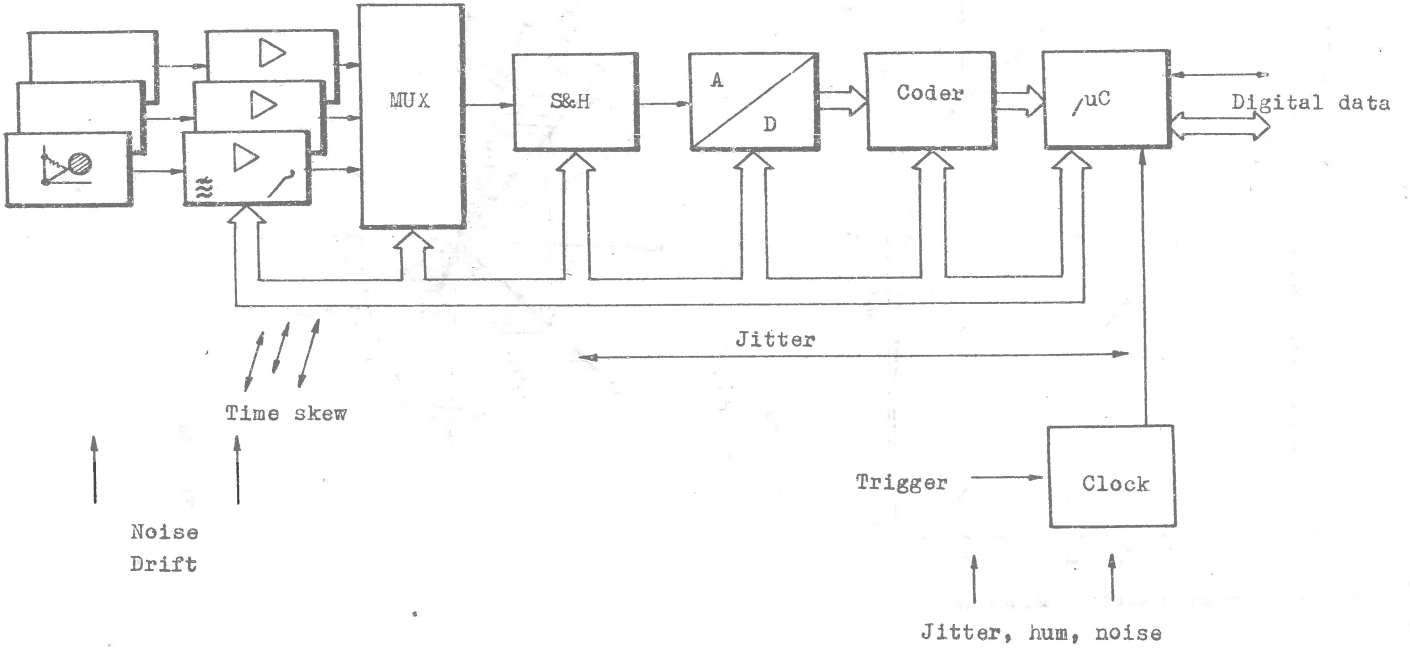

Fig. 2

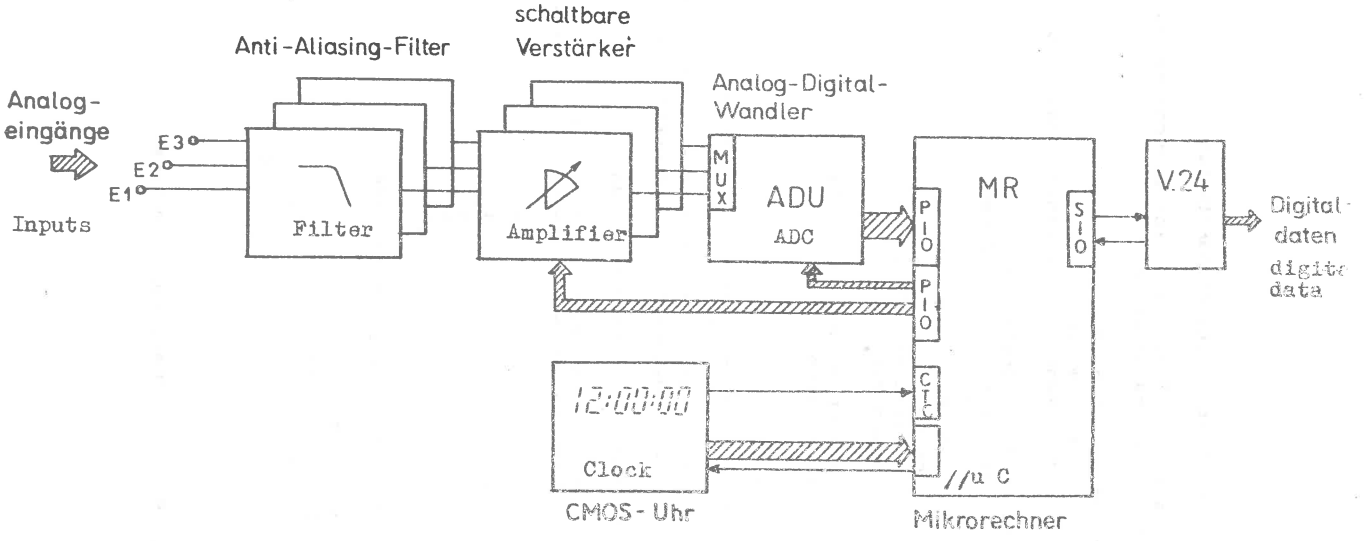
Analog-
eingänge
Inputs
E3
E2
E1
Anti-Aliasing-Filter
Filter
schaltbare
Verstärker
Amplifier
Analog-Digital-
Wandler
MUX
ADU
ADC
PIO
PIO
MR
SIO
V.24
Digital-
daten
12:00:00
Clock
CMOS-Uhr
CTC
//u C
Mikrorechner

Fig. 3

- o 8 data bits, 1 stop bit, no parity bit
- o 105 byte/s with 125 ms breaks for syncronisation after errors in transmission
- o data stream of 105 byte/s covers
  - real time information
  - data samples of seismic components
- o structure of data stream
  - 5 byte time information (BCD code)
    - second
    - minute
    - hour
    - running day (0 ... 99)
    - spare byte
  - 20 x 5 byte samples (seismic data), floating point format

- 4 bit exponent - measure for gain

gain	exponent (binary floating point)
1024	0
256	2
64	4
16	6
4	8
1	10

- 12 bit data in binary offset code

800 H ≙ 0
801 H ≙ +1
FFF H ≙ -1

.
.
.

Fig. 4 Data format and structure

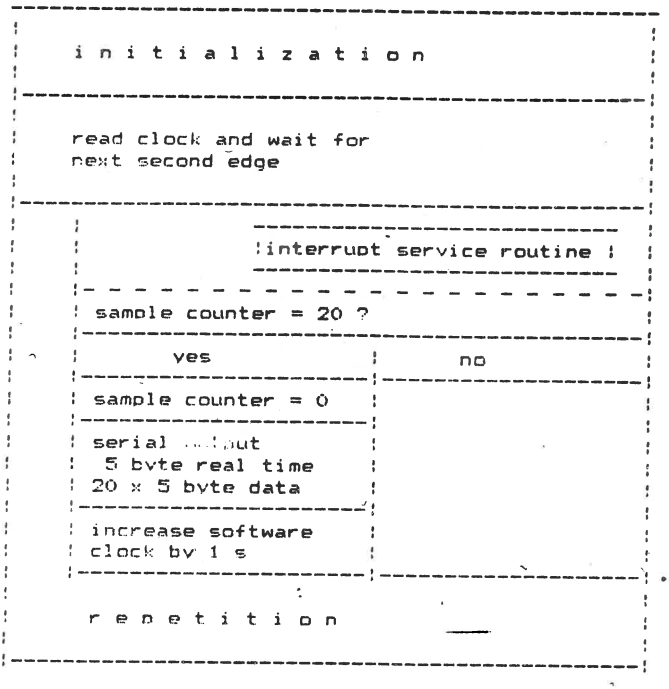

Fig. 5a Structogram of software of the sensor computer

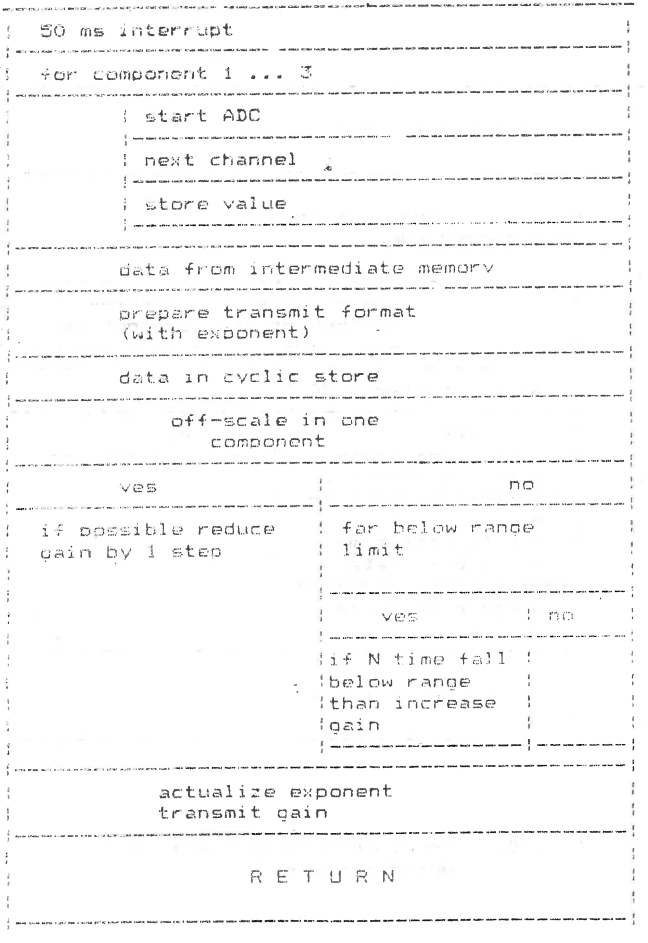

Fig. 5b Structogram of interrupt service routine

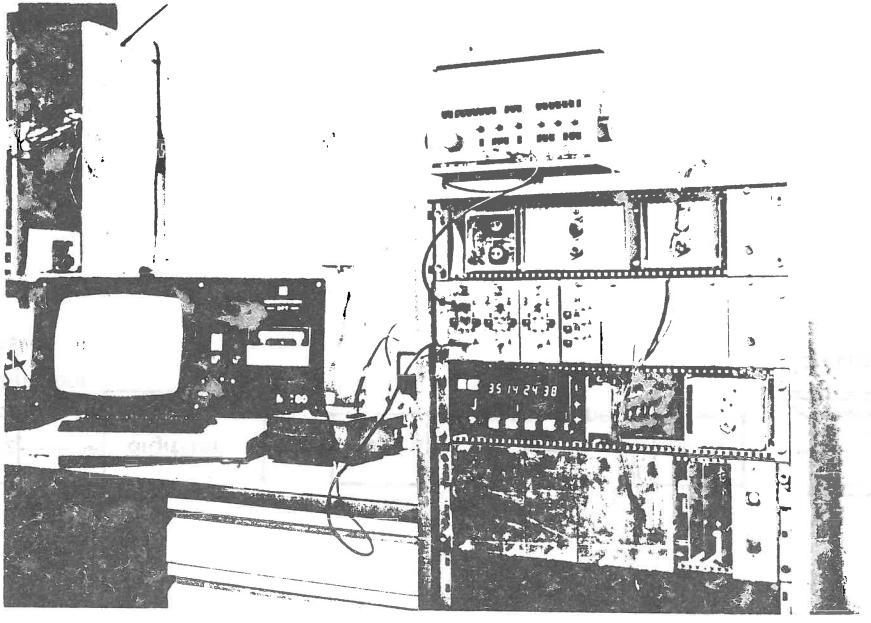

Fig. 6

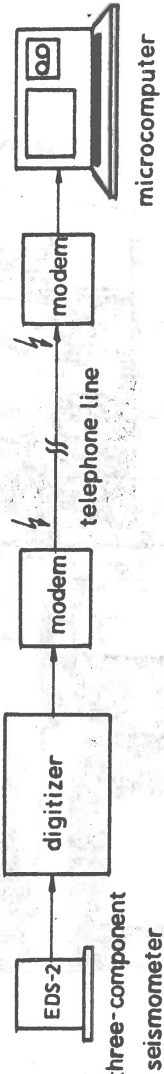
EDS-2
three-component
seismometer
digitizer
modem
telephone line
modem
microcomputer

Fig. 7

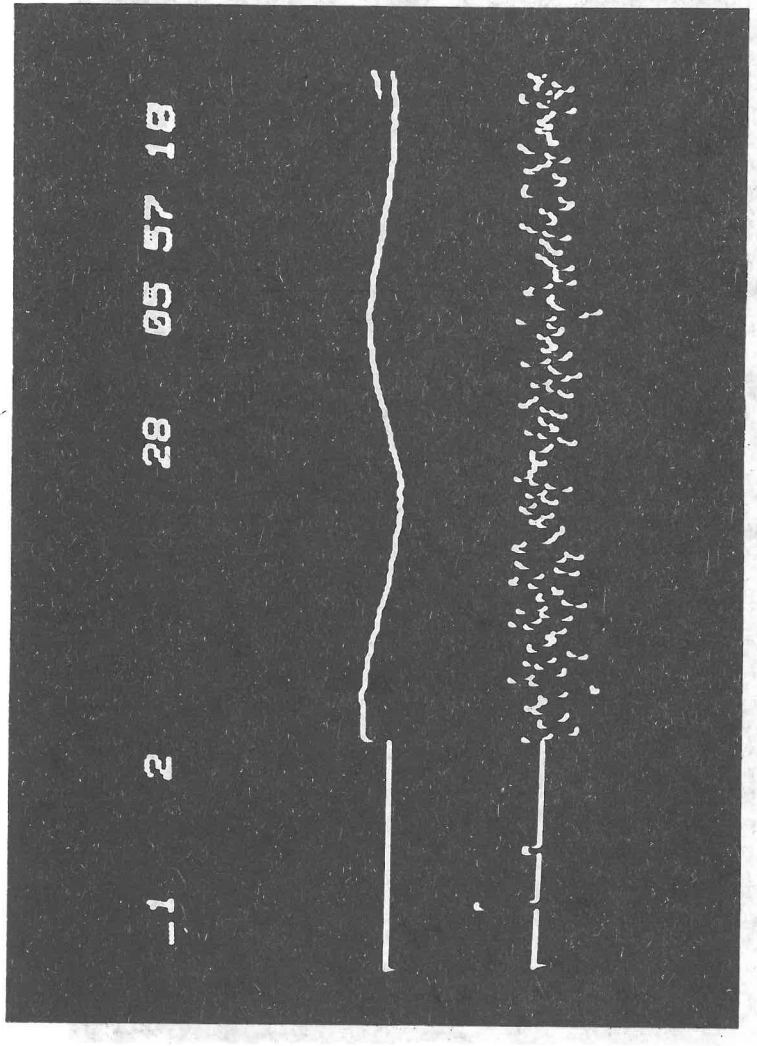

Fig. 8

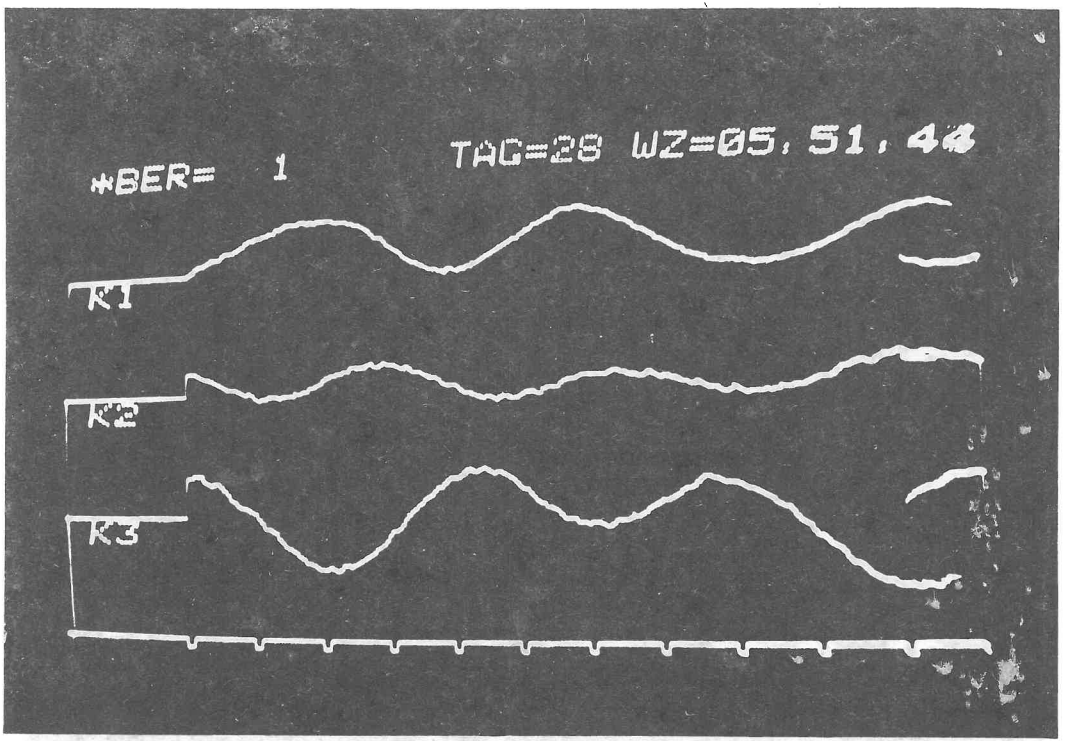

Fig. 9

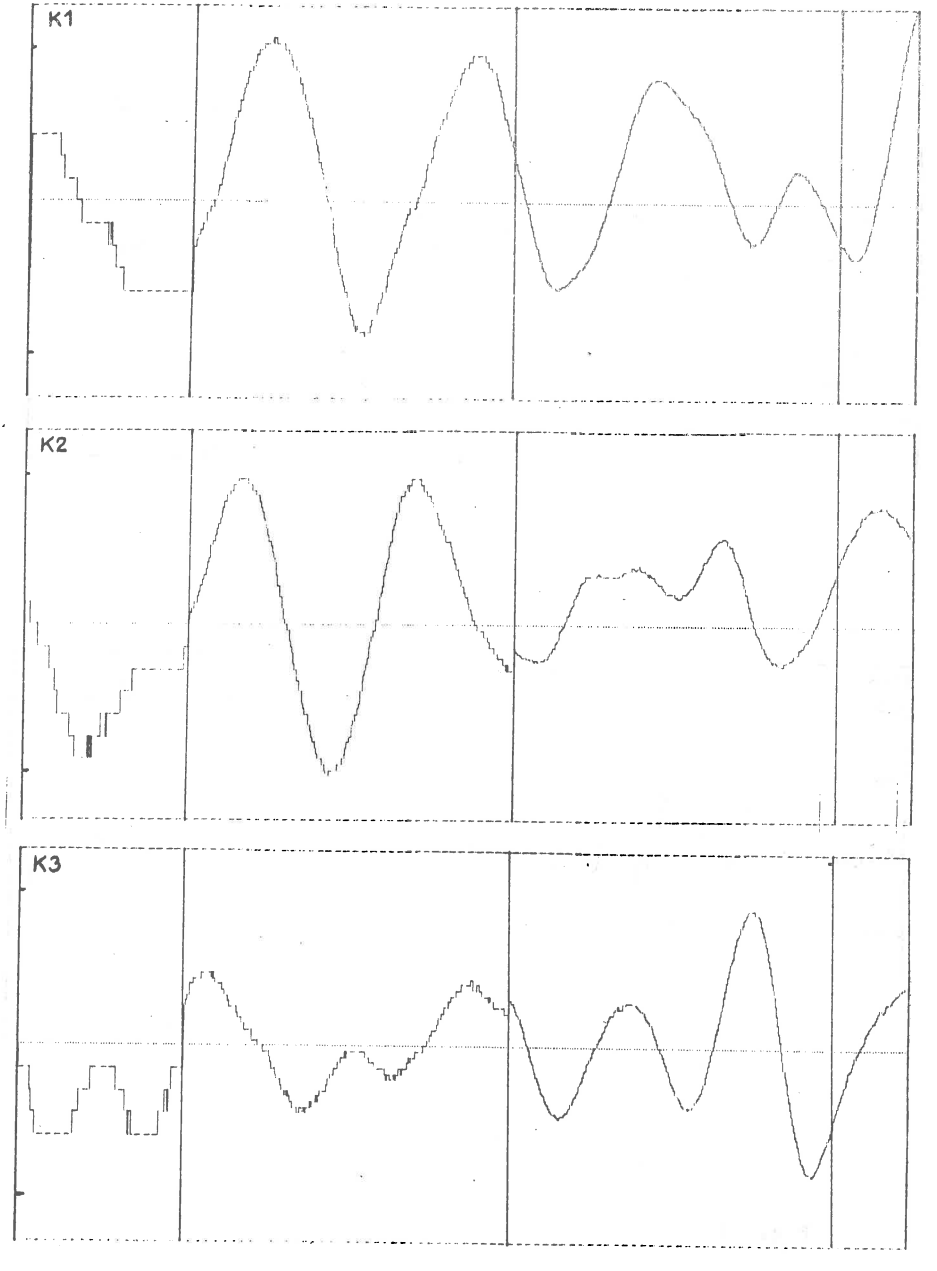

Fig. 10

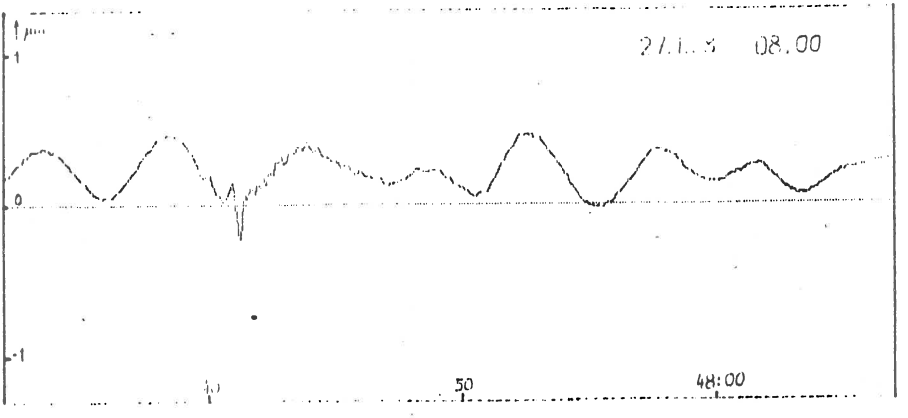

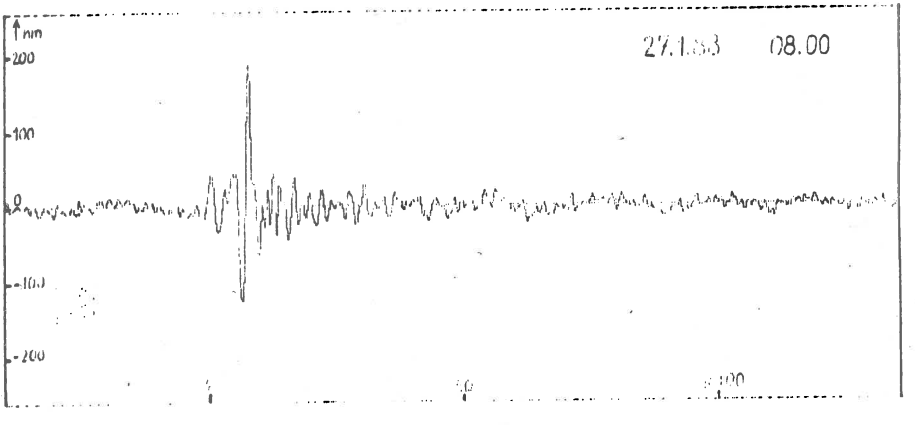

Fig. 11

On two compression methods for quasi real-time transmission of seismic data at low bit rate.

Jérôme Béquignon

European Mediterranean Seismological Centre
and *Ecole et Observatoire de physique du Globe*
5, rue René Descartes
F 67084 STRASBOURG CEDEX
FRANCE

Introduction.

Seismic networks have been operated in many areas for years. As far as emergency procedures are concerned, quasi real-time data transmission to the processing centre is needed. For small to moderate network apertures, transmission is usually performed by radio or telephone links. At larger distances, or when no reliable communications links are available, the satellite technology provides for an interesting solution. Discouragingly, either unacceptably high costs (communication satellites) or too low bit rates (scientific satellites) preclude its direct use with seismic data. thus the potential and unwealthy user must elect one of the two following strategies. The data can be processed on-site and the basic parameters (arrival times) extracted and transmitted, to the expense of a severe loss of information and control on it. Alternatively, the data can be compressed into a simpler and more compact signal, easier to transmit, with somewhat better information and greater control. The first strategy is already used in seismology [24]. The latter one has been widely investigated in speech processing, with much fewer attempts in seismology. This paper presents briefly two data compression methods, and some results obtained with real short-period seismograms. A compression rate up to 7.3:1 can be achieved with an acceptable loss of information.

Linear Prediction Theory background.

Among the numerous available compression techniques [8,18], two methods based upon Linear Prediction were investigated. This theory is of common use in exploration seismology, and a complete description may be found elsewhere [23,27]. The simplest production model is the autoregressive (AR) one. The observed signal series (x_n) is depicted as the output of a linear, all-poles filter defined by its coefficients $(a_i)_{0\le i\le p}$, with an excitation series in input (assumed as a white noise) (e_n):

$$e_n = \sum_{i=0}^{p} a_i \cdot x_{n-i}, \qquad a_0 = 1.$$

The set of parameters (a_i) is computed by minimizing the energy of the exicitation (called also innovation) series, and appears as the solution of the so-called Yule-Walker equations. For transmission purposes, they are usually transformed into an equivalent, more convenient set of parameters, the reflexion coefficients, $(k_i)_{1\le i\le p}$, which have a modulus lesser than 1 and may be coded easily.

Once these parameters are computed, the signal is filtered and the residual series (e_n) is obtained. This procedure removes from each sample x_n the linear dependencies upon the p closest previous samples. If it is efficient, the prediction gain G_p

$$G_p = 10 \log_{10}(\langle x_n^2 \rangle / \langle e_n^2 \rangle)$$

is high. For the studied seismograms, it was actually 10 dB or greater. The signal is thus represented, and may be synthesized from the parameters (k_i) and the innovation series (e_n) which has a reduced variance. The two methods to be described at once differ in the way the innovations are represented and coded.

ADPCM coding.
Since the innovation variance is smaller than the original signal one, the residual signal may be quantized in fewer bits : this is DPCM (Differential Pulse Code Modulation). The characteristics of the quantizer can be chosen according to the probability density function (pdf) of the residual signal, so that the quantization error is minimum (Lloyd-Max quantizer). Some experiments showed that the Gaussian or Laplace pdf's are acceptable approximations for the actual pdf's. To avoid the propagation of quantizing errors, the prediction is performed on quantized previous samples, thus a decoding module is included within the prediction loop.

The non-stationarity of actual seismograms arises a severe difficulty : the statistical properties of the signal change with respect to time. The cut-off threshold of the quantizer cannot be constant : high-energy bursts would be cut off, whereas low-energy frames would be dominated by quantization noise. To overcome this difficulty, the signal is assumed to have a constant pdf, but with changes in variance. The variance estimator depends only on past quantized samples, so that it may be computed either at emission or at reception. A tunable parameter controls the adaptation sensitivity [13,18]. This is ADPCM, where A stands for "Adaptive".

The output of the encoding procedure is constitued by N symbols, where $R = \log_2(N)$ is the number of bits allowed for each symbol. An additionnal compression may be performed, if all symbols do not share the same probability. This is entropy or Huffman coding. The code corresponding to each symbol has no longer a constant length : the more frequent have shorter codes, whereas others may bear longer ones. The probability law of the source must be estimated again. The resulting message has a variable length, which may be hard suited for satellite transmission.

Multipulse coding.
This method was formulated by Atal and Remde [4] in speech processing, but has been used in exploration seismology, too [11,12]. The excitation sequence is depicted as a series of isolated pulses at times t_i and amplitude b_i :

$$e_n = \sum_{i=1}^{M} b_i \cdot \delta_{in}$$

where M, the number of pulses, is much lesser than N, the number of samples within the observation window Γ.

The best pulses sequence produces a synthetic seismogram which best fits the original one, i.e. the difference has a minimum energy. The problem turns out to be linear with respect to amplitudes, but not to locations. An exhaustive test of every possible distribution is out of question, so the problem is solved by an iterative positionning of pulses. Assuming that (h_n) is the impulse response of the AR synthesis filter, and $(e_n^{(k-1)})$ the residual error with (k-1) pulses, it can be shown that the optimal position t_k gives the maximum of $|r_t^{(k)}|$, where

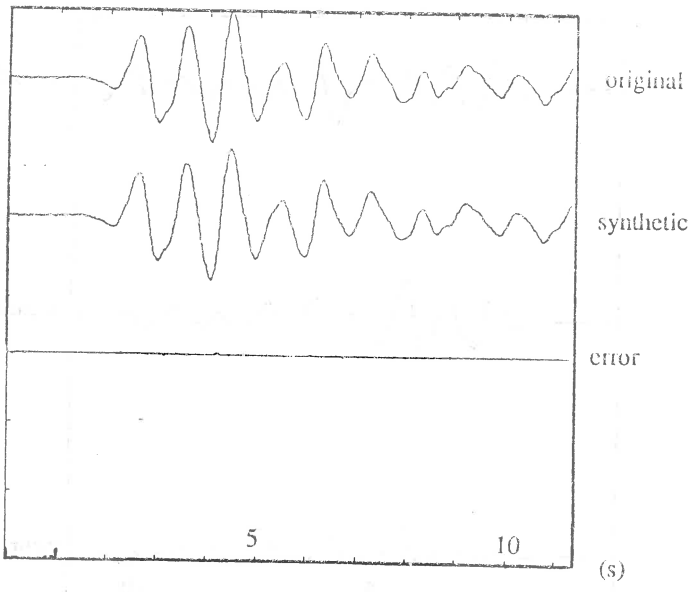

Figure 1 - 4-level ADPCM
Below, the original spectrum (solid)
the residual error spectrum (dashed).

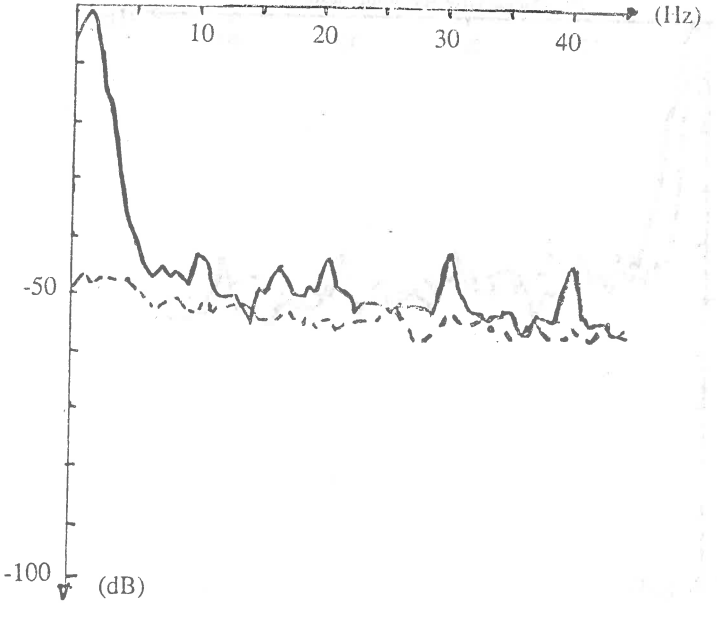

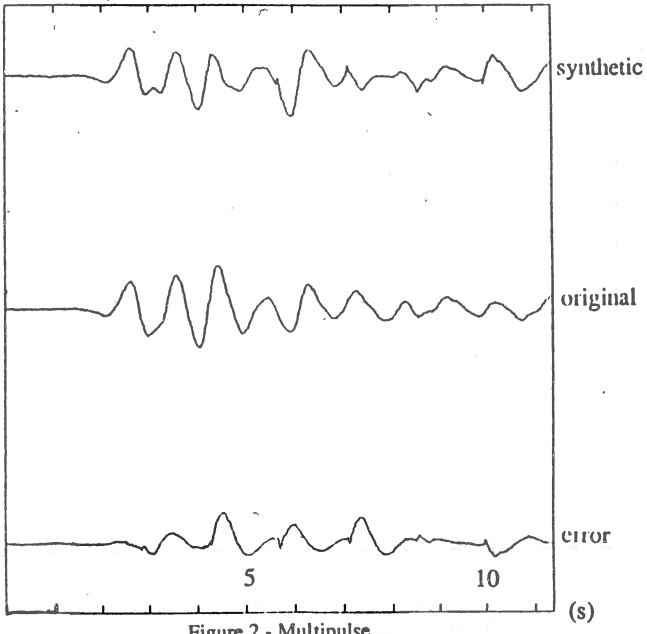

Figure 2 - Multipulse
Below, the original spectrum (solid)
the residual error spectrum (dashed).

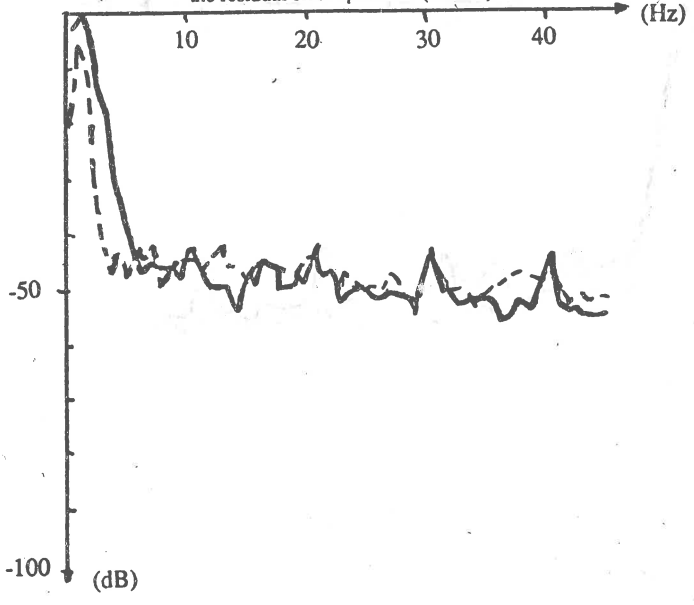

$$r_t^{(k)} = \sum_{n \in \Gamma} h_{n-t} \cdot e_n^{(k-1)}$$

is the intercorrelation between the residual error at step (k-1) and the impulse response. The corresponding amplitude is given by

$$b_k = r_{tk}^{(k)} / \Phi(t_k),$$
$$\Phi(t) = \sum_{n \in \Gamma} (h_{t-n})^2.$$

The residual errors are frequency-weighted, so that bigger errors are accepted at frequencies where the signal is strong ("perceptual" filter). The bias induced by the sequential positionning may be corrected by globally recomputing the amplitudes when all pulses are located, and solving the system

$$[R] \cdot [b] = [r],$$

where

$$R_{ij} = \sum_{t \in \Gamma} h_{n-i} \cdot h_{n-j},$$
$$[b] = (b_1, \ldots b_M)^t,$$
$$r_i = \sum_{n \in \Gamma} x_n \cdot h_{n-i}$$

The pulse locations may be optimally coded [5]. The amplitudes are coded as follows : the variance of amplitudes within a given window is computed and coded in 6 bits, then every normalized amplitude is coded separately using a 16-levels Gaussian quantizer.

Experiments and results.

The set of data was constitued by various seismograms of teleseismic, regional, local or induced (mine bursts) events, all recorded at the seismological lab of E.O.P.G.S., with a sampling period of 90 Hz. The parameters of interest are the compression ratio C, the signal-to-noise ratio SNR, and the bit rate, expressed either in bit/s or bit/sample. Care should be taken with SNR. This "objective" quality measurement is sometimes misleading : good SNR results may be of no help if arrival times are wrong, while poor SNR synthetics may contain the interesting information. Subjective criteria, as arrival timing, first motion sense, rupture restitution or spectral contents must be considered.

ADPCM was performed with a Gaussian quantizer on 8 and 4 levels. Huffman coding was simulated after 8-level ADPCM, but was unnecessary after 4-level ADPCM. A 5 coefficients AR model was used, computed by autocorrelation method and coded after Itakura and Saito [17,23], on (8+8+8+6+6) bits, on contiguous frames of 512 or 1024 samples. The results are summarized in fig.3. ADPCM worked very well with soft, low-frequency signals, and correctly with regional events (fig.1). Local events turned out to be more difficult, because of their almost-white frequency contents. Arrival times were correct to within about 1/10 s, first motion senses were almost always correct. The spectral estimates were also good, but it must be noted that noise level might be higher than the signal, at frequencies where the latter was weak. This was due to the withening effect of linear filtering. The SNR range was -14 to -41 dB for 8-level ADPCM, with a compression ratio of 3.9:1 without Huffman coding, and 4.8:1 with it. For 4-level ADPCM, the SNR range was -35 to -9 dB and the compression ratio 5.8:1.

Multipulse coding was performed using 6 pulses on sub-windows of 32 samples. On each sub-window, $\log_2\binom{32}{6} \approx 20$ bits were necessary to

coding the pulse locations, 6 bits for the amplitude variance and 4x6 bits for all the quantized amplitudes. The results were clearly worse than with ADPCM. Nevertheless, the relatively regular distribution of pulses, obtained by working on sub-windows, allowed for correct timing and first motions. The ruptures of the signal were also clearly restituted (fig. 2). The spectral estimates were poor, but here the noise level was under the signal, due to the weighting filter. The worst cases were the local events, for which the source time function is much more complex than isolated pulses. The SNR range was -11 to -5 dB with a compression ratio of 7.3:1.

method	SNR	C	rate (bit/s)	rate (bit/sample)
8-ADPCM	-41, -14	3.9:1	< 277	< 3.1
8-ADPCM + Huffman	-41, -14	4.8:1	< 225	< 2.5
4-ADPCM	-35, -9	5.8:1	< 187	< 2.1
Multipulse	-11, -5	7.3:1	< 147	< 1.7

Figure 3 - Results.

Conclusion.

Two different compression methods, both based upon linear prediction theory, were performed on real short-period seismograms of varied types. The 8-level ADPCM with Huffman coding produces good quality synthetics, thus allowing for further processing, with a moderate compression ratio. The 4-level ADPCM produces less reliable synthetics, but a somewhat higher compression ratio. Some further processing may also be performed. The multipulse coding produces low quality seismograms but high compression ratio, still acceptable as far as arrival times picking and phase recognition are concerned. This method should not be used when further processing is planned.

Acknowledgments.

I would like to thank especially J. Bonnin (CSEM-EOPG, Strasbourg), who initiated and guided this study. I am grateful to G. Poupinet (IRIGM, Grenoble), Y. Grenier (ENST, Paris), J. Le Guyader and C. Lamblin (CNET, Lannion) for their helpful comments and advices, and to M. Cara and his colleagues of the Seismological Lab (EOPG, Strasbourg), where the seismograms were recorded.

References.

[1] H. AKAIKE, "Information Theory and an Extension of the Maximum Likelihood Principle", *2nd International Symposium on Information Theory*, Tsakhadsor, Armenia, edited by B.N. PETROV and F. CSAKI, Akademia Kiado, Budapest, 1973.

[2] K. AKI, P.G. RICHARDS, "Quantitative Seismology. Theory and Methods", 2 vol., 932 p., Freeman & Co, San Francisco, CA, 1980.

[3] S.S. ALEXANDER, "Developments in Digital Seismology", *Review of*

Geophysics and Space Physics, vol. 21, n° 6, pp. 1332-1342, 1983.

[4] B.S. ATAL, J.R. REMDE, "A New Model of LPC Excitation for Producing Natural-Souding Speech at Low Bit Rate", *IEEE International Conference on Acoustics, Sound and Speech Processing 82*, pp. 614-617, 1982.

[5] M. BEROUTI, H. GARTEN, P. KABAL, P. MERMELSTEIN, "Efficient Computation and Encoding of the Multipulse Excitation for LPC", *IEEE International Conference on Acoustics, Sound and Speech Processing 84*, pp. 10.1.1-10.1.4, 1984.

[6] G. BENELLI, V. CAPPELLINI, F. LOTTI, "Data Compression Techniques and Applications", *The Radio and Electronic Engineer*, vol. 50, n° 1-2, pp. 29-53, 1980.

[7] T.E. BORDLEY, "Linear Predictive Coding of Marine Seismic Data", *IEEE Trans. on Acoustics, Speech and Signal Processing*, vol. ASSP-31, n° 4, pp. 828-835, 1983.

[8] V. CAPPELLINI (Ed.), "Data Compression and Error Control Techniques With Applications", 304 p., Academic Press, London, 1985.

[9] V. CAPPELLINI, E. DEL RE, "Data Compression Techniques for Remote Sensing Data Handling", *Proceeding of the EARSel/ESA Symposium on European Remote Sensing Opportunities, Systems, Sensors and Applications*, Strasbourg, Publ. ESA SP-233, pp. 31-36, 1985.

[10] C.H. CHEN, "Digital Waveform Processing and Recognition", 205 p., 2nd edition, CRC Press, Boca Raton, FL, 1983.

[11] Y. GRENIER, P. FABRE, "Utilisation des techniques de modélisations en P.S.V.", Final Report, A.T.P. "Géophysique Appliquée à la Prospection", 134 p., ENST, Paris, 1986.

[12] A. GUERCHAOUI, J.C. BALLUET, J.L. LACOUME, "Déconvolution de données de type sismique. Etude comparative de certaines méthodes", *XI. th GRETSI Proc.*, Nice, pp. 725-728, 1987.

[13] A. LE GUYADER, A. GILLOIRE, "Codage différentiel de la parole : algorithmes de prédiction adaptative et performances", *Annales des Télécommunications*, t. 38, n° 9-10, pp. 381-398, 1983.

[14] A. LE GUYADER, "Implantation de la quantification adaptative en précision finie", *Annales des Télécommunications*, t. 41, n° 5-6, pp. 252-259, 1986.

[15] A. LE GUYADER, P. COMBESCURE, C. LAMBLIN, M. MOULY, J.F. ZURCHER, "A Robust 16 Kbit/sec Vector Adaptive Predictive Coder for Mobile Communications", *IEEE International Conference on Acoustics, Sound and Speech Processing 86*, Tokyo, pp. 16.11.1-16.11.4, 1986.

[16] H. HOUET, J. ZSCHAU, "Environmental Data Relay via the Satellite METEOSAT", *Terra Cognita*, vol. 2, pp. 117-121, 1982.

[17] F. ITAKURA, S. SAITO, "Digital Filtering Techniques for Speech Analysis and Synthesis", *proc. of 7th International Congress on Acoustics*, Budapest, vol. 3, 25.C.1, pp. 261-264, 1971.

[18] N.S. JAYANT, P. NOLL, "Digital Coding of Waveform. Principles and

Applications to Speech and Video", 688 p., Prentice Hall Inc., Englewood Cliffs, NJ, 1984.

[19] K. KANJO, J. KASAHARA, M. TAKAHASHI, "An Application of the Adaptive Predictive Differential PCM (ADPCM) Method to the Seismic Wave Signal Compression", *Bulletin of the Earthquake Research Institute*, Tokyo, vol. **58**, pp. 647-654, 1983.

[20] N. KITAWAKI, F. ITAKURA, S. SAITO, "Optimum Coding of Transmission Parameters in PARCOR Speech Analysis-Synthesis System", *Electronics and Communications in Japan*, vol. **61-A**, n° 2, pp. 15-23, 1978.

[21] M. LEE, R. YARLAGADDA, "Reversible Seismic Data Compression", IEEE Trans., pp. 1870-1873, 1982.

[22] J.P. LEFEVRE, O. PASSIEN, "Efficient Algorithms for Obtaining Multipulse Excitation for LPC-Coders", *IEEE International Conference on Acoustics, Sound and Speech Processing 85*, pp. 25.6.1-25.6.4, 1985.

[23] J.D. MARKEL, A.H. GRAY, "Linear Prediction of Speech", 288 p., 3rd edition, Springer Verlag, Heidelberg, 1982.

[24] G. POUPINET, "Collecte de données sismologiques par satellite", *in* La Géophysique interne et l'espace, Ecole d'été, CNES, 614 p., CEPADUES, Toulouse, 1985.

[25] E.A. ROBINSON, "Multichannel Time Series Analysis with Digital Computer Programs", 298 p., Holden Day, San Francisco, CA, 1967.

[26] E.A. ROBINSON, "Statistical Pulse Compression", *Proc. of IEEE*, vol. 72, n° 10, pp. 1276-1289, 1984.

[27] E.A. ROBINSON, S. TREITEL, "Geophysical Signal Analysis", 466 p., Prentice Hall Inc., Englewood Cliffs, NJ, 1980.

[28] L.C. WOOD, "Seismic Data Compression", *Geophysics*, vol. **39**, n° 4, pp. 499-525, 1974.

Z. I. Aranovich, B. N. Kazak, C. A. Negrebetsky, M. V. Rozhkov,
R. M. Sakandelidze, I. F. Lomtatidze, A. A. Ivanashvily.

Usage of Programming Seismological Complex PUSK-2 in USA-USSR Nuclear Test Ban Verification Project.

The demands of evolution of modern experimental seismology, recent achievements in the IC technology and in the area of programming languages and operational systems evidently have reached now the stage, where it seems to exist the possibility to implement multipurpose digital seismological complexes, combining in themselves the features of seismologist's working place and ones of multipurpose data acquisition and transmission center. However, the majority of high-class devices (Lennartz, Kinemetrics etc.), which permit to collect and make some kind of data preprocessing, are essentially narrowly specialized devices, and don't let to develop universal approach to the system of geophysical observations.

We made an attempt to implement such broad approach on the base of already developed multichannel digital seismological station [1, 2], and on the base of our custom developed software, permitting to collect information from several different sensors in real time, to record it on magnetic tape, to carry out search and graphic checking of the recorded data, and also to verify the functioning of the data transmitting circuits. The described seismological complex PUSK-2 was used by the Institute of the physics of the Earth, Academy of Sciences of the USSR and Special Construction Bureau for the scientific instruments, Academy of Sciences Georg. SSR, for carrying out the joint USA-USSR Nuclear Test Ban Verification Project. The various operation and transport conditions, wide variety of the recorded seismical signals (microseismic background, chemical, industrial and nuclear explosions, local and distant earthquakes), quite simple input techique for the computers of different kind - all these features allowed us to make a conclusion about fruitfullness of this direction and about good perspectives of its further development.

The measuring core of PUSK-2 complex is the multichannel digital station, working in wide dynamic and frequency ranges (sampling rate is 100 Hz). The computing and managing core of the complex is LSI-11 compatible microcomputer "Electronica-60" with 56 Kbytes of memory, two floppy disk drives, graphic terminal, printer-plotter and two tape recorders with DMA controller. The structure of the complex is shown at Fig. 1.

Electronical seismometrical channels are high-sensitive short- and long-period three-component velocigraphs with 0.6-25 Hz and 0.02-2 Hz bandpass.

The program core of the complex is multitasking operational system MULTIFORTH, built on a base of FORTH programming language, and possessing the facilities of task priority managment, input/output interrupt processing and real time service, high speed performance and exclusively small memory requirements [3-4]. The FORTH interpreter itself operates as a background task with lowest priority. All additional routines, which are not nessesary for initial system installation and field data recording routine operation, are stored on the disk or/and on magnetic tape and can be joined to the system dictionary as soon as needed. Since FORTH allows to

build very compact programs, we used during experiments the system, constructed in such way, that the resident parts of it were: system kernel, program floating point processor, input/output device drivers, screen text editor, routines for data input from the digital seismological station, graphics software, programs for data preprocessing. Practically, all this programs constitute the loadable version of the system. Another version has been compiled for fast diagnostics of different units of the complex, in particular, station computer interface, Q-bus, tape recorders, controller, etc.

Data acquisition sequence consists of following stages: 1) data input from the digital station into the computer memory; 2) making memory image on first tape drive. Afer filling the tape data stream is switched to second recorder (automatically or manually from the keyboard). The information is recorded on tape in the seismic station format. After the process of recording is finished, data can be reformatted in order to produce more convinient data format for reading on conventional computers without any special transforming programs. This reformatting is carried out at the complex itself, when it's not in the recording mode, or at the spare complex, having also two tape recorders. It could be either a whole input tape transforming copy creation, or selectively, to select useful seismic information and not to copy different kinds of noise. The search is carried out by means of special programs of header searching and its decoding; displaying of data is carried out by means of graphic screen and printer-plotter.

During the experiments on the Soviet and US soil output tapes were read and processed on computers IBM-PC (MS-DOS operating system), PDP-11-73 (RSX-11M plus system), VAX (system VMS), MICROVAX-2, SUN (UNIX system). We had to notice, that although there were not any difficulties in tape reading, we suppose to work in future in format INTEGER*4 since we consider it to be the most convinient one (naturally, ASCII format is even more universal, but informative capacity of media will be much smaller). Besides, we choose this format after some consultations with the specialists of the University California, San-Diego, and Nevada, Reno.

Not talking in details about our sowtware, we'll only show some examples, illustrating the working of the complex PUSK-2 at Kazachstan and Nevada, mainly to make emphasis on the capability of this device.

At figure 2a-2c you can see the seismograms of three chemical explosions, which took place at the Soviet Test Site not far from Semipalatinsk, with yields of 10, 20 and 10 tons TNT, and caught by PUSK-2 at the distance of about 250 km. Each one of these seismograms has its particular features. The first one was made with tight sealing of the mine ; during the second blast there was great soil outburst, and right before the third blast the signal from a New Zeand region earthquake (1500 km to the south from N.Z., M=7) arrived. Fig.4 represents isoline maps of spectral-time surface, created by computing the amplitude spectra for every position of a time window of 5 seconds, jumping in 0.7 seconds, starting from 8 seconds before the first arrival. Every cut has been processed by homomorphic filter [5]. As it is shown, for the second blast, generated in another point, there is a slight spectral division of the direct and the reflected waves, possibly caused by the blast itself and by the geological structure of the region. The spectral-time surfaces for 1-st and 2-nd blasts are shown at fig.5a-5b.

The results of the similar experiment in the USA (PUSK-2 loca-

tion was Deep-Springs, CA, the distances from three sites of explosions were 389, 181, 188 km) are shown at fig. 3a-3b. Fig. 3a represents the seismogram of the first explosion, produced at Black Rock Desert, fig. 3b - recording of the third one from Broken Hill. We don't show the second blast seismogram because of very small signal to noise ratio (in spite of smaller distance between source and sensor compared with 1-st blast). The same seismograms were produced by american devices (installed by Natural Resources Defenc Council), located at the same place. Using of homomorphic deconvolution allowed us to extract the main spectral pitch for 1-st and 3-d blasts - correspondingly 3 and 3.5 Hz. We saw clearly the same spectral maxima after the local earthquakes records processing. These results speak strongly in favor of definitely expressed bandpass responce in Deep Springs soil around 3-4 Hz.

More brightly the capabilities of this device are displayed when analysing the recording of the nuclear explosion with announ ced yield of 20-150 Ktons TNT, recorded by PUSK-2 in Deep Springs at the distance of about 200 km. Signal-to-microseismic background ratio is about 4000. Nevertheless we have both the prehistory and all phases of the event on the same recording; clipping is absent. It's illustrated well by the maps of isolines (fig. 6), produced just like in the case of first experiment. On the upper picture the contours with energies higher, and on the bottom picture contours with energies lower than the definite level are drawn, so that an amplitude ratio of them is about 4000. Fig. 7 represents spectral-time surfaces of the input signal and same signal processe by homomorhpic filter (correspondingly upper and lower pictures) We removed spectral modulations by smoothing cepstral areas at the distance of 0.35-0.4 and 0.75-0.8 seconds from the main cepstral maximum [6] . As it can be clearly seen, the spectral maxima of different event phases all belong to the same frequency - about 1.5 Hz. It's seen both from fig. 7b, and from fig. 6a, which corresponds to the processed signal. The recordings of another kind are shown at next pictures. At fig. 8a the spectral-time surface of the local earthquake (Δ = 250 km) can be seen with well displayed spectral modulation (caused, evidently, by strong nonhomogeneousity of the origin), and fig. 8b represents the map of isolines for this surface.

Conclusion.

The described device has quite broad facilities both in sense of frequency, and in sense of dynamic characteristics; it may be used both for microseismic background recording, and for observations at the local and at the distant areas of a seismic event Flexible expandable multitasking operational system, facilities of digital data graphic control, effective programs for hardware diagnostics, producing output tape immediately "in the field" in format which is convinient for simple decoding for different computers and for different operational systems - all this allows to apply the developed hardware and software for the solution of the sophisticated problems of the modern seismology. The here cited results speak in favor of the fruitfulness and perspectives of the developed approach.

New experimental technique with improved characteristics helps us to receive more detailed information about an event, to determin its properties, wich could not be analysed reliably before. More

developed facilities of data processing allow to set experimental tasks and to answer some teoretical questions, which were unrealistic before, restricted by poor quality of experimental data and by slow processing rates.

Literature.

1. Аранович З.И., Негребецкий С.А., Серова О.А. и др. "Цифровая сейсмологическая станция станция (ЦСС) для регистрации информации в широких динамическом и частотном диапазонах". В кн.: Сейсмометры, регистраторы и сейсмометрические каналы. М.: Наука, 1985 (Сейсмические приборы, вып. 18)
2. Аранович З.И., Казак Б.Н., Негребецкий С.А., Рожков М.В. и др. "Программно-управляемый сейсмологический комплекс ПУСК-1". В кн.: Приборы м методы регистрации землетрясений. М.: Наука, 1987 (Сейсмические приборы; Вып. 19), с. 17-21.
3. Казак Б.Н., Михайловский В.М., Рожков М.В. "Многозадачная операционная система реального времени для автоматизации сейсмологических и специальных геофизических исследований". В кн.: Материалы международного симпозиума "Банки данных и автоматизация геофизических исследований", Нойбранденбург, ГДР, 1987.
4. Loeliger R.G. Threaded interpretive languages. 1981, McGraw Hill, ISBN, 0-07-038360-X. 280 pp.
5. Donald G. Childers, David P. Skinner, Robert C. Kemerait, "The Cepstrum: A Guide to Processing", proceedings of the IEEE, vol. 65, Number 10, 1977, pp. 5-23.
6. William H. Bakun, Lane R. Johnson, "The deconvolution of teleseismic P waves from explosions MILROW and CANNKIN", the Geophisical Journal of the Royal Astronomical Society, Vol. 34, No. 3, 1973, pp. 321-342.

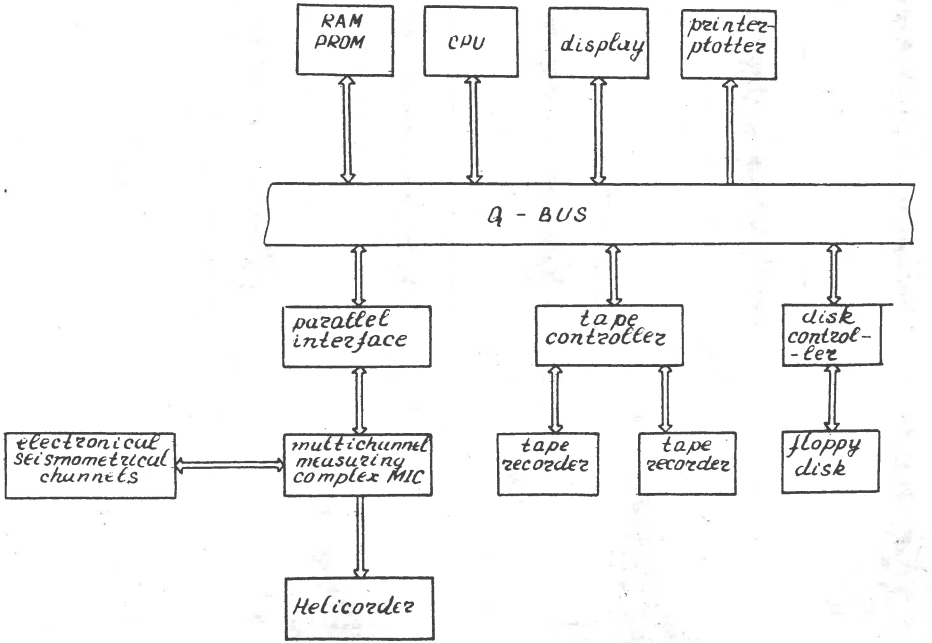

Fig. 1. Structure of PUSK-2

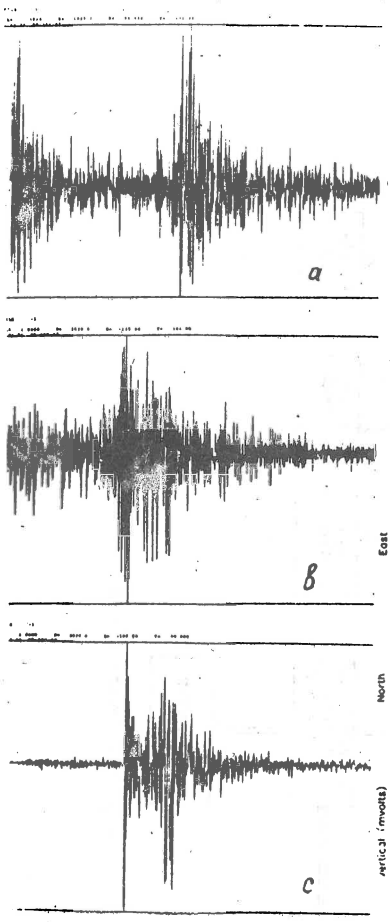
a
B
c

Fig. 2

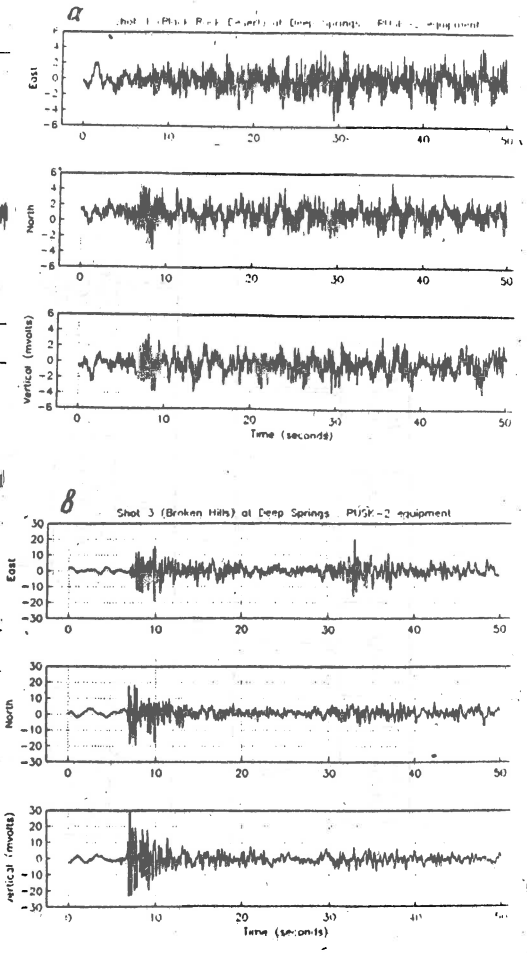
a
East
North
Vertical (mvolts)
Time (seconds)
B
Shot 3 (Broken Hills) at Deep Springs PUSK-2 equipment
East
North
Vertical (mvolts)
Time (seconds)

Fig. 3.

Fig. 4a

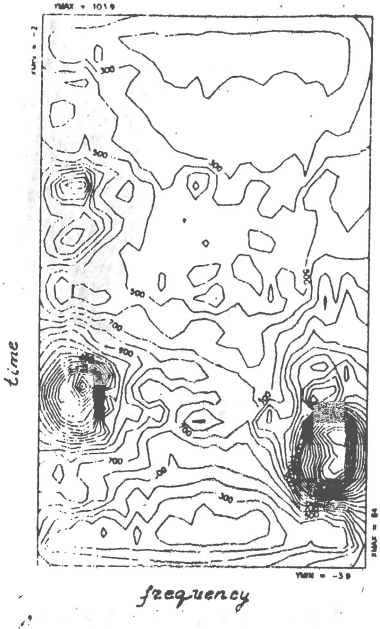

Fig. 4b

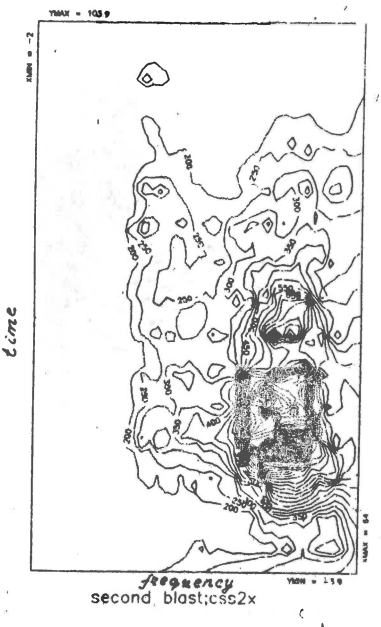

second blast;css2x

Fig. 5a

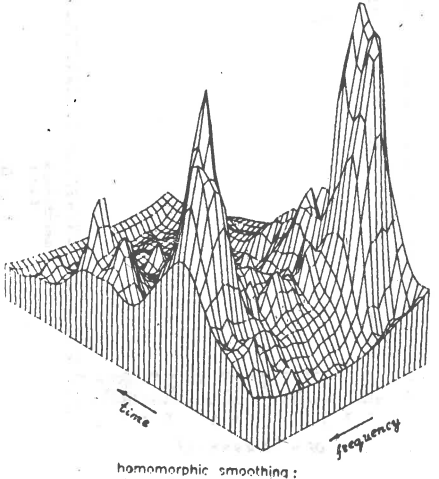

homomorphic smoothing :
first blast in Kazach.

Fig. 5b

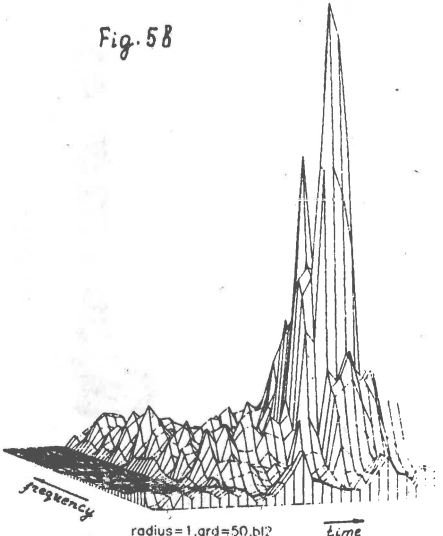

radius=1,grd=50,bl2
second blast in Kazach

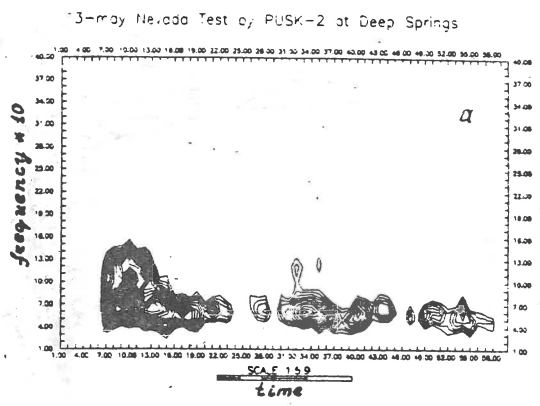
13-may Nevada Test by PUSK-2 at Deep Springs
frequency * 10
a
SCALE 1:5.9
time

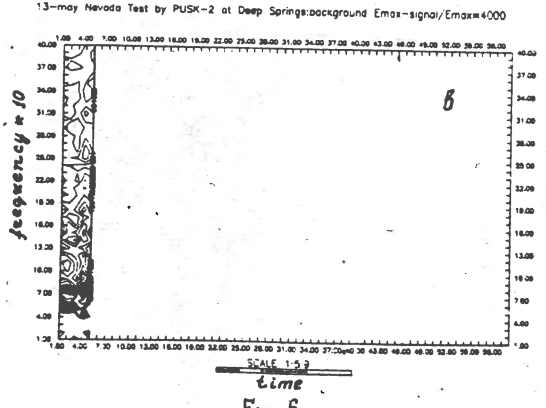
13-may Nevada Test by PUSK-2 at Deep Springs:background Emax-signal/Emax=4000
frequency * 10
б
SCALE 1:5.9
time

Fig. 6.

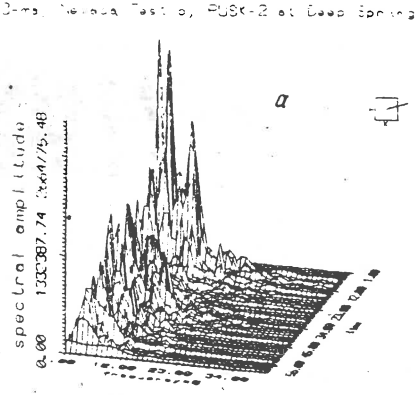
spectral amplitude
а

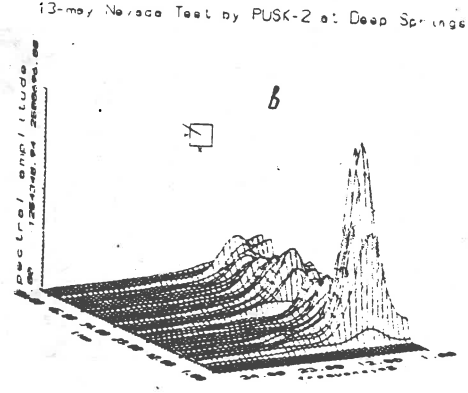
13-may Nevada Test by PUSK-2 at Deep Springs
spectral amplitude
б

Fig. 7

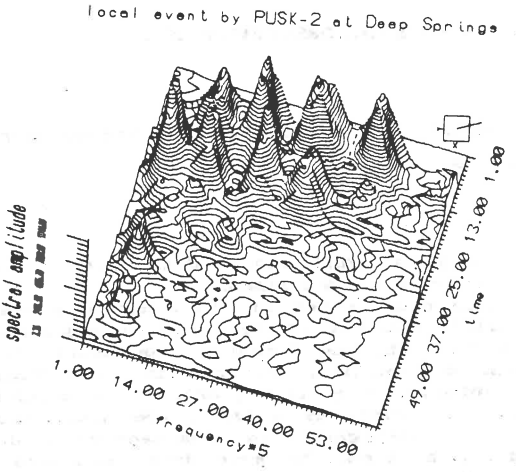
local event by PUSK-2 at Deep Springs
spectral amplitude
1.00 14.00 27.00 40.00 53.00
frequency=5
49.00 37.00 25.00 13.00 1.00
time

a

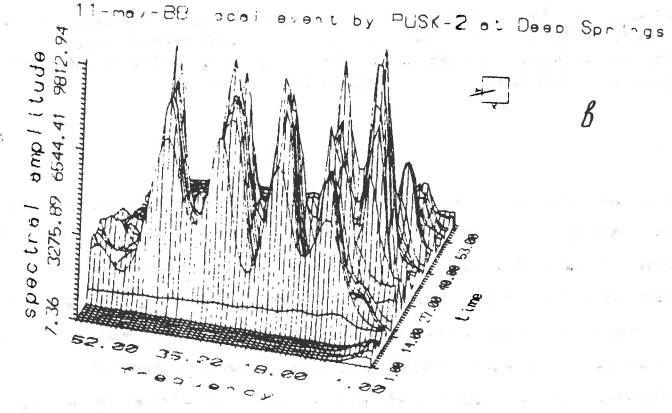
11-may-88 local event by PUSK-2 at Deep Springs
spectral amplitude
7.36 3275.89 6544.41 9812.94
52.20 35.52 18.80 1.00
frequency
1.00 14.00 27.00 40.00 53.00
time

b

Fig. 8

DATA MODEL OF A NETWORK OF GEOPHYSICAL OBSERVATORIES

Michail K. Kanarchev

Laboratory of Hydrometeorological Informatics, Hydrometeorological Service, BAS, Sofia, Bulgaria

Abstract

A conceptual scheme of a data base, which stores data from a network(s) of geophysical observatories, is described.

The data base is considered as a set of "information cubes". The entity in the data model is the set of measured or calculated values of parameters of the geophysical fields at particular moment of time. The collection of entities, arranged in a chronological order for a chosen interval (e.g. one year), is a multiple time series. These data can be present as a table. The data structure "information cube" is an aggregation of homogeneous tables (multiple time series), ordered by time. The main data structure - information cube, which is necessary to present the information in the data base, is constructed using relations in hierarchical and in normalized form. These forms of relations permit to organize a vertical hierarchy (due to the chronological order of registration and data integration by time) and horizontal fragmentation (connected with the spatial distribution of the observatories) of the data.

According to the conceptual scheme three levels of data hierarchy are defined: (1) data from one observatory, (2) data from network of observatories and (3) data from different networks (meteorological, seismic, geomagnetic, etc.).

Introduction

The data model of the observatory investigations is determined by the types of entities (measurement, observatory, etc.), their relationships and the set of attributes (parameters), which describe each entity. The relations (links) into data base frequently are presented as relational structures (tables) and as graphs (relational graphs). Depending of the presentation of the relations three basic approaches exist to the data modeling: hierarchical, network and relational (Date, 1980).

In this paper a modification of the relational approach is used. In the traditional relational model the entities and the relations are presented by means of tables (relations). This data structure is two dimensional. In the case of the observatory in-

vestigations we need more dimensions to present the evolution of the physical phenomena during the period of measurements. The most simple generalization of the tabular structure is to make an aggregation of homogeneous tables, ordered by time. This aggregation is named "information cube".

The aim of this paper is to described a logical scheme of data base of a network(s) of geophysical observatories based on the data structure "information cube".

1. Some aspects and requirements of the data model of a network of geophysical observatories

At present there is no formal theory for development of a data base, which stores data from a network(s) of geophysical observatories. The prime motivation for many geophysical organizations who consider the use of a data base management system (DBMS) is simply a desire to reduce the manual efforts required to query and update various quantities of data. Their requirements are for data-management capabilities allowing a single user (or small group) to make unpredictable queries and to present in graphical or tabular form various spatial-temporal relations for the investigated fields.

To ensure this multiple-aspect view of the data, it is necessary to synthesize an information image of the process of acquisition and storing the data from the geophysical observatories and of the methods of information extraction. The data model is a "logical" view of each entity, eg. measurement, observatory, etc., its attributes and relations in the area of interest, which in this case is a network of geophysical observatories (Tsichritzis et al., 1985). The data model on the one hand must reflect the data collection and must take into consideration the spatial-temporal nature of the geophysical fields and on the other must reflect mathematical rigor and be capable of modifications and easy implementation into computer media.

The registration of the data in case of observatory investigations is a routine process with definitive structure. This structure defines the chronological organization of the data. The

most important is to use flexible procedures of data handling, which permit to add a new information in formalized form and also the revision and the estimation of the data.

The geophysical research needed for understanding various physical phenomena can be done if a complex of methods is used. These methods must ensure the realization of various ideas of information extraction from the data, based on determined models of the investigated fields and phenomena. This process is an uninterrupted dialog between the research and the data, which can not be formalized as a whole. Consequently it is essential to organize relations between the methods, which depends mostly of the data model and the data base management system used.

The data model of the observatory investigations has two aspects: static and dynamic. The first one is linked with the description of the main entities, its attributes and the relations, who are invariant. We must point that between all categories of data in the area of interest always exist spatial-temporal relations. The second one is determined by the nature of the process of investigation of the physical fields. According to the theory of data bases the static aspect of the data model is connected with the languages named data description languages and the dynamic - with the data manipulation languages (Tsichritzis et al., 1985).

The spatial-temporal nature of the data models, whose are necessary for the Earth sciences, is the main difference in comparison with the data models, whose are supported by the conventional data base management systems for military and commercial use. This means that it must be reflected by natural way when the formalization of the data model is done and that the manipulations with the data can be done only if they fulfilled some admissible spatial-temporal relation (Kanarchev, 1986).

2. Presentation of the entities and the relations

The natural and basic entity of the data model of observatory investigations is the set of measurements at particular moment in given observatory. The attributes of this entity are: geographic

coordinates, time of measurement, measured parameters of the geophysical fields and some additional parameters which values are necessary to adjust the measurements. Let we called the basic entity "Point" (Fig. 1). The collection of points, arranged in a chronological order for a chosen interval (e.g. one year), is a multiple time series. These data can be present as a table. The length of the table is chosen according the nature of the observed phenomena and the sampling rate. It can be defined in process of generation of the concrete data base. In most cases it is equal of one year. Each row of the table corresponds to one point, one column - to the set of values of a given parameter. The rows have not a fixed data structure. It is formed in accordance with concrete needs.

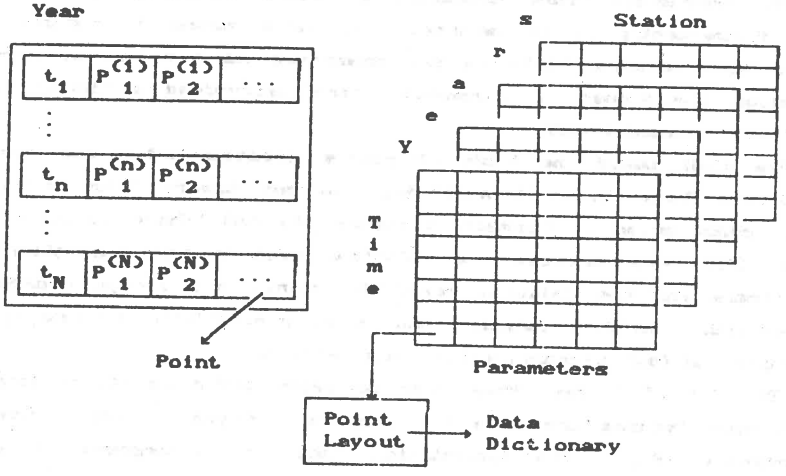

Fig. 1. The data structure – information cube and its elements.

The data structure is described in the form of table called "Point Layout" (Fig. 1). The Point Layout contains the mnemonic code, the type, the unit, the range of definition, etc. of each parameter. This is the data dictionary by means of which a link is established between the applied programmes and the data base, whereby the user receives the necessary information for

manipulation and for data control.

The attributes (parameters) are the axes of the space of the entity. To make the data manipulation more simple it is necessary that each attribute can receive only nondecomposable values.

The time of measurement is the basic parameter of the data, which characterize the sequence of the data collection. It determines the position of given point with respect to the other points, i.e. it is a link, observing the relation preceding-current-subsequent. The time of measurement is the natural key by means of which the data are retrieved. The parameters of the point depend directly or indirectly to the time of measurement. The indirect relations must be converted to direct. In the case of the ob- servatory investigations that means data must be converted as physical parameters. This operation is called normalization (Date, 1980). Consequently it is necessary to have means for manipulations with vectors, variables and constants. As a result of normalization the values of parameters are determined explicitly by the time of measurement.

We shall named the table of points, creating after the normalization, "Year" (Fig. 1). According the set theory Year is relation, constructed by normalized tuples (points). There is an essential difference between the relations used in the conventional data bases and the relation Year. The points are always ordered chronologically in this relation and it is prerequisite to use very simple and fast techniques for data retrieval.

The set of tables "Year" can be represented as "information cube", which stores the data for a number of years from a given observatory (Fig.1). The information cube is an aggregation of homogeneous relations "Year". This presentation of the data for one observatory permits a simpler and clearer way of defining various data structures using the relational operations: selection, section, etc. An analog of the first one are the annual curves, of the second one - annual changes of some parameter at given moment. The resulting data structure is a subset of the structure information cube, i.e. single value, vector, table (matrix) and set of tables (matrices). This permits to use the

existing application software without significance modifications.

The observatories and the stations are other entity of our data model. Their basic attributes are the name and the geographical coordinates. We shall called this entity "Station". An information cube is connected with each station. The information from a network of stations lying in given territory can be considered as a set of information cubes. The name of each station is unique and is assigned to the belonging cube. Two kinds of relations exist between the stations : spatial and spatial-temporal. In some cases there are also temporal relations when the spatial distribution of the stations can be neglect. For example an analog of the first one is the isoseismal map, for the second - the set of time sections of earthquake zones and for the third - the correlation curve between geomagnetic variations and the magnitude of earthquakes.

The stations are divided to several groups according the following factors: (1) type of measured data (seismic, geomagnetic, etc.); (2) sampling rate (eg., analog and digital registration of the elements of geomagnetic field in two observatories). The data from each group is stored into separate sub-data base. Each sub-data base is independent and can satisfy definitive information needs. This entity is called "Service" (Fig. 2). Each object of the type "Service" has an unique name, e.g. seismology, geomagnetism, etc. The other attributes of the object "Service" are: sampling rate, list of the stations, etc. Each Service has own data dictionary. The entity Service is an aggregation of information cubes with a definitive location.

This compact generalization of the data and their relations reflects the nature of the observatory measurements and of the investigated fields. It permits a simpler and clearer way of defining the operations between the data, irrespective of the objectives of the research task.

3. Logical scheme of the data base of a network of geophysical observatories

The data base of a network of geophysical observatories is a

set of sub-data bases "Service" and is called "Multiple-Cube".

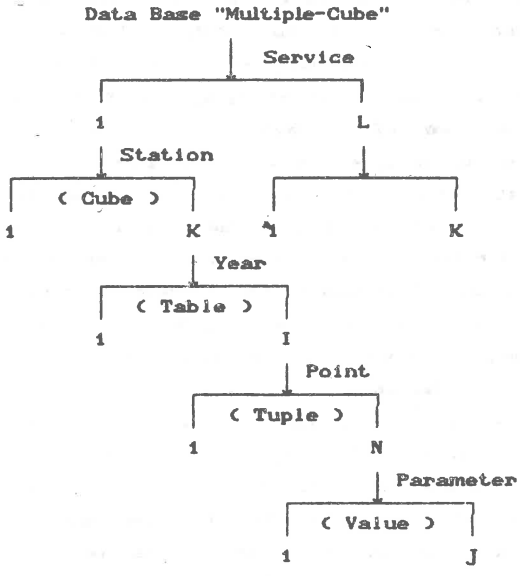

Fig. 2. Logical scheme of the data base of a network of geophysical observatories.

The logical scheme of Multiple-Cube is presented at Fig.2. It is hierarchical and consist of 5 levels. They define the following groups of operations between the data:

(1) operations with columns or values of parameters,

(2) operations with rows ("Point"),

(3) operations with tables ("Year"),

(4) operations with homogeneous cubes ("Service") and

(5) operations with heterogeneous cubes.

The main data structure - information cube - is constructing using relations in hierarchical and in normalized form (Fig.2). For example the relation Cube-Year and Cube-Year-Point is hierarchical. The relation Year is normalized.

These forms of relations (Kalinichenko, 1983) permit to

organize a vertical hierarchy of the data due to the chronological order of registration and data integration. The spatial distribution of the data is reflected using horizontal fragmentation, i.e. division of the data to a set of information cubes.

Conclusions

The described logical scheme is defined an one hand to the spatial-temporal nature of the investigated phenomena and from the other of the process of data storing and generalization. Three levels of data hierarchy are defined: (1) data from one observatory; (2) data from a network of observatories and (3) data from different networks (seismic, geomagnetic, meteorological, etc.).

The main advantages of the proposed data model are its simplicity and the natural way of presentation of the data and their relations.

The most important is that can constructed a new data manipulation language using the structure cube. This language will have a three-dimensional syntax. The operations between the data can be represented in graphical form, i.e. as operations between cubes. This will permits users to make their queries without knowledge some programing language.

References

Tsichritzis, D.C. and Lochovsky, F.H. (1985). Data Models. Moscow, Financii and statistika [russian translation].

Date, C.J. (1980). An Introduction to Database Systems. 2-nd ed. Moscow, Mir [russian translation].

Kalinichenko, L.A. (1983). Methods and Tools for Integration of Heterogeneous Data Bases. Moscow, Nauka [in russian].

Kanarchev, M.K. (1986). Digital Processing of Geomagnetic Data. Ph. D. thesis, Dep. of Geomag. and Grav., Geophysical Institute, BAS, Sofia [in bulgarian].

THE NEW TELEMETRIC SEISMOLOGICAL NETWORK OF THE NATIONAL OBSERVATORY OF ATHENS

by

PAPANASTASSIOU D., DRAKOPOULOS J., LATOUSSAKIS J.,
STAVRAKAKIS G. and G. DRAKATOS
National Observatory of Athens, Seismological Institute,
P.O. Box 20048, 118 10 Athens, Greece

ABSTRACT

The Seismological Institute of the National Observatory of Athens, started the installation of a telemetric network consisting of 17 stations for continuous seismic observations. This network covers the whole area of Greece.

In the present study a brief presentation of the telemetric network is given, also, the expected detection and location capability have been calculated. In addition the accuracy of the determination of source parameters have been investigated by applying the Monte Carlo method.

Contour maps for the expected locatability of the network and the estimated standard errors in the earthquake determination have been calculated and plotted.

INTRODUCTION

Greece, has the highest seismic activity among all countries in Europe. Most of the largest earthquakes occur along the boundaries of the subducting Mediterranean lithosphere under the Aegean sea. Furthermore some of the innumerable faults, which exist in the major area of Greece, are associated with large shallow earthquakes and some others are identified as capable faults.

The Seismological Institute of the National Observatory of Athens, is the responsible center in Greece to carry out continousely the routine seismic observations.

Since the accuracy of the earthquake parameters depends mainly on the azimuthal coverage of the recording stations, the importance of a dense seismological network in Greece is obvious.

With the rapid advancement of the seismic instrumentation technology and with increasing social needs especially after some recent disasterous earthquakes near densely populated areas, Thessaloniki (North Greece) 1978, Central Greece 1981, Kalamata (South Greece) 1986, the Institute started the installation of a modern telemetric network for continuous seismic observations. This network is consisted of 17 seismic stations. Fig. 1. shows the geographical distribution of the telemetric stations.

All the satelite stations constructed in quite places, outside of the cities, where the hard bedrock is exposed. Noise measurements are carried out in all the places prior the construction of the concrete basis where the seismometers installed.

DESCRIPTION OF THE SEISMIC TELEMETRIC SYSTEM

Teledyne Geotech developed the telemetry system. Every satelite seismological station is equipped with a sensitive short period vertical seismometer of velocity type with a mass of 5 Kg, model S 13. It has a dynamic range about 140 db and an adjustable natural frequency of 0.75 Hz to 1.1 Hz. The signals which are recording at the stations, are passing through a pre amplifier unit and are filtering into the frequency range of 0.2 Hz and 5 Hz. Afterthat are modulated and are transmitted through telephone lines to the central station of Athens. Additionaly in this station, there are in operation two horizontal seismometers of the same type. There the signals are passing through a second amplifier unit and are recording with analog form on heat sensitive paper. The existance of a cental timing system provides simultaneously accurate time at all the records.

The Digital Equipment Corporation (DEC) PDP 11/84 computer coupled with the Teledyne Geotech Seismic detection, location and analysis software, makes a sophisticated seismic data processing system (SDP).

The purpose of SDP system is to collect and process data from all the stations, Teledyne Geotech (1985). The collection of data is considered as the primary function of this system. The signals which are transmitted to the central station, first are digitizing with a rate of 50 samples/sec. Each channel of these data is processed by a event detector. This event algorithm (Veith 1978), provides ostimates of time of onset of the signal, direction of the first motion, period and maximum amplitude of the signal.

In order to reduce false detections as a result of a noisy station in the network, a network voting algorithm is utilized in addition to the signal detector. This network confirmation algorithm requires the operator to enter stations characteristics, pre event and post-event recording times and minimum number of stations required to declare an event. With this information, a unique table is generated and stored into the memory. When an event is detected on a station of the network, that stations table is utilized to determine the order and window times that the event should de detected on other stations. If the table parametrs are satisfied and the entered minimum number of stations all detect an event, then a valid event is declared by the system and data from all the stations is recorded to magnetic tape until the detector declares the event to be términated. Signal arrival times will be passéd to the event analysis program and a preliminary hypocenter and magnitude will be computed.

Visual analysis of the signals could be performed by the operator also. The user can display waveforms of the recorded data and identify up to six different phases in each channel with their associated times. Also data from other seismological stations could be added to the event file. This updated data file may then be processed by a hypocenter program for event relocation. Some other features of the system include an FFT programm, bulletin generation and focal mechanisms.

DETECTABILITY LOCATABILITY OF THE NETWORK

The knowledge of the detection location capability is a very important aspect for every seismic network. This term means the ability of a seismic network to detect and locate any earthquake which occurs in the observational area with magnitude larger than a threshold magnitude M_T and coordinates X, Y, Z.

Several methods have been developed to estimate the detection/location probability function of a seismic network.

In this work we applied a method which gives the location probability of an observational network by combining the individual detection probability of every single station. This probability is based on actual data recorded by each station.

An explanation of this method is given below. First the detection probability of every station is estimated. For this purpose a relation of the form $P(i,M_T) = f(R)$ is calculated. This relation gives the probability of the station i to detects an earthquake of magnitude M_T which occurs at a hypocentral distance R away of the station. For magnitude M_T groups of magnitudes are used, which from now on will be presented by their mean values. So the M_T values of 2.5, 3.0 and 3.5 represents the magnitude groups 2.3 till 2.7, 2.8 till 3.2 and 3.3 till 3.7 respectively. For every station and for every one of these magnitudes a plot between the percentage of the detected and located earthquakes and hypocentral distance is done. The surrounded line, extrapolated at larger distances, gave the unknown relation $P(i,M_T) = f(R)$. As data, we used all the recorded and located shocks from the network. For the majority of the stations these records covers a period longer than a year.

In order to calculate the locatable probability, we divided the observational network into small squares, 20Km by 20Km. In every square, we assumed that a single earthquake occurs with fixed magnitude M_T at different depths. Then we can calculate the locatable probability P of the network under the condition that the earthquake must be detected at more than 2 stations. So,

$$P(M_T,X) = 1.0 - (P_0 + P_1 + P_2)$$

Where X represents the position of the earthquake, and P_n means the probability that the earthquake could be detected at only n stations as follows:

$$P_0 = (1\ p_1)(1-p_2)\ldots(1\ p_n)$$

$$P_1 = p_1(1\ p_2)(1-p_3)\ldots(1\ p_n) + \ldots + p_n(1-p_1)(1-p_2)\ldots(1-p_{n-1})$$

$$P_2 = p_1p_2(1-p_3)\ldots(1-p_n) + \ldots + p_{n-1}p_n(1-p_1)(1-p_2)\ldots(1-p_{n-2})$$

Where p_i is the individual detection probability of the i station of the network

The results are shown as three dimensional maps in fig. 2(a), (b), (c) where, inside the volume shown with contours, every earthquake with magnitude greater than the fixed threshold magnitude M_T can be detected and located with a probability larger than 90%.

ACCURACY OF THE DETERMINATION OF EARTHQUAKE SOURCE PARAMETERS

There are many factors influencing the accuracy of the determination of earthquake source parameters. These include such factors as the readings of the arrival time of seismic wave phases, the travel time tables assumed which are used for the determination and the geographical relation between epicenters and the distribution of the stations. As it is well known, the epicenter can be best located when the seismic stations are regularly distributed around it. In addition, the focal depth can be accuretly obtained when the epicentral distance from at least one station is not greater than the depth. So it is obvious that the distribution of the stations plays a very significant role in the calculation of the errors which are expected in the detrmination of the sorce parameters.

We followed the Monte-Carlo method which is discribed by Skoko et al. (1966). We expanded this method so that we can calculate the errors in both the horizontal directions and also in the depth. We assumed, for the case of simplicity, that the observational accuracy is the same for all the stations and the error follows the normal distribution with a mean value of 0 and a deviation of ε^2. The equation which connects the error of the calculated parameters, the location of the stations and the travel time of the seismic waves is as follows:

$$(\partial f/\partial \Delta)_k \, dx \sin\Theta_k + (\partial f/\partial \Delta)_k \, dy \cos\Theta_k + (\partial f/\partial Z)_k \, dz + dt = \varepsilon_k$$

where

$f(\Delta, Z)$	:travel time
Θ_k	:azimuth at the true epicenter, measured clockwise from the north to the station k.
dx, dy, dz	:distance between true and calculated epicenter in X, Y and Z direction respectively.
dt	:error of the origin time.
ε_k	:observational error of arrival time at each station
κ	:index number of the station
Δ	:epicentral distance

The true epicenter is assumed to be at the origin of our coordinate system. The derivatives of the travel time are calculated using a subroutine program by assumming a horizontally uniform velocity structure. On this basis, the above equation for four unknown parameters is solved. The hypocenters are located at intervals of 20 Km both in latitude and longitude, with three cases of depths 10Km, 60Km and 100Km. Then the coefficients for the left-hand side of the equation are computed. The right-hand side terms of the equation were determined by giving values out of a series of normally distributed random numbers with a mean value of 0sec and a standard deviation of 0.3sec. Two subroutine programs are also used to give appropriate weights to the errors according to the azimuthal coverage of the epicentral and the hypocentral distance. For each hypocenter, 17 equations were given as the number of the stations. By using the least square method, the unknown parameters obtained. This procedure was repeated 100 times and the standard deviation

were calculated as the final solution for the four unknown parameters. The results were smoothed and the general trend of the errors are shown as functions of the hypocenter locations in Fig. 3, 4 and 5. In these figures, for the case of seismicity, only the total horizontal error dh (dh = $[dx^2 + dy^2]^{1/2}$) and the error of the focal depth are given.

DISCUSSION CONCLUSION

We can notice from Fig. 1 that the coverage of the stations is almost good for the covered land area except for the SW part (South West Peloponessus and West Crete) of Greece.

This affect the location capability of the network. From Fig. 2(a), (b), (c) we can conclude that shallow earthquakes (depth < 50 km) with magnitude greater than 3.0 could certainly be detected within the observational area. For earthquakes with smaller magnitudes, for instance 2.5 the network has a gap at the Southern West side of Greece. We believe that the location capability will improved with the installation of one more station in part country.

Figures 3, 4, and 5 show the theoretical errors for the horizontal distance and the focal depth as functions of hypocentral location with variouw depths. Regarding these diagrams we can get some ideas on the accuracy of the determination of earthquake source parameters. Inside the network area the errors are less than 5 km for the horizontal distance and focal depth for all the depth cases. On the other hand outside the network these errors have greater values in general. As the adopted observational errors had a standard deviation of 0.3 sec., we believe that the calculated observational errors are appropriate for earthquakes into the magnitude range of 2.5 - 3.0. So for earthquake with larger magnitude, as the arrivals are clearer, the observational errors must be smaller.

The results of the presented errors do not take into account the heterogeneity of the medium. The errors introduced from this factor will be in addition to the computed results of the present study.

REFERENCES

SKOKO, D., Y. SATO, I. OCHI, AND T. DUTTA. (1966). Accuracy of the determination of earthquake source parameters as determined by Monte Carlo method. Observation on Indian network Bull Earthq. Res. Inst. , 44, 893-900.

TELEDYNE GEOTECH (1985). Seismic Data Processing system (SDP), users\operators manuel. Garland, Texas, USA.

VEITH, K. F. (1978). Seismic signal detection algorithm. Technical Note 1, Teledyne Geotech. Garland, Texas, USA.

CAPTIONS

Fig. 1. The telemetric network of the Seismological Institute of the National Observatory of Athens.

Fig. 2. The contours show the three dimensional feature of the region, inside which earthquakes greater than the three shelled magnitudes Mt are detected and located with a probability larger than 90%. The numbers of the contours indicate in the unit of km.

(a) Mt = 2.5
(b) Mt = 3.0
(c) Mt = 3.5

Fig. 3. Theoretical errors for earthquake source parameters with a focal depth 10 km.

(a) Horizontal direction (km)
(b) Focal depth (km)

Fig. 4. Theoretical errors for earthquake source parameters with a focal depth 60 km.

(a) Horizontal direction (km)
(b) Focal depth (km)

Fig. 5. Theoretical errors for earthquake source parameters with a focal depth 100 km.

(a) Horizontal direction (km)
(b) Focal depth (km)

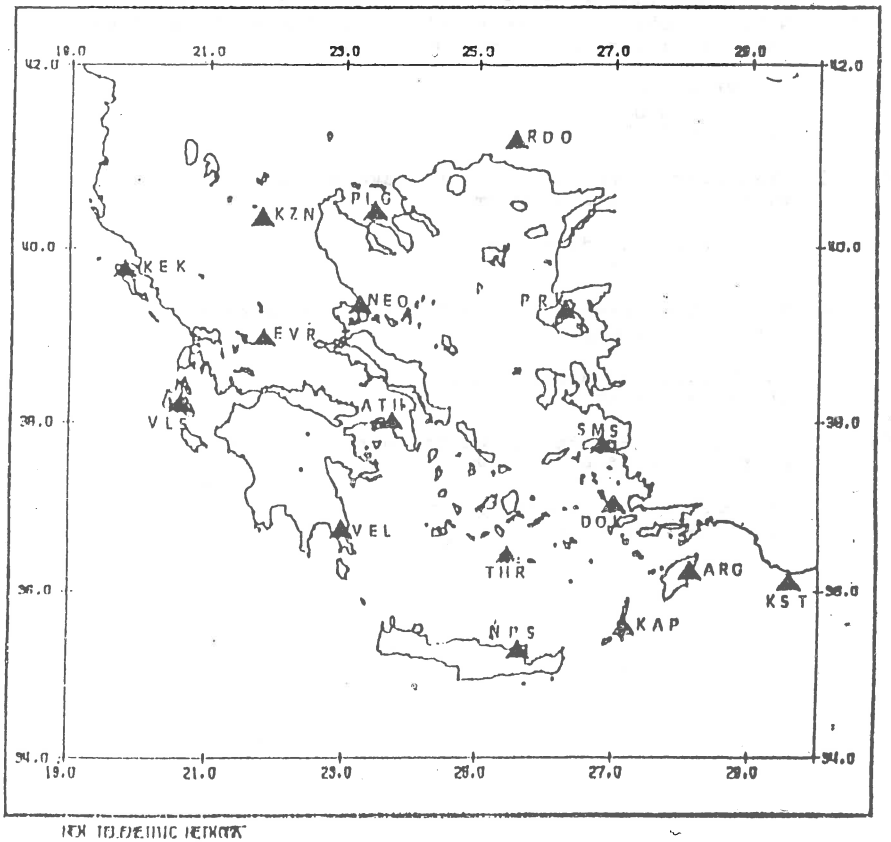
19.0
21.0
23.0
25.0
27.0
29.0
42.0
40.0
38.0
36.0
34.0
RDO
PLG
KZN
KEK
NEO
PRI
EVR
ATH
VLS
SMS
DOK
VEL
THR
ARG
KST
KAP
NPS

Fig 1

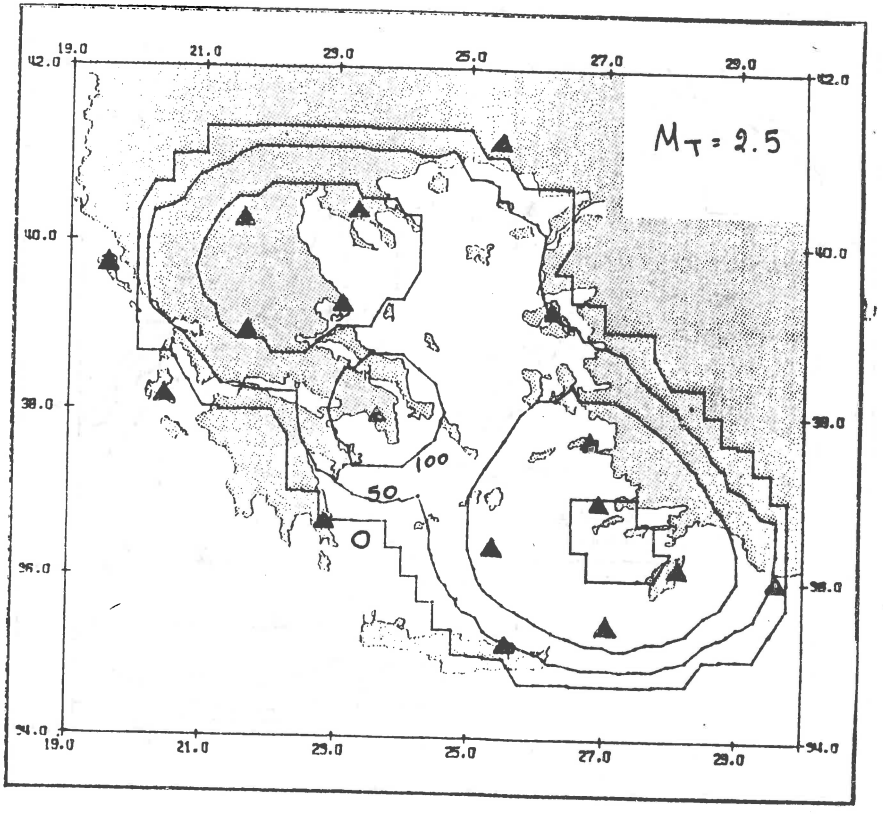

Fig 2(a)

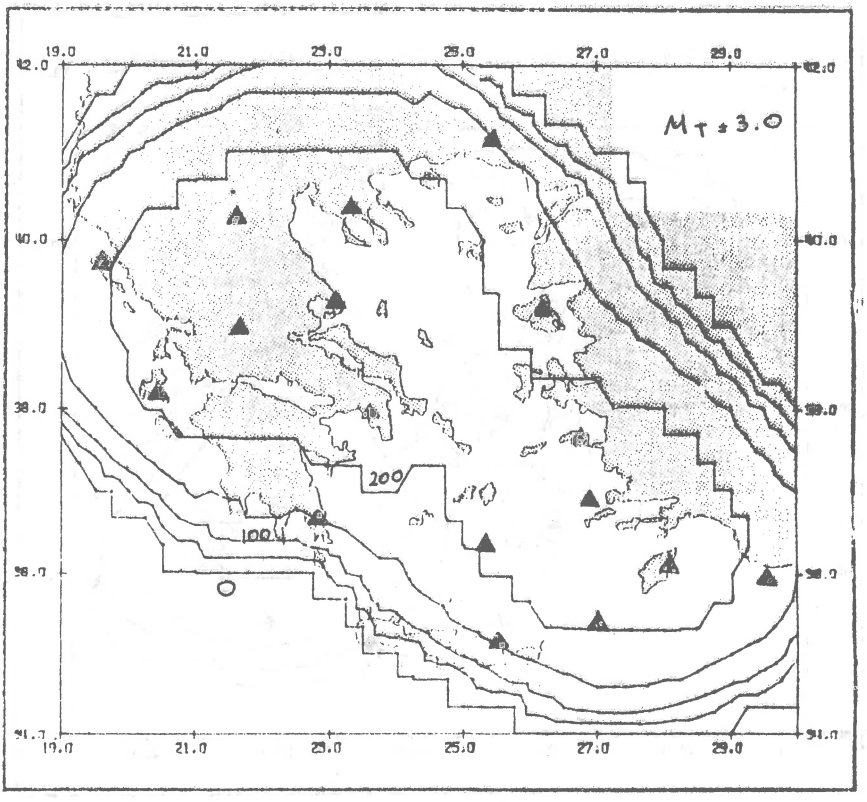

Fig 2(b)

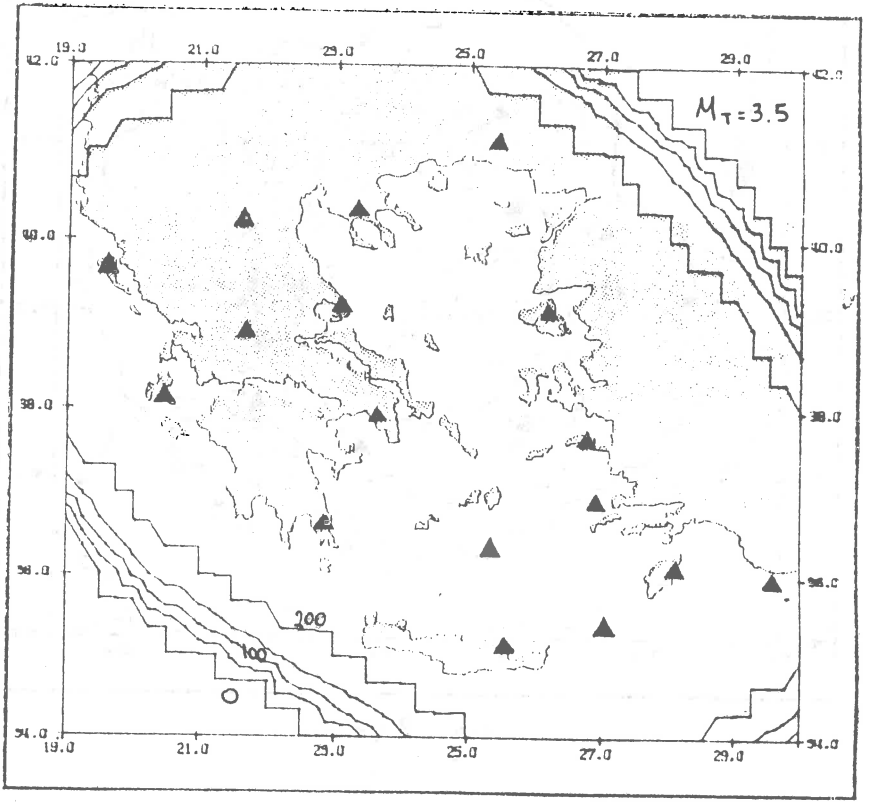

Fig 2(c)

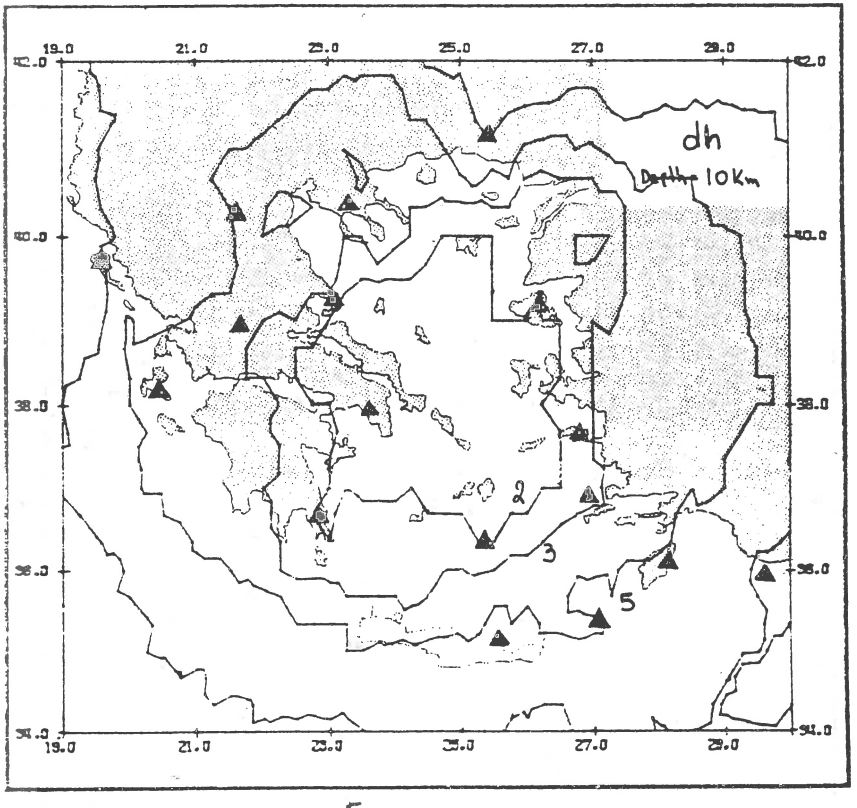

Fig 3(a)

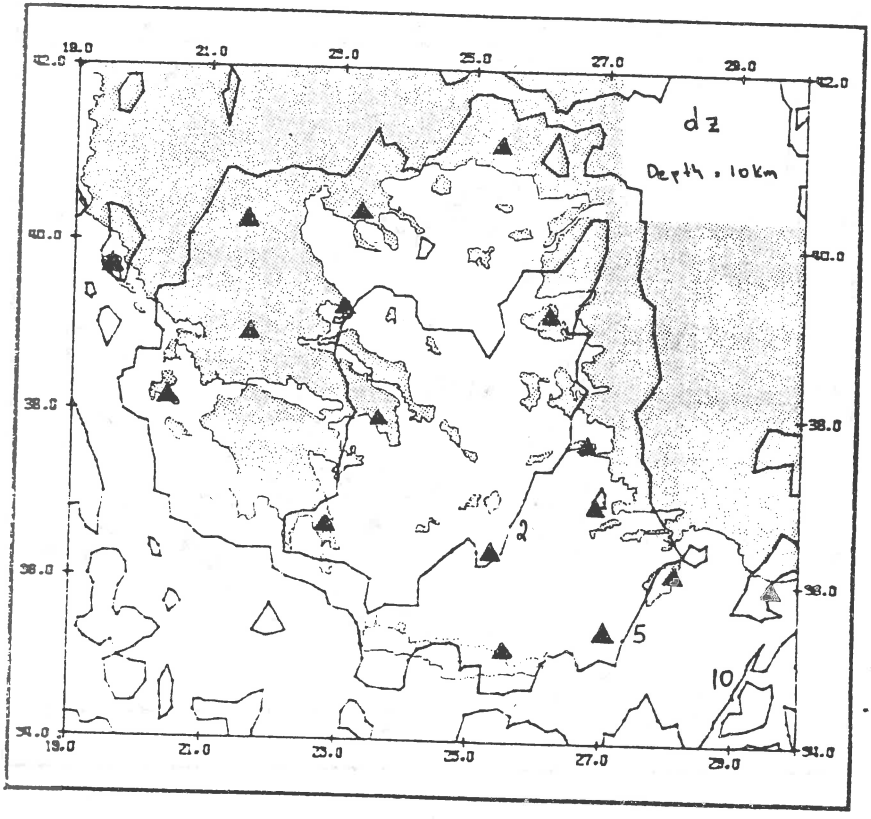

Fig 3(b)

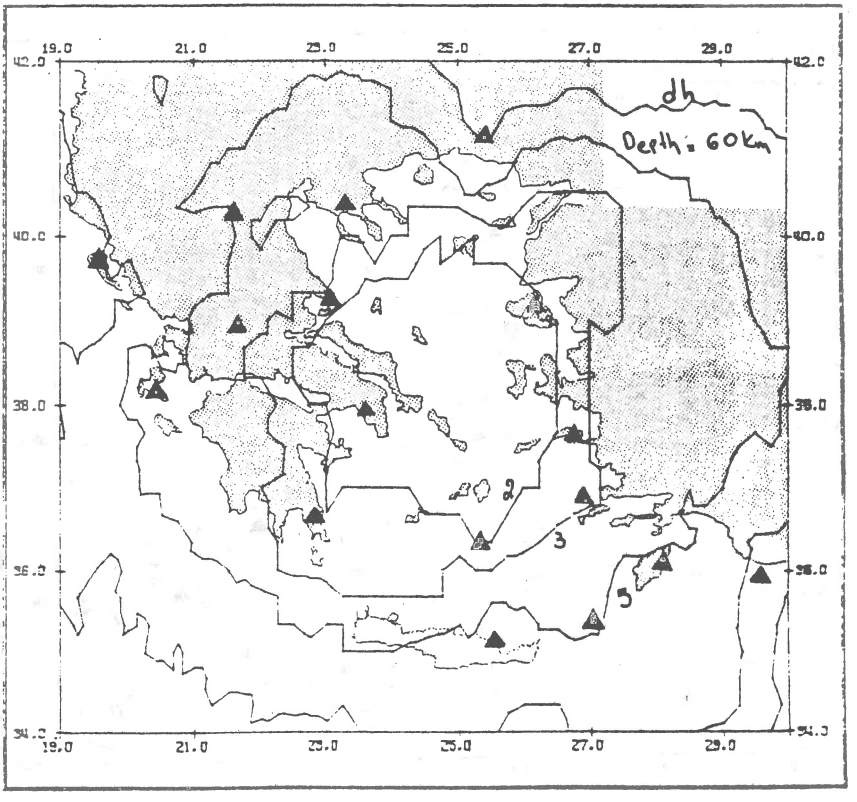

Fig 4(a)

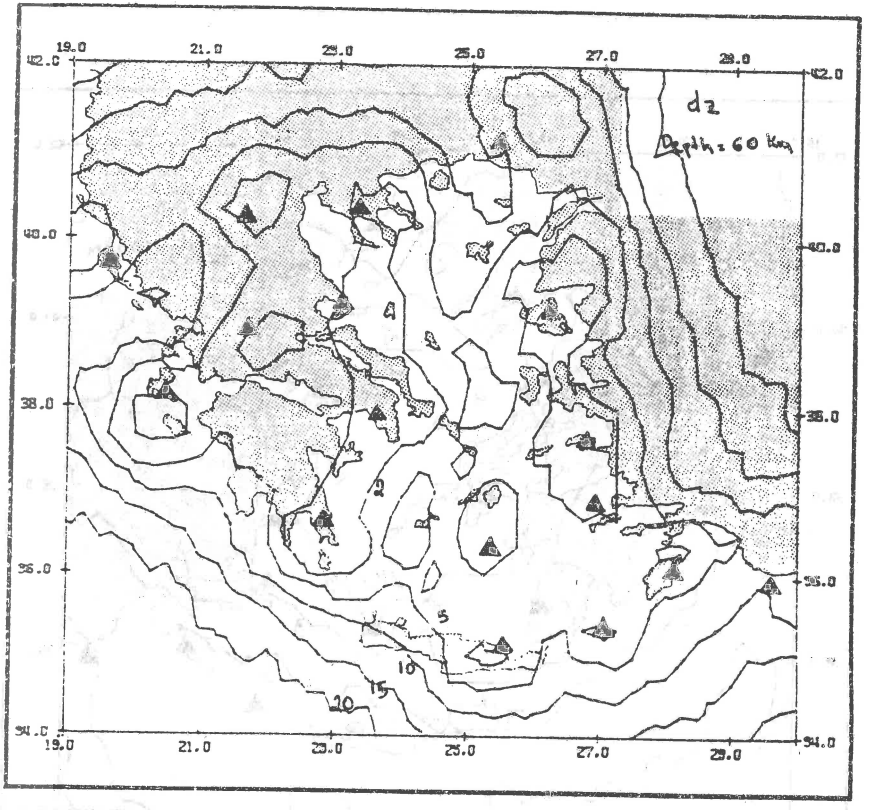
dz
Depth = 60 Km
19.0
21.0
23.0
25.0
27.0
29.0
42.0
40.0
38.0
36.0
34.0
0
5
10
15
20

Fig 4(b)

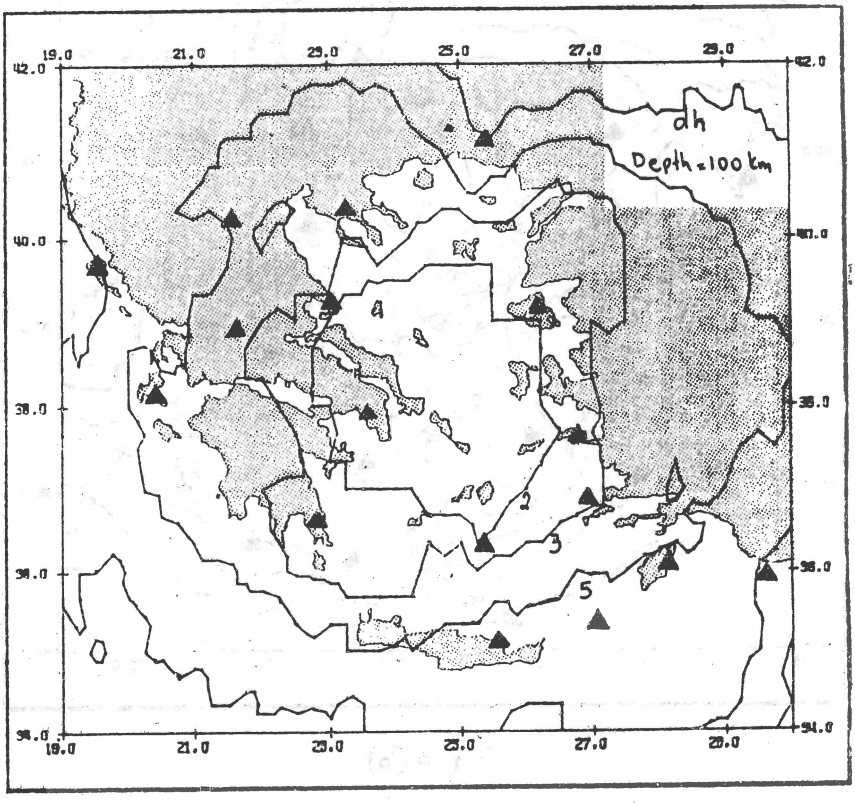
dh
Depth = 100 km
19.0
21.0
23.0
25.0
27.0
29.0
42.0
40.0
38.0
36.0
34.0
1
2
3
4
5

Fig 5(a)

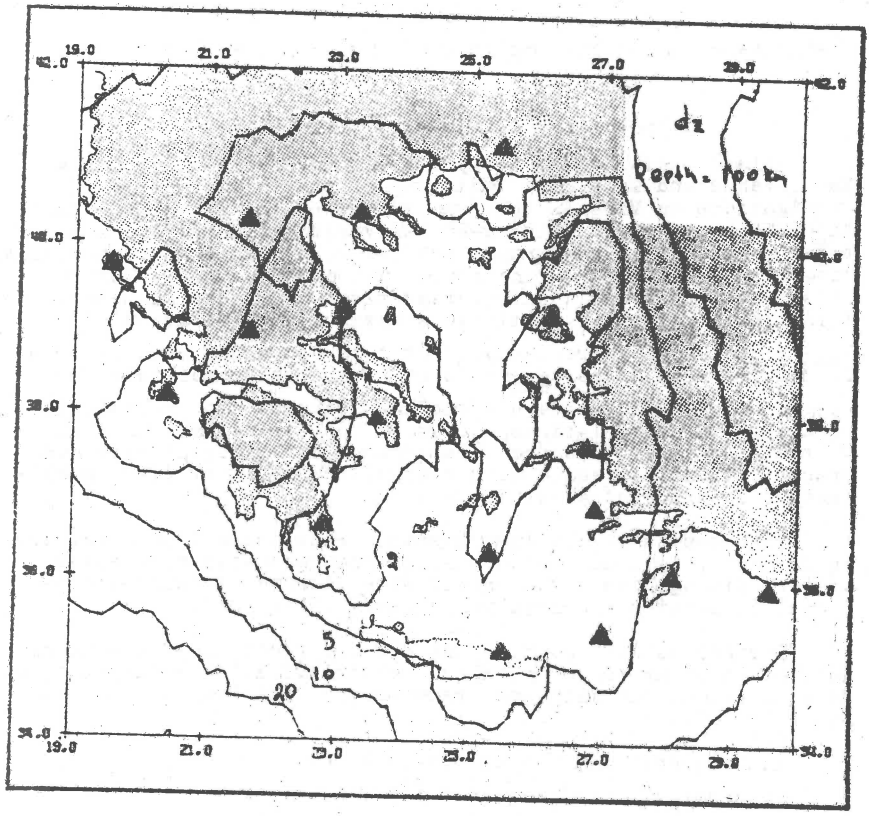

Fig 5(b)

CONSIDERATION AT ELABORATION OF THE RECEIVING-TRANSDUCING PART OF AN APPARATUS COMPLEX FOR SEISMOLOGICAL INVESTIGATIONS ON MARS

G.H. Mardirossjan

Institute of Space Research at BAS, Sofia

V.M. Fremd

Institute of Earth Physics at Acad. Sci. of the USSR, Moscow

D.D. Deneva

Geophysical Institute at BAS, Sofia

Planet seismological experiments have been made on the Moon, Venus and Mars. The beginning of the seismological investigations on Mars is the year 1976 when the USA space stations "Viking-1" and "Viking-2" delivered seismological apparatuses on it. The seismograph of "Viking-2" has been successfully disarrested and it has functioned in the course of 19 months. This seismograph had a shortperiod three-component magneto-electric transducer which permitted a maximum magnification of V_{max} = 218000 at a frequency about f_m = 3Hz and frequency band from f_{min} = 0.5 Hz to f_{max} = 10 Hz. The seismoreceiver was fixed on the hull of the descending apparatus, so it was mainly recording the oscillations caused by the strong Martian wind. On the 6 November 1976 the seismograph on "Viking-2" recorded probably a Martian quake with a magnitude of about 3 at an epicentral distance of about 110 km.

The results of the instrumental seismological observations on the Moon, Mars and Venus confirm the necessity of creating planet seismographs which should have improved technic-operational capacities and high reliability before all.

Further we will mainly consider the receiving-transducing part of an apparatus complex for seismological investigations on Mars in brief. The main requirements can be formulated as follows:

1. Frequency band: from 0.5 to 50 Hz.
2. Resolution at frequency f = 1 Hz.
   - for displacement: 5.10^{-9} m
   - for acceleration: 2.10^{-7} m/s^2
3. Dynamic range: D = 80 dB
4. Three components.
5. No need of arresting and disarresting as well as an adjustment of the zero and the natural frequency of the sensitive elements.

6. Reliable functioning at each position
7. High resistance to hit of 25-35 g.
8. Temperature range from -40° to $+40^{\circ}$C.
9. Minimal mass and dimensions.

Obviously most of the main requirements are contradictory and this circumstance requires some compromise in their solution. An apparatus seismological complex which meets these requirements will not only supply initial seismological data, but it will contribute to solving some purely technical and technological tasks.

In our opinion the above formulated main requirements can be fulfilled to a great extent using a seismoreceiver which will be specially elaborated for this aim on the basis of a three-component piezo-seismometer with general spherical or double conic inertial mass, as well as a proper electromagnetic system for an inner calibration.

The problems with the compromise solution of the contradictory requirements evolve from the basic correlations between the main parameters of each kind of seismoreceiver in particular of the piezo-seismoreceiver: its sensitivity K, the mass of the inertial element M, the capacity of the transducer C_o, the number, the dimensions and the position of the piezoelements, its natural frequency f_o, the noises and the input resistances of the prime electron amplifier and finally, the frequency range.

Let's trace out some of these correlations:

The electric sensitivity of the piezoelectric seismoreceiver for acceleration is:

$$(1) \quad k_x = \frac{M.\ddot{x}.d}{C_o}$$

where: M is inertial mass,

$\ddot{x}$ is acceleration of the apparatus frame, i.e. of the soil,

d is piezomodulus which characterizes the material of the piezo-transducer,

c is electric capacity of the piezo-transducer.

The time constant of the input chain of the prime amplifier to which the piezo-transducers are attached is as follows:

$$(2) \quad r = R_{IN}.C_o$$

where: R_{IN} is input resistance of the electron amplifier.

Formulas (1) and (2) show inverse proportionality between the piezoelements capacity C_o and the piezo-seismoreceiver sensitivity K, as well as direct proportionality between the capacity C_o and the time-constant τ which determines the lower

limit of the frequency range. The modern microcircuit electron amplifier with low noise can provide an input resistance of the order of R_I = 5Gohm. A manner to obtain higher sensitivity K_x or r , keeping the same sensitivity K_x at smaller mass M is to use a system of n piezoelements which would be joined in parallel.

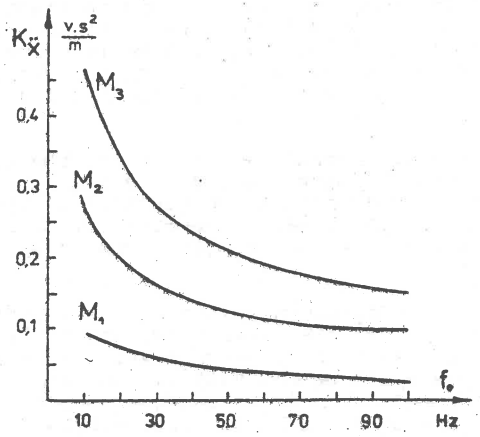

Fig. 1

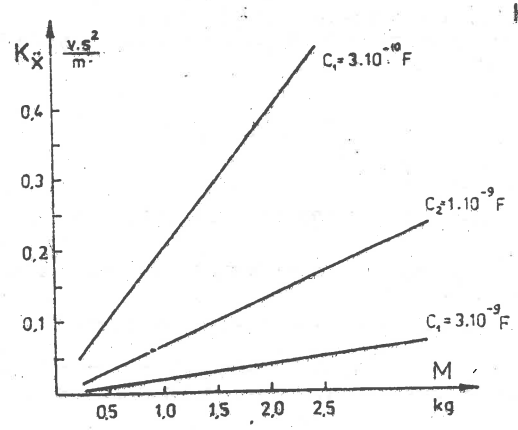

Fig. 2

Fig. 1 shows the dependence of the piezo-seismoreceiver sensitivity K on its natural frequency: $K=f(f_o)$ at three different values of the inertial mass M. The correlations between

the piezoelement rigidness, its geometric dimensions and its electric capacity, as well as the inverse proportionality between the natural frequency f_0 and the square root of the inertial mass M are taken into account.

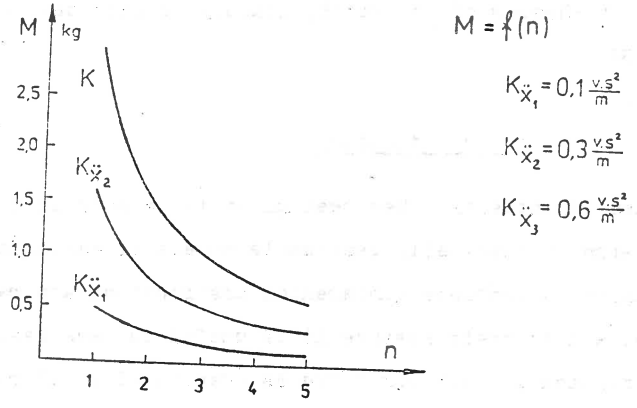

Fig. 3

Fig. 2 and Fig. 3 show the above commented dependences respectively between the sensitivity K and the inertial mass M: $K_x = f(M)$ and between the inertial mass M and the piezoelement number n: M = f(n).

Let's consider a few peculiarities of the proposed seismoreceiver. When installing the piezo-seismoreceiver the piezoelements are preliminarily pressed up with strength which exceeds the weight of the inertial mass M with an order. Taking into account that the piezoelement has elastic parameters close to the steel ones, we could count up the following exploitation advantages:

- a possibility to work at each position,
- stability at large hit accelerations,
- arresting devices not necessary

as well as low hum transverse sensitivity of the components (3-4%), a high coefficient of using the inner volume of the seismoreceiver, a possibility for an inner calibration with some different frequencies.

Conclusion: Without claiming this is a detailed analysis, we can assert that the proposed piezoelectric seismoreceiver can meet to a great degree the requirements which are demanded for the receiving-transducing part ofan apparatus complex for seismological investigations on Mars. However, at this stage the technical and technological conditions for elaboration and making of such seismoreceivers are available.

ANALYSIS OF BODY FORCE EQUIVALENTS FOR SEISMIC SOURCES

Sergei L. Yunga
Institute of Physics of the Earth, Academy of Sciences,
Moscow, USSR

1. Introduction.

Considerable attention has been given to seismic source problem in search of physically reasonable models of earthquake focal mechanism. A complete fundamental descriptions are rarely available, and in their absence it is useful to have less complete descriptions, which can serve as phenomenological representation of the source for use in fitting seismic data [1]. This last application makes it desirable for the seismic signal to depend linearly on the source representation. It has been pointed out by many authors that the solution to the problem of the seismic radiation from a suddenly occurring rupture in the earth's interior is likely to be connected with the solution to a dislocation problem [2]. An extensive review of this problem with respect to both theoretical and practical aspects is given in works [3,4].

As a result equivalent body force (EBF) formulations are extensively employed in the literature because of their simplicity, efficiency and adequacy for many practical applications. It should been noted that development of EBF models for earthquake source is usually based on a framework of elasticity and dislocation theories as developed for metals. However there are some differences in the experimentally observed behavior of metals

and frictional materials. In particular, frictional materials such as soil and rock show behavior pattern quite different from those of metallic materials. One of the distinguishing characteristics between metals and frictional materials is the existance of internal characteristic length. Thise difference must be recognized in order to develop reasonable body force equivalents for seismic sources.

Generally in fracture mechanics the EBF model is used to reduce the problem of a planar crack to a system of singular integral equations. The purpose of this paper is not to derive the radiation pattern of elastic waves irradiated by a suddenly propagated shear crack in earthquake source but to investigate only possible EBF models for earthquake source. To this end we derive EBF models in the most clear manner avoiding mathematical difficulties connected with the full analysis of the problem.

2. Method of analysis in linear elasticity.

The crack is modelled as a distribution of Mura's eigenstrains with on a priory known time dependent strength./5/. The contribution of eigenstrains to the equation of motion is shown to be equivalent to that of body forces in the following argument. The total strain ε_{ij} is regarded as the sum of elastic strain e_{ij} and eigenstrain ε^*_{ij}

$$\varepsilon_{ij} = e_{ij} + \varepsilon^*_{ij} \qquad (1)$$

where the total strain is calculated from the displacement vector u_i as

$$\varepsilon_{ij} = \frac{1}{2}(u_{i,j} + u_{j,i}) \qquad (2)$$

The eigenstrain ε^*_{ij} is direved from the jump of displacement b_i on the crack surface S and with unit normal to this surface as follows [6]

$$\varepsilon^*_{ij} = \frac{1}{2}(b_i n_j + b_j n_i)\delta(S),$$

where $\delta(S)$ is the Dirac delta function, which indicates concentration of deformation on the surface S so as

$$\int \varepsilon^*_{ij}\, dV = \int \frac{1}{2}(b_i n_j + b_j n_i)\, dS$$

The elastic strain is related to stress σ_{ij} through Hookes law as

$$\sigma_{ij} = C_{ijkl}\, e_{kl} = C_{ijkl}(\varepsilon_{kl} - \varepsilon^*_{kl}) \qquad (3)$$

where C_{ijkl} are the elastic moduli.

The equation of motion for a solid subjected to body force can be written as

$$\sigma_{ji,j} + f_i = \rho \ddot{u}_i \qquad (4)$$

Balance of momentum of moments leads to symmetry of stress tensor

$$\sigma_{ij} = \sigma_{ji} \qquad (5)$$

Here and throughout this paper a rectancular coordinate system (x_1, x_2, x_3) is employed. An index followed by a comma represents partial differentiation with respect to space variables and a superposed dot indicates material differentiation. Repeated indices denote summation over the range (1,2,3) accordingly Einstein summation convention. The foregoing equations are expressed in Eulerian representation. However, in the linear theory of elastic solids the difference between Eulerian and material (Lagrange) representations disappears since in calculating the

the time rates the convective terms are ignored [7].

Assuming now that the material is homogeneous and substituting eqn (3) into eqn (4) with $\varepsilon^*_{ij} = 0$, one notes that

$$C_{ijkl}\, e_{kj,j} + f_i = \rho \ddot{u}_i \qquad (6)$$

Also note that setting $f_i = 0$ in eqn (4) yields

$$C_{ijkl}\, \varepsilon_{kl,j} - C_{ijkl}\, \varepsilon^*_{kl,j} = \rho \ddot{u}_i \qquad (7)$$

Comparison of eqns (6) and (7) reveal that the total strain induced by an eigenstrain ε^*_{kl} is equivalent to the elastic strain induced by a body force of

$$-C_{ijkl}\, \varepsilon^*_{kl,j}$$

The total body force F^*_i ascribing to the volume V which contain all eigenstrains is defined as

$$F^*_i = \int_V -C_{ijkl}\, \varepsilon^*_{kl,j}\, dV$$

or

$$F^*_i = \int_{\partial V} -C_{ijkl}\, \varepsilon^*_{kl}\, dS_j$$

In the last formule integrand gives us the equivalent system of surface forces acting from the side of the solid media to the given volume V. Accordingly the action of the volume to the remainder part of solid elastic media has the opposite sign.

3. Method of analysis in linear elasticity with characteristic length.

Let us consider now the case than initially strong motion is arised in any small region with characteristic length . Material points contained in a small volume element, in addition to its usual rigid motion, can rotate about the centroid of the volume element in an average sence.

Balance of angular momentum gives

$$\epsilon_{k\ell r}\sigma_{\ell r} = \rho i_{k\ell}\ddot{\varphi}_k \,, \qquad (8)$$

where $i_{k\ell}$ - microinertia momehts, φ_k - rotation vector, $\epsilon_{k\ell r}$ - alternative tensor.

Assume for simplicity the case of microisotropic structute:

$$i_{k\ell} = j\delta_{k\ell} = \ell^2\delta_{k\ell}$$

By multiplying (8) by ϵ_{kmn} we put it into the form

$$\sigma_{[k\ell]} = \rho\ell^2\nu_{[k\ell]} \qquad (9)$$

where $\nu_{k\ell} = \epsilon_{rk\ell}\varphi_r$ is gyration tensor. Here we use identity

$$\epsilon_{rk\ell}\epsilon_{rmn} \equiv \delta_{km}\delta_{\ell n} - \delta_{kn}\delta_{\ell m}$$

Suppose that the stress constitutive equation (3) only determines the symmetric part of the stress tensor, i.e. write

$$\sigma_{(ij)} = C_{ijk\ell}\, e_{k\ell} \qquad (10)$$

where $a_{(\,)}$ enclosed the parenthesis indicates the symmetric part of a tensor and similarly $a_{[\,]}$ will be used to indicate the skew-symmetric part of a tensor, i.e.

$$a_{(k\ell)} \equiv \frac{1}{2}(a_{k\ell} + a_{\ell k}), \quad a_{[k\ell]} \equiv \frac{1}{2}(a_{k\ell} - a_{\ell k})$$

The total gyration $\nu_{k\ell}$ is regarded as the sum of continous gyration $\omega_{k\ell}$ and eigengyration $\nu^*_{k\ell}$

$$\nu_{k\ell} = \omega_{k\ell} + \nu^*_{k\ell}$$

where the total gyration is calculated from the displacement vector

$$\nu_{k\ell} = \frac{1}{2}(u_{k,\ell} - u_{\ell,k})$$

The eigengyration $\nu^*_{k\ell}$ is derived analogously

$$\nu^*_{k\ell} = \frac{1}{2}(b_k n_\ell - b_\ell n_k)\delta(S)$$

The stress tensor is derived as

$$\sigma_{ij} = \sigma_{(ij)} + \sigma_{[ij]}$$

Let us take now the assumption typical for couple stress theories [7,8]. As it is known the couple stress theory results as a special case of the micropolar theory when the motion is constrained so that micro- and macro-rotations coincide, that is

$$\nu^*_{k\ell} = \nu_{k\ell}$$

Note that setting (9) and (10) in eqn (4) yields

$$C_{ijk\ell}\varepsilon_{k\ell,j} - C_{ijk\ell}\varepsilon^*_{k\ell,j} + \rho\ell^2\ddot{\nu}^*_{(ij)j} = \rho\ddot{u}_i \qquad (11)$$

Comparison of eqns (6) and (11) reveal that the total strain induced by an eigenstrain $\varepsilon^*_{k\ell}$ and eigengyration $\nu^*_{k\ell}$ is equivalent to the elastic strain induced by a body force of

$$-C_{ijk\ell}\varepsilon^*_{k\ell,j} + \rho\ell^2\ddot{\nu}^*_{[ij]j}$$

The total body force F^*_i is derived as

$$F^*_i = \int_{\partial V} -\{C_{ijk\ell}\varepsilon^*_{k\ell} - \rho\ell^2\nu^*_{[ij]}\}dS_j$$

4. Conclusion. The approach is presented which takes into account not only the classical average motion but also the local motion in the small region of earthquake focus. As a result of balance laws this theory leads to nonsymmetric equivalent system of body forces.

LITERATURE

1. Backus J., Mulcahy M. Moment tensors and other phenomenological descriptions of seismic sources. - I. Continuous displacements. Geophys. J.R. astr. Soc. 1976, V.46, pp.341-361.

2. Burridge R., Knopoff L. Body force equivalents for seismic dislocatoins. Bull. Seism. Soc. Am. 1964, V.54, No 6 pp. 1875-1888.

3. Ben-Menahem A., Singh A. Seismic waves and sources. Springen-Verlag, New-York. 1981, 1108 pp.

4. Rice J.R. The mechanics of earthquake rupture. In: Physics of the Earth's interior. Amsterdam, 1980, pp.555-649.

5. Mura T. Micromechanics of defects in solids. Martinus Nijhof Publisher, 1982, 494 pp.

6. Vaculenko A.A., Kachanov M.L. Continuum theory of media with microfractures. Izvestiya AN USSR. Mechanika tverdogo tela. 1971, No 4 pp.159-166 (in russian).

7. Eringen A.C., Suhubu E.S. Non-Linear theory of simple microelastic media. I. Int. J. Eng. Sci, 1964, V.2,No 2, pp.189-204.

8. Eringen A.C. Linear theory of micropolar elasticity. Int. J. Eng. Sci, 1966, V.15, No 6, pp.909-923.

SOME STATISTICAL PROPERTIES FOR SERIES OF FOCAL MECHANISM RANDOM MATRICES

M.A. Danilova, S.L. Yunga
Institute of Physics of Earth, Moskow, USSR

SUMMARY. We have investigated the statistical properties of series random matrices of seismic sources. We repeated some results of Kagan&Knopoff's paper [3] for the statistical properties of these matrices in term of the dimensionless index Γ and then investigated these properties in term of parameter $\varkappa$ which is the intensity of average matrices. Cumulative distribution of parameter $\varkappa$ and Γ for the normalized sums of random matrices is obtained applying of Monte-Carlo simulation. Then critical values of the parameter $\varkappa_c$ were calculated from distribution of $\varkappa$ for any N elementary events on the levels $\alpha = 0.05$ and $\alpha = 0.1$.

The statistical properties of the series mechanism matrices with tectonic constraint were also investigated in the same manner. Two statistical problems are connected with seismotectonic deformation studies based on fault plane solutions. The firs one is estimation of statistical properties of the normalized sum purely random matrices of the focal mechanisms. The second problem is connected with the estimation of statistical properties of normalized sum of random matrices with the tectonic constraint i.e. in the case when random matrices are subjected by additional condition.

Seismotectonic deformation tensor can be represented in terms of the main axes of the double couple sources as:

$$M = \frac{1}{N}\sum_{k=1}^{N} m_{ij}^{k} = \frac{1}{N}\sum_{k=1}^{N}\left(t_i^k t_j^k - p_i^k p_j^k\right), \qquad (1)$$

where m_{ij}^k is focal mechanism matrix, N is number of earthquakes in the seismogenic volume and t_i^k, p_i^k are unit vectors in the direction of tension and compression of the mechanism solutions respectivly [1]. M is the average mechanism matrix. M-matrix characterizes the directivity of seismotectonic deformation tensor. The full problem of seismotectonic deformation tensor has five degrees of freedom in three-dimensional space. In ourprevious studies, describing average mechanism matrix M we used: axes of tension T and compression P of the M-matrix, intensity of M-matrix $[\varkappa = 2\,(M_{ij}\,M_{ij})^{1/2}$, $0 \le \varkappa \le 1$ and Lode-Nadai coeficient $\mu_M [\mu_M = 3M_2/(M_1 - M_3), |\mu_M| \le 1$ where M_i are eigenvalue of $M_{ij}]$.

The dimensionless index $\varkappa$ is proposed to be the main statistic for the series of the focal mechanism solutions. As it has been showed in our previous papers [1], the intensity $\varkappa$ defines the degree of agreement between the assemblage of the earthquakes being considered and the average mechanism, such that for a random orientation of the focal mechanisms, $\varkappa = 0$. If the mechanisms of all earthquakes are identical, $\varkappa = 1$. It can be mentioned that this problem is analogous to the statistical problem of Brounian motion study. Parameter $\varkappa$ multiplayed by N may be considered as a resulted parth in terms of Brounian motion in appropriate matrix space.

The main tectonic motion direction in a region can be defined from the null-axes b_{ij} of focal mechanism solutions, as it was shown by Sheigegger [2]. To consider the main tectonic motion direction we propose to introduce B-matrix as:

$$B = \frac{1}{N}\sum_{k=1}^{N} b_{ij}^{k} = \frac{1}{N}\sum_{k=1}^{N}\frac{\sqrt{3}}{2}\left(b_i^k b_j^k - \frac{1}{3}\delta_{ij}\right), \qquad (2)$$

where δ_{ij} is Kroneker symbol and $(2\,b_{ij}\,b_{ij})^{1/2} = 1$. The main tectonic motion direction corresponds to vector of B-matrix with its minimum eigenvalue.

Kagan and Knopoff [3] have investigated statistical properties of two components of seismic sources in terms of invariants of the seismic moment tensor of a realistic set of synthetic earthquakes. In the first case they proposed that a comlex earthquake is a set of individual randomly oriented elementary pure double couple sources [m = M_o diag [1,-1, 0], where M_o is the scalar moment . Then the seismic moment tensor of this complex earthquake corresponds to seismotectonic deformation tensor. In the second case the seismic moment of complex event is the sum of the compensated linear vector dipole (CLVD):
[m = $3^{-1/2}$ M_o diag [2, -1, -1].
The invariants of a symmetrical tensor m_{ij} are:

$$I_1 = tr(m_{ij}) = m_{11} + m_{22} + m_{33}$$

$$I_2 = m_{11}m_{22} + m_{11}m_{33} + m_{22}m_{33} - m_{23}^2 - m_{13}^2 - m_{12}^2 \qquad (3)$$

$$I_3 = det\,(m_{ij})$$

For a traceless tensor $I_1 = 0$, $I_2 < 0$. In the case of the double couple $I_3 = 0$, while in the case of the CLVD it is not.

In thier paper [3] Kagan and Knopoff calculated the dimensionless index as a measure of the content of the CLVD compromment in the deviatoric second order tensor:

$$\Gamma = \frac{1}{2} I_3 \left(-\frac{1}{3} I_2\right)^{-3/2} \qquad (4)$$

They noted that if $\Gamma = 0$, tensor is a double couple, since $I_3 = 0$; if $\Gamma = -1$ or $\Gamma = +1$ a source is a pure CLVD one.

If we use the above-mensioned measure μ_M and $\varkappa$ for matrix M, then: $\Gamma = 1/2\ 3^{3/2} \det(M)/\varkappa \cdot 8$ and

$$\Gamma = \frac{-\mu_M (9 - \mu_M^2)}{(3 + \mu_M^2)^3} \qquad (5)$$

Our first purpose is to estimate statistical properties of B- and M-matrices in term of index Γ, as it had be done by Kagan & Knopoff, and in term of index $\varkappa$. In this case the orientation of the focal mechanism of each individual earthquake is a puraly random one.

To study this problem we have recourse to a Monte - Carlo simulation, as proposed by Kagan & Knopoff [3]. We used a method of simulation based on the correspondence between a direction in 4-D space(of normalized quaternions) and rotations in ordinary 3-D Euclidian space. The advantage of this approach is that a uniform distribution of a direction on the unit quaternion sphere corresponds to a uniform random 3-D rotation [4].

In the practical terms, the simulation is performed as follows. We first represented the sourse as a tensor product of one (b_i) (for the CLVD sourse) or two (p_i , t_i) (for

double couple source) normalized vectors. That a point is randomly chosen on the unit quaternion sphere and we interpret the four values obtained in this way as components of a unit quaternion $q=(\varrho,\lambda,\mu,\nu)$. Because the uniform distribution of directions on the unit quaternion sphere corresponds to a uniform 3-D rotation the next source is a tensor product b'_{ij} of the new vector b'_i or m'_{ij} of the new vectors p'_i and t'_i, where $x'=Ax$ and

$$A=\begin{pmatrix} \lambda^2-\mu^2-\nu^2+\varrho^2 & 2(\lambda\mu-\nu\varrho) & 2(\nu\lambda+\mu\varrho) \\ 2(\lambda\mu+\nu\varrho) & \mu^2-\nu^2-\lambda^2+\varrho^2 & 2(\mu\nu-\lambda\varrho) \\ 2(\nu\lambda-\mu\varrho) & 2(\mu\nu+\lambda\varrho) & \nu^2-\lambda^2-\mu^2+\varrho^2 \end{pmatrix} \quad (6)$$

Repeat this procedure we may calculate B-matrix and M-matrix for any perfectly random N events.

In Kagan & Knopoff's paper this problem was solved analitically for the case of two CLVD sources for index Γ [3] as:

$$\Gamma = \mathrm{sgn}(\Gamma_m)\left[(9\cos^2\varphi-1)/(3\cos^2\varphi+1)^{3/2}\right], \quad (7)$$

where Γ is the index of the resultant source and Γ_m is the index of the primitive sources. The distribution density of the angle is $(\sin\varphi)/2$, $0\le\varphi\le\pi$. If we set $\xi=\cos\varphi$, after some manipulations, we obtain the following expressions for comulative distribution function of Γ : $F(\Gamma)=\xi$ for $\Gamma_m=1$ and $F(\Gamma)=1-\xi$ for $\Gamma_m=-1$, where Γ is defined by equation (7) and $0\le\xi\le 1$. The inversion of equation (7) gives a direct expression for the cumulative distribution function of Γ.

We also solve this problem for index $\varkappa$ and find that:

$$\varkappa=\sqrt{1+3\cos^2\varphi}/2 \quad (8)$$

Fig.1 shows the cumulative distribution of the parameter (fig.1a) and parameter $\varkappa$ (fig.1b) for the normalized sum of two random matrices b_{ij}.

In fig.2 we show the distribution of Γ for B-matrix (fig2a) and for M-matrix (fig. 2b) for a summary matrix composed of elementary tensors b_{ij} and m_{ij} respectively. In this simulations we have used 10^6 elementary events, subdivided into groups of N each. The value of Γ and $\varkappa$ was determined for each group and the distribution of this values Γ and $\varkappa$ were than obtained. It is also noted that in Kagan & Knopoff's paper [3] the standart deviation $\sigma_\Gamma=0.5768$ for N=10 and $\sigma_\Gamma=0.5797$ was found for N=1000 by using 10^4 elementary events. Our results are: $\sigma_\Gamma=0.5766$ for N=10 and $\sigma_\Gamma=0.5899$ for N=1000 by using 10^6 elementary events.

Calculated cumulative distribution of the parameter for the sum of m_{ij} - and b_{ij} -matrices coincides with the same results in Kagan & Knopoff's paper [3]. In their paper it was also shown that the value of index for the sum of the double couple sources is distributed uniformly in the interval $[-1,1]$ and it is neat uniformly for the sum of CLVD elementary sources. For large N the simulations are the same for both types of interval elementary subevents. The property of the uniformity of the distribution of for the sum of randomly rotated traceless sources will be of value when one compare the results for other types of rotational distributions [3].

As it was mentioned above the dimensionless index $\varkappa$ can be used as a measure of a similarity of real focal mechanism solution

This property is well appreciated for statistical purposes. We computed the cumulative distribution of the parameter $\aleph$ for M-matrix by a Monte-Carlo simulations. In this simulations we have also used 10^5 elementary events, subdivided into groups of N each. In fig.2c we show the distribution of $\aleph$ for M-matrix composed of elementary tensors m_{ij}, each subjected to a random rotation just in the same manner as it was discribed above.

Since the low values of parameter $\aleph$ is sometimes obtained in the calculation of M-matrices for the real focal mechanism matrix series, it is necessary to estimate the critical value of computed from the series of the random matrices m_{ij} for the comparison with the value of $\aleph$ index for the real M-matrices. The critical values $\aleph_c$ were calculated from distribution of $\aleph$ for M-matrix and B-matrix for any N elementary events on the level $\alpha = 0.05$ and $\alpha = 0.1$ (fig.3a). The critical value shows that a part $(1-\alpha)100\%$ of all normalized (average) matrices m_{ij} (or b_{ij}) computed from the series of N random matrices belongs to the interval $[0, \aleph_c]$ on the given level α.

It is clear that it's difficult to obtain the high value of parameter $\aleph$ for the sum of large N random m_{ij} -matrices. However, it's often necessary to study seismotectonic deformation in the region with the only low number of investigated earthquakes. In this case we sometimes obtained the low value of M-matrix index $\aleph$ near to $\aleph_c$ for given N.

Therefore our second object is to estimate the statistical properties of M-matrix in term of index $\aleph$ (or Γ) in the case of random matrices m_{ij} subjected by additional condition. The last one has the form inequality:

$$\mathcal{D}_{ij} \cdot m_{ij} > 0 \qquad (9)$$

where $\mathcal{D}_{ij}$ is the deviatoric part of the tensor of tectonic stress. This condition follows from the second law of thermodinamics. For a given tensor $\mathcal{D}_{ij}$ and firstly quite random matrices m_{ij}, we select only the ones that correspond to inequality (9). Matrices selected in the last manner are called here like random matrices with tectonic constraint.

The distribution of the parameter $\aleph^T$ for the sum of N random matrices m_{ij} with tectonic constraint was calculated. Then we define the critical values $\aleph^T_c$ for these matrices for various values N on the levels $\alpha = 0.05$ and $\alpha = 0.1$. The results are shown in fig.3b and permit us to express some conclusions.

The average measure $\aleph^T$ of coincidence for the random focal mechanism matrices with tectonic constraint is considerably less than 1. It is necessary to take into account the result in the tectonic investigations. In other way a mistake of the second kind occurs and in this case one may accept a rather regular process as a purely random one.

The main feature of the results presented is the minimum on the curves, as it is clear in fig.3b. This minimum corresponds to value N=30. We may obtain very high value of parameter $\aleph^T$ for the sum of N focal mechanism solutions, for $N \leqslant 30$. The critical value $\aleph^T_c$ is nearly constant and close to 0.37 for the large N. Therefore in certain sense it is the optimal quatity of the focal mechanism solutions in investigating of seismotectonic deformation.

REFERENCES

1. Kunga S.L. On the mechanism of deformation of a seismo-active volume of the Earth's crust. Izvestiya, Academy of Sciences, USSR, Physics of the Solid Earth, 1979, v.15, N 10, pp.693-699.

2. Sheidegger A.E. The tectonic stress and stress and tectonic motion direction in Europe and Western Asia as calculated from earthquake fault-plane solution. Bull. seism. Soc. Am., 1964, v.54, N 5 (part A), pp. 1519-1528.

3. Kagan Y.Y., Knopoff,L. The first -order statistical moment of the seismic moment tensor. Geophys. J.R. astr. Soc., 1985, v. 81, pp. 429-444.

4. Moran P.A.P. Quaternions, Haar measure and estimation of paleomagnetic rotation. In: Perspectives in Probabillity and Statistics, 1975, ed. Gani, J., Academic Press, London, pp. 295-301.

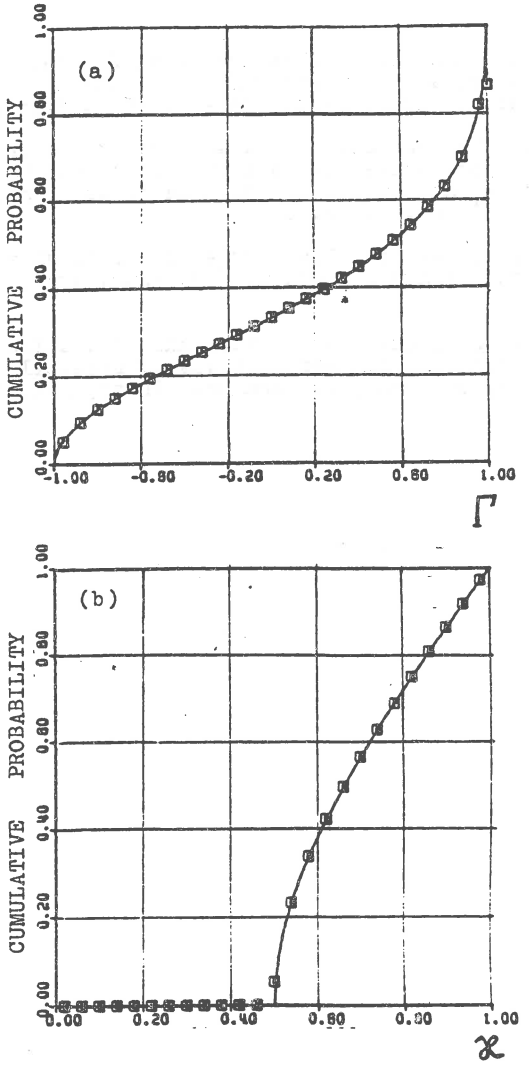

Figure 1. Cumulative distribution of parameter Γ (a) and parameter χ (b) for B-matrix composed of two elementary random matrices b_{ij}. Solid lines are analitic resolutions and points correspond to resolution by Monte-Carlo simulation. It was used 10^6 elementary events.

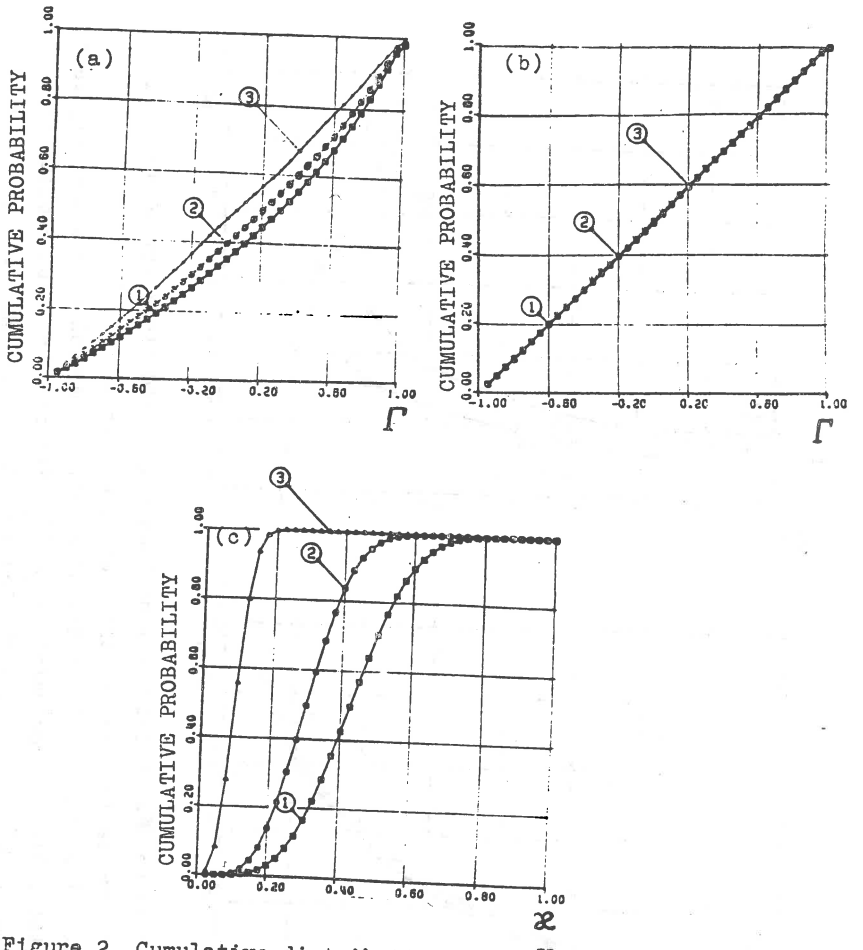

Figure 2. Cumulative distributions of parameters for B-matrix composed of N elementary random ℓ_{ij}- matrices and for average mechanism M-matrix composed of N elementary random focal mechanism m_{ij}-matrices. Distribution of parameter Γ for B-matrix is shown in fig. 2a and for M-matrix - in fig. 2b. Distribution of parameter χ for M-matrix is shown in fig.2c. Case 1, N=5, case 2, N=10, case 3, N=100.

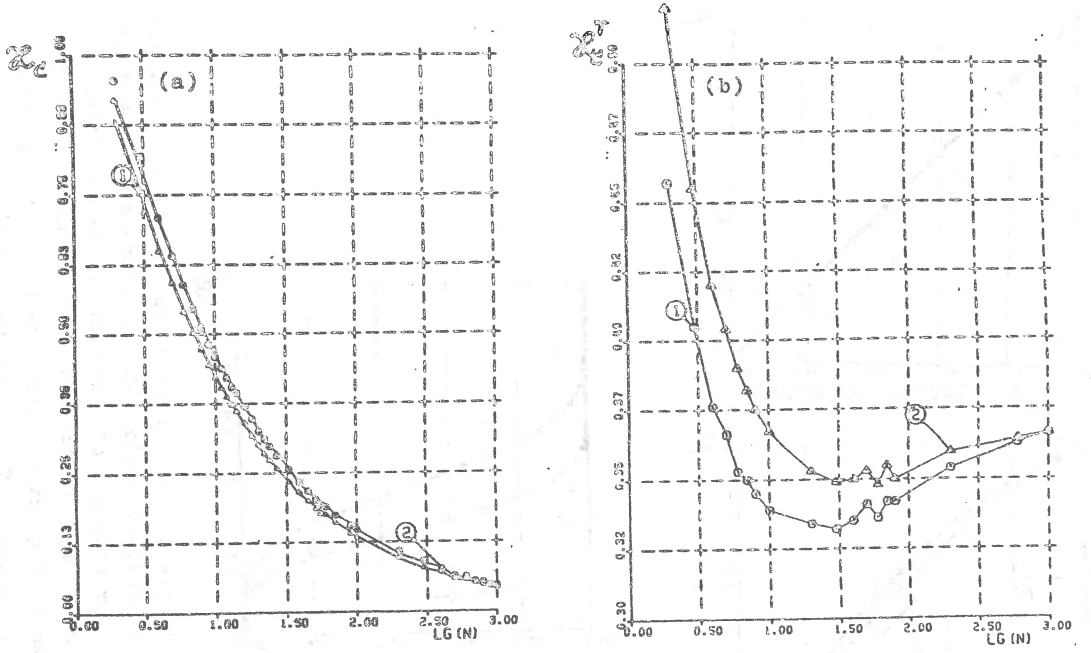

Figure 3. a) Critical value $\mathcal{K}_c$ of intensity of M-matrix (solid line) and of B-matrix (points) obtained from cumulative distributions of parameter $\mathcal{K}$.

b) Critical value $\mathcal{K}^{\Gamma}_c$ of intensity of M-matrix composed of N elementary random matrices m_{ij} with the tectonic constraint ($\mathcal{L}_{ij} \cdot m_{ij} > 0$) obtained from cumulative distribution of parameter $\mathcal{K}^{\Gamma}$. Case 1, on the level $\alpha = 0.1$, case 2, on the level $\alpha = 0.05$.

FAULT-PLANE SOLUTIONS OF THE THREE STRONGEST EARTHQUAKES IN THE SEMMERING REGION IN 1984

Dana Procházková[1], Julius Drimmel[2]

[1]Geophysical Institute, Czechosl.Acad.Sci., Prague.

[2]Central Institute for Meteorology and Geodynamics, Vienna.

Introduction

Zone Mur-Mürz-Leitha is the well-known seismoactive zone in the Eastern Alps. The strongest earthquake in the vicinity of Murau on May 5, 1201 had the intensity 9° MSK-64 /1/. In terms of the works /2-4/ this line is regarded as a manifestation of a developing hidden deep-seated fault. The analysis of historical seismicity /5/shows that this zone is divided into several active segments; one of this is the Semmering region. The quoted work also showed that in the Semmering region two kinds of aftershocks were observed. The present work concentrates on one group of earthquakes, which occurred in the Semmering region in April to July 1984, and we have processed macroseismic and instrumental data in order to observe details of the processes taking place in the focal region.

Macroseismic data processing

Macroseismic data on the earthquakes belonging to the investigated sequence were collected above all by the Central Institute of Meteorology and Geodynamics in Vienna /7/. Collected were positive reports by people of the territory of Austria for 15 earthquakes.

Only for three strongest of them was it possible to compile isoseismal maps /7/. The isoseismal map of the first of them, on Apr.15, 1984 at 10h55m UTC is in Fig.1.

We can see that the inner isoseismals are elongated roughly in the ENE-WSW direction, i.e. near the direction of the Mur-Mürz-Leitha zone in this region. Uncommon intensity increase was observed in the Donau valley. The macroseismic co-ordinates of the epicentre φ = 47.65°N, λ = 15.85°E are identical with the co-ordinates of the centre of gravity of the 6° isoseismal. On the basis of isoseismal radii, Table 1, the epicentral intensity I_o = 8.5°MSK-64 and the macroseismic focal depth h = 5km were determined by using the Kövesligethy formula, α = 0.001, as well as the Blake formula, k = 3.1, Fig. 2.

Table 1.

Date	Macroseismic data of earthquakes
15.4.1988	r_6 = 5km, r_5 = 14.1km, r_4 = 36.6km, r_3 = 79.1km
22.5.1984	r_5 = 8km, r_4 = 24.4km, r_3 = 63.4km
24.5.1984	r_5 = 10.2km, $r_{4.5}$ = 16.7km, r_4 = 32.9km, $r_{3.5}$ = 81km

The isoseismal map of the stronger shock on May 22, 1984 at 19h 33m UTC is on Fig.3. The first inner isoseismal is elongated in the NE-SW direction. The form of the second inner isoseismal is nearly circular, which does not agree with the foregoing shock under investigation. The comparison of these two isoseismal maps

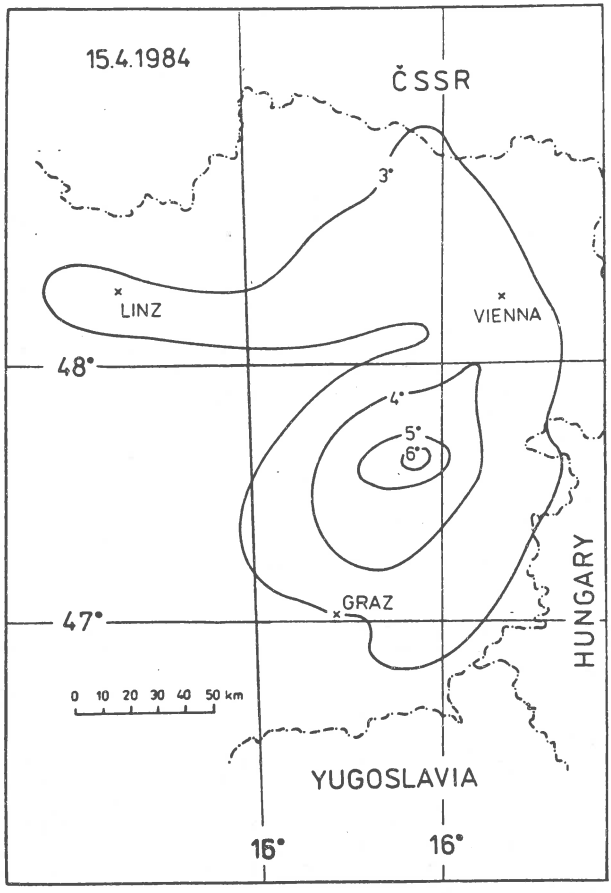

Fig.1. Isoseismal map of earthquake of Apr.15, 1984.

also shows that the local uncommon increase in the Donau valley is not observed in the case of the second studied shock.

The macroseismic co-ordinates of the epicentre φ = 47.65° N, λ = 15.85° E are identical with the co-ordinates of the centre of gravity of the 5°. isoseismal. On the basis of isoseismal radii, Table 1, the epicentral intensity I_0 = 5.5° MSK-64 and the macroseismic focal depth h = 9km were determined by using the Kövesligethy formula, α = 0.001, as well as the Blake formula, k = 3.2, Fig. 2.

The third earthquake on May 24, 1984 at 19h 56m UTC, the isoseismal map of which is in Fig. 4, was also macroseismically felt on the territory of Czechoslovakia (the Geophysical Institute of the Czechoslovak Academy of Sciences in Prague collected 144 positive reports by people of 65 localities /8/). The macroseismic co-ordinates of the epicentre φ = 47.65° N, λ = 15.85° E are

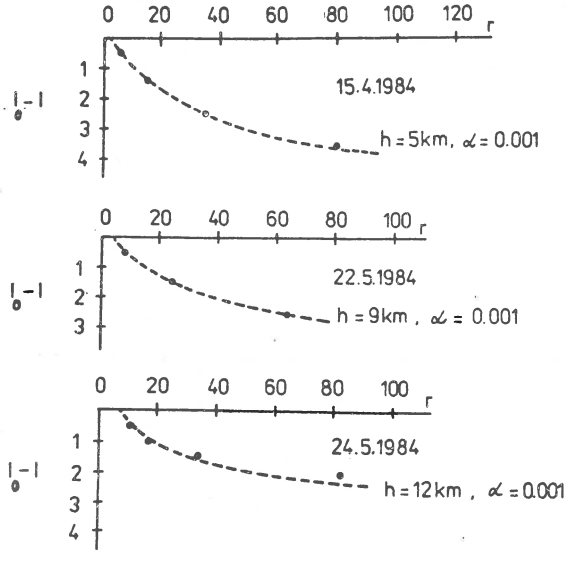

Fig.2. Intensity attenuations with epicentral distance of investigated earthquakes.

identical with the co-ordinates of the centre of gravity of the 5° isoseismal. On the basis of isoseismal radii, Table 1, the epicentral intensity I_o = 5.5° MSK-64 and the macroseismic focal depth h = 12km were determined by using the Kövesligethy formula, α = 0.001, as well as the Blake formula, k = 3.2, Fig. 2 (according to the first Vienna report I_o = 6° MSK-64). In Fig. 4, we can see that the two inner isoseismals are elongated in the direction NNW-SSE, which is near the perpendicular direction to the elongations observed in the case of the foregoing two earthquakes.

The differences among these studied shocks are in the size of the macroseismic fields (the last one has the greatest macrosismic field) and in the elongations of the remote isoseismals, especially 3° MSK-64. This mentioned isoseismal in the last case is elongated far into the Bohemian Massif. Though the elongation of remote isoseismals of earthquakes, the foci of which are in the Eastern Alps, in the Bohemian Massif is well known for a long time (see quotations in /9/), such great differences among the earthquakes with foci almost from one place are unexpected. The differences in the size of macroseismic fields can be partly explained by the increasing macroseismic focal depth of investigated shocks (5, 9, 12km) in agreement with /6/. The explanation of the differences in the isoseismal forms can only be sought in the focal mechanisms of these earthquakes and/ or the regional geology.

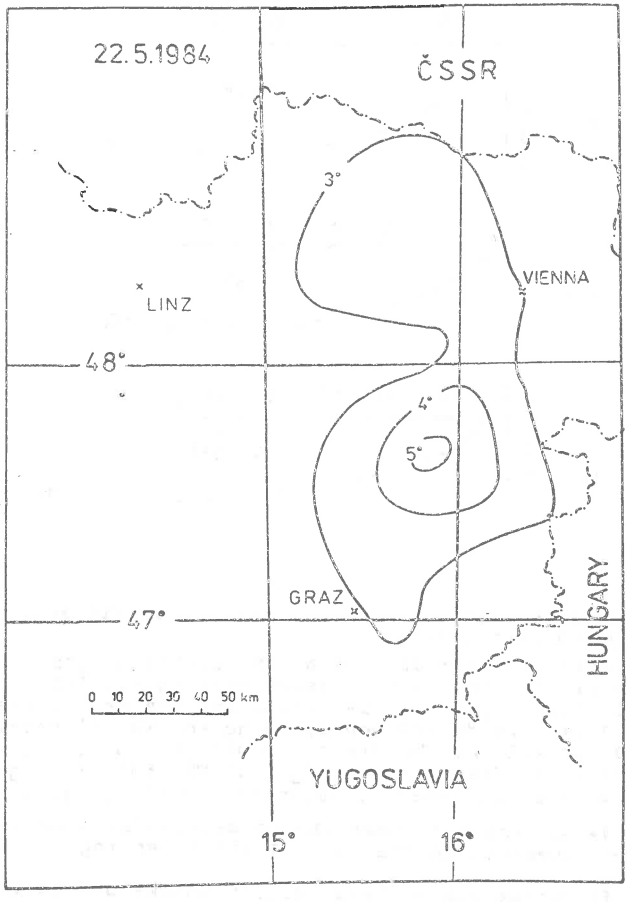

Fig. 3. Isoseismal map of earthquake of May 22, 1984.

Seismogram processing

The Bulletin of the International Seismological Centre /10/ says that the detailed studied three shocks were recorded at 130, 64 and 108 seismological stations, respectively. Except for they were recorded by several local and regional seismological stations which do not belong to the world network of seismological stations. Seismograms of some stations we obtained and used for the study.

For the three strongest shocks an attempt was made: besides the standard seismogram processing the interpretation of wave groups was also based on the multiple-shock concept in agreement with /11/. The empirical azimuthal

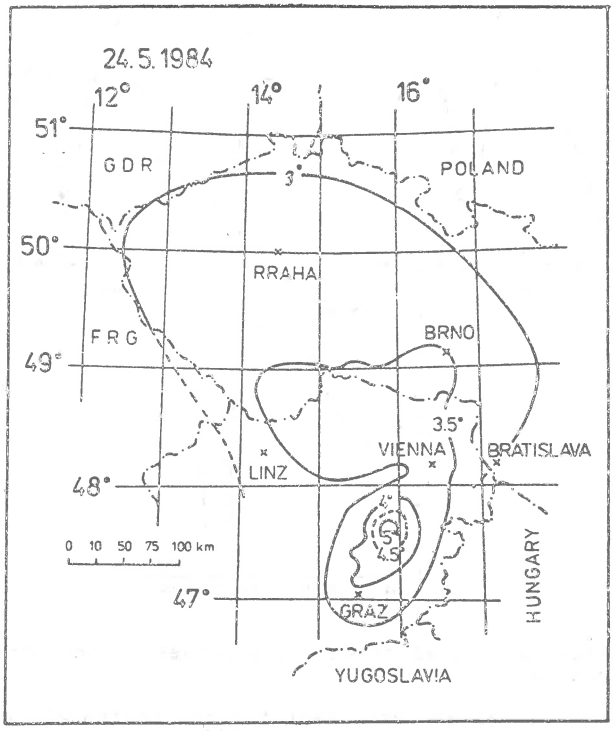

Fig. 4. Isoseismal map of earthquake of May 24, 1984.

travel-time curves showing the delay of the P_{max} with reference to first arrival times of P waves, Fig. 5, were compiled. We can see that the curves for shocks of April 15, 1984 and May 22,1984 are nearly the same and that the curve for the shock of May 24, 1984 distincly differs from both foregoing ones.

In order to obtain information fundamental to our understanding of the nature of the investigated earthquakes, fault-plane solutions of the studied three shocks were determined. To obtain them, we used the signs of the first motion of P waves. We collected 31, 11, 24 data of the ISC Bulletin /10/ and 14, 20, 14 data of the local or regional stations, some of which do not belong to the world-wide seismological network, respectively. Because we also took into account data of near seismological stations ($\Delta < 200$km), we used for the determination of the take-off angles of rays at the focus the layered model of the crustal structure of the region and the depth of the focus in agreement with /12/. As usual, we used the stereographic projection and the method described in /13/. Assuming the double-couple model we consider a fault to be represented by one of the nodal planes.

Figure 6, shows the meridians of both nodal planes, their pole- points X, Y, their intersection - point Z for the investigated shocks. We can see that the fit of the observed points and the

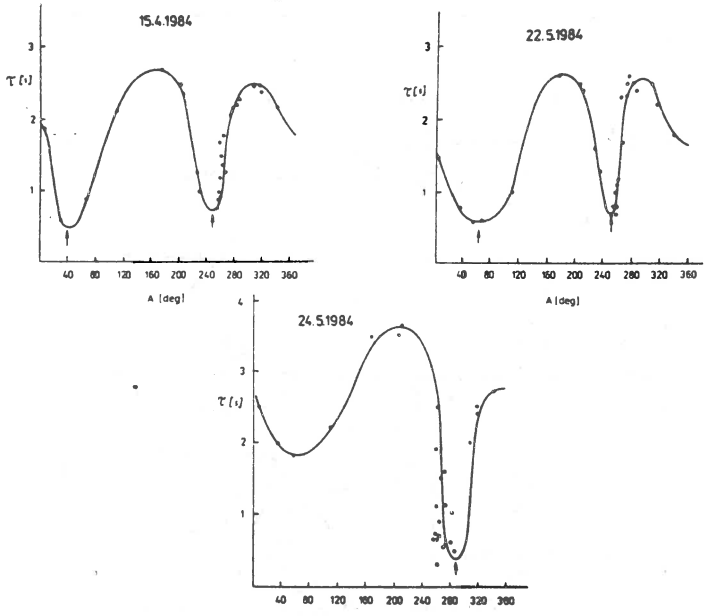

Fig. 5. Empirical azimuthal travel-time curves of investigated earthquakes.

courses of nodal planes are excellent for the earthquake of Apr. 15, 1984, good for the shock of May 22, 1984 (two points do not agree with the given solution) and sufficient for the shock of May 24, 1984 (two of five stations which do not agree with the given solution are far from the nodal planes, the rest in close to one of the nodal planes). The polar co-ordinates of the points X, Y, Z which fully describe the course of nodal planes are the following:

15.4.1984: X - A = 19°, i = 43°.
Y - A = 115°, i = 55°.
Z - A = 264°, i = 56°.

22.5.1984: X - A = 311°, i = 20°.
Y - A = 125°, i = 59°.
Z - A = 229°, i = 75°.

24.5.1984: X - A = 68°, i = 62°.
Y - A = 282°, i = 48°.
Z - A = 161°, i = 33°.

We can see that the fault-plane solutions of the first shocks are nearly the same and of the third shock quite different, which agrees with the results obtained by the macroseismic data proces-

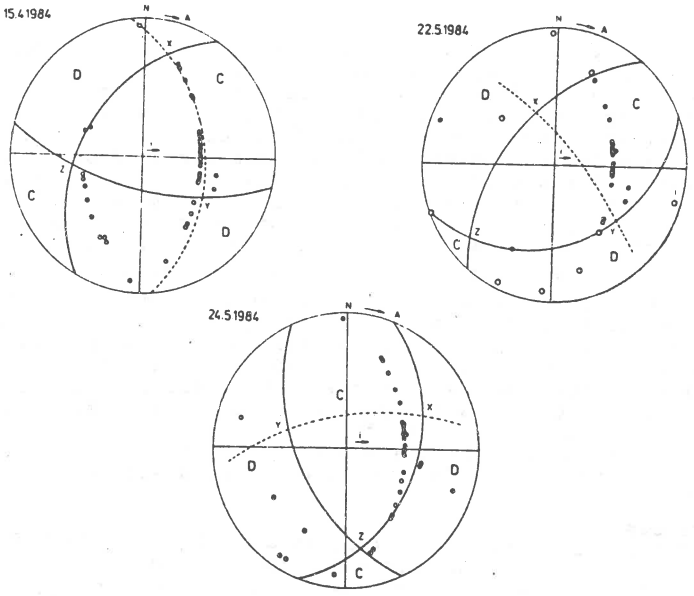

Fig. 6. Fault-plane solution of investigated shocks.

sing and non-standard seismogram interpretation mentioned above. A comparison of the course of nodal planes and the elongation of inner isoseismals (Figs. 1, 3, 4) shows that one of the nodal planes usually agrees with the elongation of inner isoseismals, which confirms the previous results.

Conclusions

A detailed evaluation of the macroseismic and instrumental data describing three earthquakes that occurred in the Semmering region in short successive periods (15.4.1984, 22.5.1984, 24.5.1984) has shown that the shocks differed in:

- Focal depth (5, 9, 12km).
- Elongation of isoseismals in the near zone (WSW-ENE, SW-NE, NNW-SSE) and partly also in the local intensity anomalies as well.
- The course of azimuthal travel time curves (close in the first two shocks under study).
- Earthquake mechanisms (similar in the first two shocks and quite different in the third shock).

The different methods of seismological data processing have revealed differences between the shocks studied. On the basis of the experience gained so far, these differences can be supposed to be due to different processes in the focal region. We can again find evidence that the character of focal processes in one place changes in time relatively quickly. A comparison of the elongation of isoseismals and the mechanism of the earthquake of 24.5.,1984 allows us to assume that the earthquake mechanism influences the shape of the macroseismic field even in the remote zone, i.e. relatively far in the Bohemian Massif may be felt the earthquakes

occurring in the region of the Eastern Alps, whose mechanisms cause a movement of blocks in planes NNW-SSE to NW-SE.

On the basis of the obtained results it can be inferred that the Semmering region lies on the point of intersection of at least three different fault systems (Mur-Mürz-Leitha, Qvarner-Semmering--Wien, NW-SE fault). Movements take place along these fault systems even in the course of one earthquake sequence. In order to extend our knowledge of the studied earthquakes, we will continue trying to determine stress drops of these earthquakes.

In conclusion it can be stated that a detailed study of individual earthquake sequences interferes with the often established idea of similarity of shocks in one focal region, which constitutes the basis of many practical applications. However, it gives a much more realistic idea of the physical processes that take place in the crust and in the upper mantle and that are responsible for earthquakes. The state of stress in a particular region is affected by the structure of the region, mainly by inhomogeneties in the structure, for one thing, and for the other, by the re-distribution of the state of stress which occurs after individual shocks, i.e. time represents a parameter of great importance.

References

/1/ J.Drimmel: Rezente Seismizität und Seismotektonik des Ostalpenraumes. In: Der Geologische Aufbau Österreichs. Springer-Verlag Wien, New York, 1980, 506.

/2/ A.V.Tchekunov, V.G.Kutchma: Glubinnaya struktura razlomov (in Russian). Geotektonika, No 5, Moskva 1979, 24.

/3/ V.I.Makarov, Yu.K.Schtchukin: Ocenka aktivnosti skrytych razlomov (in Russian). Geotektonika, No 1, Moskva 1979, 96.

/4/ D.Procházková, A.Dudek, Z.Mísař, J.Zeman: Earthquakes in Europe and their Relation to Basement Structures and Fault Tectonics. Rozpravy ČSAV, řada mat.-fyz. Academia, Praha 1986.

/5/ D.Procházková: Properties of Earthquakes in the Mur-Mürz--Leitha-Little Carpathians Region. Publ.Ser.Swiss Seismolog.Service, No 101. Zürich 1987, 147.

/6/ D.Procházková: Analýza zemětřesení ve Střední Evropě. Doctor's thesis. Geoph.Inst.Czechosl.Acad.Sci., Praha 1984.

/7/ J.Drimmel: Erdbeben in Semmering Gebiet. Erdbebendienst der Zentralanstalt für Meteorologie und Geodynamik. Wien 1984.

/8/ D.Procházková: Macroseismically Felt Earthquakes in Bohemia and Moravia in 1984. Travaux Géophysiques 1985. Academia, Praha, in press.

/9/ D.Procházková, A.Dudek: Parameters of Earthquakes Originated in Central and Eastern Europe. Travaux Géophysiques 1980, No 550. Academia, Praha 1982, 43-82.

/10/ Bulletin of the International Seismological Centre, 1984, April - July. ISC, Newbury 1986.

/11/ I.V.Gorbunova: Characteristics of Multiple Shocks. Wave Pattern, Extent and Orientation of Focal Region. Tectonophysics, 93(1983), 225-232.

/12/ I.G.Simbireva, A.S.Chepkunas: Mechanizmy ochagov zemletryasenij, opredelennye s uchetom regionalnogo stroyeniya zemnoj kory i mantii Kamchatky (in Russian). Vulkanologiya i seismologiya, No 2, 1986, 85-96.

/13/ K.Kasahara: Earthquake Mechanics. Cambridge Univ.Press., Cambridge 1981.

FAULT PLANE SOLUTIONS AND SEISMOTECTONIC DEFORMATIONS STUDY FOR THE CENTRAL BALKAN REGION

Botzev N. - Geophysical Institute, BAS, Sofia
Kunga S. - Institute of Physics of the Earth, USSR, Moscow

The study presented aims at focal mechanisms of small magnitude earthquakes determination and generalizing the data obtained to study tectonic stress and seismotectonic deformation field. Several hundred fault plane solutions were computer prepared. Averaging procedure is based on the calculation of the composite mechanism for a number of events. General pattern of regional stress field is presented.

Recent crustal large scale deformation and stresses are of special interest in geophysical studying of Central Balkan Region. A progress in understanding of this problem is of primary importence for geodynamical investigations of Bulgaria. However, for the time being there are only very limited data on stress field and seismotectonic deformation of this part of the Balkan region. The study of contemporary seismotectonic deformation process and state of tectonic stresses requires the selection of the appropriate new data concerning this kind of parameters which would have a genetic relationship with main geodynamical features.

The study presented here aims at focal mechanisms of small magnitude earthquakes determination and summarizing the data collection to derive a large acale tectonic stress field and seismotectonic deformation of Bulgaria.

The region under investigation represents a mozaic of subregions of different seismic activity and size with rather different behavior in the course of geotectonic development. The Thracian massive and Moesian platform represent the two rather stable blocks which plaed an important role in the geotectonical evolution. The folded area - Balkanides - lie between them [1]. Seismological and other geophysical information has been extensively used to investigate the seismotectonic process in this region [2]. Several geodynamical schemes such as models based on the assumption that the driving forces are external ones and are connected with movements of adjacent lithospheric plates or models with internal forces which produce gravitational sliding or at last models which involve forces that act at the bottom of the litosphere are proposed as it is known for Balkan region. The collection of new data for supporting of one or another models seems gives the possibilities for choosing the best one and have to be of great geophysical significance.

In our previous papers [3,4] first onsets of body waves recordings by mainly short period instruments were used to determine the fault plane solutions of small magnitude earthquakes for the period of time from 1983 to 1986. Additional data concerning first onsets of short period instruments recordings have been used to study focal mechanisms and to investigate the characteristic features of the stress state and deformation seismotectonic process of concidered region.

The present study is based not only on the polarity of P-

waves, but also on SH, SV - waves polarities. No others types of waves have been considerd and no the no the compressional or dilatational data enlisted in stations bulletins (ISC et al) have been used. A three layer crustal models different for North, Southwestern and Southeastern part of Bulgaria was assumed for the body waves rays calculations. Some possible others crustal models have been investigated in our previous paper [5] and it was founded that the influence of the accepted model is not of crucial importance for the problem of general directions of tension and compression stress reconstruction.

The data of first motions were plotted on an equalarea proection of the upper hemisphere of the focal sphere. The method of plotting SH, SV onsets in just the same manner as P-wave onsets was used during this study according our paper [6,7] . All the first motion readings were collected in the special data base and then fault plane solutions were computer prepared. As a typical example of one computer fault plane solution and a corresponding picture of first motions and nodal lines of focal mechanism is shown in fig.1. Dilations and compressions are represented by open and solid symbols respectively. Data of P wave first motions and SH, SV onsets are shown by circles and triangles, respectively.

A total number of 891 earthquake focal mechanisms of the Bulgarian region have been determined and taken up into the cataloque prepared for the period of time from 1983 to 1988. Due to the space distribution of seismisity completeness and balance in the regional distribution of fault plane solutions obtained have not been reached. Some regions, as for Southwestern part of Bulgaria, are over-represented by numerous determinations of sourse parameters. It isn't the case for some others parts of the region, as for its Eastern part. The distribution of numbers of focal mechanisms in different magnitude intervales are illustrated by table 1.

Tabl. 1

M	<2	2-2,5	2,6-3,0	3,1-3,6	3,7-4,1	>4,1
number of events	425	216	91	16	7	6

The differentiation foci of earthquakes with known focal mechanisms is shown by table 2.

Tabl. 2

region	number of events	A_z	ω	φ	ψ	$\varkappa$
1	642	76	158	18	218	0,15
2	160	129	60	47	91	0,14
3	79	147	86	22	66	0,17

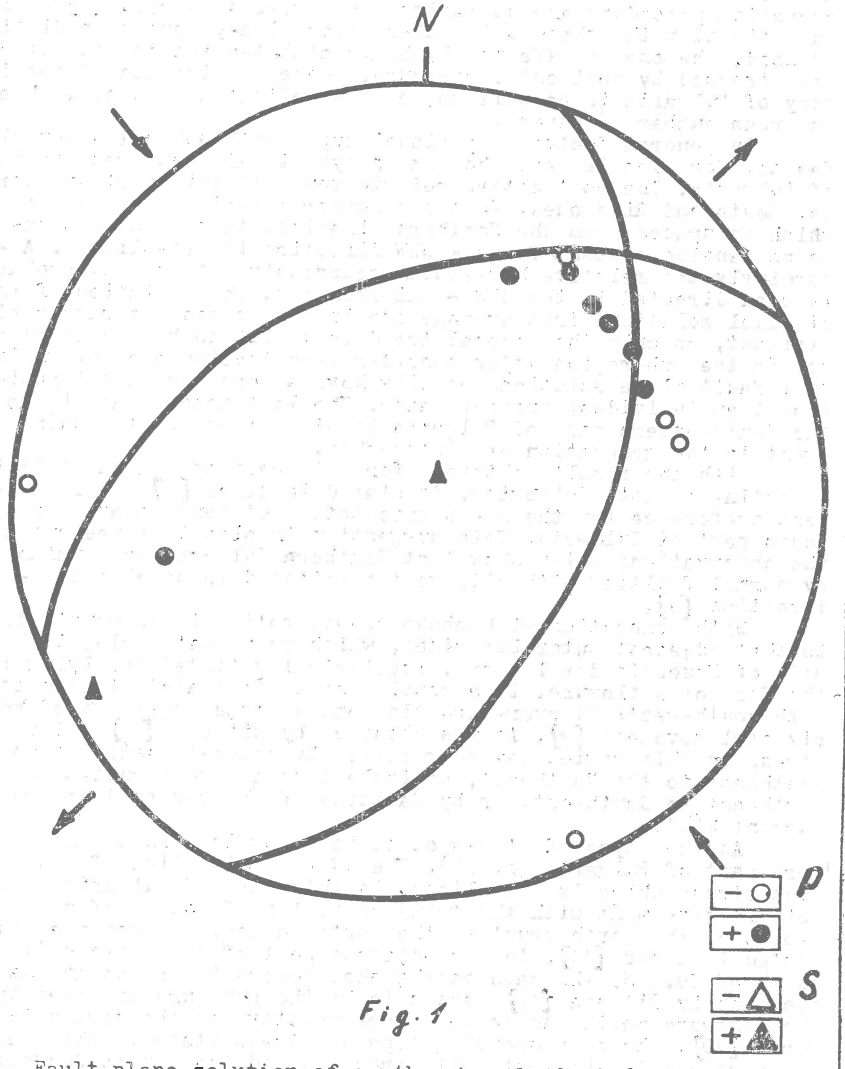

Fig. 1

Fault-plane solution of earthquake 18.12.1986, T_o = 23:39,
φ = 43,14; λ = 26,05; H = 5 km; M = 2.8

A rather great variety of fault plane solution obtained is recognised. For a determination of the regional orientation of tectonic stresses use have been made of average (or composite) mechanisms determination for the earthquakes of certain seismic areas. The regional stress directions as determined from this averaging procedure are summarized in fig.2. As a result of this investigation the three main sub-regions clealy have been distinguished, the one is affected by horizontal tension and the others are stressed by horisontal pressure. These subdivision of territory of Bulgaria is as well known in excellent agreement with a numerous number of papers.

In general features tensional type earthquakes (as normal faults, for example) are the common type in all Southwestern part of Bulgaria. The most active seismic zones of this part are Struma, Mesta and Rila ones. In the concidered part of the region which is spaced from the Northern Dinarides to the Rodop mountains tension stress of SSE - NNW direction is established. Accordingly the relative horisontal compressive stress may probably been directed in the SWW - NEE azimuths. The deviation of individual solutions from average one in many cases was rather significant, so only the general trend is useful to be presented here. In the sub-region under consideration tension axes of individual fault plane solutions usually have a more horizontal position than individual pressure axes. The last means that within the Southwestern part of Bulgaria tension stress is the main agent in the generation of earthquakes.

With the results obtained for this part of region it is interesting to note following. As stated in paper [8] it is an evident preference for the N - S orientation of tension axes in the South part of Bulgaria. This suggestion is also in agreement with the observations which show that Southern Bulgaria are dominated by normal faulting with slip vector oriented in an almost N - S direction [9].

With connection with above consideration it is wourth to note that adjacent outer Dinarides, which represent a classical domain of Mesosoic development, isoclinically folded and lying in the form of a flexure, is a complex of imbrificated structures with south-westward over-thrusting and a large amplitude of horizontal movement [9]. As was obtained by Ritsema [10] , the stress in this region may be relieved by under-thrusting from the Southwest to the Northeast, equivalent to an overthrusting from Northeast to Southwest, or by faulting of the reversed or transcurrent kind.

Another type of stress state is recognized in the Southeastern part of Bulgaria (fig.2). The NW - SE direction of compression stress which is established in this part of Bulgaria is likely in agreement with the trend of vector of motion of some blocks of the earth crust in the Northern part of Greece as suggested in paper [11]. In the adjacent part of the Western Turkey, north of 39.5 N, the main earthquakes generating agent as was proposed by Ritsema [10] seems to be the pressure excerted by the westward moving Anatolian block relative to the region in the North [10]. The corresponding type of stress state in this case the pressure in the Northwest direction and tension in Southeast one.

In the remainder and greater part of the region under in-

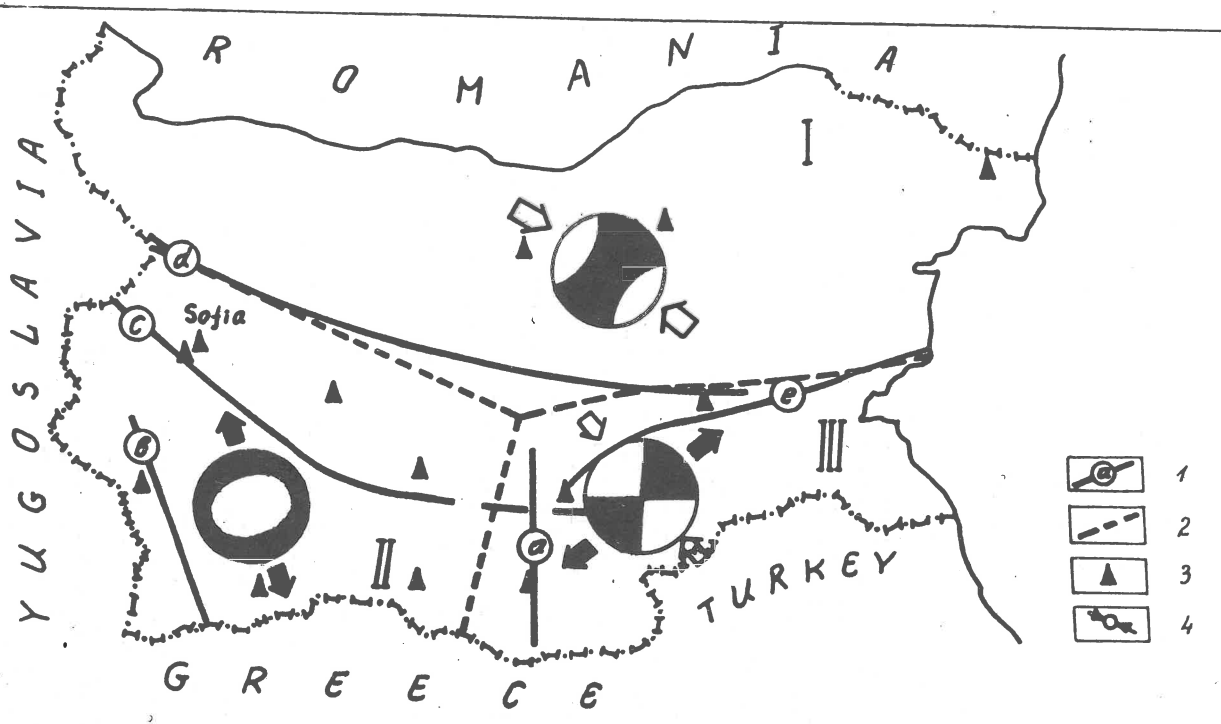

Fig. 2

Averaged mechanism sôlutions for shallow earthquakes with M>I.5; compressional quadrants are shown in black Average directions of the horisontal stresses are show on slid for P-axic and open symbols for T-axic.

vestigation, that is Nortern part of Bulgaria, the direction of general trend of compressional stress was determined as SE - NW one. The same azimuth of main compression in NW - SE direction is established also in paper [12] for sequence of 5 earthquakes with magnitudes M=4.5 - 5.0 which occurred in the region of town Strazhica in 1986, 1987. This direction is recognized also in paper [13] as the result of complex stress state investigation which was developed on the base of two independent methods. The first one was an analysys of the focal mechanism of earthquake 27.08.1982 with magnitude M=4.7. And the second method was the reconstruction of stress state with the use of shear joints in Upper Pliocen and Lower Cretaceons limestones of the Moesian platform.

The final result of presented investigation is formulated as follows. The three main regions with appreciable differences in stressed state and seismotectonic deformation was clealy recognized in the Central Balkan region. The main tectonic large scale structures and general features of geofisical fields are in agreement with recognized type of stressed state of the earth crust and with dominanted types of local movements in earthquake foci.

The data-set, prepared during this investigation and presented here in the form of generalized scheme, is the most complite set of fault plane solutions that ever has been reported for Bulgaria. A more or less clear picture has been obtained for the prevailing earthquake generating stresses in the region. However it is not well possible for present authors at given stage of investigation to go into much more details in the studying of the individual earthquake focal mechanisms even thought such an interpretation at a detail level seems to be as a natural and necessary extension of this paper. So maintainance of the information flow with the use of computer determination of focal mechanisms of current earthquakes of Bulgaria is of great importance.

The stress pattern obtained in present work is only a general type one. The suggestion is that any geodynamical model presented for Central Balkan region has to be in agreement with this stress pattern based on real focal mechanisms data.

References

1. Boncev E. The Balkanides. Geotectonic positions and Development. - Publishing house of BAS, Sofia, 1986, pp.273.

2. Dobrev T., Shchukin Yu. The Geophysical Fields and the seismic Nature of the Eastern Part of the Carpathian-Balkan Region, Moscow, Nauka, 1974, pp.170.

3. Dotzev N., Yunga S. Earthquake Source Mechanism in Bulgaria.- Izv. AN USSR, Physics of the earth, 1988, 4, pp.3-14.

4. Dotzev N., Yunga S. Estimation of the seismotectonic stress state of the Earth's crust in Bulgaria.- Izv. AN USSR, Physics of the Earth, 1988, 6, pp.55-59.

5. Dotzev N., Yunga S. Temporal Variations of Focal Mechanisms in some Regions of Strong Bulgarian Earthquake Occurrences - Bulg. Geophys. Journal, 1988, 2, pp.90-96.

6. Yunga S.L. On the focal mechanism of deformation of the seismically active part of the Earth's crust - Izv. AN USSR, Physics of the Earth, 1979, 11, pp.8-23.

7. Yunga S.L. Theoretical-methodological elements of focal mechanism determination.- Izv. AN USSR, Physics of the Earth, 1981, 4, pp.33-42.

8. Georgiev Tz. Fault plane Solutions Pressure and tension Axes for some Earthquakes in South-western Bulgaria.- Bulg. Geophysical Journal, 1987, 3, pp.102-107.

9. Seismotectonic analysis and map of SFR Yugoslavia-Proceedings of the seminar on the seismotectonic map of the Balkan Region, Dubrovnik, 17-26, Apr. 1973, UNESCO, Skopje, 1974, pp.158-213.

10. Ritsema A.R. The earthquake mechanisms of the Balcan Region K.N.M.I. De Bilt, The Netherlands, 1974, UNESCO, Survey of the seismicity of the Balkan Region, UNDP Project, RER/70/ /172/.

11. Papazachos B., Moudrakis D., Psilovikos A., Leventakis G. Focal properties of the 1978 earthquakes in the Thessaloniki area.- Bulgarian Geophys. J., 1980, 1, pp.72-80.

12. Christoskov L., at all, Seismological Features of the Region of the 1986 Earthquake Sequence.- Bulgarian Geophys. Journ. 1988, 2, pp.73-89.

13. Shanov S., Tz. Georgiev, B. Dimitrov Contemporary tectonic stress field in North-East Bulgaria.- Review of the Bulgarian Geological Society, vol.XLIX, part 1, 1988, p. 39-46.

THE STATE OF STRESS UNDER THE MERIDIONAL CARPATHIANS

M. C. Oncescu, L. Ardeleanu, E. Popescu

Center of Earth Physics and Seismology, P.O. Box MG-2, Bucharest-Măgurele, Romania

Introduction

The Meridional Carpathians form the highest elevations in the Eastern Carpathians and can be roughly defined geographically between 45° - 46° N and 22° - 26° E. They are bounded eastward by the Vrancea Mountains, where the Eastern Carpathians form a pronounced arc, bending from a W-E direction to a SE-NW direction.

The tectonics of the Carpathian Arc is not very well understood, especially that one of the Meridional Carpathians. Two micro-plates are considered to be in contact in this region: the Inter-Alpin Sub-Plate and the Moesian Platform (see Figure 1); nevertheless, it is surprising that this contact that generated the high elevations is now characterized by a very low seismic activity. It is the scope of this study to analyse the state of stress under the Meridional Carpathians on the base of the few earthquakes that occured in this region in the last years.

This study is divided in two parts: first, the determination of the regional stress tensor starting from the slip vectors given by fault plane solutions, and second, the determination of source parameters of some digitally recorded events.

Data

The data used in this study come from 13 earthquakes occured in the period 1983 - 1986, with epicenters between 45° - 46° N and 22° - 26° E, and clearly recorded at the 16-station Romanian telemetered network (see Table 1). All stations are equiped with Teledyne-Geotech S13 seismometers (vertical component, with T_0 = 1 s) and are radio-linked to a central recording station where digital data acquisition is also performed.

It is worth mentioning that four events (No. 2, 3, 4, 7) in the eastern part of the region under investigation (namely, under Bucegi and Ciucaş Mountains, close to Vrancea region) have sub - crustal depth. The individual locations of all events are obtained using both P and S wave arrival times (see the last column of Table 1).

The fault plane solutions are determined using P wave first motion signs, both from the telemetered stations and from other local seismic stations.

A number of 5 events were digitally recorded at the telemetered seismic stations, which allowed the determination of source parameters. The digitization rate is 50 Hz, but anti-alias filters cut frequencies greater than 12.5 Hz; at the lower end, we considered frequencies up to 0.5 Hz.

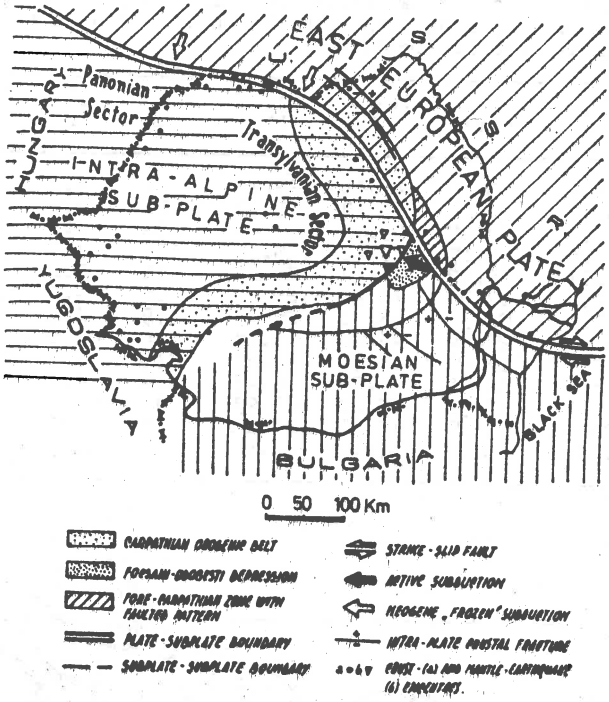

Fig. 1. Sketch of the three tectonic units in contact under the Carpathian Arc (after Constantinescu et al,1976)

Fault plane solutions and stress tensor

The obtained fault plane solutions are presented in Figure 2 and Table 2, and excepting the subcrustal events No. 2, 3 and 4, all represent a normal faulting with a N-S extension. Due to the small number of P signs and to the proximity of the hypocenters, we determine composite fault plane solutions in the case of pairs 2-3, and 5-6.

Gephart and Forsyth (1984) present a robust method to invert individual focal mechanism data in order to obtain the regional stress tensor. The method minimizes the sum of absolute values of the rotation angles around any axes needed to bring into coincidence the observed and predicted slip directions (with senses). A predicted slip direction corresponds to a certain orientation of the three principal stress axes $\sigma_1 < \sigma_2 < \sigma_3$ and to a certain ratio $R = (\sigma_2 - \sigma_1)/(\sigma_3 - \sigma_1)$.

If the fault plane is not 'a priori' known, the method automatically distinguishes between the two possibilities when searching for the best fit.

Table 1. List of earthquakes used in this study (in order of decreasing longitude). N is the number of arrival times used in locations.

No.	Date	Origin time	Lat.N (°)	Lon.E (°)	h (km)	M_D	N
1	830409	00:16	45.55	25.99	7	3.7	12P + 9S
2	860117	04:28	45.58	25.98	71	2.3	5P + 6S
3	840115	00:47	45.64	25.91	54	3.3	4P + 7S
4	840326	23:17	45.42	25.83	71	3.2	10P + 9S
5	850204	02:57	45.57	25.80	10	3.0	5P + 3S
6	861010	17:16	45.40	25.80	10	4.8	12P + 9S
7	850201	06:35	45.40	25.34	59	3.6	7P + 8S
8	861202	22:44	45.06	25.24	30	3.8	8P + 6S
9	831114	16:22	45.11	25.29	30	3.3	8P + 3S
10	840520	20:58	45.52	24.43	22	4.5	10P + 4S
11	830904	13:39	45.04	23.93	12	4.4	11P + 8S
12	850206	12:27	45.27	23.13	5	3.5	8P + 4S
13	851021	18:33	45.19	22.56	5	3.3	5P + 3S

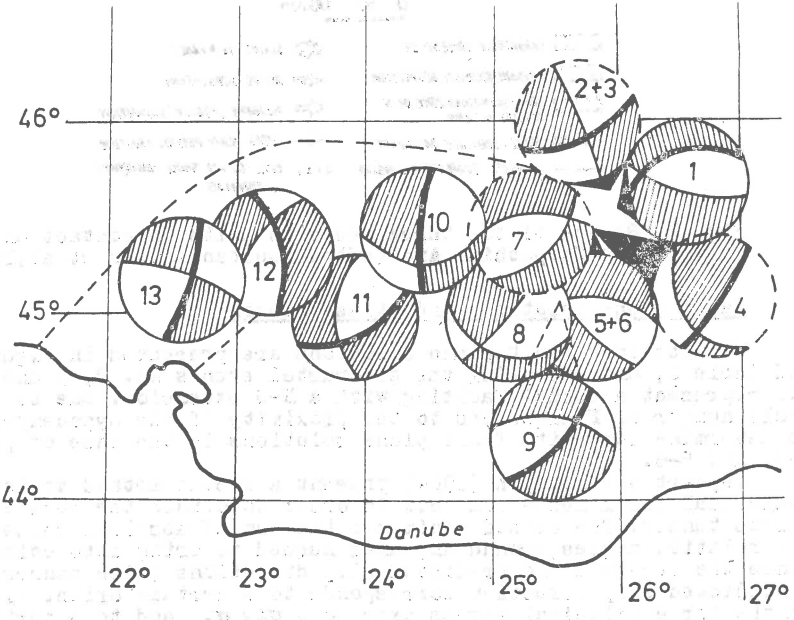

Fig. 2. Fault plane solutions in a stereographic projection on the lower hemisphere; hatched areas correspond to compressions (+). The numbers are those from Table 1; thick curves mark the identified rupture planes. Events with sub-crustal depths are denoted by dashed circles.

Table 2. Fault plane parameters; φ is the dip direction and N is the number of first motion signs.

No.	Rupture plane φ	δ	$\|r\|$	Auxiliary plane φ	δ	$\|r\|$	N	Score (%)
1	347	21	2	190	71	10	14	100
2+3	162	73	3	72	88	15	8	87
4	133	83	5	255	11	11	10	100
5+6	251	46	16	21	56	20	17	88
7	358	49	18	145	46	20	8	100
8	328	84	7 ?	198	10	7 ?	9	100
9	143	66	6	13	35	10	8	100
10	275	86	2	170	14	22	24	79
11	149	77	3	273	22	19	20	80
12	83	59	2	295	36	8	11	100
13	105	83	2	12	66	31	6	100

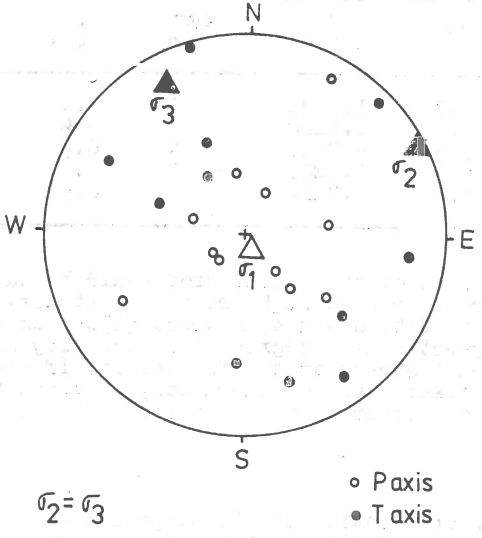

Fig. 3. Individual P and T axes and principal stress axes in a stereographic projection on the lower hemisphere.

In the present application we used 11 fault plane solutions presented in Table 2, together with the two possible rotation angles $|r|$. The main result of the inversion is presented in Figure 3; this describes a biaxial stress state with horizontal tractions and vertical compressions. The model stress tensor does not fit the slip directions of events 5+6, and 7, a fact that can be explained by a local inhomogeneity in stress under

the Bucegi Mountains. As can be observed from Table 2, the misfit angles $|r|$ vary between 2° and 7°, with an average of about 4°. Errors of a few degrees are less than the uncertainty of the focal mechanism determinations, which in these cases is estimated to be of the order of 10° - 20°. The rupture plane could not be identified in case of event No. 8, due to the proximity of its B axis with σ_2 axis (Gephart, 1985).

Source parameters

Using the classical spectral theory of seismic sources of Brune (1970), the following source parameters were computed: seismic moment M_0, stress drop $\Delta\sigma$, source radius r and final dislocation u. The obtained results are listed in Table 3. More striking among them is the low stress drop (between 1 and 20 bar, irrespective on depth). We mention for comparison that for the same source model, Oncescu (1986) obtained significantly larger stress drop values for Vrancea intermediate depth earthquakes (up to an order of magnitude larger).

Table 3. Source parameters; N is the number of P + S waveforms.

No.	h (km)	M_D	M_0 (dyn·cm)	$\Delta\sigma$ (bar)	r (km)	u (cm)	N
1	7	3.7	1.0E21	1	0.8	0.2	16
4	71	3.2	1.1E20	1	0.4	0.1	6
9	30	3.3	8.7E20	4	0.5	0.3	7
10	22	4.5	1.3E22	20	0.6	2.2	11
11	12	4.4	1.8E21	5	0.5	0.8	12

These low values of the stress drop could be due either to a low initial stress or to a high frictional stress. Because of the low attenuation determined by Oncescu (1986) under these mountains, we suggest a high degree of homogeneity and thus a low final frictional stress on the faults. So, if the low seismic activity is also taken into consideration, we think that low initial stresses characterize the deep roots of the Meridional Carpathians.

Discussion

The vertical orientation of the compression axis can be due either to the gravity of the mountains themselves, or to a subduction of the Moesian Platform under these mountains. The great depth of some events in the eastern part (54 to 71 km) and a positive P wave velocity anomaly of 1% - 3% put into evidence by Oncescu et al (1984) may favor the idea of a subduction stopped in an initial stage under the Meridional Carpathians.

Moreover, Oncescu (1987) obtained almost the same stress orientations for the eastern part of the Moesian Platform, a fact that supports the continuity of the stresses acting within the Moesian Platform and its margins. The low relative motion of the Moesian Platform with respect to the Inter-Alpine Sub-Plate is in agreement with the low seismic activity characterized by events

with small-to-moderate magnitudes. Nevertheless, one should not forget that an earthquake with $M \simeq 6.5$ (I_o = VIII) occured at about 45.5°N and 24.6°E on January 26, 1916, so that this region deserves further attention.

Acknowledgments. We thank J.W. Gephart for permitting the use of his stress inversion programs.

References

Brune, J.N., 1970. Tectonic stress and the spectra of seismic shear waves from earthquakes. J. Geophys. Res., 75, 4997-5009.

Constantinescu, L., Constantinescu, P., Cornea, I. and Lăzărescu, V., 1976. Recent seismic information on the lithosphere in Romania. Rev. Roum. Géol. Géophys. Géogr., Géophys., 20, 33-40.

Gephart, J.W., 1985. Principal stress directions and the ambiguity in fault plane identification from focal mechanism. Bull. Seismol. Soc. Am., 75, 621-625.

Gephart, J.W. and Forsyth, D.W., 1984. An improved method for determining the regional stress tensor using earthquake focal mechanism data: application to the San Fernando earthquake sequence. J. Geophys. Res., 89, 9305-9320.

Oncescu, M.C., 1986. Some source and medium properties of Vrancea (Romania) seismic region. Tectonophysics, 126, 245-258.

Oncescu, M.C., 1987. On the stress tensor in Vrancea region. J. Geophys., 62, 62-65.

Oncescu, M.C., Burlacu, V., Anghel, M. and Smalbergher, V., 1984. Three-dimensional P-wave velocity image under the Carpathian Arc. Tectonophysics, 106, 305-319.

IRPINIA, ITALY, 1980 EARTHQUAKE: WAVEFORM MODELLING OF STRONG MOTION DATA

P. Suhadolc[1], F. Vaccari[1] and G. F. Panza[1,2]

1) Istituto di Geodesia e Geofisica, Università di Trieste, Trieste, Italy.
2) International School for Advanced Studies, Trieste, Italy.

ABSTRACT

Several strong motion records of the Irpinia (Southern italy) 1980 earthquake have been modelled for a total time duration of about 180 s with the use of the multimode summation of waves of P-SV type. If waveform modelling is applied to unfiltered accelerations the best that can be done, at present, is envelope matching. The early phase of the studied event seems to be formed by at least twelve episodes representing the rupture of asperities of different sizes. The space-time distribution of such episodes suggests that the rupturing process did propagate in a bilateral fashion.

INTRODUCTION

With the expanding possibilities of computing synthetic seismograms, waveform modelling has gained more and more recognition also in source studies. The first applications have been made in the low-frequency range using teleseismic surface waves (Kanamori, 1970a; 1970b) or normal oscillation (e.g. Gilbert and Dziewonski, 1975; Dziewonski et al., 1981) data. Langston and Helmberger (1975) proposed a method to model the source using waveform data of body-wave phases, which extended the modelling to much shorter periods. These studies, however, were aimed at obtaining the focal parameters in the point source approximation.

The availability of digital accelerograms, combined with the increasing demand from structural engineers for more quantitative methods of analysis and interpretation, makes the development of efficient theoretical tools for the construction of synthetic records at high frequency very important.

In recent years synthetic waveform modelling of real ground motion (Spudich and Archuleta, 1987) allowed to model the behavior of earthquake sources for frequencies up to 1 Hz. With the possibility of modelling high frequency data the attention is presently concentrated in the analysis of the complexity of earthquake sources in space and time. This task is mainly achieved by modelling strong-motion data (e.g. Hartzell and Helmberger, 1982; Olson and Apsel, 1982; Takeo, 1987; Suhadolc et al., 1988).

Usually, the frequency content of the strong motion records is broadband. That is, the acceleration amplitude spectra are roughly constant over a range of frequencies from 5 Hz down to 0.5 Hz or less. At lower frequencies the amplitude decreases with decreasing frequencies. The point where this occurs, called corner frequency, f_o, depends primarily on the duration of the strong shaking or equivalently on the size of the source, with the longer motions, from larger earthquakes, delivering more energy at lower frequencies.

The computation of synthetic signals of long duration having a broadband frequency content can hardly be done using the ray approach (see, e.g., Chapman, 1985; Cerveny, 1985). At present, a very suitable tool for this

purpose seems to be the modal summation (Panza, 1985; Panza and Suhadolc, 1987), which has already been applied at lower frequencies (Liao et al., 1978) and recently at frequencies up to 10 Hz (Panza et al., 1986; Suhadolc et al., 1987; Suhadolc and Chiaruttini, 1987). By summing the modes of oscillation of a given structure, approximated with flat parallel layers, and using realistic models for the seismic source it is easy to construct, for given frequency and phase velocity bands, complete synthetic seismograms. The use of Rayleigh modes (P-SV waves) gives the vertical and radial components, while the use of Love modes (SH waves) gives the transverse one.

Considering shallow sources, the construction of complete synthetic accelerograms using mode summation, can be conveniently performed by using models of the earth with elastic and anelastic properties specified to depths of the order of 100 km, a representative value of the thickness of the lithosphere. The handling of structural models extending to these depths in an efficient way, makes it possible to synthesize early P-wave arrivals without the necessity of introducing any unrealistic high-velocity half-space with the consequent generation of spurious S-wave arrivals as in the case of the locked mode approximation (Harvey, 1981). Moreover, the computation is, in practice, not limited to layered models, since it is possible to simulate gradients by means of a sequence of many thin layers without loosing computational efficiency.

IRPINIA, ITALY, 1980 EVENT

Initial choice of parameters

The earthquake source behavior is relatively well understood by waveform matching synthetic and observed ground motions for frequencies up to 1 Hz. At higher frequencies, smaller scale details of the earthquake source process and of the structure surrounding the source volume become essential for a deterministic prediction of the strong ground motion, therefore usually a statistical approach is taken to predict ground motion for frequencies above 1 Hz (see, e.g., Boore and Joyner, 1978; Boatwright, 1982; Koyama, 1985).

In the following we discuss a direct method which makes use of the deterministic computation of synthetic signals at high frequency to outline the rupturing process of an earthquake, by showing its application to the November 23, 1980 Irpinia earthquake (M_S = 6.9) in southern Italy (for a detailed discussion of this event see Bernard and Zollo, 1988; Westaway and Jackson, 1987).

The basic crustal model used to compute synthetics is the "A" model proposed by Del Pezzo et al. (1983). The model (Fig. 1) has been modified: at the top, where we have introduced a positive gradient in the P- and S-wave velocities of the first 8 km to obtain a more realistic modelling of the sedimentary sequence, and at the bottom, where more layers have been added in order to model the lithosphere (Panza et al., 1980). Due to the difficulty in measuring, particularly at high frequencies, the intrinsic attenuation of the Earth in a physically meaningful way (Panza et al., 1986; Panza, 1988), a frequency independent Q (Knopoff, 1964) has been assumed in all the layers. Q values in the crustal layers have been choosen according to the average estimates given by Knopoff (1964), and in the subcrustal region according to the average values given by Craglietto et al. (1987).

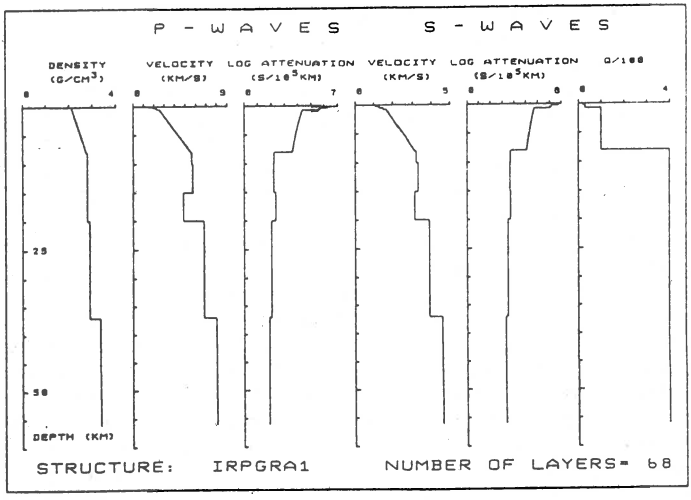

Fig. 1. Structure IRPGRA1 used in the modelling of the 1980 Irpinia event. To minimize the effect of anelasticity we have chosen the relation $Q_\alpha = 2.5\ Q_\beta$ between the quality factors for P- and S-waves. In the figure only Q_β is plotted.

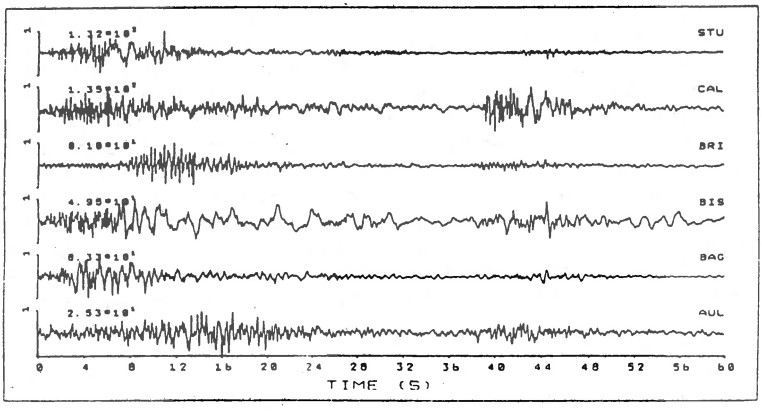

Fig. 2. Observed accelerations, after Gaussian filtering with a cut-off frequency at 10 Hz, due to the 1980 Irpinia, Italy, earthquake. From top to bottom, the signals refer to the stations: Sturno (STU), Calitri (CAL), Brienza (BRI), Bisaccia (BIS), Bagnoli (BAG), Auletta (AUL). For station locations see Fig. 3a. The maximum zero-to-peak ground acceleration in units of cm/s^2 is given in the upper left part of each record. The zero of the time axis does not coincide with the earthquake origin time.

The time series (Fig. 2) which were analyzed are the strong ground motion recordings (Berardi et al., 1981) of the Ente Nazionale Energie Alternative - Ente Nazionale Energia Elettrica (ENEA-ENEL). These time series have been preliminarly filtered with a cut-off frequency of 10 Hz using a Gaussian filter.

Since the source-receiver distances are comparable with the fault length and the event is a complex one, we have decided to limit ourselves to P-SV waves. Therefore we will use only the vertical components recorded at the six accelerometric stations closest to the epicentral area (Fig. 3a). The analysis will be restricted to the first 30 s of the recordings. The cut-off frequency of computation - 10 Hz - largely exceeds the limit - a few Hz - below which the present knowledge of the elastic and anelastic properties of the crust allows a deterministic modelling of wave propagation. In the comparison between synthetic and observed accelerograms we will therefore give more relevance to envelope fitting rather than to single peaks matching. Peak-to-peak modelling seems to be more appropriate when applied to ground velocities and displacements.

Comparing the duration of the observed ground motion with the examples of "complete" synthetic signals obtained for comparable distances (see Panza and Suhadolc, 1987) one can clearly see that the single-point source is by no means a realistic representation of a large earthquake's source process in the near field. Moreover, looking at the recordings we note that the accelerations at Auletta are particularly low if compared to the ones obtained at Brienza, a station located almost in the same direction but at a larger distance. This fact cannot be explained in terms of different geological setting (Mostardini e Merlini, 1986), but rather contains very useful information to constrain the orientation of the point-sources used to model the strong motion records.

The fault strike, oriented N140°E, is taken to be almost parallel to the axis of the Apennine chain; the fault length, as deduced from the spatial distribution of aftershocks (Deschamps and King, 1984), is taken equal to 70 km. Initially, thirteen evenly spaced locations have been selected along the fault; subsequently three more had to be added in near the Brienza station (Fig. 3a). The spacing of these locations - hereafter called epicenters - is 5.7 km. Point sources of different hypocentral depth and size are placed in correspondence of each epicenter.

It has been shown by Suhadolc et al. (1988) that to model the observed recordings, sources with finite durations and a mechanism having a rake of 240° on a fault dipping 70° to the NE had to be taken into account. For the sake of simplicity the duration of 0.6 s has been kept constant for all the point sources. Moreover, Suhadolc et al. (1988) found that rupture velocities smaller than the S-wave velocity in the pertinent layers constrain the location of the shock activating the rupturing process around epicenter G.

Waveform modelling of accelerograms traces

In this paper the point sources will be used to represent braking asperities (Kanamori and Stewart, 1978), but their interpretation in terms of the barrier model (Das and Aki, 1977; Aki, 1979) is equally possible. It is well known, from the representation theorem, that the effect of lateral variation can be represented by point sources, therefore in the analysis we are making some caution is necessary in the meaning which can be given to the obtained sequence of point sources. In any case we consider quite remarkable

that even considering horizontally homogeneous model, i.e. neglecting the effect of lateral variations the synthetic signals of Fig. 4 have been obtained superimposing the effects of only twelve point sources, properly distributed in space and time (Fig. 3b and Fig. 3c). Such a sequence of point sources can therefore be considered as a schematic representation of asperities of different size even if some of them may originate by the modelling of phases arising from lateral heterogeneities. However it seems possible to outline the overall rupturing process as it did propagate in a bilateral fashion, probably along a path schematized by the dotted line in Fig. 3b, with a subsonic velocity. The fracturing process, deduced from this modelling, nucleates with a point source of relatively small seismic moment, even if earlier nucleations with an even smaller size, as predicted by theoretical crack models (e.g. Knopoff and Chatterjee, 1982; Chatterjee and Knopoff, 1983), cannot be excluded. The downward propagating fracture gives rise to the maximum energy release, located just above a layer with high P- and S-wave velocities which may correspond to the methamorphic layer of the continental crustal model proposed by Mueller (1977). The distribution of point sources simulating the fracture propagation upwards and to the NW from the nucleation point seems to be quite regular both in space and time. This part of the fracturing process can be therefore assumed almost continuous. The southeastern branch of the fracture, on the other hand, is not so well linked in time and space with the main central fracture process and could be well assumed to represent an almost "independent" subevent. The later parts of the strong motion records are modelled by means of some shallow point sources, with varying seismic moment, simulating the stopping of the rupture within the sedimentary cover and very likely some effect of lateral heterogeneities. In fact, the seismic moments of these shallow sources are significantly smaller than the ones of the sources simulating the beginning of the rupturing process, and the very relevant effect in all the record is due to their shallow depth.

The final synthetic signals are shown in Fig. 4. This figure is made up of six parts, each corresponding to one of the six stations considered. In each part of the figure the individual synthetic signals due to the twelve considered point sources, as seen at the corresponding station, are shown on the top. In the lower part of the figure two records are shown: above, the superposition of the twelve synthetic contributions, below, the observed accelerograms Gaussian filtered with a cut-off frequency of 10 Hz. Due to the absence of absolute time on strong motion records the shift between the last two time series is arbitrary and we have deliberately not chosen the one which may give the best accord between the synthetic and the observed accelerations.

Five point-sources have been used to model the initial part of the recordings. Without affecting the theoretical signals at the other considered stations, the remarkable peak acceleration observed at Sturno (Fig. 4f) at about 11 s has been modelled with a 2 km deep point source located at epicenter K. The long-period oscillation, which appears in the experimental time series recorded at Sturno between 5 and 8 s after the starting of the record, has been modelled by adding a signal corresponding to a normal-fault point-source, 2 km deep in epicenter I. This is the only point source with a focal mechanism different from all the others. The fault strikes in a direction perpendicular to the Apennines chain, and the rake is 270°. This reorientation is necessary in order to modify the waveform of the Sturno record without affecting those obtained so far at Bagnoli (Fig. 4b), Bisaccia (Fig. 4c) and Calitri (Fig. 4e)

stations. The existence near epicenter I of a fault orthogonal to the main one has been also suggested by Crosson et al. (1986) to explain the vertical movements observed in the region after the earthquake. Other solutions (e.g. Bernard and Zollo, 1987; Westaway and Jackson, 1987) might be of course possible, but up to now we have not investigated the parameters space in detail.

The energy maximum, concentrated between 8 and 14 s after the starting of the observed Brienza (Fig. 4d) record, cannot be due to point sources located in correspondence of epicenters A to M, as can be deduced from an analysis of the possible P- and S-wave travel times. It must be therefore associated with one or more point sources becoming active many seconds after the first one and close to the station itself. Placing these point sources in correspondence of epicenters X, Y, W (Fig. 3a) and properly spacing them in time and depth, produced at Brienza a peak acceleration three times larger than that at Auletta, as required by the experimental data.

In general, some signals with higher (3 Hz) frequency content should be added to the obtained synthetic records, especially at Brienza, Calitri and Sturno stations. This lack of high frequencies is due to the fact that the source duration of all point sources has been kept equal to 0.6 s.

The relative amplitudes of the envelopes of the theoretical accelerograms, however, agree quite well with those of the experimental records. The Auletta station synthetics (Fig. 4a), as a consequence of the value assumed for the rake value, is also nicely reproduced both in the peak value and in the waveforms. Only the Bagnoli theoretical signal (Fig. 4b), in spite of the fact it resembles the recorded waveform, has a relative peak value, which is larger than in the observed case. A possible explanation could be found in the geological setting of that station which is sitting on the calcareous Apennine platform, not present in correspondence of the other stations (Mostardini e Merlini, 1986).

The waveform fitting can be obviously improved considering a larger number of point sources, but a close waveform matching at these frequencies is not significant, at least until a better understanding of the high-frequency behavior of earthquake rupturing will be achieved, and until the structural parameters will be known on the scale of the involved wavelengths. This in turn requires the development of codes for the treatment of detailed two- and three-dimensional laterally heterogeneous structures, presently in progress (Vaccari et al., 1988).

CONCLUSIONS

The availability of good quality strong motion data produced by the ENEA-ENEL network allows a quite detailed modelling of the earlier part of the rupturing process which characterized the Irpinia 1980 earthquake. From the first 30 s of record of the six stations closest to the seismogenetic area it is possible to identify twelve point sources, which can be grouped into three main rupturing episodes. The distribution in space and time of such episodes indicates that the rupture did propagate in a bilateral way, even if the southernmost part of the rupture can be taken as an independent episode. The waveform fitting can be obviously improved considering a larger number of point sources but, at present, we consider not significant a close waveform matching at frequencies higher than a few Hz. To be able to use in a deterministic way

gh frequency information it is in fact necessary to better understand the gh-frequency behavior of earthquake rupturing and to know and consequently to del the lateral variations of the structural parameters to the scale of the volved wavelengths.

Scaling the observed and synthetic acceleration peaks according to the ocedure described in Suhadolc et al. (1987) a value of about 2.4×10^{25} dyn cm found to be released by the considered twelve sources. This scalar sum of ocal" seismic moments is obviously smaller than the overall seismic moment termined in the far field. The "local" stress drops can be as high as a few ndred bar, however estimates of the ruptured area obtained in this study gether with the far field seismic moment determination yield an average ress drop between 20 and 40 bar.

KNOWLEDGEMENTS

This research has been financially supported by ENEA contract N. 3972 erie III).

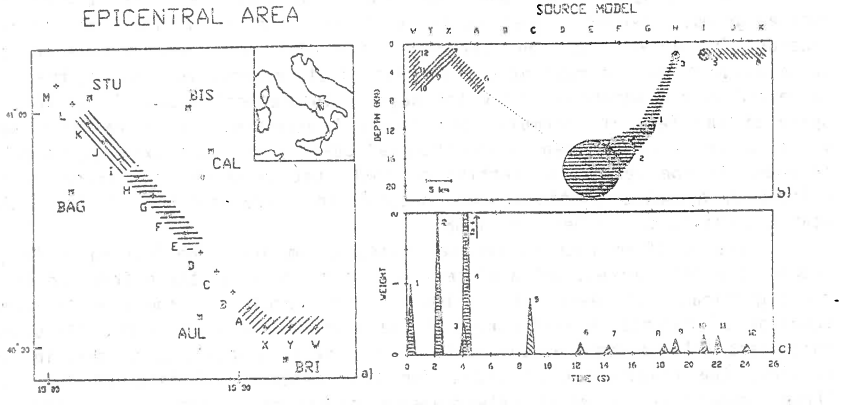

ig. 3. a) Map showing the positions of the epicenters (+), used in the onstruction of the synthetic signals of Fig. 4, and the considered trong-motion stations (*). b) Distribution in space of point sources used to onstruct the synthetic signals of Fig. 4. The radii of the circles around the ypocenters are proportional to the size of the corresponding point source. c) ime distribution of the point sources shown in Fig. 3b. The heights of the riangles are proportional to the size of the corresponding point sources. In he figure the three different hatchings denote the three rupture events in hich the overall rupturing process can be subdivided.

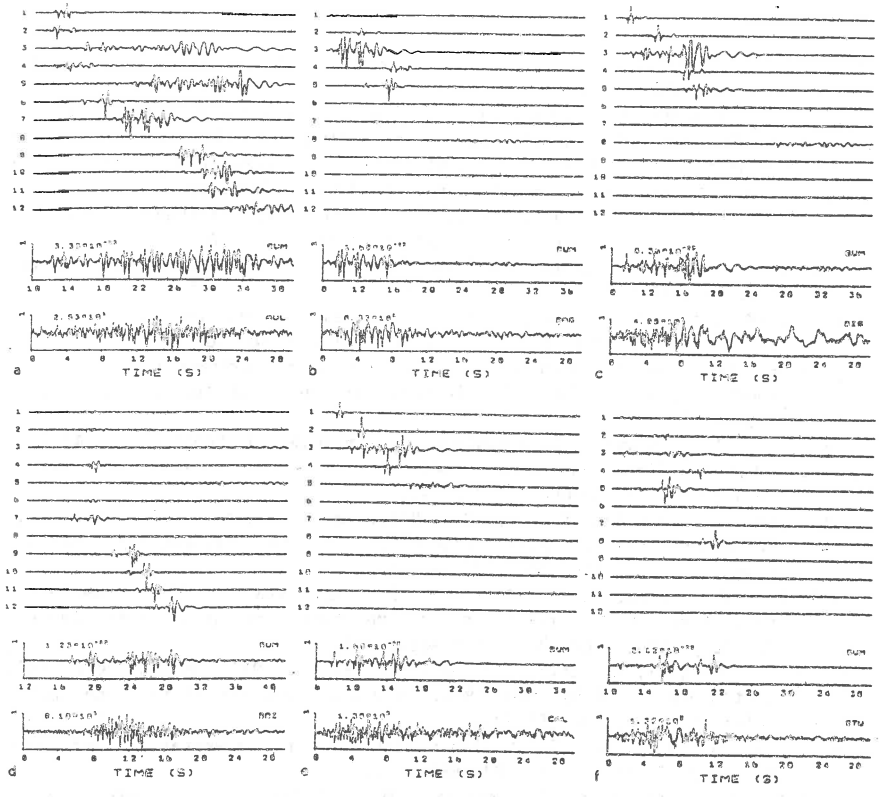

Fig. 4. For each of the six stations, the synthetic accelerations relative to the twelve point sources, their superposition (SUM) and the recorded series are shown. The locations, weights and time shifts are reported in Fig. 3b and Fig. 3c. The fault strike, dip and rake of all sources are respectively 310°, 70° and 240°, except for point source number 5, whose values are 40°, 70° and 270°. The amplitude of each synthetic trace, in units of cm/s^2, corresponds to a seismic moment $|M_0| = 1$ dyn cm. The zero-to-peak acceleration, in units of cm/s^2, is given in the upper left part of the record.

REFERENCES

Aki, K., 1979. Characterization of barriers on an earthquake fault. J. Geophys. Res., 84:6140-6148.

Berardi, R., Berenzi, A. and Capozza, F., 1981. Campania-Lucania earthquake on 23 November 1980 accelerometric recordings of the main quake and relating processing. In: "Contributo alla caratterizzazione della sismicità del territorio italiano". ENEA-ENEL, Roma, pp. 1-103.

Bernard, P. and Zollo, A., 1987. The Irpinia (Italy) 1980 earthquake: detailed analysis of a complex normal fault. Submitted to BSSA.

Boatwright, J., 1982. A dynamic model for far-field acceleration. Bull. Seism. Soc. Am., 72:1049-1068.

Boore, D. M. and Joyner, W. B., 1978. The influence of rupture incoherence on seismic directivity. Bull. Seism. Soc. Am., 68:283-300.

Boschi, E., Mulargia, F., Mantovani, E., Bonafede, M., Dziewonski, A. M. and Woodhouse, J. H., 1981. The Irpinia earthquake of November 23, 1980. EOS, 62:330.

Cerveny, V., 1985. Gaussian beam synthetic seismograms. J. Geophys., 58:44-72.

Chapman, C. H., 1985. Ray theory and its extension - WKBJ and Maslov seismograms. J. Geophys., 58:27-43.

Chatterjee, A. K. and Knopoff, L., 1983. Bilateral propagation of a spontaneous two-dimensional anti-plane shear crack under the influence of cohesion. Geophys. J. R. astr. Soc., 73:449-473.

Craglietto, A., Panza, G. F., Mitchell, B. and Costa, G., 1987. Anelastic properties of the crust in the Mediterranean area. 19th General Assembly IUGG, Vancouver, Abstracts, 1:70.

Crosson, R., Martini, M., Scarpa, R. and Key, S. C., 1986. The southern Italy earthquake of 23 November 1980: an unusual pattern of faulting. Bull. Seism. Soc. Am., 76:381-384.

Das, S. and Aki, K., 1977. Fault planes with barriers: a versatile earthquake model. J. Geophys. Res., 82:5658-5670.

Del Pezzo, E., Iannaccone, G., Martini, M. and Scarpa, R., 1983. The 23 November 1980 southern Italy earthquake. Bull. Seism. Soc. Am., 73:187-200.

Deschamps, A. and King, G. C. P., 1984. Aftershocks of the Campania-Lucania (Italy) earthquake of 23 November 1980. Bull. Seism. Soc. Am., 74:2483-2517.

Dziewonski, A. M., Chou, T.-A. and Woodhouse, J. H., 1981. Determination of earthquake source parameters from waveform data for studies of global and regional seismicity. J. Geophys. Res., 86:2825-2852.

Gilbert, F. and Dziewonski, A. M., 1975. An application of normal mode theory to the retrieval of structural parameters and source mechanisms from seismic spectra. Philos. Trans. R. Soc., London, Ser. A, 278:187-269.

Hartzell, S. H. and Helmberger, D. V., 1982. Strong-motion modeling of the Imperial valley earthquake of 1979. Bull. Seism. Soc. Am., 72:571-596.

Harvey, D. J., 1981. Seismograms synthesis using normal mode superposition: the locked mode approximation. Geophys. J. R. astr. Soc., 66:37-69.

Kanamori, H., 1970a. Synthesis of long-period surface waves and its applications to earthquake source studies - Kurile Islands earthquake of October 13, 1963. J. Geophys. Res., 75:5011-5028.

Kanamori, H., 1970b. The Alaska earthquake of 1964: Radiation of long-period

surface waves and source mechanism. J. Geophys. Res., 75:5029-5040.
Kanamori, H. and Stewart, G., 1978. Seismological aspects of the Guatemala earthquake of February 4, 1976. J. Geophys. Res., 83:3427-3434.
Knopoff, L., 1964. Q. Rev. Geophys., 2:625-660.
Knopoff, L. and Chatterjee, A. K., 1982. Unilateral extension of a two-dimensional shear crack under the influence of cohesive forces. Geophys. J. R. astr. Soc., 68:7-25.
Koyama, J., 1985. Earthquake source time-function from coherent and incoherent rupture. Tectonophysics, 118:227-242.
Langston, C. A. and Helmberger, D. W., 1975. A procedure for modelling shallow dislocation sources. Geophys. J. R. astr. Soc., 42:117-130.
Liao, A., Schwab, F. and Mantovani, E., 1978. Computation of complete theoretical seismograms for torsional waves. Bull. Seism. Soc. Am., 68:317-324.
Mostardini, F. and Merlini, S., 1986. Appennino Meridionale. Sezioni geologiche e proposta di modello strutturale. 73° Congresso Società Geologica Italiana, 30 Settembre-4 Ottobre 1986, Roma.
Mueller, S., 1977. A new model of the continental crust. In: "The Earth's Crust", J. Heacock (Editor). Am. Geoph. Un. Monogr. 20, pp. 289-317.
Nakanishi, I. and Kanamori, H., 1984. Source mechanism of twentysix large shallow earthquakes (M 6.5) during 1980 from P-wave first motion and long-period Rayleigh wave data. Bull. Seism. Soc. Am., 74:805-818.
Olson, A. H. and Apsel, R. J., 1982. Finite faults and inverse theory with applications to the 1979 Imperial valley earthquake. Bull. Seism. Soc. Am., 72:1969-2001.
Panza, G. F., 1985. Synthetic seismograms: the Rayleigh waves modal summation. J. Geophys., 58:125-145.
Panza, G. F., 1988. Attenuation measurements by multimode synthetic seismograms. To be published in: "Digital Seismology and Fine Modelling of the Lithosphere", R. Cassinis, G. Nolet and G. F. Panza (Editors), Plenum Press.
Panza, G. F., Mueller, St. and Calcagnile, G., 1980. The gross features of the lithosphere-asthenosphere system in Europe from seismic surface waves and body waves. PAGEOPH, 118:1209-1213.
Panza, G. F. and Suhadolc, P., 1987. Complete strong motion synthetics. In: "Seismic Strong Motion Synthetics", B. A. Bolt (Editor), Computational Techniques, 4:153-204, Academic Press.
Panza, G. F., Suhadolc, P. and Chiaruttini, C., 1986. Exploitation of broadband networks through broadband synthetic seismograms. An. Geophys., 48:315-328.
Spudich, P. and Archuleta, R. J., 1987. Techniques for earthquake ground-motion calculation with application to source parametrization of finite faults. In: "Seismic Strong Motion Synthetics", B. A. Bolt (Editor), Computational Techniques, 4:205-265, Academic Press, Orlando.
Suhadolc, P. and Chiaruttini, C., 1987. A theoretical study on the dependence of the peak ground motion acceleration on source and structure parameters. In: "Strong Ground Motion Seismology", M. O. Erdik and M. O. Toksoz (Editors), NATO ASI, Series C, 204:143-183, Reidel, Dordrecht.
Suhadolc, P., Vaccari, F. and Panza, G. F., 1988. Strong motion modelling of the rupturing process of the November 1980 Irpinia, Italy, earthquake.

In "Seismic Hazard in Mediterranean Regions", J. Bonnin et al. (eds.), 105-128. Kluwer Academic Publishers, Dordrecht, Boston, London.

Takeo, N., 1987. An inversion method to analyze the rupturing processes of earthquakes using near-field seismograms. Bull. Seism. Soc. Am., 77:490-513.

Vaccari, F., Gregersen, S., Furlan, M. and Panza, G. F., 1988. Synthetic seismograms in laterally heterogeneous, anelastic media by modal summation of P-SV waves. Submitted to Geophys. J.

Westaway, R. and Jackson, J., 1987. The earthquake of 1980 November 23 in Campania-Basilicata (southern Italy). Geophys. J. R. astr. Soc., 90:375-443.

SEISMOGENIC FAULTING IN CENTRAL BALKANS

Gorbunova I. - Institute of Physics of the Earth, Moscow, USSR
Dobrev T. - Higher Institute of Mining and Geology, Sofia, Bulgar
Dotzev N. - Geophysical Institute, Sofia, Bulgaria
Shchukin Y. - Research Institute of Geophysics, MosboW, USSR

Utilization of a new approach to the interpretation of seis mogrammes from 63 earthquakes in the Central Balkan area gives t possibility to determine the destribution way of the fault in th earthquake source as well as the size of the source zones.

A map with unujual showing manner of the epicenters introduced and through conditional marks are shown the sizes alongate earthquake source, and the way of rupture (movement) of the faul is presnted some seismotectonic conclusions are done.

INTRODUCTION. On present-day seismic maps, an earthquake epicent is marked by a point described by coordinates φ and λ. In orc to differentiate earthquakes by their magnitude, circumferences varying radii are usually drawn around these points. At the same time, many studies have shown that the focus of an earthquake i not a point, but a three-dimensional volume, and one quite large in the case of strong earthquakes. The dimensions and orientatic of earthquake foci are, therefore, key criteria in determining t activeness and spatial location of the process of seismogenic fa ting.

This paper shall present a new map of epicentres in the Ce tral Balkan region, on which they are depicted by arrows indicat the direction in which the dislocations spread, while the length of the arrows relatively corresponds to the size of the earthqua focus for a particular magnitude. The data have been obtained fr the seismograph traces for weak earthquakes and have been interpreted by a new technique.

I. ELEMENTS OF THE TECHNIQUE AND RESULTS OF ITS APPLICATION

The technique is based on a new approach to the interpretation c seismograph traces from earthquakes in the region and examines the spreading of the dislocations in the focus of an earthquake [4 - 6]. The technique takes into account the dynamics of the process taking place within the focus by separating the P_{max} - waves and S_{max} - waves after a time interval τ measured from the beginning of the shock during the general dislocation. On th seismograph traces, these are the maximum amplitude wave groups A_{PImax} and AS_{max}.

Such a physical-wave approach to the interpretation of seismograms is, essentially, a representation of an extended focus of definite dimensions as a linear sequence of point-like source which "enter" the shock wave generation process in in sequence, while the maximum energy of emission occurs at intervals of time τ, whene the number of the "entering" sources is at its maximu [7]. In this case, seismograms look like gowing amplitude shifte in the time interval from the first arrival to the maximum number of entries. The propriety of such a depiction is confirmed b the results from experiments modering the physics of an earth - quake focus. Thus Vassileva's model, based on the dislocation ir a man-made crack shows clearly that the full displacement does

not occur at once but is a discrete process beginning with weak movements [8].

The identification of P,Smax - waves as focal is done by means of azimuthal travel timetables. In contrast to the more conventional timetables in use the asimutal one $t_{Pi} = f(A_z, \Delta = const)$ expresses the dependence of the time of travel of the focal waves P_i (where i = 1,2,... max) which are generated in sequence after the first entry not only to the direction in which the waves spread but also to the extension of the dislocation and speed at which it travels. And since the form of the asimuthal travel timetable differs from the conventional quasi-linear one this allows the waves generated by the focus to be separated from the waves which have crossed its borders into the Earth's interior. The latter's azimuthal travel timetables are linear and parallel the azimuthal axes while the travel timetables of the focal waves have a sinusoid form greatly extended along the azimuth of the dislocation (theoretically it is a sine curve). In this case the degree to which the azimuthal travel timetable is extended is determined by the extension of the dislocation and the speed at which it appears. The drawing of azimuthal traveltables essentially rules out the possibility of forming the maximums of the P-waves and S-waves by just adding up the values for the various types of waves reflected and reflected as they travel through the Earth's interior [9].

Azimuthal travel time curves are plotted by excluding the time of the waves' travel with the help of the travel timetables used to determine the parameters of the point of the hypocentre from the first arrivals of P-waves. The anisotropy of the medium is measured from the temporal deviations, i.e. the difference between the wave's real travel time from the origin to the station and the ideal time calculated on the basis of a model travel time table. The exclusion of the wave's travel time is done by relating station-measured times of travel to an epicentral distance using the formula:

$$t_{P\ max} = (\Delta = 70\ km) = t_{P\ max} - (t_{P2} - t_{P1} + t_o) \pm f_k$$

where: $t_{P max}$ are the station - observed times of P max wave travel; t_{P_1} is the time of Pmax-wave travel over a fixed epicentral distance, e.g. Δ =70 km on the travel time curve; t_{P_2} is the time of Pmax wave travel from origin to station according to the travel timetable; t_o is the time at the source obtained by defining the initial hypocentre from the first arrival of P-waves; f_k - the difference in the actual time of wave travel from origin to station and the time calculated from the travel timetable. These times are plotted as a function of the azimuth from the initial hypocentre defined from the first arrivals of P-waves at the station. This however is done only when it is certain that that the station has recorded the very first arrivals of P-waves [10]. The entire procedure can nevertheless be greatly simplified by plotting the azimuth value along the abscissa and the values of the differences Pmax-P along the ordinate. In fact seismology has long described and interpreted Pmax and Smax as focal waves.

The azimutal travel timetables for a part of the Central Balkans on Fig.1 show that the seismograms' maximum values pertain to the process of seismogenic faulting at the focus. In 70% of the cases, the directions thus obtained fall in within 30° with

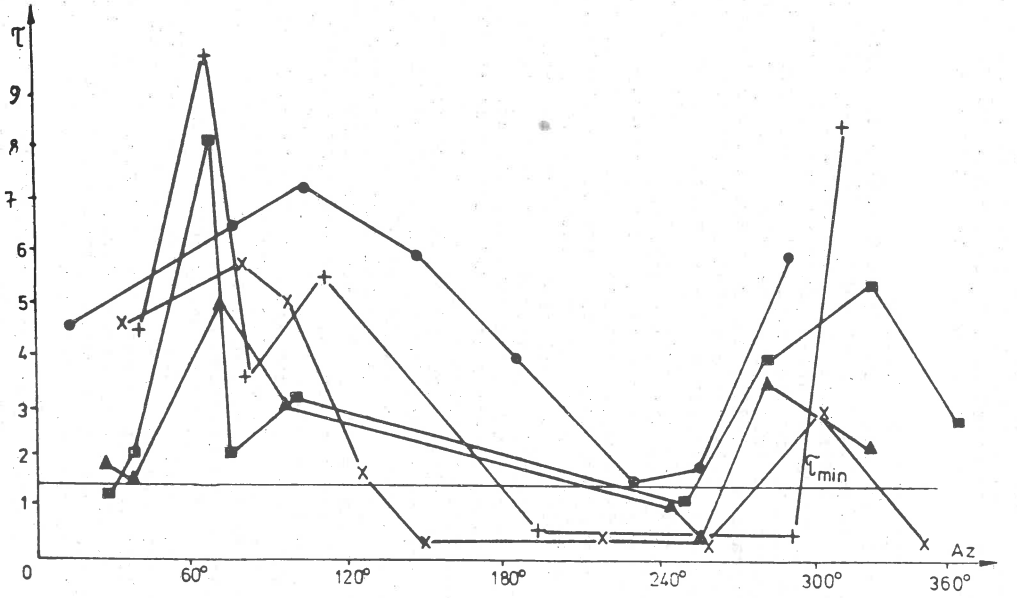

Fig.1

Azimuthal travel timetables for five weak earthquakes in different seismically active zones and with different dislocation orientation.

the azimuths of the nodal plane determined by the initial station registration of P-waves and S-waves [23]. The same precision has been achieved in determining the nodal planes when defining the mechanism of an earthquake. Moreover, the graphs in Fig.1 show clearly the maximum values corresponding to earthquakes in the different epicentral zones and the directions of dislocation dislocation distribution determined from these maximum values, which are logically attributed to the tectonic peculiarities of the region.

II. DATA USED AND DISCUSSION OF RESULTS

II.1. DATA USED. Data were used from 63 earthquakes of magnitude 1 to 3 registered in Bulgaria between January 1983 and November 1986. The magnitude was determined using the formula [11] depending on the time over which the seismograph traces were recorded. The earthquake coordinates and the origin times were obtained with the help of Bulgaria's National Operative Telemetric System for Seismological Information, NOTSSI, and software for PDP-11 desined by D. Solakov. The telemetric system equipment had identical amplitude/frequency characteristics. The earthquake mechanisms were defined by S. Yunga and N. Dotzev [23] by a technique and a set of software specially developed and designed by S. Yunga.

The azimuthal travel time curves and the parameters 1, c and A of the extended focus were obtained through the processing of more than 500 seismograms made by the vertical seismographs S 13-Z, used on all seismic stations in Bulgaria (Fig.2).

II.2. DISCUSSION OF RESULTS. A simplified version was used to plot the azimuthal travel timetables as graphs of time differences in wave travel Pmax-P, depending on the azimuth. The azimuthal travel timetables for the different seismically active zones and the direction of dislocation are shown on Fig.1. The maximum values of the azimuthal travel timetables and of the opposite spread of the dislocation proved different for the different seismic areas.

The chart illustating the parameters of the focal extension of weak earthquakes (Fig.2) in the central part of the region (between 42 to 43° N and 24 to 25° E) shows the different directions of faulting. Observable here are dislocations oriented to the northeast, northwest, southwest and southeast, as well as dislocations in opposite directions (Fig.3). The heterogeneity of the field of dislocations reflects the complex tectonic links and interactions in the Earth's crust on the territory of Bulgaria.

The dislocation distribution shows predominant orientations in various directions of this seismically active zone (Plovdiv - Chirpan). In the west-located foci, practically all dislocations have a west-northwest orientation while dislocation orientation in the northwest-located foci is much more diverse. To the southwest nearly all foci have a complicated dislocation structure at an angle to the predominant southwest-southeast directions. To the east a sufficiently stable northeast orientation of the dislocation distribution is observable.

Regularities of three dimentional orientation of the lineal sources of weak earthquakes and distribution of regional seismological structures and lineaments are shown on Fig.4.

III. DIMENSIONS OF EARTHQUAKE SOURCES.

The dimensions of the sources were determined using the azimuthal travel time curves and the formula suggested by [4 - 6]:

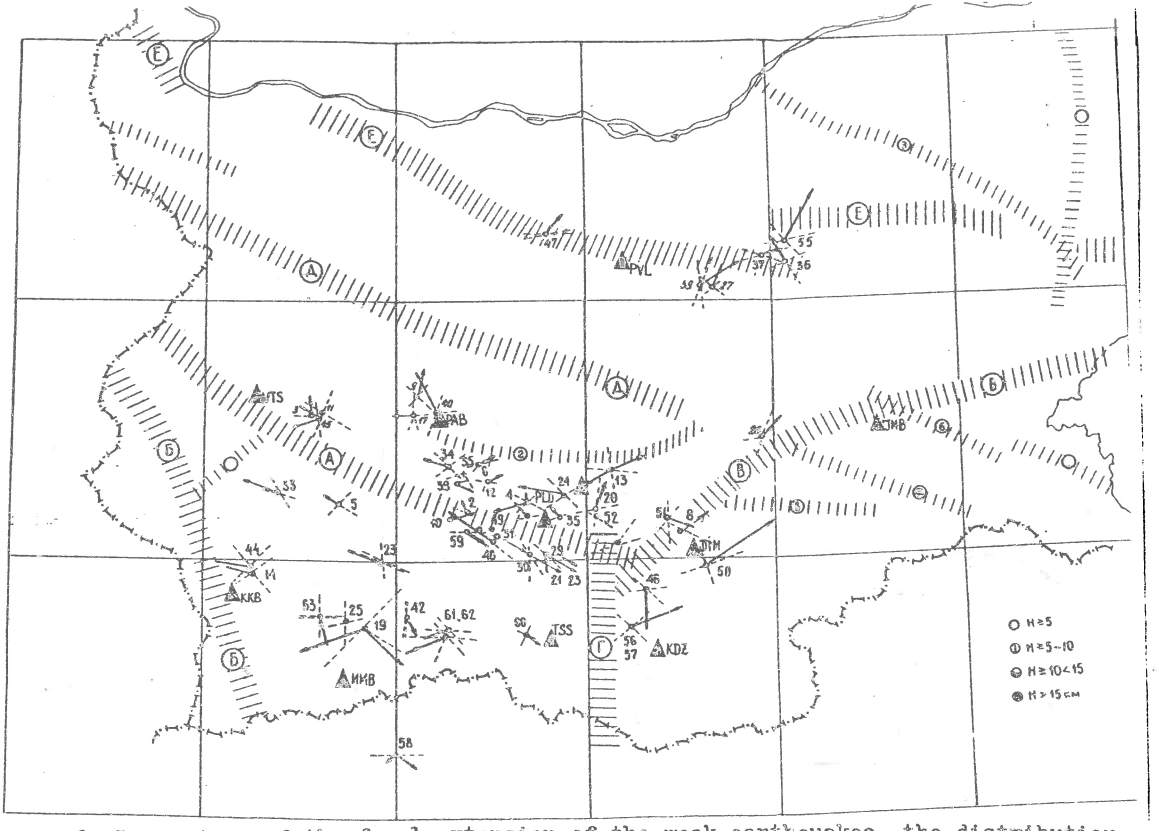

Fig.2. Parameters of the focal extension of the weak earthquakes, the distribution and direction of faulting, obtained using the technique proposed by the authors.

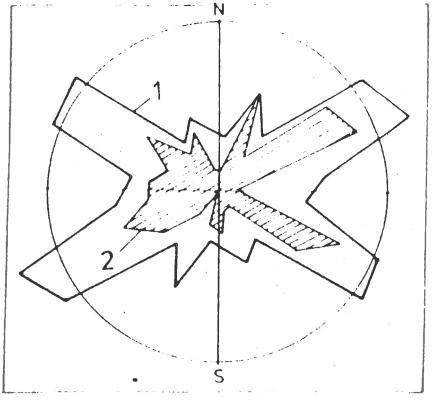

Fig. 3

Typical spread of dislocation in sources of weak (M = 1 to 3) earthquakes (1) and of opposite-direction spreading (2) obtained from the analysis of the data.

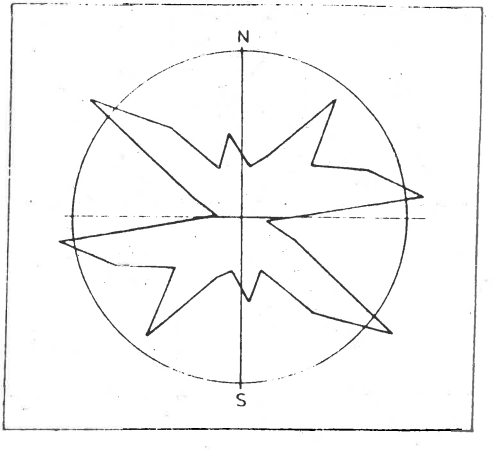

Fig. 4

Spatial orientation of regional seismogenic lineaments and of anomalies in relation to the density of weak earthquakes.

$L = Vp/2\ (\tau max - \tau min)$; $C = Vp\ (\tau max - \tau min)/(\tau max + min)$.

This is discussed in detail in [6]. Suffice it to examine in brief the term "earthquake source". There are two views on its meaning: according to one, surface dislocations correspond to the size of the source [13-16]. Theoretically such a source is examined by Kostrov [7]. In his opinion the medium is elastic outside the zone of destruction. According to the other view the source of seismic waves is much larger in size than the zone of destruction [17-22].

A source determined on the basis of Pmax-waves has proven larger than a source including only the zone of destruction. Notably such a view is expounded in the works of Byorly [17], Knopoff [18], Keilis-Borok [19], Gurrevitz, Nersesov et al. [20]. Keilis-Borok has calculated the size of the source on the basis of earthquake machanics using the values of shearing stresses wich are equal to zero at definite points in space. Gurrevitz, Nersesov et al. include not only the dislocation, but also the area of cracking and plastic deformations of the medium. According to their calculations the source area exceeds many times the size of the dislocation.

Gurrevitz [20] has performed certain calculations in studying the regularities pertaining to the fragmentation of an ideal elastic medium. According to these calculations the radius of the sphere within which seismic energy is generated is 2 to 3 times greater than the radius of the sphere of dislocation. In performing calculations for a medium of more realistic elastic and plastic properties Bullen [21] finds that the source should exceed something like twice the area of dislocation. The same conclusion is reached by Aptikaev [22], who has studied the ehergy damping along the amplitudes of earthquakes and explosions. On the basis of this experimental fact he delineates three zones: a zone of dislocation (focal zone) with a radius R_o; an inner zone (emiter) with a radius R_e and an intermediate zone with a radius R_i. The radius of the inner zone where the material of the medium is deformed under high dynamic tensions and plastic deformations are observable is two to three times greater than the radius of the zone of destruction. The radius of the intermediate zone $R_i = 6R_e$.

The dimensions of sources calculated by us coincide with the abovecited calculations of the size of the intermediate zone (zone of seismic emission formation). Our studies shown further that the maximum phase which characterizes the emission in the source does not correspond to the end of the dislocation. It is formed in the area surrounding the dislocation which is about twice larger. Therefore there are no reasons to equate a source with the size of a dislocation when grading earthquakes by their energy E on thebasis of the maximum values A/t in the groups of P-waves and S-waves. The approximate radius R of the focal zone which forms the seismic emission may be represented by the formula: $\lg R_{[km]} = 0.3\ \lg E_{[J]} - 2.02$, and the length of the dislocation proper, by the formula: $\lg R_{[km]} = 0.3\ \lg E_{[J]} - 3.02$.

The dependence between the volume V of the source and the energy class may be expressed as follows: $\lg V_{[km^3]} = 0.86\ \lg E_{[J]} + 1.14$.

CONCLUSION. Appying the technique evolved by the authors the spatial and temporal laws regulating the contemporary seismic process in the formation of weak and strong earthquake foci may be used to predict the direction in which seismic dislocation the predominant field of tectonic tensions and its variants will develop.

BIBLIOGRAPHY

1. Riznichenko, Yu. Methods of Detailed Seismic Studies. In: Tr. IFZ AN SSSR. Nauka, 1960, No. 9(176), pp.162-190.
2. Earthquakes in the USSR in 1979. Moscow, Nauka, 1979, pp. 124-146.
3. Earthquakes in the USSR in 1975. Moscow, Nauka, 1975, pp. 95-116.
4. Gorbunova, I. Defining Source Length and Dislocation Direction by Means of Seismograph Traces. Dokl. AN SSSR, 1981, vol. 261 pp. 836-839
5. Gorbunova, I. Interpretation of P- and S-waves from Earthquakes with Extended Sources. Interpretation of Seismological Observations. Moscow, Nauka, 1983, pp. 88-101.
6. Gorbunova, I., Kal'metieva, Z. Experimental Characteristics of Source Emission During Weak Earthquakes. Frunze, Ilim., 1988, 100 pp
7. Kostrov, B. Tectonic Earthquake Source Mechanics. M., 1975, 147pp.
8. Vasilyev, Yu. Modeling of the Seismic Seam. In: Izv. AN SSSR, "Fizika Zemli series, No. 3, 1986, pp. 11-18.
9. Epiffansky, A. Algorithm for the Plotting of Precise Systematic Seismic Traces for Any Dipolar Source. Computer Use in Seismic Practice. Moscow, Nauka, 1984, pp. 100-116.
10. Gorbunova, I., Pastorov, A. On the Divergence of Kynematic Earthquake Parameters as per Observations by Regional and World Station Networks. In: Izv. AN SSSR, Fizika Zemli, 1983, pp. 22-31.
11. Samardjieva, E., Christoskov, L. On the Eastablishment of a Unified Earthquke Magnitude Classification System on the Basis of Late-period Seismograph Traces at a Distance of up to 10. In: Mladezhki naouchen prinos, S., BAS, 1985, pp. 72-87.
12. Dineva, S. A Study of the Dynamic Characteristics of Earthquake Sources in the Carpathian-Balkan Region. Dissertation, M. 1986, pp. 24
13. Riznichenko, Yu. Dimensions of the Crust Earthquake Source and the Seismic Moment. In: Issl. po fizike zemletr. M., Nauka, 1976, 9-27.
14. Sadovsky, M., Pissarenko, V., Steinberg, V. On the Dependence of Energy on the Seismic Source's Volume. Dokl. AN SSSR, 1983, V. 271, 3.
15. Sadovsky, M. Once More on the Dependence of a Seismic Source's Volume on Its Energy. Dokl. AN SSSR, 1984, Vol. 275, No. 5, pp. 1087-1088.
16. Steinberg, V. On Source Parameters and the Seismic Effect of Earthquakes. Izv. AN SSSR, Fizika Zemli, 19, No. 7, pp. 49-64.
17. Byorly, P. Symposium on Earthquake Mechnism, Ottawa, 1960, pp. 303-304
18. Knopoff, M. Energy Release in Earthquake. Jeogr. J. RAS, V. I, 1, 1958.
19. Keilis-Borok, V. A Theoretical Analysis of the Relationship Between Earthquake Energy, the Size of the Displacement at the Source and the Size of the Source. Otchet TKSE, IFZ AN SSSR, I, 4, 1957, CH. III
20. Gurrevitz, G., Nersesov, I., Kuznetsov, A. On the Application of the Law of Earthquake Recurrence. In: TISSS, D., 1960, No. 6, pp. 41-80.
21. Bullen, K. An Introduction to Theoretical Seismology. M., 1966, 46 pp.
22. Aptikaev, F. Determining the Energy of Seismic Sources. In: Eksperimentalnaya seismologia. Moscow, Nauka, 1971, pp. 59-65.
23. Dotzev, M., Tunga, S. Earthquake Source Mechanism in Bulgaria. In: Izv. AN SSSR: Fizika Zemli series, 1988, No. 4, pp. 3-14.

DYNAMICAL EARTHQUAKE PARAMETERS FOR THE BALKAN REGION AND THEIR INTERRELATION

N.V.KONDORSKAJA
Institute of Physics of the Earth, Moskow, USSR
S.DINEVA
Geophysical Institute, Sofia, Bulgaria

INTRODUCTION

The present work is devoted to the investigation of the relations SEISMIC MOMENT-VERSUS-MAGNITUDES MPV, MPV_S, MLV, MLH, MSV for the earthquakes in the Balkan region on an average for all earthquakes and for each faulting type (thrust, normal, strike-slip).

DATA

Dynamical characteristics: seismic moment and different types of magnitudes used in this paper are presented in table I.

SEISMIC MOMENT The values of seismic moment are determined from the long-period P-wave spectra, obtained on the basis of the analyses of the seismograms from stations of the Unified System for the Seismological Observations (USSO) in the USSR (Dineva, 1989).

MAGNITUDES The determination of the values of all magnitudes is based on data from the stations of the USSO and some other European countries (ČSSR, DDR, Poland) equipped with reliable and high sensibility unified seismographs. With the exception of magnitude MPV_S, which is determined from the records of short-period seismographs (type A according to the international classification), all the rest magnitudes are determined from the records of middle- and long-period seismographs (types B and C according to the same classification).

The calibrating functions, recommended by Vanek et al. (1962) were used for determination of magnitudes MPV, MPV_S and MLH, but calibrating functions, obtained by Christoskov et al.(1983)-for magnitudes MSV and MLV.

TABLE 1

NUM-BER	DATA OF EARTHQUAKE YEAR	MON	DAY	COORDINATES (ISC)		h [m]	To h:min (ISC)	Mo.10^{18} [N.m]	MPVs	MPV	MSV	MLH	MLV	TYPE OF FAULT PLANE SOLUTION
1	1969	01	14	36.11	29.11	22	23:12	2.65± 1.36	5.96±0.08	6.49±0.06	5.90	5.87±0.10	6.18±0.21	strike-slip
2	1969	03	28	38.66	28.46	9	01:48	50.30	6.18±0.38	6.67±0.09	5.63	6.50±0.08	6.65±0.06	strike-slip
3	1970	03	28	39.21	29.51	18	21:02	25.20	6.61±0.08	7.35±0.10	6.89	7.25±0.14	7.35±0.19	normal
4	1970	04	08	38.34	22.56	23	13:50	8.11± 0.95	6.21±0.11	6.36±0.03	6.01±0.08	5.84±0.07	6.10±0.08	thrust
5	1971	05	12	37.64	29.72	30	06:25	3.36± 1.13	6.11±0.05	6.39±0.07	6.08	6.05±0.07	6.13±0.08	normal
6	1971	05	04	35.15	23.56	14	21:39	1.76	6.52±0.12	6.83±0.07	6.68±0.05	6.08±0.09	6.17±0.03	thrust
7	1971	09	13	37.96	22.38	75	04:13	3.39± 0.45	6.11±0.12	6.34±0.10	6.16±0.05	5.55±0.09	5.72±0.16	strike-slip
8	1975	03	17	40.48	26.08	18	05:35	1.15	5.55±0.11	6.40	-	5.68±0.05	5.75±0.11	normal
9	1975	03	27	40.45	26.12	15	05:15	4.28± 1.50	6.39±0.11	6.54±0.07	6.40	6.50±0.07	6.65±0.04	normal
10	1975	06	30	38.49	21.62	3	13:26	0.10	5.63±0.07	6.05±0.19	-	5.33±0.07	5.42±0.05	strike-slip
11	1976	05	11	37.45	20.36	10	16:59	20.92± 5.43	6.15±0.05	6.71±0.05	6.36±0.10	6.46±0.10	6.59±0.07	normal
12	1976	06	12	37.52	20.58	17	00:59	1.48± 0.40	5.96±0.09	6.01±0.09	5.84±0.07	5.60±0.12	5.55±0.11	thrust
13	1977	03	04	45.83	26.72	86	19.21	112.90±34.72	6.63±0.10	7.24±0.04	7.04±0.10	6.91±0.09	6.94±0.06	thrust
14	1977	08	18	35.27	23.52	47	09:27	1.02	6.25±0.14	6.11±0.12	5.73±0.08	5.28±0.05	5.34±0.08	strike-slip
15	1977	09	11	34.95	23.05	4	23:19	0.98	6.02±0.06	6.09±0.08	6.10±0.11	6.09±0.06	6.08±0.06	thrust
16	1977	11	03	42.12	24.03	11	02:22	0.98± 0.36	5.72±0.20	5.83±0.07	-	5.26±0.14	5.46±0.08	normal
17	1978	05	23	40.73	23.25	9	23:34	3.39± 0.90	6.06	6.09±0.05	5.50	5.55±0.12	5.85±0.08	normal
18	1978	06	20	40.78	23.24	16	20:03	15.60± 4.40	6.20±0.08	6.71±0.05	6.10±0.01	6.44±0.10	6.59±0.06	normal
19	1979	04	15	42.04	19.05	4	06:19	16.38± 3.71	6.61±0.10	6.93±0.06	6.78±0.04	7.06±0.06	7.21±0.08	thrust
20	1979	04	15	42.29	18.68	7	14:43	1.10± 0.26	5.97±0.05	5.87±0.08	5.56±0.06	5.75±0.10	5.80±0.09	normal
21	1980	05	02	35.63	29.76	38	05:30	4.52	5.65±0.06	6.04±0.11	-	5.26±0.09	5.47±0.04	strike-slip
22	1980	07	10	39.44	22.65	22	19:38	1.00± 0.23	5.60±0.05	6.22±0.21	-	5.50±0.10	5.60±0.09	normal
23	1981	02	24	38.23	22.97	18	20:53	13.32± 2.92	6.53±0.06	6.97±0.06	-	6.82±0.08	6.84±0.09	strike-slip
24	1981	02	25	38.17	23.12	30	02:53	9.49± 0.91	6.31±0.07	6.75±0.07	-	6.56±0.06	6.50±0.05	strike-slip
25	1981	03	04	38.24	23.26	32	21:58	8.56± 0.52	6.28±0.05	6.47±0.05	-	6.39±0.09	6.41±0.07	strike-slip
26	1981	03	05	38.20	23.12	31	06:59	1.06± 0.83	5.75±0.05	6.16±0.16	-	5.33±0.09	5.33±0.08	strike-slip
27	1981	03	07	38.19	23.27	33	11:34	0.79	5.83±0.05	6.10±0.16	-	5.32±0.05	5.18±0.02	normal
28	1981	03	10	39.38	20.75	32	15:16	2.25	5.80±0.06	6.20±0.06	-	5.59±0.09	5.47±0.08	strike-slip
29	1981	04	26	36.53	30.65	76	14:13	1.63	5.79±0.05	5.93±0.08	-	4.99±0.08	5.00±0.07	strike-slip
30	1981	06	28	37.82	20.13	13	17:20	1.14	5.68±0.06	5.97±0.08	5.36±0.12	5.57±0.06	5.58±0.05	strike-slip
31	1981	07	03	39.54	20.67	41	21:42	0.53	5.67±0.05	5.94±0.09	5.12	5.45±0.07	5.28±0.06	normal
32	1981	08	13	44.85	17.33	16	02:58	0.69	5.83±0.05	5.90±0.09	5.45	5.77±0.08	5.90±0.05	thrust
33	1981	12	19	39.24	25.23	10	14:10	24.05±11.95	6.66±0.06	6.73±0.06	6.78	7.19±0.09	7.26±0.14	thrust
34	1981	12	27	39.24	25.23	10	17:39	4.54± 0.60	5.91±0.04	6.18±0.06	-	6.52±0.11	6.69±0.12	strike-slip

RESULTS

The parameters of the moment-magnitude relations for all earthquakes and for each type of faulting (thrust, normal and strike-slip) are presented in table 2.

COMPARISON OF THE RELATION $M_o = f(MLH)$ WITH SIMILAR ONES OBTAINED BY OTHER AUTHORS The found relation $M_o = f(MLH)$ is presented as line I in fig.I. The moment- M_s relations of Giardini et al. (I984) for the Mediterranean, based on the data of centroid-moment tensor, North (I974, I977) for Eastern Mediterranean and Riznichenko (I976) for the whole world are given on this figure by lines 2,3 and 5 respectively. The moment- M_s relation of Aki (I967) based on the assumption of ω^{-2} decay is also shown (line4).

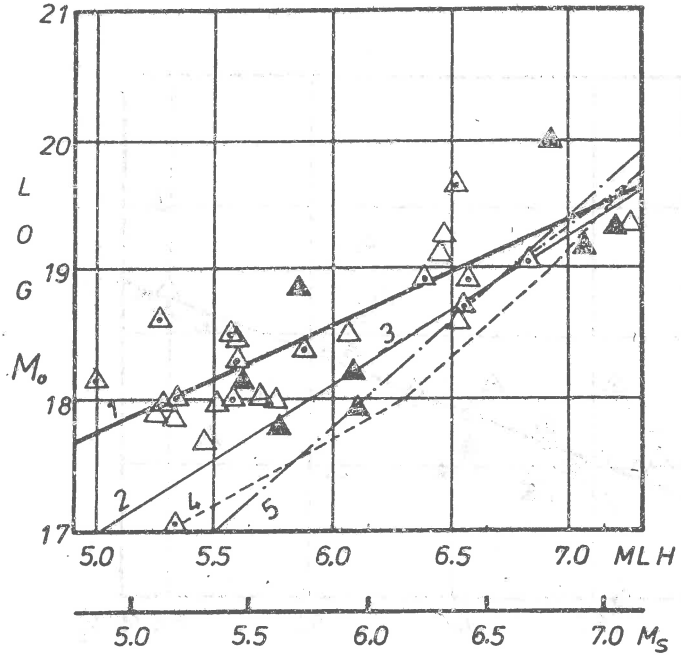

Figure I. Seismic moment M_o (N.m) as a function of surface-wave magnitude MLH. The symbols used indicate the type of faulting (△ - normal; ▲ - thrust; ◬ - strike-slip).

The closest relation to (I) is that of Giardini et al. with a slight shift to the smaller seismic moments, which does not exceed the accuracy of determination of M_0. A good coincidence is observed between relation (3) and the present data. As far as relation (5) is concerned, only for large earthquakes MLH ≥ 6.0 a good coincidence between it and relation (I) takes place. For small earthquakes (MLH ~ 5.5) relation (5) predicts M_0 values I4 times smaller than given by relation (I). The data shown, though considerably scattered, with only one exception, are with a higher moment values than predicted by relation (4) over the magnitude interval up to MLH = 7.0. For instance, for earthquakes with MLH < 6.4 relation (4) predicts M_0 values 5 - I0 times smaller than given by relation (I). For MLH > 7.0 a close coincidence exists between relation (4) and the presented data.

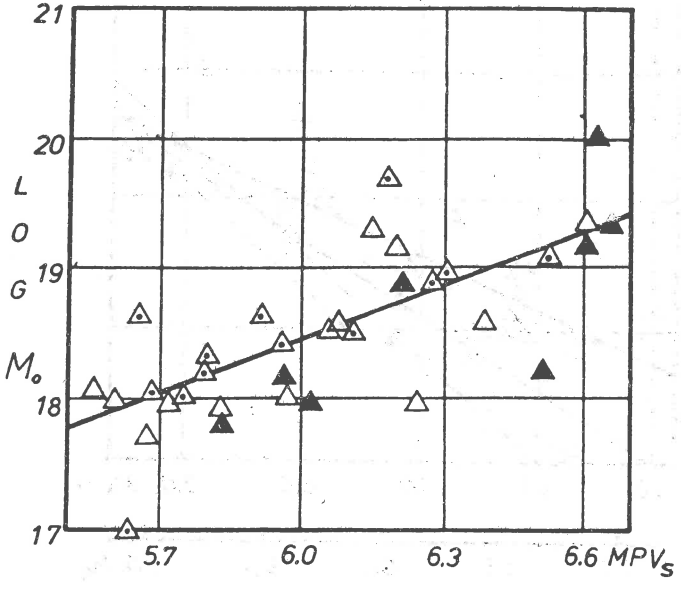

Figure 2. Seismic moment M_0 (N.m) as a function of body-wave magnitude MPV_S. Symbols identify faulting type as in fig.I.

COMPARISON OF THE RELATIONS MOMENT-VERSUS-MAGNITUDE FOR EARTHQUAKES WITH DIFFERENT FAULTING TYPE It was found, that in general, for all relations at smaller magnitudes (MLH ≤6.5), thrust earthquakes have M_o values lower than those of strike-slip and normal earthquakes (see table 2). (The type of faulting is determined from fault-plane solutions of Dineva, I986.) The difference is about 2 - 3 times, but for relation $M_o = f(MPV_s)$ it reaches 4 and 5 times, respectively for strike-slip and normal earthquakes (fig.2). For these magnitudes the difference between seismic moments of strike-slip and normal earthquakes is insignificant. The values M_o for strong earthquakes - MLH > 6.5 do not depend upon the faulting type.

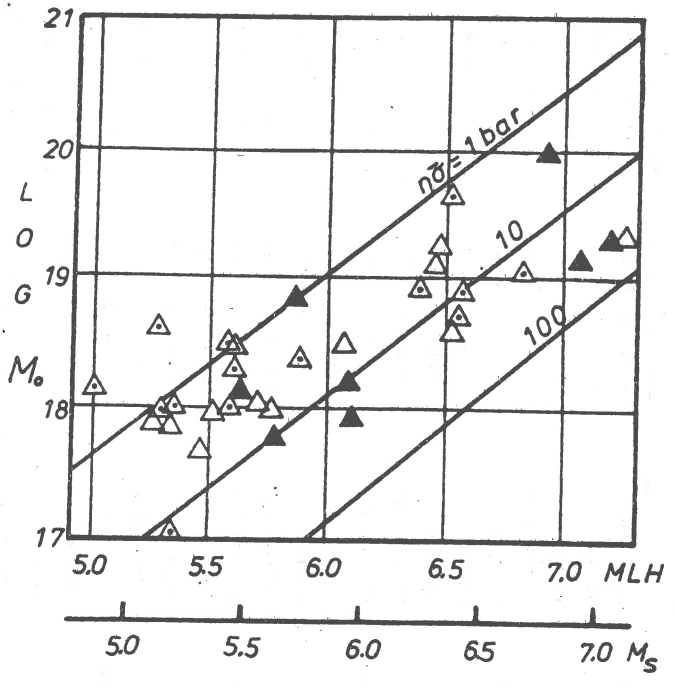

Figure 3. Seismic moment M_o (N.m) as a function of surface-wave magnitude MLH. The straight lines are for constant apparent stress. A rigidity of 3×10^{11} dyne/cm^2 is used. Symbols identify faulting type as in fig.I.

TABLE 2

PARAMETERS OF REGRESSIONS MOMENT - VERSUS - MAGNITUDE

REGRESSION		COEFFICIENTS a	COEFFICIENTS b	COEFFICIENT OF CORRELATION	STND.ERR. OF SQR.	NUMBER BER
Mo = a + bMPVs	ALL EVENTS	10.21 ± 1.45	1.37 ± 0.24	0.71	0.46	34
	THRUST	6.87 ± 3.49	1.88 ± 0.55	0.81	0.50	8
	NORMAL	10.71 ± 2.27	1.30 ± 0.38	0.74	0.41	12
	STRIKE-SLIP	9.96 ± 2.95	1.42 ± 0.49	0.64	0.51	14
Mo = a + bMPV	ALL EVENTS	10.21 ± 1.06	1.31 ± 0.16	0.81	0.38	34
	THRUST	9.96 ± 1.32	1.35 ± 0.36	0.84	0.46	8
	NORMAL	11.02 ± 1.20	1.18 ± 0.19	0.89	0.27	12
	STRIKE-SLIP	9.20 ± 2.55	1.46 ± 0.40	0.72	0.46	14
Mo = a + bMLH	ALL EVENTS	13.68 ± 0.67	0.81 ± 0.11	0.79	0.40	34
	THRUST	12.44 ± 1.92	0.99 ± 0.30	0.80	0.51	8
	NORMAL	13.57 ± 0.86	0.83 ± 0.14	0.87	0.29	12
	STRIKE-SLIP	14.01 ± 1.22	0.77 ± 0.21	0.73	0.46	14
Mo = a + bMLV	ALL EVENTS	13.68 ± 0.64	0.80 ± 0.10	0.80	0.39	34
	THRUST	12.37 ± 1.87	0.99 ± 0.29	0.81	0.49	8
	NORMAL	13.61 ± 0.70	0.81 ± 0.12	0.91	0.25	12
	STRIKE-SLIP	14.00 ± 1.21	0.76 ± 0.20	0.73	0.45	14
Mo = a + bMSV	ALL EVENTS	13.68 ± 1.26	0.82 ± 0.82	0.67	0.67	21
	THRUST	11.67 ± 2.21	1.11 ± 0.34	0.79	0.52	8
	NORMAL	NO CORRELATION				5
	STRIKE-SLIP	13.26 ± 1.33	0.90 ± 0.22	0.86	0.34	8

APPARENT STRESSES On the plot M_o-versus-MLH with straight lines are presented relations $M_o = f(MLH)$ for constant apperent stress (fig.3). As is shown, in general, earthquakes with MLH < 6.0 have values of an apparent stress I - IO bars. Only two earthquakes with MLH < 5.5 have $\eta\bar{\sigma}$ < I bar (about 0.2 bar). The largest apparent stresses (IO - 30 bars) are observed for earthquakes with MLH > 6.0. According to the classification of Kanamori and Anderson (I975) inter-plate earthquakes have $\eta\bar{\sigma} \sim$ IO to 20 bars, "average" - $\eta\bar{\sigma} \sim$ 30 bars, and intraplate - $\eta\bar{\sigma} \sim$ 50 bars. Taking into account this classification the majority of earthquakes under investigation belong to the inter-plate earthquakes, and the rest earthquakes - to the "average".

REFERENCES

AKI K. Scaling law of seismic spectrum. - J.Geophys. Res., I967, v.72,N 4, p.I2I7-I23I.

CHRISTOSKOV L., N.V.KONDORSKAYA, J.VANEK Earthquake magnitude in seismological practice: PH, S and L waves, Praha, Acad. Nakl. Československe Akademie VED, I983, II3 p.

DINEVA S. Seismic moment of some strong earthquakes in the Carpathian-Balkan region (I969-I98I). -Bulg.Geophys.J., I989, v.XIV, N 2.(in press, in Russian)

DINEVA S. Investigation of the dynamical parameters of the earthquakes in the Carpathian-Balkan region, Thesis, Institute of Physics of the Earth, Moskow, USSR, I986. (in Russian)

GIARDINI D., A.M.DZIEWONSKI, J.H.WOODHOUSE, E.BOSHI Systematic analysis of the seismicity of the Mediterranean region using the centroid-moment tensor method. - The O.G.S. Silver Anniversary Volume (A.Brambati and D.Slejko - Eds.), Trieste, I984,p.I2I-I4I.

KANAMORI H., D.ANDERSON Theoretical basis of some empirical relations in seismology. - BSSA, I975, v.65, N 5, p.I073-I095.

NORTH R.G. Seismic slip rates in the Mediterranean and Middle East. - Nature, I974, v.252, N 5484, p.560-563.

NORTH R.G. Seismic moment, source dimensions and stresses associated with earthquakes in the Mediterranean and Middle East. - Geophys.J.R.astr.Soc., I977, v.48, p.I37-I6I.

RIZNITCHENKO Y.V. Source dimensions of crust earthquakes and the seismic moment. - In: "Investigation on the physics of earthquakes", Moskow, Nauka, p.9-27. (in Russian)
VANEK J., V.KARNIK, A.ZATOPEK, N.V.KONDORSKAYA, J.V.RIZNITCHENKO, E.F.SAVARENSKY, S.S.SOLOVEV, N.V.SHEBALIN Standartization of magnitude scale. - Izv. AN SSSR, Ser.geofiz., 1962, 2, p.153-158. (in Russian)

SOME ENGINEER CONSIDERATIONS FOR STRONG MOTION DURATION DEFINITION

Marin Kostov, *Central Laboratory for Seismic Mechanics and Earthquake Engineering, BAS, Sofia*

1. INTRODUCTION

The main characteristics of seismic excitation the engineers need for earthquake resisitant building design are the maximal (or effective) acceleration, frequency content, and duration of seismic motion. When the design acceleration and frequency content of seismic motion are relatvely well defined and there are many methods for their engineer usage, the duration of motion is not explicitly included in the nowadays design codes and engineering praxis. It is known that seismic motion duration plays an important role in the lightly damped system analyses, liquefaction potential assessment, nonlinear structural analyses, in some interaction problems etc.

The existing strong motion duration definitions are based mostly on seismological considerations. They are aimed to clarify in the first line problems conected with the source mechanism study, magnitude or energy determination but they have less applications in the structural response analyses. There are basically two types of strong motion duration definitions. The first one defines the duration as time interval between the first and the last passage of predefined acceleration level - usually 0.05g [1]. The second one is based on the commulative energy computation by integrating the square of accelerations. According to the last definition the duration is defined as time interval needed to accumulate a certain prescribed part of total energy (power) - e.g. 95% [2] or 90% [3]. Bolt [4] has used both definitions on a band pass filtered sinusoidal components of seismic motion. In the presented paper the strong motion duration is determined taking into account the structural dynamic characteristics. The duration is defined as a time interval needed for dissipating some prescribed part of the total seismic input energy of single degree of freedom system (SDFS).

2. ENERGY BALANCE OF SDFS

The force equilibrium equation of SDFS subjected to seismic excitation is :

$$F_i(t) + F_{vis}(t) + F_{e,pl}(t) = F_{inp}(t) \qquad (1)$$

where

$F_i(t)$ is the inertia force,

$F_{vis}(t)$ is the viscose damping force,

$F_{e,pl}(t)$ is the linear or nonlinear restoring force,

$F_{inp}(t)$ is the excitation force.

Multiplying both sides of (1) by relative velocity $v(t)$ and integrating over the time t, the energy equilibrium equation is obtained :

(2) $$E_{kin}(t) + E_{vis}(t) + E_{e,pl}(t) = E_{inp}(t)$$

In the case of linear SDFS and translatory motion, the terms of equation (2) can be expressed :

(3) $$E_{kin}(t) = \frac{mv^2(t)}{2}$$ - kinetic energy

(4) $$E_{vis}(t) = c\int_0^t v^2(\tau)d\tau$$ -dissipated viscose energy

(5) $$E_e(t) = \frac{kx^2(t)}{2}$$ - potential energy

(6) $$E_{inp}(t) = -m\int_0^t a_g(\tau)v(\tau)d\tau$$ - input energy

where :
c is the viscose constant, k is the system stiffnes, m is the mass, $a_g(t)$ is the acceleration time history. In the case of nonlinear SDFS (5) must be replaced by :

(7) $$E_{e,pl}(t) = \int_0^t F_{e,pl}(\tau,x)v(\tau)d\tau$$

If for the case of simplicity an elastic-plastic force-displacement relation (fig.1) is assumed, (7) can be further divided into two integrals:

(8) $$E_e(t) = \frac{kx_e^2(t)}{2},$$

$$x_e(t)=x(t)-x_{pl}(t) \; ; \; |F_{e,pl}| < F_e = kx_e,$$

(9) $$E_{pl}(t) = F_e\int_0^t v_{pl}(\tau)d\tau$$ - hysteresis energy,

where F_e is the ultimate elastic force, x_{pl} is the plastic part of the displacement, x_e is the elastic part of the displacement.

When t tends to infinity the kinetic and the potential energy (stored energy) tend to zero. In the same time E_{inp} and the dissipated energy ($E_{dis} = E_{vis} + E_{his}$) reach a constant value. According to the energy conservation law $E_{inp} = E_{dis}$, when E_{kin} and $E_e = 0$.

In fig.2 the build up plots of the input energy, the dissipated energy and the sum of potential and kinetic energy (stored energy) for an elastic-plastic SDFS are drawn. The natural period of the initial elastic system is T=0.5s. Seismic excitation is applied by accelerogram "Imperial Valley", comp.N90E, El Centro (1940) earthquake, scaled to 0.1g. It can be seen that after the excitation stops, the stored energy tends to zero and $E_{inp} = E_{dis}$.

The input energy build up is more irregular compared to the dissipated energy one. During the excitation input energy shows a lot of peaks and valleys, caused by the steady change of energy flow. In the E_{inp} and E_{dis} plots three different regions can be separated. The first region is in the very beginning and is characterized by a small amount of dissipated energy. In the second region there is intensive energy input, respectively energy dissipation. The third region shows a relatively small change of the input (dissipated) energy and dying up of the kinetic and the potential energy. Obviously the second region of the input (dissipated) energy build up is the most important for the structural response. In fig.3 similar plots are shown. They are computed for four SDFS with natural periods in the elastic stage T=0.04s., T=0.2s., T=0.8s. and T=2.0s.(damping - 5%). A synthetic accelerogram is used, corresponding to an earthquake with a magnitude 5.7, source debth 7.5km. and epicentral distance 7.5km. One can clearly distinguish the different time of energy dissipation by the four systems. Considering the stiff system (t=0.04s.) the time for energy dissipation is very short. The input energy grows up to its maximal value for a very short time, practically immediately after the maximal acceleration of the ground motion strikes. The long period system (T=2.0s.) behaves in a different manner. The energy dissipation lasts a long time even after the excitation stops. Looking at the time of the last excursion in the plastic range there is a big difference again. For the stiff system the last excursion practically coincides with the time when the maximal ground acceleration occurs. For the long period system this happens some 20s. later (inspite of the low acceleration value of ground shaking at the time).

3. STRONG MOTION DURATION DEFINITION

The duration of seismic excitation depends both on earthquake characteristics as magnitude, epicentral distance, source debth, source mechanism, local soil conditions and structural dynamic characteristics - natural period of vibration, damping, ductility. For this reason the significant for structural response duration of ground shaking could be determined as a time interval the systems need for dissipation of the main part of seismic input energy. For SDF - systems this time can be drawn as a plot, similar to the response spectra. Let's call this plot a duration spectrum. In fig.4 a mean and maximum duration spectra of 10 generated accelerograms [5], corresponding to an earthquake with a magnitude 6, source debth 7.5km and epicentral distance 15km. are shown. The local soil conditions correspond to stiff soils. These spectra are obtained using linear SDFS with 5% damping. The significant duration is defined as a time interval needed for 90% (from 5 upto 95%) dissipation of maximal seismic input energy. For comparison the effective duration (t_{eff}) using the commulative energy definition is also determined (from 5 up to 95%). The mean t_{eff} is 5.3s. and the max. t_{eff} is 6.7s. These values are plotted as dashed lines in the same figure. For short period systems (approximately up to T=0.5s.) there is a good correlation between

the by commulative energy computed duration and that, obtained by the new definition. For long period systems the both definitions differ significantly. The long period systems need more time to dissipate the seismic input energy. It means that for these systems the dynamic analysis must be carried out considering the whole (even longer) duration of the seismic excitation.
In fig.5 mean seismic excitation duration spectra for elastic-plastic SDFS are shown. The yield level is 0.8 and 0.5 of the corresponding maximal elastic force for linear SDFS with 5% of critical damping. The spectra in fig.5 show some lower values compared with the duration by linear SDFS. This can be explained by the dissipated hysteresis energy, which considerably contributes to a faster seismic input energy dissipation. The figure shows again that for long period systems the time needed for energy dissipation is longer.

4. DISCUSSION AND CONCLUSIONS

The proposed definition of the significant for structure response duration of seismic motion is a furter development of the nowadays used in the seismology duration definitions. The main advantage of the new definition is the possibility to take into account the dynamic properties of the structures. One and the same seismic motion can be classified as "short" or "long", depending on the structure considered. Possibly the proposed definition could be used for multi degree of freedom systems. In this case the duration used might be that corresponding to the first natural period of vibrations.
The proposed definition could be possibly used in two ways. The first way is to develop statistically based relations for the strong motion duration, depending on the earthquake magnitude, epicentral distance, local soil conditions, structural natural period of vibrations, damping and ductility.
The second way of application is connected probably with the seismic microzonation studies. In this case a good assessment of the duration spectra could be obtained based on the comprehensive studies of the local seismic sources, site soil conditions and the dynamic properties of the structures to be designed.
In both cases the duration presently defined can be a good help for engineers by dynamic analyses and can contribute to the reasonable decrease of nonlinear analysis computational costs. It can be also used for artificial accelerogram generations or real accelerogram selection in dynamic structural analysies.

5. LITERATURE

1. Page, R.A., Boore, D.M., Dietrich, J.N., Estimation of Bedrock Motion of Graund Surface, USGS Profesional Paper, 941A, 1975.
2. Husid, R., Median, H., Rios, J., Analysis de Terramotos Norte-americanos y Japonseces, Revista del IDIEM, 8, Chile, 1969.
3. Trifunac, M.D., Brady, A.G., A Study of the Duration of Strong Earthquake Ground Motion, Bull. Seism. Soc. Am., 65, 3, 1975.
4. Bolt, B.A., Duration of Strong Ground Motion, 5 World Conf. on Eart. Eng., v1, Rome, Italy, 1973.
5. Kostov, M., A Model for Seismic Motion Generation, Bulg. Geoph. Jour., v8, 3, 1987.

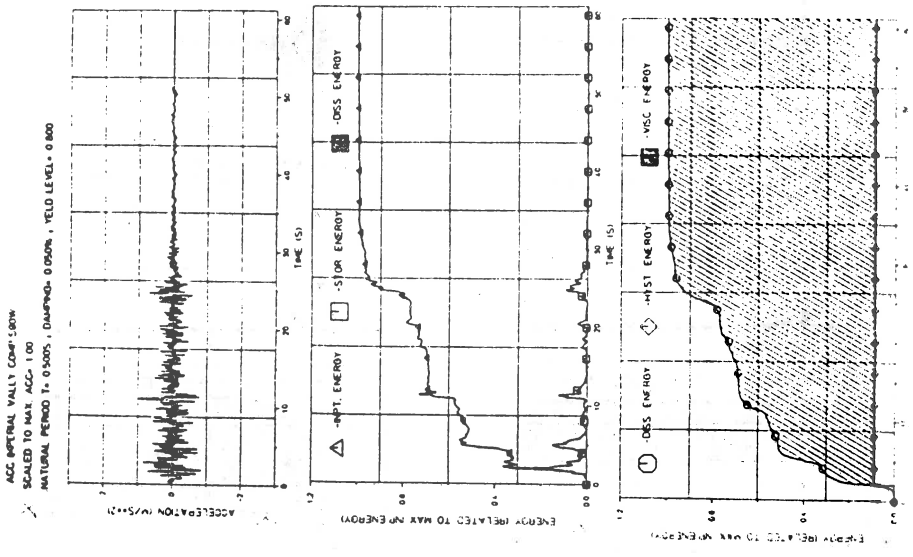
ACC IMPERIAL VALLY CONTROL
SCALED TO MAX ACC= 1.00
NATURAL PERIOD T= 0.500S , DAMPING= 0.050% , YELD LEVEL= 0.800
ACCELERATION (M/S**2)
TIME (S)
-KPT. ENERGY
-STOR ENERGY
-DSS ENERGY
ENERGY RELATED TO MAX KP ENERGY
TIME (S)
-DSS ENERGY
-HYST ENERGY
-VSC ENERGY
ENERGY RELATED TO MAX KP ENERGY

fig.2

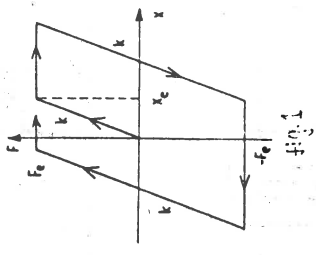
x
k
k
k
x_e
f_e
$-f_e$

fig.1

ACCTIME HISTORY, SIMULATION NO. 1
SCALED TO MAX. ACC= 1.00
NATURAL PERIOD T= 0.0400 , DAMPING= 0.020 , YIELD LEVEL= 0.600

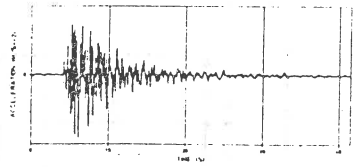

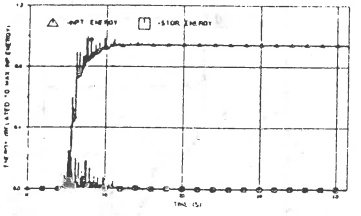

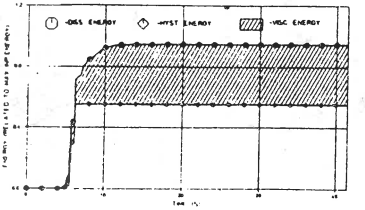

ACCTIME HISTORY, SIMULATION NO. 1
SCALED TO MAX. ACC= 1.00
NATURAL PERIOD T= 0.0505 , DAMPING= 0.020 , YIELD LEVEL= 0.600

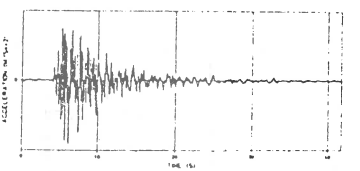

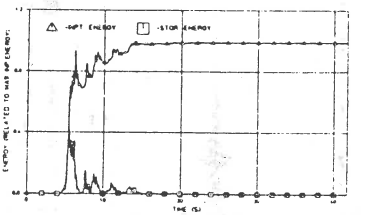

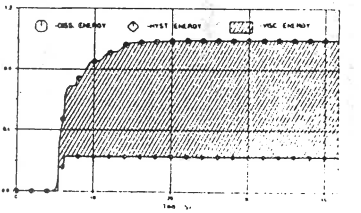

ACCTIME HISTORY, SIMULATION NO. 1
SCALED TO MAX. ACC= 1.00
NATURAL PERIOD T= 0.0505 , DAMPING= 0.020 , YIELD LEVEL= 0.800

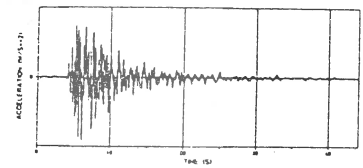

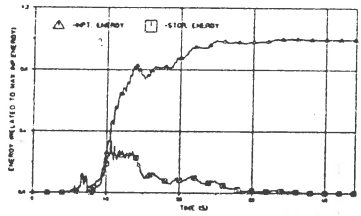

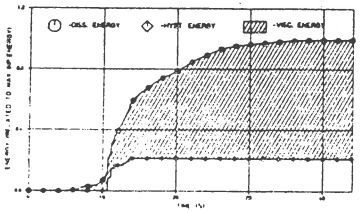

ACCTIME HISTORY, SIMULATION NO. 1
SCALED TO MAX. ACC= 1.00
NATURAL PERIOD T= 2.0000 , DAMPING= 0.020 , YIELD LEVEL= 0.800

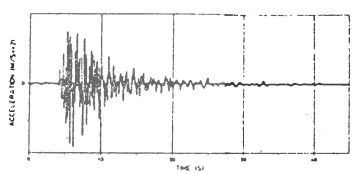

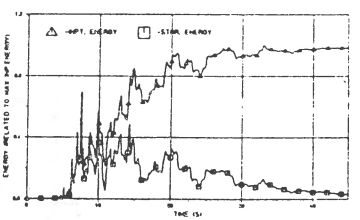

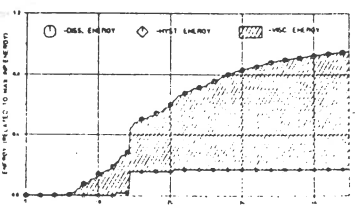

DURATION SPECTRA

viscose-elastic SDFS

solid line - mean and maximal duration

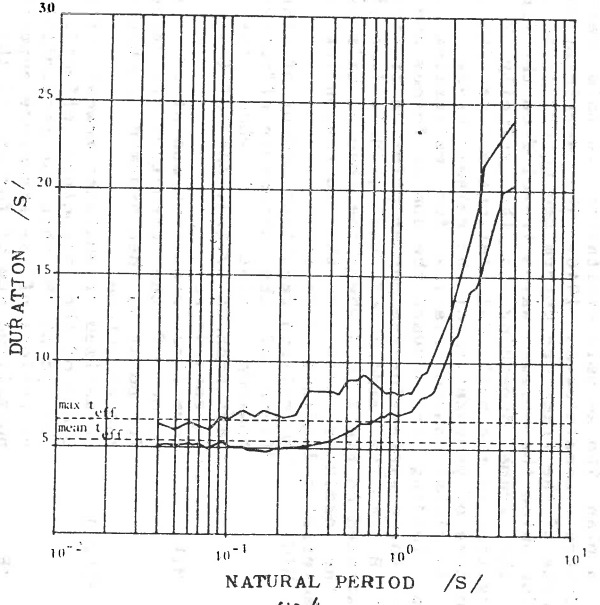

fig.4

DURATION SPECTRA

elastic-plastic SDFS

solide line - yeld level 0.8

dashed line - yeld level 0.5

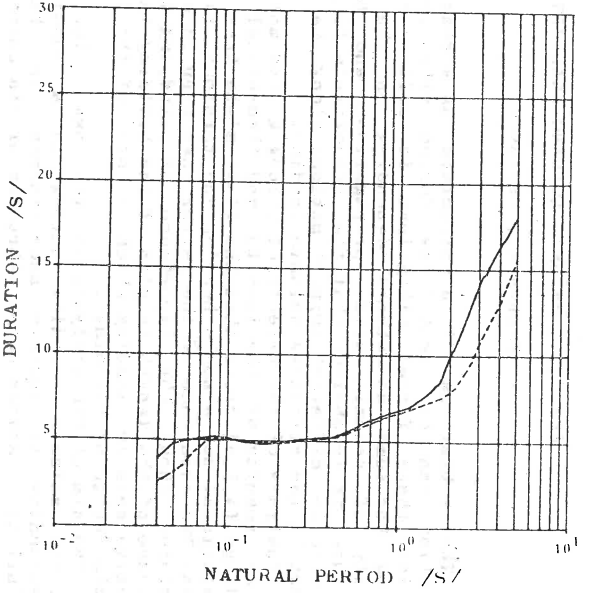

fig.5

EFFECTIVE SEISMIC LOADING ANALYSIS

Kaneva A., Tzenov L.

The vibrations of a structure as a result of the seismic excitation can be treated as forced vibrations. The loading exciting these forced vibrations is called effective seismic loading. For some structures depending on the soil conditions, velocity of seismic waves propagation, and the length of the structure, it is obvious that the structure's foundation would be subjected to different support motions along its length that would reflect in the effective seismic loading.

Analysis of the effects of strong ground motions [1,2,3,7] as well as results of the in-situ and theoretical investigations of buildings [4,5,6] prove that the floor slabs take part not only in translational but also in bending and torsional vibrations in their planes. The existence of the latter ones even in symmetric building structures shows the importance of studying the problem of the influence of the length in plan of the building in determining the effective seismic loading which is one of the first steps in the seismic design of buildings.

The aim of the analysis is to answer the question if the effective seismic loading acting on a considered structure, corresponding to certain accelerogram, is changing when the possibility of asynchronous vibration of its supports is taken into account.

Using the procedure in [8] the effective seismic loading is determined for a one story four-bay frame (Fig.1) considered as long in plan. The seismic excitation in this case, corresponds to El Centro accelerogram 1940. The accelerations at different supports of the frame are determined according to the delay in time Δt for which the seismic waves travel from the first up to support i of the frame depending on the velocity V of seismic wave propagation in the soil. Calculations are carried out for different velocities of propagation of the seismic waves.

As global characteristics for estimating of the effective seismic loading are assumed the sum of forces and resultant moment of the force system for the corner point A of the girder and for point B in the middle of the girder. Some of the results are illustrated on Fig.2 to 8 where the abscise axis is the time in sec and the ordinate axis is the corresponding normalized global characteristic designed as follows:

- M(d) - normalized resultant moment of the normal to the plane of the structure effective seismic loading towards point A, when the possibility of asynchronous vibrations of the structure supports is considered
- M(k) - normalized resultant moment of the normal to the plane of the structure effective seismic loading for point A, when assumed synchronous vibrations of the structure
- M(L/2) - normalized resultant moment of the normal to the plane of the structure effective seismic loading for point B when the possibility of asynchronous vibrations of the structure supports is considered
- AR - normalized sum of forces of the effective seismic loading in the plane of the structure when the possibility of asynchronous vibrations of its

supports is considered

AR/Y - ratio of the sum of forces of the effective seismic loading in the plane of the structure with asynchronous effect considered towards the case when it is neglected

Comparing the results for M(d) for velocities of seismic wave propagation V=200m/s (Fig.2), V=500m/s (Fig.3), V=1000m/s, V=4500m/s (Fig.4) to those for M(k) (Fig.5), it is evident that taking into account the length in plan of the building changes its effective seismic loading. The differences between M(d) and M(k) increases when the velocity V becomes lower, i.e. when the building becomes "longer" in plan or when time for traveling of the seismic waves from the first to the last support increases. And on the contrary, when velocity V is higher these differences diminish. For example for the case considered, when V=4500m/s (Fig.4) the differences between M(d) and M(k) are negligible and when V=5600m/s M(d) and M(k) are identical, so in practice for velocities V=4500m/s and higher the building considered should be assumed as "short" in plan when asynchronous vibrations of its supports are not possible.

The results for the sum of forces for different velocities V of seismic wave propagation are analogous.

The other global characteristic for estimating the effective seismic loading M(L/2) indicates the existence of torsion in the structure as a result of the seismic excitation considered. Fig.6 and 7 show that at certain times M(L/2) takes considerable values. Here it is necessary to note that not only for this case but for every symmetric structure assumed as "short" in plan the moment M(L/2) always equals zero.

The analysis in the plane of the frame demonstrates that the maximum value of the effective seismic loading, determined when the possibility of different support motions is considered, is smaller than that when synchronous motion of all supports is assumed, i.e. when the building is "short". But this does not give us enough grounds to consider that the effective seismic loading is more favorable for the building when taking into account its length in plan; for example the ratio AR/Y (Fig.8) can reach rather high values.

Main conclusion of the investigation carried out is that taking into account the possibility of asynchronous vibrations of the supports of a structure as a result of a certain seismic excitation could effect qualitatively the respective effective seismic loading. That is why a building should not be accepted as seismically safety if its design is carried out assuming the building as "short" in plan, i.e. on the base of customary procedures, while in fact it is necessary the possibility of asynchronous vibrations of its supports to be considered. In other words, before determining the effective seismic loading, depending on the velocity of seismic waves propagation in the site soil and the structure itself, it is necessary to establish if the structure should be assumed as "long" in plan.

References

1.Korchinski J.,L.Tzenov, Investigation of buildings in seismic regions of Bulgaria,"Stroitelstvo",1967/6 (in Bulgarian)
2.Vibrational method for testing of residential and industrial buildings,Series "Zhilie zdanij",Center for scientific and technical information on civil engineering and architecture,Moscow,1967 (in Russian)
3.Shapiro G.A. et al.,Analysis of nonlinear behaviour of residential and industrial buildings using vibrational apparatus,Moscow,1969 (in Russian)
4.Brankov G.,S.Sachanski,L.Tzenov et al.,Basic conclusions from the 4 of March 1977 earthquake,III Nat. congress on theor. and applied mechanics, Varna,1977 (in Bulgarian)
5.Korchinski J.,L.Borodin et al.,Seismic building construction, izd."Visshaya shkola",Moscow,1977 (in Russian)
6.Tzenov L., Reduction of seismic vulnerability of structures, BAS,Sofia,1982 (in Bulgarian)
7.Dumanoglu A.,R.Severn, Multiple support base excitation of structures, Proc.VII ECEE,Greece,1982
8.Tzenov L., Effective seismic loading on long in plan structural systems,"Stroitelstvo",1986/8 (in Bulgarian)

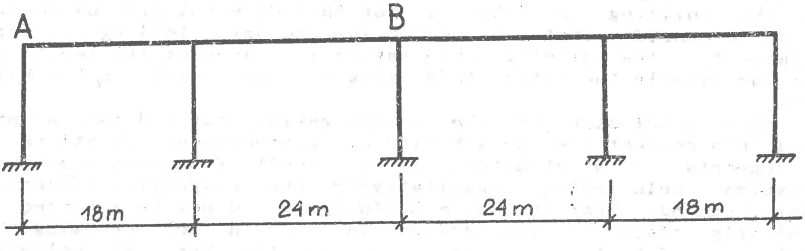

Fig.1

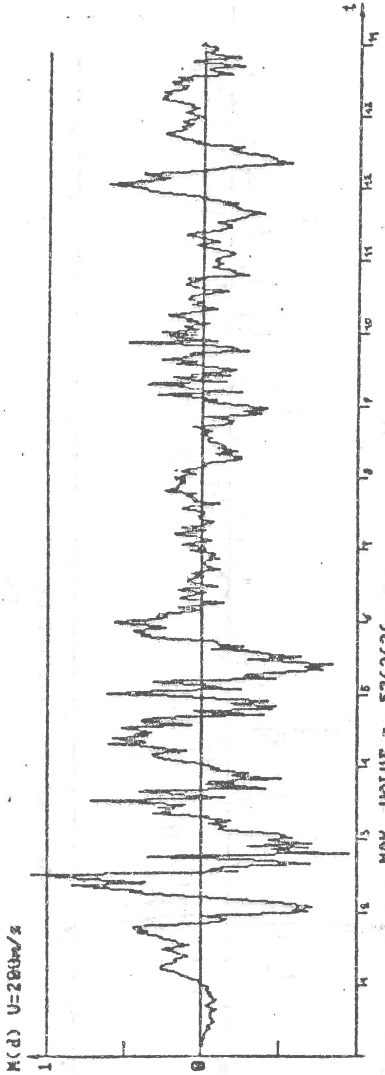
M(d) U=200m/s
1
0
MAX. VALUE = 5763636

Fig.2

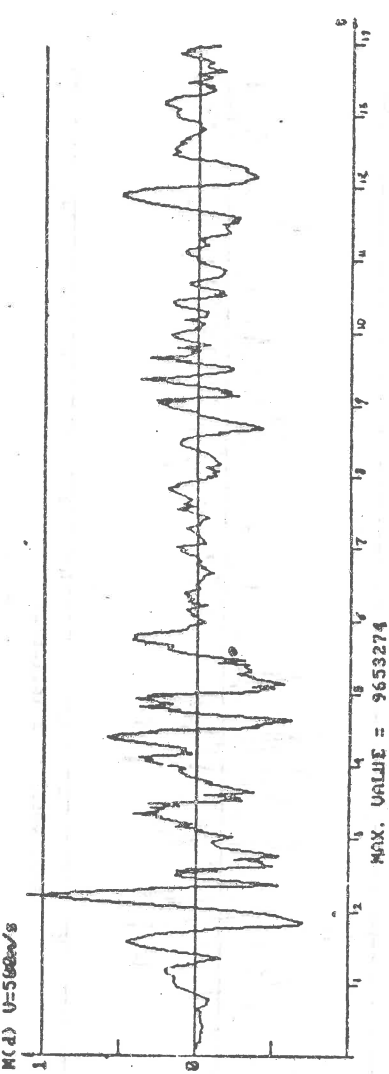
M(d) U=500m/s
1
0
MAX. VALUE = 9653274

Fig.3

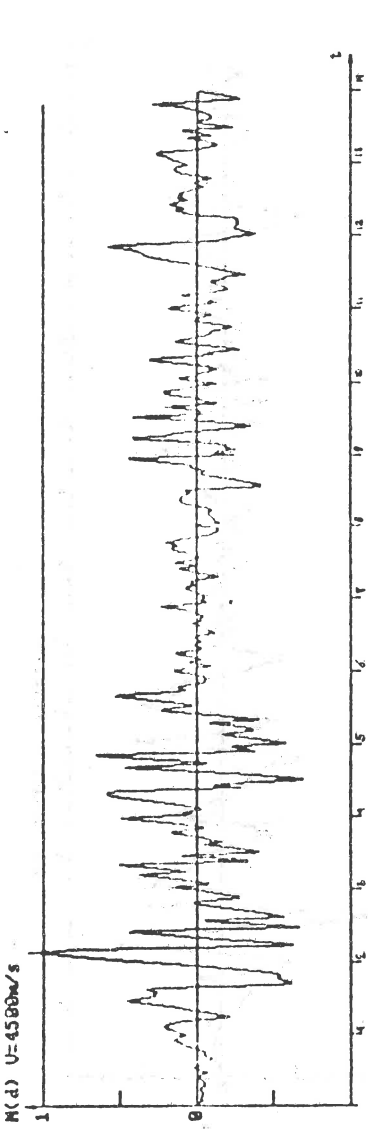
M(d) V=4580w/s
1
0
t
MAX. VALUE = 1.16112E+07

Fig.4

M(w)
1
0
t
MAX. VALUE = 1.205518E+07

Fig.5

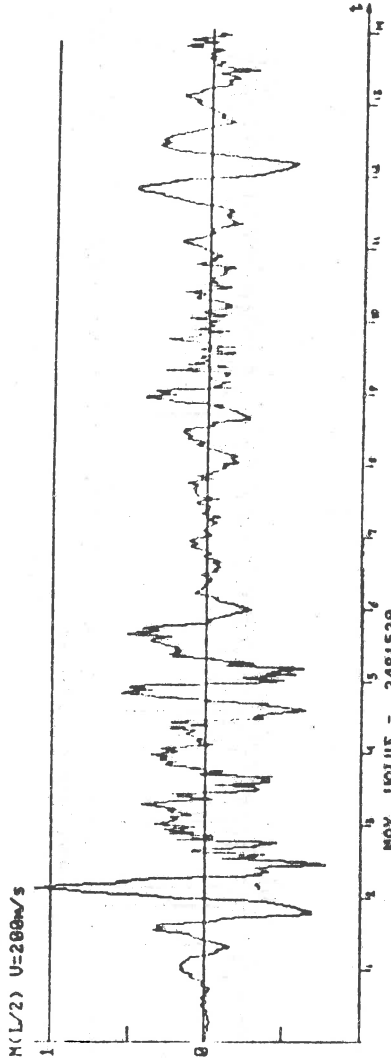
M(L/2) U=200m/s
1
0
MAX. VALUE = 3481530
t

M(L/2) U=500m/s
1
0
MAX. VALUE = 4162650
t

FIG 6

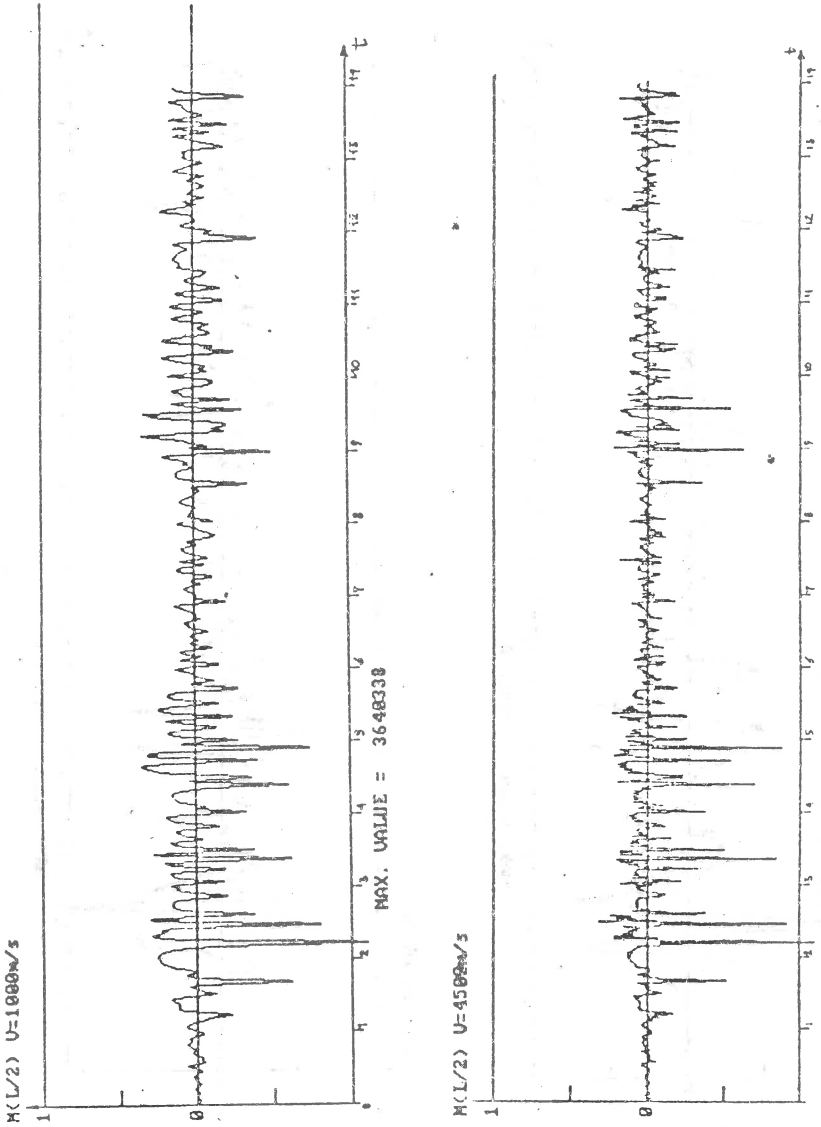
M(L/2) V=1000m/s
1
0
MAX. VALUE = 3648338
t
M(L/2) V=4500m/s
1
0
MAX. VALUE = 2768292
t

Fig 7

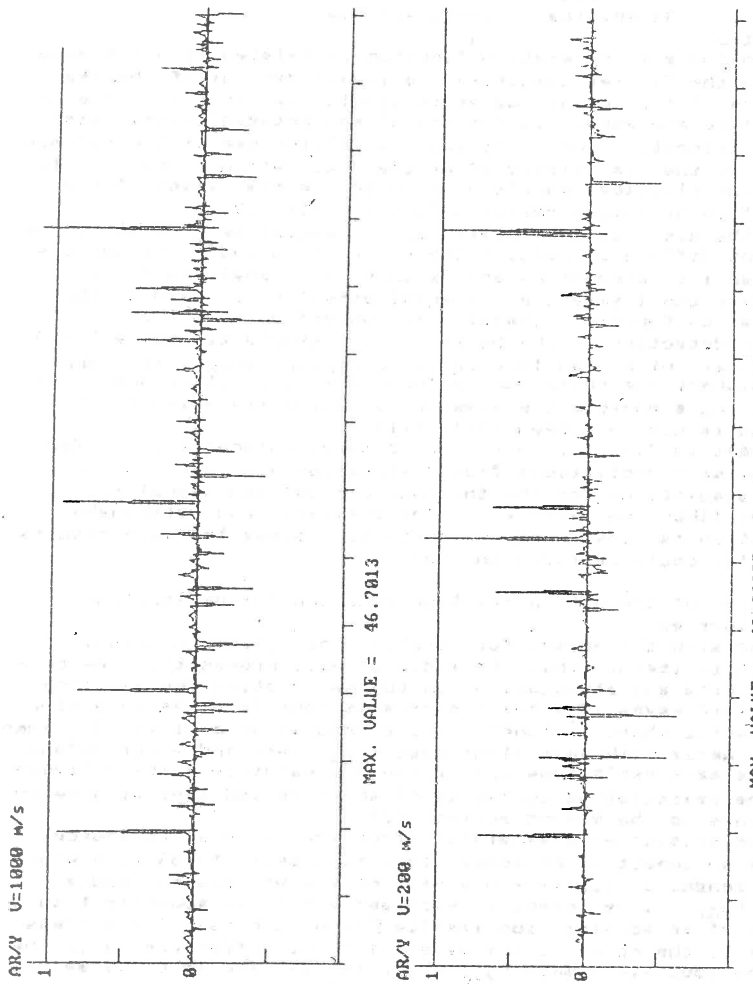
AR/V U=1000 m/s
1
0
MAX. VALUE = 46.7813
AR/V U=200 m/s
1
0
MAX. VALUE = 48.02857

Fig 8

AUTOCORRELATION FUNCTIONS OF SHORT PERIOD P - WAVES GENERATED BY DISLOCATION AND POINT SEISMIC SOURCES

L.Christoskov,E.Levy,A.Milev
Geophysical Institute,Sofia

I.Introduction.

As is known,the autocorrelation function is related with the power spectrum by the Fourier transform.The investigations of the spectral features of the seismic waves is widely used in the seismological practice and especialy for comparison between seismic signals from dislocation and point sources [1].The use of the seismic signal within the time period after the dislocation process is typical for the classical models used in the determination of the power spectrum or autocorrelation function [1,7,10].
Since the the dislocation process can be several seconds long,a very important difference between the dislocation and point sources is not taken into account,especialy in P-waves analyses.On the other hand,in the literature a special attention is paid to the autocorrelation function generally in connection wuth the P and S -wave detection on the background of stochastic noice [13], or for maximal entropy analyses[8].In explosion from earthquake separation,where the comparison between the dislocation and point sources is indispensable,the question of autocorrelation function application is not developed [4,6,11,14].

An attempt to find the connection between autocorrelation features of seismic oscilations from dislocation and point sources with some assumptions for the the source model and signal propagation is described.The application for explosion and earthquake identification is considered.The exposition gives the main results while details could be found in [15].

II.Definition of the autocorrelation function for dislocation and point sources.

1.Background premises for modeling the seismic process.

1/ It is assumed,that the media of wave propagation has certain elasticity and attenuation due to the friction.The exciting of the seismic waves in a point source is considered as an action of sufficiently short δ-function-type impulse on a limitted volume of elastic media with equivalent mass M_{eq_θ} .Here and after "b"and "e" indexes mark explosions and earthquake parameters respectively

2/The registrating system is of short-period type with velocity responce to the ground moution [2].

3/The seismic wave generation from the dislocation source is assumed as an impact of consequently acting segments SS with width Δx and lenght U -fig.1,upon a part of the propagating media with mass M_{eq_e} .The impact of each segment SS is equivalent to the action of an acceleration impulse δ-function type.The process is similar to the point source generation.The difference is in the size of the equivalent mass M_{eq_e} which is assumed to be larger than M_{eq_θ} due to the finite value of the SS segment dimencion.

2.Definition of the autocorrelation function $R_\beta(\tau)$ for point source.

After some mathematical operations and substitutions for the auto correlation function $R_B(\tau)$ of a point source signal we obtain:

$$R_B(\tau) = e^{-K_B\tau} \cdot \cos(\omega_B \cdot \tau)$$

where $K_B = \omega_B / 2Q$, Q is the quality factor of the media; ω_B is a function of: M, of the attenuation properties and elasticity of the media [15]. [4,6]

In the further investigations of the autocorrelation properties of the processes, the mean value $\overline{R_{\theta max}}$ of the autocorrelation function amplitudes $R_{\theta max}$ is used given by the expresion:

$$\overline{R_{\theta max}} = \frac{1}{\tau_{max}} \cdot \int_0^{\tau_{max}} R_{\theta max}(\tau) \cdot d\tau = \frac{1}{K_B \cdot \tau_{max}}$$

where τ_{max} is the maximum value of the correlation interval.

3. Definition of the autocorrelation function $R_{\theta}(\tau)$ and its parameters for dislocation source.

After corresponding mathematical operations we obtain:

$$R_{\theta 1}(\tau) = e^{-K_\theta \tau} \cdot \frac{\sqrt{\left[e^{-K_\theta \theta} \cdot (e^{2K_\theta \tau} - 1) \cdot \sin(\omega_\theta \theta)\right]^2 + \left[2 - e^{-K_\theta \theta}(e^{2K_\theta \tau} + 1) \cdot \cos(\omega_\theta \theta)\right]^2}}{2 \cdot (1 - e^{-K_\theta \theta} \cos \omega_\theta \theta)} \cdot \cos(\omega_\theta \tau + \varphi') =$$

$$= R_{\theta 1 max}(\tau) \cos(\omega_\theta \tau + \varphi')$$

$$R_{\theta 2}(\tau) = e^{-K_\theta \tau} \cdot \frac{\sqrt{\left[(e^{K_\theta \theta} - e^{-K_\theta \theta}) \cdot \sin(\omega_\theta \theta)\right]^2 + \left[2 - (e^{K_\theta \theta} + e^{-K_\theta \theta}) \cdot \cos(\omega_\theta \theta)\right]^2}}{2 \cdot (1 - e^{-K_\theta \theta} \cdot \cos \omega_\theta \theta)} \cdot \cos(\omega_\theta \tau + \varphi'') =$$

$$= R_{\theta 2 max}(\tau) \cdot \cos(\omega_\theta \tau + \varphi'').$$

Here $R_{\theta 1 max}(\tau)$ and $R_{\theta 2 max}(\tau)$ are the envelopes of the corresponding trigonometric functions. φ' and φ'' are determined by the expresions:

$$\varphi' = arctg\left[\frac{e^{-K_\theta \theta} \cdot (e^{2K_\theta \tau} - 1)}{2 - e^{-K_\theta \theta} \cdot (e^{2K_\theta \tau} + 1)} \cdot tg(\omega_\theta \theta)\right]; \quad \varphi'' = arctg\left[\frac{e^{K_\theta \theta} - e^{-K_\theta \theta}}{2 - (e^{K_\theta \theta} + e^{-K_\theta \theta})} \cdot tg(\omega_\theta \theta)\right]$$

θ is the dislocation time; K_θ and ω_θ are analogical to K_B and ω_B but always $\omega_B > \omega_\theta$.

III. Comperison between the mean maximum values of the autocorrelation functions $\overline{R_{\theta max}}$ and $\overline{R_{B max}}$ for dislocation and point sources respectively.

The following theoretical ratio was calculated

$$Q_1 = \frac{\overline{R_{\theta max}}(\theta, \omega_\theta, K_\theta)}{\overline{R_{B max}}}$$

for $\tau_{max} = 20$ sec and $\mu = \frac{\omega_\theta}{\omega_B} = 1$. Fig.2 shows the results. The oscillatory nature of $Q(\theta)$ is obvious. It is possible $\overline{R_{\theta max}}$ to be less than $\overline{R_{B max}}$ for small values of θ. Taking into account that realy $\mu > 1$, the real ratio between $\overline{R_{\theta max}}$ and $\overline{R_{B max}}$, $Q = \mu Q_1$ can reach substantional values, as it is shown in fig.3 for $\mu = 1{,}25$, $K_\theta = 0{,}4$, $\omega_\theta = 2\pi$ [rad]. The last fact shows that it is possible to establish a criterion for identification of dislocation and point sources on the basis of $\overline{R_{\theta max}}$ and $\overline{R_{B max}}$.

IV.Experimental results.

Twelve events have been investisated,6 of them/from 1 to 6/are explosions and 6 -earthauakes located in the Middle Asia Region. Fis.4 shows the locations and the resistration point -st.VTS.The two sroups of events are of approximately equal depths,respectively 0 km.for the explosions and from 0 to 15 km for the earthauakes.

Fis.3 shows the points correspondins to the real values of and Q /marked with circles/.It is obvious the substantial coincidence for the parameter values used:k =0,4; μ=1,25; Ω_e=2π 1/sec. The coincidence confirms the theoretical results.

The last three parameters are mean values for the 6 earthauaks The values of $2R_{max}$ for the 12 events are sraficallu displayed on fis.5.An demarcatins interval 53% < $2R_{max}$ <57% can be defined, above which the events of the treated masnitude interval can be considered as eartauakes and below which -as explosions.This confirms the possibility of establishins a masnitude dependent criterion for identification of explosions and earthauakes ,anknown from the literature [4,9,11,14].

V.Conclusions.

1.The ratio Q between the mean maximum values of autocorrelation functions for lonsitudinal waves from dislocation and point sorces is oscillatory increment function of the dislocation time Θ-fis.2.

2.The larser values of Q are related to the smoller radiation frequense from the elementary sesment SS ,fis.1,of the dislocation source in comparison with the frequence of the point source.

3.The larser values of Q are related also to the larser time of radiation due to the finite value of the dislocation time Θ.The influence of this factor is the reason for the oscillatory nature and the increase of Q ,when Θ takes larse values.

4.The experimental results obtained on the basis of twelve events verifu the theoretical conclusions-fis.3.

5.An additional criterion for seismic events identification can be established on the basis of the above mantioned results-fis.5.

REFERENCES

1.Аки К., П. Ричардс, Количественная сейсмология, М, Мир, 1983.

2.Леви Е., Вероятностни характеристики на екстремумите при сума от квази хармоничен сигнал и гаусов шум, Бълг. геофиз. сп., 1986, №1, т. XII.

3. Ризниченко Ю.В., Размеры очага корового землетрясения и сейсмический момент, Исследования по физике Земли, М, наука, 1976, с.9-55.

4.Родин Г., Сейсмология ядреных взрывов, М, Мир,1974.

5.Харкевич А. А., Основы радиотехники, М, Связь, 1963.

6.Христосков Л., Ал. Милев, Върху дискриминационите параметри за телесеизмични сигнали от земетресения и взривове, Сборник доклади, Юбилейна научна сесия "25 години геофизичен институт" , БАН, 1985,С.

7. Aki K., Scaling Law of Seismic Spectrum, Journal of Geoph.. Res. v.72,1967, N 4, 1217 - 1231.

8. Barrodale I., R. Ericson, Algorithms for Least Square Linear Prediction and Maximum Entropy Spectral Analysis, Geophysics,45,N 3 1985.

9. Dalhman O., H. Israelson, Monitoring Undergraund Nuclear Explosions Elsevier, Amsterdam, 1977.

10. Haskell N., Total Energy and Energy Spectral Density of Elastic Wave Radiation from Propagating Faults, Bull. Seism. Soc. Am., 56, 125-140, 1966.

11. Husby E., S. Makkelteit, Indentification of Seismic Sources- Earthquake or Undergraund Explosion, NATO Advanced Study Institute, Oslo, 1980 .

12. Johnson R., T. McEvelly, Regional Study with Broadband Data, The VELA Program, A Twenty-Five Year Review of Basic Research, Ed. Ann Kerr, Defence Advance Research Project Agency, USA, 1985.

13. Stamler W., Application of Prediction Error Filters for the Detection of Weak Teleseismic Events, IEEE Trans. Geosci. Remote Sens., 19, 222-230, 1981.

14. The VELA Program, A Tweny-Five Year Review of Basic Research, Ed. Ann Kerr, Defence Advance Research Progects Agency, USA, 1985.

15. Christoskov, L. V, E. Levy, A. Milev, Autocorrelation functions of short period P-waves generated by dislocation and point seismic sources. Bulg. Geoph. Journ., 1988, N4.

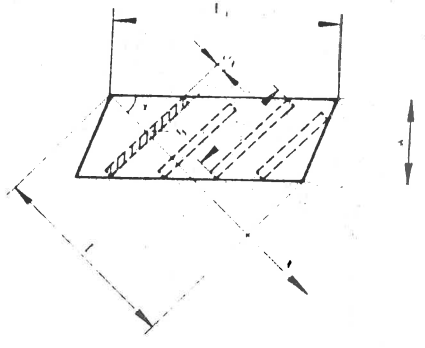

Fig.1

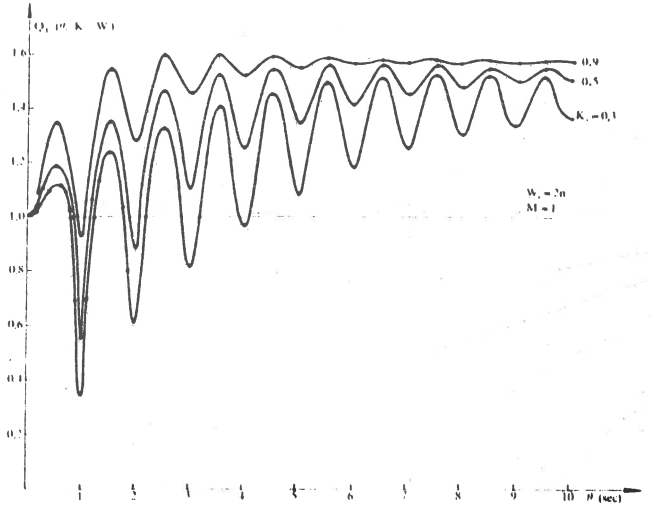

Fig.2

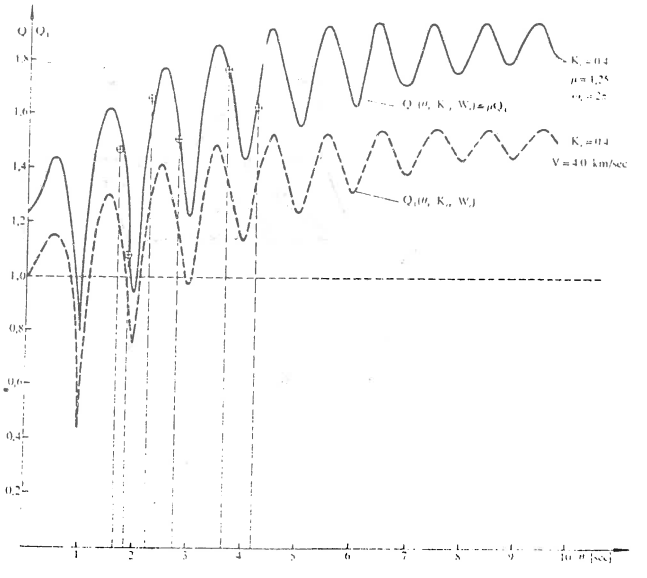
Q/Q1
1,8
1,6
1,4
1,2
1,0
0,8
0,6
0,4
0,2
1
2
3
4
5
6
7
8
9
10
t (sec)
K1 = 0.4
μ = 1,25
Q1 = 25
Q (t, K1, W1) = μQ1
K1 = 0.4
V = 4.0 km/sec
Q1(t, K1, W1)

Fig. 3

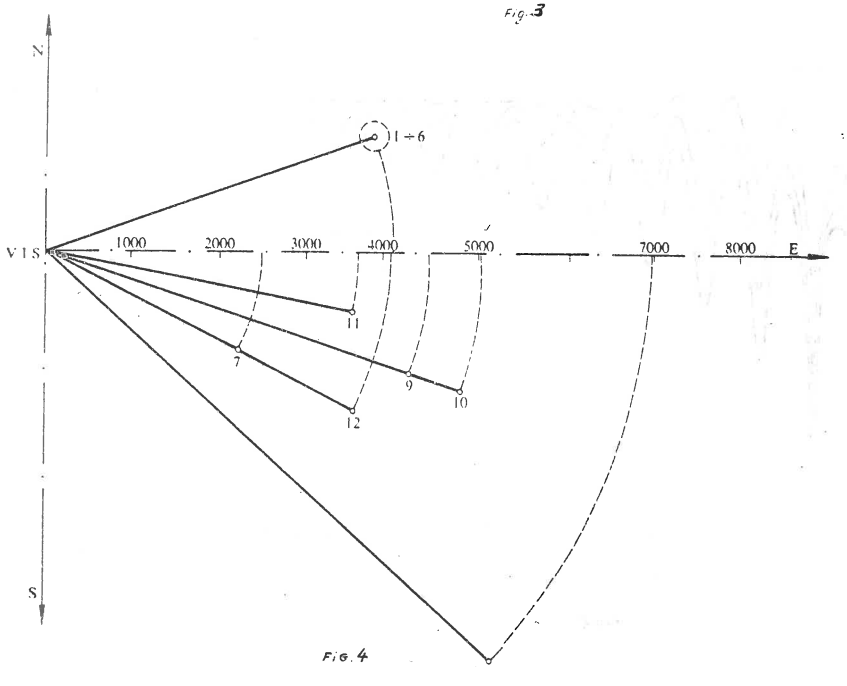
N
S
VIS
1000
2000
3000
4000
5000
7000
8000
E
1 ÷ 6
7
9
10
11
12

Fig. 4

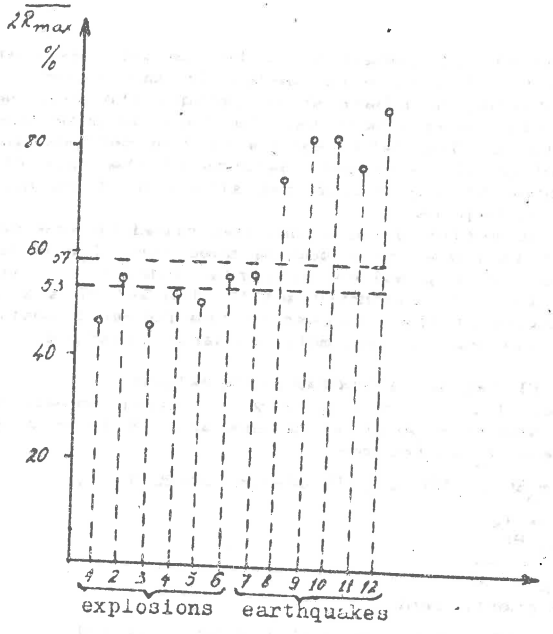
$\overline{2R_{max}}$
%
80
60
57
53
40
20
1 2 3 4 5 6 7 8 9 10 11 12
explosions
earthquakes

Fig. 5

GENERATION OF STRONG MOTION ACCELEROGRAMS FOR STRUCTURAL BEHAVIOUR PREDICTION

Marin Kostov - *Central Laboratory for Seismic Mechanics and Earhtquake Engineering, BAS, Sofia*

1. INTRODUCTION

To predict the structural behaviour under seismic excitation a reliable strong motion data base is needed. In many cases in order to overcome the existing data base shortcomings, the engineers try to generate artificial ground motions. For this purpose there are many methods available. The main feature of the methods seems to be their phenomenological character. Because of the lack of data, one tends to combine strong motion registrations from different seismic and tectonic regions.

The model for strong motion generation, described in the paper is a physical one. It is based on a source spectrum. The model is a further development of a previous author's model [1], incorporating ideas from Boor [2] and McGuire [3]. The author's attention has been drawn because of the succsess of the former investigators in predicting RMS and peak ground motion characteristics.

2. A MODEL FOR ARTIFICIAL ACCELEROGRAMS GENERATION

The model equation (1), accounting only for shear waves, defines the acceleration spectrum $A(\omega)$ at a distance R from a seismic source with a moment M_o as follows:

$$A(\omega) = CM_o S(\omega,\omega_c) P(\omega,\omega_m) TL(\omega) \exp(-\omega R/2Q_\beta) \quad , \tag{1}$$

where C is a constant:

$$C = \frac{R_{\theta\varphi} \cdot PR}{4\pi \cdot \rho \cdot \beta^3 \cdot R}, \tag{2}$$

$R_{\theta\varphi}$ - directivity coefficient,

PR - reduction coefficient for partitioning the motion into two horizontal components,

ρ - mass density,

β - shear wave velocity,

Q_β - quality factor for S waves,

$S(\omega,\omega_c)$ is the source spectrum:

$$S(\omega,\omega_c) = \frac{\omega^2}{1 + (\omega/\omega_c)^2}, \tag{3}$$

It corresponds to ω - square model. For other cases it is possible the ω - cube model to give better results.

$P(\omega,\omega_m)$ is a lowpass filter representing the high frequency

attenuation in the source region:

(4) $$P(\omega,\omega_m) = [1+(\omega/\omega_m)^{2s}]^{-1/2},$$

ω_m = 10 up to 15 Hz; s = 4.

TL(ω) is a bandpass filter, which represents the transfer function of the local geology system.
Following Boor [2], a transient accelerogram can be produced by windowing a shot-noise process with the function:

(5) $$w(t) = at^b \exp(-ct).H(t)$$

where
H(t) is the Heavyside's step function, a,b,c, - constants defined in [2] and [4]

(6) $$a = (e/\varepsilon T_v)^b ,$$

$$b = -\varepsilon \ln\eta(1+\eta(\ln\varepsilon-1)) ,$$

$$c = b/(\eta T_v) ,$$

$$\varepsilon = 0.02, \qquad \eta = 0.05 .$$

T_v is the width of the window, assumed $T_v = 2T_D$. T_D is the duration of strong shaking [2], $T_D = f_c^{-1}$.
There are two sets of parameters governing the model - the characteristics of the geological system and the source characteristics. The first set of parameters defines the transfer function TL(ω). These parameters are: body wave velocities, mass densities, dampings and geometrical characteristics for all geological strata. Depending on the complexity of the geological system, a proper level of model sophistication can be chosen. According to our experience, in many cases the simple horizontally stratified viscoelastic medium is a good representation of the geological system.
The second set of parameters - M_o and ω_c can be alternatively replaced by other source characteristics as moment-magnitude and the effective stress drop $\Delta\sigma$ [2,5]. In some ranges the moment-magnitude can be replaced by other kinds of magnitude. In this report as parameters governing the source spectrum the moment-magnitude and the effective stress drop are used:

(7) $$M = 2/3 \log M_o - 10.7,$$

$$f_c = 4.9.10^6 \beta (\Delta\sigma/M_o)^{1/3}.$$

3. NUMERICAL REALISATION

It is known that the local geology parameters cannot be determined with great accuracy. They significantly vary in space and to some extend in time too. Similarly the seismic moment and the stress drop cannot be calculated accurately. In order to involve in the computation the different accuracy level and the possible variation of the model parameters, they are considered as random numbers with an appropriate kind of distribution. The numerical realisation of the model is done by the Monte-Carlo method. It means that playing dice on all independent model parameters a sample of artificial accelero- grams will be generated. On their basis a lot of ground motion characteristics can be derived -

maximum or RMS acceleration, velocity and displacement, duration, a various number of spectra, etc.
All characteristics generated are represented by a sample, which has the number of values corresponding to the number of generations done. The more the generations, the bigger the sample, respectively - the greater the statistics reliability. The procedure of generating artificial ground motions follows the sheme:
1. Random number generations, according to the distribution of the independent model variables.
2. Shot-noise generation and windowing with function (5).
3. FFT.
4. Scaling of the Fourier-spectrum by eq.(1).
5. FFT^{-1}, accelerogram.
6. Baseline correction, integration - velocigram, seismogram.
7. Determination of max. and RMS values, response spectra, etc.
8. Updating, statistics.
The procedure steps from 1 to 8 will be repeated according to the number of generations desired.

4. DATA BASE FOR MODEL VERIFICATION

Earthquake sequence Friuli, 1976 is used for model verification [7]. Two sites - San Rocco and Forgaria Cornino, respectively on stiff and soft soils are chosen. Only registrations of events of a magnitude greater than 5 are selected (Tables 1 and 2). The earthquake source characteristics are placed in Table 3. The geology characteristics are shown in Tables 4 and 5. All model input characteristics are assumed to be equally distributed. Because of the small epicentral distances, a maximum acceleration more than 0.2g is expected. That is why an equivalent-linearization procedure [6] concerning the surface soil layers is applied.

5. STRUCTURAL BEHAVIOUR PREDICTION

On the basis of the real earthquakes data, an artificial data base is generated by the model former described. Both the generated data base and the real accelerogram data are used for structural behaviour determinations. Viscose-elastic and elastic-plastic single degree of freedom systems (SDFS) are firstly analysed. The second step includes nonlinear investigation of two 5 and 10 story reinforced concrete frames. In the last step of the analysis the behaviour of 5, 10 and 20 story shear walls with different first natural period of vibration (T=0.4s., T=0.8s., T=1.6s., T=2.4s.) is investigated.
As a criterion for the structural behaviour prediction success the comparisson between various structural response parameters obtained by generated and real accelerograms is used. The following response parameters are compared: maximal accelerations, velocities, displacements, plastic displacements, plastic rotations, required ductility, maximal base bending moments and shear forces, input energy. The comparisons are made in a statistical sense - i.e. mean, mean + one standard deviation, and peak values are compared.
In fig.1 various response spectra comparisons are shown. There is a very good fit between spectra obtained by generated and real

In fig.1 various response spectra comparisons are shown. There is a very good fit between spectra obtained by generated and real accelerograms, it means there is a very good SDFS response prediction.
In fig.2 comparisons between predicted and real (obtained by real accelerograms)response parameters for frame structures are shown. With some exceptions there is a good prediction again. Some significant differencies are obtained for the girders required ductility .
In fig.3 results from the third step of analysis (shear wall behaviour) are shown. The predicted behaviour deffer quantitatively from the behaviour under real accelerogram excitation but there is not a qualitative conflict.
As a whole the results obtained show that generated by the described model accelerograms could be used as a data base for comprehensive structure analyses.

5. CONCLUSIONS

The model for strong seismic motion generation has been proved to generate motions from different seismic sources. The positive experience collected allowed the following conclusions:
- seismic motion for an arbitrary site, accounting for the local seismicity and geology structure can be generated,
- the ground motion can be easily scaled,
- the seismic motion generated can be calculated by the desire level of confidence,
- the model input characteristics can be varied to study the structure response.

The comprehensive proof of the possibility to use generated seismic motion for structural behaviour prediction shows that in most cases the artificial accelerograms, generated by the described model have got the features of the real accelerograms and they could be used for structure analyses. The structural response parameters predicted by generated accelerograms generally agree with the response parameters obtained by real accelerograms.

6. LITERATURE

1. Kostov M., Simulated Regional Response Spectra ,Bulg. Geophys. Jour.,11,3,1983.
2. Boore D.,Stochastic Simulation of High Frequency Ground Motion based on Seismological Models of Radiated Spectra, Bull. Seism. Soc. Am., 75/61, pp.1865-1874, Dec.1983.
3. McGuire R.C.,T.C. Hanks, RMS Accelerations and spectral Amplitudes of strong Ground Motion during the San Fernsndo, California Earthquake, Bull. Seism. Soc. Am.,70, pp. 1907 - 1919, 1980.
4. Saragoni, G.R.,G.S. Hart, Simulations of artificial earthquakes, Earth. Eng. Struc. Dyn., 2, pp. 249-269, 1974.
5. Hanks T.C., H. Kanamori , A Moment-Magnitude Scale, J. Geoph. Res., 84, pp 2348-2350, 1979.
6. Seed H.B., I.M. Idriss, Influence of Soil Conditions on Ground Motions during Earthquakes, J. Soil Mec. Found. Div., ASCE, 85, SMI, 1969.
7. Scherer R.J., G.I. Scheuller, Friuli Earthquake Sequence of

able 1.

riuly earthquake sequence, sellected registrations on site
rgaria Cornino

Time of occurrence	M	R [km]	H [km]	Comp	max.a [g/10]
76.09.11	5.3	20.6	6.	NS	1.0000
16.31.10				WE	1.1429
76.09.11	5.6	19.4	6.	NS	1.3131
16.35.01				WE	2.3382
76.09.15	5.9	15.9	5.	NS	2.6367
03.15.19				WE	2.1934
76.09.15	6.0	15.8	7.	NS	3.5404
09.21.18				WE	3.3503
76.09.16	5.3	6.1	8.	NS	2.4557
23.48.07				WE	2.0139
76.05.11	5.0	7.6	6.	NS	1.9192
22.43.60				WE	3.1185

able 2.

riuly earthquake sequence, sellected registrations on site
an Rocco

Time of occurrence	M	R [km]	H [km]	Comp	max.a [g/10]
76.09.11	5.3	20.6	6.	NS	0.3403
16.31.10				WE	1.7151
76.09.11	5.6	19.4	6.	NS	0.8024
16.35.01				WE	0.9555
76.09.15	5.9	15.9	5.	NS	0.6045
03.15.19				WE	1.3556
76.09.15	6.0	15.8	7.	NS	1.3092
09.21.18				WE	2.5106

able 3

riuli earthquake sequence, parameters of sellected events

Time of occurrence	Source depth [km]	Directivity coeff.		Stress drop ($N/m^2 . 10^5$)		Moment magnitude	
	h	$\bar{R}_{\theta\varphi}$	$\sigma_{R_{\theta\varphi}}$	$\bar{\Delta\sigma}$	$\sigma_{\Delta\sigma}$	$\bar{M}$	σM
76.09.11 16.31.10	6.	0.7	0.1	15.	5.	5.2	0.25
76.09.11 16.35.01	6.	0.7	0.1	17.	5.	5.5	0.25
76.09.15 03.15.19	5.	0.7	0.1	15.	5.	5.9	0.25
76.09.15 09.21.18	7.	0.7	0.1	15.	5.	6.0	0.25
76.09.16 23.48.07	8.	0.7	0.1	15.	5.	5.2	0.25
76.05.11 22.43.60	6.	0.7	0.1	18.	5.	5.0	0.15

Table 4.

Geology profile characteristics, site Forgaria Cornino

Layer No	Layer thickness [m]		S-wave vel. [m/s]		Density [kg/m^3]		Q-value	
	$\bar{h}$	σ_h	$\bar{\beta}$	σ_β	$\bar{\rho}$	σ_ρ	$\bar{Q}_\beta$	σ_{Q_β}
1	5.	1.	200.	50.	1800.	100.	20.	5.
2	21.	2.	600.	100.	2100.	100.	50.	5.
3	500.	50.	900.	100.	2100.	100.	100.	10.
4*	-	-	2500.	100.	2500.	100.	200.	20.

* halfspace

Table 5.

Geology profile characteristics, site San Rocco

Layer No	Layer thickness [m]		S-wave vel. [m/s]		Density [kg/m^3]		Q-value	
	$\bar{h}$	σ_h	$\bar{\beta}$	σ_β	$\bar{\rho}$	σ_ρ	$\bar{Q}_\beta$	σ_{Q_β}
1	30.	5.	600.	100.	2000.	100.	50.	5.
2	2000.	200.	2500.	100.	2200.	100.	100.	10.
3*	-	-	3000.	100.	2400.	100.	200.	20.

* halfspace

NONLINEAR RESPONSE SPECTRA
ELASTIC-PLASTIC MODEL, YIELD LOAD= 0.600
REAL DATA
SIMULATED DATA
ACCELERATION (M/S**2)
VELOCITY (M/S)
DISPLACEMENT (M)
INPUT ENERGY (M/S)**2
NATURAL PERIOD T (S)

FRAME C. 10 STORY, 2 BAY, NOT-023
BASE MOTION FRIULI EARTHQUAKE, FORGARIA CORNINO
STRUCTURAL RESPONSE ENVELOPES

**SOLID LINE : REAL DATA
**DASHED LINE: SIMUL DATA

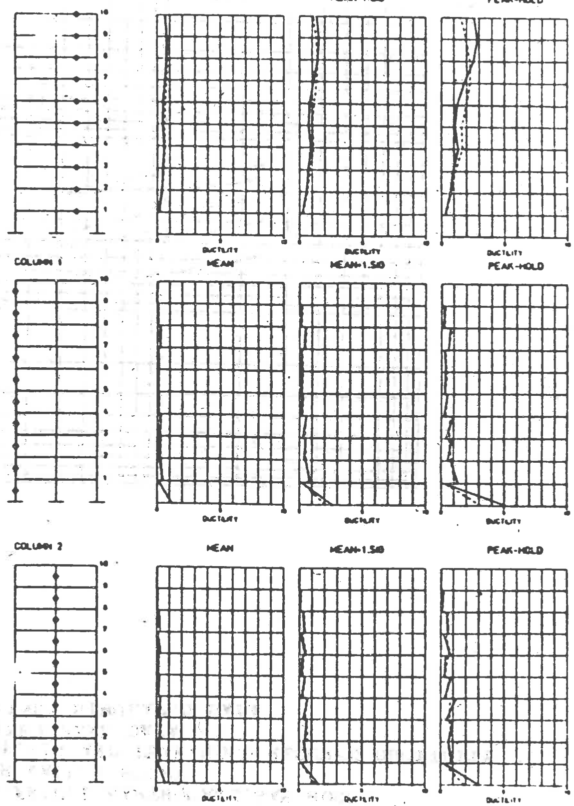

FRAME C. 10 STORY, 2 BAY, NOT-023
BASE MOTION FRIULI EARTHQUAKE, FORGARIA CORNINO
STRUCTURAL RESPONSE ENVELOPES

**SOLID LINE : REAL DATA
**DASHED LINE: SIMUL DATA

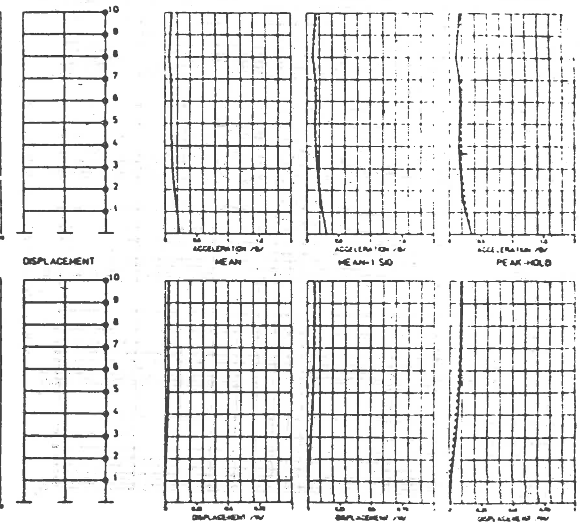

	MEAN		MEAN+1 SD		MEAN-HOLD	
	REAL	SIMUL	REAL	SIMUL	REAL	SIMUL
BASE SHEAR /KN/	265.42	287.27	380.48	404.66	576.40	679.40
BASE MOMENT /KNM/	3313.10	3806.00	5123.80	5832.60	6812.00	7167.00
BASE ACC. /G/	0.23	0.23	0.31	0.31	0.35	0.35

BASE MOTION:FRIULI EARTHQUAKE,SAN ROCCO
SINGLE SHEAR WALL 5 STORY
MEAN, MEAN+1.SIG AND PEAK-HOLD REQURED DUCTILITY
... SOLID LINE: REAL DATA
... DASHED LINE: SIMULATED DATA

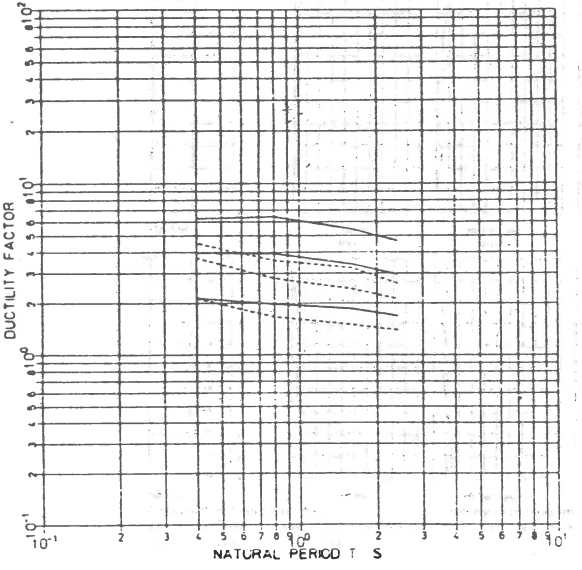

BASE MOTION:FRIULI EARTHQUAKE, SAN ROCCO
SINGLE SHEAR WALL 5 STORY
MEAN. MEAN+1.SIG AND PEAK-HOLD
ACCUMULATED PLASTIC ROTATION
... SOLID LINE: REAL DATA
... DASHED LINE: SIMULATED DATA

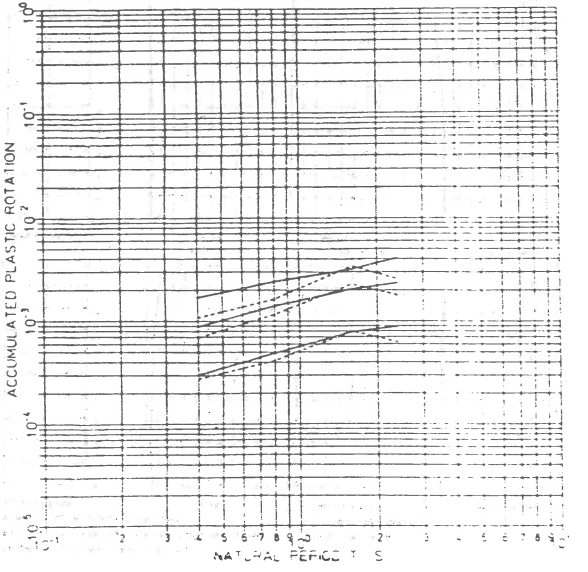

fig.3

SOURCE PARAMETERS OF SELECTED EARTHQUAKES IN CENTRAL AND WESTERN MARGIN OF AFAR

By

Fekadu Kebede and Otta Kulhánek
Seismological Department
Uppsala University
Box 12019, S-750 12
Uppsala, Sweden

ABSTRACT

Spectral analysis of 196 short-period and long-period vertical- and horizontal component seismograms from ten earthquakes in central Afar and in its western margin is performed to determine dynamic source parameters and to discuss their tectonic implications. For the earthquakes under study, the stress drop varies from 1.8 to 30.7 bars while the seismic moment varies from 2.2×10^{24} to 1.54×10^{26} dyne-cm. In general, low stress drop values are obtained. It is observed that there is an increase of stress drop with the increase of moment-magnitude which in turn is obtained from the calculated average seismic moment. Energy estimates show that the mode of energy release is different in the two regions. The variation may indicate that different tectonic processes are involved in the two regions. The slip rate obtained for the Serdo area is of the order of 1.8 cm/yr and is in close agreement with spreading rates obtained by others for the Red Sea and Gulf of Aden while it is somewhat higher than that of central Afar and the Ethiopian rift.

(The full text has been submitted to Tectonophysics for publication)

ANALYSIS OF THE KALAMATA, GREECE, STRONG MOTION RECORDS AND CORRELATION WITH THE OBSERVED DAMAGES

by

Carydis, P.[1], Drakopoulos, J.[2], Kalogeras, J.[2], Mouzakis, H.[1], Taflambas, J.[1], and Vougioukas, M.[1]

1. INTRODUCTION

On September 13th, 1986, Kalamata and the surrounding area were struck by a very strong and destructive earthquake. According to the Seismological Institute of Athens the epicenter was located about 20 km north of the city and the local magnitude was calculated equal to 5.5 R. The earthquake was followed by a large number of aftershocks, the strongest of which occurred on September 15th, 1988. The epicenter was located about 15 km north of the city and the local magnitude was calculated equal to 4.8 R.

The city of Kalamata is located in SW Peloponese, Greece, and it is the administrative and commercial center of the area with a population of about 20000 people. The soil is alluvium and the city lays along the banks of the Nedon dry river. During the last two centuries the surrounding area has been struck by four earthquakes, shown in figure 1.

The earthquake of September the 13th caused the death of 21 people, the wounding of 300 people and the total destruction of the 44% of the Kalamata buildings.

In this study we present the results of the processing of some of the accelerograms that were obtained during the aftershock sequence. More specifically we have calculated the values of ground acceleration, velocity and displacement, and the response spectra of the recordings. Furthermore a correlation between the results and the observed damages caused by the main shock was performed.

2. DATA AND METHOD

The permanent strong ground motion network of the Seismological Institute of Athens at Kalamata and the surrounding area consists of four accelerographs, SMA 1 type, which are installed in Kalamata, Sparti, Kiparissia and Pilos (figure 1). the main shock of the seismic sequence triggered the Kalamata and Sparti accelographs. The Kalamata instrument was triggered in addition by fifteen aftershocks. The Seismological Institute of Athens installed two more instruments in the city of Kalamata at sites with different observed damages, but no reliable record was obtained because of the small magnitude of the recorded shocks. The seven well recorded earthquakes which have been used in the present study are shown in Table 1.

The strong ground motion instrument at Kalamata is installed at the basement of the 3 storey building of the Telecomm-

---

1) National Technical University of Athens, Laboratory of earthquake Engineering, Patision 42, GR 106 82, Athens.
2) National Observatory of Athens, Seismological Institute, P. O. Box 20048, GR 118 10, Athens, Greece.

nication Company. The building is a stiff structure with a reinforced concrete load - carrying system. The longitudinal component of the instrument has an E - W orientation.

The methodology that was followed for the processing of the records was the one that the Laboratory of Earthquake Engineering, National Technical University of Athens, uses and is based on the methodologies by Trifunac and Lee (1973), Petrovski and Naumovski (1979), Hudson (1979), Basili and Brady (1978) and Jennings and Nigam (1968). The main steps of the method are the following:

a) First the production of the contact copy of the record is made, which is magnified three or four times in order to be digitized.

b) The digitization process is performed manually, with the crosshair following the middle of the line of the copy. The digitization is made on unequal time intervals, picking prominent points on the records such as peak values and points of inflection.

c) A computer plot of the digitized data at the same scale as the original record is used to check the digitization accuracy. By superimposing the two accelerograms incorrect points are identified and corrected.

d) Computer processing of strong motion accelerograms. The steps involved are these:

i) Start with the uncorrected accelerogram digitized at unequal time intervals.

ii) Interpolate equally spaced time data to facilitate digital filtering.

iii) Extend accelerogram at beginning and end to permit ORMSBY low pass filtering in order to remove high frequency noise.

iv) Calculate derivatives of X.

v) Substitute in transducer equation to find true ground acceleration.

vi) Remove linear trends in acceleration and velocity by least squares fit.

vii) Extend record for digital filering.

viii) Filter through ORMSBY low pass filter by unequal weight running average.

ix) Interpolate points at same time ordinates as input accelerogram and subtract from input to produce high pass filtered accelerogram, thus performing baseline adjustment.

x) Eliminate linear trends again by least squares fit producing final form of the corrected accelerogram.

xi) Integrate accelerogram, eliminate linear trends, filter through low pass filter to produce final corrected ground velocity.

xii) Integrate again and filter through low pass filter to produce final corrected ground displacement.

e) For digital calculation of the response spectra we use the Nigam and Jennings method (1978).

In the present case, because of the bad developing of the film, it was impossible to obtain a contact copy. So, the digitization was made straight from the original many times and by many users. Then the best one was selected.

The cut - off frequency of the low pass filter was

determined by using the USGS and Basili and Brady (1978) procedures.

3. RESULTS

After the digitization and the correction of the recordings done we obtained the maximum ground values (Table II). We finally obtained the responce spectra of the shocks. In fig. 2 and 3 the responce spectra of the main shock and the largest aftershock for 0%,2%,5%,10% and 20% damping and for the three components are shown. The 5% damping (the middle line) generally corresponds to buildings made of reinforced concrete.

For the main shock the value of the spectral acceleration for the longitudinal component varies between 0.4 and 0.6g for natural periods between 0.15 anp 0.7 sec. The peak value is about 0.6g for period about 0.3 sec. The vertical component shows a peak value of the order of 1.5g corresponding to a natural period of 0.18 sec. The acceleration for the transverse component varies between 0.6 and 1.0g for natural periods between 0.15 and 0.7 sec and reaches a peak value of 1.0g for a natural period of 0.28 sec. The peak spectral velocities are considerably high for the horizontal components (60 cm/sec for the longitudinal component and 85 cm/sec for the transverse), while for the vertical component the peak value is 40 cm/sec. As for the displacements, the two horizontal components show peak values of about 15 cm, while the vertical one is about 7.5 cm.

For the major aftershock and for the longitudinal component the higher spectral acceleration values vary between 0.6 and 1.0g for natural periods between 0.15 and 0.7 sec, with a peak value of about 1g at 0.32 sec. For the vertical component and for values of natural period between 0.1 and 0.7 sec the spectral acceleration varies between 0.15 and 0.5g and shows a peak value of 0.51g at 0.3 sec. The transverse component shows spectral accelerations between 0.2 and 0.35g for natural periods between 0.15 and 0.5 sec with a peak value of 0.33g at 0.25 sec. The peak spectral velocities for the longitudinal, vertical and transverse components are 67, 20 and 18 cm/sec respectively and the peak spectral displacements are 7, 2.8 and 2.5 cm respectively.

Table III shows the maximum spectral acceleration for 5% damping, for each of the shocks analyzed.

4. CORRELATION OF THE RESULTS AND THE OBSERVED DAMAGES

According to the relation connecting the natural period with the number of storeys of the building after Carydis and Mouzakis (1986), almost all buildings in Kalamata have natural periods between 0.1 and 0.7 sec, that is values that coincide with the area of the peak spectral accelerations caused by these earthquakes.

In order to calculate the seismic coefficient developed to the buildings of Kalamata during the earthquake, we use the following steps: We select a 7.5% damping (the mean value of 5% and 10%). For values of natural periods between 0.1 and 0.7 sec, the values of spectral accelerations observed, vary

for the longitudinal component (east - west direction) between 0.4 and 0.5g, while for the transverse component (north - south direction) vary between 0.55 and 0.85g. The relation connecting the seismic coefficient with the spectral acceleration is:

$$\varepsilon = \frac{1.2\ SA / g}{1.75\ Q}$$

where: ε is the seismic coefficient
1.2/1.75 = 1.42 is the safety factor
SA is the spectral acceleration for 5% damping
Q is the quality factor of the structure and varies between 1 and 6.

In this particularity case we considered three of buildings, for which Q = 5 (good quality, ductile construction), Q = 3 (medium quality, reinforced concrete buildings) and Q = 1.5(common adobe structures or bad quality buildings from reinforced concrete). Table 2 shows the seismic coefficients developed for each of the two horizontal components and for the three quality coefficients confederated From the point of view of seismicity the area of Kalamata is placed to zone II and the seismic coefficient according to the soil category is 0.06 for soil α, 0.08 for soil β and 0.12 for soil γ.

We estimate that buildings with a load bearing system of reinforced concrete, constructed according the Earthquake Resistant Code of 1959, an corresponding to Q=3, suffered a seismic coefficient considerably higher than the one they had been studied for, for the north-south orientation (transverse component), while for the east-west orientation (longitudinal component) they suffered a seismic coefficient almost equal to the one they had been studied for. But because of the fact that the coefficient Q=3 assumes considerable inelastic deformation, the damages to the east-west direction were also extensive. The load bearing masonries, which are studied for the same seismic coefficient that is in use for other constructions, suffered during the main shock quite higher seismic coefficient than those used for their study. We also have to take in account the vertical component for which the spectral acceleration is quite high for the low periods, characterizing the various parts of the buildings (roofs, floors etc).

As far the above conclusions are concerned, we are reserved as to the fact that the results are extracted from the recordings of one single instrument. while for more accurate results more than one instruments are required.

REFERENCES

BASILI, M. and BRADY, G.,(1978), Low frequency filtering and the selection of limits for accelerograms corrections, 6th ECEE,
September 18-22, Dubrovnic, Yugoslavia.
CARYDIS, P. and MOUZAKIS, H.,(1986), Small amplitude vibration measurements of building undamaged, damaged and repaired after earthquakes. Earthquake Spectra , vol.2.

no.3.

COMNINAKIS, P.E. and PAPAZACHOS, B.C., (1986), A catalogue of earthquakes in Greece and the surrounding area for the period 1901-1985, Univ. Thessaloniki, Geophys. Lab., Publ.no.1.

HUDSON, D.E., (1979), Reading and interpreting strong motion accelerograms, EERI monograph.

NIGAM, N.C. and JENNINGS, P.C., (1968), Digital calculation of the responce spectra from strong motion earthquake records, EERL, California Institute of Technology, Pasadena.

PETROVSKI, D. and NAUMOVSKI, N., (1979), Processing of strong motion accelerograms, Part I:Analytical methods, Institute of Earthquake Engineering and Earthquake Seismology, University Kiril and Metodij, Skopje, Yugoslavia.

TRIFUNAC, M.D. and LEE, V., (1973), Routine computer processing of strong motion accelerograms, EERI, California Institute of Technology, Pasadena.

TABLE I : PARAMETERS OF THE EARTHQUAKES, THE ACCELEROGRAMS OF WHICH WERE USED IN THE PRESENT STUDY

CODE NUMBER	DATE	ORIGIN TIME	Φ° N	λ° E	M_L (ATH)
S1	13 SEP	17:24	37.10	22.19	5.5
S2	13 SEP	18:30	37.11	22.14	3.3
S3	13 SEP	22:40	37.12	22.16	3.6
S4	14 SEP	22:48	37.15	22.04	3.4
S5	15 SEP	05:15	37.22	22.01	3.2
S6	15 SEP	11:41	37.08	22.07	4.8
S7	15 SEP	12:47	37.09	22.04	3.6

TABLE II: MAXIMUM SPECTRAL ACCELERATION FOR 5% DAMPING

CODE NUMBER	COMPONENT	ACCELERATION (g)
S1	L	0.635
	V	1.491
	T	1.007
S2	L	0.124
	V	0.102
	T	0.100
S3	L	0.117
	V	0.079
	T	0.092
S4	L	0.102
	V	0.071
	T	0.062
S5	L	0.109
	V	0.087
	T	0.072
S6	L	0.986
	V	0.513
	T	0.331
S7	L	0.133
	V	0.098
	T	0.113

TABLE III: MAXIMUM PEAK GROUND VALUES

CODE	COMP	ACC/TIME (g/sec)	VEL/TIME (cm*sec^{-1}/sec)	DISPL/TIME (cm/sec)
S1	L	0.22/4.2	34.35/3.53	8.94/4.03
	V	0.32/3.11	14.21/2.86	4.02/3.09
	T	0.29/3.67	33.00/3.47	7.18/3.66
S2	L	0.04/1.03	3.06/1.21	3.29/6.35
	V	0.03/1.02	1.59/8.69	1.30/9.60
	T	0.03/1.04	2.60/11.21	2.67/5.24
S3	L	0.05/0.98	1.99/4.53	1.92/5.78
	V	0.02/1.07	1.11/7.00	0.32/6.75
	T	0.04/1.02	2.20/11.85	1.71/4.19
S4	L	0.04/0.64	2.47/0.53	1.15/9.99
	V	0.02/0.71	4.56/7.97	5.35/6.00
	T	0.02/0.79	1.47/0.71	1.07/9.10
S5	L	0.05/0.68	3.41/0.63	0.81/1.31
	V	0.02/0.27	1.19/9.79	1.53/3.31
	T	0.03/0.68	2.60/8.88	0.73/8.51
S6	L	0.32/2.44	26.75/2.30	4.15/2.41
	V	0.16/1.88	7.91/2.12	1.05/2.12
	T	0.10/2.26	9.50/1.63	1.24/1.87
S7	L	0.05/1.22	1.71/1.33	0.41/6.39
	V	0.03/0.22	0.81/5.10	0.27/7.95
	T	0.03/1.19	2.72/11.11	3.33/9.41

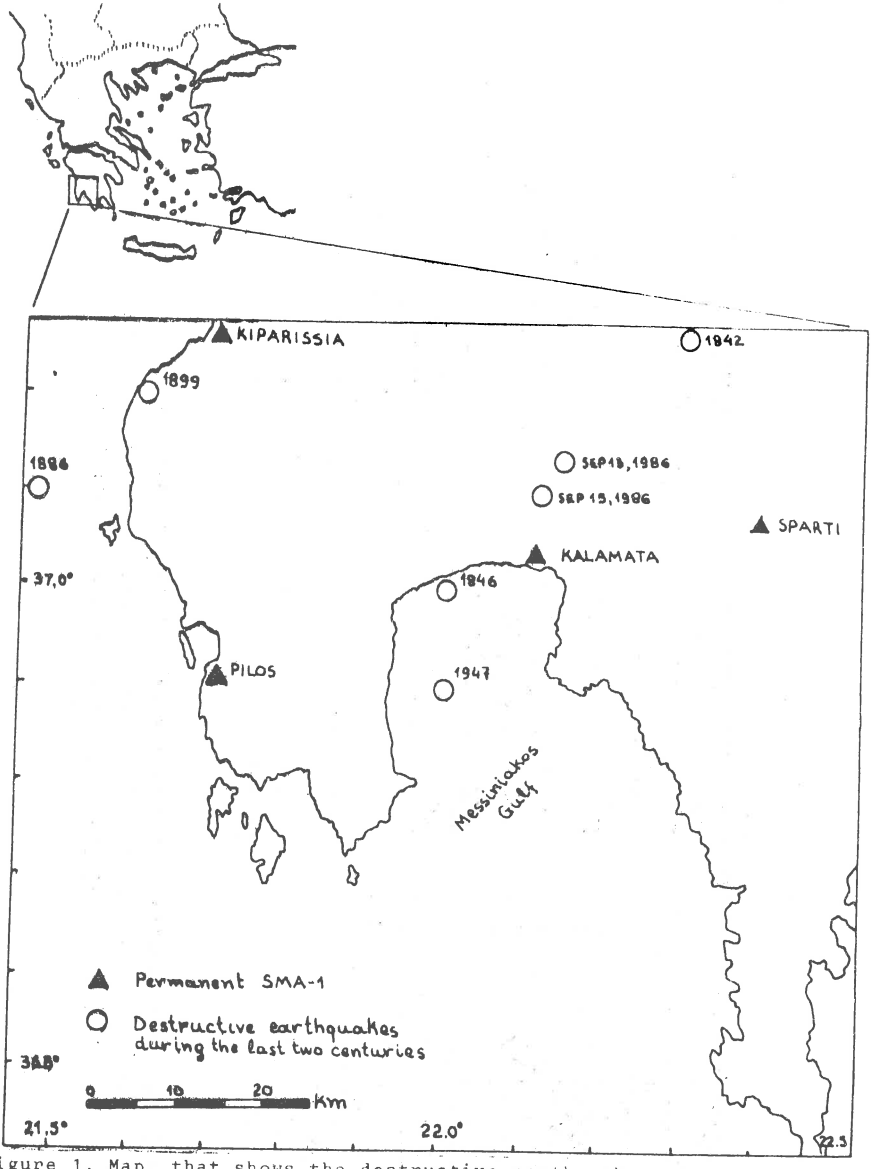

Figure 1. Map, that shows the destructive earthquakes around Kalamata, Greece, during the last two centuries and the permanent strong ground motion network of the National Observatory of Athens in the area.

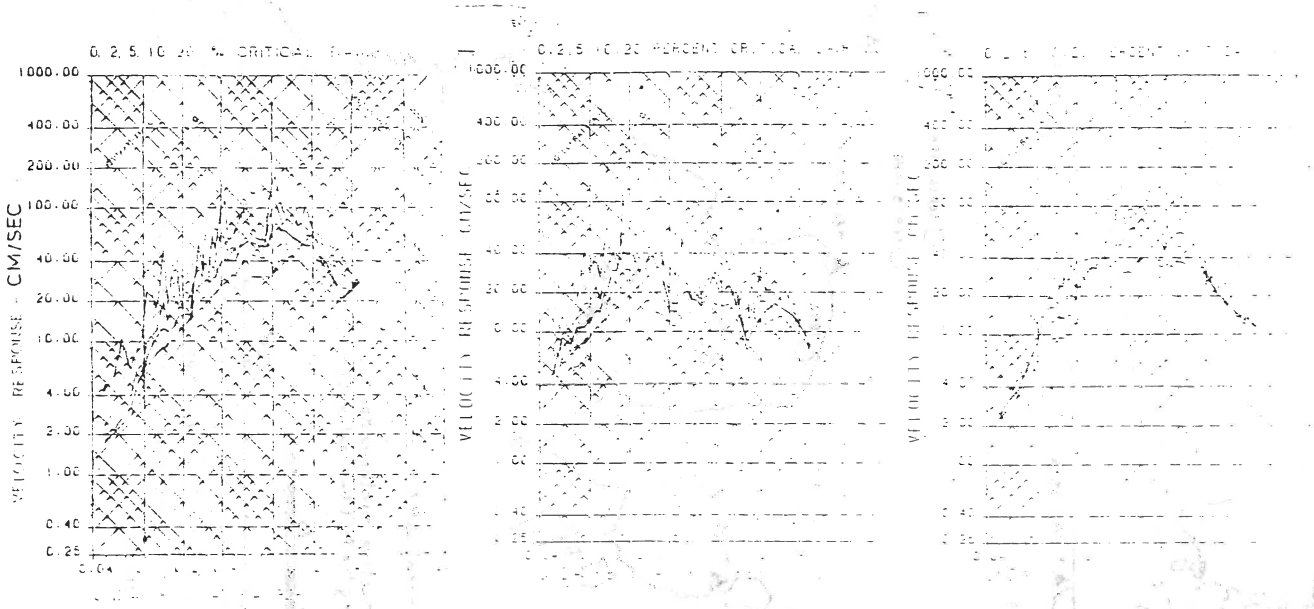

Figure 2. Responce spectra of the main shock occured at Kalamata on the 13th of September 1986. From left to right Long, Vert and Tran components. The middle line shows the spectra for 5% damping.

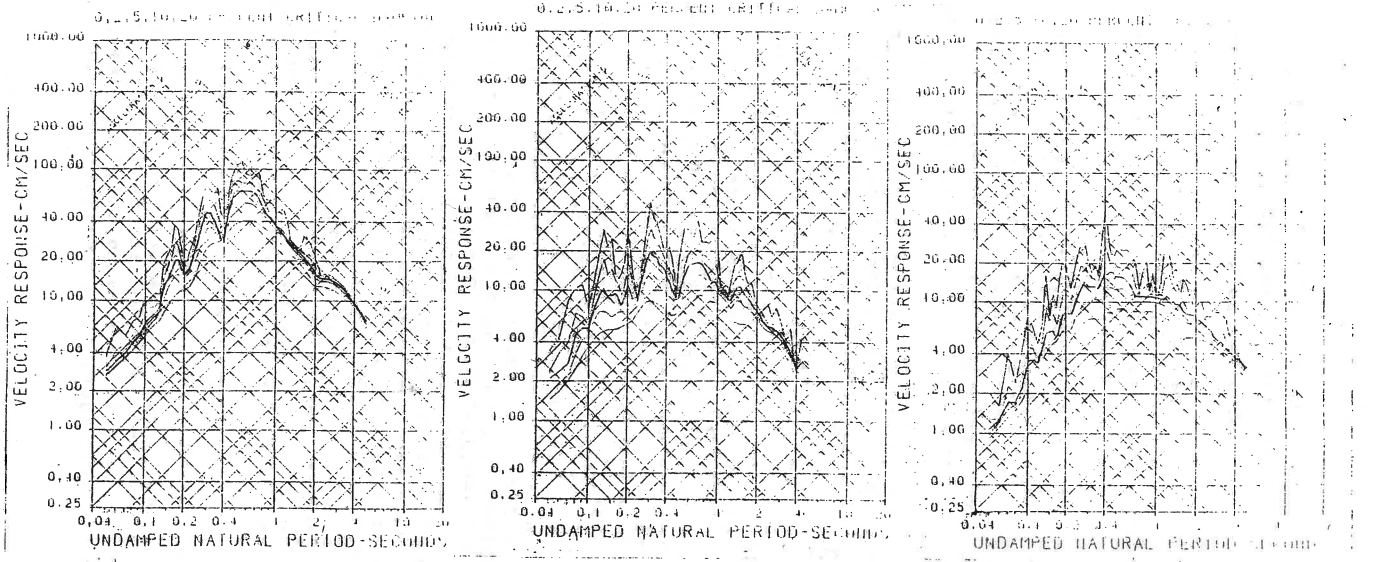

Figure 3. Responce spectra of the major aftershock occured at Kalamata on the 15th of September 1986. From left to right Long, Vert and Tran components. The middle line shows the spectra for 5% damping.

Properties of Selected Long-Period Microseismic Storms (Sept.1987 - Jan.1988) Recorded by the Průhonice Seismological Station

D. Knaislová, D. Procházková

Geophysical Institute, Czechosl. Acad. Sci., Prague

In Czechoslovakia, the microseisms have been systematically researched since 1948 (Zátopek 1960). At the Prague seismological station the records of the Wiechert seismograph were used to follow the microseisms. Since 1968 they have been measured at the Průhonice seismological station, where the Kirnos (1968 - 27.1. 1979) and the SKD (since 27.1.1979) instruments are in operation (Procházková 1978).

We defined a microseismic storm as a short-term enhancement of microseism amplitudes and we systematically studied them on the basis of records of seismic station Průhonice (PRU, $\varphi = 49°59.3'$ N, $\lambda = 14°32.5'$ E, h=302m) and data of the time period 1968-1980. The following findings were obtained:

1) Microseismic storms are manifest by a sudden increase in amplitude and period of both horizontal components.
2) Microseismic storms occur either separately or in sequences and individual storms are sometimes difficult to identify.
3) Individual microseismic storms last from one to several days and have nearly the same form - a sudden increase of amplitudes to some maximum and a decrease. Their more detailed pattern was not investigated.
4) Microseismic storms differ in size. For the purpose of classification we can use the quantity $A=A_2-A_1$, where A_2 is the maximum amplitude recorded in the horizontal component during the storm and A_1 is the largest horizontal amplitude determined with the aid of the smooth envelope curve of the dot diagrams, the method constructing dot diagrams was described by Zátopek (1956); A=0.05-2.80 μm. Periods T=4-9 s.
5) Severe microseismic storms occur less frequently than weak ones. For Průhonice seismological station and the time period 1968-1980 we obtained $\log N=0.92-1.64A$, where N is the number of microseismic storms of size A in μm, $A \in (0.05, 2,80)$ (Knaislová, Procházková 1985).

In this paper we give special attention to microseismic storms that occurred on Sept.28-30,1987, Oct.25-27,1987 and Jan.17-20,1988 (Darbyshire 1988). The constants of all components of an SKD instrument recording at the Průhonice seismological station are:

$T_s = 24.6$s, $T_g = 1.2$s, $D_s = 0.5$, $D_g = 0.1$, $\sigma^2 = 0.21$,

$T_m = 0.2$-20s, $V_m = 900$-1000.

The behaviour of microseismic activity is expressed in terms of amplitudes and periods of two horizontal and one vertical components measured at the principal meteorological times, i.e. 0h, 6h, 12h and 18h UTC, Table 1. The measurements were only

omitted in case in which an earthquake distorts the microseismic noise. In the vicinity of the maximum trace amplitudes we carried out 3 hourly readings in a 20 minute interval, centered at the hour, Table 2.

The variations of the amplitudes and periods during the microseismic storms in both horizontal and one vertical components based on Table 1 are illustrated by dot diagrams, Fig.1. The last selected storm was in the PRU seismological station followed by another microseismic storm, which was characterized by higher amplitudes in all three components than the foregoing one, therefore we also measured that storm. The amplitude and period ranges are in Table 3. The main characteristics of the investigated storms are:

- Sept.28-30,1987: size A=0.6 μm, maximum on Sept.30 at 00h, the period corresponding to the maximum amplitude is 8s, $A_{max}(Z) > A_{max}(NS) > A_{max}(EW)$.
- Oct.25-27,1987: size A=0.7 μm, maximum on Oct.26 at 00h, the period corresponding to the maximum amplitude is 8s, $A_{max}(Z) = A_{max}(NS) = A_{max}(EW)$.
- Jan.17-20,1988: size A=0.8 μm, maximum on Jan.18 at 00h, the period corresponding to the maximum amplitude is 8s, $A_{max}(Z) = A_{max}(NS) = A_{max}(EW)$.
- Jan.20-28,1988: size A=2.9 μm, maximum on Jan.24 at 12h, the period corresponding to the maximum amplitude is 8s, $A_{max}(Z) > A_{max}(NS) > A_{max}(EW)$.

The last mentioned storm belongs to the most severe storms that were recorded in the Průhonice sesmological station in the time interval 1968-1980 (Knaislová, Procházková 1985). The patterns of the investigated microseismic storms agree with the pattern of the foregoing once which occurred in the time interval 1968-1980.

The variations of amplitudes and periods during the 3 hourly time intervals centered around the maximum phase based on measurements of every 20 minutes (Table 2) are illustrated in Fig.2. We can see that:

- Sept.28-30,1987: one maximum 0.6 μm on Sept.30 at 00h, simultaneously in all components, a period increase is only during the maximum phase, the duration of the maximum phase is smaller than 20 minutes.
- Oct.25-27,1987: several local maxima, the main maximum 0.7-1.0 μm on Oct.26 at 01h 40m in all components, a period increase is during the whole interval, the duration of the maximum phase is probably smaller than 2 hours.
- Jan.17-20,1988: one maximum 1.1 μm on Jan.18 at 00h 40m, a period increase is during the whole interval, the duration of the maximum phase is probably smaller than 1 hour.
- Jan.20-28,1988: several local maxima, the main maximum 2.1-3.2 μm on Jan.23 at 23h 40m (Z > NS > EW), a period increase is during the whole interval, the duration of the maximum phase is probably smaller than 2 hours.

We can conclude that the selected microseismic storms differ y their size and time duration. The first three discussed storms abe nearly the same size. The maximum amplitudes are either al- ost the same in all components or relation $A_{max}(Z) > A_{max}(NS) >$ $_{max}$(EW) applies. This difference could indicate different sour- es of the studied microseismic storms. Detailed investigations f the maximum phases of microseismic storms allow us to deter- ine more precisely the maxima of microseismic storms, we can bserve several local maxima and one main maximum which is in all omponents. During the maximum phase of microseismic storms, pe- iod increases are observed. The duration of the maximum phase f microseismic storms varies between several minutes to several enths of minutes.

able 1.
[s] - period, A [μm] - amplitude, K - recorded quality factor, ime - [UTC].

omponent		NS			Z			EW		
ate	Time	K	T	A	K	T	A	K	T	A
icroseismic storm Sept.27-Oct.1,1987.										
ept.27	12	3	5	0.3	3	5	0.3	3	5	0.2
	18	3	5	0.3	3	5	0.3	3	5	0.2
ept.28	0	3	5	0.3	3	6	0.3	3	5	0.2
	6	3	5	0.2	3	5	0.2	3	5	0.2
	12	3	5	0.2	3	4	0.2	3	4	0.2
	18	3	5	0.3	3	5	0.3	3	4	0.2
ept.29	0	3	5	0.3	3	5	0.3	3	5	0.2
	6	3	8	0.5	3	8	0.6	3	8	0.4
	12	3	5	0.3	3	6	0.3	3	6	0.3
	18	3	8	0.5	3	8	0.7	3	8	0.4
ept.30	0	3	5	0.6	3	8	0.6	3	7	0.5
	6	3	5	0.4	3	6	0.4	3	7	0.4
	12	3	5	0.4	3	5	0.4	3	5	0.3
	18	3	5	0.3	3	5	0.5	3	5	0.2
ct.1	0	3	4	0.2	3	5	0.3	3	5	0.2
	6	3	4	0.2	3	4	0.2	3	4	0.2
icroseismic storm Oct.25-Oct.31,1987.										
ct.25	0	3	4	0.2	3	4	0.2	3	4	0.2
	6	3	4	0.2	3	4	0.2	3	4	0.3
	12	3	4	0.3	3	4	0.2	3	4	0.1
	18		t.t.			t.t.			t.t.	
ct.26	0	3	8	0.5	3	8	1.0	3	8	0.7
	6	3	8	0.5	3	8	0.7	3	8	0.5
	12	3	7	0.6	3	8	0.7	3	8	0.6
	18	3	7	0.5	3	8	0.6	3	7	0.6

Jan.23	12	3	6	0.6	3	5	0.7	3	6	0.6
	18	3	6	0.6	3	6	0.5	3	6	0.5
Jan.24	0	3	6	0.6	3	6	0.7	3	6	0.7
	6	3	6	0.9	3	6	0.8	3	6	1.0
	12	2	8	2.5	(2)	8	2.9	(2)	7	1.7
	18	(2)	7	2.1	2	8	1.7	2	6	2.2
Jan.25	0	(2)	6	2.0	(2)	6	1.7	(2)	6	1.9
	6	(2)	6	1.7	(2)	6	1.8	(2)	6	1.2
	12	3	6	1.2	3	6	1.2	3	6	0.9
	18	3	6	1.0	3	7	1.1	3	6	0.8
Jan.26	0	3	6	1.0	3	6	0.9	3	6	0.8
	6	3	6	0.7	3	6	0.6	3	6	0.6
	12	3	6	0.5	3	6	0.5	3	5	0.5
	18	3	5	0.4	3	5	0.5	3	5	0.4
Jan.27	0	3	5	0.3	3	6	0.4	3	5	0.3
	6	3	5	0.4	3	5	0.3	3	5	0.2
	12	3	4	0.2	3	5	0.3	3	4	0.2
	18	3	5	0.3	3	5	0.3	3	5	0.3
Jan.28	0	3	4	0.3	3	4	0.3	3	5	0.3
	6	3	4	0.2	3	4	0.3	3	4	0.2

Table 2.
T[s] - period, A[μm] - amplitude, K - recorded quality factor, time - [UTC].

Component		NS			Z			EW		
Date	Time	K	T	A	K	T	A	K	T	A
Maximum phase of microseismic storm of Sept.27-Oct.1,1987.										
Sept.29	22.20	3	5	0.4	3	5	0.4	3	5	0.2
	22.40	3	5	0.3	3	6	0.3	3	5	0.3
	23.00	3	6	0.3	3	5	0.3	3	5	0.4
	23.20	3	5	0.3	3	5	0.5	3	5	0.2
	23.40	3	5	0.3	3	5	0.4	3	5	0.3
Sept.30	00.00	3	5	0.6	3	8	0.6	3	7	0.5
	00.20	3	4	0.3	3	5	0.3	3	5	0.3
	00.40	3	5	0.3	3	6	0.3	3	6	0.3
	01.00	3	6	0.3	3	5	0.4	3	5	0.2
	01.20	3	5	0.3	3	6	0.4	3	5	0.2
	01.40	3	4	0.2	3	5	0.3	3	4	0.2
Maximum phase of microseismic storm of Oct.25-31,1987.										
Oct.25	22.20	3	7	0.5	3	8	0.6	3	8	0.5
	22.40	3	6	0.5	3	8	0.7	3	8	0.4
	23.00	3	7	0.6	3	8	0.7	3	8	0.7
	23.20	3	8	0.5	3	8	0.5	3	8	0.5
	23.40	3	8	0.7	3	8	0.7	3	7	0.7
Oct.26	00.00	3	8	0.5	3	8	1.0	3	8	0.7
	00.20	3	7	0.5	3	8	0.6	3	7	0.5

Oct.26	18	3	7	0.5	3	8	0.6	3	7	0.6
Oct.27	0	3	8	0.7	3	8	0.6	3	7	0.4
	6	3	7	0.5	3	7	0.7	3	7	0.4
	12	3	6	0.6	3	6	0.6	3	6	0.5
	18	3	6	0.4	3	6	0.4	3	6	0.3
Oct.28	0	3	6	0.5	3	7	0.5	3	6	0.5
	6	3	6	0.4	3	5	0.5	3	6	0.4
	12	3	6	0.4	3	6	0.5	3	6	0.3
	18	3	5	0.3	3	5	0.3	3	5	0.3
Oct.29	0	3	5	0.3	3	6	0.5	3	5	0.4
	6	3	5	0.4	3	5	0.5	3	5	0.4
	12	3	5	0.6	3	6	0.6	3	5	0.5
	18	3	6	0.6	3	6	0.6	3	5	0.4
Oct.30	0	3	5	0.6	3	6	0.6	3	6	0.7
	6	3	5	0.5	3	5	0.5	3	5	0.4
	12	3	5	0.7	3	5	0.5	3	5	0.4
	18	3	5	0.5	3	5	0.4	3	5	0.4
Oct.31	0	3	5	0.4	3	5	0.3	3	4	0.2
	6	3	4	0.2	3	4	0.3	3	4	0.2
	12	3	4	0.2	3	4	0.3	3	4	0.2
Microseismic storms Jan.17-Jan.28,1988.										
Jan.17	0	3	6	0.3	3	6	0.3	3	5	0.3
	6	3	5	0.2	3	6	0.3	3	5	0.3
	12	3	6	0.4	3	6	0.4	3	6	0.3
	18	3	8	0.6	3	8	0.8	3	6	0.3
Jan.18	0	3	8	0.8	3	8	0.8	3	8	0.8
	6	3	8	0.8	3	8	0.8	3	8	0.7
	12	3	8	0.7	3	8	0.8	3	8	0.7
	18	3	7	0.7	3	7	0.7	3	8	0.7
Jan.19	0	3	5	0.7	3	7	0.7	3	6	0.5
	6	3	5	0.7	3	5	0.7	3	5	0.5
	12	3	5	0.6	3	6	0.5	3	5	0.4
	18	3	5	0.5	3	5	0.5	3	5	0.4
Jan.20	0	3	5	0.5	3	5	0.5	3	5	0.4
	6	3	5	0.6	3	6	0.3	3	5	0.4
	12	3	6	0.5	3	6	0.4	3	6	0.4
	18	3	6	0.7	3	6	0.7	3	6	0.4
Jan.21	0	3	7	0.7	3	6	0.7	3	6	0.5
	6	3	6	0.7	3	6	0.7	3	6	0.6
	12	3	6	0.7	3	6	0.7	3	6	0.5
	18	3	6	0.7	3	6	0.8	3	6	0.6
Jan.22	0	3	6	0.7	3	6	0.5	3	6	0.5
	6		t.t.			t.t.			t.t.	
	12	3	6	0.7	3	6	0.7	3	5	0.4
	18	3	6	0.7	3	6	0.7	3	6	0.5
Jan.23	0	3	6	0.7	3	6	0.7	3	6	0.5
	6	3	6	0.6	3	6	0.6	3	6	0.7

Oct.26	00.40	3	6	0.5	3	8	0.8	3	8	0.7
	01.00	3	8	0.7	3	8	0.9	3	8	0.7
	01.20	3	7	0.5	3	8	0.8	3	8	0.7
	01.40	3	7	0.7	3	8	1.0	3	8	0.8
Maximum phase of microseismic storm of Jan.17-20,1988.										
Jan.17	22.20	3	8	0.7	3	8	0.8	3	8	0.7
	22.40	3	8	0.7	3	8	0.8	3	7	0.7
	23.00	3	8	0.7	3	8	0.7	3	8	0.7
	23.20	3	8	0.7	3	8	0.7	3	7	0.5
	23.40	3	8	0.7	3	8	1.0	3	8	0.5
Jan.18	00.00	3	8	0.8	3	8	0.8	3	8	0.8
	00.20	3	8	0.7	3	8	1.1	3	7	0.7
	00.40	3	8	1.0	3	8	1.0	3	8	0.8
	01.00	3	7	0.7	3	8	0.7	3	8	0.7
	01.20	3	8	0.7	3	8	0.9	3	8	0.8
	01.40	3	8	1.1	3	7	0.8	3	8	0.7
Maximum phase of microseismic storm of Jan.20-28,1988.										
Jan.24	10.20	2-3	6	2.4	3	7	2.2	3	7	2.2
	10.40	3	6	2.9	3	7	3.0	3	7	1.7
	11.00	3	7	2.3	3	7	2.4	3	7	1.7
	11.20	3	7	3.2	3	8	1.7	3	6	1.9
	11.40	3	7	2.4	3	7	2.2	3	7	2.2
	12.00	3	8	2.5	3	8	2.9	3	7	1.7
	12.20	3	6	2.3	3	7	2.2	3	7	1.7
	12.40	3	7	2.9	3	7	3.2	3	7	2.1
	13.00	3	6	2.3	3	7	3.2	3	7	1.9
	13.20	3	7	2.8	3	7	2.2	3	6	2.0
	13.40	3	6	2.7	3	7	2.0	3	7	1.8

Table 3.

Date	Amplitude range [m]	Period range [s]	Maximum amplitude [m]	Storm duration [hours]
Sept.28-30, 1987	0.2-0.6	4-8	0.6	30
Oct.25-27, 1987	0.2-0.7	4-8	0.7	114
Jan.17-20, 1988	0.2-0.8	4-8	0.8	54
Jan.20-28, 1988	0.2-2.9	4-8	2.9	162

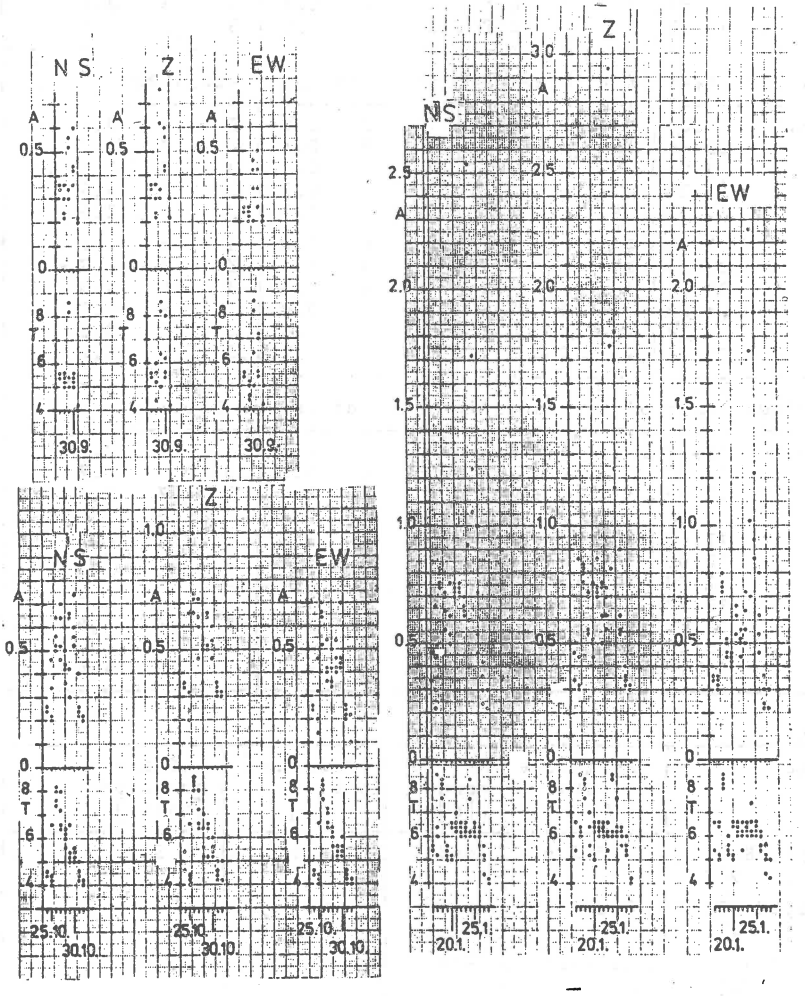

Fig.1.

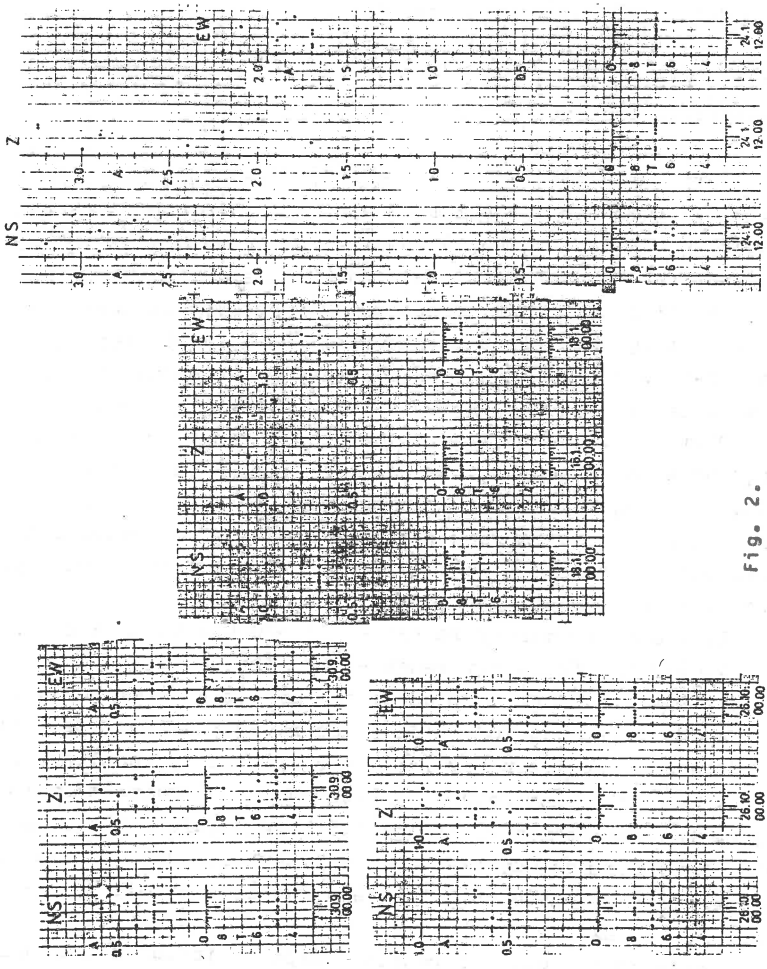

Fig. 2.

References

Darbyshire J. (1988): Proposed Cooperation on Study of Microseismic Storms of Long Period. IASPEI Activity Report.

Knaislová D., Procházková D. (1985): Behaviour of Microseisms at the Průhonice Seismological Station. Travaux Géophysiques 1983, No 582. Academia, Praha 1985, 51-93.

Procházková D. (1978): Relation between Microseisms Recorded at Seismic Stations Praha and Průhonice. Studia geoph.et geod., 22, 362.

Zátopek A. (1956): Sur les microséismes de Praha. Publ. du BCIS, Sér. A, Tr. Sc., 1956, 183.

Zátopek A. (1960): Les microséismes de Praha au cours de l'Année Géophysique Internationale. Studia geoph. et geod., 4 (1960), 233.

SEISMOACOUSTIC BOREHOLE EQUIPMENT

Dimitar Mihailov
Geophysical Institute, Sofia , Bulgaria

During the earthquake swarm of I986/87 in and around town Strazhica followed the earthquake of 7.I2.I986, underground sounds were heard by many witnesses in the seismoactive a rea, as autor included. These sounds appeared spontaneosly, lasted for several minutes and disappeared suddenly, but sometimes ended in earthquake. All that time the standard Willmore Seismometer S-I3 was at work having recorded microseismic noise of increased level and of a characteristic pulsating type.

Obviously, there exist processes of considerable higher frequencies overstepping the possibilities of a standard equipment. This enjoined the design and production a seismoacoustic borehole equipment for ceaseless recording of seismoacoustic emissions and noises, and this at a very short time. The specifica tions of the equipment are:

I. Proper frequency ra nge - I3 -30 000 Hz in 3 subranges.

2. Working frequency range - I9 -I2 000 Hz.

3. Dynamic range - 86 dB at two levels at every 40 dB.

4. Ga in - from $I0^3$ to $I0^9$, according the characteristic.

The working frequency range was limited by peculiarities of the geological structure by heterogeneous sedimentary rocks and by the chosen manner of the borehole module fixing, which determined the maximum frequency of the seismoacou..ic signals in the ground capable of being recorded in a stable mode - about I3 000 Hz.

The seismoacoustic borehole equipment includes the followed functional modules/ Fig.I/:

I. The borehole module contains sensors, preamplifiers, filters, buffers and power supply.

2. The surface module consisting of conditionic amplifier, filters, detectors, adder, intelligence event detector, additional equipment controler and recorders, a nd power supply.

3. Signa l recorders of every channel, 40-channel parallel

spectro-analyzer with own memory and serial recorder, magnetic type recorder with pla yback, time and printer.

This seismoacoustic borehole equipment opperation as follows:

The signal from the sensors which is proportional to the ground vibration velocity or acceleration is amplified by respective preamplifier and is filtered in order to get the frequency cha racteristics for each of the three subranges. The signals from every channel are distributed between two levels at every 40 dB with an additional amplifier and the sixth signals are conveyed along a cable through the insulated buffers. The power supply is simmetrical with a floating common point insulated from the ground. All amplifiers into the borehole module have constant amplification. In the absence of seismoacoustic emissions and noises the spectral densities of the acoustic and thermal noises in each channel are equalized in the surface module. Naturally, amplitude-frequence characteristic obtained is nonlinear - fig.2.

The signals of the same level from every three channels are added with empirically received coefficients and processed by the intelligence event detector at a constant signal-noise relation I,3. The detector actuates an output for the true value of the event with a probability of 82%. Detection time is less than 0,24 s for the all working frequency range.

The signals recorders from every channel record continuously the root mean square value and the maximum signal amplitude with a minute at the end with the same minute.

During a seismoacoustic emission or event as well as an earthquake, the absolute detection time - hour, minute, second is typed too. Also, a type record is made of an event containing signal.

The installation of the borehole module: An additional vibrator whose specification is known was installed at the bottom and wassjust attached tothe sites of the borehole at a depth of 32 m. Then an acoustic isolation was lowered and the borehole module was installed on it together with a container fulled of 100 kg concrete with acoustic properties near to those of surround rocks. On achieving the possibly best contact the borehole

was fulled up with inert material for acoustic isolation and for recovering of nominal geological charge.

The performance of this equipment started in March I987 and lasted for seven months. About I3 000 events were recorded, of which about 6 000 were of artificial origin - transport vibrations, blasts and others, seismoacoustic emissions and signals without following earthquake - about 2 300, and with following earthquake - about 3 000. About 2 000 are with unknown origin for the time being.

The materials of these observations are being processed but some preliminary results and conclusions can be given even now:

I. An acting prototype of a seismoacoustic borehole equipment has been designed and experimented enabling the establishment of technical and technological requierements for this kind of testings and designs.

2. Seismoacoustic emissions in the epicentral zones of a seismoactive ragion have been recorded.

3. Acoustiv signals arriving at the observation point from I to 6 seconds prior P-wave for more than 80% of the aftershocks have been recorded.

4. Zones of the sources of the acoustic signals have been determined as follows:

4.I. Low frequente emissions and signals down 300 Hz - from zones with tectonic mouvements at distances up to about I0 km.

4.2. Medium frequency / I00 - 3 000 Hz / - from rock areas where the equipment was installed - about 300 m.

4.3. High frequency / 600 - 20 000 Hz / - mainly from the zone deformed in the boring. These sourses are obviously connected with the relax and are manifested during seismic affects from earthquakes and blasts and others.

4.4. Seismoacoustic signals of unknown nature - about 20%.

5. It has been established that the aftershocks of the earthquake generate their own aftershocks, each of which generating seismoacoustic emissions and signals. Their energies, their prevailling frequencies, their generating volumes, the intervals between the events and so on have a structure similar to a fracthal one. It is possible to observe up to 5 - 6 stable levels of these struc-

tures.

6. There have been identified trigger mechanizms of 67 earthquakes of a magnitude larger than I,5. 5I earthquakes were triggered by artificial seimic causes, and I6 - by other geophysical processes.

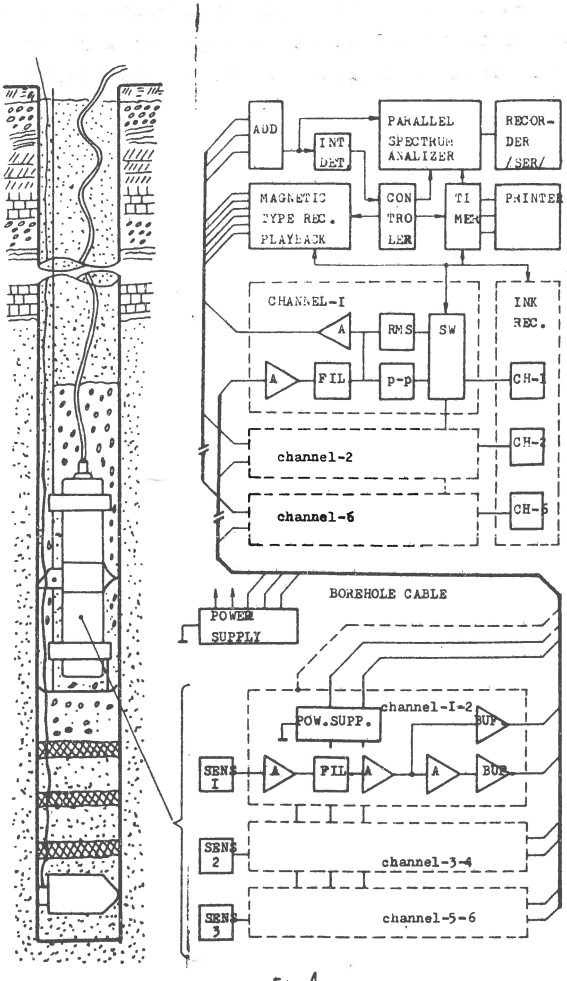
ADD
INT DET
PARALLEL SPECTRUM ANALIZER
RECOR-DER /SER/
MAGNETIC TYPE REC. PLAYBACK
CON TRO LER
TI ME
PRINTER
CHANNEL-I
A
RMS
SW
A
FIL
p-p
INK REC.
CH-1
channel-2
CH-2
channel-6
CH-6
BOREHOLE CABLE
POWER SUPPLY
channel-I-2
POW.SUPP.
BUF
SENS I
A
FIL
A
A
BUF
SENS 2
channel-3-4
SENS 3
channel-5-6

Fig.1

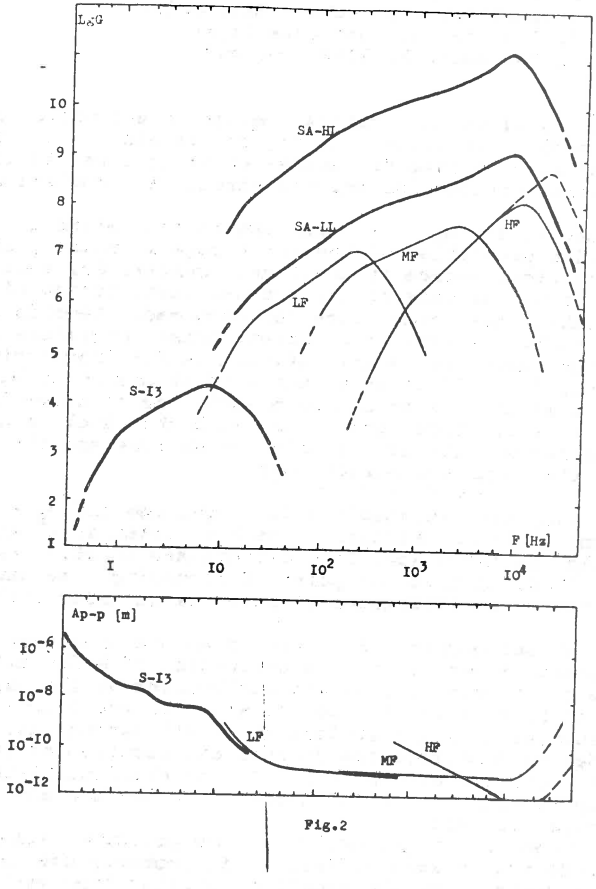
L.G
10
9
8
7
6
5
4
3
2
1
SA-HL
SA-LL
MF
HP
LF
S-I3
F [Hz]
1
10
10^2
10^3
10^4
Ap-p [m]
10^-6
10^-8
10^-10
10^-12
S-I3
LF
MF
HF

Fig.2

EVALUATION OF MAGNITUDE OF SMALL EARTHQUAKE IN A SEISMIC NOISE FIELD

T. Stojanov, L. Christoskov
Geophysical Institute - BAS, Sofia
O. Chavroskin, Institute Physic
of the Earth AS SSSR, Moscow

The possibility of using artifical noises in evaluation of tensions in the medium for large city regions is also of interest. Great quantity of precise data for noises of natural and artifical origin is sometimes suitable for solving structural problems as well (1).

In this paper an attempt has been made at evaluating in a new way the informative properties of the anthropogenic noises, acting as a powerful artifical source of local earthquakes. For this purpose a comparative analysis of the diurnal distribution of some local earthquakes' characteristics has been made. Records of shocks, registered by stations in different noise conditions have been selected: the temporary seismic station is far from artifical noise sources, SS "KDZ" is in a region of strong noise background. The measured and averaged double amplitude of noise in the one-hour interval of the time identifical with the shock, has been accepted as a characteristic of the noise conditions and the difference between the magnitude evaluations

$$\Delta M = M_A - M_B,$$

where M_A is the temporary seismic station magnitude and M_B - the magnitude determined in SS "Kurdjali" has been taken as a parameter for comparing the influence. Only earthquakes in close region of no more than 50-60 km from the point of recording were studied so as to avoid the noise influences of other large industrial centres.

Recordings of seismographs S-13 with standart amplitude - frequence characteristics were used; the evaluation of M for all shocks was made by the duration of the earthquakes on the basis of the general methods, accepted at the centere. For the period of 1985-1986 a histogram of ΔM distribution of all earthquakes, was drawn up in order to determine the diurnal distribution of the magnitude evaluations difference (fig. 1). The obtained histogram does not correspond with the law of normal distribution and is displaced to the right of zero.

The displacement in the direction of the positive values of the ΔM magnitude evaluations difference is probably due to a systematic error in determining the magnitude arising from various seismic conditions. The origin of the three maximums in the histogram and their nature need special studing.

The processing of the diurnal distribution of the magnitude evaluations difference was carried out by dividing the 24 hour-period into two-hour intervals in wich the average value of ΔM, the dispersion (σ^2) and the mean square error were determined. The established dependencies of those parametres on the time of day are shown on fig. 2.

The graph of the function of the mean value of the magnitude evaluation differences $\Delta \bar{M}_i$ ($i = 1,2,3....$). Fig. 2a and the curve of the average diurnal level of noise (fig. 2b) change almost synchronously within the 24 hours and this is especially visible du-

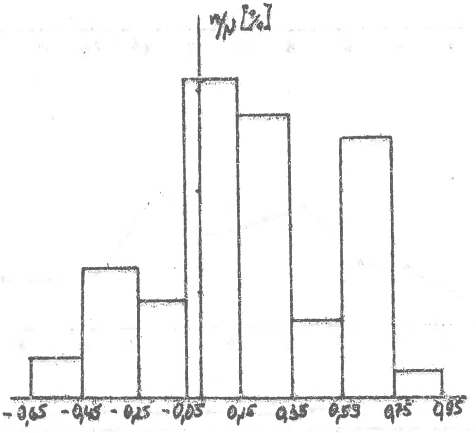

Fig. 1.: Diurnal distribution of the magnitude evaluations difference

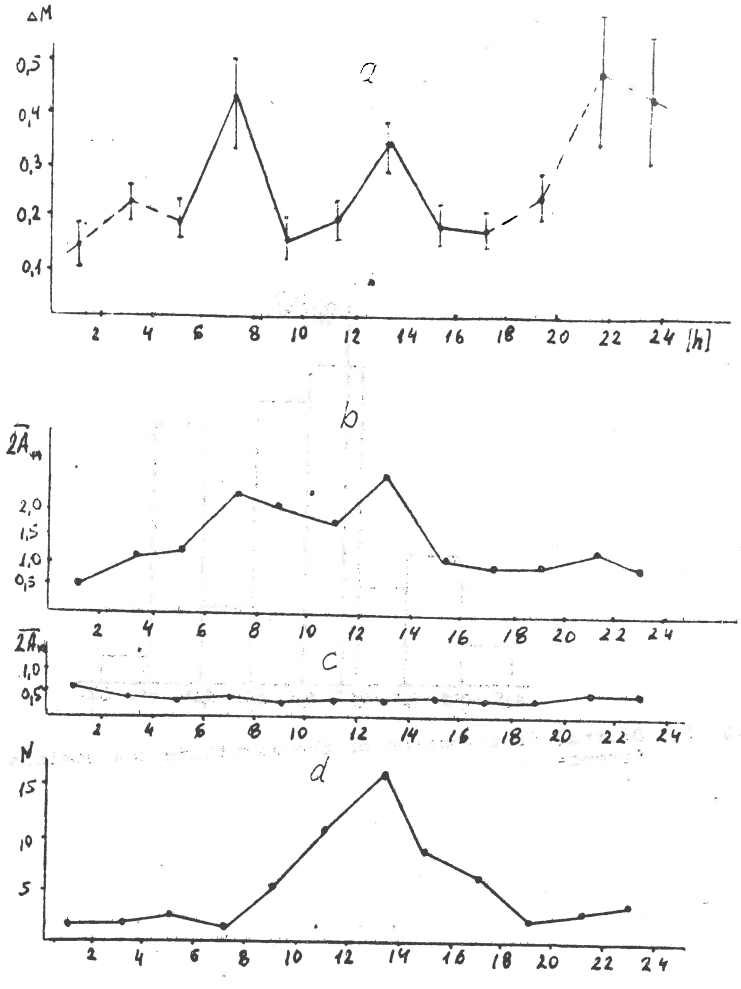

Fig. 2.: Dependence of the mean valne of the magnitude differences $\Delta \bar{M}$ (a); level of the anthropogenic noise (b); diurnal variations of noise at the temporary seismic station (c); distribution of the number of earthquakes over 24 hours (d).

ring daytime.

A possible explanation may be that the artifical noise field, generated by industry, transport and power engineering mainly during daytime, constantly brings part of its energy into the medium near the large city. That effect results in the activisation of the medium microdefects.

The strong artifical seismic noise, generated by large cities and acting as a powerful distributing vibrator on the medium eases the tensions through series of microseisms wich increase the number of structural deffects in the medium. The body waves of nearly earthquakes are propagated through such medium with losses of energy [2].

These reasons results in the reducing of the earthquake magnitude evaluation, calculated at the "noisy" station and hence in the increase of the $\Delta \overline{M}$ parametre (fig. 2a and 2b).

At primary processing of the seismological data the measuring of the earthquake recording duration brings in its error to the effect of "shortering" in the presence of noise. If this error is not taken into account in the algorithm for determing of M, the above mentioned varations of ΔM could be result of this incompleteness. The variation of ΔM on the figure is 0,15 till 0,5 magnitude units.

The coefficient of correlation between $\Delta \overline{M}$ and the double amplitude of noise has been calculated for the most active period of the day (between 7 a.m. and 7 p.m.) and it proved to be $0,68 \pm 0,06$ while for the whole 24 hour period it is lower 0,52.

The diurnal variation of noise in the temporary station is shown on fig. 2c and it undergoes almost no visible changes. Calculations have indicated that the coefficient of corelation between the number of microtremors (fig. 2d) and the noise variation for the same period at SS "KDZ" is very low - 0,34 for the 24-hour period.

The peculiarities shown above need a more detailed analysis with the help of records of more prolonged observations and data collected at a greater number of stations

The results will probably help in specifying the station corrections.

This paper is an attemp at explaning of the interaction of an artifical noise field with a seismic wave. It is not meant to give an answer to all exceptionally complex and incompletely investigated questions, connected with the effects of seismic noise.

References

1. Bungum H.; Hjortenberg E.; Risbo T.: "Use seismic oscilation, generation from power station, for study of variations of seismic velocities"; "Study of the Earth by nonexplosion seismic sources", "Nauka", M, 1981 (in Russian)

2. Alexandrov S.T.; Camburcev A.C.: "About nonlinear interaction seismic waves from impulse source" (in Russian)" Institute Fyz. Zemly SSSR, M, 1983, Nr. 13

VERTICAL SEISMIC NOISE AT STATIONS ON THE TERRITORY OF BULGARIA

T. Stojanov, L. Christoskov
Geophysical Institute - BAS

1. Introduction

The microseisms of different periods are of different origin and are connected with the registration point (1,2,3). Some studies on a group of stations have showen the possibility of finding monochromatic components in the seismic noise, even over great distances (4,5). Interesting results have been obtained in investigating the noise at the regional seismic networks, whose seismimetres are located in boreholes (6).

2. Data and apparatuses

The NOTSSI system allows digital registration of seismic events, that have occured on the territory of Bulgaria and its near vicinity, and their collecting on magnetic bands. All stations of the network are equipped with vertical short-period seismometers S-13 with standart characteristics. Data from stations Plovdiv (PLD), Pavlikeny (PVL), Jambol (JMB), Preselentsy (PSN), Vitosha (VTS), Dimitrovgrad (DIM), Kardzaly (KDZ) and temporary seismic stations have been used in this study.

Each observation of noise represents a registration of microseisms for an interval of 30 seconds preceding the beginning of an earthquake.

Information from all measurements is accumulated at the centre, where it can be digitally processed by a PDP-11/34 computer.

For the studied period from 1.1.1986 till 31.12.1987 more than 760 records from 8 stations were processed. The recordings were selected in accordance with their regular distribution during the 24 hours and during the different seasons of the year.

3. Method of analysis

The method of measuring the noise level is the following: the maximum peak to peak amplitude in the 30 second interval was measured for each seismogram and this was then averaged by hours and months. Thus the mean maximum amplitude is an evalution of the seismic noise level at stations of different geographical location.

At the next stage of the digital processing of the seismic noise its spectrum was calculated by Furrie's transformation (7). The spectra were computed by means of a computer programme, permitting spectrum evaluation by 1024 points length. The frequency of discretisation was 50 Hz in the range 0 to 6 Hz (with dividing capability 0,048 Hz). The purpose of the present digital spectral analysis was to obtain the first representative data for monochromatic components in the noise spectrum for the different seismic stations on the territory of Bulgaria.

4. Results

On the basis of the maximum amplitude analysis during the definite lenght interval the results in the table 1 were obtained. According to the results in the table, stations TSS, PLD and JMB have the lowest noise level, and stations PSN and DIM - the highest. The main frequency peaks are concentrated in a narrow frequency band for stations TSS and DIM; in a wider one for sta-

Table 1. Average noise level at some seismic stations on the territory of Bulgaria for 1987.

Stat.	A_{max} Day	Number of occurr.	A_{max} / A_{min}	$A_{max} - A_{min}$	Δf [Hz]
PLD	0,77	86	3,45 0,22	3,23	1,40-3,10
PVL	4,91	86	10,34 0,33	10,01	0,05-5,03
IMB	0,98	84	7,65 0,15	7,5	0,39-2,17
TSS	0,39	82	0,94 0,11	0,83	0,05-0,68
PSN	5,11	86	18,19 0,63	16,54	0,64-2,86
VTS	2,55	85	6,58 0,38	6,2	0,20-1,81
DIM	11,21	80	30,88 0,64	30,24	2,10-2,70
KDZ	3,97	81	9,41 0,92	8,89	0,05-2,56

tions VTS, PLD, PSN and the widest being for PVL and KDZ.

Stability to amplitude level variations is greatest for stations TSS, PLD and VTS, and the most dynamic for the studied period are DIM and PSN. The noise level at the quietest point of observation and noise level at the noisiest one differ more than 32 times.

The different spectrum evaluations of noise at the seismic stations, calculated on the basis of the digital seismograms for a quiet regions in the absence of strong athmospheric disturbances on a day free of local seismic events, are shown on fig. 1. The greatest number of monochromatic peaks is to be found in the spectra of KDZ, PLD, TSS; stations VTS and JMB have single prevailing peaks, especially DIM, whose peak of 2 Hz is of industrial origin.

The annual variation of the seismic noise level is shown on fig. 2. The average maximum amplitude of the noise records is plotted for each month of 1987, only for May it is the mean amplitude value for a single free of labouractivity day - the 1st of May. The low noise level during that day, served as a comparison for the stations with high level of anthropogemic noise (PVL, KDZ, JMB, PLD). An exception are stations TSS and VTS where the variations are clearly connected rather with the atmospheric disturbances due to their mountainous location. The high level at station DIM for the month of May is probably due to the constant industrial process not far from the point of registration. The depth of the minimum in May could give an initial estimation for the contribution of industry and transport to the general noise at the above mentioned stations.

The noise variations at station PVL with a maximum during the summer months are equal to those made for this season in 1975 According to the evaluations in 1987 for the last 12 years the noise level at the same station has increased by about 25% in comparison with 1975 (8).

The great number of numerical seismograms for 3.4.1987 allawed showing several instances of three - dimensional representation of the diurnal noise variations (fig. 3a). Three - dimensionalgraphs for the same stations (respectively TSS) are drawn up on fig. 3b, for a holiday like Mayday.

Stations TSS is stable with respect to the prevailing frequences of maximum radiated energy for the day and night hours.

A 10 times lower level of noise can be seen on Fig. 3. - Station TSS beimg the quietest of all for this period.

An instance of uninterrupted 24-hour spectral components variation is shown for station PLD on 3.4.1987 on fig. 4. The rapid morning increase of noise amplitudes amd their different behavior afterwards is clearly observable in an ordinary warkday. Here the higer amplitudes decrease about midday and stay high till about 22 hours local time.

This figure represents a demonstration of the seismic noise in a large industrial centre in this country.

5. Remarks and conclusions (Coumentaries)

The results obtained characterise same regular components in the seismic noise spectrum corresponding to a different concentration of microseismic energy.

There are stations considerably varying in noise aspect on the multiform relief of this country. Some of them are characterised by a nurrow-band spectrum and constant level for the studied pe-

Fig. 1.: Spectra of some seismic stations in Bulgaria on a quiet day.

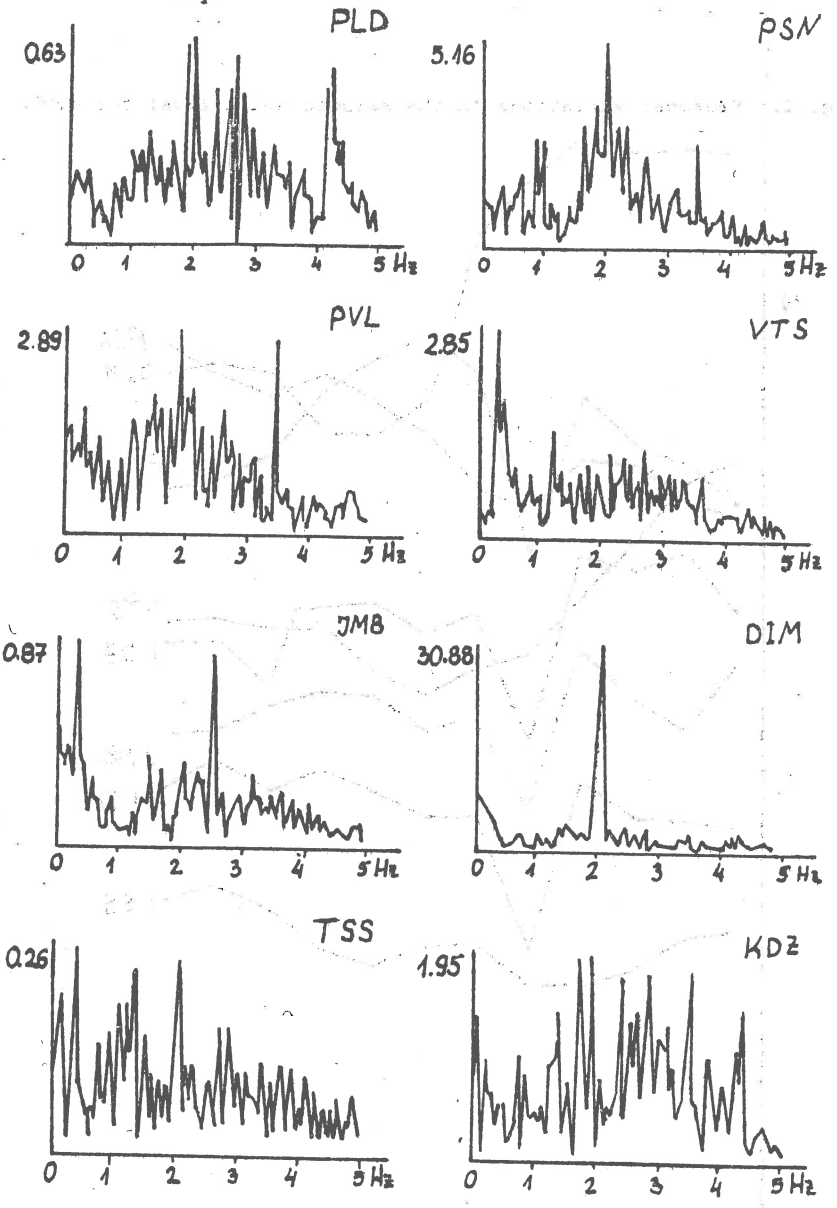

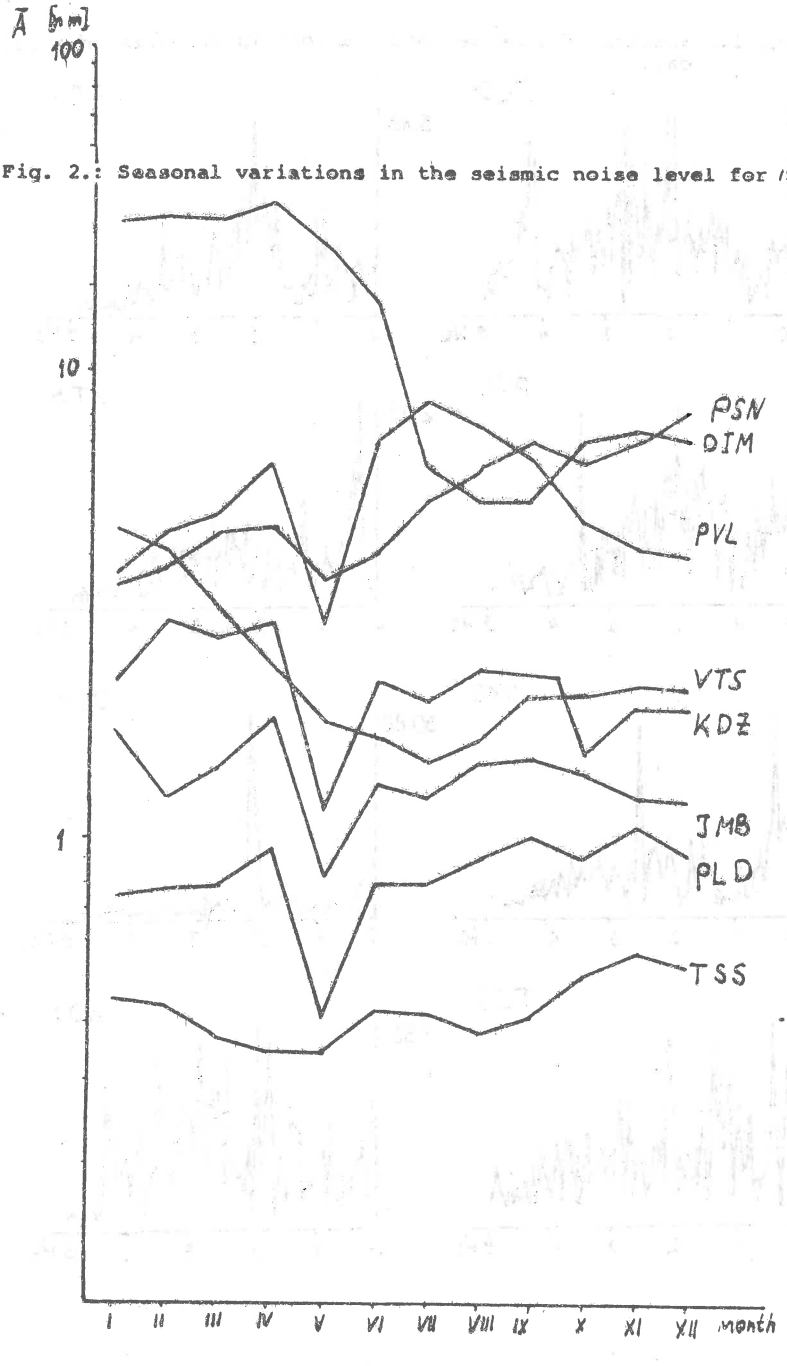

Fig. 2.: Seasonal variations in the seismic noise level for 1986.

TSS

Fig. 3a: 24-hour variations of seismic noise at station TSS on 03.04.1986, Friday (workday) night and day.

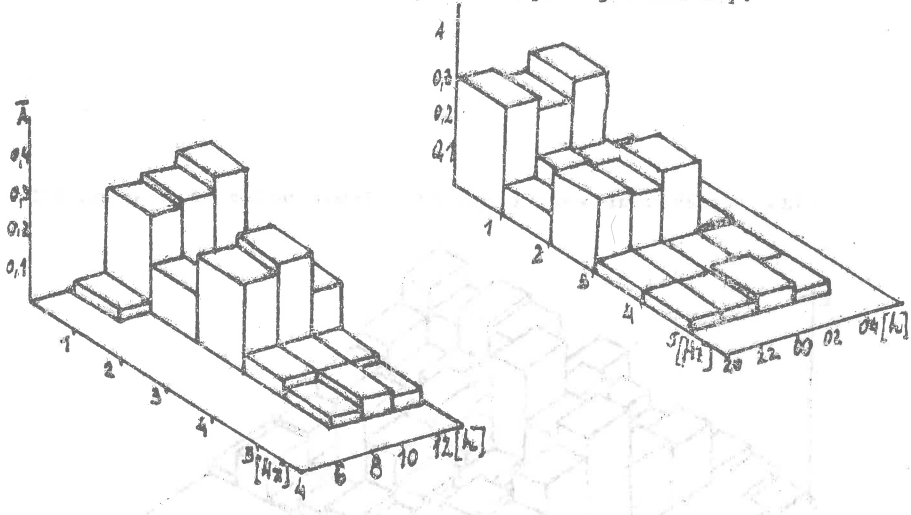

Fig. 3b: 24-hour variations of seismic noise at station TSS on 01.05.1986 (holiday), night and day.

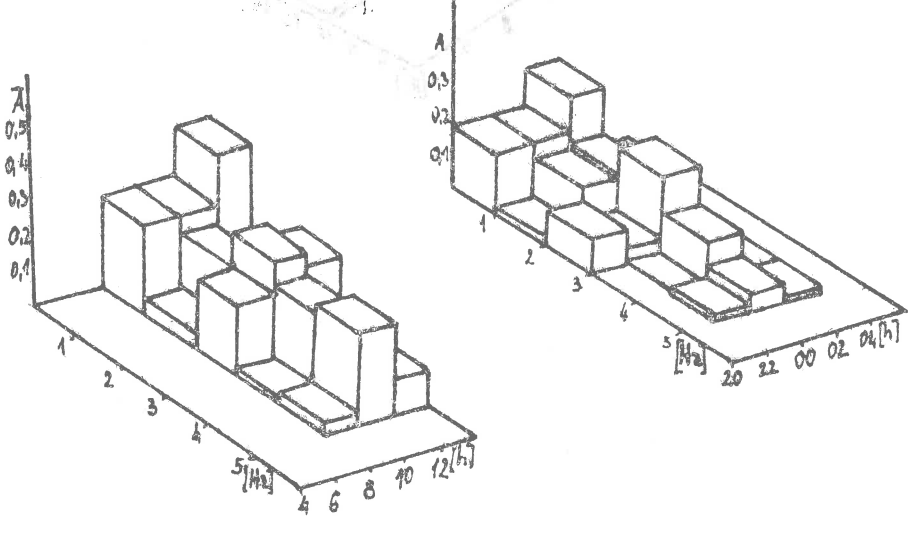

Fig. 4.: 24-hour variations of seismic noise at station PLD.

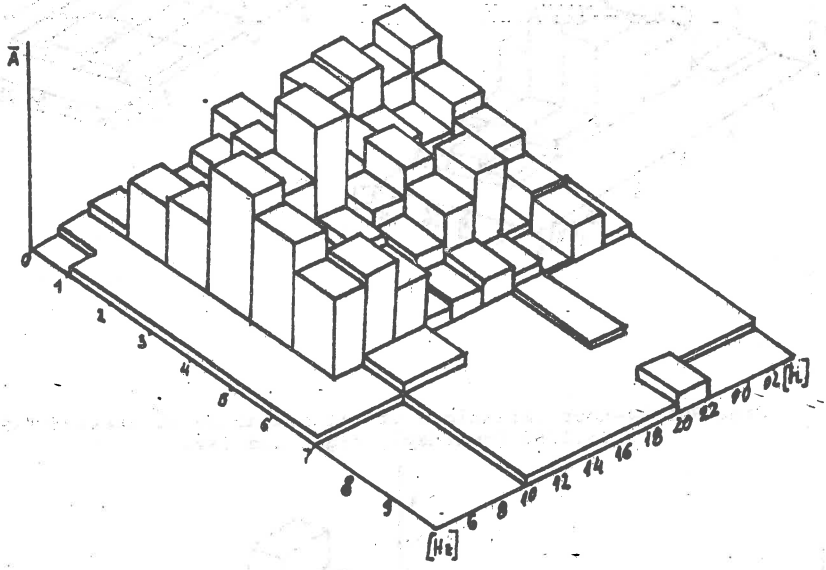

riod (TSS, PLD, JMB, VTS); others by a spectrum of wider band and accidental realisations of monochromatic peaks (PSN, PVL).

The noise measurements used in this paper show monthly variations in the seismic noise field level at the different NOTSSI system stations on the territory of Bulgaria.

The difference between the lowest and the highest noise field intensity on the territory of Bulgaria is up to 280 times for the studéed period.

The spectral evaluations analysis allowed drawing up 24-hour variations of some Bulgarian stations.

References

1. K.Kanai, T.Tanaka: "On Microtremors", Bull. Earthq. Res. Inst., Vol (39), 1961
2. G.Frantti, D.Wiilis, J.Wilson: "The Spectrum of Seismic Noise", BSSA, Vol. 52, Nr.1, 1962
3. E.Hjortenberg, J.Hjelme: "Seismic Noise at Danish Stations in Relation to Detection": Publ. Inst. Geophys. Pol. Acad. Sci., A-9, (135), 1980
4. E. Hjortenberg, T. Risbo: "Monochromatic Components of the Seismic Noise in the NORSAR Area", Geophys. I.R.Astr. Soc., 1975, 42
5. E. Hjortenberg: "Monochromatic Components of the Seismic Noise in the 1-3 Hz Band", Publ. Inst. Geophys. Pol. Acad. Sc., A-5, (116), 1977
6. P. Rodgers, St. Taylor, K. Nakanishi: "System and Site Noise in the Regional Seismic Test Netwerk from 0,160-20 Hz", BSSA, Vol. 77, Nr. 2, 1987
7. Users/Operators Manual for Seismic Data Processing System. Teledyne Geotech, Garland, Tx. 1981
8. L. Christoskov, Tz. Georgiev: "Some Statistical Characteristics of Seismic Short Period Microseisms", Contemporary Geophys. Problems - BAS, 1975

NONLINEAR EFFECTS AT THE PROPAGATION OF SEISMIC WAVES

T. Stojanov, L. Christoskov
Geophysical Institute - BAS

1. Introduction

The non-linear wave events in different media and systems a mainly described by the four most familiar nonlinear wave equations (1): of Cortevig - de Friz, of sinus - Goran, the nonlinear equation of Shredinger and a system of spring masses described by Teday. It is important that they all have solitons describing a different wave characterized by a peculiar behaviour and called soliton. Thus, a soliton is a separate wave with a stable profile propagating in a dispersing medium and manifesting properties of a particle (2).

2. Nonlinear effects in seismic wave fields

Nonlinear seismology is in its starting, investigating stage of its development which determines the particular methods and problems of the studies.

There is a limited number of theoretical elaborations wich are treating the problem of discovering seismic solitons as separate one - parameter waves (3). Experimentally such a soliton of the envelope is observed before the strong earthquake in Chile in 1960 according to the recordings in Pasadena (USA) (4)(Lund). Thus, most generally the conditions for a soliton formation are: the availability of velocity dispersion leading to dephasing of the monochromatic components and a nonlinear change of the wave shape leading to shortering the duration of wave package. As a result of the joint action of these two many-direction processes a stable wave (soliton) is formed.

3. Selection and processing of the used observation data

In order to find out nonlinear seismic effects a series of investigationes are carried out on seismic recordings in real medium on the territory of Bulgatia and part of the territory of the USSR. Records of microseismic storms and of distant earthquakes by the National Operativ System and by the photo-recording instruments in the Bulgarian Stations: VTS, PSN, MMB, KDZ, PVL, PLD and the Soviet PUL, MOS, ASH are used.

The initial evaluation of characteristic amplitudinal pecularites in the wave packages was realized on records of microseisms with sources in the Black Sea and the Baltic, and for earthquakes at teleseismic distances with M 5 - 7,2 a predominatingly from the regions of Iran, Turkey, Thailand and Southern Greece. The ocuration of the wave packages was from 1,5-8 seconds and their parameters below were measured: Amplitude A, period of the carrying frequency T, and the time duration at level 0,7 from the amplitude $\tau_{0,7}$. They were determined the mean duration $\bar{\tau}_{0,7}$, mean period $\bar{T}$, and all the other mathematical operations were made on a personal computer "Prawetz" 82.

For the description of the nonlinear properties of the envelope of wafe fields we proceed from the Shredinger's equation (5).

The solutions of the one-dimension equation of Shredinger are analysed according to their stability depending on the dispersion coefficient b and the nonlinear β_3 .

The analysis of the solutions of the Shredinger's equation

most generally shows thah for an indication of a soliton sign in the seismic wave fields it is necessary to investigate the connection between the width (continuity) of the package and its amplitude.

In fig. 1a the above dependence is shown for microseismic storms n Baltic Seas, fig. 2a-for an earthquake in Taiwan.

The parameter of nonlinearity β_3 can be determined by graphs and by formula to β_3.

$$\beta_3 = \frac{4}{\omega} \cdot \frac{d\omega}{d(A^2)}$$

By the same method was determined the coefficient of dispersion. The graph dependence for b is shown in fig. 1b; for the wave packeges of an earthquake in Taiwan in fig. 2b.

$$\bar{b} = \frac{\omega_0^3 \bar{\tau}_{0,7}^2}{4\pi} \cdot \frac{d\omega}{d\bar{\tau}_{0,7}}$$

4. Results

As a result of the analysis from 24 processed records of microseisms three cases are reflected and 5 results are indicated from 101 processed records of strong earthquakes (table 1). For each separate example in the different columns we have plotted the equations of the straight lines with their respective error σ and the coefficient of correlation r with their perespective value by the t criterion.

In the last column of table 1 according to the analysis for stability of the solution of the Shredinger equation the signs of $\bar{b}$ and β_3 are compared. In six of the cases according to condition $\bar{b} < 0$; $\beta_3 > 0$ a soliton of the envelope of the seismic wave packages exists and two of them, indicated in the table, satisfy condition $\bar{b} > 0$, $\beta_3 < 0$ for the appearance of three - dimension soliton.

Also the comparatively near valwes of the coefficients $\bar{b}$ and β_3, make an impresion, at wich we may consider that in these cases the non-linear phase modulation (compressing the wave package) is balanced with the medium dispersion (expanding the package).

An additional possibility for testing the results in table 1. is given by common condition that the value of the product of the amplitude with the square of the time size of the wave package is constant ($A\bar{\tau}_{0,7}^2$ = const.). The estimation obtained for the respective wave fields are shown in table 2. The percent deviation from condition: $A\bar{\tau}_{0,7}^2$ = const., has different, quite fluctuating valwes but the mean percent deviation for all cases is about 20%. We consider results as satisfactory taking into account the qualitative indication of a nonlinear object.

5. Commentary notes

As a result of the first carried out initial investigations for searching for soliton properties in Bulgaria, some preliminary conclusions can be drawn.

3 of the generally 24 cases about the microseisms and 5 of the 101 about the earthquakes are answering the criteria for solitons of the envelope in the present investigation. This shows that clearly expressed soliton properties in the seismic fields are comparatively rarely observed.

For us remains open the question, whether the soliton properties a rare manifestation in the propagation of the seismic waves or the manner of looking for such properties is imperfect, taking into account that the real medium should favour the origination of non-linear effects.

It is expedient at a positive indication for solitons to

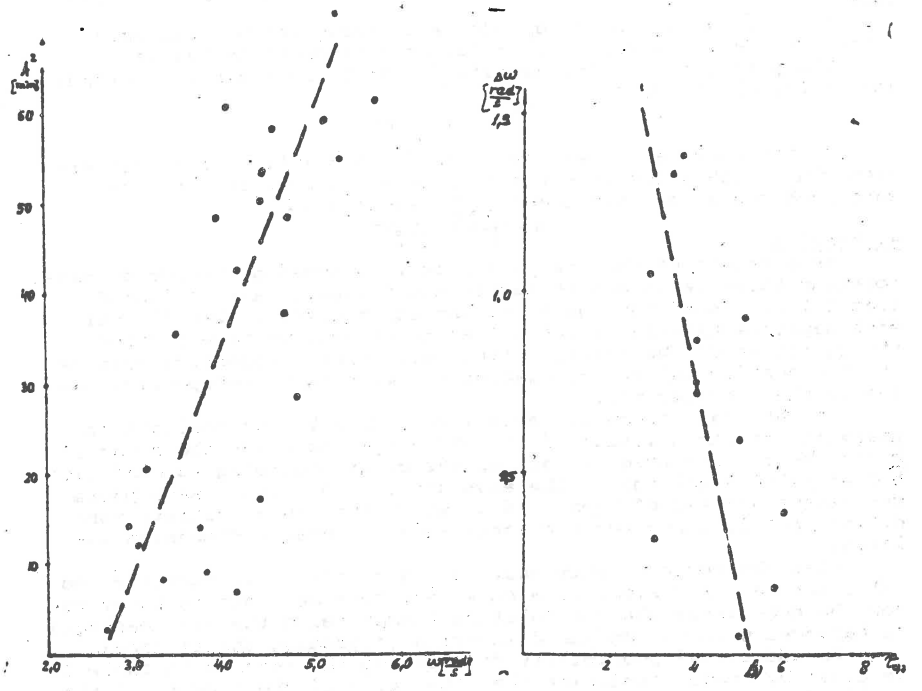

Fig. 1.: A graph of the investigation of the soliton properties of the seismic wave packages envlope from a microseismic storm with a source in the Baltic Sea, in seismic station PVD for E - W component.
a) dependence of the amplitude square A^2 of the carrying frequency of the wave package .
b) dependence of the frequency difference $\Delta\omega$ on the semi-width of the wave package $\tau_{0,7}$

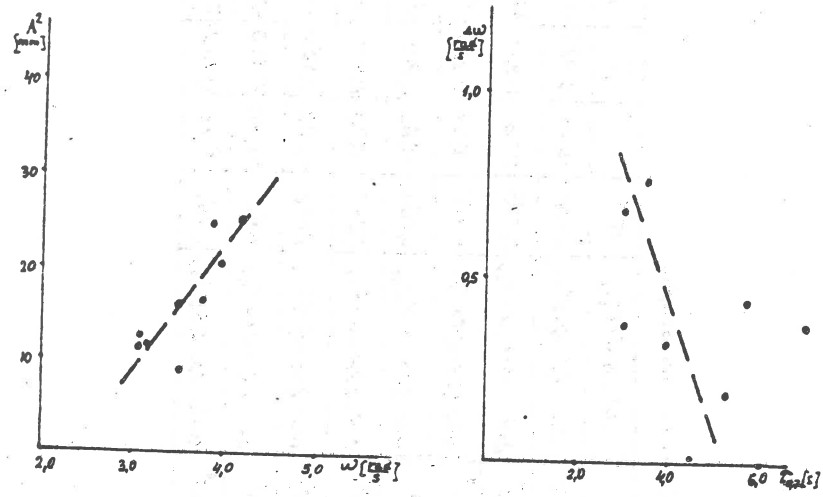

Fig. 2.: A graph of investigation of the soliton properties of the seismic wave packages envelope in the coda an earthquake in Taiwan of 14.11.1986 with M 7,2 for station VTS
(a) and (b) like fig. 1.)

Table 1.: Determination of the parameters $\bar{b}$ and β_3 by the graphs from each stations.

seismic event	station	component	$A^2 = A^2(\omega)$	σ^2	r	P	β_3	$\Delta\omega = \Delta\omega(\tau_{0,7})$	σ^2	r	P	$\bar{b}$	β_3, $\bar{b}$
microseism storm 14/15.11. 1986.	PSM	N-S	$A^2 = -1,25 + 0,032\omega$	0,019	0,49	0,975	$1,33 \cdot 10^{9}$	$\Delta\omega = 1,1 - 0,19\tau_{0,7}$	0,014	-0,45	0,975	$-5,86 \cdot 10^{9}$	$\bar{b}<0; \beta_3>0$
	PSN	E-W	$A^2 = 3,4 - 0,51\omega$	2,863	-0,72	0,990	$-5,2 \cdot 10^{8}$	$\Delta\omega = -0,31 + 0,24\tau_{0,7}$	0,058	0,68	0,995	$3,4 \cdot 10^{8}$	$\bar{b}>0\ \beta_3<0$
	PUL	N-S	$A^2 = -44,7 + 18,8\omega$	191,77	0,73	0,990	$1,26 \cdot 10^{8}$	$\Delta\omega = 3,25 - 0,53\tau_{0,7}$	0,410	-0,67	0,950	$-134 \cdot 10^{8}$	$\bar{b}<0\ \beta_3>0$
earth-q.uake in Taiwan 14.11.1986 M=7,2	VTS	E-W	$A^2 = -31,4 + 136,1\omega$	8,73	0,87	0,950	$5,5 \cdot 10^{6}$	$\Delta\omega = 1,85 - 2,81\tau_{0,7}$	0,062	-0,62	0,975	$-7,5 \cdot 10^{6}$	$\bar{b}<0\ \beta_3>0$
	MMB	E-W	$A^2 = -104 + 28,1\omega$	8,21	0,88	0,990	$2,16 \cdot 10^{6}$	$\Delta\omega = 1,48 - 0,29\tau_{0,7}$	0,037	-0,88	0,950	$-3,26 \cdot 10^{6}$	$\bar{b}<0\ \beta_3>0$
	KDZ	E-W	$A^2 = -11 + 0,48\omega$	248,62	0,44	0,900	$4,89 \cdot 10^{6}$	$\Delta\omega = 1,58 - 0,19\tau_{0,7}$	1,072	-0,08	0,550	$-5,42 \cdot 10^{6}$	$\bar{b}<0\ \beta_3>0$
	PUL	N-S	$A^2 = -41 + 16,4\omega$	16,2	0,43	0,900	$1,29 \cdot 10^{7}$	$\Delta\omega = 1,2 - 0,18\tau_{0,7}$	0,890	-0,48	0,900	$-2,47 \cdot 10^{6}$	$\bar{b}<0\ \beta_3>0$
earthquake in Greece 7.1.83 M=5,5	MMB	Z	$A^2 = 20,6 - 24,4\omega$	120,08	-0,52	0,975	$-8,48 \cdot 10^{6}$	$\Delta\omega = -1,5 + 0,58\tau_{0,7}$	1,261	0,43	0,950	$7,4 \cdot 10^{6}$	$\bar{b}>0\ \beta<0$

Table 2.: The deviations from $\bar{A} \cdot \bar{\tau}_{0,7}^{2}$ = const. for the cases from table 1.

seismic event	station	compon.	$\bar{A} \cdot \bar{\tau}_{0,7}^{2}$	$\pm \sigma$	% deviate from $\bar{A} \cdot \bar{\tau}_{0,7}^{2}$ = const.
micro-seism storm 14/15.11. 1986	PSN	N-S	15,0	1,9	12,6
	PSN	E-W	8,9	2,1	22,0
	PUL	N-S	18,7	3,1	16,1
earthquake in Taiwan 14.11.86. M=7,2	VTS	E-W	50,7	10,2	20,2
	MMB	E-W	133,7	45,4	32,9
	KDZ	E-W	68	7,9	11,5
	PUL	N-S	98,4	18,9	20,2
earthquake in Greece 7.1.83 M=5,5	MMB	Z	33,1	9,2	27

make additional profile (or areal) investigations in order to localize the sections wich are responsible for the formation of strong non-linear properties of the medium.

References

1. Scott E.: "Nonlinear electric-magnit waves", Moscow, "Mir", 1986, pp. 47 (in Russian)
2. Jamb G.L.: "Elements of Soliton Theory", Moscow, "Mir", 1983, pp 10 (in Russian)
3. Rabinovich M.: "Introduction in theory of oscilation and waves", Moscow, "Mir", 1964, pp 306 (in Russian)
4. Lund F.: "Interpretation of the Precursor to 1960 Great Chilean Earthquake as a Seismic Solitary Wave", PAGEOPH v. 121, Nr. 1, 1983, pp 19
5. Ciprakov V.: "Problems in nonlinearyty seismology", Moscow, "Mir", 1987, pp 142 (in Russian)

MICROSEISMIC STORMS IN THE ATLANTIC JANUARY 1-3 AND FEBRUARY 29 - MARCH 3, 1984.

O.V.Pavlov, V.N.Tabulevich, L.A.Drugova, G.M.Troshina*

Institute of the Earth's crust, Siberian Branch, AS USSR
664033 Irkutsk, USSR

*Siberian Energetical Institute, Siberian Branch, AS USSR,
664033 Irkutsk, USSR

The article aims to demonstrate the efficacy of methods of seismic location of sources of microseismic vibrations (SMV) in context with observations of the Hydrometeorogical service.

We have repeatedly suggested a build-up of a World network for a reliable location of SMV and the singular phenomena arising simultaneously with stormy microseisms (radiation of infrasound by standing sea waves, excitations of the atmosphere and ionosphere and oth.) [1,2]

Undoubtedly, the location of SMV could be considerably precisized, provided the stations would be located in different directions around the "epicentre" of the microseisms.

As yet however work on SMV location was limited by observations of microseisms by seismic stations of the USSR [3]. This is obviously a less advantageus a case. Nevertheless even with this "unilateral" station pattern we succeeded to perform locations of SMV with sufficient precision.

The direct problem of determining the field of displacements and velocities from a source given is completely determined (of course, accounting for heterogeneity of the Earth crust, elastic constanss, the Fermi principle etc.). The inverse problem of determining the location of SMV belongs to the class of the so called incorrect problems of mathematical physics. In general it can not be solved unambiguously. There exist methods however, which allow to obtain solutions up to a certain degree of reliability. In our case such methods consist in subordinating the problem to the conditions of frequency synchronism and the application of the concept of power discrepancy [2] .

Seismic stations 1,2...s, which have recorded vibrations from one and the same SMV, have to show a synchronous variation and equality of periods of vibrations (T) at any instant given (t) of the fundamental term of the spectre:

$$T_1 = \varphi(t), \quad T_2 = \varphi(t) \quad \ldots\ldots \quad T_s = \varphi(t) \qquad (1)$$

$$T_1 \approx T_2 \approx \ldots\ldots T_s \qquad (2)$$

Usually a set of seismic station is selected, for which the coefficient of interrelation γ in expression (1) has a sufficient value and the variation of periods ΔT is insignificant ($\gamma = 0{,}8$, $\Delta T = 0{,}3$ s).

The power (energy) of every seismic process, similar to earthquakes, explosions mechanic vibrators and natural sources of excitation (waves, wind etc.) is an invariant quantity. It does not depend on the system of measurement and on the location (sites) of the

seismic stations. Velocities and times of propagation of seismic waves may vary in dependence of the structure of the medium, but the energy, developed in the source, will be constant.

If we have 1,2...s seismic stations, due to which the powers of the SMV is determined, then

$$W_1 = W_2 = \ldots\ldots W_s \,. \tag{3}$$

The differences of powers are to be zero. Under actual conditions the discrepancy of powers will be

$$H = \sum_{j=1}^{s-1} \sum_{i=j+1}^{s} (W_i - W_j)^2 . \tag{4}$$

The amplitude of microseisms in every station

$$A_i = \sqrt{W\,(1+\beta R_i^{-1,5})} \Big/ \sqrt{D R_i}\, \exp[\alpha(T) R_i] . \tag{5}$$

$\alpha[T]$ being the damping coefficient, D a constant depending on the properties of the medium and the period of vibration, β is a constant of composition of the vibrations, characterizing the share of body and surface waves in the micrcseisms.

Denoting $\sqrt{\frac{W}{D}} = W'$ and

$$\varphi(R) = \sqrt{R}\, \exp[\alpha(T) R] \Big/ (1+\beta R^{-1,5})$$

we obtain for s stations:

$$\begin{aligned} W_1' &= A_1 \varphi(R_1) \\ W_2' &= A_2 \varphi(R_2) \\ &\ldots\ldots\ldots\ldots \\ W_s' &= A_s \varphi(R_s) \end{aligned} \tag{6}$$

To obtain the coordinates of SMV and its power we chose on the Earth surface a lattice which is to contain the presumed SMV.

The discrepancy of power and distance are computed for every point of the lattice. R is determined accounting for the Earth sphere [2]. the computer searches a point in the lattice, for which the discrepancy of power H has a minimum. This point coorresponds to the SMV with the coordinates φ, λ and a power W.

The field of power discrepancies visually demonstrates the process of searching the coordinates of SMB (fig.1,2). For a SMV theoretically given the PD H_{min}, at any number of stations is to be zero. Actually the input data are subjected to errors and the PD for a set of three stations will be

$$H_3 = (W_1 - W_2)^2 + (W_2 - W_3)^2 + (W_3 - W_1)^2 \tag{7}$$

The location of SMV - H_{min} in the lattice determined due to data of three or n stations is to have the same coordinates. Obviously, the reliability of the result increases with the number of input data. Fig.-s 1 and 2 show the field of discrepancies in the coordinates φ, λ, H for two cases:

1. The determination was performed under precize conditions 1 and 2 with $\tau = 0,95$; $\Delta T = 0,1$ s. Fig.1a shows the discrepancy field for three and fig.1b for four seismic stations. The PD was $H_{min} = 8.10^{-3} W$ Js^{-1} for three stations and $H_{min} = 1,5.10^{-3} W$ Js^{-1} for four stations. The coordinates were $\lambda = 30$ deg E, $\varphi = 75$ deg .
2. In the determinations an error in amplitudes was introduced

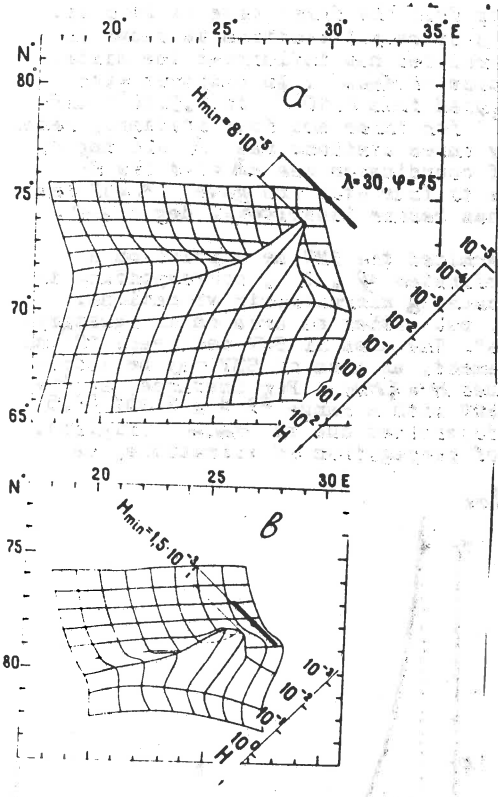

Fig.1 Variation of the power discrepance of coordinates φ, λ for SMV having φ =75deg. λ =30deg.E.
a- H determined due to three,
b- due to four seismic stations.

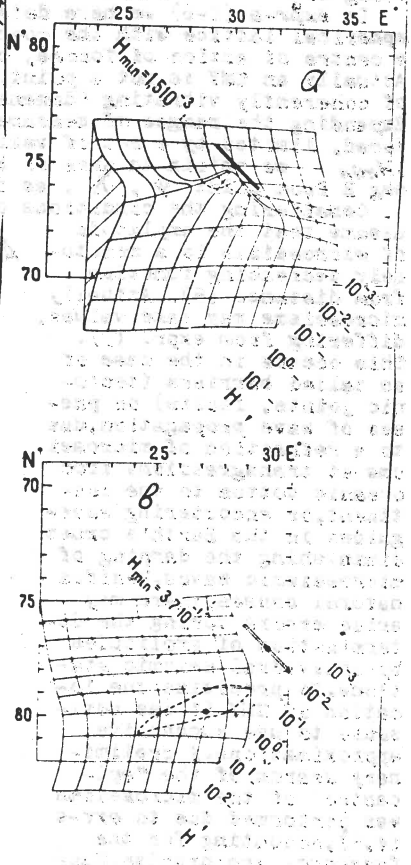

Fig.2 Variation of the power discrepancy H accounting for error in amplitudes
a-calculation of H performed due to three stations,
b-due to four stations.

Amplitudes were taken, differing from the first case by 20 p ct. The field of discrepancies for 3 or resp.4 stations is shown in fig.-s 2a and 2b. The error introduced has influenced the distributions of the PD and the location of H_{min}. As compared with the first case the PD has increased from 8.10^{-3} to $1,5.10^{-3}$ and from $1,5.10^{-3}$ to $3,7.10^{-3}$ W Js^{-1} for three and four stations, resp. The location of SMV obtained by three stations was λ =26 deg E; φ =78 deg, i.e. the decline of coordinates was $\Delta\lambda$=1-4 deg E; $\Delta\varphi$ =3 deg N. Determination due to four stations gave λ =32 deg E; φ =76 deg N. The decline has become lower: $\Delta\lambda$=2 deg E; $\Delta\varphi$ = 1 deg N.

In expr-s (4-6) we have determined the SMV as a point on a spherical lattice with the coordinates φ, λ, corresponding to a centre of action of forces, causing microseismic vibrations. Actually an SMV is not a point, but rather an area on an equatory of coherently vibrating "domens". The area of SMV can reach 10^2 km^2. Expanding the ranges of measurement, an area of SMV may be introduced, limited by a set of values $H \leq \xi H_{min}$. For instance, at $H = 3H_{min}$ we obtain an area of SMV with a range ± 3 deg N and $\pm 1,5$ deg E from point φ, λ, as determined due to H_{min} (fig.2b).

Considering the conditions of propagation of vibrations, we assume that the amplitude of microseisms is a monotonely decreasing function from distance (5). Actually microseisms may take values, differing from expr. (5). This occurs in the case of so called barriers (tectonic joints, faults) on passes of wave propagation, due to a refraction of microseisms at transgressions from oceanic bottom to the continent, or encoutering waveguides in the Earth's crust diminishing the damping of microseismic waves. Besides natural causes, there may arise errors during the determination of amplitudes by individual seismic stations. To precisize the location of SMV it was advisable to use successive approximations. A preliminary search of the "epicentre" of the microseisms was performed due to exr-s (4,5), acounting for the frequency synchronism. Successive precision of coordinates and an evaluation of errors was performed by means of comparison of the curve

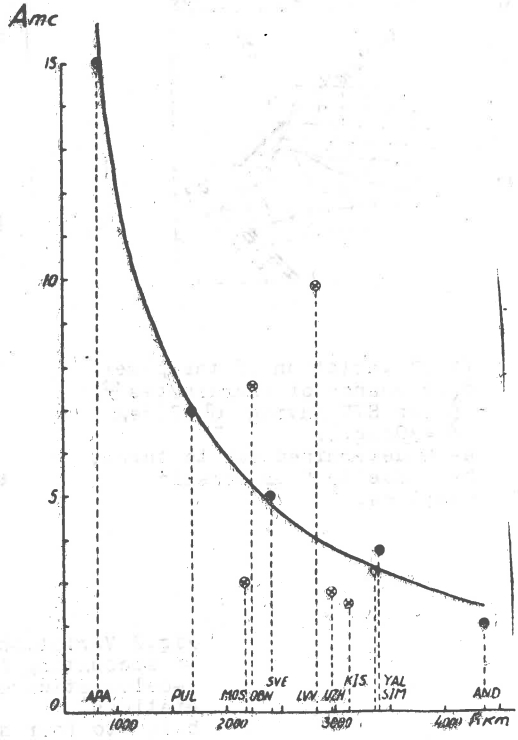

Fig.3 Theoretical decrease of amplitudes of microseisms due to expr.(5) and actual amplitudes of microseisms for stations.

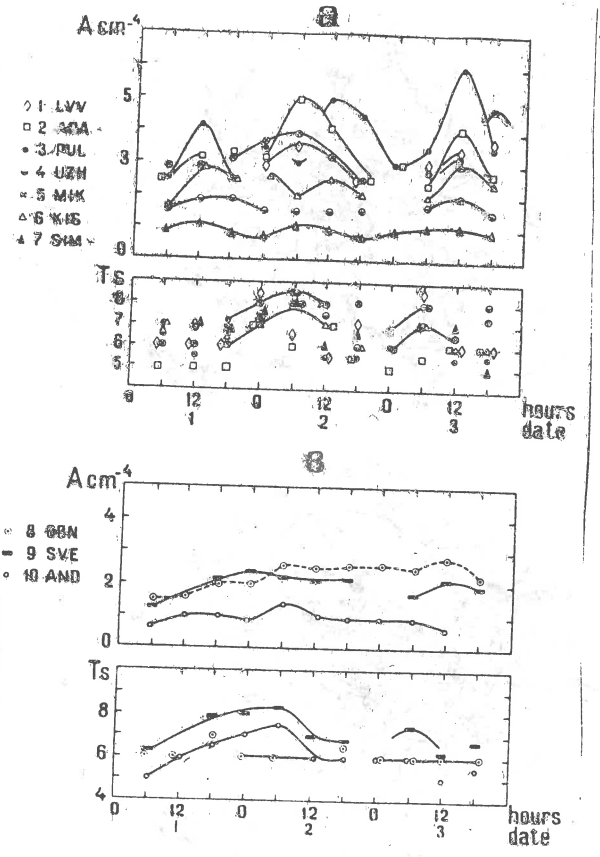

Fig.4 Periods (T) and amplitudes (A) of microseisms from a storm, occured January 1-3, 1984 in the Northern Atlantic. Abbreviation of seismic stations:
a. 1-Lvov(LVV), 2-Apatity(APA), 3-Pulkovo(PUL), 4-Uzhorod(UZH), 5-Minsk(MIK), 6-Kishinyov(KIS), 7-Simferopol (SIM),
b. 8-Obninsk(OBN), 9-Sverdlovsk(SVE), 10-Andijan(AND).

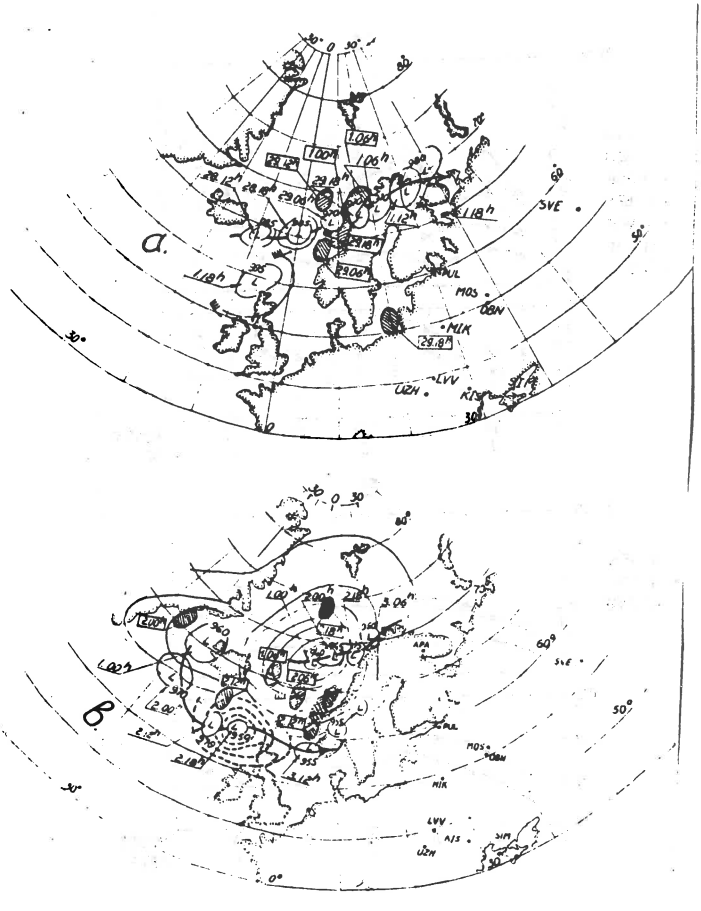

Fig.5 Displacement of cyclones in the North Atlantic and SMV. By arrows displacements of cyclones are shown. Dates show the sites of atmospheric lows (L). Shadowed ovals show the sites of SMV, their data are given in rectangles. Symbols of stations are given in fig.4 captian.
a - Meteorologic situation Febrruary 28,29 - March 1, 1984.
b - Meteorologic situation January 1-3, 1984.

of theoretical decrease of amplitudes (5) with actual values, recorded by stations. As an "epicentre" of SMV and its power the first approximation was taken. Fig.3 gives a comparison of theoretical (full line) and actual amplitudes of microseisms (point and crosses) for a SMV, recorded 12h October 24, 1983 and having the coordinates φ=75 deg N λ=30 deg E; W=10^{17} Js. From fig.3 it may be seen, that stations Apatity, Pulkovo, Sverdlovsk, Simferopol, Andijan have recorded amplitudes of vibrations close to theoretical values. Stations Uzhgorog, Kishinyov reported amplitudes, declining by 20-30p ct. and stations Moscow, Obninsk and Lvov showed values differing by a factor of two from the theoretical. These stations were further excluded from the set of stations used for determinations with exp(5)

From the full Bulletin of stormy microseisms of 1984 [3] we have chosen two extra intensive storms January 1-3 (fig.40 and February 29, March 1-3 (Fig.6).

Storm January 1-3, 1984. A complicated meteorological situation has arisen January 1-3, 1984 above the Northern part of the Atlantic (fig.5). January due first a deep cyclone with a pressure 940 mb (=0-3 deg E, =67-69 deg.) was moving in a N-E direction (shown by an arrow). At the same time at the shores of Greenland another cyclone has originated (960 mb), which has gradually deepened and has moved in an Eastward direction towards Great Britain. Its Location 18h January 2 is shown by dotted lines.

The SMV, and therefore sources of generation of infrasound are shown by shadowed areas. The location was performed due to stations Apatity, Pulkovo, Sverdlovsk, Moscow, Obninsk, Minsk, Lvov, Kishineyov , Uzhgorod, Simferopol.

Fig.4 shows variations of periods and amplitudes of microseisms at the stations mentioned. Areas SMV January 1.06h and 12h January 2 were located at the rear part of the cyclone in the ocean and at the Scandinavia shores. One of the SMV January 2 12h was located in the area of convergence of opposite winds of the northern and southern cyclones. The maximum power of SMV was recorded Jan.2 12h. It was equal to 3,2.10^{17} Js .

Storm February 29, March 1-3, 1984. Fig.6 shows diagrams of amplitudes and periods of microseism of the Atlantic, recorded by seismic stations of the USSR. On fig.5a the movement of the cyclone is shown and a location of SMV is given. Characteristic is the position of the SMV along the Scandinavian coast and in the open ocean. These SMV had periods 6,5-8,0 s. The maximum power was recorded 29.1.12h, it equalled 2,6.10^{17} Js . 29 at 18h a SMV was recorded in the Baltic sea with a period of microseisms 5 s.

Along with locations of SMV due to microseismic data in the present work, as well as in previous papers, data of the Hydrometeorological service USSR were involved.

By means of SMV location unusual phenomena are disclosed, occurring in the atmosphere and the ocean. Areas of radiation of microseisms, of standing waves, variations of physical properties of the atmosphere, areas of disturbance of propagation of radiowaves and increasements of geomagnetic storms are located. These phenomena are not observed by satellites.

The SMV location, performed for cyclones January 1-3 and February 29 and March 1-2, 1984 enables to evaluate the extra ordinary phenomena mentioed above by means of observations, carried out in point of the Earth surface, remote from SMV.

References

1. Tabulevich V.N. Complex investigations of microseismic vibrations. Novosibirsk,"Nauka",1986, 149 p., (in Russian).

2. Tabulevich V.N., Brandt I.S., Troshina G.M.
On excitation sources of microseismic vibrations in the North Atlantic Ocean and the North Western Pacific Ocean, Fourth Report of the IASPEI, Commission on Microseisms, Ed.H.Korhonen, Inst. of Seismology, Univ. of Helsinki, Report 3-5, 1981, p.43-60.

3. Tabulevich V.N., Drugova L.A. Bulletin "Observations of microseismic vibrations by seismic stations of the USSR for 1984" Irkutsk, Inst. of the Earth Crust, ICD-B2 Moscow, 1987, 257 p. (in Russian).

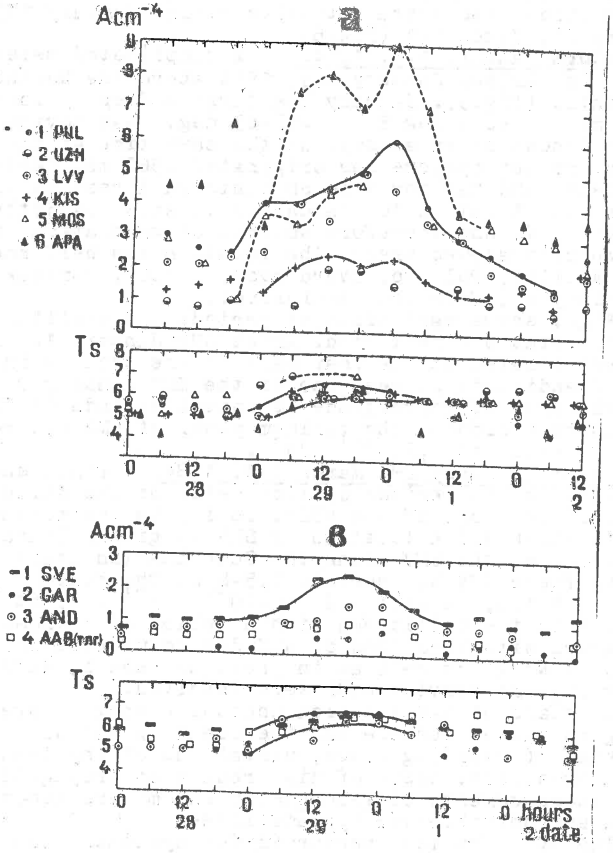

Fig.6 Variation of amplitudes and periods of microseismic vibrations for February 29, March 1-3, 1984. Symbols of seismic stations in caption to fig.4. Additionally: Moscow (MOS), Garm (GAR), Talgar (AAB).

CERTAIN COMMON PROPERTIES AND PECULIARITIES OF PROCESSES OF STRONG EARTHQUAKE PREPARATION

B.G.Pustovitenko, A.G.Kamenobrodsky, E.I.Porechnova

Inst.Geoph.Ac.Sc.Ukr.SSR, Simferopol;
State University by M.V.Frunze, Simferopol

For the strongest earthquakes of different regions a phenomenon of migration of the weak shock epicenters to the zone of a future strong earthquake has been established /1-5/.

For a discription of spatial distribution of the weak shock epicenters we have introduced the quantity r_i (i=1,2...N), where r_i is the distance between the strong (main) earthquake epicenter and consistently occured previous and following epicenters of the weak shocks. The representative shocks, which differ by an energy level from the main shock by 2-4 orders and are located on the area commensurable with size of the zone of preparation of a strong shock of such magnitude, are considered to be weak.

Temporal motion of the process is represented by the function $r(t)$, constructed according to the discrete values r_i. In order to exclude random fluctuations the diagrams $r(t)$ were smoothed three-times by 5 points. For the weak active Crimean region the diagrams $r(t)$ were used without this method of smoothing. The diagrams $r(t)$ have the characteristic maxima and minima. All investigated strong earthquakes of the Crimea were turned out to be corresponding in time to the minima of the functions $r(t)$ /5/.

Now let's consider the diagram $r(t)$ from a position of the development process of an earthquake preparation on the example of the earthquake of Hait (fig.1). After finishing the strong earthquake and aftershock succession the weak shock epicenters are gradually moving away from the focal zone to the outlying districts: r_i increase up to the limit values at some moment t max. At this time seismicity becomes weak in the focal zone, the seismic "calm" phase comes. Then this process begins to displace again (to drawn up) to the focal zone, gradually localizing in it: $r_i \to r_{min}$. Sometimes the seismic "calm" comes again before the main shock -utter lack of the weak shocks on the whole investigated territory, a mean-urgent herald /2,6/. Probably, r_{max} and t max characterize size of the

zone and time of this "calm" in the zone of preparation and r min and t min characterize size of the focal zone and time of the second "calm" immediately before the onset of distruction at the source.

This phenomenon of gradual drawing up the weak shocks to the main shock zone is a sign of an earthquake preparation.

Quantitative characteristics of the diagrams $r(t)$ have appeared to be different for the earthquakes of a different energy level and, namely, the stronger main shock was, the larger distance r max the weak shock epicenters were removing away at and much time t max was between r max and the main shock moment.

For the Crimean earthquakes it has been established /4,5/, that the parameters of the extreme values $r(t)$: r max, r min, δt max, δt min, and also the difference $\delta r = r$ max $- r$ min ("amplitude") were directly connected with the main shock magnitude in the range M=3,5÷6,8. The values δt max $= t_0 - t$ max and δt min $= t_0 - t$ min - are the time intervals from the main earthquake moment t_0 to the correspondent points of the extrema r max and r min, corresponding to t max and t min. The equations of regressions have the next form:

$$\lg \delta \tau = (0,91 \pm 0,09) + (0,14 \pm 0,02)\, M \quad (1)$$

$$\lg r \text{ min} = (0,56 \pm 0,09) + (0,16 \pm 0,02)\, M \quad (2)$$

$$\lg \delta t \text{ max} = (0,92 \pm 0,11) + (0,40 \pm 0,02)\, M \quad (3)$$

Dependence of the quantitative parameters of this sign upon the strong earthquake magnitude allows to distinguish different processes of preparation of the events of different energy levels. For the regions with considerably different seismotectonic processes similar dependences may differ, but a common tendency of connection of the sign parameters with the magnitude must be preserved. Examination of the separate earthquakes of the Middle Asia and Kamchatka has shown, that the real magnitude values of the earthquakes and the estimated ones according to δr of the functions $r(t)$ with use of the formulae (1) are close to each other. Apperently, size of the earthquake zones of different regions doesn't differ considerable. At the same time, time of development of the process and velocity of drawing up the epicenters in the Middle Asia and Kamchatka have appeared to be 2-4 times higher, than in the Crimea.

Using all common properties of processes of an earthquake preparation discribed above it may be possble to find those places in the region, to which the weak shock epicenters are drawing up. For this purpose the investigated area is scanned by the following way. Knots

of a coordinate net are successively (over 1° or 0°5) taken for the main shock epicenter, and the distances r_i are measured relative to every j-th conventional epicenter. Further, a family of diagrams $r_j(t)$ is constructed, and the parameters (δr_j, δt_j, $r_{j\,min}$ and so on) are estimated and plotted on the map of the region correspondingly the location of an j-th conventional epicenter. It appeares, that the strong earthquake epicenters are disposed near the areas outlined by the extreme values δr, δt_{max} and the least values r_{min}. In this way, the zones of preparation of the strongest earthquakes ($M \geqslant 7$) of the Kuril-Kamchatka and Middle Asia regions (fig.2) and the appreciable Crimean earthquakes ($M \simeq 4$) have been retrospectively restored.

In the regions with complex tectonics and in the presence of many cross fractures of the earth crust the drawing up of the weak shock epicenters to the place of a future fault may occure differently along each of the fractures (structures). Also, intensity and velocity of seismic processes, to all appearence, are different in the nearest and remote zones of preparation. That is why in order to construct the diagrams $r(t)$ it is not necessary to use all weak shock epicenters, but those only, which are on the areas of definite configuration. Two configurations have been considered:

1. It was suggested, that some volume of the earth crust, surrounding a source on all sides uniformly, took place in a source area formation. On the plan this is a circle or a ring with a center in the examined earhquake epicenter. The circle radius and ring width are the variable quantities.

2. It was suggested, that some volume of the earth crust, adjoining to the linear (stretching) structure of the earth crust took place in a source area formation. On the plan this is a band of an apprpximitely right-angled form. The weak shock epicenters were picked out in the bands with dimensions corresponding to the zone preparation. These bands included the main shock epicenter and were oriented along each of the cross fractures and also in the intermediate directions.

Let's illustrate the method described above on the example of processes of the strongest earthquake preparation of the Middle Asia and Kuril-Kamchatka regions. For the earthquake in Hait (1949, M=7,4 , φ=39°,2 , λ =70°,8) intensity of the processes appeared to be different in the structures of different orientation. In connection with it data selection was conducted in the rectangles 600×300 km,

located along the meridian, on latitude and dragonally. More distinctly the earthquake preparation sign is displayed in the variant with meridional orientation ($\delta r \sim 150$ km) (fig.1). Investigation of dependence δr on the dimensions of a circular zone of data selection shows, that δr is small in the nearest and remote zones ($\Delta < 200$km and $\Delta = 600 \div 900$ km), where the processes are either irregular or subjected to the influence of the neighbouring large earthquake sources.

For the Kamchatka earthquake of 1971 (M=7,8 , φ =55°,9 , λ =163°,4) the diagrams $r(t)$ are different for the zones located along and across the main tectonic structures: velocity of migration along the seismic zone $\sim$ 22 km/yr, across it $\sim$ 9 km/yr.

For the earthquake of 1969 (M= 8,2 , φ =43°,3 , λ =147°,8 , Shikotan) the variant with a circular zone of data selection appeared to be the best one. Apparently, some volume of the earth crust relatively evenly surrounding the earthquake source, took part in this considerable event preparation. Velocity of migration of the weak shock epicenters there is about 44 km/yr.

CONCLUSION

The investigated strongest earthquakes of the different seismic active regions display one common property of their preparation processes: monotony of the process of drawing up the weak shocks to a future strong earthquake zone. Dependence of the quantative parameters of the sign on a magnitude allows to differ processes of preparation of the events of different energy levels. Due the method of scanning the whole region and mapping out the sigh parameters, there is a possibility to single out the zones, to which the seismic process is drawing up, i.e., to localize the place of a future main earthquake. For the regions with complex tectonics it is necessary to take into account a possible difference of the seismic processes along and across the main structures and also in the nearest and remote zones, adjoining to the place of a preparing earthquake.

On the example of the Crimea, the Middle Asia, the Kuril and Kamchatka it has been shown, that velocity of migration of the weak shock epicenters to the zone of a future strong earthquake is different not only for the different seismic active regions but also for the separate earthquakes within the single region and, apparently, it is connected with local seismotectonic conditions of a concrete structure.

REFERENCES

1. Моги К. Предсказание землетрясений. М.: Мир, 1988. 382с.
2. Нерсесов И.Л., Пономарёв В.С., Тейтельбаум Ю.М. Эффект сейсмического затишья при больших землетрясениях. //Исследования по физике землетрясений. М.: Наука, 1976. с. 149-169.
3. Соболев Г.А., Завьялов А.Д. Локализация сейсмичности перед Усть-Камчатским землетрясением 15.XII.1971г. //Изв. АН СССР, Физика Земли, 1984, № 4, с. 17-84.
4. Pustovitenko B.G., Kamenobrodsky A.G. Investigation method of processes of strong earthquake preparation //Europ. Seismol. Commission XX General Assembly, Abstracts. Moscow, 1984, p. 32 .
5. Каменобродский А.Г., Пустовитенко Б.Г., Поречнова Е.И. Пространственно-временные распределения эпицентров слабых толчков как индикатор подготовки сильных землетрясений. //Изв. АН СССР, Физика Земли, № 10, 1987. с. 3-10.
6. Прогноз землетрясений. № 3 / отв. редактор Садовский М.А., Душанбе-Москва: Дониш, 1984. 216с.

LEGENDS TO THE FIGURES

Certain Common Properties and Peculiarities of Processes of Strong Earthquake Preparation

B.G.Pustovitenko, A.G.Kamenobrodsky, E.I.Porechnova

Fig.1. The diagram $r(t)$ of the earthquake in Hait, 10.VII.1949, M=7,4 .

Fig.2. Re-establishing of the zone of preparation on the example of the earthquake in Markansu, 11.VIII.1974 (φ=39°,39 , λ=73°,86 , M=7,3).
Isolines: 1- δr , 2- $r$min, 3-crossing of the areas of extreme values δr, $r$min , 4- the earthquake epicenter.

Fig.3. The data selection zones and correspondent diagrams $r(t)$ of Kuril-Kamchatka region. The dotted-line shows the zone boundaries of data selection of the weak earthquakes, participating in preparation of the strong earthquakes:

a- Kamchatka, 1971 , M=7,8
b- Iturup , 1973 , M=7,5
c- Shikotan , 1969 , M=8,2

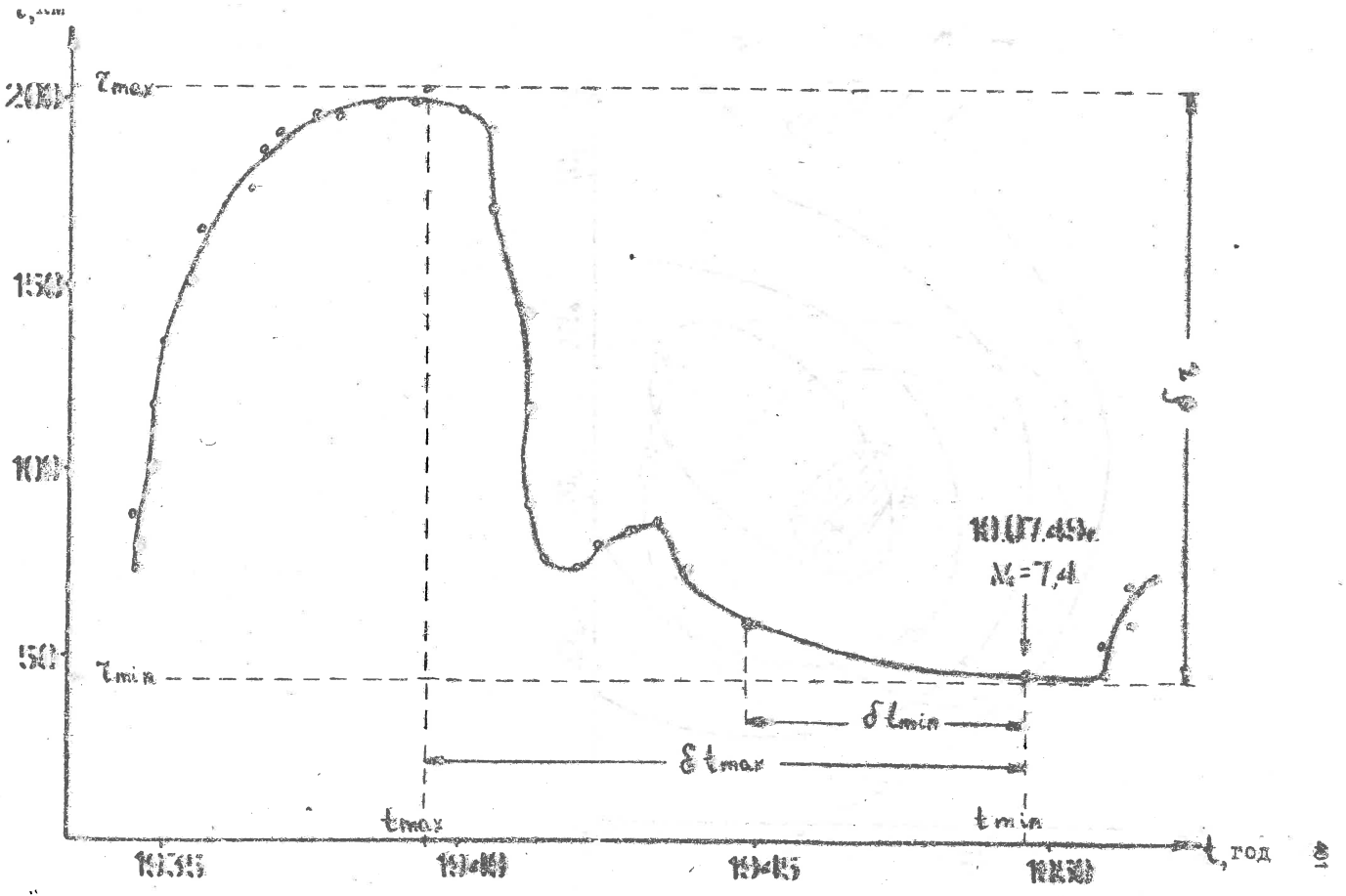
T, K
200
150
100
50
Tmax
Tmin
δ tmin
Σ tmax
tmax
tmin
t, год
N=7,4

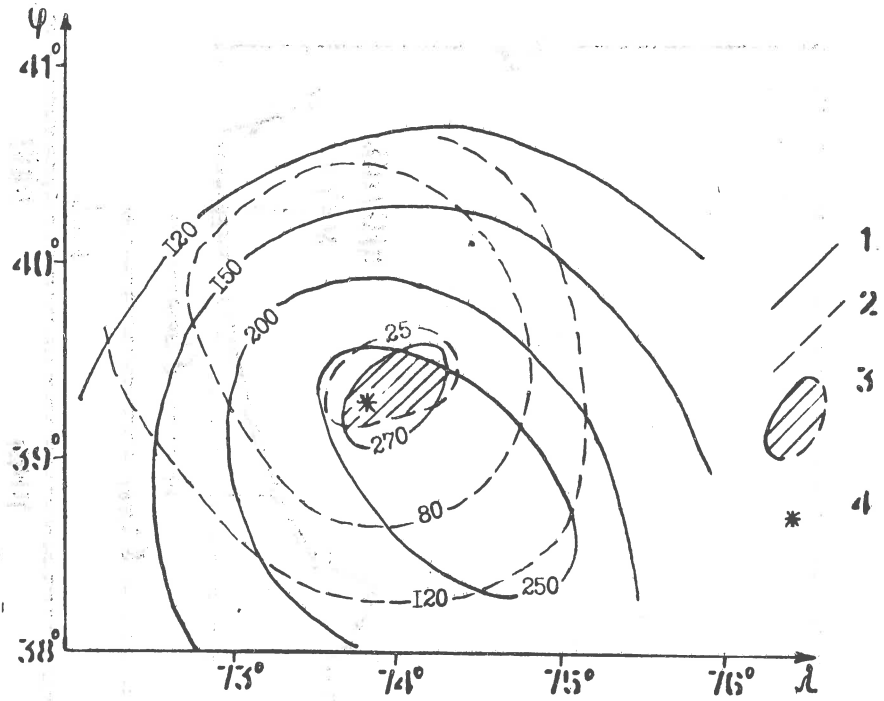
φ
41°
40°
39°
38°
73°
74°
75°
76°
λ
120
150
200
25
270
80
120
250
1
2
3
4

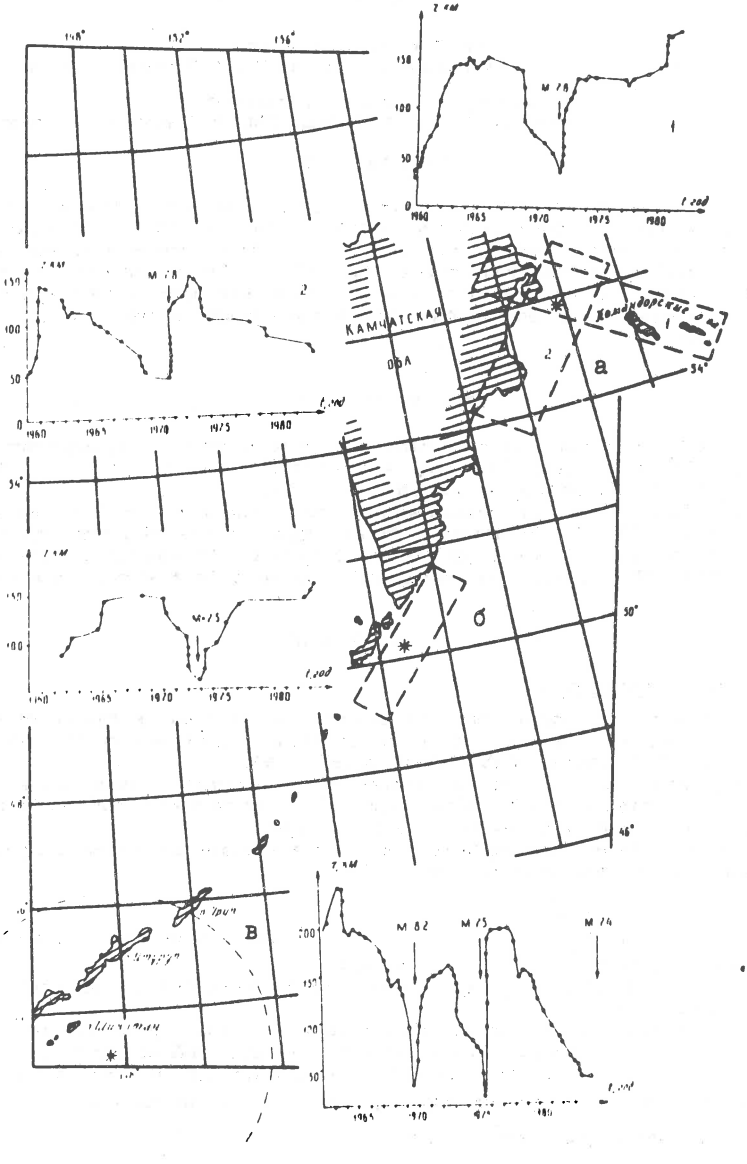
M 7.8
M 7.8
M 7.5
M 8.2
M 7.5
M 7.4
КАМЧАТСКАЯ
ОБЛ
Командорские о-ва
а
б
в
1
2
54°
50°
46°
1960
1965
1970
1975
1980
t год

ANOMALIES OF CODA WAVE PARAMETERS CORRELATED WITH LARGE VRANCEA INTERMEDIATE EARTHQUAKE OCCURRENCE

Victoria Oancea, Olivia Bazacliu
Center of Earth Physics and Seismology, P.O.Box MG-2, Bucharest, Romania

Georgeta Mihalache, Al. Dumitrascu
Department of Mathematics, INCREST, Bd. Pacii 220, 79622 Bucharest, Romania

INTRODUCTION

Studies regarding the earthquakes from different seismic regions in the world (Kurile-Kamcatka, California, Vrancea) pointed out anomalies in the time behaviour of some coda wave characteristics in the period preceding the occurrence of strong events in the area (Chouet, 1979; Gusev and Lemzikov, 1980, 1984 a,b; Oancea and Bazacliu, 1988).

In this paper, the temporal variation of two coda wave parameters is analysed: its envelope shape and its frequency content, for the intermediate earthquakes of the Vrancea region, Romania.

OBSERVATIONAL DATA

A set of 345 intermediate Vrancea earthquakes which occurred during September 1981 - December 1986 are analysed. The events have duration - based magnitudes $3.0 \leq M_D \leq 7.0$ and depths $61 \leq h \leq 201$ km (Radu et al., 1984; Radu, 1988).

The analogue and digital seismograms of three stations of the Romanian seismic network (MLR, CFR and TLB) are used. The seismograms are velocity recordings obtained with a short-period S-13 seismometer (vertical component). The epicentral distances range between 80 and 200 km; MLR is the nearest station, providing the best results in our study.

DATA ANALYSIS

A. Coda envelope shape

The analysis regarding the coda envelope shape is based on the method proposed by Gusev and Lemzikov (1980) for the Kurile-Kamcatka region and on previous results obtained for the Vrancea region (Oancea and Bazacliu, 1988).

The parameter α, describing the deviation of the envelopes of individual earthquakes from the mean envelope built for a "normal period", is obtained as described in Oancea and Bazacliu (1988). Briefly, it consists in the following steps:

- the peak-to-peak amplitudes A of the coda envelope are read on every analogue recording, at 5 s interval, beginning after the time

$$t_c = t_s + 2(t_s - t_p) \qquad (1)$$

from the origin time (t_p, t_s = the arrival times of P and S waves) and till the recording amplitude decreases to twice the noise amplitude;

- the dependences $\log A(\log t)$ are obtained for every event (t = the time measured from the origin time);

- the mean envelope for a normal period (characterized by the absence of strong earthquakes) is built; in our study, the chosen normal period is 1982 January-May;

- the deviations of the individual envelopes $\log A_i(\log t)$ from the mean one $\log \bar{A}(\log t)$ are estimated, by computing the parameter α from the relation:

$$\log A_i(\log t) - \log \bar{A}(\log t) = \alpha_i t + \beta_i \qquad (2)$$

where β_i characterizes the recording level;

- the dependences $\alpha(t)$ are plotted for each station; based on their similarity, a mean dependence $\bar{\alpha}(t)$ over the three stations is obtained;

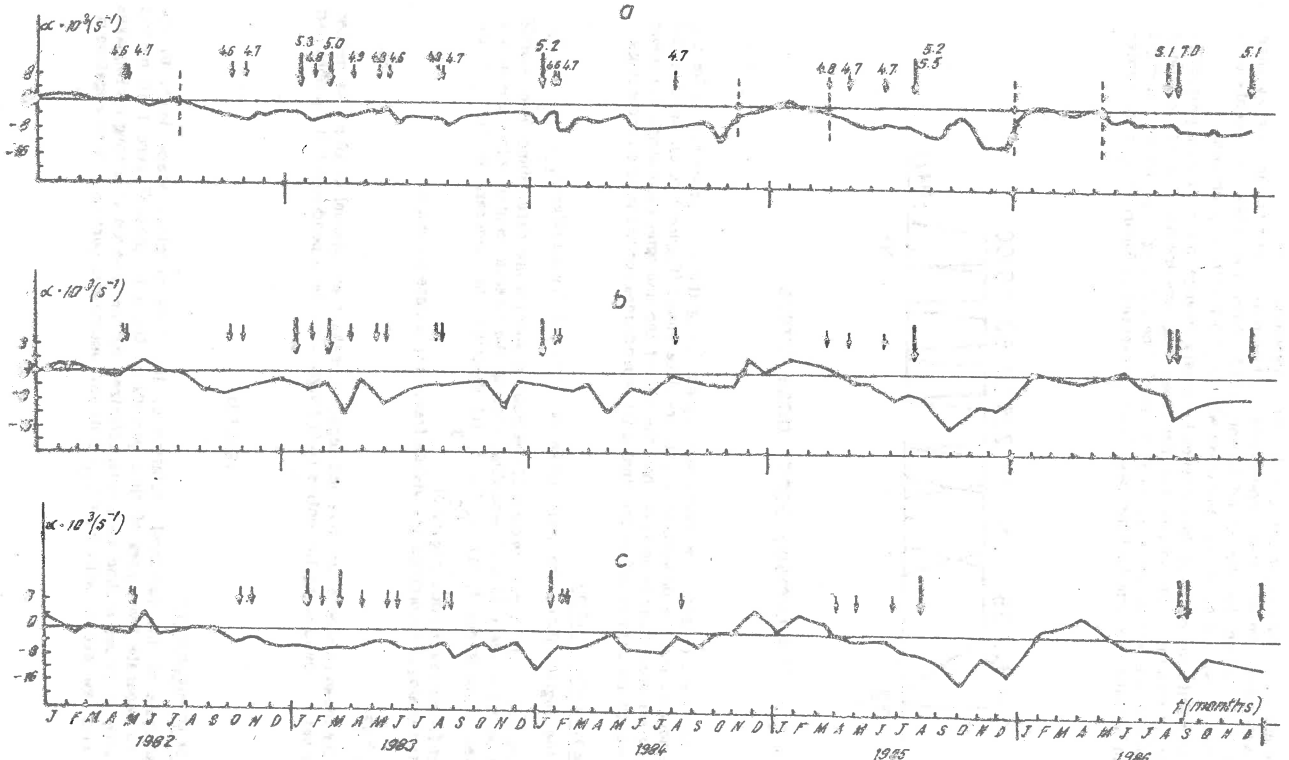

Fig. 1. The temporal variation of the parameter α, for the original seismograms (a) and for the recordings filtered in the second (b) and third (c) frequency bands.

- the anomalies noticed on the α (t) dependences are analysed.

Figure 1 a presents the smoothed dependence α (t) obtained using the moving average procedure for MLR station, for the period January 1982 - December 1986. The events with $M_D > 4.5$ are marked with small arrows and those with $M_D \geq 5.0$ with large arrows.

In order to clarify the cause of the evidenced anomaly: change in the medium properties or in the spectral content of the source, the digital seismograms are band-pass filtered and so the influence of the source spectrum is eliminated. The filtering is performed in eight frequency bands, using the Ormsby band-pass filters presented in Figure 2 (f_c = the center frequencies).

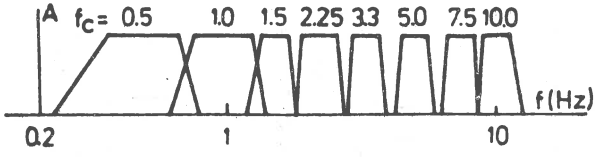

Fig.2. The Ormsby band - pass filters.

The α values are obtained for every seismogram, using the same procedure as for the original seismogram and the dependences α (t) are determined (Figure 1 b, c). Because the number of digital recordings is smaller than the one of the analogue recordings, the mean values on a month are used to define the final α (t) dependences for the filtered recordings.

B. Coda frequency content

Using the digital data, the first three predominant frequencies f_{p_1}, f_{p_2} and f_{p_3} corresponding to the first three maxima of the Fourier spectra are determined. The Fourier spectra are built for every 10 s of recording, moving the interval center with steps of 5 s. The obtained dependences f_{p_1} (t), f_{p_2} (t), f_{p_3} (t) describe the decrease in time of the predominant frequency in coda (Figure 3).

Using the analogue recordings, the visible frequency is determined, as:

$$f_v = \frac{n}{10} \qquad (3)$$

where n is the mean number of positive and negative peaks in an interval of 10 s. The center of the interval is moved along the entire coda length and the dependence f_v(t) is obtained (Figure 4).

RESULTS

A. Coda envelope shape

The analysis of the temporal variation of the coda envelope shape leads to the possibility to separate two types of time periods on the α (t) plots (Figure 1 a): normal periods - with α values around zero (characterized by the absence of strong earthquakes ($M_D \geq 5.0$) and few events with $4.5 < M_D < 5.0$) and anomalous periods - with negative α

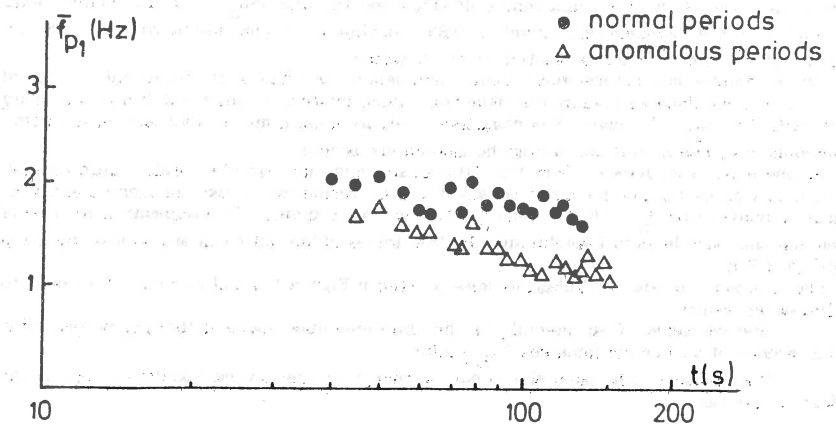

Fig. 3. The dependence of the predominant frequency on time, in coda.

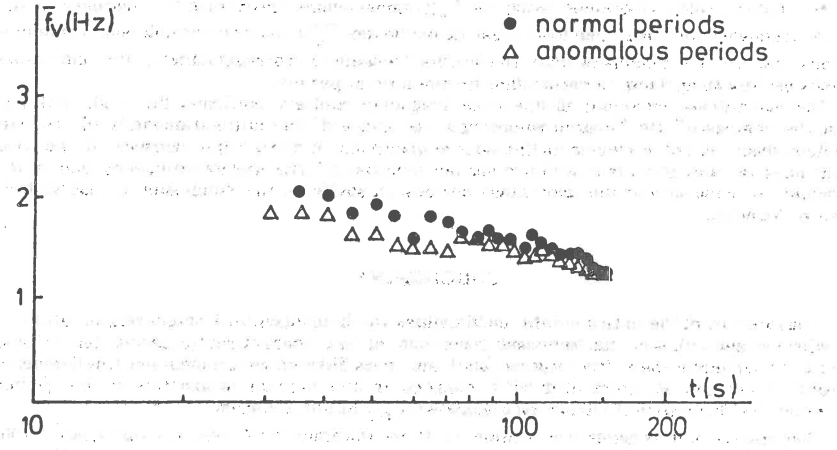

Fig. 4. The dependence of the visible frequency on time, in coda.

values (characterized by the occurrence of strong earthquakes ($M_D \geq 5.0$) and many events with $4.5 < M_D < 5.0$) (Oancea and Bazacliu, 1988). In Figure 1 a the dashed vertical bars are the limits of the time periods separated by the α values.

The anomalous periods precede strong earthquakes; α values returns to values around zero after the earthquake, except the situations when another strong event follows or many events with $4.5 < M_D < 5.0$ occur. The negative α values mean a more rapid decrease in time of the coda envelope amplitude, during the anomalous periods.

On the α (t) plots derived from the filtered seismograms, similar results are obtained. Figure 1 b, c presents the temporal variation of the parameter α for the second and third frequency bands (with f_c = 1.0 Hz and f_c = 1.5 Hz, respectively). The separation in normal and anomalous periods is noticeable and also the limits of the intervals are almost the same as in Figure 1 a.

The similarity of the α(t) dependences plotted in Figure 1 a and Figure 1 b, c leads to the following results:

- the existence of an anomaly of the coda envelope shape in the period preceding the occurrence of strong earthquakes ($M_D \geq 5.0$);
- the cause of the anomaly is not a change in the source spectrum, but in the medium properties.

B. Coda frequency content

Using the dependences f_{p_i} (t) which describe the decrease of the predominant frequency in coda, a difference between the plots corresponding to the earthquakes occurred in the normal and anomalous periods is noticed. Two mean dependences $\overline{f_{p_i}}$ (t) for the two types of periods (normal and anomalous) are determined and plotted (Figure 3). It can be seen that the predominant frequencies corresponding to the anomalous periods are less than those corresponding to the normal periods.

A similar result is obtained using the f_v(t) dependences describing the decrease of the visible frequency in coda. The two mean dependences $\overline{f_v}$(t) on the normal and anomalous periods lead to the conclusion that the visible frequencies corresponding to the anomalous periods are less than those corresponding to the normal periods.

The anomalous behaviour of the coda frequency content confirms the result obtained from the analysis of the filtered recordings: the cause of the noticed anomaly of the coda envelope shape is not a change in the source spectrum. A more rapid decrease of the coda amplitudes (as was obtained) would mean an increase of the source frequency and of the frequency in coda during the anomalous periods, opposite to the conclusion of our analysis (Figures 3 and 4).

CONCLUSIONS

The analysis of the intermediate earthquakes which occured in Vrancea region allows us to evidence anomalies in the temporal behaviour of two characteristic parameters of coda waves: the envelope shape (for original and band-pass filtered recordings) and the frequency content. They can be correlated with changes in the medium properties in the periods preceding the occurrence of strong earthquakes ($M_D \geq 5.0$) in the area.

The results of this paper are similar to those obtained by Gusev and Lemzikov (1980, 1984 a, b) for the earthquakes of the Kurile-Kamcatka region. They concluded that the anomalies evidenced in the envelope shape and in the visible frequency are explained by the increase of the effective absorbtion in the medium.

REFERENCES

Chouet, B., Temporal variation in the attenuation of earthquake coda near Stone Canyon, California, Geophys. Res. Lett., 6, 3, 143-146, 1979.

Gusev, A.A. and Lemzikov, V.K., Preliminary results of the investigation of the coda envelope variations for near earthquakes. before the Usti-Kamceatka earthquake in 1971. Vulkanologhiya i Seismologhiya, 6, 82-95, 1980 (in Russian).

Gusev, A.A. and Lemzikov, V.K.. Anomalies in the characteristics of coda waves of weak earthquakes in the Kurile-Kamceatka zone, Vulkanologhiya i Seismologhiya. 4, 76-90. 1984 a (in Russian).

Gusev, A.A. and Lemzikov, V.K., Temporal variations of the coda envelope shape of near earthquakes. Abstracts of the XIX-th General Assembly of the European Seismological Commission, Moscow, October 1-6, 1984. 36, 1984 b.

Oancea, V. and Bazacliu, O.. The temporal variation of the coda envelope shape for Vrancea intermediate earthquakes. Gerlands. Beitr. Geophysik. 97. 2494-2497. 1988.

Radu, C.. Catalogue of intermediate Vrancea earthquakes with $M_D \geq 3.0$ occurred during 1985 January 1 - 1988 June 30. Manuscript, 1988 (in Romanian).

Radu, C., Ardeleanu. L. and Tenea, L.. Catalogue of intermediate Vrancea earthquakes with $M_D \geq 3.0$ occurred during 1977 June 1 - 1984 December 31, Internal Report 30.81.8/85. II, A_3, 1985 (in Romanian).

SEISMOLOGICAL INDICATIONS FOR PREPAREDNESS STAGES OF 1986 EARTHQUAKES IN CENTRAL NORTH BULGARIA

Rumiana Glavcheva, Ludmil Christoskov
Geophysical Institute - BAS, Sofia, Bulgaria

Abstract
The variation of the seismic activity in time and space has been studied. Two intervals of activation have been observed in-between 1976 - 1986. These intervals are specified as possible preparedness stages.

Two sequences occured in the Gorna Oryakhovitsa seismic zone , Central North Bulgaria, in 1986-1987. Their main shocks were of magnitudes 5.1 and 5.7 on February 21 and December 7, 1986, respectively (Christoskov, Glavcheva et al., 1988).

The source location and the size of the events are not unexpec - ted, since events of magnitude up to 7.0 could be realized in this zone (Boncev, Bune, Christoskov et al., 1981). Some con - siderations on the possibility of predicting the main events are discussed below.

The Gorna Oryakhovitsa zone has been defined by seismological and tectonic data (Grigorova, Grigorov, 1964; Boncev, 1971). The latest strong earthquake occurred in 1913 (M=7). The after- shock activity continued up to 1916. Since that time the seis - micity has been characterized by a gradual decreasing of the energy released. The strongest earthquake is of M=4 in 1963 . This zone is in a seismic quiescence of moderate events for 72 years, or at least for over than 20 years.

The possibility of studying the seismic activity of a low energy level is restricted by the abilities of the seismic stations net- work. For the period 1916-1968 a complete information about felt earthquakes ($M \geq 2.5$) is collected. Since 1968 the majority of local events with $M \geq 2$ have been recorded instrumentally. Since 1971 all events of $M \geq 2$ and since 1982 all events of $M \geq 1.7$ have been located with an adequate accuracy as far as the epicen- tre coordinates are concerned. This is not the case with the depth determinations which are in fact rather approximate.

On the basis of this data set the time variations of the event num- ber, the thickness of seismoactive layer, the annual energy relea - sed and the mean value of the energy for a single event are studied. The results are shown in Figure 1. It is evident that since 1976 an active period has set in in the zone. In the years 1976-1981 the annual energy released is 15.5 times bigger than in the pe - riod of 1971-1975. The number of seismic events has grown up to 6 times in comparison with the previous period of time. The gene- ral trend of activation is characterized by some periodicity in the energy release with a period of 4-5 years. Since 1982 this period has become twice shorter. This fact and the effect of a certain decrease of the total activation may specify the interval 1982-1985 as a separate preparedness stage prior to the 1986 earthquakes.

Fig.1. SEISMIC PATTERN CHANGES IN TIME

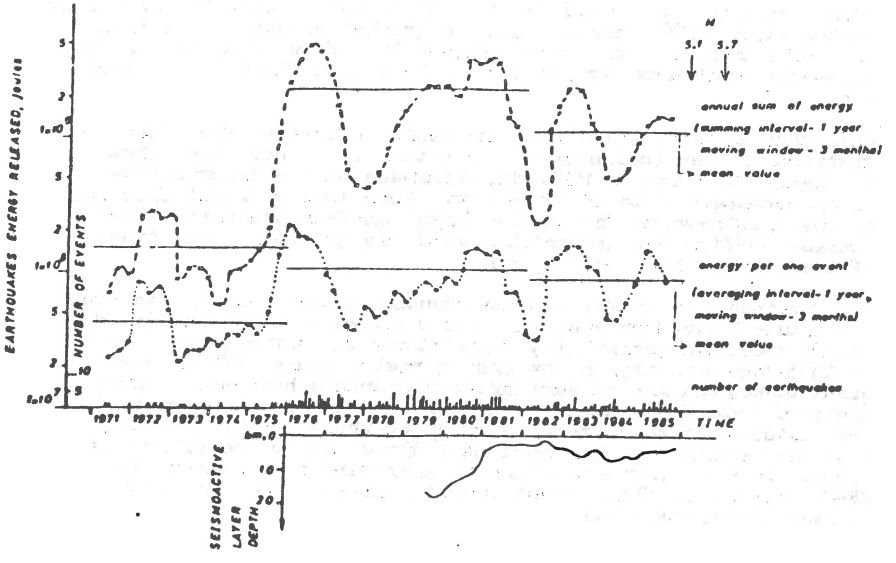

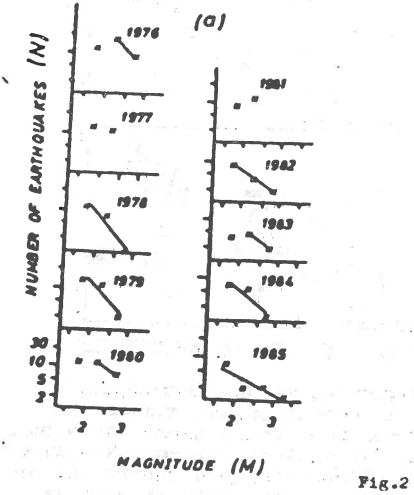

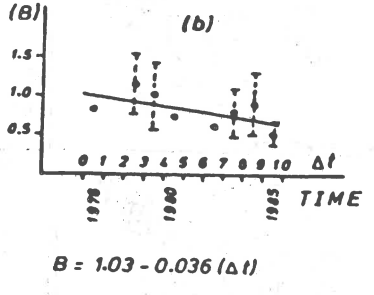

Fig.2

(a) ANNUAL RECURRENCE GRAPHS $\log N = A + BM$ of all the Eqs registered

(b) TIME CHANGES OF THE SLOPE "B"

An attempt is made to obtain the recurrence graphs for the earthquakes since 1976 (Figure 2a). The graphs' slopes have a trend of a slow decrease with time (Figure 2b). This tendency may be connected with some variations of the stress field in the whole zone.

Considering the precision of the depth estimates, the time variations of the thickness of the active layer only are shown in Figure 1. Prior to 1981 the thickness of the seismoactive layer decreased from 15 to 1-2 km. Since 1982 a slight increase of the thickness of the active layer has been observed. These changes confirm the assumption about the possible variations of the stress field in the zone.

The distribution of the microearthquake epicentres is presented in Figure 3 for five specific time intervals which correspond to the observed periodicity from Figure 1. In the years 1967 to 1975 the activity is low and sporadic. since 1976 a subsequent concentration of earthquake epicentres has been observed. Spots of relatively higher epicentre density are seen near to the future aftershock zones during the whole period 1976-1985. They are located in the south-west direction to the aftershock zones. More over, their shape has a prominent extension in NE-SW direction. This orientation is inherited by the later formed aftershock zones.

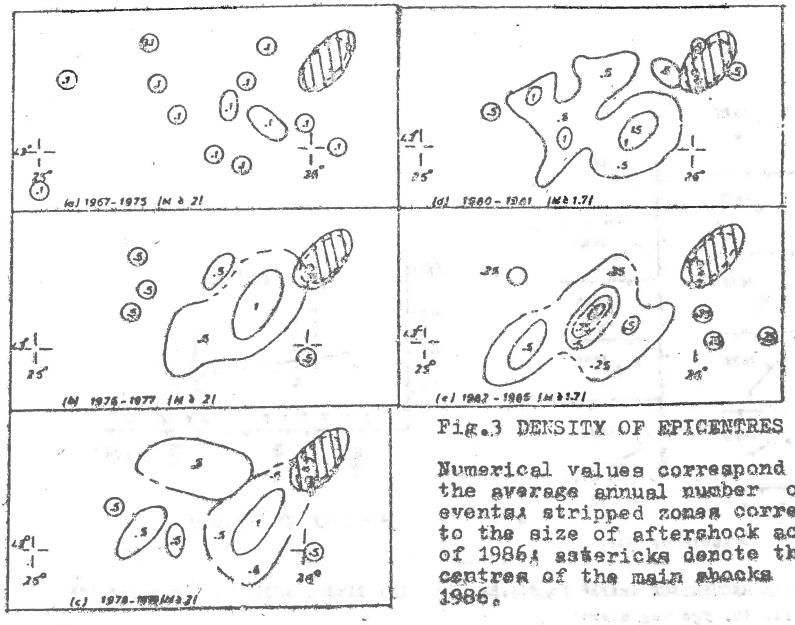

Fig.3 DENSITY OF EPICENTRES

Numerical values correspond to the average annual number of events; stripped zones correspond to the size of aftershock activity of 1986; astericks denote the epicentres of the main shocks in 1986.

At the initial stage (1976-1979) these spots are very close to the aftershock zones. Since 1980 the size of the spots of the high density has been reduced and the spots appear at a certain distance in the same south-west direction from the area of the further strong activation (Fig.3d, e).

As follows from Figure 1 and Figure 3, 1976 might be assigned as the beginning of the active preparedness process.

In addition, the distribution of the seismic energy released in the Gorna Oryakhovitsa zone is considered. It could be seen from Figure 4 that the annual energy realized confirms in general the trend in the seismicity pattern presented in Figure 3 and briefly discussed above.

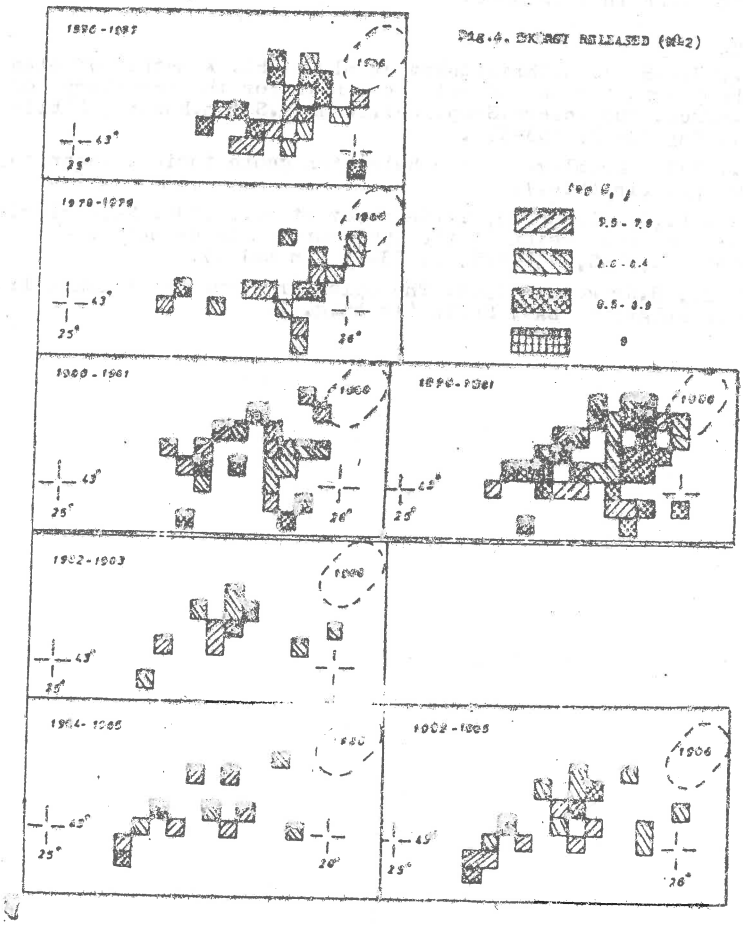

Fig.4. ENERGY RELEASED (ergs)

The results from Figure 3 and Figure 4 show that the seismic activity in the last four years before 1986 is continuously reduced in the vicinity of the future active zone.

In conclusion, it could be emphasized that a ten-year active preparedness period is specified. It is characterized by a general increase of the seismic activity and a subsequent decrease of the slope of the magnitude-frequency graph. Two separate stages of this process may be defined: the first one (1976-1981) is typical with a concentration of the activity near to the future aftershock zone and a relatively bigger thickness of the seismogenic layer; the second stage is characterized by a certain reduction of the micro-activity (energy and number of events), receding of the active spots from the future aftershock zone and an obvious decrease of the thickness of the seismogenic layer. The observed pattern might be of use in understanding the further cases of quiescence and/or activation in the Gorna Oryakhovitsa zone for the purpose of earthquake forecasting in this zone.

References

Bončev E., V.I.Bune, L.Christoskov et al., 1981. A method of elaboration the prognostic map of seismic zoning for the territory of Bulgaria.-Proc. 2nd Intern.Symp.Anal.Seism.a.Seism.Hazard, Liblice, Czechosl., May 18-23, 553-573.

Bončev E., 1971. Problems of the Bulgarian geotectonics. Technics, Sofia, 202 pp. (in bulg.).

Christoskov L., R.Glavcheva, Tz.Georgiev et al., 1988. Seismological features of the region of the 1986 earthquake sequence. - Bulg.Geophys.J., BAS, vol.XIV, 2, 73-89 (in bulg.).

Grigorova E., B.Grigorov, 1964. The epicentres and the seismic lineaments in Bulgaria. BAS, Sofia (in bulg.).

DEVELOPMENT OF THE FOCAL ZONE OF THE CRIMEA EARTHQUAKE ON JULY 5, 1984

B.G.Pustovitenko, S.A.Kapitanova, T.A.Panteleeva

Department of Seismology, Inst.Geoph.Ac.Sc.Ukr.SSR, Simferopol

By seismological signs the area of a preparing earthquake was singled out in the central part of the Crimean region in 1983 with M=5±1 /1/. This earthquake occured on July 5, 1984 in the earth crust of the Black Sea region within the prognosticated coordinates with the energy class K=11,4 ;MLH=3,7 , and intensity of 3-4 on the coast /2/.

The main shock was accompanied by the number of repeated shocks unusual for this energy level and forestalled by the foreshock succession. More than 200 shocks with $K \geqslant 5$ were registered in the focal zone during six months. Such splash of a seismic activity level in the Crimea wasn't observed since the time of abatement of the aftershock process of the destructive earthquake of 1927 with M=6,8 /3/.

The process of energy release was complex and multiple with several periods of stiring up and calm (fig.1). On the whole, the shock series of 1984 may be attributed to the following type of succession: foreshocks- a main shock - aftershocks. An energy gap between the main shock and the strongest foreshock and aftershock accounted for Kf=1,9 , Kaf=0,7 , respectively.

The focal zone was stretched in near the latitudinal direction along the main seismogenerating structures of the continental slope region of the Black Sea and was divided into two local subzones: a foreshock zone (block I) and an aftershock one (block II) (fig.2 a). The focal zone extent is more than 20 km in the latitudinal direction and about 15 km in the meridional direction. Predominant depths of the sources in the block I were within 10÷17 km, and in the block II - 20÷25 km (fig. 2b,3).

Spatial localization of the hypocenters of the whole of the series of the earthquakes had some common features with the destructive earthquake succession of 1927: /3/ I-the strong foreshock and the main shock had different focal zones by orientation and size; 2-the seismological zone of the whole of this succession had a submur-

sion from west to east ; 3- the strongest foreshocks and aftershocks (K ≥ 10) migrated along the zone and on the depth (fig.2b). This migration velocity in the eastern direction accounted for 1,2 km during twenty-four hours and in the opposite direction was less by one order.

Let us regard different stages of the focal zone development. The process of accumulated energy release and preparation for the main fault began in the western part of the focal zone (in the block I) at the depth of 10-20 km nine days before the main shock (stage I, fig. The foreshock area in the period from June 24 to July 2 (03h.17min) was stretched in the west-eastern direction with Az=320°(140°) and its extent was 15 km (stage I). Three days before the main shock this process of medium destruction displaced to the eastern part of the zone (to the block II) at the depth h=20-25 km (stage 2). The azimuth of the largest stretched part of this new foreshock zone with the extent L=11km was preserved (Az=320° or 140°). The main shock occured on July 5 at 03h,07min at the depth of 18 km on the edge of the second aftershock zone. The repeated shocks, followed by the main shock during the first twenty-four hours (stage 3) formed a compact zone at the depth of about 25 km near the main fault with the aftershock zone orientation in the eastern direction with Az=70°(250°) and L=7 km. The most part of accumulated energy released during this period. The next stage of release (stage 4) enveloped the whole of the focal zone (block I and II) and continued during three months yet. Isolation of the western and eastern subzones was preserving as before and practically their main contours didn't change on the plan and depth. On October 5 the process of energy release ended with a comparatively strong shock with K=10 in the northern part of the block I.

Extent of the zone of the medium destruction in the sources of the separate earthquakes with K > 9 have been investigated with use of the azimuth travel time curves of the maximum phase and period of a longitudinal wave by the methods /4/. The azimuth travel time curves of the moment differences of arrival time of the maximum amplitude of the wave P(t pm) record and the first arrivals (tp) at the group of stations surrounding the source are represented in the fig.4.

For the six earthquakes the azimuth travel time curves had two maxima, that allowed to conclude in accordance with theoretical notions, that the process of development of this destruction occured in

the form of a double-directed fault. Azimuthal distribution of the periods in the P-max wave (Tm) repeats the form of the azimuth travel time curves (t pm-tp).

The main shock had the double-directed fault with the azimuths of propagation 140° and 245° and extent of the wave radiation zone 12 km and 6 km, respectively, with the velocity of breaking 6,0 and 5 km/sec. It is interesting to note, that these values coinside with orientation and extent of the foreshock zone immediately before the main shock (stage 2) and with the aftershock zone, formed during the first twenty-four hours of the maximum release (see fig.3). The strongest aftershocks inherited one of the fault directions of the main shock, namely, in the azimuth 140°; the foreshocks of the second stage had the one-directed fault oriented close to latitude.

Space-time distribution of the source dynamic parameters also gives some notion about peculiarities of thesource zone development. The values of seismic moments (Mo), circular dislocation radii (r_o) and faulted stresses ($\Delta\sigma$) received by Fourier spectra with use of the dislocation model of Brune have been considered /5/. To exclude dependence of the source parameters on the earthquake energy not the values were considered, but their deviations $\delta \lg M_o$, $\delta \lg r_o$, $\delta \lg \Delta\sigma$ relative to the average long-time dependences for the Crimean earthquakes: $\bar{M}_o(K)$, $\bar{r}_o(K)$, $\Delta\bar{\sigma}(K)$ [6] $\delta \lg M_o = \lg M_{oi} - \lg \bar{M}_o$

There are certain common similarities and peculiarities of the source parameters of all these earthquakes.

For the majority of these earthquakes of the both foreshock and aftershock periods the underestimated values of the seismic moments Mo and size of a fault r_o and faulted stresses $\Delta\sigma$ (fig.5) are typical. Some deviations from the common tendency were observed in the process of development of the focal zone and, probably, were connected with peculiarities of the medium in the eastern and western parts of the zone (blocks I and II).

The beginning of the process was characterized by the underestimated values of Mo and r_o. Two days before the main shock (when the release process transfered into the block II) the values $\Delta\sigma$ became two times as large and Mo and r_o approached to their average long-time values. During the forth stage of the focal zone development the sources with small dimensions of fault and underestimated values of seismic moment appeared in the blocks I and II. For all this, the average deviations $\delta \lg M_o$ were larger in the block II, than in the block I. These variations in behaviour of the source parameters of the foreshock and

aftershock subzones can be explained by the difference of the source radiation orientation relative to the seismic stations in the different periods and by the properties of the deep medium where the seismic faults have occured. The whole complex of earthquakes of the focal zone of 1984 with the volume of 3000 km^3 for 3,5 months made a contribution to the tectonic deformation equal to $4 \cdot 10^{-8}$, that was by 2 orders below the medium deformation during the earthquake of 1927 with M=6,8.

C O N C L U S I O N

The earthquake of 1984 occured in the zone of the joint of the most travelling structures of different extent in the central part o the Crimean region. Development of the process was occuring in the latitidinal direction, passing from the higher levels of the crust to the lower levels. The focal zone was shaping through the several stages, each of those had its own peculiarities; the main shock had a double-directed fault. The foreshock period prepared the medium for the fault formation and extension into the sourth-eastern direction in the time of the main shock. The aftershocks occured on the whole along the second fault in the time of the main shock, namely, into near the latitudinal direction. The majority of the weak shocks as well as the main shock were more high-frequency, had the underestimated values of the fault dimensions in comparison with the shocks of the same energy level of past years.

The total volum of the destructed medium in the time of the earthquake series of 1984 accounted for 3000 km^3, that was equivalent by energy to a stronger earthquake with K=14 ($M \approx 5,5$), as it was expected in /1/.

The complex character of the investigated genetically connected group of the earthquakes resembles to the destructive earthquake succession of 1927 occured there, but with another lower energy level.

REFERENCES

1. Пустовитенко Б.Г.,Каменобродский А.Г. Исследование процессов подготовки землетрясений по распределению эпицентров слабых толчков //Геофиз.журн.1984.Т6, №4 с.44-52
2. Пустовитенко Б.Г.,Кульчицкий В.Е.,Пантелеева Т.А. Землетрясения Крыма.//Землетрясения в СССР в 1984г.М.:Наука, 1987, с.19-27
3. Пустовитенко Б.Г.,Кульчицкий В.Е.,Аверьянова В.Н.,Шебалин Н.В. Об особенностях очаговых зон сильных крымских землетрясений 26 июня и 11 сентября 1927 года.// Вопросы инженерной сейсмологии, вып.18, М: Наука, 1976. с.103-114.
4. Горбунова И.В.,Кальметьева З.А.- Новые характеристики протяжённости очаговой области близких землетрясений -Изв.АН СССР, сер."Физика Земли", №3, 1982, М.34-46с.
5. Brune J.N. Tectonic stress and the spectra of seismic shear waves from earthquakes. // J.Geophys.Res. - 1970, 75,p.4997-5009
6. PustovitenkoB.G., Kamenobrodsky A.G., Kulchitsky V.E., Panteleeva T.A., Porechnova E.I. Regional aspects of seismic precursors display of the earthquake in the Crimea on May 28, 1983. // European seismological commission XIX General Assembley. Abstracts, Moscow, 1984, p.32

Legends to the Figures

Development of the Focal Zone of the Crimea Earthquake on July 5, 1984

B.G.Pustovitenko, S.A. Kapitanova, T.A.Panteleeva
Department of Seismology, Inst.Geoph.Ac.Sc.Ukr.SSR,
Simferopol

Fig.I. Time motion of the energy release (in the values of the energy class K).

Fig.2. Space-time structure of the focal zone.
a - a general plan of the focal zone.
The circles denote the earthquake epicenters of different values of the energy classes K.
b -migration of the strongest earthquake epicenters along the zone and at the depth.

Fig.3. Different stages of the focal zone development in the plan of (φ, λ) and at the depth h. The solid circle denotes the main shock epicenter.

Fig.4. The azimuth travel time curves of the P(a) waves and their periods (δ). Special notion is used for every value.

Fig.5. Changing of the deviations of the dynamic parameters of the sources $\delta lg M_o$, $\delta lg r_o$ and $\delta lg \Delta\sigma$ in time in the blocks I and II of the focal zone.

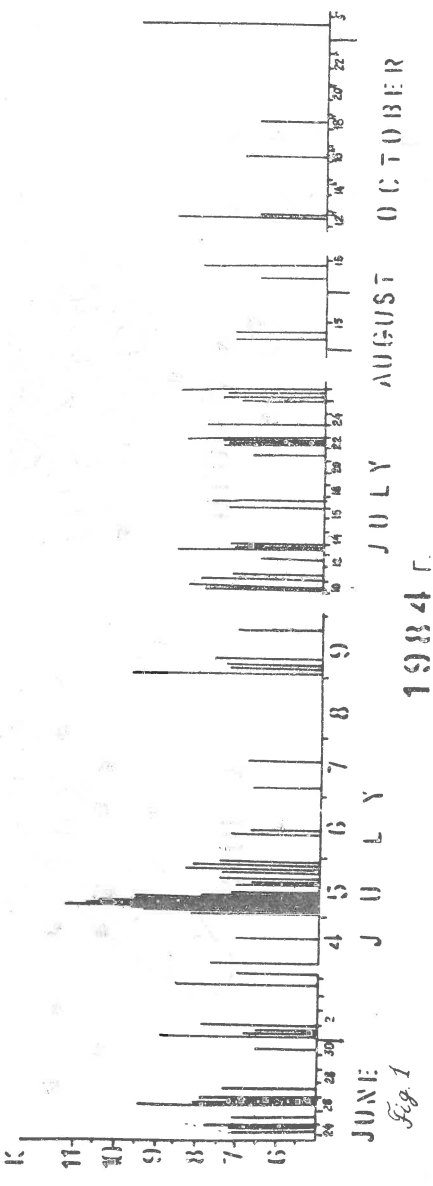

Fig. 1

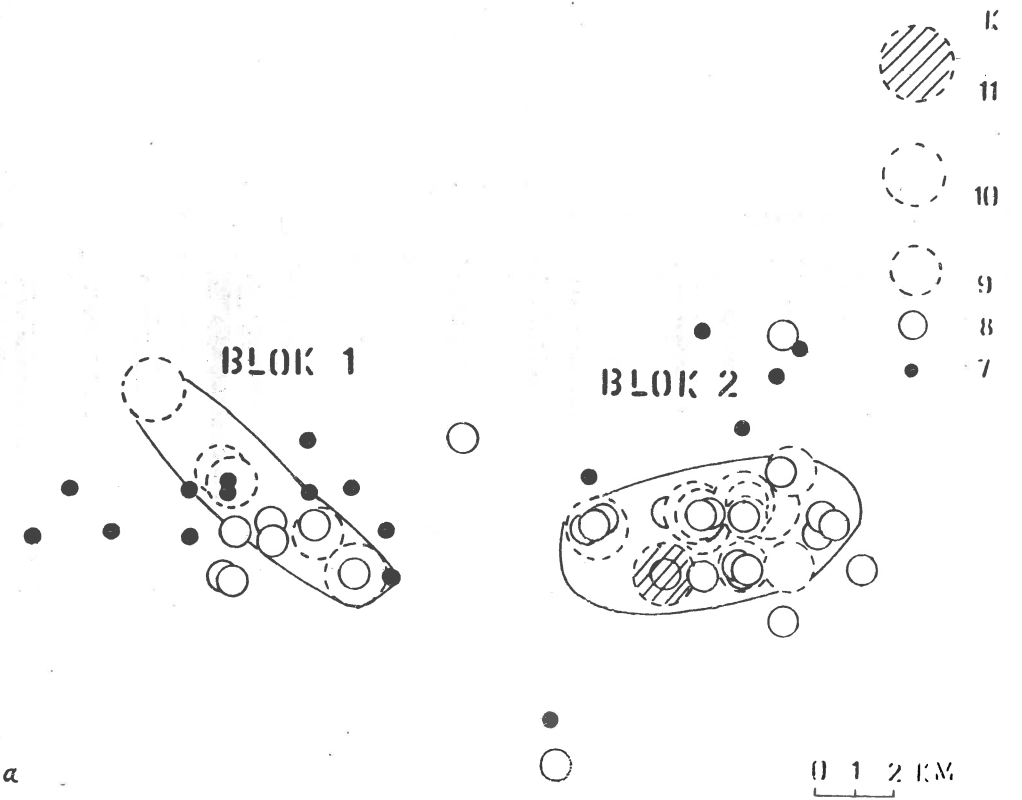

Fig 2a

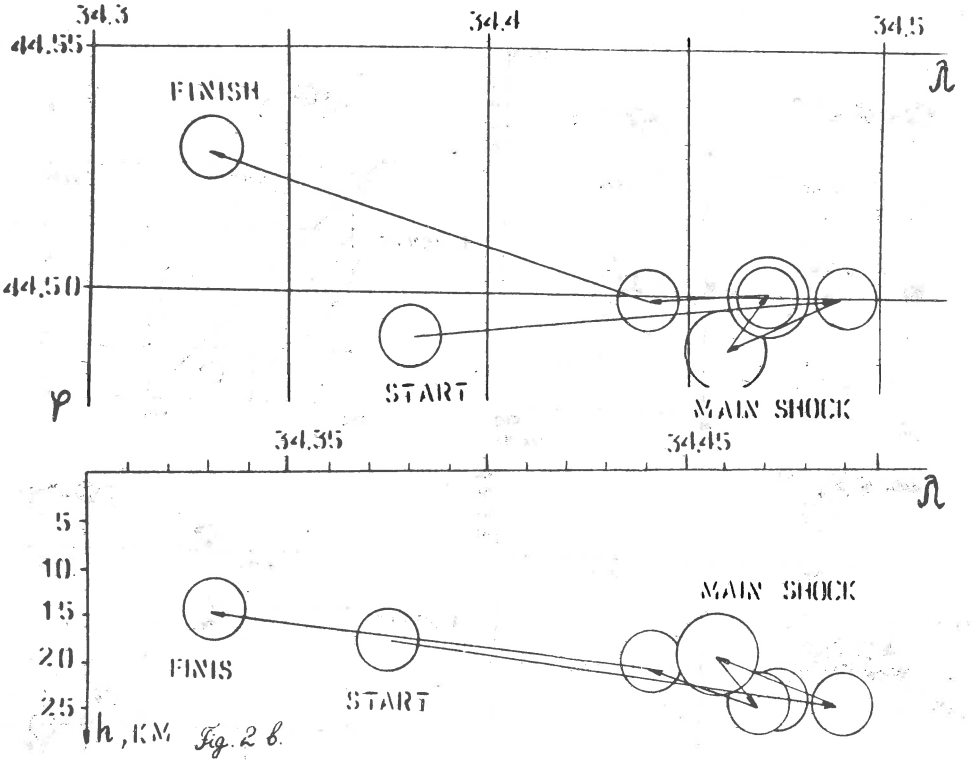
34.3
34.4
34.5
44.455
44.450
φ
λ
FINISH
START
MAIN SHOCK
34.395
34.495
λ
5
10
15
20
25
h, KM
FINIS
START
MAIN SHOCK

Fig. 2 b.

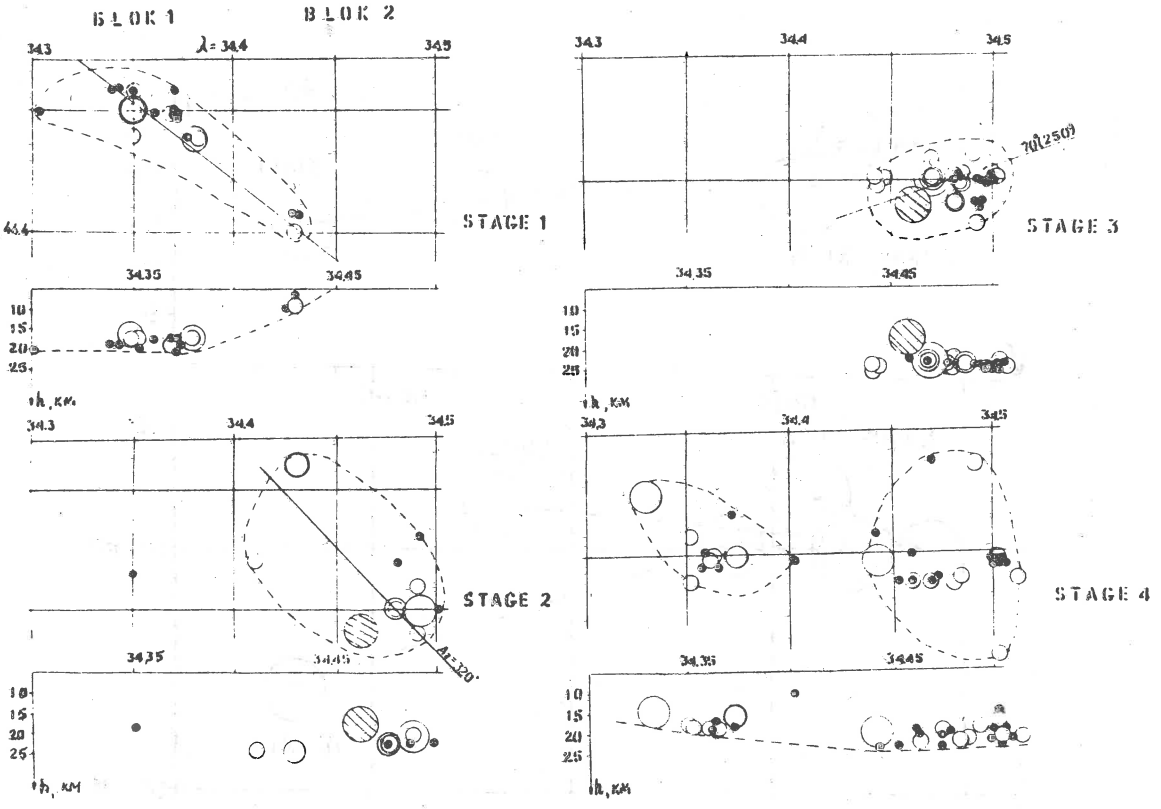
BLOK 1
BLOK 2
λ = 34.4
34.3
34.5
44.4
34.35
34.45
10
15
20
25
h, KM
STAGE 1
STAGE 2
STAGE 3
STAGE 4
70(250)
Δλ=320

Fig. 3

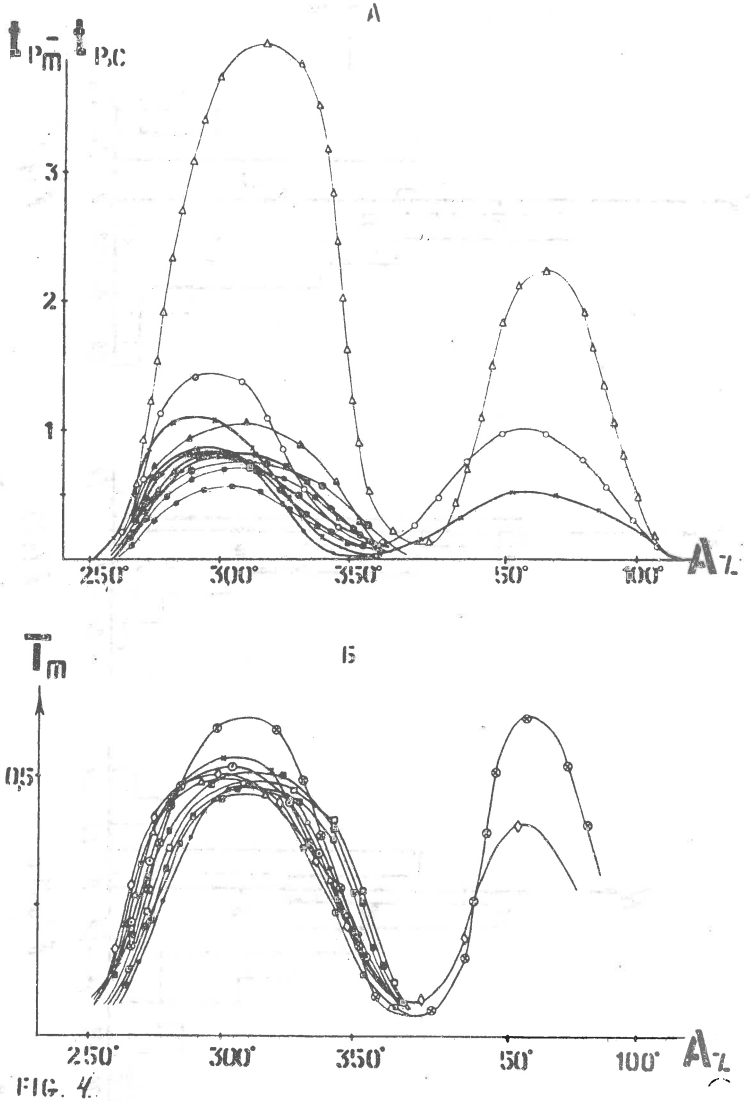

FIG. 4.

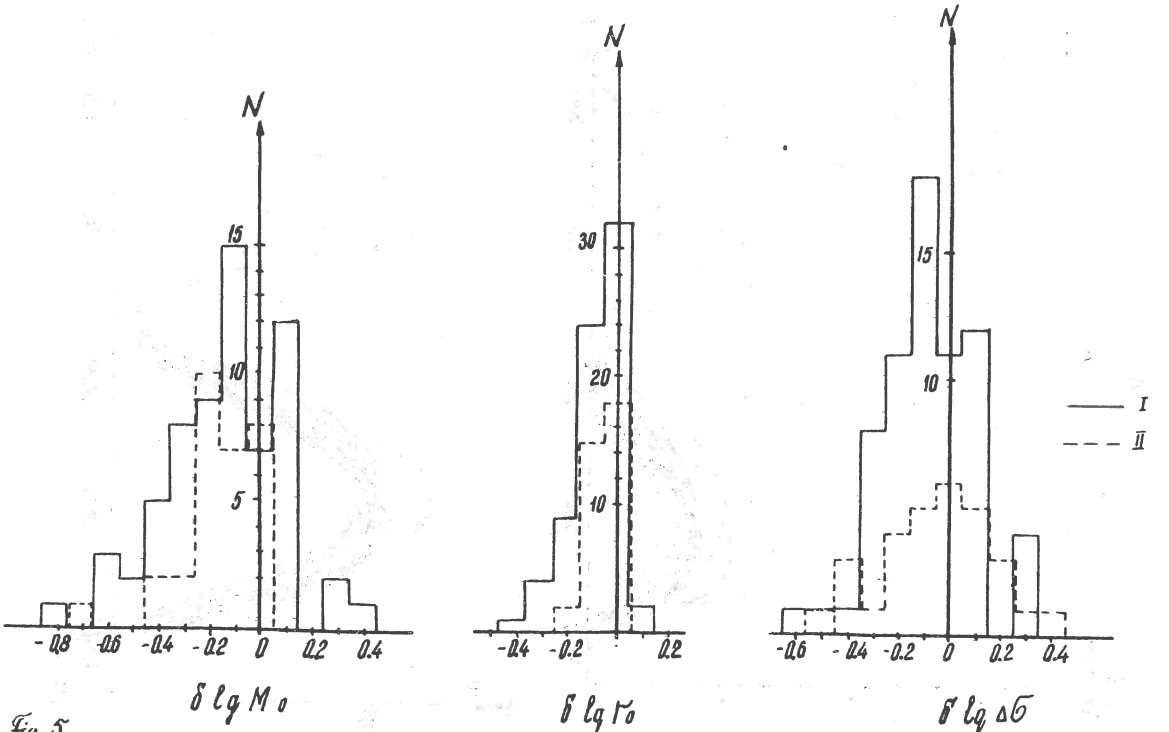
N
15
10
5
-0.8
-0.6
-0.4
-0.2
0
0.2
0.4
δ lg M o
N
30
20
10
-0.4
-0.2
0.2
δ lg r o
N
15
10
-0.6
-0.4
-0.2
0
0.2
0.4
δ lg Δδ
I
II

Fig. 5.

EVALUATION AND PURPOSE OF ELECTROTELLURIC MEASURIMENTS IN THE MAIN ETHIOPIAN RIFT

Klaus Meyer[1] and Laike M. Asfaw[2]
1. Seismological Department, University of Uppsala, Sweden
2. Geophysical Observatory, Addis Ababa University, Ethiopia.

Abstract

In the fall of 1987 two electrotelluric stations were installed in the central part of the Main Ethiopia Rift (MER), the first stations of this kind in Africa. The main purpose for monitoring the electrotelluric field (ETF) is the recent interest for anomalies in the ETF preceding earthquakes. An earlier work suggests that geophysical processes at a critical state of the stress field in the earthquake preparation zone may involve changes in the apparent resistivity and would hence produce different (anomalous) induction effects in the ETF prior to discharge of the accumulated stress. In order to find a causal connection between seismic energy release and anomalous behaviour of the ETF, we propose a continuous evaluation of the apparent resistivity, employing simultaneous geomagnetic and electrotelluric measurements. At any time, the variation of the apparent resistivity may then be correlated with the seismic energy release in the region. Sites for the stations have been chosen within an area of recent high seismic activity at the eastern escarpment of the MER.

Introduction

Systematic continuous monitoring of the electrotelluric field, ETF, with special emphasis on anomalous ETF variations prior to earthquakes, has been carried out primarily in Kamchatka and Central Asia (Garm), USSR. For instance, Fedotov et. al. (1970), Myachkin et. al. (1972), Sobolev (1975) and Meyer and Ponomarev (1987) report irregularities in the ETF from some hours to some days before earthquakes in Kamchatka. Corresponding irregularities were not found in the geomagnetic recordings in Kamchatka. In Europe, the ETF has been systematically monitored since 1981 at sites distributed in Contintental Greece (Varotsos and Alexopoulos, 1984). Short-duration anomalies (Varotsos and Alexopoulos, 1984a,b, Meyer et. al., 1985) and long-duration anomalies (Meyer, 1984, Thanassoulas and Tselentis, 1986, Ralchovsly and Komarov, 1988) prior to imminent earthquakes are reported from the Balkan area. Some other ETF measurements and anomalies preceding earthquakes are reported from China (Raleigh et. al., 1977, Noritomi, 1978 a,b) and from the USA (Corwin and Morrison, 1977).

Summarizing previous investigations, it seems that the electrotelluric method can contribute to the problem of earthquake forecast and to explanations of the physics in the earthquake source area. Recent discussions, especially initiated by the Greek VAN experiment (Varotsos and Alexopoulos, 1984 a,b) have encouraged other countries to install electrotelluric stations, mainly to test the statistical significance of occurrence of ETF forerunners to earthquakes in various seismically active regions.

The Main Ethiopian Rift constitutes the northern part of the East African Rift, a region of high seismicity. Seismological conditions in Ethiopia render therefore good possibilities to study the ETF and probable relations to seismic activity. The recent high seismic activity in the central part of the Main Ethiopien Rift is concentrated to its eastern escarpment (Laike, 1986, Fekadu and Meyer, 1988), manifested by three earthquake sequences between 1981 and

1985. Thus, it was decided to install electrotelluric stations in this particular part of the rift.

Installation of ETF stations

The Wendogenet - Awasa basin is the site chosen for electrotelluric monitoring (Fig. 1). The region is located in the central part ot the Main Ethiopian Rift, at its eastern escarpment. The largest earthquakes in this area during the last 40 years are given in Table 1. In June 1986, a seismic mobile station was installed at Wendogenet, the seismic readings of which clearly indicate that the area is currently seismically active. Microearthquakes occur practically every day, many of them are felt.

TABLE 1

Recent important earthquakes in Wendogenet - Awasa area.

Date	Latitude	Longitude	Magnitude
6 September 1944	7.2	38.5	6.0
14 July 1960	7.2	38.5	6.3
11 January 1972	7	38	4.0
2 December 1983	7.03	38.6	6.2

The Wendogenet - Awasa basin is formed by volcano-tectonic sinking of regional extent (Di Paula, 1972). The eastern caldera at which the electrotelluric stations are located, forms also the eastern escarpment of the rift where numerous hydrothermal manifestations can be observed. The most recent volcanic centres of Urgi and Chabbi, few kilometers to the west of the stations, occur in the Corbetti caldera which forms part of the Wonji Fault Belt. This fault belt is a quaternary Volcano-tectonic lineament extending along the length of the rift and having width between 2 and 8 kilometers (Lloyd, 1977; Mohr, 1966).

The two stations installed (Fig. 1), separated by about 2 km, include two dipoles each. The dipoles, oriented east-west and north-south, have a length of 100 m. As to the selection of electrodes we preferred the $Pb\text{-}PbCl_2$ type described by Petiau and Dupis (1980). To avoid any disturbances by daily temperature variations the electrodes are buried 2 m into the conglomerate of sediments (gravel, sand, clay). This provides also good contact during the dry season of the year. For the time being, the recording units are analogue. Power is supplied from 12 V batteries. Test recordings reveal that the diurnal variations are in the order of some hundred μV (several mV/km).

Resistivity variations related to seismic energy release

The effect of tectonic stress release by earthquakes on the resistivity in a seismically active region has been mentioned reported earlier. For instance, Barsukov (1972), Barsukov and Sorokin (1973), Mazella and Morrison (1974) and Niblett and Honkura (1978), have described apparent resistivity changes of up to 24 % prior to earthquakes. Continuous rock resistivity measurements in active mines in Poland show that the resistivity can change up to one order of magnitude prior to the rockbursts induced by the mining activity (Stopinski and Teisseyre, 1982). Among the investigations mentioned above, Niblett and Honkura (1978) used the magnetotelluric method to derive the apparent resistivity. The other workers employed direct resistivity measurements.

Previous analysis of ETF data, i.e. the interpretation of forerunners in terms of physical processes in the earthquake source region, suggests basicly two different causes. Varotsos and Alexopoulos (1984 a,b) ascribe certain ETF anomalies to a source effect. Heterovalent impurities in ionic crystals cause interstitials which form electric dipoles. By changing the imposed stress field, the dipoles re-orientate into a new state of thermodynamic equilibrium, the time process of which may be fast under certain stress conditions. The resulting change of polarization is equivalent to the emmission of an electric current (see Varotsos and Alexopoulos, 1986, chapt. 7). On the other hand, Meyer and Teisseyre (1985, 1987) explain ETF anomalies by variations of the electromagnetic induction due to resistivity changes, related to opening and closing of cracks and water transport between cracks. They also account for possible anisotropy effects, relating the resistivity response of a stress system to the principal axes of a the fault plane of the impending earthquake. According

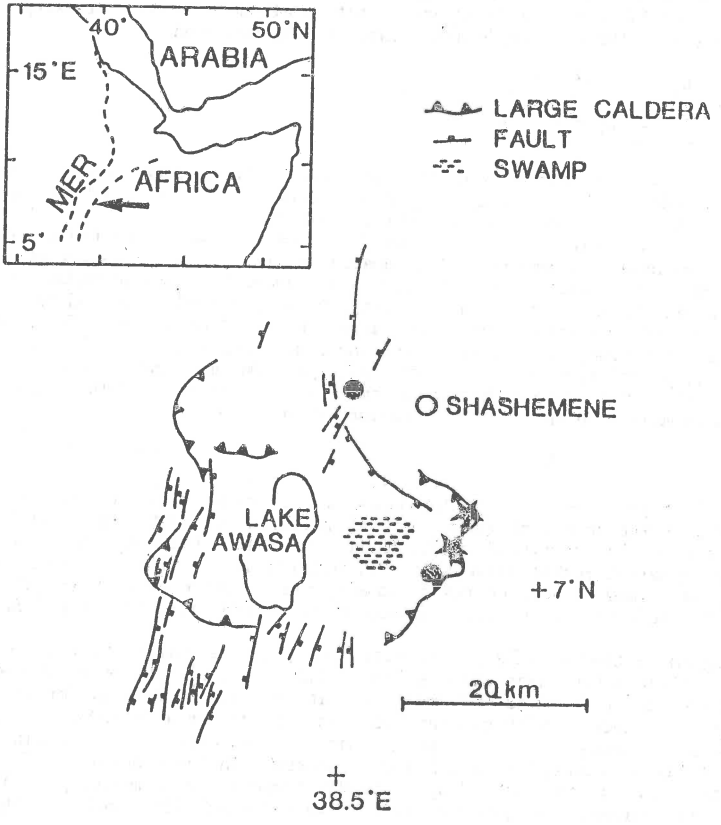

Tectonic features in the Wendogenet - Awasa region, eastern escarpment of the central part of the Main Ethiopian Rift, MER (see inset). Solid circles show earthquakes from Table 1. ETF station sites are denoted by a star.

to the extended dilatancy anisotropy model, EDA, one might expect such effects over large areas (Crampin et. al. 1984). Resistivity changes are also proposed by Barsukov (1972) who related observed resistivity decrease to rock fracturing under stress and subsequent increase of the relative volume of the electro-conducting pore liquid. Teisseyre (1983) attempts to explain observed resistivity changes in Polish copper mines prior to rockbursts. In an area of dry dilatancy the resistivity increases slowly but decreases abruptly with the start of a water percolation process.

The ETF variations reflect both the source processes (emmission of electric current) and the parametric changes of the transmitting medium (for instance resistivity changes). Below we sketch a procedure for investigation of the ETF.

1. Employing the magnetotelluric method we derive the apparent resistivity from simultaneous analysis of the ETF and the geomagnetic field, the data of which are available from a 3-component station at Addis Ababa. Following Rikitake (1966) the two fields are related by the equation

$$E_x = (\mu\rho p)^{\frac{1}{2}} H_y$$
$$E_y = -(\mu\rho p)^{\frac{1}{2}} H_x \qquad (1)$$

were E and H are ETF and geomagnetic field intensities, respectively, ρ is apparent resistivity, μ is magnetic permeability and p is an algebraic operator, $\delta/\delta t$. A complete procedure of estimating apparent resistivities from ETF and geomagnetic field data is described by Chouliaras and Rasmussen (1988). We propose continuous estimates of the apparent resistivity over longer periods of time (years), to reveal a possible time dependance. Any time dependance of apparent resistivities may then be related to stress conditions and processes at different stages prior, during and after the event occurrence (for instance: stress accumulation, crack orientation and crack density, electrokinetic phenomena, percolation process, stress release). One measurable process is the stress release by earthquakes. The seismic energy release is related to the earthquake magnitude through the relation (Båth, 1979)

$$\log E = a + b\,M \qquad (2)$$

where E is seismic energy, M is earthquake magnitude and a,b are constants. We can estimate the amount of seismic energy released per unit time (even for microearthquake activity) and relate these measures to the time variations of computed apparent resistivities. Any correlation of time variations of apparent resistivities and seismic energy release may be interpreted in terms of physical processes (parametric changes) in the seismically active region.

2. Using the estimated apparent resistivities, one can calculate the residual electric field (Chouliaras and Rasmussen, 1988). The investigation of the residual of the ETF can easily reveal variations which have a different nature than those connection with geomagnetic induction. After a thorough discussion on possible sources of electric noise, the interpretation of the remaining residual may show anomalies which are connected with the generation of electric currents, such as those caused by crack development, creep motion or emission of electric currents described earlier by Varotsos and Alexopoulos, 1986 (reorientation of dipoles in ionic crystals).

Acknowledgements

This research is conducted jointly by the Seismological Department, University of Uppsala and the Geophysical Observatory, University of Addis Ababa. The project is financed by the Swedish Agency for Research Cooperation with Developing Countries, SAREC, under contract 9.49 SAREC 87/221. We are grateful to Laust B. Pedersen, Uppsala, for suggestions and discussion on the Pb - $PbCl_2$ electrodes and to Leif Eriksson, Geological Survey of Sweden, for the review of this work.

References

Barsukov, O.M. and Sorokin, O.N., 1973. Variations in apparent resistivity of rocks in the seismically active Garm region. Izv., Earth Physics, 10, 100-102.

Barsukov, O.M., 1972. Variations of electric resistivity of mountain rocks connected with tectonic causes. In: E.F. Savarensky and T. Rikitake (Editors), Forerunners of Strong Earthquakes. Tectonophysics, 14(3/4): 273-277.

Båth, M., 1979. Introduction to Seismology. Birkhäuser, 2nd ed., 428 pp.

Chouliaras, G. and Rasmussen, T.M., 1988. The implication of the magnetotelluric impedance tensor to earthquake prediction in Greece. Tectonophysics, in press.

Corwin, P.F. and Morrison, H.F., 1977. Self-potential variations preceding earthquakes in California. Geophys. Res. Letters, 4, 171-174.

Crampin, S., Evans, R. and Atkinson, B.K., 1984. Earthquake prediction: a new physical basis, in Proceedings of the First International Workshop on Seismic Anisotropy, Suzdal, 1982, ed. Crampin, S., Hipkin, R.G., & Chesnokov, E.M., Geophys. J.R. Astr. Soc., 76, 147-156.

Di Paola, G.M., 1972. Geology of the Corbetti Caldera area. Bull. Volcan., Vol. 34, No. 2,pp. 497-506.

Fedotov, S.A., Dolbilkina, N.A., Morozov, V.N., Myachkin, V.I., Prebrazensky, V.B. and Sobolev, G.A., 1970. Investigation on earthquake prediction in Kamchatka. Tectonophysics, 9, 249-258.

Fekadu, K. and Meyer, K., 1988. Recent seismic activity and deployment of mobile stations in the Main Ethiopian Rift. Seismolog. Dept. Uppsala, Techn. Rep. 9 pp.

Laike, M.A., 1986. Catalogue of Ethiopian earthquake parameters, strain release and seismic risk. ESTC-SAREC B and D report, in press.

Llyod, E.F., 1977. Geological factors influencing geothermal exploration in the Langano region. Privatley circulated report, 73 pp.

Mazzella, A. and Morrison, H.F., 1974. Electrical resistivity variations associated with earthquakes on the San Andreas fault. Science, 185: 855-857.

Meyer, K., 1984. Large variations of the electrotelluric field prior to a major earthquake in Greece. Presented at the EGS 1984, Moscow. Procedings EGS 1984, in press.

Meyer, K., Varotsos, P., Alexopoulos, K. and Nomicos, K., 1985. Efficiency test of earthquake prediction around Thessaloniki from electrotelluric precursors. Tectonophysics, 120, 153-161.

Meyer, K. and Ponomarev, A., 1987. Electrotelluric forerunners to earthquakes in Kamchatka. Tectonophysics, 138, 341-347.

Meyer, K. and Teisseyre, R., 1985. Electrotelluric periodic anomalies prior to large imminent earthquakes. IASPEI, Tokyo. Acta Geophys. Pol., 36, 4 (1988), in press.

Meyer, K. and Teisseyre, R., 1987. Observation and qualitative modelling of some electrotelluric earthquakes precursors. IASPEI, Vancouver. Subm. to Phys. Earth Plan. Int.
Mohr, P.A., 1966. Chabbi Volcano. Bull. Volcan. Vol. 29, pp. 797-816.
Myachkin, V.I., Sobolev, G.A., Dolbilkina, N.A., Morozov and Preobrazensky, V.B., 1972. The study of variations in geophysical fields near focal zones of Kamchatka. Tectonophysics, 14, 287-293.
Niblett, E.R. and Honkura, Y., 1978. Time dependence of electromagnetic transfer functions and their association with tectonic activity. 4th Workshop on Electromagnetic Induction, Murnau, FRG, 17 pp.
Noritomi, K., 1978a. Geoelectric and geomagnetic observations and phenomena associated with earthquake in China, in Proceedings on the chinese Earthquake Prediction by the 1977 Delegation of the Seismological Society of Japan, pp 57-87, Seismol. Soc. Japan, Tokyo, (in Japanese).
Noritomi, K., 1978b, Application of precursory geoelectric and geomagnetic phenomena to earthquake prediction in China, Chin. Geophys. (Am. Geophys. Union), 1. 377-391.
Petiau, G. and Dupis, A., 1980. Noise, temperature coefficient, and long time stability of electrodes for telluric observations. Geophys. Prospecting, 28, 792-804.
Ralchovsky, T.M. and Komarov, L.N., 1988. Periodicity of the earth electric precursor before strong earthquakes. Tectonophysics, 145, 325-327.
Raleigh, B., Bennet, G., Craig, H., Hanks, T., Molnar, P., Nur. A., Savage, J., Scholz, C., Turner, R. and Wu, F., 1977. Prediction of the Haicheng earthquake. Eos, Trans. Am. Geophys. Union, 58: 236-272.
Rikitake, T., 1966. Electromagnetism and the Earth's Interior, Elsevier, Amsterdam, 308 pp.
Sobolev, G.A., 1975. Application of electric method to the tentative short-term forecast of Kamchatka earthquakes. Pure Appl. Geophys., 113, 229-235.
Stopinski, W. and Teisseyre, R., 1982. Precursory rock resistivity variations related to mining tremors. Acta Geophys. Pol., 30(4).
Thanassoulas, C. and Tselentis, G.A., 1986. Observed periodic variations of the Earth's electric field prior to earthquakes in N. Greece. 8th European Conf. Earthquake Eng., manuscript, 6 pp.
Teisseyre, R., 1983. Premonotory mechanism and resistivity variations related to earthquakes. Pure Appl. Geophys., 121(2), 297-315.
Varotsos, P. and Alexopoulos, K., 1984a. Physical properties of the variations of the electric field of the earth preceding earthquake, I. Tectonophysics, 110, 73-98.
Varotsos, P. and Alexopoulos, K., 1984b. Physical properties of the variation of the electric field of the earth preceding earthquake. II. Determination of epicenter and magnitude. Tectonophysics, 110, 99-124.
Varotsos, P. and Alexopoulos, K., 1986. Thermodynamics of point defects and their relation with bulk properties. North-Holland Phys. Publ., 474 pp.

PRESENT STATE OF EARTHQUAKE PREDICTION RESEARCH IN ROMANIA USING NATURAL FIELDS

C.Demetrescu, M.Ene, M.Andreescu, D.Burst, C.Haradja.
Institute for Earth's Physics, Bucureşti - Măgurele ,
P.O.Box MG-2, Bucharest, Romania

INTRODUCTION

After the damaging earthquake of March 4, 1977, the Institute for Earth's Physics developed studies on precursory changes in the temporal variation of some natural fields of the Earth; our group initiated geomagnetic, self potential and radon measurements. Since 1985 a cooperative research in earthquake prediction with Japanese universities has been in progress; ground water temperature, crustal deformation, self potential and radon measurements have been developed within the frame of this project. In Figure 1 the location of sites where the measurements have been carried out is presented.

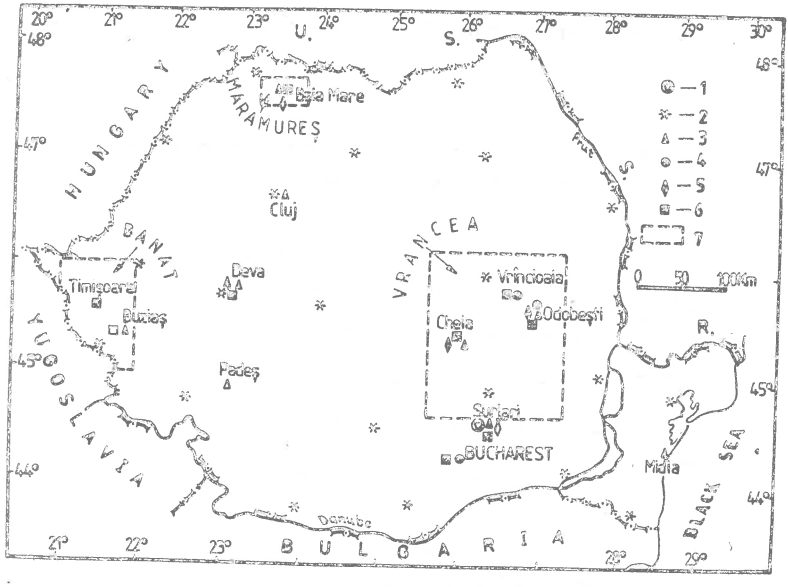

Fig.1 Sites and test areas to monitor precursory changes in the temporal variation of some natural fields. 1-Surlari Geomagnetic Observatory ; 2- secular variation repeat stations;

3- recording proton magnetometer stations ; 4- ground water temperature measurements; 5- self potential stations; 6- radon cup stations; 7-tectonomagnetic arrays (repeat stations). Full symbols - equipment in operation; open symbols-planned site.

GEOMAGNETIC MEASUREMENTS

Three types of geomagnetic measurements are currently being carried out by our group. In the chronological order of their initiation, they are: (a) measurements of geomagnetic elements H,Z, F,D, once a year in a network of 21 repeat stations fairly uniformely distributed over Romania (initiated in 1964 to monitor the secular variation, by Atanasiu et al. (1974)); (b) total field (F) measurements, several times a year, in 3 tectonomagnetic arrays of 9, 16 and 17 repeat stations (initiated in 1979); (c) F measurements in an array of 4 continuously recording proton magnetometers (initiated in 1983).

A previous analysis (Demetrescu et al., 1983) of total field measurements in the tectonomagnetic array " Vrancea " of 17 stations, which is placed in the area in which earthquakes are by far more numerous than in the other two investigated areas, revealed both some correlations between magnetic variations and earthquakes and the limits of this approach. In Figure 2 the temporal variation of differences between the total fiels at several stations

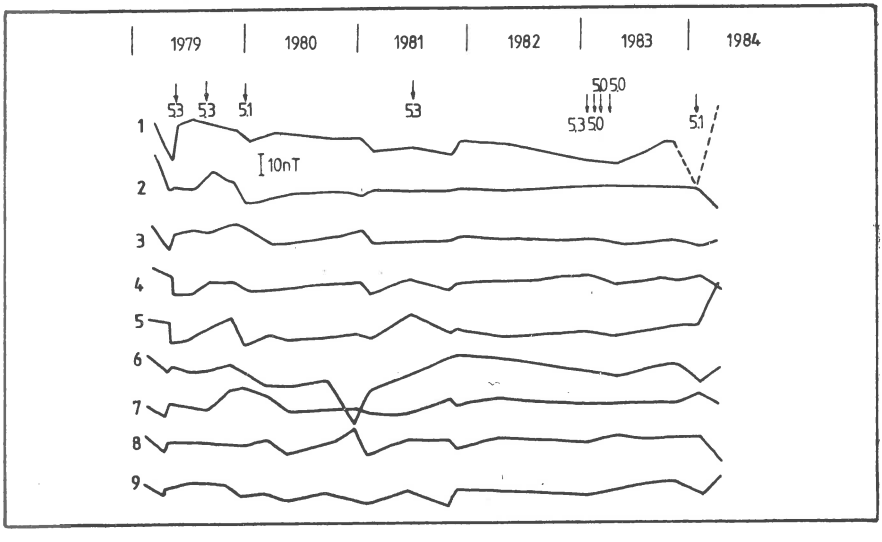

Fig.2 Tectonomagnetic data for "Vrancea" array, 1979 - 1984.

of the array and Surlari Geomagnetic Observatory is shown together with intermediate earthquakes with M_L 5.o. The total field was measured by means of proton magnetometers with an accuracy of 1 nT. Data were corrected for diurnal variation using records at the geomagnetic observatory, as well as for differential magnetic induction effects (Demetrescu and Andreescu, 1983).

In the analysed interval no definite conclusion could be reached: a few coincidences of magnetic variations with crustal and intermediate earthquakes were noticed, but other magnetic variations were not followed by earthquakes. The maximum magnitude of crustal earthquakes was 4.6 and of intermediate earthquakes was 5.3. Anyway, the interval between measurements appears to be too large as compared to the frequency of occurence of crustal earthquakes with 3.5 M 5.o. Of course, a longer series, with more significant earthquakes is needed before a definite conclusion could be reached. We would continue such measurements to look for long term precursors to greater seismic events. However, a preliminary inspection of a longer series of data showed no definite correlation with the 7.o intermediate earthquake of August 3o, 1986.

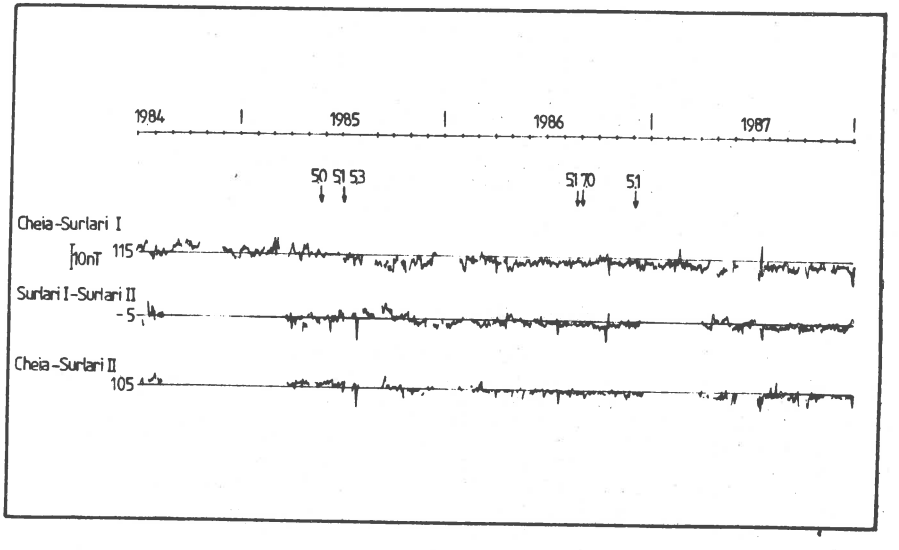

Fig.3 Dayly average of raw differences of the total field at continuously recording stations.

Since 1983 we have run a network of 4 recording proton magnetometers with a hope to detect, beside long term tectonomagnetic signals, short ones as well. The hourly and dayly averages of the differences between F values at different stations are monitored and further cleaned of residual electromagnetic effects by using the Wiener predictive filtering of Davis et al. (1981). In Figure

3 we show as an example the dayly averages of the raw differences between two proton magnetometers (sensitivity o.o1 nT, digital output) at Cheia and Surlari II, in the interval 1984-1987. A comparison with the Bobrov type recordings at the geomagnetic observatory (Surlari I) is given as well, in order to emphasize the quality of the proton magnetometer data. Again, a preliminary visual inspection of the plot does not reveal any long term precursor to the intermediate 3o August 1986 magnitude 7.o earthquake.

To end this paragraph we note the rather complicated magnetic conditions in the area of Vrancea array, which add to the difficulties one is faced with when trying to find tectonomagnetic effects of earthquakes occuring at depths greater than 6o km: (a) four types of magnetic basement (hercino-kimmerian, proterozoic-caledonian, baikalian and alpine) burried under kilometers of sediments (amounting to 17 km in the Focşani Depression) or flysch, and (b) the existence of a conductivity anomaly in the area contributing to a high noise in the data.

SELF POTENTIAL MEASUREMENTS

Two stations were installed in 1984 at Cheia and Odobeşti. The electrodes, lead plated with a surface of 1 m^2, are burried at a depth of 2 m. The distance between electrodes is about 5om. The earth's potential is recorded on paper. Since 1986, Nagoya University equipment, with unpolarizable electrodes, installed by Prof. Hitoshi Mizutani within the frame of the cooperative research in earthquake prediction with Japanese universities, parallels the former one, in order to detect possible electrode polarization and other unwanted effects. The electrodes are made of lead electrolysed in KCl solution, covered by $PbCl_2$, placed in a vinyl chloride pipe of 3o cm, filled with a mixture of plaster and $PbCl_2$ (chikogern).

RADON MEASUREMENTS

In the interval 1978-1983 the radon concentration in soil was monitored at 4 stations - 2 in the Vrancea area and 2 in areas charecterized by shallow earthquakes (Zoran, 1983). The radon cup method of King (1978) was used. In Figure 4 (Zoran, 1983) the monthly averages of the track density normed with respect the average value for the entire interval are displayed, together with intermediate earthquakes with M 5.o. The similarity of the variation at Cheia and Vrîncioaia in the Vrancea area and some possible correlation with earthquake occurence encouraged us to resume such determinations. The new series started in July 1988 within the frame of the Romanian - Japanese cooperation (Prof. Hideki Shimamura, Hokkaido University), in a much larger network in Vrancea area.

GROUND WATER TEMPERATURE MEASUREMENTS

In November 1985 high precision quartz thermometers (Shima-

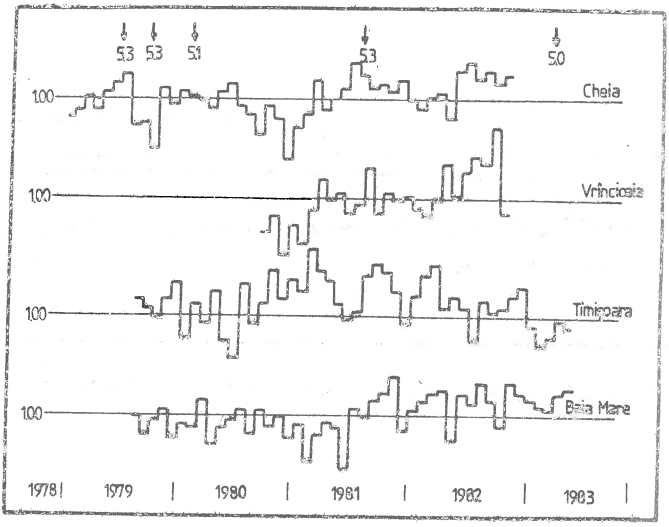

Fig.4 The variation of Radon concentration in soil at some Romanian stations

mura, 1980) were installed at 3 locations in Romania (2 in Vrancea area, 1 in Bucharest) by Prof.Hideki Shimamura, Hokkaido University, within the frame of the mentioned Romanian - Japanese cooperative programme, to monitor ground water microtemperature changes. In Figure 5 the records taken in 1986 are shown, together with atmospheric pressure changes. The Vrancea earthquakes of August 30 and December 16, 1986, are marked as well. The possible correlation of the variation at Odobeşti (ODA) with the earthquakes occurrence was interpreted by Shimamura (1987) as in Figure 6. To further check the sensitivity of Odobeşti area, another borehole was drilled reaching a deeper aquifer and a second temperature sensor is now in operation at ODA.

CONCLUSION

Our paper is but a progress report on the present state of the earthquake prediction research in Romania using natural fields. We consider our results rather encouraging, though not very convincing, and hope that such measurements as described, together with seismological studies (Mârza, this symposium) and other types of studies (e.g. crustal deformation and gravity changes), would eventually prove useful in the prediction of large Vrancea intermediate earthquakes.

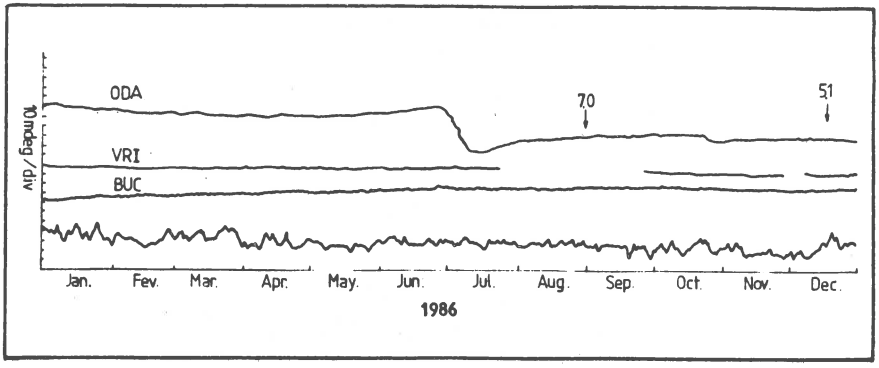

Fig.5 Recorded groundwater microtemperature variations in 1986.

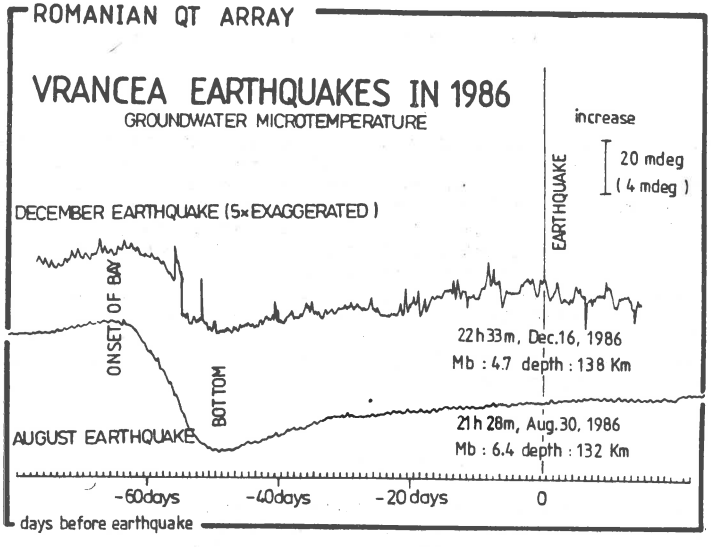

Fig.6 Interpretation of ground water temperature changes in 1986 (Shimamura, 1987).

REFERENCES

Atanasiu, G., Neştianu, T., Demetrescu, C. and Anghel, M., 1974. The secular variation of the geomagnetic elements H, Z and F between 1958-1972 in Romania, Rev.Roum, Géol., Géophys., Géogr., Géophysique, 18: 59-65.

Davis, P.M., Jackson, D.D., Searls, C.S., McPherson, R.B., 1981. Detection of tectonomagnetic events using multi-channel predictive filtering, J.Geophys. Res., 86: 1731-1737.

Demetrescu, C. and Andreescu, M., 1983. Magnetic induction model for correcting tectonomagnetic array data, Proceedings, International Symposium on Earthquake Prediction, Bucharest, April 1983.

Demetrescu, C., Ene, M., Andreescu, M., Anghel, M. and Smalberghер, V., 1983. Total field measurements in the tectonomagnetic array " Vrancea " between 1979-1983, Proceedings, International Symposium on Earthquake Prediction, Bucharest, April 1983.

King, C.Yu, 1978. Radon emanation on San Andreas Fault, Nature, 271, 516-519.

Shimamura, H., 198o. Precision Quartz Thermometers for Borehole Observations, J.Phys.Earth, 28, 243-26o.

Shimamura, H., 1987. Report at the Annual Meeting of the Seismological Society of Japan, Tokyo, April 1987.

Zoran, M., 1983. Studies on Radon concentration in soil, in Demetrescu et al., Internal Report, Institute for Earth's Physics, Bucharest.

NEUROPSYCHIC COMPLAINTS IN THE PERIOD OF THE EARTHQUAKE IN VRANCEA 1986

O. Kolev, I. Ivanov

Institute of Neurology, Psychiatry & Neurosurgery, Sofia

Tz. Ralchovsky, D. Deneva

Geophysical Institute, Acad. G. Bonchev Str., block 3, Sofia 1113, Bulgaria

Unusual animal behaviour before earthquakes has been known since hoary antiquity. Moreover, the responses of each biological species in different regions of the world and in different times have been similar [Evernden, 1976; Nikonov, 1980; Rikitake, 1978; Group of earthquake research, 1984]. The anomalous animal behaviour reflects the changes of geophysical and geochemical fields in the earth's crust and the atmosphere prior to the seismic event. A detailed survey of the possible stimuli as well as the animal and human sensory thresholds for them obtained by laboratory studies is reported by [Buskirk et al., 1981].

The capabilities of humans as bioindicators are more limited due to the higher sensory threshold and the numerous social stimuli. Complaints of sick persons with damaged cardio-vascular systems is known in the period before strong earthquakes. A laryngeal irritation preceding near moderate earthquakes or strong ones at longer distances in the period of two weeks before the event with a culmination on the eve is reported by [Tzvetkov et al., 1985]. But the reliability of this precursor is doubtful because of the unpresentative character of the data.

The aim of this work is to study the state of the patients in the clinic of neurology and psychiatry in Sofia in the period before the earthquake on 30 August 1986, at 21 h 29 min in Vrancea region, Rumania (M_{LH} = 6.9; h = 139 km [NEIS]). In Sofia, at an epicentral distance of 410 km it was felt to be of IV-V grade according to the scale of MSC-64.

Immediately after the earthquake 67 patients were interviewed about their sensations in the course of 24 hours preceding the earthquake. They are distributed into 4 groups as follows:

I group: patients with peripheral vestibular disfunctions - 12 individuals.

II group: patients with functional diseases of the central nervous system (CNS) /neurosis - 4 individuals, diencephalic syndrome - 6 individuals/.

III group: patients with mental illness - 33.

IV group: patients with organic damages of the CNS (patients with insultus in an intensive care department-12).

The inquiry was performed according to the following scheme: 1. Dizziness sensations; 2. Auditory changes; 3. Neurovegetative complaints; 4. Psychoemotional state.

The obtained results in percent with respect to the symptoms occurring in the four groups of patients are as follows:

I group: 33.3% - systematic dizziness; 75% - unsystematic dizziness; 33.3% - instability; 33.3% - noise; 33.3% - cardiac complaints; 50% - gastrointestinal complaints; 41,1% - respiratory complaints; 25% - headache; 50% - internal tension.

II group: 60% - dizziness; 20% - noise; 60% - cardiac complaints; 60% - gastrointestinal complaints; 70% - respiratory complaints; 50% - headache; 50% - formication of the extremities; 20% - dryness in the mouth; 90% - anxiety and internal tension; 60% - unmotivated fear; 10% - spontaneous weeping; 60% - insomnolence; 20% - weakness.

III group: 3% - cardiac complaints; 9% - gastrointestinal complaints; 6% - anxiety; 9% - unmotivated fear; 3% - sombre mood; 51.1% - sleeping during the earthquake; 27.3% - awake from the shaking during the earthquake; 21,3% were awake before the beginning of the earthquake.

IV group: without any changes during the period preceding the earthquake (66.7% were asleep; 33.3% - awake from the shaking).

The established disorders in the patients under observation are probably a response to a complex of stimuli including an anomaly of geoelectrical field in the period of a few hours prior to the shock which was registrated in Geophysical Observatory "Vitosha". An increase of the electroteluric potential by 70 mV/m has been observed. Its effect has been added to the influence of the natural low frequency electromagnetic emissions whose intensity had increased by 4-5 mV prior to the earthquake.

DISCUSSION: The abundance of symptoms with the patients of the first group could be considered as a result of earthquake precursors' influence on the vestibular system. The irritative state of the affected vestibular structures allows a higher sensitivity of the vestibular receptors. The vegetative symptoms in this group are reactions of the autonomic nervous system, i.e. an expression of the vestibular-vegetative reflexes. The fact that four individuals of this group complained of experiencing a shock before it actually had occurred, supports the hypothesis that the vestibular structures take part in mechanisms for

detection of precursors.

Disturbances in the functioning of the limbic system and the diencephalon are presented in the second group. The lymbic system receives sensory information from the periphery and transfers it to the upper structures. One of the functions of the limbic system is to estimate the sensory inputs and in accordance with them to stimulate the behaviour, the emotions and the vegetative responses. We suspect that the functional disorders in these cases are the reason for the high sensitivity leading to an increase of the sensory information. On the other hand they cause intensified vegetative and psychoemotional responses.

The small number of complaints in the third group, we suppose, is a result of a medication by neuroleptic, antidepressant and hypnotic drugs.

The absence of changes in the subjective state of the patients of IV group could be explained by the organic stage of damage of the central nervous system.

We presume that the registrated electro-teluric potential and electromagnetic emission changes in the process of preparing of the earthquake are stimuli for the receptory system related to the vestibular analyzer. This hypothesis is supported by the fact that humans under electromagnetic emissions show vestibular complaints [Holodov, 1982]. According to laboratory data the threshold sensitivity to electric fields is about 1 v/m. We suppose that individuals with functional disorders of the vestibular analyzer have a lower threshold. Nevertheless, the electric fields are a part of the geophysical stimuli which can influence humans.

CONCLUSION: This study shows that the vestibular system participates in perceiving of geophysical changes prior to earthquakes. Most probably the changes of the electrotelluric potential and the electro-magnetic emissions are part of a combination of factors stimulating the sensory system.

REFERENCES

Buskirk, R.E., C. Frohlich, G. Latham, 1981 Unusual animal behaviour before earthquakes: A review of possible sensory mechanisms, Rev. Geoph. Sp. Res., vol. 19, No 2, 247-270.

Evernden /ed./, 1976 Proc. Conference 1, Abnormal animal behaviour prior to earthquakes, US Geological Survey, Menlo Park, California.

Group of earthquake res., 1984 Some characteristics of animal behaviour prior to earthquakes; Earthquake prediction, proc. of Intern. symp. earthquake prediction, TERRAPUB, Tokyo, UNESCO, Paris.

Holodov, J.A. Brain in electromagnetic fields (in Russian), 1982, Nauka, Moscow, p. 120.

NEIS - earthquake data report, 1986.

Nikonov, A.A. Seismicity and animal behaviour (in Russian), 1980, Zeml. vsel., 6, 31-35.

Rikitake, T., 1978 Biosystem behaviour as an earthquake precursor, Tectonophysics, 51, 1-20.

Tzvetkov, I., E. Tzvetkova, 1985 Bioseismology (in Bulgarian), Priroda, 34, 6, 8-14.

Continuous Evaluation of Seismic Hazard Induced by the Deposit Extraction in Selected Mines in Poland.

Głowacka Ewa, Kijko Andrzej
Institute of Geophysics, Polish Academy of Sciences
01-452 Warsaw, ul. Księcia Janusza 64

Introduction

Tremors of rockmass occurring in underground mines are typical examples of induced seismic activity caused by the rock deformation due to the extraction of some of its volume. The dependence of seismic activity on the extracted deposit volume has long been known from observations /e.g., Sklenar et al., 1975/. In 1985 on the basis of earlier solution of Randall /1971/and Mc Garr /1976 / Kijko introduced the dependence of seismic activity on the amount of extracted deposit as a deterministic relation, and he also pointed out that it is necessary to interpret this dependence as a probabilistic relation.

This paper will briefly present the way of deriving a probabilistic relation between seismic activity of the rockmass and the size of the extracted volume of the deposit.

The derived relation was tested in the chosen region of coal mine "Wujek" and in the copper basin region in Poland.

Formulation of the problem

In 1985 Kijko has found the following relation between the total amount of the released seismic energy and volume V of the extracted deposit

$$\Sigma E = C \cdot V^B. \qquad (1)$$

Parameters C and B depend on the kind of mining works and the state of rockmass. Formula (1) was derived using statistical relationships, so it is also of statistical character and can be used for regions of a large number of shocks.

The seismic hazard is understood as the sum of seismic energy released through time Δt_i (during which volume ΔV_i has been extracted). To evaluate the hazard, we will calculate the following values:

1) $$(\Sigma E)_i = C \cdot V_i^B - C \cdot V_{i-1}^B \qquad (2)$$

$(\Sigma E)_i$ is the most probable sum of seismic energy expected through

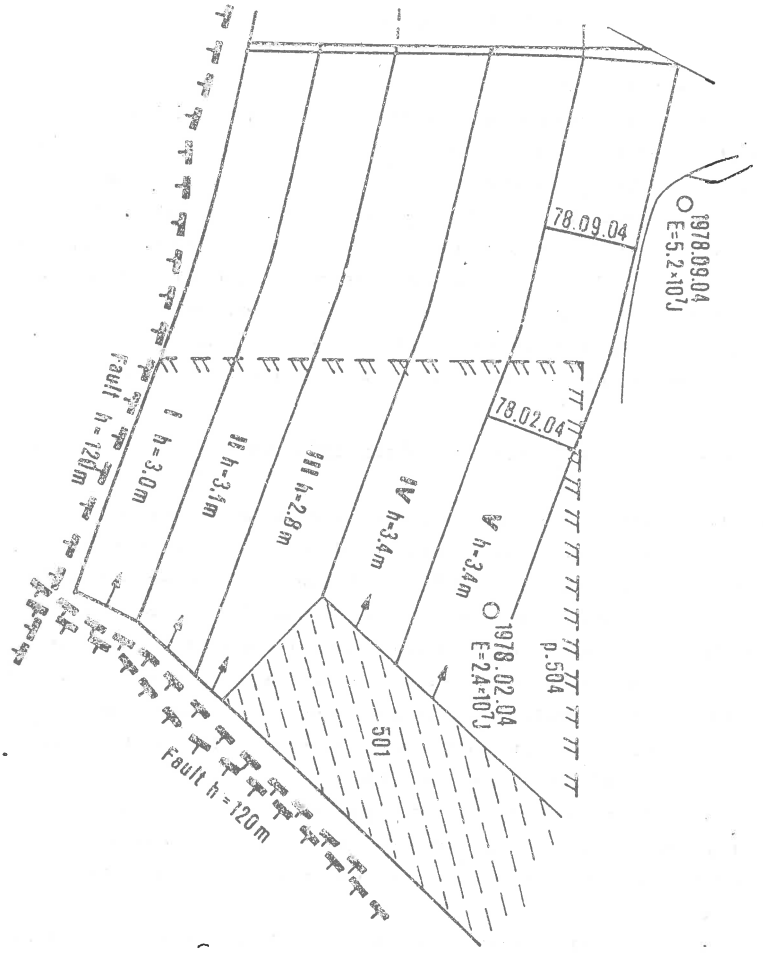

Fig. 1. A sketch of the geological and mining situation in a chosen region of seam 501 at the "Wujek" Coal Mine.
/ Głowacka, Syrek, Kijko, 1985 /.

time Δt_i, associated with mining of $\Delta V_i = V_i - V_{i-1}$. Constants C and B are calculated for the former course of function (1), i.e., for t_{i-1}

2) $$(\Sigma E)^a_i = (\Sigma E)_i + \Delta E_{i-1} \qquad (3)$$

- $(\Sigma E)^a_i$ is the most probable sum of energy expected through time Δt_i plus the amount of energy accumulated in the rockmass: $\Delta E_{i-1} = (\Sigma E)_{i-1} - (\Sigma E)_{i-1}$. Quantity $(\Sigma E)_{i-1}$ is the real sum of the seismic energy released in time t_{i-1}. Equation (1) is of statistical character. We assume additionally that the distribution of (ΣE) around the most probable value described by equation (1) has a character of normal distribution with a standard deviation σ. Let $P(E_j) = P(\Sigma E > E_j)$ mean that the most probable value of the seismic energy sum exceeds the threshold E_j. We can then calculate

3) $$P(E_j) = 1-(1/\sigma\sqrt{2\pi}) \int_0^{E_j} \exp(-(1/2\sigma^2)(E-\Sigma E^a)^2)dE, \qquad (4)$$

The above algorithm for seismic hazard evaluation has been applied in some regions of coal mines (Głowacka et al. 1987) and copper mines (Kijko et al. 1985) in Poland and Czechoslovakia (Głowacka et al. 1988). The results obtained for these regions show that the estimation of seismic hazard as a function of the extracted rock amount has a character of a long-term forecast. Combined with the results of measurement of other geophysical fields, presented in a probabilistic manner, the method may be quite effective in the forecast of shocks.

The goal of this work is to present some of the results obtained for the part of seam 501 in the coal mine Wujek in Upper Silesia and for a region of copper mines in Lubin-Głogów Area.

Results

Figure 1 shows the sketch of geological and mining situation of chosen region of seam 501 in coal mine "Wujek" in Upper Silesia. Practically there is no tectonic perturbation in this area. The basic deposit of seam 501 was excavated in 1974-1979 at 5 retreating longwalls with a mechanized support with caving. During the exploitation there occurred 2 tremors with the energy of 10^7J, 68 tremors with the energy of 10^6J, about 500 tremors with the energy of 10^5J and several thousands of smaller events.

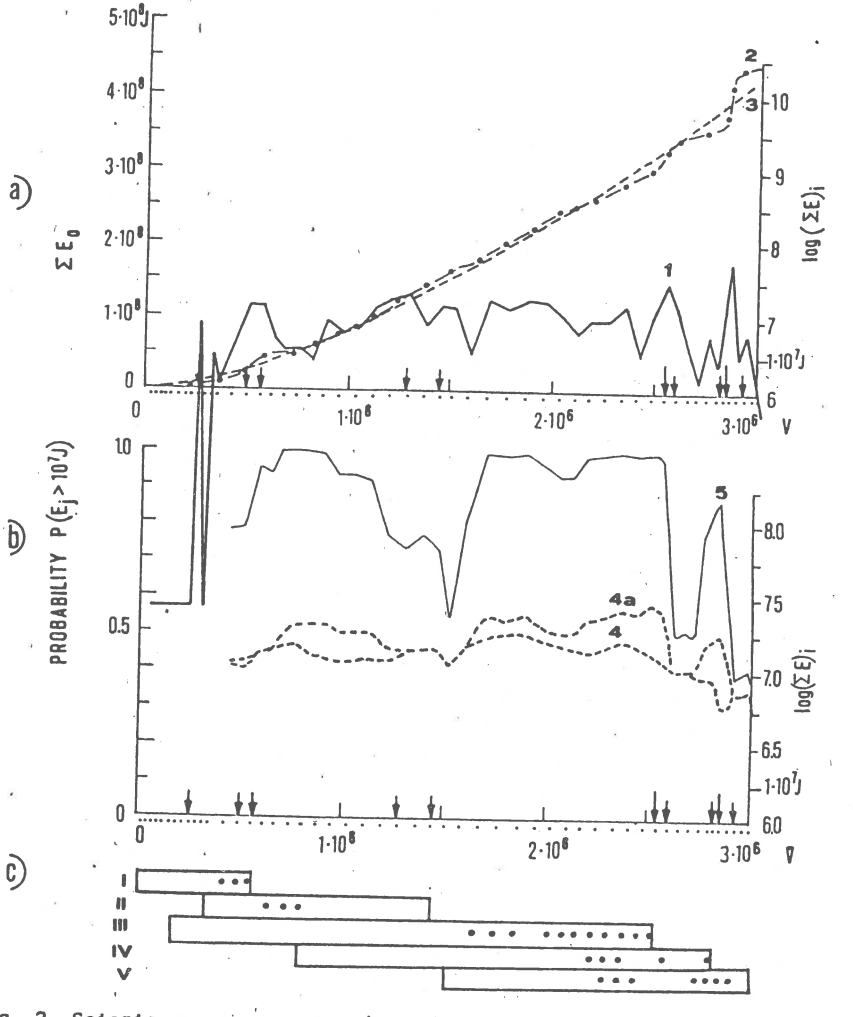

Fig. 2. Seismic energy versus volume of extracted lock for the chosen region of the "Wujek" Coal Mine. /Głowacka, Syrek, Kijko 1985/. Arrows mark the tremors with energy bigger than 10^7 J and $5 \cdot 10^6$ J.

Curve : 3 - energy calculated from the relation $E = C \cdot V^B$,
5 - probability of exceeding the energy 10^7 J.

c/ The course of extraction at valls I-V. Dots mark the periods with increased energy accumulation. Other explanation as in Fig. 3.

The analysis of the seismic hazard for each of the walls separately and for the whole region was done. The results of seismic hazard evaluation for whole region is presented in fig. 2. One can notice several months long periods of increasing accumulation /where curves 4 and 4a diverge/ and increased probability preceding tremors with energies greater than 10^6J. In lower part of the figure 2c dots mark the periods of energy accumulation occurring at particular walls. It can be seen that tremors with energy greater than 10^7J were preceded by accumulation at 2 or 3 longwalls at the same time, so they had more regional nature, unconnected directly with the extraction of individual walls. This means that the region where very strong seismic events are originated considerably exceeded the dimension of longwalls and that one should look for an explanation of this phenomenon to the extraction of the whole region rather then that of single wall.

The second of discussed area is the copper basin region. The mining started here 25 years ago and till 1987 there was about 2500 tremors with energy bigger then 10^5J, about 100 tremors with energy bigger then 10^7J and 9 tremors with energy bigger then 10^8J. The biggest earthquake with magnitude 4.5 occurred in March 1977.

The relation (1) was derived on the assumption of Gutenberg-Richter relation. The study of energy and magnitude distributions of induced shocks in Polish mines pointed to the bimodal character of these distributions (Dessokey 1984, Kijko et al. 1987). The characteristic shape of shock distribution gave grounds for dividing the shocks into two classes. The low-energy shocks are in time and space associated directly with the excavation, while the large shocks result from accumulation of deformation over larger area and for a longer time. A tectonic origin of major shocks cannot be excluded either.

The study of energy-frequency distribution done by Stankiewicz (1988) shows that the bimodal model fits the observations for the copper basin very well. The lower limit of major tremors is the energy $E = 10^9$J.

The bimodal distribution of shocks suggest that the preparation regions for small and big tremors differ substantially from each other. Then the parameters C and B in our equation /1/

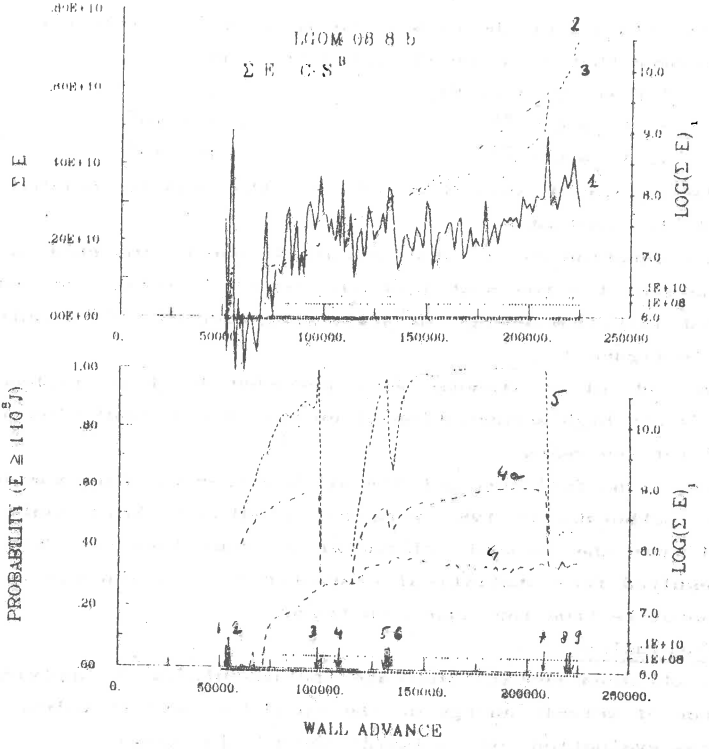

Fig. 3. Seismic energy versus extracted rock area for the Copper Basin Area in 1968-1987 / Curve 1 - monthly sums of seismic energy, 2 - total seismic energy, 3 - energy calculated from the relation, $\Sigma E = C_1 \cdot S^{B_1} + C_2 \cdot S^{B_2}$ 4 - predicted seismic hazard calculated from relation / 2 /, 4a - predicted seismic hazard, taking into account the energy accumulation calculated from relation /3/, 5 - probability of exceeding the energy 10^8J /.

Tremors : 1 - 1977.02.03, 2 - 1977.03.24,
3 - 1980.03.07, 4 - 1980.12.21,
5 - 1982.08.01, 6 - 1982.09.12,
7 - 1986.10.25, 8 - 1987.05.31,
9 - 1987.06.20

for the two classes of shocks will be different. In this connection it was assumed that equation /1/ takes the form:

$$\Sigma E = (\Sigma E)_1 + (\Sigma E)_2$$

$$(\Sigma E)_1 = C_1 \cdot S^{B1} \qquad E < 10^{8} J \qquad (5)$$

$$(\Sigma E)_2 = C_2 \cdot S^{B2} \qquad E \geq 10^{8} J$$

where the excavated area $S = V/h$ and the working height h is assumed to be constant.

Since equation /5/ is statistical, it can be inserted as well into equations for the most probable expected energy sum and for the probability that energy 10^{8} J will be exceeded. The result can be seen in figure 3.

Four out of 9 tremors were preceded by high probability ($P > 0.7$) and high accumulation of energy. The accumulation period can last for few years.

There is no full forecast for all big tremors. For example the big two rockbursts in 1987 were not predicted. This could have resulted from the tectonic character of some tremors. This also could resulted from statistical character of relation (1) and (5) which cannot be true for separated tremor.

Conclusions

The obtained results indicate the usefulness of applying the dependence of seismic energy on the excavated deposit volume for a continuous evaluation of seismic hazard in mines.

It was shown that for high-energy tremors the area of energy accumulation preceding a tremor covers several longwalls and the accumulation period can last several years.

The result of study of bimodal distribution were taken into account for the relationship between seismic energy and extracted deposit amount.

With a view to the energy accumulation, the evaluation of seismic hazard has a character of long-term forecast.

It is proposed that the Bayes formula should be used for evaluating the seismic hazard in order to take into account at the same time the progress of extraction and the results of measurements by different geophysical methods. These measurements or evaluations can act as intermediate and short-term precursors.

References

Aki, K., A probabilistic synthesis of precursory phenomena. In Earthquake Prediction, An International Review, (ed. Simpson, D. W., Richards P. G.,)(American Geophys. Union, Washington D. C. 1981)566-574

Dessokev M. M., (1984) Statistical model of Seismic Hazard Analysis for mining tremors and natural earthquakes, PUBL. INST. GEOPHYS. Pol. Acad. Sc. A-15 (174)

Głowacka E., Rudajev V., Bucha V., (1988) An attempt of continuous evaluation of seismic hazard induced by deposit extraction for the Robert Field in the "Gottwald" mine in Kladno, Publs. Inst. Geophys. Pol. Acad. Sc. M-10, (212)

Głowacka E., Syrek B., Kijko A., (1985)Dynamic evaluation of the seismic hazard in "Wujek" coal mine (in Polish) ACTA MONTANA 75 p. 5-20

Kijko A., (1985), Theoretical model for a relationship between mining seismicity and excavation area, ACTA GEOPHYS. POL. 33, 231-242 Kijko A., Głowacka E., (1985), Związek aktywności sejsmicznej górotworu z eksploatacja w kopalniach LGOM-u. Materiały I krajowej konferencji naukowo-technicznej: Zastosowanie metod geofizycznych w górnictwie kopalin stałych. t II, s. 101-106.

Kijko A., Drzezla B., Stankiewicz T., (1987) Bimodal character of the distribution of extreme seismic events in Polish mines, Acta Geophys. Pol., 35

McGarr, A., (1976), Seismic moments and volume changes. J. GEOPH. RES. 81, 1487-1494

Randall, M., J., (1971), Shear invariant and seismic moment for deep-focus earthquake. J. GEOPHYS. RES. 76, 4991-4992

Rikitake, T., Earthquake Prediction (Elsevier, 1976)

Sklenar, J., Rudajev, V., (1975), Application of some seismic methods for the evaluation of stress-strain condition in the rock mass. ACTA MONTANA 32, 211-230.

Stankiewicz T., (1988), A stochastic model for the occurrence of mining tremors, Acta Geophys. Pol., 36, (in press).

EARTH'S ELECTRIC POTENTIAL VARIATIONS BEFORE STRONG EARTHQUAKES

Tz.M. Ralchovsky, L.N. Komarov,
B.K. Ranguelov, D.D. Deneva

Geophysical Institute-BAS, Acad. G. Bonchev Street,
block 3, 1113 Sofia, Bulgaria

1. Introduction

In the Geophysical Observatory "Vitosha" (φ = 42,6°N, λ = 23,2°E) situated near Sofia, continuous observations of the electric potential differences between electrodes placed not very deep under the surface are carried out since the beginning of 1986. The Earth's electric potential (EEP) is measured after amplification and filtration to a frequency of up to 0,3 Hz, the registration being analog one with a velocity of the recorder 1 cm/hour. The purpose of the observations is to find out characteristic changes of EEP preceding the earthquakes in the area. On the basis of the EEP changes many authors have endeavoured for a higher final goal, namely to realize earthquake prediction (Fedotov et al. 1970, Coe 1971, Sobolev 1975, Varotsos and Alexopoulos 1984 a,b) which, so far, cannot be considered as reached. Experimental data with varied characteristics continue to be obtained both as a result of the used methods and apparatuses, and as a result of the different local geological and tectonic conditions under which the natural observations are carried out (Miyakoshi 1986, Meyer and Ponomarev 1987, Ralchovsky and Komarov 1987, Meyer and Piriola 1987).

2. Experimental Data

As stated above the EEP observation is realized in the Geophysical Observatory "Vitosha" (VTS) by pairs of electrodes fixed in the earth's surface and connected with the measuring amplifier and analog recorder. The data about EEP thus obtained are compared with the data on the earthquakes that have occurred in the region of the Balkan Peninsula in 1986 and they are given in Table 1. The NEIS catalogs and the Bulgarian seismological system NOTSSI have been used. All earthquakes in this area with a magnitude M 4,5 for the whole 1986 have been selected. This magnitude limitation is needed because of the high seismicity of the region and the lack of strict criteria about the space-time correlation between the earthquakes and the EEP-variations. This limitation in no case can solve the problem of the space-time correlation but gives good reason, at least in a qualitative aspect, to assume that the earthquakes with a higher magnitude could have a better expressed electrodynamical effect. In Table 1 there are standard data about all 29 earthquakes in 1986, being the epicentral distance, h - source depth, and the last column with the respective signs (+,-,/) gives an idea of the EEP effect whether it was observed or not.

Fig. 1 is connected with Table 1 on which in a schematic map of the Balkan Peninsula the place of the earthquakes under consideration are shown and denoted with the respective numbers. The dotted circles denote the scale distances (in km) from the observation-VTS.

On all figures below copies of the EEP-registrogrammes are shown, in some figures being insignificantly smoothed in time intervals near the earthquakes under consideration. On the horizontal axis is time (UT), and on the vertical axis is the relative change of EEP intensity in mV.

In Fig. 2 a part of the original record of EEP on 18.02.86 is presented. Up to 09.00 UT the record is of a quiet character followed by an apparent increase of EEP level with about 5-7 mV followed by a longer recovery phase. It is namely in this phase that the earthquake occurs (EQ) at 14:34 UT with a magnitude 4,7 at a distance about 200 km from VTS. The EEP changes which are similar to the one described below will be called anomalies.

Fig. 3 connected with the first earthquakes of the sequence that have destroyed the town of Strazhitza on the territory of Bulgaria (Ralchovsky et al. 1986). The main shock with M = 5,1 is at 05 39 UT followed by two aftershocks (AEQ). The development of the anomaly in EEP starts about 6 hours before the main shock, reaching maximum (u 10 - 12 mV) at 03:00 UT. During the recovery phase the earthquake and the aftershocks occur, the recovery level being higher than the initial quiet values.

Fig. 4 is part of the original EEP recording at the time near the earthquake on 03.03.86/01:24 UT denoted by an arrow. In the period indicated two more events have occurred on the same place with a smaller magnitude which are also noted on the record. The earthquake is 7-8 hours after the start of the anomalous EEP increase, after passing through the maximum phase which has developed at the background of a general EEP level increase. As in Fig. 3 here we fall in a more complex anomalous variation connected with a few consecutive earthquakes at one and the same place. It is seen that the anomaly develops until the last one of the three earthquakes after which the EEP level is stabilized with a higher value than the initial one. Now the intensity of the anomaly is about 35 mV.

Fig. 5 is a copy of the analogue EEP record near the moment of a shock with a magnitude 5,2 on 15.03.86/08:46 UT. The anomaly in the behaviour of the electric potential is obvious and has an interesting impulse form. The earthquake is in its maximum at the second weaker impulse followed by the recovery phase until about 18:00 UT. The maximal intensity of the anomaly is about 55 mV.

Fig. 6 shows the EEP change for a period of 4 days and nights connected with a sequence of 5 earthquakes occurring in one and the same area at about 300 km from the place of observation. The earthquakes are "strung as a necklace" at the background of the developing anomaly, the strongest shock being during the highest maximum, followed by an abrupt drop of the potential. The anomaly intensity is about 50 mV. Because of technical reasons the

record has been broken 4 hours after the earthquake which is denoted with a dash-dot line, after which the record is renewed.

Fig. 7 is connected with the strongest destructive earthquake in the region of the Balkan peninsula during the last few years with M = 6,9 occurred in Vrancea on 30.08.86/21:28 UT. A number of electric effects can be ascribed to this earthquake which will be considered below. The anomaly which has developed immediately before the EEP main shock is shown in Fig. 7. In the period of development of the anomaly one more earthquake falls - at 19:15 UT which will not be considered now. The main shock of the Vrancea event is in the peak of the impulse maximum, followed by an abrupt drop and recovery of the initial level. Similar impulses, probably connected with the preparation of this strong earthquake, start appearing on the EEP records even on 19.08.86 and continue during the whole period to the main shock, initially with a big frequency of occurrence decreasing to one per day, about 70 hours before the earthquake itself.

The distribution of these impulses in the time is shown in Fig. 8. Besides them Fig. 8 presents also one more peculiarity in the EEP behaviour. This is a slow increase of the background level which has also started on 19.08.86 during the day of occurrence of the first impulse. The background level variations are shown with a dashed curve and the vertical segments mark the distribution and intensity of the impulses.

Fig. 9 shows an extremely intensive EEP-anomaly with a similar development and form as the previous cases, but connected with a relatively weak earthquake on 27.10.96 with M = 4.5 at a significant distance from VTS. As seen the earthquake falls in the plateau of the anomaly maximum followed by a continuous drop and recovery of EEP-level.

3. Discussion and Conclusion

From the cases shown here a big part of the earthquakes that have occurred in 1986 in the region of the Balkan Peninsula correlate with characteristic anomalous EEP variations.

From 29 earthquakes with M 4,5 for three of them /(1),(2), (3)/ we have no data about EEP. Having in mind that the earthquakes are local events by preparation and realization for 5 cases /(6), (10), (11), (12), (22)/ the epicentral distance is relatively big and we may suppose that their preparation cannot be reflected on the EEP behaviour observed in VTS. Further on statistics shows that 2/3 of the occurred earthquakes have precursory EEP-anomalies and only for 7 cases there is no EEP-effect.

The question of the EEP-reliability and how they are connected with the earthquakes that have occurred after them remains controversial. The results reported so far show a wide deviation of the preceding time of EEP-effect occurrence before a given earthquake. For the different authors it varies from months to hours which makes the correlation of the effect with the earthquake very low. In the intermediate time interval it is possible that a great number of earthquakes can occur especially in seismoactive zones. It is also possible that EEP-changes may occur due to meteorological factors, geomagnetic variations,

tidal variations, artificial disturbances. In other words the indirect connection of the EEP-effect with the earthquake creates problems with the space-time correlation of the events. A better understanding and reliability could be obtained if a relative simultaneousness of the two events is observed, i.e. in a definite phase of the EEP-anomaly development the earthquake occurs. In the cases indicated by us there is a certain definiteness of the earthquake since the EEP-anomaly development. The earthquakes occur during the peak of the anomalous change maximum immediately before the abrupt drop of the intensity or after the maximum of realization in the phase of the gradual recovery of the potential initial level.

As seen from the experimental data the EEP-anomaly can be also connected with cases of single earthquakes as well as with a sequence of earthquakes from one and the same source. As a rule the EEP change continues until the occurrence of the last earthquake irrespective of its magnitude. This fact indicates that the tectonic energy turns into electrodynamical one until the last stage of the deformation strain falling. Evidently this is the more complex case of occurrence of a precursor EEP-change.

The existence of two cases of EEP-anomaly, namely at a single earthquake, and at a sequence of earthquakes, complicates the obtaining of simple estimations for the different parameters characterizing the seismic and electric events.

Generalizing the experimental data thus presented, it should be noted that:

- EEP anomalous variations are recorded developing, as a rule, in hours (2-9 hours) before a given earthquake and the single case of a destructive earthquake (30.08.86/M=6,9) shows that anomalous "impulses" in EEP can be observed about ten days before the earthquake;

- the earthquakes occur in two definite phases in the EEP-anomaly development, namely: in the anomaly maximum followed by the abrupt drop of the potential or during the recovery phase of the anomaly;

- the intensity of the anomalous changes significantly exceeds the background noise remaining approximately within the interval 6-60 mV for the different earthquakes.

REFERENCES

1. Coe, R., Earthquake Prediction Program in the People's Republic of China, EOS, Trans.Amer.Geophys. Union, 52, 940-943, 1971.

2. Fedotov, S. et al., Investigation on earthquake prediction in Kamchatka,Tectonophysics, 9, 249-258, 1970.

3. Meyer, K. and R. Piriola, Anomalous electroteluric residuals prior to a large imminent earthquake, Tectonophysics 125, 371-376, 1986.

4. Meyer, K. and A. Ponomarev, Electroteluric forerunners to earthquakes in Kamchatka, Tectonophysics, 138, 341-347, 1987.

5. Miyakoshi, J., Anomalous time variation of the self-potential

in the fractured zone of an active fault preceding the earthquake occurrence, J. Geomag. Geoelectr. 38, 1015-1030, 1986.

6. Sobolev, G., Application of electric method to the tentative short-term forecast of Kamchatka earthquake, Pageoph, 113, 229-235, 1975.

7. Ralchovsky, T. and L. Komarov, Earth electric activity in August-September 1986 and a strong earthquake in Vranchea, Bulg. Geophys. J., XIV, 1, 78-85, 1988.

8. Varotsos, P. and K. Alexopoulos, Physical properties of the variations of the electric field of the Earth preceding earthquakes, I, Tectonophysics, 110, 73-98, 1984.

9. Varotsos, P. and K. Alexopoulos, Physical properties of the electric field of the Earth preceding earthquakes. Determination of epicenter and magnitude, Tectonophysics, 110, 99-125, 1984.

10. Ralchovsky, T. et al. An experimental result for the earth electric potential and the earthquakes, Compt.rend.Acad.bulg. Sci., 39, 11, 61-63, 1986.

FIGURE CAPTIONS

Fig. 1 A scheme of the location of epicentres of earthquakes with M 4,5/1986 and observatory "Vitosha" (VTS).

Fig. 2 A copy of EEP registrogram on 18.01.1986, the time of the earthquake (EQ) with M=4,7 is denoted by an arrow.

Fig. 3 A copy of EEP registrogram for the earthquake on 21.01.1986 with M = 5,1: AEQ denotes the times of the occurred aftershocks.

Fig. 4 A copy of the EEP registrogram for three consecutive earthquakes on 03.03.1986.

Fig. 5 A copy of the EEP registrogram for the earthquake on 15.03.1986.

Fig. 6 EEP smoothed values for the period 02.05-05.05.1986.

Fig. 7 Impulse EEP change for the earthquake in Vrancea on 31.08.86

Fig. 8 Distribution of the impulses near the earthquake in Vrancea for the period 16.08-16.09.1986.

Fig. 9 A copy of the EEP registrogram for the earthquake on 27.10.1986.

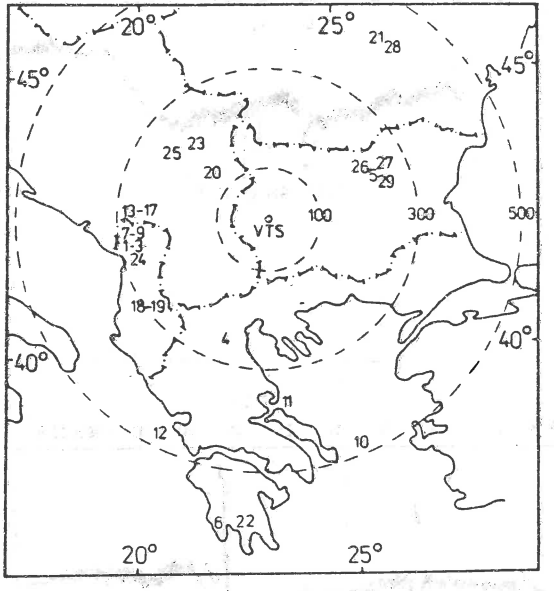

FIG.1

TABLE – 1

BALKAN PENINSULA EARTHQUAKES 1986 , (M ≥ 4,5)

No	DATE 1986	GT	φ °(N)	λ °(E)	Δ /KM/	h /KM/	M	F
1	08.01.	14 50	42,3	19,8	280	10	5,0	-
2	08.01.	15 18	42,3	19,8	280	10	5,0	-
3	08.01.	20 57	42,3	19,9	280	11	5,0	-
4	18.02.	14 34	40,7	22,0	200	26	4,7	-
5	21.02.	05 39	43,3	29,5	230	25	5,1	-
6	22.02.	21 11	36,6	21,9	720	33	4,8	-
7	03.03.	01 24	41,9	20,3	250	23	5,0	-
8	03.03.	12 36	41,9	20,3	250	23	4,9	-
9	15.03.	08 46	41,1	20,0	300	10	5,2	-
10	25.03.	01 41	38,4	25,1	500	5	5,1	-
11	07.04.	02 59	38,8	23,3	400	12	4,8	-
12	22.04.	20 33	38,4	20,5	490	57	4,5	-
13	02.05.	10 19	42,2	19,7	280	10	5,1	-
14	03.05.	04 37	42,3	19,9	270	10	5,1	-
15	03.05.	09 17	42,4	19,9	280	10	5,0	-
16	04.05.	00 30	42,3	19,9	280	10	5,1	-
17	04.05.	21 16	42,2	19,9	280	10	5,3	-
18	25.06.	20 44	41,2	19,5	300	28	4,7	-
19	18.08.	01 48	41,5	20,0	280	10	4,9	-
20	30.08.	19 15	43,4	21,9	140	10	5,1	-
21	30.08.	21 28	45,6	26,3	420	139	5,9	-
22	13.09.	17 24	37,0	22,2	620	23	5,9	-
23	05.10.	08 55	43,7	20,9	280	10	4,5	-
24	27.10.	22 32	41,9	19,5	300	13	4,5	-
25	01.12.	00 08	43,3	20,9	220	10	5,0	-
26	07.12.	14 17	43,3	25,6	350	38	5,6	-
27	08.12.	14 44	43,3	26,0	390	10	4,5	-
28	15.12.	22 38	45,6	30,4	420	148	4,8	-
29	15.12.	17 16	43,3	26,0	390	10	4,8	-

+ - effect ; - - no effect ; / - no data

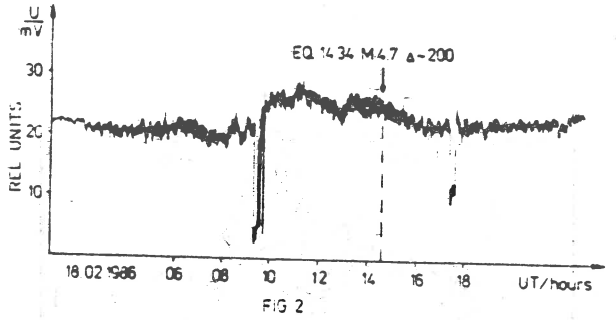

FIG 2

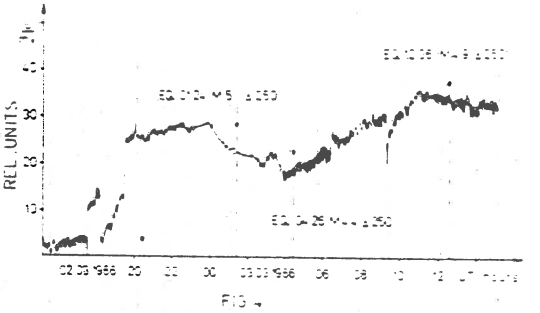

FIG 4

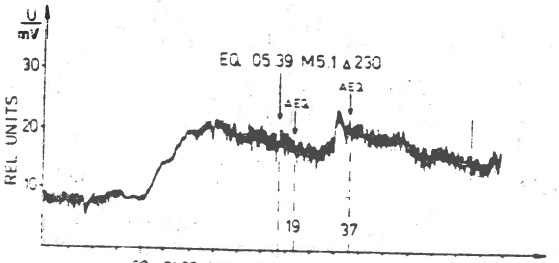

FIG 3

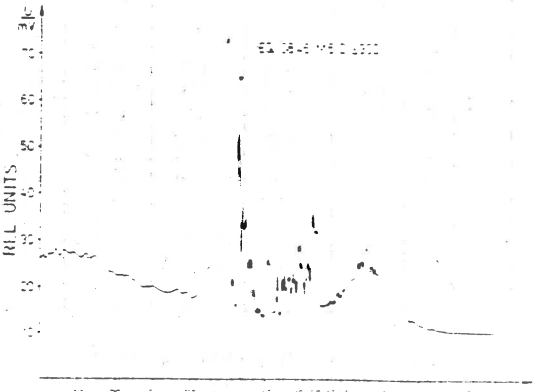

FIG 5

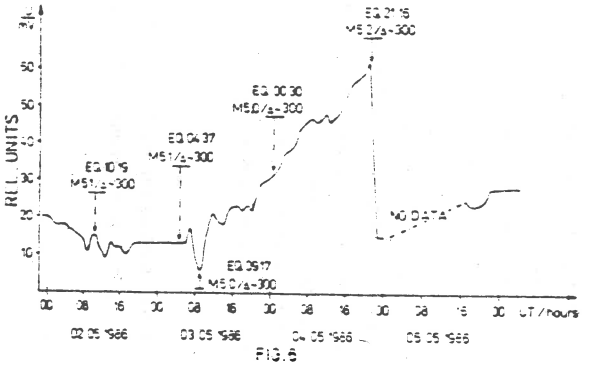

FIG.6

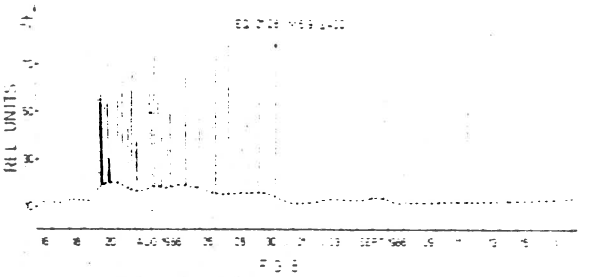

FIG.8

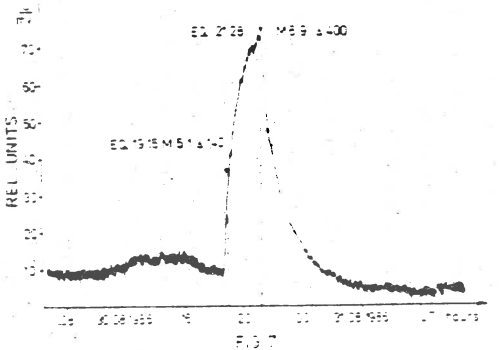

FIG.7

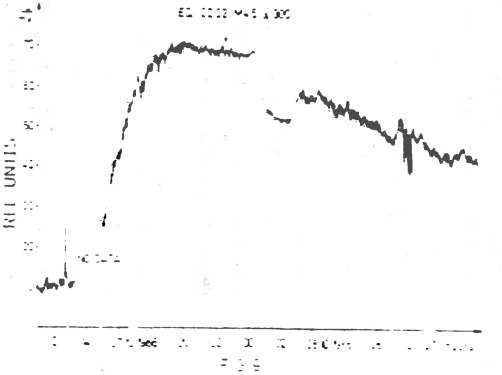

FIG.9

Seismic observations in the Mudurnu Valley Test Area at the North Anatolian Fault Zone

E.Weigelt, H.Berckhemer, B.Baier
Inst.f.Meteorologie u. Geopysik, Frankfurt a.M.,FRG
R.Ates, A.Yatman, O.Ozel
Earthquake Research Institute, Ankara, Turkey

Within the Circum-Mediterranean seismic belt the North Anatolian fault zone (NAFZ) is characterized by a geographically well defined seismic activity and, therefore, particulary suited for research on phenomena in the earthquake preparation zone.

Along the NAFZ three regions of high seismic energy density can be recognized.
The first one is at the eastern end around Erzurum where North- and East Anatolian fault zone join. The second zone is around Karabük and Tosya, where the NAFZ changes direction. The thirt zone of high seismic activity lies at the western end of the NAFZ, in the region south of Adapazari.
Here the NAFZ splits into a northern branch running through the Bay of Izmit into the Marmara Sea, and a southern fault system which can be traced at the surface from Abant Lake in the east along the Mudurnu valley and finds a possible continuation in the Iznik-Mekece fault zone.

In the branching region the tectonic stile of the NAFZ changes from right lateral strike slip to normal faulting. This is not only evidenced by fault plane solutions of larger earthquakes but also by the composite fault plane solutions of 60 micro earthquakes as shown in Fig.4. The considerable number of data inconsistent with the best fit solution indicates the transitional character of the tectonic regime.

Seismicity investigations (1800 to 1980) show, that major earthquakes (M>5) occure in time intervals of 10 to 20 years around the Mudurnu valley.

The frequency of occurrence of medium to large earthquakes in a small area and the apparently high and continuos stress accumu - lation makes this region favorabel for the Turkisch- German project for earthquake prediction research.

Within this project observations of micoearthquakes around the Mudurnu valley provide basic data for the other experiments and for studies on relations between low magnitude seismicity and larger shocks.

Five seismograph stations (ASA, BZT, CAK, INE, KOG) were installed around the Mudurnu valley and are operating since October 1984. This net was enlarged by the stations MEC (since May 1988), ESE and DOG(since October 1988) (s.Fig 1.).

The stations are equiped with short period Willmore Mark 3-seismometers; T_0 = 1.4 and with the longterm tape recording system MLR-78 developed and built in the Frankfurt Institute of Meteorology and Geophysics. This analog recording system is working continuously over three weeks with an internal battery power supply. Timing is achieved by coded crystal clocks set and syn - chronized by DCF long wave radio signal (Bonanomi Telecode).

The tapes are evaluated in Ankara and Frankfurt searching for earthquakes by amplitude trigger. Using P- and S- arrival times the epicenters are calculated by the computerprogram Fasthypo.

About 850 lokal earthquakes were registrated in the test area during 1985 to 1987, with ML< 3.0. Just a few events had ML>3.0 up to 4.2. Magnitude ML is calculated from the signal duration.

Fig.2 shows the number of earthquakes per month in the time of 1985 to 1987. An increase in the rate of earthquakes can be re - cognised in May 1986 from averagely 15 to 25 events per month and again an increase in June 1987 up to 35 events per month.

The epicenter distribution for 1985 to 1987 (Fig.3) shows concentration of activity in the south-western part of the test area and especially an accumulation along the western part of the fracture zone of the last big earthquake (22.Jul.1967; M=7.2).

The eastern part of the test area and fracture zone seem nearly free of earthquakes.
Also a westwards migration of the center of activity at a rate of 10-15 km/year is appearand.

The depth of the earthquakes is low, generally about 5 to 10 km.

Some earthquake swarms with nearly identical signal shape were registrated around Tasburun.

Composite fault plain solutions of about 60 microearthquakes show right lateral striks slip with some tendency to normal faulting. (Fig. 4). Inconsistences in the solution indicate variations in the tectonic behaviour in the Mudurnu region.

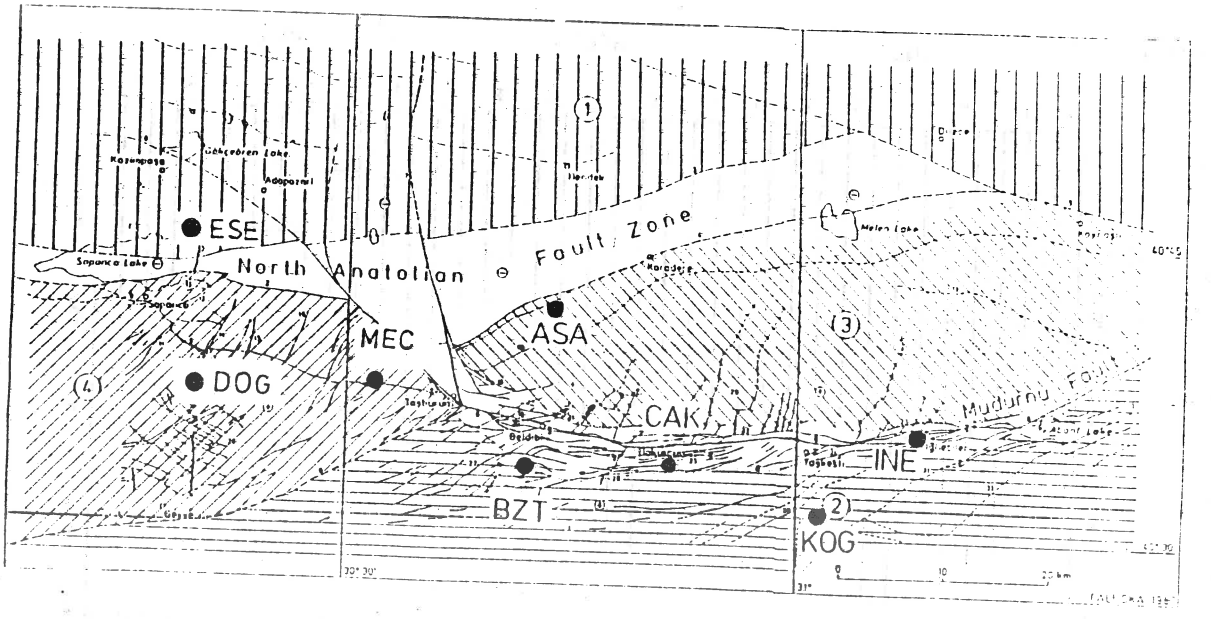
ESE
North Anatolian Fault Zone
MEC
ASA
DOG
CAK
INE
BZT
KOG
1
2
3
4

Figure 1.

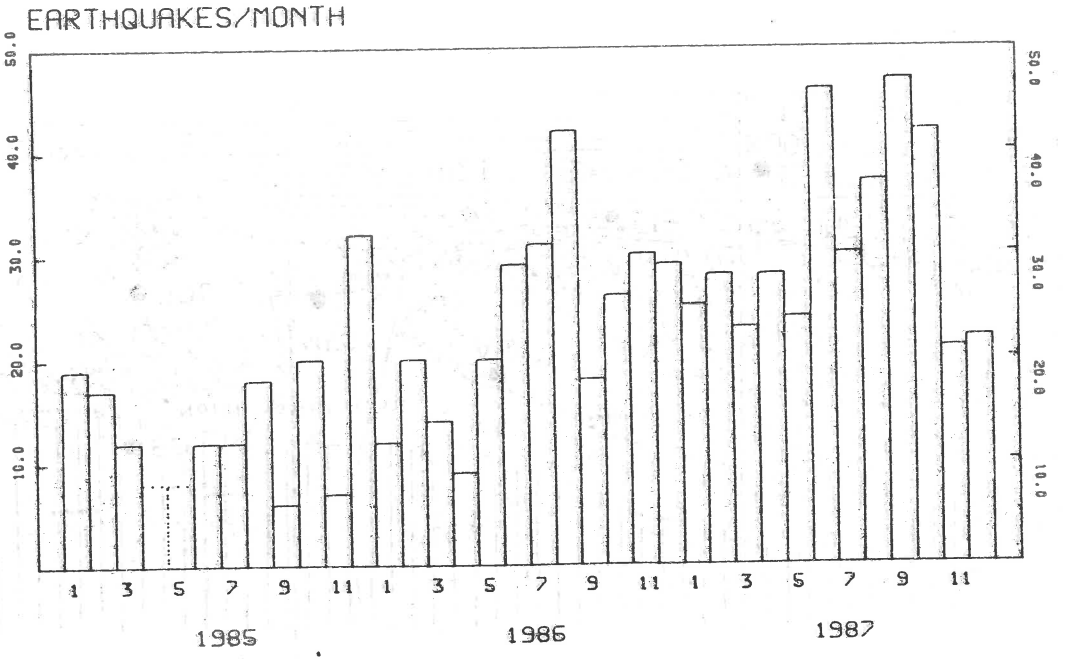
EARTHQUAKES/MONTH
50.0
40.0
30.0
20.0
10.0
1 3 5 7 9 11 1 3 5 7 9 11 1 3 5 7 9 11
1985
1986
1987

Figure 2.

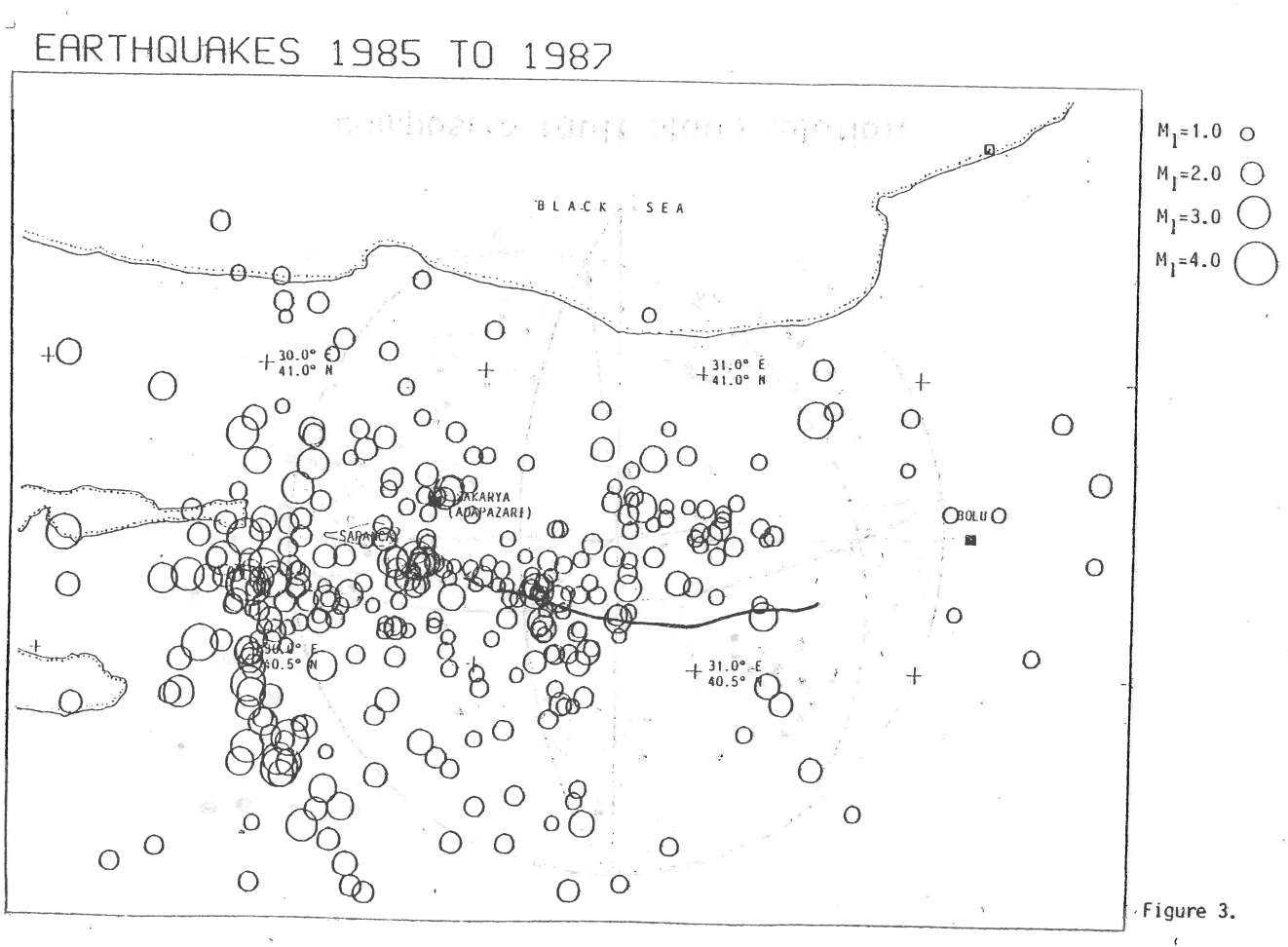
EARTHQUAKES 1985 TO 1987
BLACK SEA
30.0° E
41.0° N
31.0° E
41.0° N
SAKARYA
(ADAPAZARI)
SAPANCA
BOLU
30.0° E
40.5° N
31.0° E
40.5° N
M1=1.0
M1=2.0
M1=3.0
M1=4.0

Figure 3.

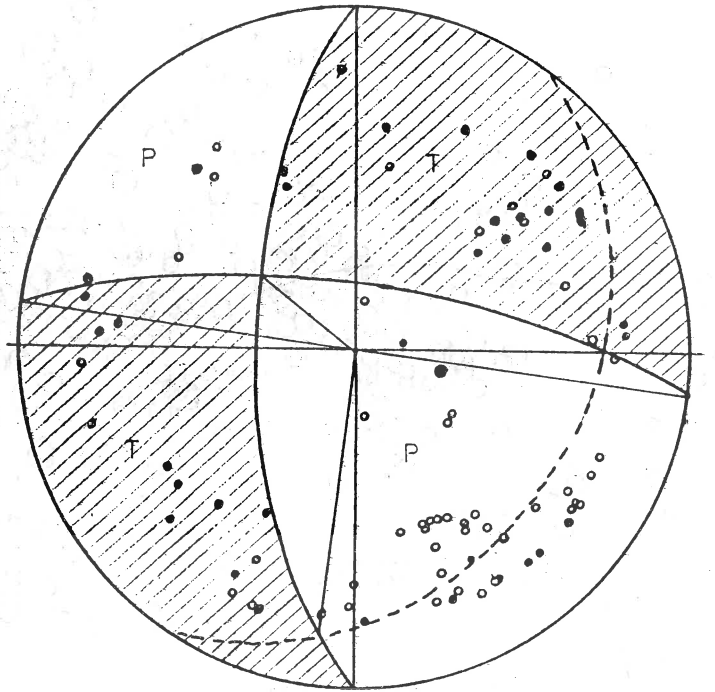

composite fault plane solution

Figure 4.

Evidence for Mechanical Properties Variations in the Friuli Seismic Area

Mao, W.J., Ebblin, C.,* Zadro, M.

Institute of Geodesy and Geophysics
University of Trieste, Italy

* Department of Physics
University of L'Aquila, Italy

Abstract

Three different methods and two kinds of data were used to investigate the mechanical parameter time variations in the Friuli seismic area in the years following the destructive 1976 earthquake.

The Earth tidal strains were extracted from three horizontal, longitudinal--strain--8--years records (1979--1986) in the Friuli seismic area by the filter method (Mao et al., 1988). The areal strain factor, where the tidal loading effects are negligible, shows significant time variations: amplitudes in 1986 being about 50 percent of those in 1979 (Table 1).

The rock mechanical properties modifications, estimated in terms of the local shear and bulk modulus variations, were obtained considering the envelope of the tidal strain signals.

The detection of near-field seismic velocity changes from microearthquake data is usually difficult owing to small errors in the hypocentral location and the arrival measurement for single event brings about a large velocity uncertainty. The simultaneous inversion for hypocenter location and seismic velocities of the arrival time data of the local seismometric network yielded satisfactory results and displayed velocity changes in good agreement with the estimates above (Fig. 1).

However although bulk modulus and seismic velocity change compatibly, shear modulus does not. This may be because the velocity changes are average values within the microearthquake network, whereas tidal strains mainly reflect the medium properties around the Villanova station.

Of particular interest appears the change in the velocities and the elastic parameters which started in March 1982, about 11 months before an earthquake of magnitude 4.1, the largest event from 1979 to 1986, which occurred under the seismic network on Feb. 10, 1983. When the earthquake occurred the change of the velocities and of the bulk modulus had reached about 3 percent and 50 percent, respectively. After the earthquake, the velocities and K started to turn to values like those observed before the event and the recovery time was nearly equal to that of the deviation. Similar results were also reported by Mikumo et al. (1978).

It also appears noteworthy that the earthquake occurrence is marked by a bulk modulus increase in contradiction with the dilatation hypotheses.

Many earthquakes of M<4 occurred under the Friuli microearthquake network during 1978 to 1986 but did not bring about evident velocity and elastic parameter changes. This would indicate that, in the Friuli seismic area, the velocities and tidal strain amplitudes display evident changes only prior to earthquakes of M>4 and that the latter changes are more sensitive than the former ones, supporting the theoretical results obtained by Beaumont and Berger (1974).

Table 1. Areal Strain Factor (h-31)

wave	areal strain T Am.	areal strain O Am.	h-31 *	phase lag (degree)
1979 June - November				
M_2	1.178	1.026	0.314	14
O_1	1.085	0.717	0.238	4
1986 May - October				
M_2	1.163	0.473	0.147	6
O_1	1.064	0.476	0.165	11

T and O denote theoretical and observed tides.
The unit of areal strain amplitude is 10^{-8}.

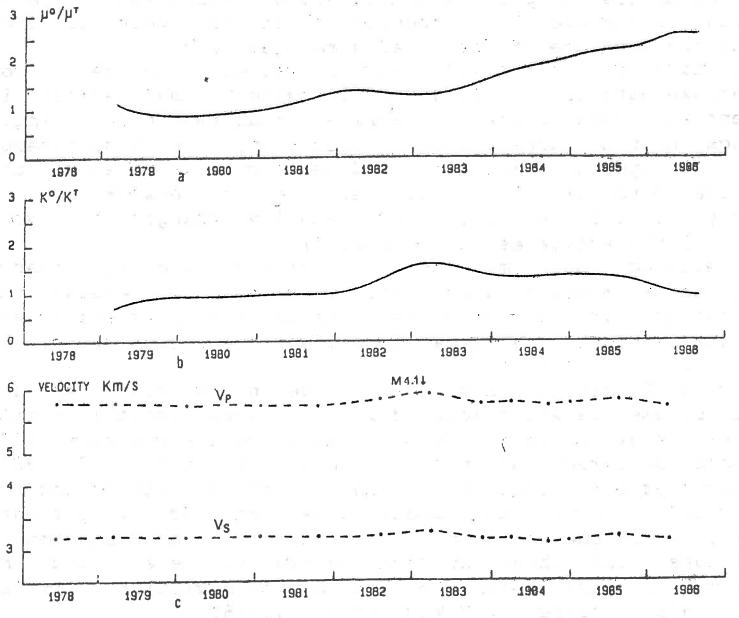

Fig. 1. Temporal variations of the shear modulus (a), of the bulk modulus (b) and of the seismic velocities (c).

Ackowledgments

One of the authors (W. Mao) has carried out this work with the support of the ICTP Programme for Training and Research in Italian Laboratories, Trieste, Italy. This research has been supported by MPI 6H0 Prof. Zadro and CNR 610 87,00852,05 Prof. Ebblin funds.

References

Beaumont, C. and Berger, J., 1974. Earthquake prediction: modificationof the Earth tide tilts and strains by dilatancy, Geophys. J. R. astr. Soc., 39, 111-121.

Mao, W. J., Santero, P., and Zadro, M., 1988. Long and middle term behaviour of the tilt and strain variations in the Friuli area, NE Italy, submitted to PAGEOPH.

Mikumo, T., Kato, M., Doi, H., Wada, Y., Tanaka, T., Shichi, R., and Yamamoto, A., 1978. Possibility of temporal variations in earth tidal strain amplitudes associated with major earthquakes, in: Earthquake Precursors: Proceedings of the U.S.-Japan Seminar on Theoretical and Experimental Investigations of Earthquake Precursors, Kisslinger, K., and Suzuki, Z., eds, Central Academic Publishers of Japan, Tokyo, 123-136.

This paper has been submitted to Tectonophysics.

Evidence for Mechanical Properties Variations in the Friuli Seismic Area

Mao, W.J., Ebblin, C.,* Zadro, M.

Institute of Geodesy and Geophysics
University of Trieste, Italy

* Department of Physics
University of L'Aquila, Italy

Abstract

Three different methods and two kinds of data were used to investigate the mechanical parameter time variations in the Friuli seismic area in the years following the destructive 1976 earthquake.

The Earth tidal strains were extracted from three horizontal, longitudinal--strain--8--years records (1979--1986) in the Friuli seismic area by the filter method (Mao et al., 1988). The areal strain factor, where the tidal loading effects are negligible, shows significant time variations: amplitudes in 1986 being about 50 percent of those in 1979 (Table 1).

The rock mechanical properties modifications, estimated in terms of the local shear and bulk modulus variations, were obtained considering the envelope of the tidal strain signals.

The detection of near-field seismic velocity changes from microearthquake data is usually difficult owing to small errors in the hypocentral location and the arrival measurement for single event brings about a large velocity uncertainty. The simultaneous inversion for hypocenter location and seismic velocities of the arrival time data of the local seismometric network yielded satisfactory results and displayed velocity changes in good agreement with the estimates above (Fig. 1).

However although bulk modulus and seismic velocity change compatibly, shear modulus does not. This may be because the velocity changes are average values within the microearthquake network, whereas tidal strains mainly reflect the medium properties around the Villanova station.

Of particular interest appears the change in the velocities and the elastic parameters which started in March 1982, about 11 months before an earthquake of magnitude 4.1, the largest event from 1979 to 1986, which occurred under the seismic network on Feb. 10, 1983. When the earthquake occurred the change of the velocities and of the bulk modulus had reached about 3 percent and 50 percent, respectively. After the earthquake, the velocities and K started to turn to values like those observed before the event and the recovery time was nearly equal to that of the deviation. Similar results were also reported by Mikumo et al. (1978).

It also appears noteworthy that the earthquake occurrence is marked by a bulk modulus increase in contradiction with the dilatation hypotheses.

Many earthquakes of M<4 occurred under the Friuli microearthquake network during 1978 to 1986 but did not bring about evident velocity and elastic parameter changes. This would indicate that, in the Friuli seismic area, the velocities and tidal strain amplitudes display evident changes only prior to earthquakes of M>4 and that the latter changes are more sensitive than the former ones, supporting the theoretical results obtained by Beaumont and Berger (1974).

Table 1. Areal Strain Factor (h-31)

wave	areal strain T Am.	areal strain O Am.	h-31	phase lag (degree)
1979 June - November				
M_2	1.178	1.026	0.314	14
O_1	1.085	0.717	0.238	4
1986 May - October				
M_2	1.163	0.473	0.147	6
O_1	1.064	0.476	0.165	11

T and O denote theoretical and observed tides.
The unit of areal strain amplitude is 10^{-8}.

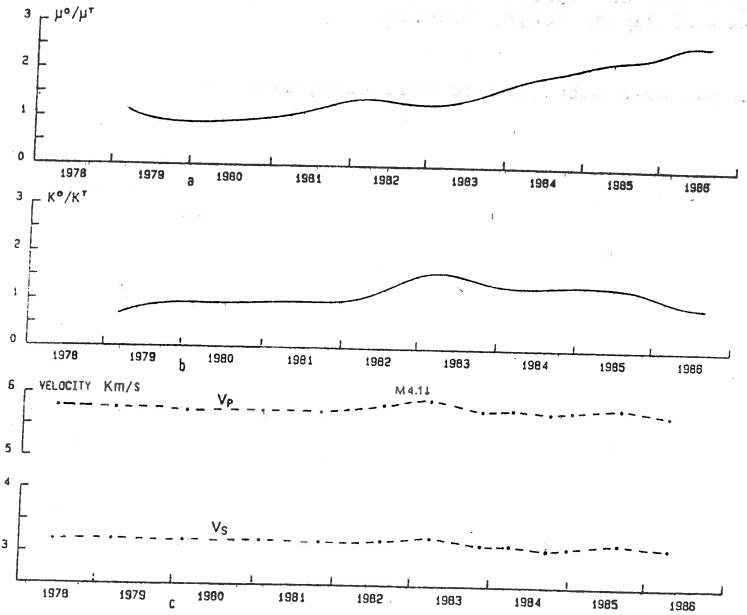

Fig. 1. Temporal variations of the shear modulus (a), of the bulk modulus (b) and of the seismic velocities (c).

Ackowledgments

One of the authors (W. Mao) has carried out this work with the support of the ICTP Programme for Training and Research in Italian Laboratories, Trieste, Italy. This research has been supported by MPI 6H0 Prof. Zadro and CNR 610 87,00852,05 Prof. Ebblin funds.

References

Beaumont, C. and Berger, J., 1974. Earthquake prediction: modificationof the Earth tide tilts and strains by dilatancy, Geophys. J. R. astr. Soc., 39, 111-121.

Mao, W. J., Santero, P., and Zadro, M., 1988. Long and middle term behaviour of the tilt and strain variations in the Friuli area, NE Italy, submitted to PAGEOPH.

Mikumo, T., Kato, M., Doi, H., Wada, Y., Tanaka, T., Shichi, R., and Yamamoto, A., 1978. Possibility of temporal variations in earth tidal strain amplitudes associated with major earthquakes, in: Earthquake Precursors: Proceedings of the U.S.-Japan Seminar on Theoretical and Experimental Investigations of Earthquake Precursors, Kisslinger, K., and Suzuki, Z., eds, Central Academic Publishers of Japan, Tokyo, 123-136.

This paper has been submitted to Tectonophysics.

A METHOD OF MAP COMPILATION FOR EXPECTED EARTHQUAKES ON A COMPLEX OF SEISMOLOGICAL PRECURSORS

Sobolev G. A., Chelidze T. L. *, Zavyalov A. D., Slavina L. B. and Gotsadze O. D. *

Institute of Physics of the Earth, USSR Academy of Sciences, B. Gruzinskaya, 10, Moscow, 123810 (USSR)
*Institute of Geophysics, Georgian SSR Academy of Sciences, Z. Rukhadze, 1, Tbilisi, 380093 (USSR)

Intensive searching of earthquake precursors beginning from the 1960-s resulted up to now in the data collected on several dozens of precursory events in geophysics. The effectiveness of each precursor determined as the ratio of earthquake density in alarm time (or over an area) to the average earthquake density for the period (or over an area) of observations, as a rule, does not considerably exceed the prediction effectiveness in random forecasting. The earthquake prediction experience of today suggests that combination of various precursors to estimate a prognostic situation increases the prediction effectiveness several times.

The basis of the suggested complex analysis of seismological precursors of earthquakes of energy class K≥12.5 is the Bayesian principle of revealing of time-space regions of increased probability of expectation of a large earthquake from the combination of parameters (map of expected earthquakes).

Information basis for the developing the method of compilation of the map of expected earthquakes was formed by the catalog of Caucasian earthquakes of energy classes K≥8.5 for the period 1962-1985. As prognostic features the following seven parameters are used (see Table 1): the density of seismogenic fractures K_{sf} (Zavyalov, 1986) the slope of recurrence curve ε_γ (Zavyalov, 1984), the number of weak earthquakes in a time unit as seismic quiescence ε_n and activation ΔN, the ratio of onset times of elastic waves ε_τ (Slavina and Tagizade, 1984), the seismic energy releas $\Delta E^{2/3}$ and ΔE (Keilis-Borok, 1959). These parameters were chosen using the ideas on the physics of earthquake source which are based on the model of avalanche-unstable fracturing. This concept describes the process of preparation of a large earthquake as a result of cooperative development of faults at different scale levels. All prognostic features were presented as space-time distributions of anomalous deviations from a respective background level and had retrospective statistical estimates of prediction effectiveness presented in Table 1.

To compile the map of expected earthquakes the region

under study was divided into elementary seismoactive cells, in each of them the values of every prognostic parameter were calculated (Likov et al., 1984). The probability of expectation

Table 1.

Results of retrospective test of parameters included in the map of expected earthquakes in the Caucasus.

No	Parameter	Critical level	Probability of detection $P(K_i \mid D_1)$	Probability of false alarm $P(K_i \mid D_2)$	Precursor time, years
1	K_{sf}	12.2	0.55	0.22	7.7 ± 4.4
2	ε_y	$+2\sigma$	0.78	0.46	3.0 ± 2.3
3	ε_n	-1σ	0.61	0.32	5.9 ± 3.2
4	ΔN	$+2\sigma$	0.56	0.32	4.4 ± 3.3
5	ε_τ	$\pm 3\sigma$	0.75	0.23	3.3 ± 1.9
6	$\Delta E^{2/3}$	$+2\sigma$	0.56	0.47	4.2 ± 3.7
7	ΔE	$+2\sigma$	0.63	0.54	5.8 ± 3.3

T_{pr}=4.9 ± 1.7

of a large earthquake with a combination of prognostic precursors available in the elementary cell was calculated by the Bayes formula

$$P(D_1 \mid K) = \frac{P(D_1) * \prod_{i=1}^{n} P(K_i \mid D_1)}{P(D_1) * \prod_{i=1}^{n} P(K_i \mid D_1) + P(D_2) * \prod_{i=1}^{n} P(K_i \mid D_2)}$$

where $P(D_1)$ is the unconditional stationary probability of occurrence of large earthquake in a spacial cell examined; $P(D_2)=1-P(D_1)$ - the unconditional stationary probability of non-occurrence of large earthquake in the spacial cell examined; K_i - the presence of the i-th prognostic precursor in the cell.

The area under study was differentiated with respect to the value of unconditional stationary probability with due account of the data on fault tectonics and velocities of vertical motions.

Figure presents the map of expected earthquakes for the Caucasus from the 1962-1980 data. It can be considered as prognostic one for a period of 1981-1985. During this period on

the area confined by the map eight earthquakes took place with 12.5≤K≤13.3. Larger earthquakes were not recorded.

Tables 2 and 3 estimate the effectiveness J of a retrospective forecast from the map of expected in 1980 earthquakes, for the combined map and the maps of separate methods. Each of eight large earthquakes in 1981-1985 was considered retrospectively predicted if the region of its preparation (a circle with the radius R=5*L, where L is the rupture length in the source calculated empirically by the formula $\lg L_{km}=0.244*K-2.266$) covered more than a half of a spacial cell with the respective value of η. Here η is the ratio of conditional probability of the expectation of a large earthquake to unconditional one; N_p is the number of retrospectively predicted earthquakes; N_Σ is the whole number of large earthquakes occured during the observation time in the area under study S_Σ. The alarm area S_{al} was calculated with the same rule kept in mind, but, instead of the cell area, the areas πR^2 of the circles described around the cells' centre entered S_{al}.

Table 2.

The effectiveness of the map of expected earthquakes in the Caucasus as of 1980 from the 1981-1985 test results.

$\eta=\frac{P(D_1 \mid K)}{P(D_1)}$	9	8	7	6	5	4	3
N_p/N_Σ , %	12.5	12.5	37.5	62.5	62.5	75.0	87.5
S_{al}/S_Σ , %	5.5	6.7	11.2	12.4	13.4	19.6	23.5
$J=\frac{N_p/N_\Sigma}{S_{al}/S_\Sigma}$	2.3	1.9	3.3	5.0	4.7	3.8	3.7

Table 3.

The effectiveness of separate parameters from the 1981-1985 test results.

	ε_τ	K_{sf}	ε_y	ε_n	ΔN	$\Delta E^{2/3}$	ΔE	Mean
N_p/N_Σ , %	25.0	69.0	75.0	87.5	12.5	56.0	25.0	47.0
S_{al}/S_Σ , %	10.0	20.0	59.0	53.0	26.0	42.0	35.0	35.0
$J=\frac{N_p/N_\Sigma}{S_{al}/S_\Sigma}$	2.5	3.4	1.3	1.7	0.5	1.3	0.7	1.6

The comparison of Tables 2 and 3 shows that the map of expected earthquakes compiled from a combination of precursors, worked more effectively than the maps compiled from separate prognostic features.

At present, the map of expected earthquakes in the Caucasus for 1986-1990 is tested. On 13 May, 1986 in the Caucasus in the region of Dgavahet Highland an earthquake of energy class K=14 took place in the zone where the conditional probability $P(D_1|K)$ six times exceeded the unconditional one.

REFERENCES

Keilis-Borok V.I., 1959. On estimation of the displacement in an earthquake source and of source dimensions. - Ann.geofis., v.12, No.2, pp.205-214.

Likov V.I., Sobolev G.A. et al., 1984. Metodika viyavleniya razvivauschegocya zemletryaseniya po kompleksu seismologicheskikh parametrov. In: Prognoz zemletryaseniy. Donish, Dushanbe-Moscow, No.5, pp.127-138 (in Russian).

Slavina L.B., Tagizade T.T., 1984. Prostranstvennovremennoe raspredelenie parametra $\Sigma[\Delta V_p/V_s]$ v zonakh zhivuschikh glubinnikh razlomov. In: Prognoz zemletryaseniy. Donish, Dushanbe-Moscow, No.5, pp. 209-216 (in Russian).

Zavyalov A.D., 1984. Naklon grafika povtoryaemosti kak predvestnik silnikh zemletryaseniy na Kamchatke. In: Prognoz zemletryaseniy. Donish, Dushanbe-Moscow, No.5, pp.173-184 (in Russian).

Zavyalov A.D., 1986. Parametr koncentracii seismogennikh razrivov kak predvestnik silnikh zemletryaseniy Kamchatki. Vulkanologiya i seismologiya, No.3, pp.58-71 (in Russian).

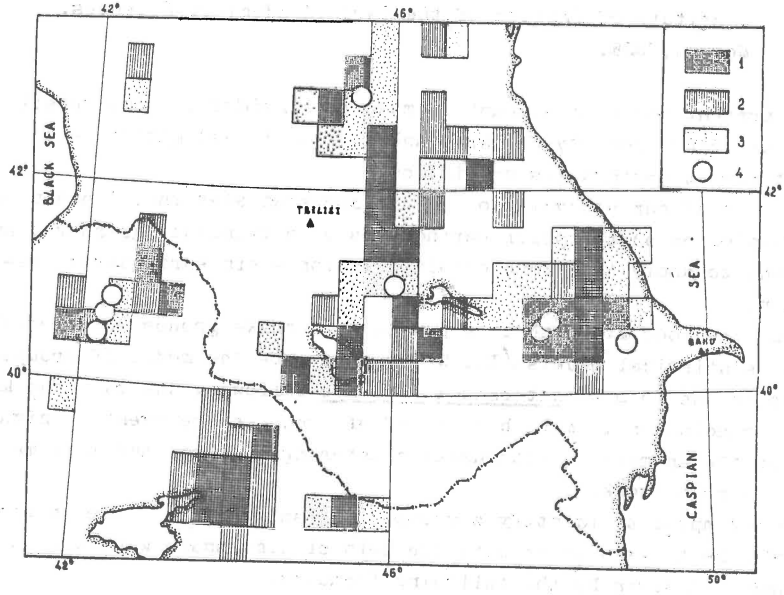

The map of expected earthquakes in the Caucasus compiled from a combination of seismological precursors as of 1980 with the 1981-1985 earthquakes plotted. 1,2,3 - zones of 0.70, 0.63 and 0.56 values of conditional probability of occurrence of earthquakes correspondingly; 4 - earthquakes epicenters.

THE MODEL FOR SEPARATION OF EARTHQUAKE GROUPS AND ITS APPLICATION TO LONG-TERM PREDICTION.

G.A.Sobolev, V.Yu.Vasiliev, V.V.Ratushny, A.D.Zavyalov
Institute of Physics of the Earth, Academy of Sciences,
Moscow, USSR.

In present paper an attempt is made to consider in some detail the clustering property of earthquakes. Such investigation is of importance in earthquakes prediction.

The aim of our study is to investigate spatial-temporal behaviour of grouping parameter prior earthquakes with magnitude greater than 5.0, and to apply technique obtained in long-term earthquakes prediction.

Some previous attempts to separate earthquake groups were based on the statistical models /I/. We suggest here the model of grouping events in the form of aftershock sequence following the main shock. Such a conclusion is made because of aftershocks are events, which reflect the anomalous earthquakes clustering in space and in time near the main shock.

We attempted to identify a group of seismic events close in space and time to each other with the help of time-space window: (T,R). The model is given by the following formulas:

$$T(K) = A \cdot 10^{BK} \quad (\text{hr}) \qquad (I)$$

$$R(K) = C \cdot L \quad (\text{km})$$

where $Lg(L) = 0.244 \cdot K - 2.266$ following Yu.V.Riznitchenko, L - fault length(km), K - energetic class of earthquake.

The result of such aftershocks investigation are general constants A,B,C, which are used then to define grouping events before large earthquakes with $K \geq 12.5$, or magnitude $M \geq 5.0$.

ALGORITHM FOR AFTERSHOCKS DETERMINATION.

In the earlier technique to separate aftershocks Gardner J.K. and Knopoff L. /2/ suggested empirical windowing procedure; ProzorovA.G., Shreider S.Yu. /3/ presented an algorithm to remove after-

shocks based on the hypothesis of the normal distribution of aftershocks around the main event.

Let us consider in some detail the new method describing aftershocks in space and time. The technique was applied to the Caucasus catalog of earthquakes with magnitude M ≥ 2.5 (K ≥ 8.5) for the time period 1962-1985.

The most important earthquake parameters such as origin time, energy/magnitude, depth and etc., are considered to be the target parameter in this visualization procedure. Therefore every event from the catalog is presented by means of colour point in three-dimensional space (X,Y,Z), where Z - is value of chose target parameter, and (X,Y) - are coordinates of earthquake in mercator projection. Point with coordinates 41.0 N/46.0 E corresponding to (0,0) km, is the center of the map.

The cloud of these points that we named "image" prepared and stored in a computer data base and with the aid of special computer programs could be reflected at the colour screen. Such a technique is allowed to use different image processing methods. Fig.1 shows the map of Caucasus catalog epicenter density for the period 1962-1985 years. It should be noted here that the number of earthquakes hitted in the definite space point is considered as a target parameter. The result of applying two-dimensional smooth filter as the image processing procedure is presented at Fig.2 and Fig.3.

Now let us consider the procedure for identifying aftershocks, occuring near the large event in both space and time. For this purpose aftershocks "image" of the form above is constructed and computed in those coordinates: Time(X-axis) - Distance(Y-axis). The point with coordinates T=0,R=0 is the main shock. After processing it(map) by filter with II x II -points window we obtain T,R-boundary values in hours and km, choosing the largest coherent aftershock area. In our study about 25 earthquake sequences have been analysed using this method to obtain the set of T,R-values. Two examples are demonstrated at Fig.4.

A plot of the duration T(in hours) of all aftershock sequences was made as a function of the energetic class of the largest shock in the sequence. A linear regression line to the Lg(T) data of the form (I) was found to be reasonable approximation. The extent of the aftershock zone was estimated from the distance-class data R(K) of the form (I). A linear regression line was selected similiar

way to T(K) bounds. This procedure was programed for computation in such a way that the general constants A,B,C are obtained and the window T(K),R(K) of the form(I) were applied to determine the grouping events.

CLUSTERING ANALYSIS.

Let us to analyse the results of retrospective applying the window procedure to the Caucasus catalog of earthquakes. The behaviour of the grouping parameter which is determined as: ratio of grouping earthquakes to the total number of them in working area during specified sliding time interval is considered. The value of the grouping parameter is related to the end of sliding time interval which is moved with I-year step. The size of working area considered as a square with side equal 6L, IOL, 20L and with a center at the epicenter of main shock is investigated. L - is fault length as mentioned above.

It should be pointed out some results of analysis of the grouping parameter behaviour before the large earthquake with $K \geq 12.5$ (magnitude $M \geq 5.0$).

First: the absence of grouping events during 6-8 years before main shock is noted (about 70 per cent), Fig.5.

Second: the presence of grouping events for 3-5 years prior the large earthquake is noted (about 30 per cent), Fig.6.

Some strong earthquakes investigated were named "incorrect" because of there were other large shocks closed to the first one. Plot of grouping parameter in this case is demonstrated at Fig.7.

CONCLUSION.

I.The technique to process the catalog data and to separate grouping earthquakes is designed.

2.The two main tendencies of grouping parameter behaviour are obtained, that are follows:

a) the absence of grouping events during 6-8 years before main shock;

b) the presence of grouping events for 3-5 years before main shock.

3.The use of grouping characteristic for the long-term prediction of large earthquakes seems to be promising.

REFERENCES

1. Dzievonski A.M.,Prosorov A.G. Selfsimilarity of the clustering of earthquakes. -In: Mathematical modelling and interpretation of geophysical data. M.;Nauka,1984,p.10-21.(Computational seismology; Iss.16).
2. Gardner J.K.,Knopoff L. Is the sequence of earthquakes in southern California, with aftershocks removed, Poissonian? Bull. Seism. Soc. Amer.,1974,v.64,No 5,p.1363-1367.
3. Prosorov A.G.,Shreider S.Yu. A statistical analysis of positive influence for normal earthquakes in Tien-Shan and Pamir-Alay. -In: Mathematical models in seismology and geodinamics. M.;Nauka, 1986.(Computational seismology; Iss.19).

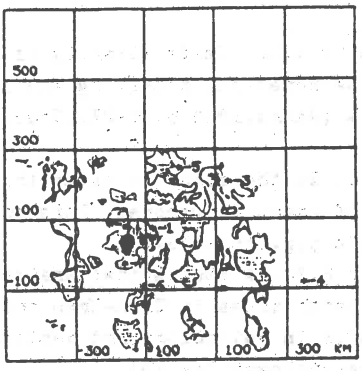

The map of the Caucasus catalog 1962-1985 epicenter density.

Fig.I

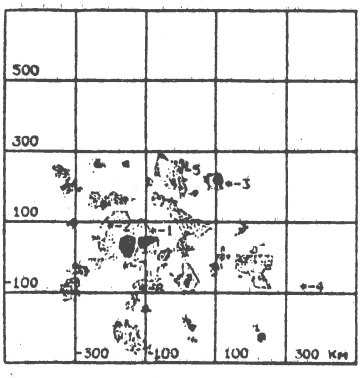

Processing the map of epicenter density with 5*5 - Filter.

Fig.2

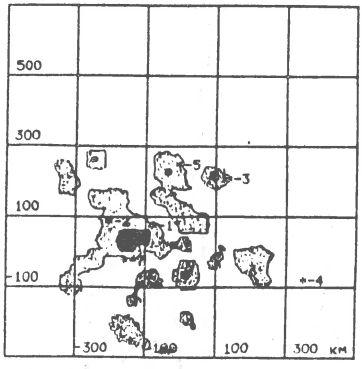

Processing the map of epicenter density with 11*11 - Filter.

Fig.3

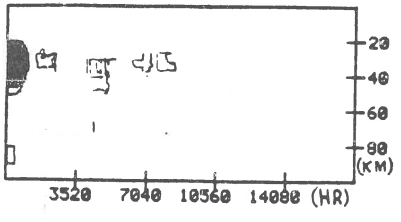

EARTHQUAKE 28.7.1976 (K=14.7)

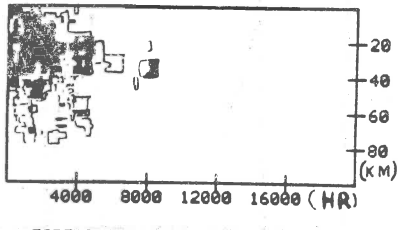

EARTHQUAKE 24.11.1976(K=16.0)

Space-time aftershock images.

Fig.4

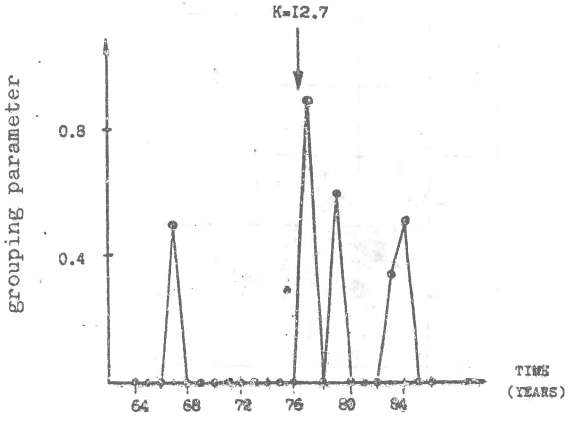

GROUPING PARAMETER BEFORE I976.4.29 EARTHQUAKE(K=I2.7)
WITH I-YEAR TIME INTERVAL

Fig.5

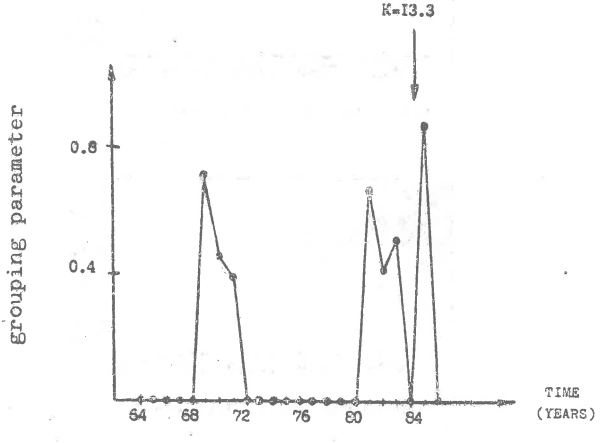

GROUPING PARAMETER BEFORE I984.9.I8 EARTHQUAKE(K=I3.3)
WITH 3-YEAR TIME INTERVAL

Fig.6

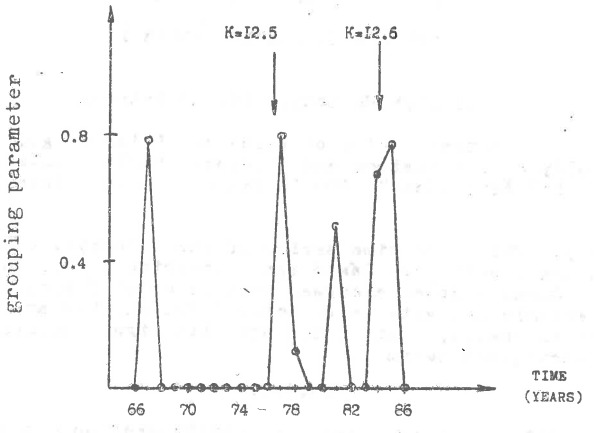

GROUPING PARAMETER BEFORE I984.3.4 EARTHQUAKE(K=I2.6)
WITH I-YEAR TIME INTERVAL

Fig.7

CHANGES OF MINERAL SPRINGS DURING THE EARTHQUAKE SWARM 1985/86 IN WESTERN BOHEMIA

Oldřich Novotný, Ctirad Matyska

Department of Geophysics and Meteorology,
Faculty of Mathematics and Physics, Charles University,
V Holešovičkách 2, 180 00 Praha 8, Czechoslovakia

Summary: The long time series of the intensity of the mineral springs in the Františkovy Lázně spa, covering the period 1984-88, is presented. Considerable changes were recorded during the period of increased seismic activity in December 1985. Another appreciable changes of the intensity, but of the opposite sign, occured two years after the earthquake swarm.

1. Introduction

It has often been reported that earthquakes have been accompanied by changes of the underground water regime [1-3]. Such investigations can also be carried out in the town of Františkovy Lázně in Western Bohemia owing to the regular measurements taken by the personnel of the spa. For about 20 mineral springs the following quantities are regularly measured (once a week): the discharge of mineral water in litres per minute, its temperature, the content of dissolved carbon dioxide and the contents of mineral substances. The Františkovy Lázně spa is located close to the epicentres of the earthquake swarm 1985/86. For most earthquakes the epicentral distance was less than about 15 km.

This paper is a continuation of former studies [4,5], where only shorter time series of the mineral water discharge were presented.

2. Changes in the discharge of mineral water

The depths of boreholes that the mineral water discharges from, are different for the individual springs, varying from several meters to about 100 m. The mineral springs are influenced by internal geological factors and, moreover, by meteorological factors as well as by the pumping of the water for the spa purposes. The meteorological factors mainly affect the shallow springs. Besides, no remarkable changes of the shallow spring discharge were observed during the period of increased seismic activity. That is why we have taken into account only several deep springs which seemed to be influenced exclusively by deep geological phenomena. Here we shall confine ourselves to the changes of discharge only.

Figures 1 to 4 show the discharges of mineral water from the following springs during the period November 1984 - February 1988 (the numbers in brackets are the depths of the springs): Glauber I (29m), Glauber II (32m), Glauber III (53m), Glauber IV (93m), Kostelní (30m). The measurements were carried out once a week. It is evident from Figs. 1-4 that the outpouring of the corresponding mineral springs were changed significantly during the period of increased seismic activity in December 1985. For example, if we take the mean outpourings in November 1985 as 100%, then the mean outpourings in January 1986 were increased by 38% for Glauber III, by 40% for Glauber IV and

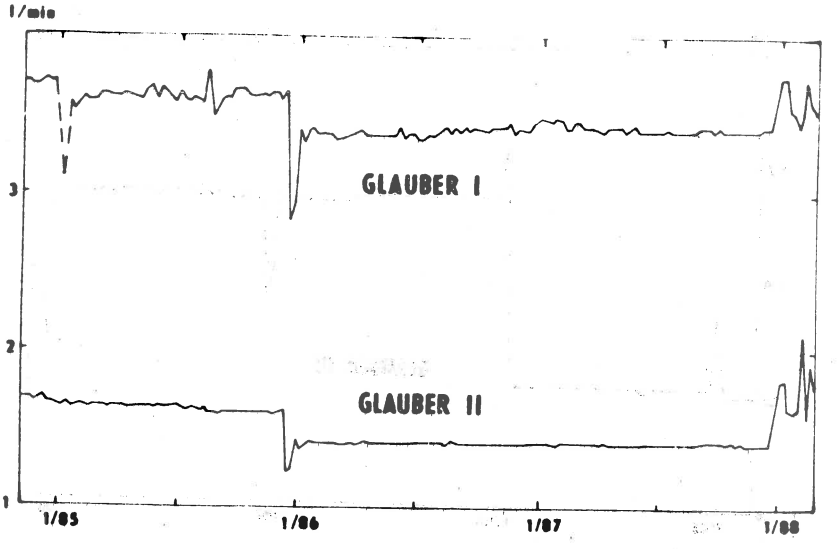
l/min
3
2
1
GLAUBER I
GLAUBER II
1/85
1/86
1/87
1/88

Fig.1

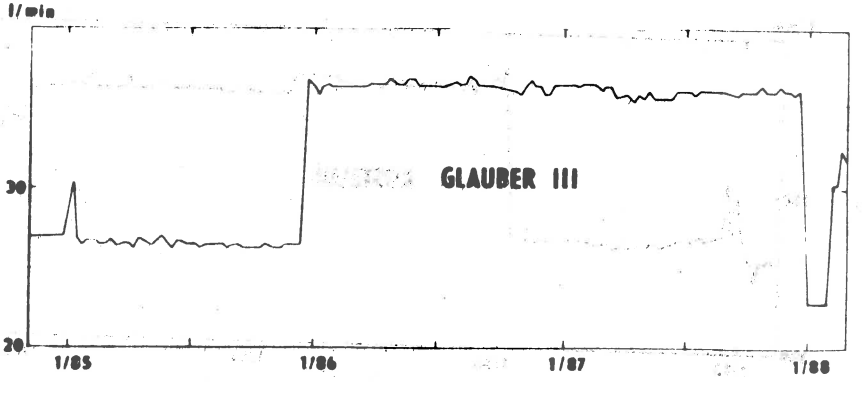
l/min
30
20
GLAUBER III
1/85
1/86
1/87
1/88

Fig.2

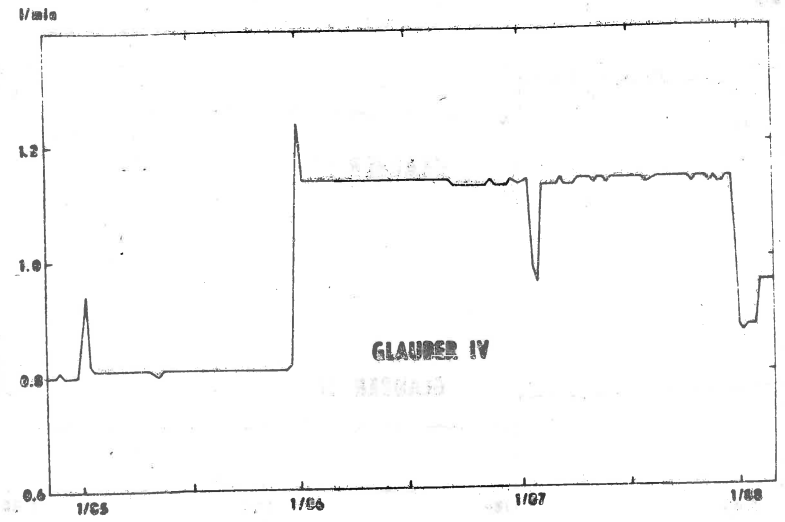
l/min
1.2
1.0
0.8
0.6
GLAUBER IV
1/85
1/86
1/87
1/88

Fig.3

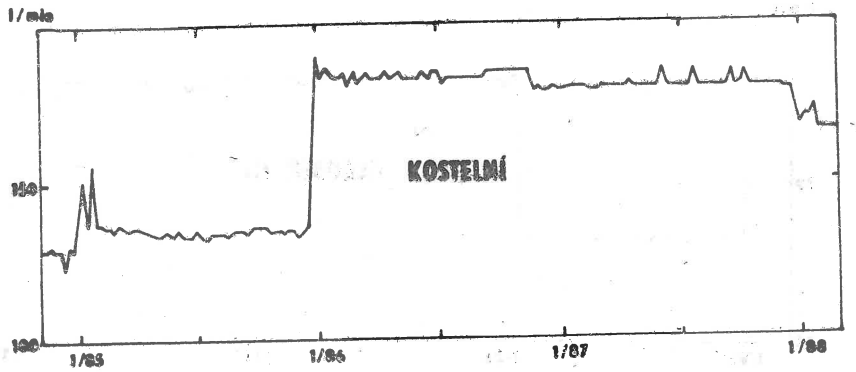
l/min
KOSTELNÍ
1/85
1/86
1/87
1/88

Fig.4

by 37% for Kostelní [5]. Let us mention that the detailed change of Glauber III in December 1985 is presented in [4,5]. As to other deep springs D14 (31m) and Adler (26m), it was observed that the changes in December 1985 were much smaller.

It is worth noting that other abrupt changes of the water regime, but of the opposite sign, occured in the beginning of 1988, i.e. two years after the last earthquake swarm.

3. Conclusions

It is highly probable that the changes of the mineral water regime in December 1985 can be attributed to the increased seismic activity. These changes are not directly connected with the beginning or end of the earthquake swarm, but may be related to the strongest shocks in December 1985. On the other hand, the later significant changes in the beginning of 1988 were not accompanied by any remarkable seismic activity of the region.

We have no clear physical explanation of the observed phenomena. Although a possible relation between the earthquake swarm and the release of carbon dioxide from the Earth's crust in this region has been proposed in [5], this hypothesis cannot be proved on the basis of the present data. The fundamental question, whether changes of the water regime in this region might play a role of earthquake precursors, cannot be answered as well. For this purpose, more detailed measurements (e.g. once a day or more frequently during the period of increasing seismic activity) ought to be taken. Nevertheless, we believe that the study of the mineral water regime is important for understanding the physical processes leading to earthquake swarms in this region.

Acknowledgements: The data used in this contribution were obtained by the personnel of the Františkovy Lázně spa. We especially thank Mrs. I. Matějková and Mrs. M. Kočí for providing the records of measurements.

References

[1] B.A. Bolt: Earthquakes. W.H. Freeman and Company, San Francisco 1978.

[2] I.G. Kissin: Zemletryaseniya i podzemnye vody. Nauka, Moscow 1982.

[3] G.A. Mamlanov (ed.): Gidrogeoseysmologicheskie predvestniki zemletryaseniy. Fan, Tachkent 1983.

[4] O. Novotný, O. Čadek, J. Zahradník: Změny vydatnosti minerálních pramenů ve Františkových Lázních v souvislosti se zemětřesením. In: Proceedings of the seminar on the earthquake swarm, Mariánské Lázně, April 1986.

[5] O. Novotný, O. Čadek, J. Zahradník: Changes of the mineral springs in Františkovy Lázně spa in connection with the earthquake swarm 1985-86. In: Proceedings of the Workshop on Earthquake Swarm in Western Bohemia December 1985 - February 1986, December 1-5, 1986.

SEISMIC ACTIVITY AND PIEZOMETRIC LEVEL VARIATIONS IN THERMAL WATERS IN SOFIA

P.PETROV, S.SHANOV, V.VUTKOV, M.TSHATALOVA, S.SOKOLOVA

Geological Institute - Sofia 1113, Bulgaria

INTRODUCTION

Within the complex of seismic prognosis investigations, the study of underground waters regime and its relation with the seismic activity, holds a place apart. The increased interest in the hydrodynamic indicators is due to their comparatively high informativeness for the strained and deformation state of rock massifs and to the possibility for their immediate observation and registration.

During the last 20 years seismogeodynamic test areas have been built in the USSR, the USA, Japan, China and other countries, including also seismohydrogeological stations for studying underground waters regime as a part of the wide complex of investigations for the purposes of seismic prognosis. The systematic study of the seismic regime of underground thermal waters in Bulgaria started 10 years ago by collaborators from the Geological Institute of the Bulgarian Academy of Sciences.

A subject of investigations are the hydrodynamic, temperature and hydrogeochemical effects of thermal water sources - springs and boreholes at strong seismic areas. One of the seismohydrogeological points is the borehole with thermal water in the centre of Sofia and the results from the investigations and their processing are a subject of the present study carried out in order to interprete the daily, long years measurements and to find the correlations with the seismic manifestations of local and neighbour seismic areas. A modification of the method of inverse probability is applied in order to select a comparatively weak efficient signal against strong disturbing noises.

BRIEF INFORMATION ABOUT GEOLOGY AND HYDROGEOLOGY OF SOFIA VALLEY

Sofia valley is a complex tectonic graben of a continued geological development. It has been formed between two main fault zones direct North-West - South-East, limiting the graben from North and South by the flanking mountains - the Balkan, the Ljulin, the Vitosha and Lozen Mountains, the Ihtiman ridge of Sredna Gora. The graben has been filled in mostly with Tertiary alluvium-lake sediments of a maximum thickness up to 1,3 km. The underlying stratum formed from Mesozoic sedimentary, volcanosedimentary, volcanic and magmatic rock formations. In the central part of the graben the so called Sofia horst is to be found.

A hydrogeological artesian basin with fresh, cold and thermomineral waters has been formed in the valley and the slopes of the flanking mountains. The thermomineral waters under pressure have been accummulated in the pore-fracture system of the Mesozoic underlying rock stratum and in the pore sediments of the Neogenic cover of the graben. The thermal waters have different temperature reaching 83^{o}C. The geothermal field in the valley is characterized by high temperatures in depth, geothermal gradients and an active

hydrothermal regime.

The borehole in the centre of Sofia (Sofia centrale borehole), where seismohydrogeological investigations are made, is of depth 490,7 m. It crosses the thin Quaternary and Neogenic cover over the Sofia horst and reveals the thermal waters of the natural mineral spring of a temperature 47°C accummulated in the senonien sedimentary volcanic series.

Sofia neogenic graben is characterized by comparatively high seismic activity, manifested through distructive earthquakes in 1818, 1858, 1917. The strong earthquakes of local and neighbour focuses caused considerable changes in the debit, pressure and the temperature of the waters of Sofia mineral spring (Вацов,1902; Радославов,1918).

INITIAL DATA

The present study uses data from daily measurements of the piezometric level fluctuations in the Sofia central borehole. The water level is reported from the borehole issue (zero point). Variations of the piezometric level reflect the total ascendency of the natural, exogenic factors (atmospheric pressure, seasonal changes in the hydrostatic pressure, the amount and distribution of the rainfalls) as well as endogenic processes (first of all - redistribution of stresses in the Earth's crust). Therefore, to report the actual endogenic effect, the data for the water level variations should be cleared from the disturbing factors (noises).

To define the influence of the atmospheric pressure /P/ over piezometric level /H/, the experimental diagram for 1978 has been worked out under Shepard's method (Девис,1977). A linear correlation between ΔH and ΔP is established for the months VI, VII, IX, X, XII (Fig.1).

Barometric effectiveness (n_{ef}) has been calculated under the formula:

$$\Delta H = n_{ef}.\Delta P \qquad /1/$$

where ΔH and ΔP are the variations of the piezometric level and of the barometric pressure. It has been calculated that if the atmospheric pressure is changed by 1 XPa, the piezometric level changes 1-2 cm.

A subject of investigations are also the magnitudes of the seasonal variations of the piezometric level depending of the amount and daily distribution of the rainfalls.

A basis for the investigation are the data for the piezometric level variations in 1977. This year is characterized by a strong seismic activity. The strong earthquake on 04.03.1977 with a M = 7,1 and an epicentre in Vrancha /Roumania/ sharply raised the piezometric level of Sofia central borehole (Бранков,1983). The raise continued for a long time enabling approbation of the method of inverse probality at a strong seismic stimulation of the piezometric indicator.

NOISE CORRELATION EVALUATION

Defining noise statistical parameters, attention must be paid to the selection of initial data, which should not contain anomalous and correlative observations. Practically, it is impossible to simply divide the observed variations into anomalous and non-anomalous (Fig.2).

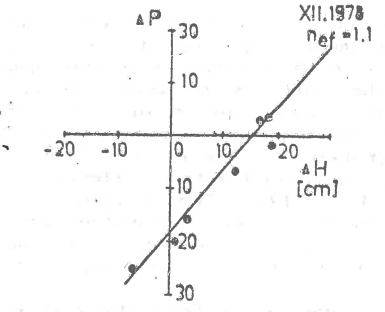

Fig.1 Linear correlation between piezometric level variations /ΔH/ and the barometric variations /ΔP/.

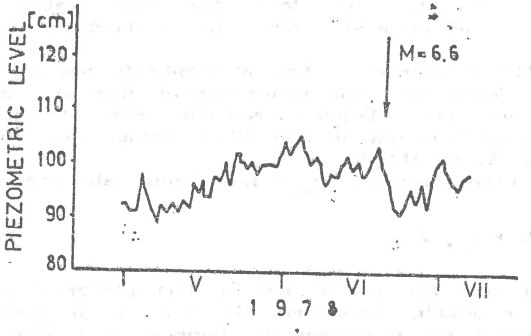

Fig.2 Variations of the piezometric level of Sofia central borehole during May-June 1978. The relationship between these variations and the earthquake with M = 6,6 in Greece is not clear.

The absence of noise correlation could be most objectively determined by means of the autocorrelation function (Демидович,1969):

$$R(\mu) = \frac{1}{m - \mu} \sum_{j=1}^{m-\mu} f(x_j).f(x_{j+\mu}) \qquad /2/$$

m - number of observations; μ - interval between the initial day and the day of comparison.

$$f(x_j) = \bar{f} - f_{rec}(x_j) \qquad /3/$$

$$\bar{f} = \frac{\sum_{j=1}^{m} f_{rec}(x_j)}{m} \qquad /4/$$

Ratio $R_H = \frac{R(\mu)}{R(0)}$ is the normalized autocorrelation function. Time interval, of which the correlation considerably decreases /at $R_H(\mu) \approx 0{,}3$/, is called radius of correlation.

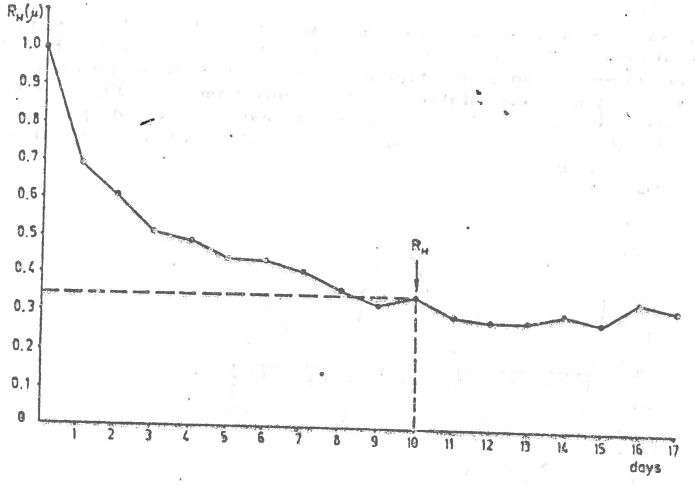

Fig.3 Autocorrelation function of the noises for the period from 01.04.1977 to 31.10.1977. R_H is the radius of correlation for the noises.

The radius of correlation between noises should be several times smaller than duration of the expected anomaly. The radius of correlation of the disturbing noises for Sofia central borehole has been calculated on the basis of data from 214 days (01.04.1977 to 31.10.1977). It is 10 days at $R_H \approx 0{,}35$ (Fig.3). This means that any anomaly of a shorter period than 10 days will be in the noise correlation zone and it will be difficult to be selected on the background of the disturbing noises.

Investigations showed as well that noises are subordinated to the normal law of distribution and the

assumption for noise uniformity is probable with reliability 99,9 %. These are the required prerequisites to use the method of inverse probability.

SELECTION OF THE EXPECTED ANOMALY BEFORE EARTHQUAKES

For the purposes of the present investigation several terms are laid to the expected anomaly of the piezometric level variations in order to be of benefit for the short-term prognosis of earthquakes: 1/ if the noise correlation radius at the piezometric level is minimum 10 days, the expected anomaly should be of a duration at least 20 days; 2/ to be as a prognosis, it should have faded several days before the earthquake; 3/ since piezometric variations before the earthquake reflect the process of stresses increase in the Earth's crust and probably this process is speeded before an earthquake, then the change per time unit of the piezometric level should increase; 4/ since the investigation will be made with normalized data, model anomaly should have dispersion $\sigma^2=1$.

To work out the model anomaly, we used the piezometric level variations of Sofia central borehole, registered 30 days before three strong earthquakes on the Balkan peninsula. After the relevant calculations, the diagram on Fig.4 was obtained. The average value of the anomaly is 0, dispersion is 1 and duration 21 days, that is, it corresponds to the stipulated conditions.

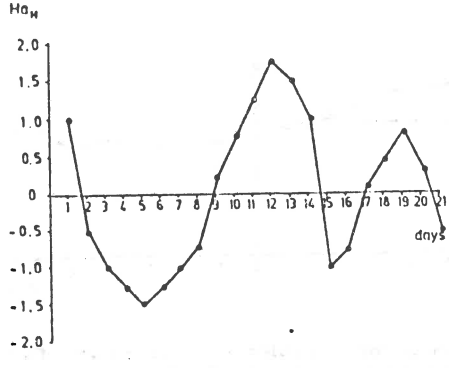

Fig.4 Normalized model of the expected anomaly.

METHODS OF CALCULATION

The optimum irreversible operation for separation of week signals on the background of strong noises is the one which is realized through mutual correlation of the input function and the effective signal. The task is formulated as follows: A certain discrete distribution of the meanings F(x) of the observed event is given. It is known that at a given interval of the measurements the searched determinated anomaly a(x) is present, it has been complicated by noises f(x) of certain statistical properties. The observed meanings should be evaluated in a sense, whether there is or not any effective anomaly. The concrete solution is based on the Bayes' formula of the inverse probability (Демидович,1969;

Шнитин, 1979), taking into consideration the fact that the dispersion of the expected anomaly is equal to the noise dispersion (since the data for an interval of 21 days have been normalized).

The correlation is obtained by interval, constant step multiplication of the observed meanings $F(x_j)$ by m ordinates of the expected anomaly and the received products are summarized:

$$K_f = \sum_{i,j=1}^{m} F(x_j).a(x_i) \qquad /5/$$

For the purposes of investigation this amount is attributed to the final measurement of the data interval. The curve plotted according to meanings of the cummulative function K_f will contain the entire information of effective anomalies. Maximums will define the intervals where probably there is an anomaly and after which an earthquake could be expected. Probability of an anomaly could be expressed as follows:

$$p = \frac{e^{tk - r}}{e^{tk - r} + 1} \qquad /6/$$

e^{tk-r} is the coefficient of probability and in the concrete case tk is the cummulative function K_f, r is half of the lenght of the expected anomaly (r=10,5 for the case). To be sure that there is any anomaly, p should be of value higher than 0,5. Our investigations show that for the concrete case we could consider an anomaly any time when the cummulative function becomes more than 0.

RESULTS FROM THE INVESTIGATION

Initially, we processes the recording for the daily changes of the piezometric water level of Sofia central borehole for the period 28.01.1977 to 04.01.1978. After calculating the diagram of the cummulative function K_f, we got 29 relative maximum values higher than zero; in only 20 of the cases the probability for an anomaly was higher than zero. One day before the earthquake in Vrancha, this probability reached 99 % and before the strongest eathquake in Velingrad the probability was 7 % three days before the earthquake itself. Upon a thorough analysis of all known earthquakes within a radius of 600 km around Sofia for the period of investigation, we selected those events which most probably influenced Sofia borehole. In fact, this selection contains a certain subjective element since it is difficult to define the event which dominated with its influence on Sofia borehole. Besides, it is possible that there is a complex influence from several regions where earthquakes originate. Nevertheless, this data provides possibility to search certain empirical regression relationship for the prognosis of the forthcoming event of a satisfactory accuracy, in respect of the date, strenght and probable distance from Sofia. Using standard methods, the following regression equations have been worked out:

$$M = 3{,}884 + 0{,}078\ K_f \pm 20\ \%$$

The cummulative function is the starting point for making prognosis of the earthquake magnitude M.

$$Na = 3,483 + 0,1934\ K_f \pm 3 \qquad /8/$$

This regression provides possibility to estimate approximately the date of the event. It will be Na days from the moment when the anomaly becomes positive.

$$N = 1,114 + 0,4363\ Na \pm 3 \qquad /9/$$

Some justification for the date could be made using this regression between Na and the days N to the event, after the curve reached its maximum. Distance regressions appeared to be insignificant and this problem is still outstanding.

CONCLUSION

To chek the possibilities of thus selected methodological approach, we processed every day the data from the level measurements in Sofia borehole in January and February 1987. During this period there were 5 earthquakes (Fig.5). For the first day of the prognosis - 21.01.1987 the cummulative function is positive, the result was that between 21st and 26th of January an earthquake of M=3,6 to 5,3 was expected. An earthquake was registered with an epicentre in Strajitza on the 21st of January of M=3,8. The next event, again in the region of Strajitza of M=3,2 did not show any anomaly of the K_f diagram. The next anomaly on the 5th of February provided grounds for expecting an earthquake of a magnitude 3,4 to 5,1 on the 9th or 10th of February. There was registration of an event with M=3,9 on the 10th of February in Greece at about 500 km from Sofia. Another anomaly of K_f followed. It gave good reasons to make a prognosis of an earthquake of a magnitude between 3,3 and 5,0 of most probable date - 13th of February 1987. An earthquake of M=5,1 was registered on this date on the territory of Albania.

On the 18th of February especially strong anomaly K_f was registered, reaching its maximum on the 23rd of February. It was determined that the most probable event could be expected on the 24th or 25th of February 1987 of a M=3,8 to 5,6 with 50 % probability. An earthquake was registered on the 25th of February of M=3,3 on the territory of Yugoslavia about 200 km to the West of Sofia.

It is evident from the above that the non-standard approach selected is perspective and provides possibility for a short-term seismic prognosis. To improve effectiveness of prognosis evaluations, it is necessary: 1/ to specify the form of the emperically worked out expected anomaly; 2/ with the receipt of new data, we could continuously correct the coefficients of the empirical relations between K_f,M,N,Na; 3/ to make comparative investigations also with the data of the other seismohydrogeological centres.

With the improvement of the interpretation method, measurements of the piezometric levels of the deep thermal waters in the seismic areas of Bulgaria could be used reliably to make a prognosis of the earthquakes.

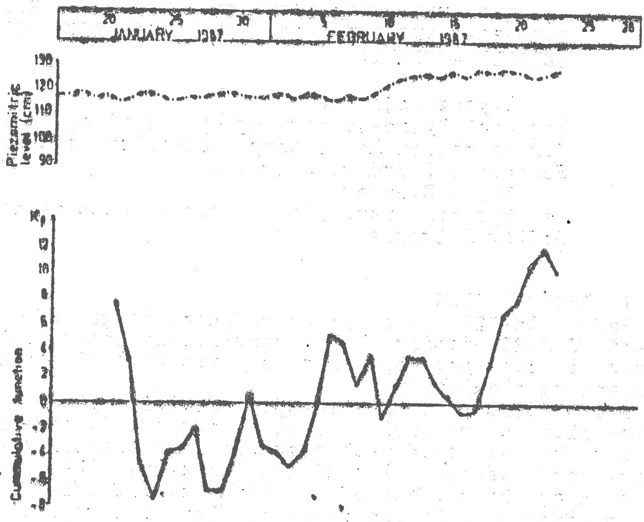

Prognosis – expected erthquakes	Interval-days					
	Date	23.01.1987		9-10.02.1987	13.02.1987	24-25.02.1987
	Magnitude	M=3.6÷5.3		M=3.8÷5.1	M=2.3÷5.0	M=3.8÷5.0 P≥50%
Registred erthquakes	Date	21.01.1987	29.01.1987	10.02.1987	13.02.1987	25.02.1987
	Magnitude	M=3.8	M=3.2	M=3.9	M=4.1	M=3.3
Region of erthquake		Strajitza	Strajitza (Bul.)	Greece	Albania	Copaonic (Yug.)
Estimation of the prognosis		+	–	+	+	+

Fig.5 Prognosis for January and February 1987.

REFERENCES

Бранков Г.(гл. ред.),1983 Земетресението Вранча - 1977 г. Последствията в Н Р България - Изд.БАН,София, 428.

Вацов С.,1902 Землетресения в България през XIX век София, 95.

Девис Д.,1977 Статистика и анализ геологических данных Мир,Москва, 572.

Демидович О.А.,1989 Выделение слабых геофизических аномалий, статистическим способом. - Недра, Москва, 112

Никитин А.А.,1979 Статистические методы выделения геофизических аномалий. - Недра, Москва, 280

Радославов Б.М.,1918 Мини, кариери и минерални води в Софийски окръг. - София, 189.

CONCENTRATION VARIATIONS OF ATMOSPHERIC RADON DAUGHTERS AND THEIR POSSIBLE CONNECTION WITH SEISMIC ACTIVITY

Miyana Adjemova
Regional Hydro-Meteorological Service, Radioactive Contamination Laboratory, Bulgarian Academy of Sciences, Plovdiv, Bulgaria
Sasho Elenkov
Geophysical Institute, Bulgarian Academy of Sciences, Sofia, Bulgaria

I. INTRODUCTION

Radon /Rn-222/ is an inert radioactive gas of earth origin, a part of U-238 family. It is continuosly generated by the earth, because it can leave spontaneously tis site of generation, not interacting chemically.

The problem of radon transport from its place of generation to the place of measuring is quite essential, especially when it is to be connected with possible communicatin signals, preceding earthquakes. A lot of studies assume that radon is transported near the surface of the earth by diffusion which limits its transport within the range of about one meter.

In connection with the uranium deposits found at comperatively greater depths, it has been made clear that there must be a mechanism of migration whith is cinsiderably faster than diffusion /1, 2, 3/.

The radon concentration variations in soil in connection with seismic activity also sugest transport of radon at great distances /4, 5, 6/.

Kristiansson and Malmqist's study/7/ prove the existance of long-distance transport in general. The quite different radon concentration near the surface of the earth /0,2m/ show that diffusion is not a dominating form of transport. Therefore radon is not ingected into the free atmosphere only by its diffusion through the upper soil level.

Regardless of the complex borden-line exchage between the low atmosphere and the soil and the influence of many parametres, radon concentration varoations, which can not be explaned with the effect of meteorological parametres and horisontal transport of air masses, are observed. That is why it is considered that in studying radon daugthers concentration variations in the atmospheric air, the velosity of exhalation from the soil showed not be altogether ignored.

Due to the relatively small contribution of thoron in the air the term radon daughter products is widely used, implying radon and thoron inductions.

II. EXPERIMENTAL METHOD

Radon is measured inderectly by its beta-decay products/Pb-214 and Bi-214, having a half-life 26,8 and 19,8 min respectivety they are quicly attached to the larger aerosole particles within the range of one or two minutes. Thus the transport of the radio-

active atoms into the atmospheric air is carried by aerosol particles which have acquired radioactive properties.

Taking air samples is carred out at 2 meters above the earth surface by means of a filter method. The gross beta activity of the aerosoles on the filter of 20 cm^2 of exposition area is measured daily using conventional measuring tecnique. The measurement data are corrected for artifical radioactivity which can sometimes also be present on the filter.

Data for the total beta activity of radon daughter products in the atmospheric air in Sofia, Plovdiv, Pleven, Varna and Burgas are used in this paper. These concern the period from 1979 till 1986.

III. CORRELATION BETWEEN RADON DAUGHTERS CONCENTRATION AND METEOROLOGICAL PARAMETRES

The essential influence of the meteorological parametres on radon concentration variations in the air can be seen from the studies in this field. The following basic elements are discussed here: temperature in the ground air layer, atmospheric pressure, air humidity, wind direction and quantity of precipitation.

1. Radon daughters concentration /RDC/ -temperature

It has been definitly proved that there is no connection between these two values. The correlation coeficient varies with no definite pattern from k=-0,2 to k=0,4 for the different months of the studies period.

2. RDC - atmospheric pressure

Negative correlation betwwen these values, varying from moderate to noticeable, has been observed. The correlation coefficient varies in the range k=-0,1 - k=-0,6.

3. RDC - humidity

Moderate positive relation is observed with these two values. RDC correlate with humidity within the range k=0,2 to k=0,4.

4. RDC - precipitation

A negative relation between the average monthly values of precipitation and RDC is observed. K=-0,36.

5. RDC - wind direction

Due tothe great difference in radon concentration over the mainland over large water surfaces in the presence of horizontal transfer, the air masses over the points of observation are respectively enriched or depleted in radon. When air masses are transfered from the west and the north qurter there is a drop in RDC and when they are from the south and east qurter RDC rises.

It has become clear from these analyses that meteorological parametres influence RDC in the air in a different way and to a different extent. this determines the difficulty in analysing the observed irregularities. Expert evaluation of overall synoptic situation at the moment of their registration is necessary.

The situation during the earthquakes in the region of Strazhitsa is an example of such aproach and an evaluation of its results.

IV. EXPERIMENTAL DATA

The annual variation of RDC values for 1986 at point Plovdiv isshun on fig. 1. A considerable rise in RDC is clearly observed at the end of the year. It shoued be noted that these data would

not have seemed strange at all, having in mind the annual RDC variations in the air, if their absolute values haven t exceed 1,5 - 2 times the measurements for the same months during the whole 8-year period.

The monthly variation of the data for December 1986 at point Plovdiv is shown on fig.2. The increase in the values during the period immediately preceding the shocks on 07.12.1986 and strongest aftershock on 18.12.1986(M=5.7 and M=4.6 respectively) is clearly observed.The same increases are also observed at the other measuring points.(fig.3,4,5,6)

Another interesting fact should be noted here.The investigations establishes no mutual dependence of the date measured at different points.This only natural having in mind the varying condition - geological,location,relief,altitude etc these points situated at.That makes the fact that in December 1986 there is a positive correlation for the Rn concenntration values measured at the different points all the more interesting.This can be very well seen on fig.3-6 whith shows the curves of RDC variations. These concidences hint that the observed anomalous rises are due to processes connected with the preparation and the realisation of the above mentioned earthquakes.If this true these anomalies in RDCin the atmospheric air could be considered as precursory indication.An evaluation of the synoptic situation at the moment of their registration should be made in order to confirm or discard suth a statement.During the first ten days of December 1986 the weather in country was determined by an anticyclon over south of Europe.On December 4^{th},5^{th},6^{th} and 7^{th} warm air from the Mediterrane penetrated into the country.Temperatures rose.Atmospheric pressure was higher than normal.The weather was dry and sunny.In general this synoptic situation doesn't favour RDC rise in the atmosphere.In this case the explanation that the observed increase is due to insensified Rn transport from the deep layears of the earth's crust stands to reason.

The situation in relation to the earthquake of February 21^{th} 1986 in the same region is considerably less clear.Anomalous increases ware observed only at the nearest measuring points- Plovdiv and Pleven.The complex synoptic situation in the country might be a possible reason for that.From February 17^{th} till Feb.22^{th} the weather was determined by a vast and slow-moving Mediterranean cyclon Our country was at it's head where separate shallow cyclon whire winus and related to them frontal systems pass.The weather was unstuble predominantly overcast with occasional breaks in the clouds and slight rain over many places.Atmospheric pressure variations were insignificant.Al this complicated to a great extend the vertical transfer of Rn and its interpretations respectively.

V.CONCLUSIONS

RDCin the air is to a considerable extent influenced by the variations in the dynamics of the atmospheric processes,yet not allof the variation can be explaned by these changes.

An intense Rn exhalation due to processes going on the deep layers of the earth's crust and related to the preparation and realisation of seismic events is to be supposed.

It is necessary to stady the dependence of RDC variations on the changes in the seismic conditions in so far as the processes causing these changes are analagous to those, resulting in a

stong earthquake realisation.

The authors consider the observation on RDC in the athmospheric air a good short-term precursor,provided it is in combination with observation of underground waters and soil gas.It is well known that the influence of meteorogical parameters on the latter two is many times weaker and the variations with are not caused by tectonic processes are insignificant.

REFERENCES

1. Fleicher,R.L.,Hart,H.R.,and Mogro-Campero,A.,1980, Radon emanation over an ore body: Search for long-distance transport of radon: Nucl Instr.Meth. v.173, p.169-181.

2. Fleischer,R.L.,and Mogro-Campero,A.,1979, Radon enhancements in the earth: evidence for intermittent upflows?: Geophys.res. Lett. v.6, p361 -364.

3. Fleischer,R.L.,and Mogro-Campero,A.,1979, Integrated radon mapping in the earth - Assessment of the Rn-220 signal and its exclusion: Geophysycs, v.44, p.1541-1548.

4. Birchard ,G.F.,Libby,W,F.,Soil radon concentration changes, preceding and following four magnitude 4,2-4,7 earthquakes on San Jacinto fault in Southern California: JGR, v.85,NB6,p.3100-3106

5. King,Chi Yu,1980, Episodic radon changes in subsurface soil gas along active faults and possible relation to earthquakes, JGR v.85,NB6, p.3065-3078.

6. Mogro-Campero,A.,Fleischer,R.L., Likes,R.S.,1980, Changes in subsurface radon concentration associated with earthqoukes, JGR v.85, NB6, p. 3053-3057.

7. Kristiansson,K.,Malmqvist,L., 1982, Evidence for nondiffusive transport of Rn-222 in the ground and a new physical model for the transport, Geophysyks,v.47,NO 10,p.1444-1452.

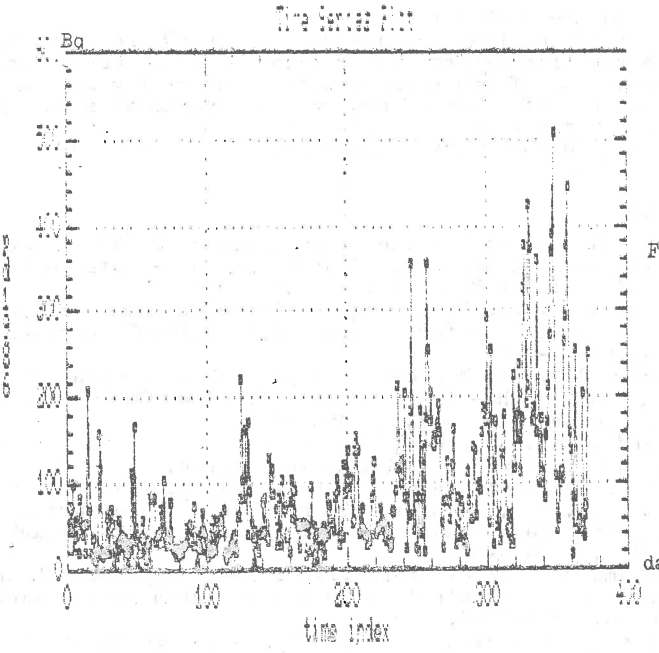
Time Series Plot
Bq
days
time index
0
100
200
300

FIG. 1

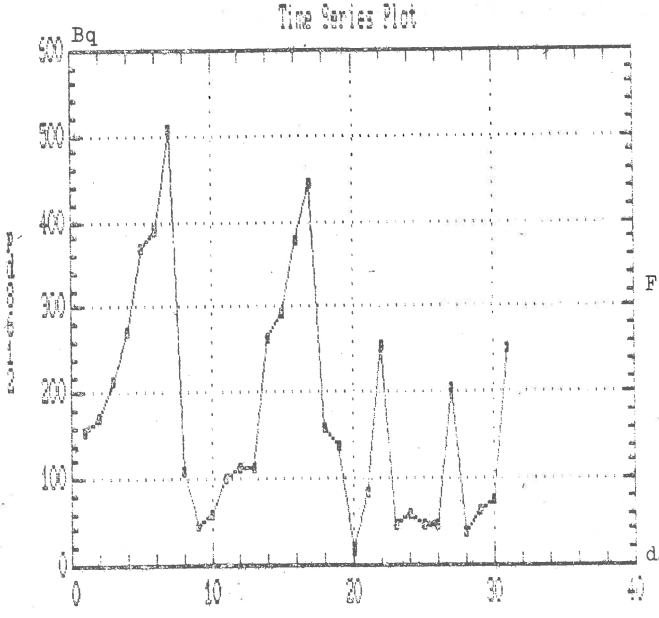
Time Series Plot
Bq
days
0
10
20
30
100
200
300
400
500

FIG. 2

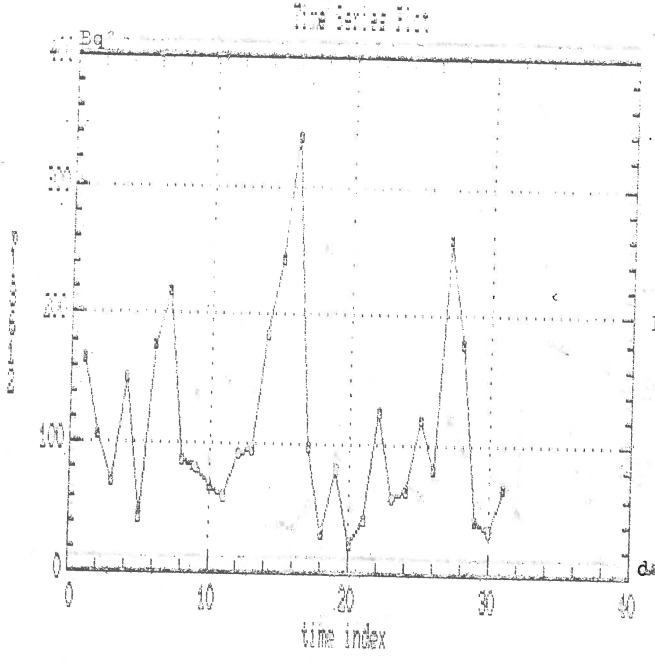
Time Series Plot
Bq
0
100
200
300
0
10
20
30
40
days
time index

FIG. 3

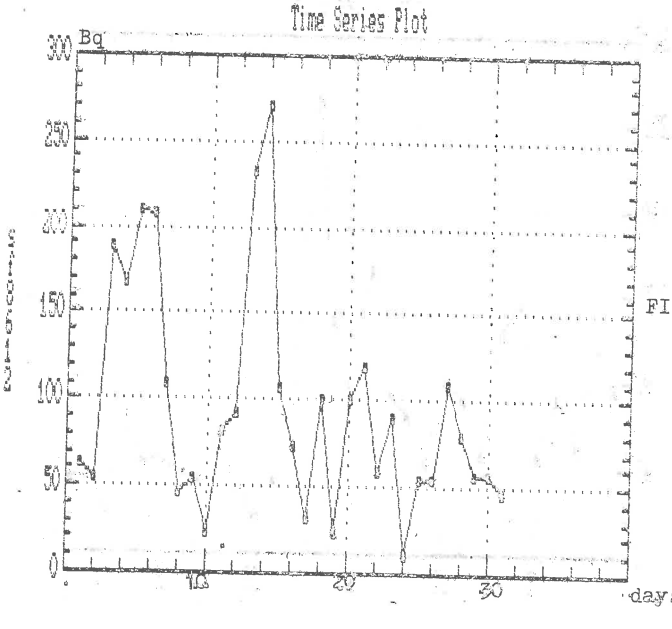
Time Series Plot
Bq
300
250
200
150
100
50
0
10
20
30
days

FIG. 4

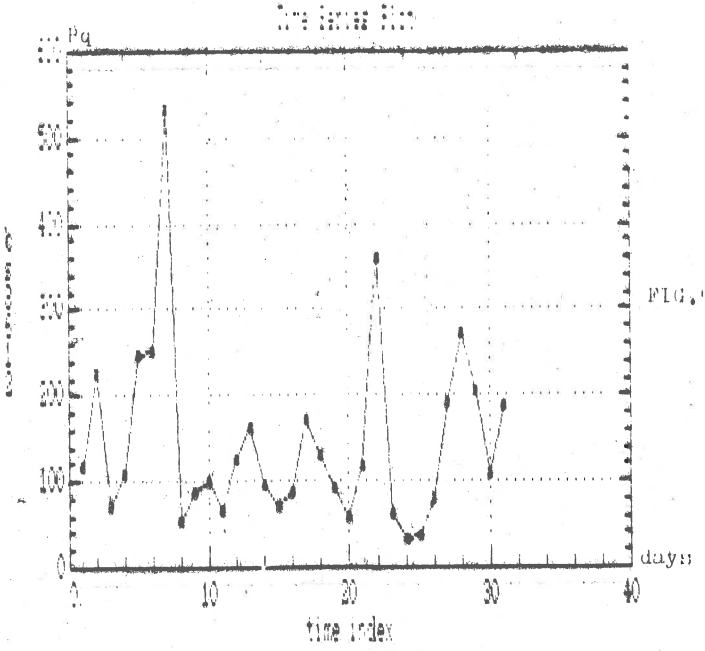
Time Series Plot
Bq
500
400
300
200
100
0
0
10
20
30
40
days
time index

FIG.5

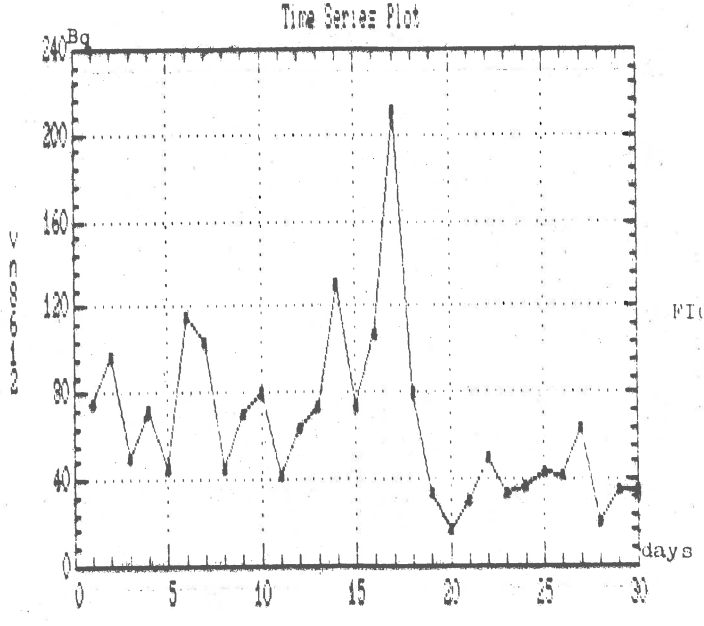
Time Series Plot
Bq
240
200
160
120
80
40
0
0
5
10
15
20
25
30
days

FIG.6

H-3 USE IN GEOCHEMICAL PRECURSORS STUDY

K.KOSTADINOV, Y.YANEV - UNIVERSITY OF SOFIA, RADIOCHEMICAL LABORATORY

L.ADGAROVA - REGIONAL HYDRO-METEOROLOGICAL SERVISE - PLOVDIV

S.ELENKOV - GEOPHYSICAL INSTITUTE - SOFIA

Rn-222 is an inert radioactive gas of the uranium-238 family, being a daughter of Ra-226.It is well known, that rate of emanation of Rn depends on the state of stress in the medium.In response to new fractures and compression of the old ones,the equilibrium of the contact between rocks and circulating gases and waters is destroyed,which leads either to their enrichment,or depletion of radon.

The emanation of radon is eased in places conected with tectonic disturbances where its vertical migration may present a usefull information for preparation of a given earthquake.

To discriminate other interfering factors however is necessery to have a long-term measurment on a given underground water in order to estimate the normal variations in the radon concentration.A much simpler method to select the most suitable springs for constant radon measurment is to determinate the transient time of the water in the system,i.e. to determine the age of the water as well as it's possible fast contact with surfase waters.This can be done in many different ways but the most accurate of them are the isotops metheds.

For this purpose environmental isotopes like H-3,C-14,Si-32,Cl-36,Th-230 can be succesfully used.In cases where it isnecessary to establish fast contact between surfase and underground waters in a given hidrological system,the isotopes of hydrogen and oxygen are of great use.Tritium is the most suitable for this purpose because it is radioactive and can be measured very sensitively.

Hydrogeological situation

The interest in the seismic activity of the Upper Thracian Valley in Bulgaria is not occasional.This valley represents a very large negative strctura - a tectonic trench.To the south it is separated from the Rhodopes by the Maritza fault.To the north it is restricted by a bunch of faults which are vailed by comparatively young sediments.To the east fault or flexture is bordered by the Chirpan break.It's foundation has a strongly marked block structure,petrographically represented by granites, granodiorites and sienites.In the town of Plovdiv the footing blocks rise up to 130 metres above the ground(the Plovdiv hills) and only 8 km.to the north this same footing arise 1000m deep.The Upper Thracian fault is filled with neogenic and plioplaystocenic materials.

The complicated tectonic construction is responsible for the strong seismic activity of this region as well as for the great number of diferent thermal and subthermal underground waters.

In this research the results of tritium measurements in underground waters selected for earthquake prediction are discussed.Most of the studied waters are from deep wells which are considered well protected from the influence of environmental factors.All waters are selected in such a way that they are situated within the range of the largest tecto-

nic disruptions, which predetermines the possible seismogenic fluctuations in the chemical and isotope composition.

Application of environmental tritium for dating of groundwater

The direct dating of groundwater with tritium by using an equilibrium value Ao according to the well known exponention low of radioactive decay for it's concentration in the surface waters (i.e.in precipitation) is practically impossible after 1952 as a results of large disturbances due to the nuclear weapon testing in the atmosphere. Nevertheless the tritium content may setve as an useful indication to distinguish "old" waters (i.e.before 1952) from freshly recharged waters for the last few years. The "old" waters which have been in contact with the atmosphere before 1952 must have, a tritium concentration ranging from 0 to 3-4 TU. A good practical guide for this latitude is that old waters certainly contain less that 3-4 TU, which means that they are 30-40 years old.

By the end of the 60-ies is was still possible to make a good difference between very young waters with high tritium content (1000TU) and waters with practically 0 TU. At present this is very difficult to be done because the tritium concentration in the precipitation have strongly decreased. As a result a confusion may arise when trying to interpret some tritium results for waters of mixed type may well be in the range of the tritium concentration of present precipitations. In this case it is necessary to have a longer series of H-3 measurements in precipitations in order to establish the tritium input function for the last few years and to correlate in with the changes of the H-3 concentration in the thermal springs.

Results and discussion

The analysis of tritium in the samples from underground waters from the Thracian valley was carried out according to the method used by IAEA Isotope Hydrology Laboratory in Vienna, which includes;

1. Preliminary distillation of the samples to discard dissolved and suspended material;
2. Electrolytical enrichment of tritium by a factor of 18-20;
3. Liquid scintillation measurement of the enriched samples and calculation of the initial activity. According to results of the analysis to tritium concentration the investigated waters can be divided into three different "types".

1. Old waters with a transient time more than 30 years. The zero trituim activity is a good idication of relatively slow recharge and practically of no contact with the surface water for the last 30 years.
2. Waters of the "mixed" origin with thritium content between 2 and 10 TU. Their low but measurable tritium concentration can be attributed to infiltration of small quantities of contemporary water in the well. A more precise explanation may be given by more prolonged measurement in the order to see some seasonal changes, if any at all.
3. Waters with high tritium concentration. In this case the waters are recharged for a small period of time and their tritium concentration is that of precipitations of the last several years.

Conclusions

For the purpose of the seismic prediction by means of Rn-222 we propose to use the tritium dating method in order to distinguish old from young waters and in this way to eli-minate the thermal springs which can be

influenced by current changes in environmental conditions.The best suited for this purpose are the underground waters with practically zero tritium content.Concerning the investigated waters of "mixed" type with tritium content between 2 and 10 TU it is necessary to conduct a more profound investigation of the possible changes in the tritium concentration in order to establish a reliable picture of their contact with surfase waters and to conclude their suitability to Rn-222 monitoring.

REFERENCES

1.Chi-yu King Radon Monitoring for Earthquake Prediction in China Earthq.Predict. Res. 3 (1985) 47-68
2.Eriksson E. Radioactivity in Hydrology, Nuclear Radiations in Geopysics,Springer-Verlag,Berlin-Heidelberg,1962
3.IAEA,Isotope Hydrology Lab.Service,Manual19 ,1976
4.Guidebook on Nuclear Techniques in Hydrology,Technical Report Series ,91 1968

ANALYSIS OF TEMPORAL VARIATION OF d-RATIO, b-COEFFICIENT AND $e_{\Delta T}$ - AVERAGE ENERGY, AS PRECURSORS OF VRANCEA INTERMEDIATE EARTHQUAKES

C.Radu, Luminiţa Ardeleanu
Center of Earth Physics and Seismology, P.O.Box MG-2
Bucharest, Romania

INTRODUCTION

The Vrancea seismic region, the most important seismic area in Romania, offers unique conditions in the world, for the prediction of intermediate earthquakes, due to the peculiarities of isolation, concentration and periodicity of its seismic activity.

The Vrancea region is located at the Carpathian Arc Bend, defined by the coordinates φ =45.7°N and λ =26.6°E. The distribution of epicentres shows two distinct and parallel zones, oriented N35°E (Radu, 1974):

- the zone of intermediate earthquakes, with the area of 95 x 6o km^2, characterized by events with depth h=6o-2oo km and M_{max}=7.5;
- the zone of normal earthquakes, characterized by events with h<6o km and M_{max}=5.2; a minimum of seismic activity is observed within depth interval h=4o-7o km.

The detailed study of the seismicity of this region showed that the intermediate earthquakes with M>5.o present a great interest for seismic prediction, because they are associated with some precursory phenomena (Radu and Mârza, 1982). From the series of these phenomena we shall analyse only three of them: the ratio d, the coefficient b and the average energy $e_{\Delta T}$. The state of the art of these researches, initiated by authors in 1982, is presented further on.

DEFINITIONS

. The parameter d represents the ratio between the total durations of oscilation D, recorded on the horizontal (NS and EW) and vertical (Z) components at a certain seismic station (Malamud, 1974):

$$d_{N,Z}=\frac{D_{NS}}{D_Z} \quad ; \quad d_{E,Z}=\frac{D_{EW}}{D_Z} \tag{1}$$

. The coefficient b characterizes the magnitude-frequency relation:

$$\log N = a - bM \tag{2}$$

For the determination of b-coefficient the following relation was used (Utsu, 1964):

$$b = \frac{\log e}{\bar{M} - M^*} \tag{3}$$

where $\bar{M}$ represents the mean magnitude and M^*- the minimum magnitude from the considered series.

. The average energy $e_{\Delta T}$ reprezents the ratio between the total energy of the representative earthquakes and their number, for the time interval ΔT (Belelovsky, 1982):

$$e_{\Delta T} = \left. \frac{\sum_{i=1}^{N} E_i}{N} \right|_{\Delta T} \qquad (4)$$

The magnitude M adopted for classification is of M_{GR} type. The seismic energy E was determined using the relation :

$$\log E = 11.8 + 1.5\ M \qquad (5)$$

OBSERVATIONAL DATA

In order to point out the predictive content of the three previously mentioned parameters - d, b and $e_{\Delta T}$, two data sets were analysed :

- the series of Vrancea intermediate earthquakes with $1.9 \leq M < 7.0$, occurred during the period June 1977-May 1988 (for the ratio d, coefficient b and index $e_{\Delta T}$);
- the series of Vrancea intermediate earthquakes with $4.0 \leq M < 7.4$, occurred during 1935-1988 (for the coefficient b only).

The durations of oscillation D, were measured on the recordings of Cheia (MLR) seismic station equipped with DD_1 short period instruments (Z, NS, EW components).

The values of the magnitude M, were taken from the Catalogue of Romanian earthquakes (Radu, 1974, 1988; Radu et al., 1985).

For the study of temporal variation of the three parameters, the method of moving average was applied, using windows of different widths, as follows: for the ratio d - 10 events with a step of 5 events; for the coefficient b - 10, 15 and 20 events with a step of 5 events; for the index $e_{\Delta T}$ - 30, 60 and 90 days with a step of 30 days. The mean values of the parameters were assigned to the end of the window. The occurrence time of the earthquakes with $M \geq 5.0$, considered for prediction, were marked by vertical bars or circles.

RESULTS

The results obtained since 1982 up to date, concerning the predictive content of the three parameters (Radu and Ardeleanu, 1982; Radu et al., 1984a, 1984b) can be summarized as follows :

. The ratio d. The analysis of temporal variation of the ratio d, leads to the following remarks (Fig.1):

- the plots representing the variation of $d_{N,Z}$ and $d_{E,Z}$ ratios are similar both in shape and in phase;
- the major seismic activity (earthquakes with $M \geq 5,0$) is concentrated in the periods of minimum values of the ratio d, when 1-4 strong earthquakes occurred;
- the representative maxima of the ratio d - $M_1, M_2, \ldots, M_6$, define time intervals T=1.43/1.67; 1.23/1.23; 1.10/1.10; 1.07/1.83 3.67/2.92 years, which may be useful in the estimation of the periods of minimum values (bay-shaped) of the ratio d, and therefore of the periods of possible intensive seismic activity.

. The coefficient b. The existence of a significant variation of b-coefficient with focal depth, for Vrancea earthquakes (b_n = 0.97, b_i=0.78, b_{n+i}=0.84/Radu, 1974), imposed a separate analysis of intermediate earthquakes. The following two cases were analysed:

1. The temporal variation of the coefficient b for the series of earthquakes with $4.0 \leq M < 7.4$, occurred during the period 1935-1988/134 events. The analysis of Fig.2 leads to the following

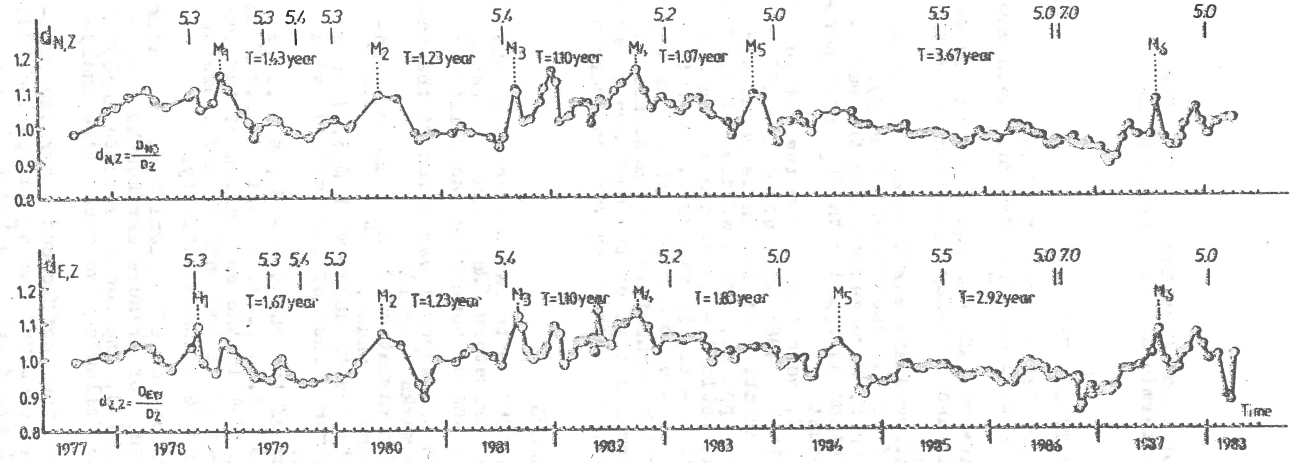

Fig.1 - Temporal variation of the ratio d (Vrancea - h=60-200 km ; 1977 June - May 1988 ; $1.9 \leq M \leq 7.0$) ; moving window - 10 events.

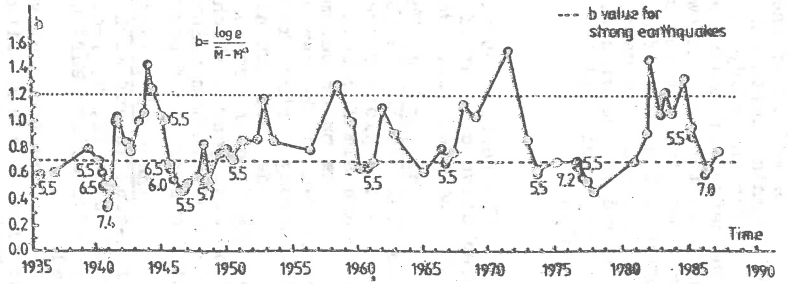

Fig.2 - Temporal variation of the coefficient b (Vrancea - h=60-200 km ; 1935-1988 ; $4.0 \leq M \leq 7.4$) ; moving window - 10 events.

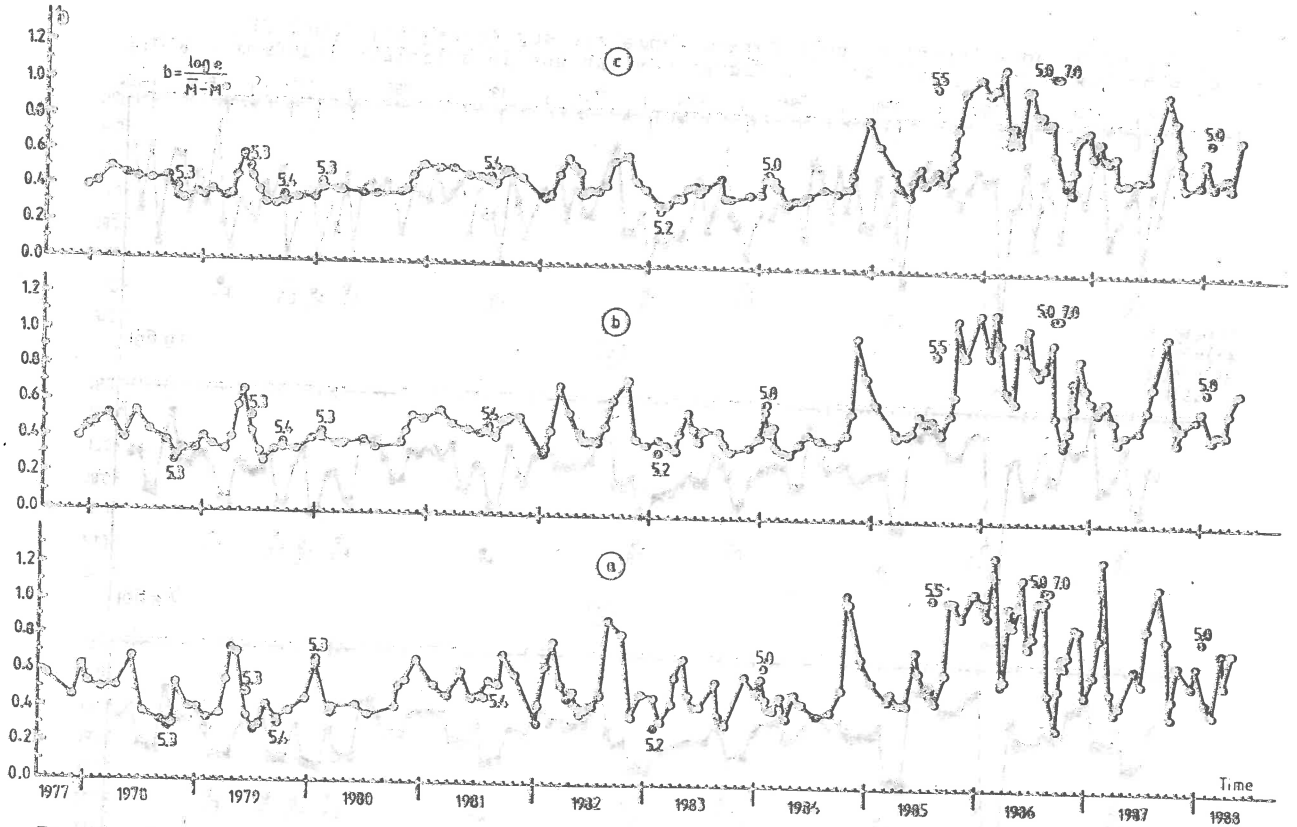

Fig.3 - Temporal variation of the coefficient b (Vrancea - h=60-200 km; June 1977-May 1988; 1,9≤M≤7,0) for different moving windows (a=10, b=15, c=20 events).

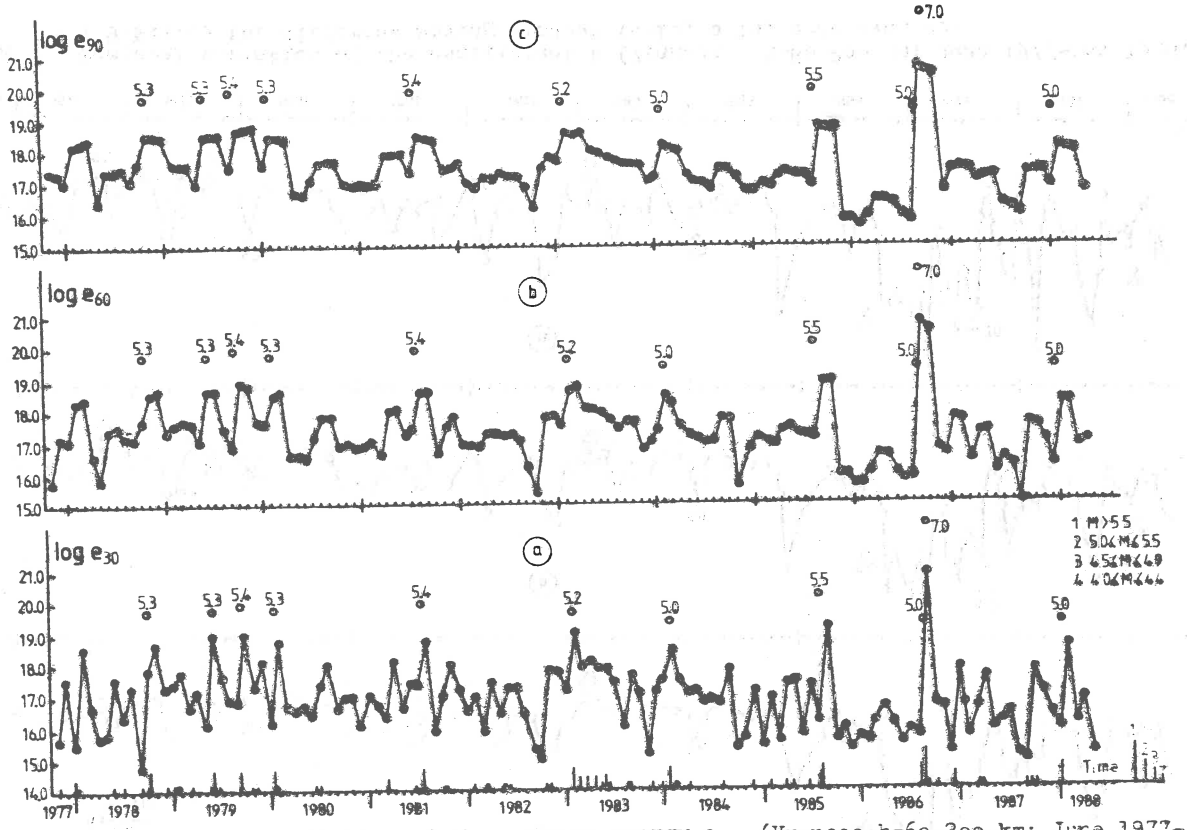

Fig.4 - Temporal variation of the average energy $e_{\Delta T}$ (Vrancea-h=60-200 km; June 1977-May 1988; 1.9≤M≤7.0) for different moving windows (a=30, b=60, c=90 days);

remarks:

- the major seismic activity (earthquakes with M>5.5) is concentrated in the periods of minimum values of b-coefficient. We note the marked maxima preceding the earthquakes of 1945 (b=1.45/M=6.5, 6.o), 1977 (b=1.57/M=7.2) and 1986 (b=1.5o/M=7.o);
- the periods of minimum values of b-coefficient, corresponding to the earthquakes with M>5.5 (excepting 1945 March 12/M=5.5; 1985 August 1/M=5.5) are characterized by values equal or smaller than those obtained from the magnitude - frequency relation for strong earthquakes (b=o.7o/Radu and Ardeleanu, 1982);
- the maxima of the function b(t) seem to reflect the intensity of the future seismic activity, that is, after a significant maximum (b>1.2) the occurrence of a strong earthquake (M>5.5) is possible.

2. The temporal variation of the coefficient b for the series of earthquakes with 1.9<M<7.o occurred during the period June 1977-May 1988/8o4 events. The analysis of Fig.3 leads to the following remarks:

- the major seismic activity (earthquakes with M>5.o) is concentrated in the periods of minimum values of b-coefficient, when 1-3 strong earthquakes occurred;
- the existence of a high (b=1.5o) and "agitated" maxima before the major earthquake (M=7.o) of August 3o, 1986.

. The average energy $e_{\Delta T}$. The analysis of temporal variation of the average energy $e_{\Delta T}$ leads to the following remarks (Fig.4):

- the function $e_{\Delta T}$ has a qvasiperiodic character;
- the minima of the function $e_{\Delta T}$ are located before strong (M>5.o) and moderate (M>4.o) earthquakes, and for strong earthquakes they are observed in a larger range of ΔT;
- the curves $e_{\Delta T}(t)$ obtained using small and large windows complete each other ; in the first case the minima are more pronounced and clearly localized in time, but in the second case the streng earthquakes are pointed out.

Based on these remarks, the function U(t) defined as:

$$U(t) = U_{\Delta T_{min}, \Delta T_{max}}(t) = \sum_{\Delta T_{min}}^{\Delta T_{max}} e_{\Delta T}(t) \qquad (6)$$

was computed, which cumulates the effect of individual time series.

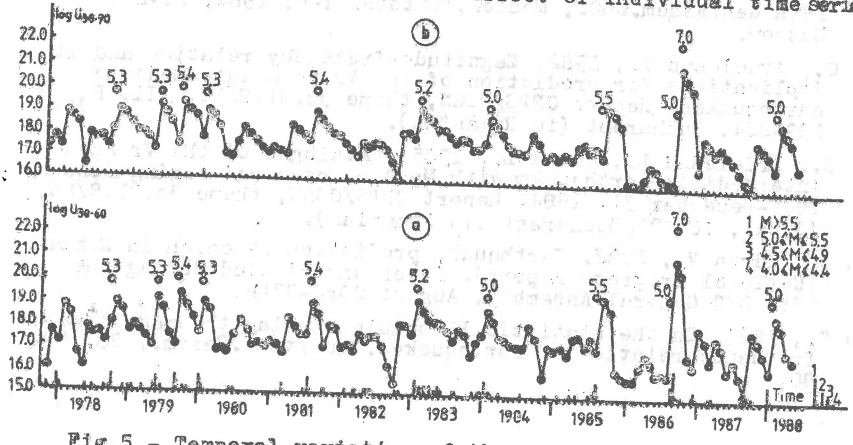

Fig.5 - Temporal variation of the function U(t)

In Fig.5 the functions $U_{30-60}(t)$ and $U_{30-90}(t)$ are presented. The pronounced minima can be noticed before earthquakes with M ≥ 5.o. We remark the clear anomaly associated with the major (M=7.o) earthquake of August 3o, 1986.

CONCLUSIONS

The temporal variation of the parameters d, b and $e_{\Delta T}$ provide useful information for the prediction of Vrancea intermediate earthquakes.

The major seismic activity (earthquakes with M≥5.o) is concentrated in the periods of minimum values of the ratio d and coefficient b, and follows a minimum of the average energy $e_{\Delta T}$ (or the function U(t)).

REFERENCES

Bellelovsky M.L., 1982. The average energy of earthquakes within ΔT interval and its use in prediction in Earthquake Prediction, 1, 88-1o9, Donish, Dushanbe (in Russian).

Malamud A.S., 1974. On a possible precursor of strong earthquakes. DAN Tadj. SSR, 1, 31-34 (in Russian).

Radu C., 1974. Contribution à l'étude de la séismicité de la Roumanie et comparaison avec la séismicité du bassin méditerranéen et en particulier avec la séismicité du sud-est de la France. Thèse Dr.Sci., 453 p., Univ.Strasbourg, France.

Radu C., 1988. Catalogue of the Vrancea intermediate earthquakes with M_D≥3.o, occurred during the period January 1, 1985-June 3o, 1988. Manuscript, CFPS, Bucharest (in Romanian).

Radu C., Apolozan L., Tenea L., 1984 a. The ratio d and the coefficient b-possible precursors of the Vrancea intermediate earthquakes. Report CFPS/CSEN, theme 3o.81.8/84, I, 423-441, Bucharest (in Romanian).

Radu C., Apolozan L., Tenea L., 1984b. Contributions to the prediction of the Vrancea intermediate earthquakes. Abstracts, 19th Gen.Assem.ESC., Moscow, October 1-6, 1984, 23-24, Moscow.

Radu C., Ardeleanu L., 1982. Magnitude-frequency relation and its implications for prediction of the Vrancea intermediate earthquakes. Report CFPS/CSEN, theme 3o.81.8/82, III, B_3, 199-224, Bucharest (in Romanian).

Radu C., Ardeleanu L., Tenea L., 1985. Catalogue of the Vrancea intermediate earthquakes with M_D≥3.o, occurred during June 1, 1977-December 31, 1984. Report CFPS/CSEN, theme 3o.81.8/85, II, A_3, 16-42, Bucharest (in Romanian).

Radu C., Mârza V., 1982. Earthquake prediction research in Romania (National Progress Report). Paper distributed during the 18th ESC General Assembly, August 23rd-27th.

Utsu T., 1964. On the statistical formule showing the magnitude-frequency relation of earthquakes. Quart. J.Seism., 28, 79-88.

CASE HISTORY OF AN ANTICIPATED EVENT: THE MAJOR (m_w = 7.0) VRANCEA (ROMANIA) EARTHQUAKE OF 1986

V.I. Marza, V. Burlacu, A. Pantea, Zina Malita
(Center for Earth Physics and Seismology (CEPS), Bucharest, Romania)
Georgeta Mihalache, Al. Dumitrascu
(Department of Mathematics, INCREST, Bucharest, Romania)

1. Introduction

Analysis and discussion of a variety of precursory seismicity patterns (p.s.p.) belonging to all temporal developmental stages of the preparatory (geo)phisycal process leading to the damaging major subcrustal Vrancea, Romania, earthquake (eq) of August 30, 1986 (epicenter = 45.5N/26.4E; depth = 144 km; m_w = 7.0, M_w = 7.3, M_L = 7.0; I_o = VIII½) is performed and documented, clearly proving that the eq would not has been unexpected. The salient features of Vrancea seismogenic region (VSR) and the tectonic setting have been presented elsewhere (Purcaru, 1979; Apostol et al, 1985; Constantinescu & Marza, this issue; etc). The seismological data base used for this study is the earthquake master catalogue of Constantinescu & Marza (1980, 1984), permanently uptated and completed on the basis of the data supplied by real-time telemetred seismic network of Romania, centered on VSR.

2. The Vrancea 1986 Major (m_w = 7.0) Subcrustal Earthquake related Precursors

A synoptic precursors' presentation is listed in the Table 1. In the following we shall present, discuss, comment and analyse the distinct p.s.p. contained in the Table 1.

Table 1. The Vrancea 1986 major subcrustal earthquake related precursors

DISCIPLINE	CLASSIFICATION	REMARKS
1. Regularity pattern 1.1. Periodicity/cyclicity 1.2. Paired occurence	Long-term	'A priori' reporting (Marza et al. 1977; Marza 1982)
2. Preseismic quiescence	Long-term	Real-time monitoring (Apostol et al. 1985, Marza 1982)
3. Hypocentral migration/progression	Long-term	'A priori' reporting (Marza et al. 1985, 1986a)
4. b-slope change	Medium-term	Real-time monitoring
5. Abnormal crustal activity (activation)	Medium-term	'A priori' reporting (Marza et al. 1986b)
6. Anomal subcrustal event (August 4, 1986)	Medium- to short-term	'A posteriori' reported
7. Foreshocks	Short-term	'A posteriori' reported

2.1. Regularity patterns in recurrence of major ($M_{GR} \geq 6.8$) VSR eqs., these patterns are characteristic for long-term strong ($M_{GR} \geq 6.8$) seismicity of VSR, and Fig.1 is a descriptive presentation of them. Fig. 1.A depicts overall series of events, whereas Fig 1.B presents a decomposition of the previous (which are randomly distributed) series into 3 nonrandom components. So the ordinate of the Fig. 1.B is the absolute calendarial year of occurrence, and the abscissa represents the relative years in each century. From the Fig. 1.B there are evident two salient regularity pattern: (1) a remarcable (quasi)periodicity of strong events ($M_{GR} \geq 6.8$) with a mean intersequence time $\Delta t \approx 100$ yr (and a standard deviation roughly 10% of the mean), and (2) paired occurrences, especially in the M3 band of maximum activity. This last feature, i.e. paired occurrences, was an early reason to consider that a possible second strong shock is in store (Marza et al. 1977, Marza 1982).

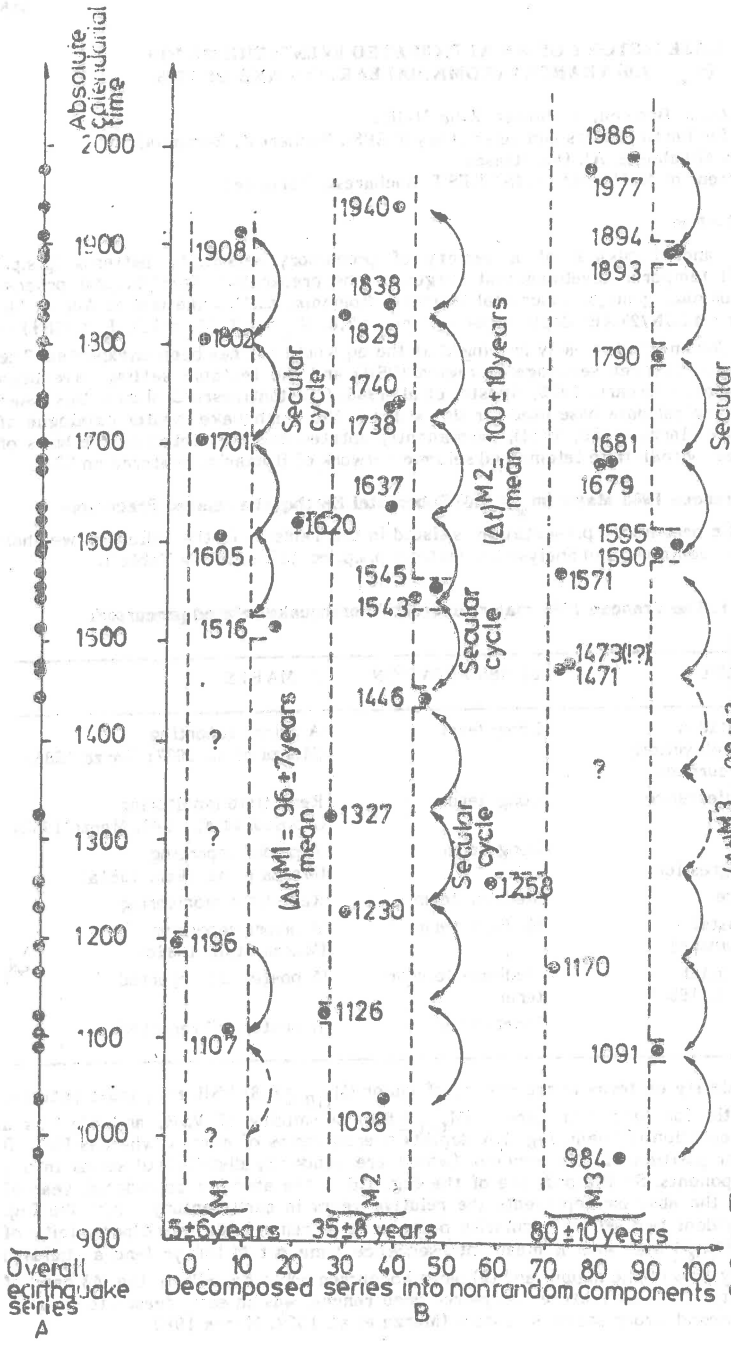

Fig. 1. Overall and decomposed components projections of strong ($M_{GR} \geq 6.8$) Vrancea subcrustal earthquake time series reflecting occurrence regularities (Combined and updated after Purcaru, 1979 and Márza, 1982)

2.2. Preseismic quiescence in minor VSR seismicity. As the former strong shock in VSR (that is, 1977 March 04, $m_w = 7.2$) was preceded by a quiescence pattern (Marza 1979, termed in that paper: 'seismic gap' (of the second kind, cf Mogi, 1979)), and moreover the subsequent larger shocks in VSR (i.e. $M_L \geq 5$) were in large proportion preceeded by quiescence patterns (Marza 1982, 1984 Apostol et al. 1985) we started a monitoring action in order to detect such patterns. In this respect by the February 1980, in the depth range of 120 to 145 km was reported a quiescent area (Marza 1982, Apostol et al. 1985) which lasted more than initially hypothesis (Marza 1982), but ended on 30 August 1986 with a major event in the same depth range. Fig.2 is a space (depth)-time diagram reflecting the quiescence pattern roughly in the depth range 120-145 km. Initially we were waiting to observe a simpler pattern, as before the former large eq, i.e. 1977 event (Marza, 1979), but the present reported pattern has been found more complex, one explanation being the better resolution threshold (3.7 to 4.0 (M_{GR}) for former case, as compared with 3.8 (M_L) roughly equivalent with 3.3 (M_{GR}) for latter event). This pattern with alternation of high seismicity followed by a sudden quiescence is considered significant relative to the behaviour of background seismicity and may be an intermediate term precursor. We consider this quiescence precursor as unambiguously identified because: (1) the precursor has a limited spatial extent and nearby regions have no quiescence; (2) the precursor is no man-made because no detection change or magnitude estimation procedure have been implemented since 1980. Similar patterns, quiescence-resumption/activation-quiescence etc., have been reported also by Ishida & Kanamori (1980). The observed precursory time of quiescence pattern is 2383 days, in good agreement with the computed one of 2188 day, as predicted by Marza (1981) model.

2.3. Hypocentral migration/progression of larger ($M_L \geq 5$) VSR mainshocks. This pattern was inferred based on the study of behaviour of VSR mainshocks in the period 1978-86 (Table 2).

Table 2. The full sequence of larger subcrustal Vrancea earthquakes ($M_L \geq 5$) during january 1978 - august 1986

SERIAL NUMBER OF EVENT IN THE SEQUENCE	DATE	ORIGIN TIME (UTC)	LOCATION EPICENTER (°N)	(°E)	DEPTH (km)	M_L	REMARKS
1	1978 JAN 31	07:40:14	45.715	26.457	136.4	5.1	It belongs to ping-pong stage
2	OCT 02	20:28:52	.725	.479	164.3	5.2	ditto
3	1979 MAY 31	07:20:06	.552	.327	120	5.3	ditto
4	SEP 11	15:36:54	.560	.298	154.3	5.3	ditto
5	1980 JAN 14	15:07:54	.780	.600	141	5.1	ditto
6	1981 JUL 18	00:02:58	.685	.421	166.1	5.4	It belongs to progression stage
7	1983 JAN 25	07:34:50	.749	.637	149.8	5.3	ditto
8	MAR 11	06:29:25	.645	.535	151.5	5.0	ditto
9	1984 JAN 20	07:24:22	.502	.394	132.4	5.1	ditto
10	1985 JUN 21	16:50:45	.638	.466	124.4	5.0	ditto
11	AUG 01	11:17:36	.789	.772	118.6	5.2	ditto
12	AUG 01	14:35:04	.727	.623	93.5	5.5	ditto
13	1986 APR 27	00:04:35	45.474	27.079	14.3	5.1	Crustal event
14	AUG 16	06:41	.549	26.368	146.8	5.2	Foreshock
15	AUG 30	21:28:36	.540	.431	144.0	7.0	Mainshock

Fig.3 is a plot of this pattern, in the abscissa is plotted the serial number of sequence events (cf. Table 2), that is it is proportional with time (but with no constant rate). From the plot

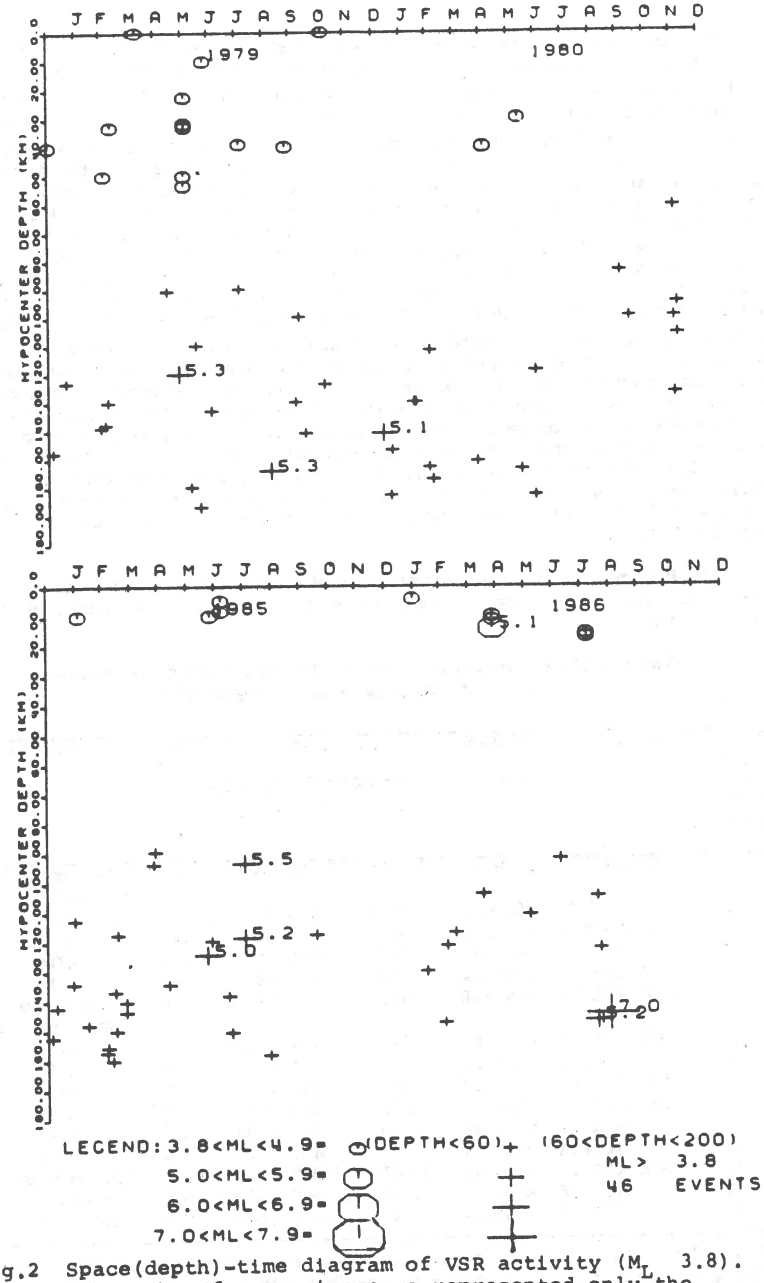

Fig.2 Space(depth)-time diagram of VSR activity (M_L 3.8). (For sake of convenience we represented only the beginning and the end periods of the pattern).

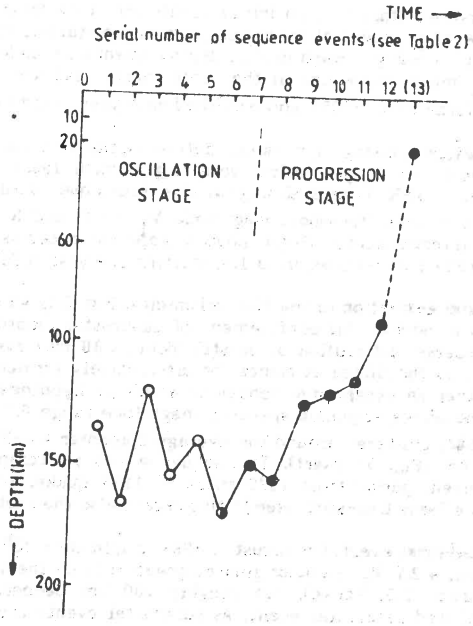

Fig.3 Hypocentral migration/progression pattern of VSR larger ($M_L \geq 5.0$) mainshocks during the period Jan.1978 - Aug.1986.(See also the Table 2).

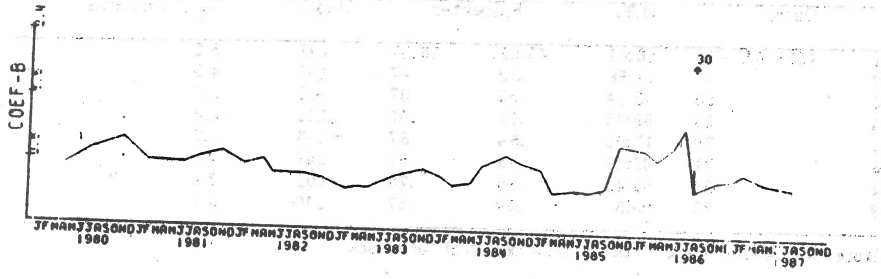

Fig.4 b-value fluctuations. Vertical arrow marks the day of 1986 major earthquake. The vertical doted bars show one standard deviation.Magnitude threshold $M_L = 3.2$

we easily may see two distinct stages: (i) an initial oscillation stage (ping-pong behaviour) and (ii) a very distinct upward hypocentral migration/progression starting in 1981 at a depth of 166 km and gradually progressing toward crustal depths, eventually ending with a 5.2 M_L foreshock and the 7.0 m_w major mainshock at the depth roughly 145 km. This pattern was firstly reported in 1985 (Marza et al. 1985), and published next year (Marza et al. 1986a).

2.4. b-slope fluctuation showing high values before mainshock. As b-value changes has got increased popularity in eq prediction work (e.g., Smith 1986) we were on-line searching b-value changes in VSR using a sliding-window technique (Utsu 1965, Aki 1965) with N = 20 events in the window (threshold magnitude M_L = 3.2) and K = 10 events step, with value plotted at the interval center. Fig.4 shows b-slope computed as described above, clearly pointing out an increase in b-values ($b \approx 1.5$) starting one year before mainshock.

2.5. Abnormal crustal activation in the VSR seismicity. Fig. 5 is an epicentral plot of activity. Two features are evident: (a) confinement of subcrustal (depth $\geq$ 60 km) events (symbol +) and rather disperse distribution of crustal (depth < 60 km) events. VSR crustal activity generally is low, so the Sihlea sequence (or alternatively termed Sihlea swarm of roughly 150 events) is rather an exceptional behaviour which we hypothesised is precursory to 7.0 m_w mainshock. The Sihlea sequence spaned a magnitude range 0.9 to 5.1 M_L during April 27 to August 27, 1986, clustered around the average epicenter 45.5N/27.1E and in the hypocentral range 5-25 km (Fig. 5; insert). This sequence was an exceptional and unique pattern during the interevent period from 1977 shock to 1986 quake, and we interpreted (Marza et al. 1986b) it as a "sensitive-spot" (see in this regard also the section 2.6).

2.6. An anomal subcrustal event. On august 4, 1986, origin time $23^h41^m37^s$, epicenter 45.3N/27.0E depth 105 km, a 2.7 M_L event originated practically on the vertical line of the "sensitive-spot" (see section 2.5, above), but roughly 100 km deeper. This is also an exceptionally case of isolated subcrustal event, as subcrustal events are confined west to this site (Fig. 5).

2.7. Foreshocks, finally, during August 16-23, 1986 eight foreshocks (Table 3) occurred in the magnitudinal range 2.4-5.2 M_L (N.B., the detection threshold for subcrustal eqs is $\approx$ 2.4 M_L).

Table 3. Foreshocks of the 30 august 1986 Vrancea (Romania) earthquake

	Data	O.T.	Epicenter		Depth	M_L	Remarks
1	1986 AUG 16	06:41	45.55;	26.37	147	5.2	
2	17	11:56	.68	.47	105	4.5	?
3	20	05:34	.55	.37	165	3.0	
4	20	09:08	.53	.57	122	3.8	
5	20	17:00	.64	.67	143	3.7	
6	21	02:11	.56	.54	147	4.0	
7	22	03:43	.60	.70	102	2.4	?
8	23	05:50	.69	.57	140	3.1	

Note: A question mark (?) point out a doubtful foreshock

3. Brief discussion

The majority of the above presented p.s.p., i.e. subsections (2.1) to (2.5) have been 'a priori' detected and reported. Moreover, the p.s.p. belonging to items 2.3, 2.6 and 2.7 are new original/genuine p.s.p. observed in V.S.R. The premonitory information supplied by the above p.s.p. data has been much richer than for the case of the former major (m_w = 7.2) event of 1977, and pointed out the variability of precursors' appearance.

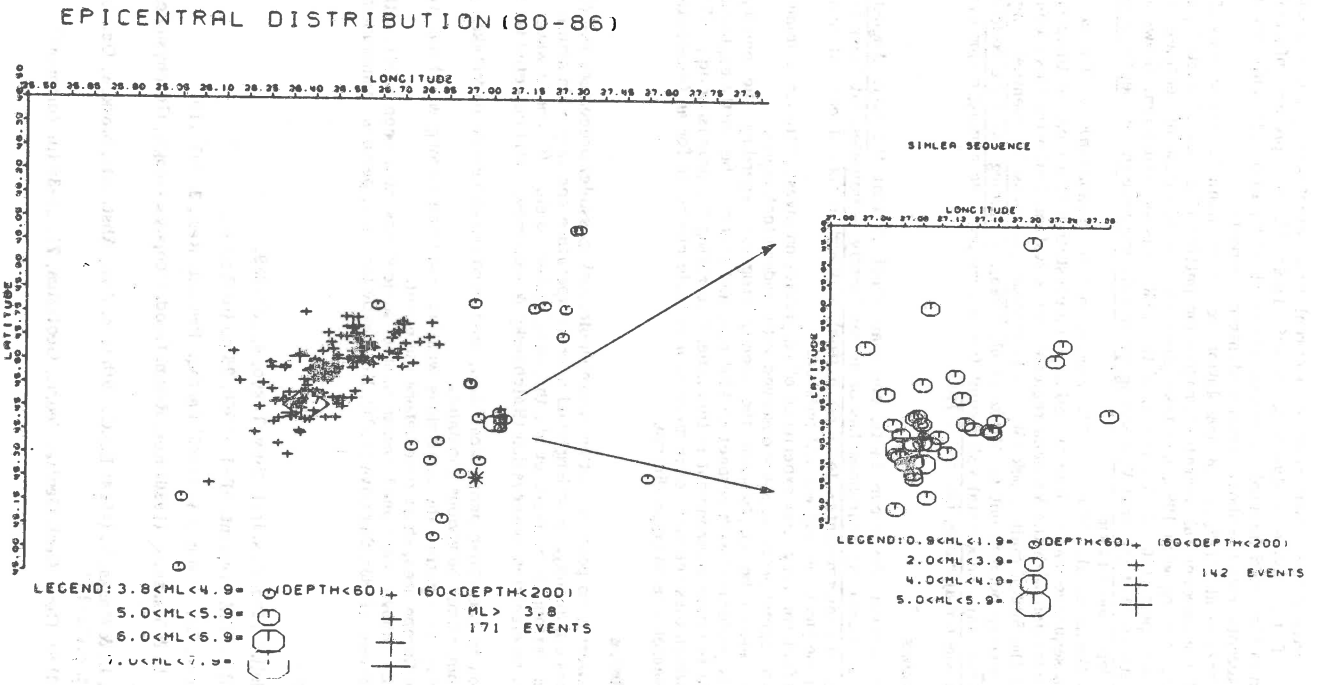

Fig.5 Epicentral plot of VSR activity. Magnitude cut-off : M_L = 3.8 . Into insert is an expanded plot of Sihlea sequence (magnitude threshold : $0.9M_L$). One may also see the anomalous subcrustal event (*).

The main merits of the present research are: real-time detection and data collection, timely reporting of the above analysed p.s.p. (cf. Table 1), and proper informative (re)interpretation in the CEPS internal reports (Marza et al. 1985, 1986b). It is illustratively to present two excerpts from the above mentioned internal reports.

Firstly, Marza et al. (1985, p. 28, translation from Romanian): "...On the basis of the interpretation of the hypocentral migration/progression pattern (Fig. 4.4 of quoted paper) one observe that, starting with 1981, one take place an intensification of tectonic stress build up in the lower part (140-160 km depth) of the VSR. This asertainement allows us to advance the hypothesis that the next VSR strong quake will originate in this depth range..." In fact observed depth was 144 km.

Secondly, Marza et al. (1986b, p. 22, translation from Romanian): "... The seismic activity of Sihlea sequence may be interpreted as a manifestation of a local tectonic stress system, but in connexion with the Vrancea regional stress system. Following this ideea one may assume that the Sihlea main shock (M_L = 5.1) represents a possible eventual stage of the progression pattern pointed out by Marza et al. (1985), remaining valid the conclusion concerning the next major subcrustal VSR event" (i.e. a very probable coming major event). Indeed the event was a major one, i.e., m_w = 7.0.

4. Conclusions

Taking in account the above facts, one may conclude that the 1986 August 30, m_w = 7.0, Vrancea (Romania) mainshock has been confidently anticipated (at least in the frame of a long -to intermediate- term prediction), although a formal commitment for evaluation and subsequent warning was not pursued.

This is in fact the very first experience of eq prediction investigation in Romania for which many seismological precursors are observed with modern techniques.

Finally it should be emphasized the steady progress regarding the earthquake prediction results performed with respect to VSR eqs, and this may be partly explained by the very suitable tectonic environment in this zone, reiterating the promising eq prediction avenue in VSR, which thus one self-recommend as a suitable candidate for an (international) experimantal research site on eq prediction.

5. Miscellanea

It is noteworthy to point out other nonseismological (possible) precursors associated with 1986 Vrancea eq, namely: an underground microtemperature anomaly (Shimamura 1986, personal communication; Demetrescu et al., this issue) detected close (Odobesti water-well) to the epicenter, an electrical observation (Ralchovsky & Komarov, 1987) detected far from the epicenter.

In addition to the above geopyisical data, post card questionnaire undertaken after the eq, brought out animal behaviour anomalies.

It is worthy to mention the anomalous weather condition (strong wind) manifested over the Eastern Europe area, short time before the event.

Besides the above mentioned research, the subject has also been dealt with by: Anghel (1980), Enescu (1983), Sagalova (1987), Kormakov (Sobolev, personal communication, 1988).

References

Aki, K. (1965) Bull.Earthq. Res. Inst. Univ. Tokyo, 4, 237-239,

Anghel M. (1980) ICEFIZ Preprint, EP-13-1980, 29 pp (in Romanian)

Apostol A., Arsene, Gr. & Marza V. (1985) Earthq. Predict. Res., **3**, 105-119.

Constantinescu, L. & Marza, V. (1980) Rev. Roum. Geod. Geophys. Geogr., Geophysique, **24**, 193-234.

Constantinescu, L. & Marza, V. (1984) E.S.C. 19th Gen. Ass., Abstracts, Moskow, October 1-6, 1984, p.176-177.

Enescu, D. (1983) St. Cerc. Geol. Geofiz. Geogr., Geofizica, **21**, 24-30 (in Romanian)

Ishida, M. & Kanamori, H. (1980) Bull. Seism. Soc. Am., **70**, 509-527.

Marza, V. (1979) Tectonophysics, **53**, 217-222.

Marza, V. (1981) Proc. 2nd I.S.A.S.S.H., Liblice, Czechoslovakia, May 18-23, 1981, p. 117-132, Prague.

Marza, V. (1981) Premonitory purport of seismicity fluctuations. Global-scale manifestations with particularization and emhasis on Vrancea region. Romania, Ph. D. Thesis, Univ. of Bucharest, 189 pp. (in Romanian with a English abstract).

Marza, V. (1984) E.S.C. 19 th Gen. Ass. Abstracts, Moskow, October 1-6, 1984, p. 43-44.

Marza, V., Irimescu, D., Pantea, A. & Anghel, M. (1977) CEPS Report, Theme 30.77.1./1977, Pt. II, Chapt. 8, p. 118-132 (in Romanian).

Marza, V., Burlacu, V. & Pantea, A. (1985) CEPS Report, Theme 8054/1985, Chpt. 4, p. 12-28 (in Romanian).

Marza, V., Burlacu, V. & Pantea, A. (1986a) Terra Cognita, **6**, Abstaret S20.15, p. 424.

Marza, V., Burlacu, V., Pantea, A. & Malita, Zina (1986b) CEPS report, Theme 30.86.3/2986, Phase II, (June, 1986), Chpt. A2, p. 11-22.

Mogi, K. (1979) Pageoph, **117**, 1172-1186.

Purcaru, G. (1979) Phys. Earth. Planet. Inter., **18**, 274-284.

Ralchovsky, Tz. M. & Komarov, L.N. (1987) Bulg. Geophys. J. **13**, 59-65 (in Bulgarian with Russian and English abstracts).

Sugalova, E.A. (1987) Geophys. J., Kiev, **9**, (6), 84-9 (in Russian).

Smith, W.D. (1986) Geophys. J.R. astr. Soc., **86**, 815-838.

Utsu, T. (1965) Geophys. Bull. Hokkaido Univ., **13**, 99-103 (in Japonese with English abstract).

SOME FEATURES of SEISMICITY prior to STRONG AFTERSHOCKS

S. S. Arefiev, R. E. Tatevosyan, M. V. Shebalin

Institute of Physics of the Earth, USSR Academy of Sience, B. Gruzinskaya, 10, Moscow, 123810 (USSR)

Large earthquakes are in many cases accompanied by aftershocks and about 10% of them provoke another large earthquake (within the range from several hours to several months). By observations in epicentral zones we try to solve the problem of predicting the future behavior of a source. Such a prediction is of high social and economic importance and has much in common with the general problem of earthquake prediction but seems to be less complicated, because the site of probable next strong shock is bounded by the epicentral zone of the first one.

Three types of seismic source behavior after the main shock, can be distinguished, which differ in their social and economic consequences: the first one (Ashkhabad type) has the aftershock swarm of relatively weak shocks; the second (Tashkent type) has longtime aftershocks sequence and some of them can achieve the main shock by their local destructive effects; and the third (Gazli) type: when a large earhquake is followed by the next even stronger one. The physical background of this distinction is still unclear.

There are some advances in this field, but, on the whole, the problem is far from being solved. In this paper, we suggest a possible approach to solving the problem, using the catalogue of aftershocks of Gazli earthquake March 19, 1984, only.

Three strong earthquakes $M \geq 7.0$ since 1976 took place in Gazli region in April 8, 1976 ($M = 7.0$), May 17, 1976 ($M = 7.3$), March 19, 1984 ($M = 7.2$). All the three are accompanied by a heavy aftershock swarm: in last case 1500 shocks were registered during two months of observations, and 891 of them have $K \geq 8.5$ ($K = 1.8M + 4$). The latter were registered without omissions [1].

The epicentral map of those events is shown in Fig. 1a. One can see that the cloud of aftershocks is isometric in shape.

From the aftershock sequence we selected 6 strong aftershocks

(K ≥ 12.5, M ≥ 4.7), see Fig. 1b. Two of them (the strongest one including) took place during the first day (March 20, 1984, 03h 49m, K = 12.6; March 20, 1984, 06h 28m, K = 13.5). One aftershock (April 1, 1984, 09h 47m, K = 12.8) was on the edge of the zone and there are only two events near it, so we have not any suitable data for analysis. Therefore, we had to consider only 3 strong aftershocks.

Event 1: March 30, 1984, 14h 25m, depth = 24.5 km, K = 13.0

Event 2: April 11, 1984, 23h 30m, depth = 7.5 km, K = 12.9

Event 3: April 28, 1984, 23h 33m, depth = 5.0 km, K = 13.3

To discuss the seismic regime before and after these events we will use basic regime parameters: activity A_{10} and fractionality γ [2]. We will also use the Morishita index for determining the level of clustering of space distribution of the aftershocks [3, 4].

The whole work was performed in two steps. The first one was the consideration of regime parametrs for the zone as a whole.

The temporal variations of A_{10} and γ for the zone are shown in Fig. 2a, b (the arrows show the times of strong aftershocks origin). We can not see any stable features in the seismic regime connected with strong aftershocks.

Temporal variations of the Morishita index for the zone as a whole are even less pronounced and are not given hear. It follows that either the whole zone is not involved in preparing strong aftershocks, and we have to locate more correctly the spatial limits within which we calculate the parameter of the seismic regime or our method is unfeasible.

The general dependences of γ (fractionality) and the Morishita index on the depth are well mutual correlated (Fig. 2c, d), so we can presume some physical relationship between the fractionality of media, and the level of clustering of ruptures (seismic events).

The more complicated second step is determining more close the temporal and spatial limits, of sub-zones belonging to Events 1 - 3 These limits must be as narrow as needed to exclude the effect of the preparation of other strong aftershocks. We chose the 24 km side square around each epicenter of Event 1 to 3 which is approxima-

tly equal to the size of its preparation zone or to 3 times rupture length of the source [5].

The limitation on depth (H = 18km) was provided after analysis of the aftershok's depth distribution. We can observe that in depth the whole active space clearly subdivided in two layers with the boundary at the depth of 18 km. For the first Event (H = 24.5km) we select shocks within the lower layer that is deeper than 18km, for others two (H = 7.5, H = 5km) H ≤ 18km (see Fig. 1b).

Theese three group of events form three subcatalogues. Each of these subcatalogues is devided into two parts: "before" and "after" the strong event. The "before" events were assumed to be 100 previous shocks and "after" the next 100. The number of 100 events permit the adequate application of the mentioned technique. In case if the actual number of shocks was less than 100, we were obliged to make our conclusions with necessary reservation. Time variations of A_{10} and γ for this sub-catalogues were calculated. As a zero time we assume the time of origin of the stong aftershocks.

The maps of epicenters, which meets the above mentioned limits, Morishita indeces and A_{10}, γ graphs "before" and "after" Event 1 are shown in Fig. 3a. The "before" interval includes only 25 aftershocks, 22 from them covers only one fourth of the whole zone space. For this quarter the index shows a random spatial distribution of aftershocks, though the whole arrea is characterised by a fairly high level of clustering. The "after" interval displays a random space-distribution.

The same set of parameters for Event 2 is shown in Fig. 3b. The "before" level of clustering is higher than "after".

Before Event 2 you see a bay-form time behavior of γ against the background of decline in activity (see Fig. 3b). This bay is formed 8 days before the Event and achieves its minimum (γ = 0.33) before 5 days. During the last day before the shock fractionality increases to 0.51.

For Event 3 (see Fig.3c) "before" has almost the same level of clustering as Event 2. The "after" interval shows a higher level of clusering. But the "after" interval has only 54 events which isn't a sufficient sample. The bulk of events are displaced NW of the zone under consideration (33 events) and have a random

distribution.

Bay before Event 3 (Fig. 3c) began earlier (12 days), achieves minimum before 5 days and has a deeper bottom (γ = 0.27). The shock occurs when γ increases to 0.46. The variation of A_{10} is in antiphase with γ.

It can be said with some reservasions that the level of shocks clustering is higher before than after the strong events, and vice versa. At the same time we can observe slightly pronounced for the size ca 5 km increas of clustering level "before" and decreas of clustering level "after" the Event, this size corresponding with the source size of the Event (dashed vertical line at I_δ vers L graphs, Fig. 3).

The fractionality temporal variation in the Event 2 preparation zone shows a slight bay again, which was formed, when Event 3 occured in the neighbourhood. The occurence of Event 2, too could be seen in the same way in the γ time variation graph of Event 3. But for a neighbour event the bay is less expressive, compared whith the given one.

The most complicated problem in predicting strong aftershocks is pre-establishing of zones in which the events are prepared. The size of the zone can be derived from statistical data on rupture lenghts. Then we can scan whole territory, on the basis of the square whose size was established and the bay-form of gamma time variations in antiphase with the activity and high values of Morishita index would point to preparation of a strong aftershock.

CONCLUSION

1. The preparation zone of a strong aftershock is not the whole area but only its rather limited surroundings.

2. Bay-shaped fractionality temporal variations are formed before strong aftershock which are in antiphase with activity temporal variations.

3. The level of clustering of aftershocks is higher before than after strong aftershocks especialy for the specific size of the source itself. This conclusion is not very reliable.

4. The distribution with depth the clustering level and of the fractionality are mutualy correlated.

REFERENCES

1. Gazly earthquakes 1976 and 1986. FAN, Tashkent, 1986, 368p.
2. Arefiev S.S., Tatevosyan R.E., Shebalin N.V. On inherent structure of Caucasus seismicity. - In: Voprosy inzhener. seismologee, M.: Nauka, 1987, n. 28, p. 126-146.
3. Ouchi T., Uekawa T. Statistical analysis of th espatial distribution of earthquakes before and after large earthquakes. - Phys. of the Earth and Planet. Inter. (preprint, 1985, 30p.)
4. Arefiev S.S., Shebalin N.V. On estimation of clustering Caucasian earthquekes. DAN USSR, v. 298, n. 6, p. 1349-1352, 1988.
5. Riznichenko Yu.V. Source size of crustal earthquakes and seismic moment. - In: Issledovanya po fizike zemletryaseniy. M.: Nauka, 1976, p. 9-27.

ILLUSTRATIONS

Fig. 1. Map of epicenters of the aftershocks and cross-section in depth (a); strong aftershocks with spatial limits which form sub-catalogues (b).

Fig. 2. Fractionality (a) and activity (b) temporal variations for the whole zone; Morishita index (c) and fractionality (d) vs depth for the whole zone.

Fig. 3. Maps of epicenters and Morishita indeces before and after Event 1; fractionality and activity temporal variations in spatial limits (see fig. 1, b) (a); the same set of the parameters for Event 2 - (b) and Event 3 - (c).

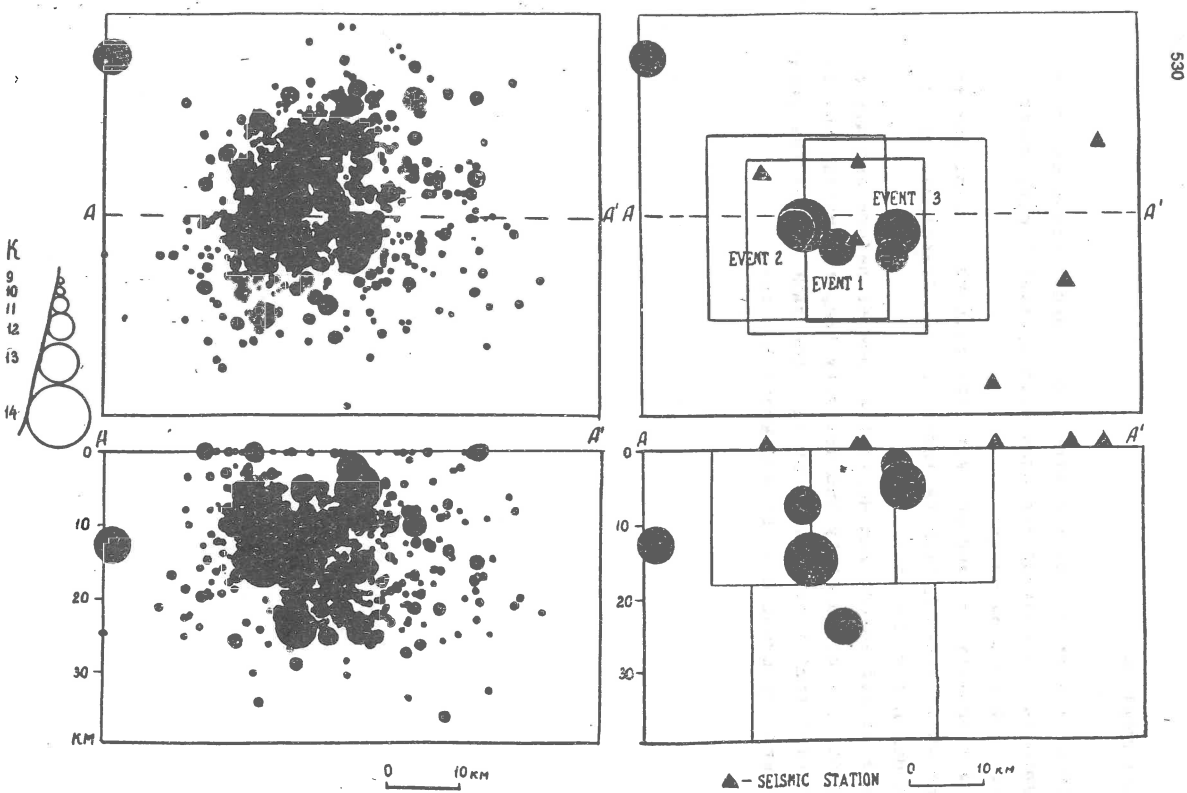

Fig. 1. Map of epicenters of the aftershocks and cross-section in depth (a); strong aftershocks with spatial limits which form sub-catalogues (b).

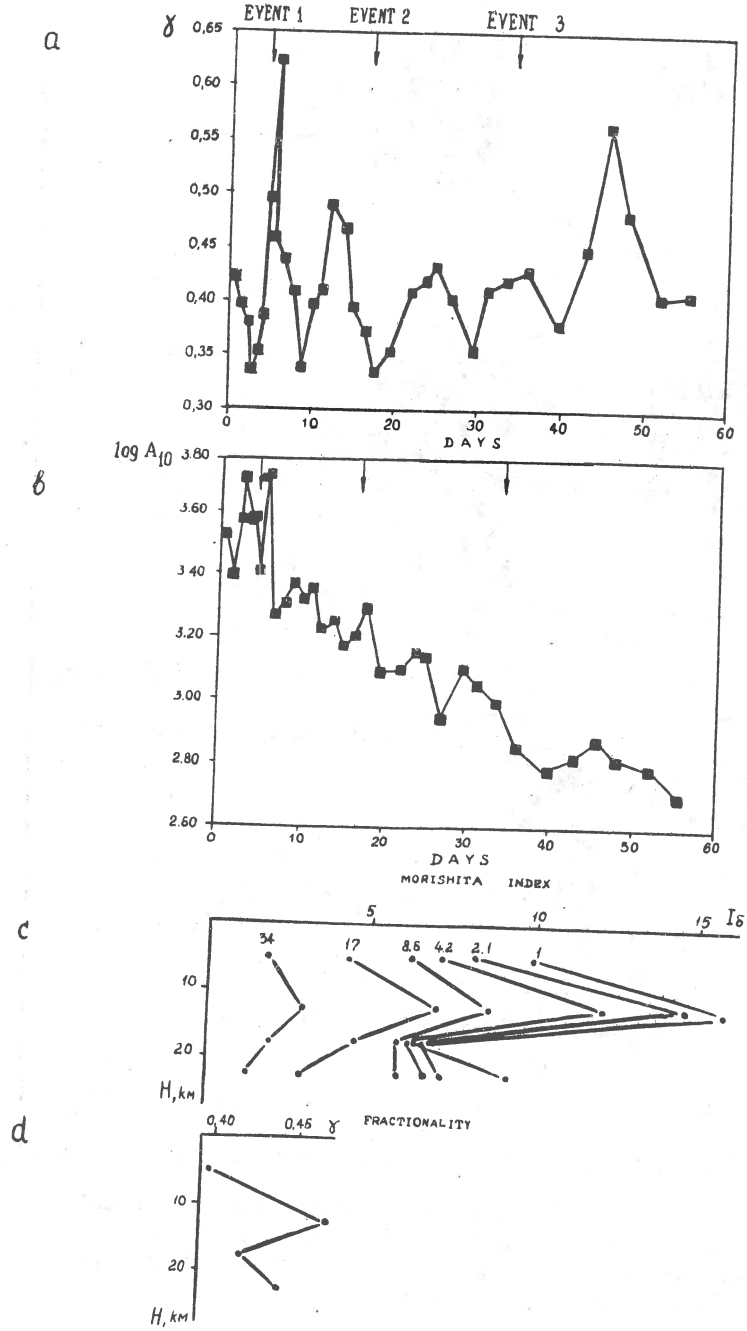

Fig. 2. Fractionality (a) and activity (b) temporal variations for the whole zone; Morishita index (c) and fractionality (d) vs depth for the whole zone.

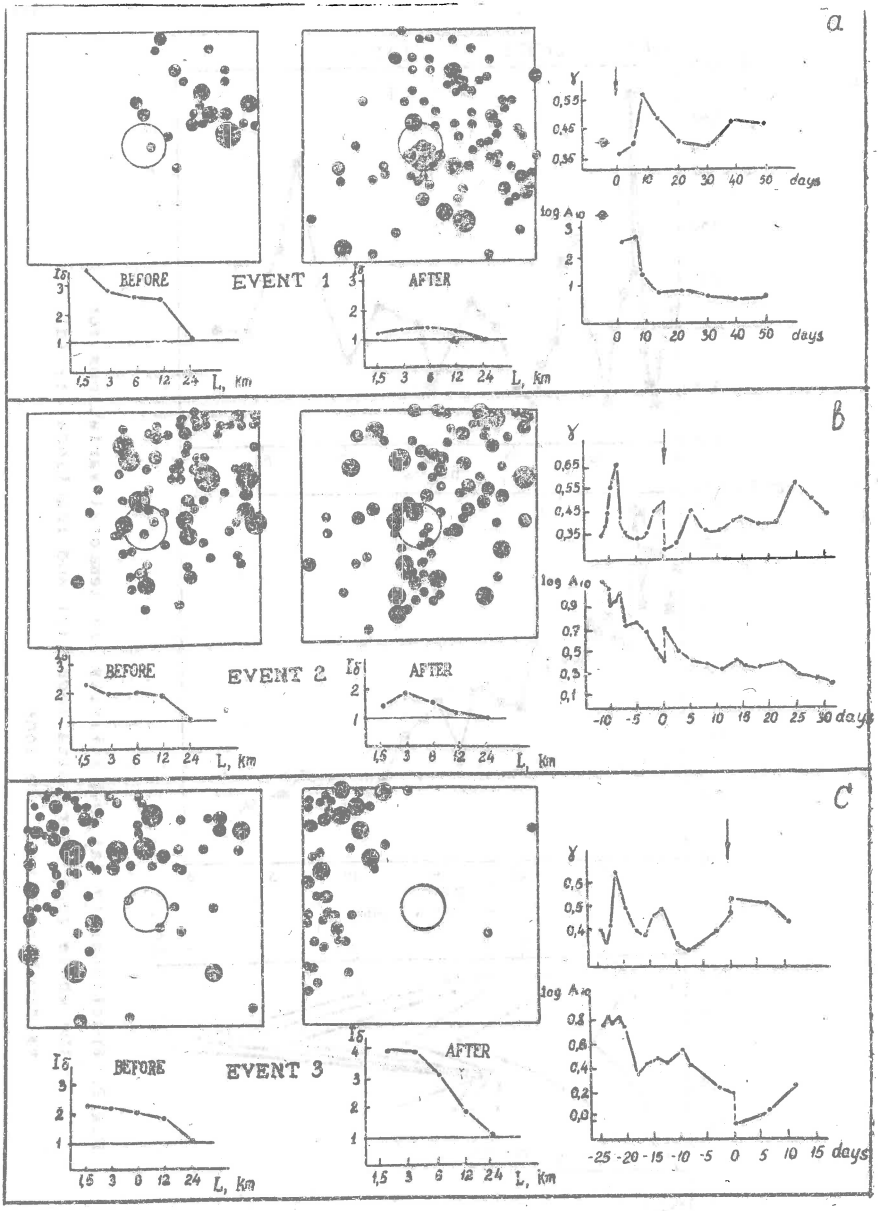

Fig. 3. Maps of epicenters and Morishita indeces before and after Event 1; fractionality and activity temporal variations in spatial limits (see fig. 1, b) (a); the same set of the parameters for Event 2 - (b) and Event 3 - (c).

THE MAIN SEISMOACTIVE FAULTS IN ALBANIA

Shyqyri Aliaj: Seismological Center,
Tirana, ALBANIA

INTRODUCTION

In Albania are distinguished two large domains with different recent regime: the external domain of compressional regime and the internal one of tensional regime.

In this paper we intend to point out the main seismoactive faults determining their seismic potential as well.

Generally, in Albania the seismoactive faults are such faults that dislocate the Earth's Crust, but, only behind the Adriatic collision, in the Pre-Adriatic depression, the seismoactive faults goes up to the Upper Mantle.

The high seismic potential zones of Albania are correlated with the present deformations occuring more at a linear belt of compressional regime behind the Adriatic collision (Adriatic--Ionian seismogenous belt) and, in few active zones of tensional regime, in the inner part of orogen (Korça-Ohri-Dibra, Gollobor-da and Shkodra seismogenous zones).

1. SCHEME FOR THE NEOTECTONIC STRUCTURE

The Alpin orogen of Albania, called Albanides, is bordered by the Adriatic plate in the Adriatic and Ionian seas (fig.1). The passage from the Aegean subduction zone to the Adriatic collision one is made at the Ionian Islands of Greece (D. Sorel, 1976).

In the orogen of Albanides there are distinguished two great domains of different present tectonic regime: the external domain of compressional regime and the internal one of tensional regime (Aliaj, 1982).

Some transversal fault zones intersect the structure of the Albanides.

The external domain, presented by folds, reverse faults up to thrusts and strike-slips, includes the structures of Sazani, Ionian, Kruja zones and the Pre-Adriatic marginal depression. In southern Albania this domain reachs a width of 100 km (fig. 1).

The Pre-Adriatic depression, due to oblique collision between the Adriatic plate and Albanides orogen, is oblique to the orogen of the external domain.

The internal domain, presented by a horst-graben structure, is situated NE of external domain and includes the new structure of Krasta-Cukali, Albanian Alps, Gashi, Mirdita and Korabi zones. The horst-graben structure is developed behind the front of the great overthrusts, which ceased being active during the neotectonic stage (fig. 1).

The microtectonic studies and the earthquakes focal mechanism solutions prove that the external domain suffers a compressional regime of NE to SW direction, nearly normal to Adriatic collision zone, while the internal one suffers a tensional regime of NNW to SSE direction, paralel to the zone of Adriatic collision (fig. 2).

2. THE MAIN SEISMOACTIVE FAULT ZONES AND THEIR SEISMIC POTENTIAL

This seismotectonic analysis is carried out for each longitu-

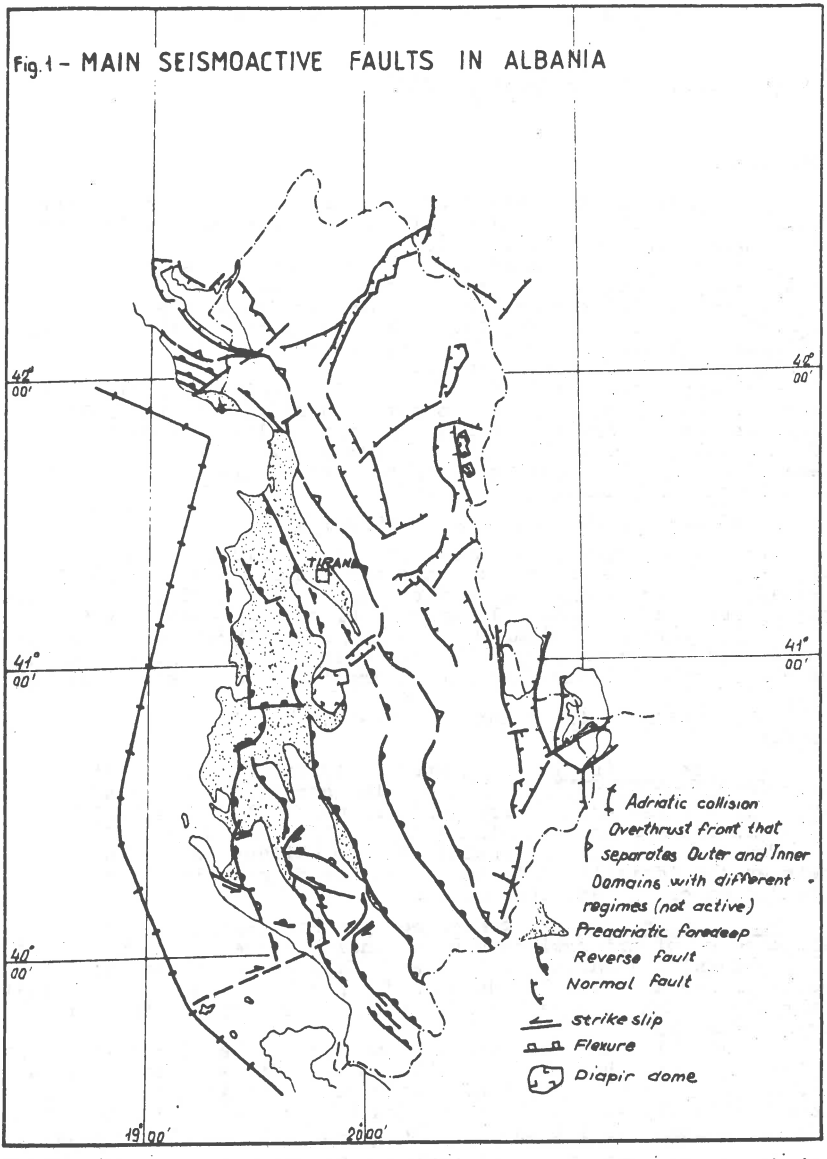

dinal and transversal seismoactive fault zone, determining their expected seismic potential as well.

2.1. The longitudinal seismoactive faults

The main longitudinal seismoactive fault zones (from W to E)

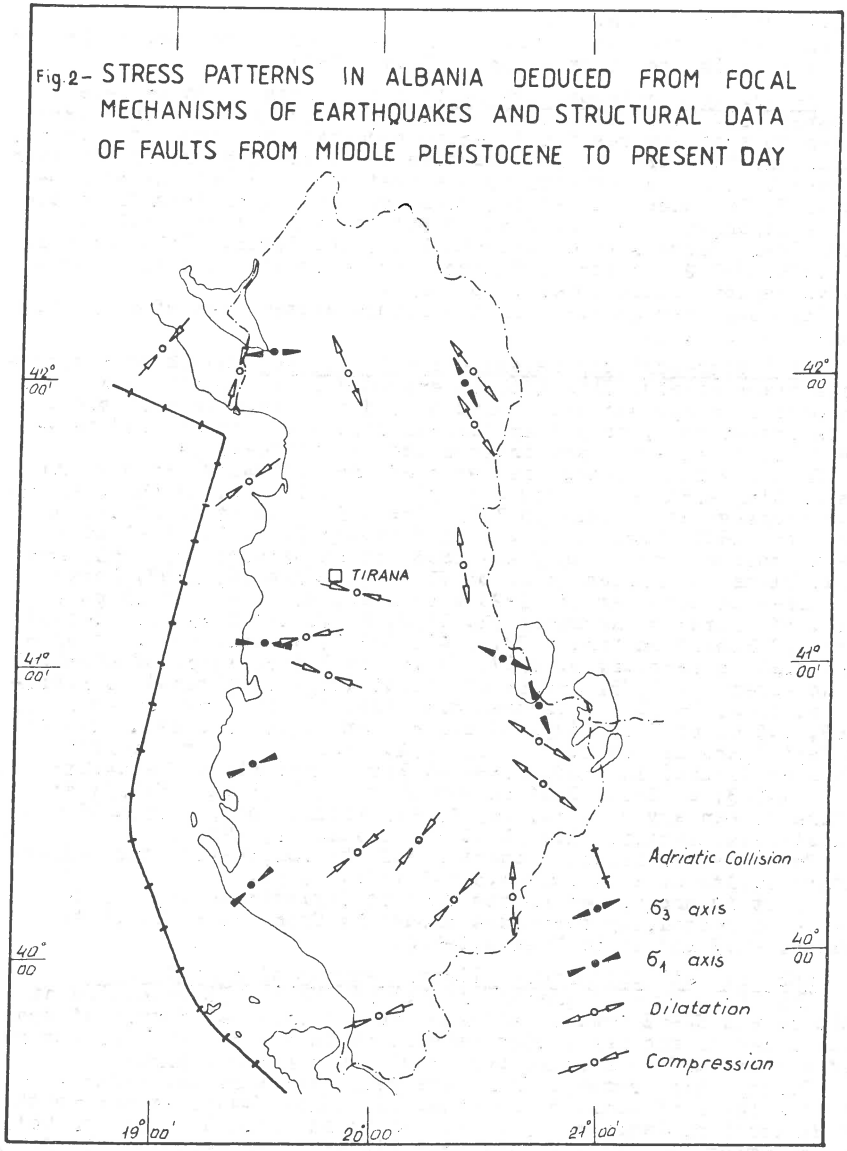

are:

1. The Adriatic seismoactive fault zone (North of Shkodra-Peja transversal), 2. The Ionian-Adriatic fault zone (South of Shkodra-Peja transversal), 3. The seismoactive fault zone of Shkodra-Mati-Librazhdi-Bilishti, and 4. The seismoactive fault of

Korça-Ohri-Dibra (fig. 3).

The two firsts are situated in the external domain, while the two latters in the internal one (Aliaj, 1987).

The Adriatic seismoactive fault zone (North of Shkodra-Peja transversal). This seismoactive fault zone is extended in a narrow orogen belt of compressional regime bordering the zone of Adriatic collision. The Adriatic seismoactive fault zone, presented by some reverse faults and thrusts, is the most potential of the seismoactive fault zones. The earthquakes recorded along this fault are of the strongest ones occurred in this domain as: on April 6, 1667, Io=10 degrees (near Dubrovnik), (Mihajlovic, 1947); on April 15, 1979, M=7.2 and Io=9.5 degrees, the epicenter was at Tivar - -Budva region (Sulstarova, Muço 1983).

This zone may generate in the future earthquakes of Mmax$>$7.0 (7.0-7.4) as well.

The Ionian-Adriatic seismoactive fault zone (South of Shkodra--Peja transversal). This zone is extended in a relative broad orogen belt of compressional regime behind the Adriatic collision. It is presented by many longitudinal faults of thrusts and reverse fault types which are intersected by strike-slips.

In these fault zones are recorded the following earthquakes (respecting each fault from W to E): at Apollonia, in the year 217, Io=9 degrees; at Durrës, in 1273, Io=9; in 1153 at Butrinti; on April 16, 1601, Io=9 at Vlora; on February 11, 1872, Io=9 at Sagiada-Konispol; on January 19, 1833 and on October 12, 1851, Io= =9, at Vlora; at Kudhës (dep. of Vlora) on June 14, 1893, Io=9; at Durrës on December 17, 1926 with M=6.2 and Io=9; at Llogara (dep. of Vlora) on November 21, 1930, M=6.1 and Io=9; at Cakrani (dep. of Fieri) on August 23, 1940, M=5.5; at Selo (dep. of Gjirokastra) on February 9, 1967, M=5.6; at Dhivër (dep. of Saranda) on November 22, 1975, M=5.5; at Ndroqi (dep. of Tirana) on February 4, 1934, M=5.6; at Izvor-Rabie (dep. of Tepelena) on April 3, 1969, M=5.6; at Vrap (dep. of Tirana) on August 19, 1970, M=5.5; at Kepi i Rodonit on August 26, 1852, Io=8; at Ura e Beshirit (dep. of Tirana) in 1860, Io=8; at Kepi i Rodonit on September 16, 1975, M=5.3; at Drini Gulf on November 22, 1985 with M=5.5; at Tirana on January 9, 1988, M=5.4, etc. (Sulstarova, Koçiaj, 1975 ; Sulstarova, Koçiaj, Aliaj, 1980 ; Sulstarova, 1986).

The expected seismic potential of the Ionian-Adriatic seismoactive faults zone is Mmax=5.5-6.9 (fig. 3, 5).

As it is shown, behind the zone of Adriatic collision, the degree of seismicity decreases gradually from Mmax=6.0-6.9 to Mmax=5.5-5.9 and up to Mmax=5.0-5.4.

Shkodra-Mati-Librazhdi-Bilishti seismoactive fault zone

This is a zone of graben faults of WNW to ESE extention at Shkodra and NW-SE onward, situated in the internal domain of tensional regime and has a high seismicity in the graben depression of Shkodra and an average one in his southeastern part.

During this century, there are generated such earthquakes as: at Klos (dep. of Mati) on November 16, 1929, M=4.9; at the south of Bilishti on January 18, 1958, M=4.7; at Macukull (dep. of Mati) on September 23, 1977, M=5.0; near Librazhdi on February 28, 1982, M=4.9; etc. The strongest earthquake generated in this zone is the one of June 1, 1905 at Shkodra, M=6.6 and Io=9 degrees (Sulstarova, Koçiaj, 1975 ; Sulstarova, Koçiaj, Aliaj, 1980 ; Sulstarova, 1986).

In this zone, at the depression of Shkodra, North of Shkodra

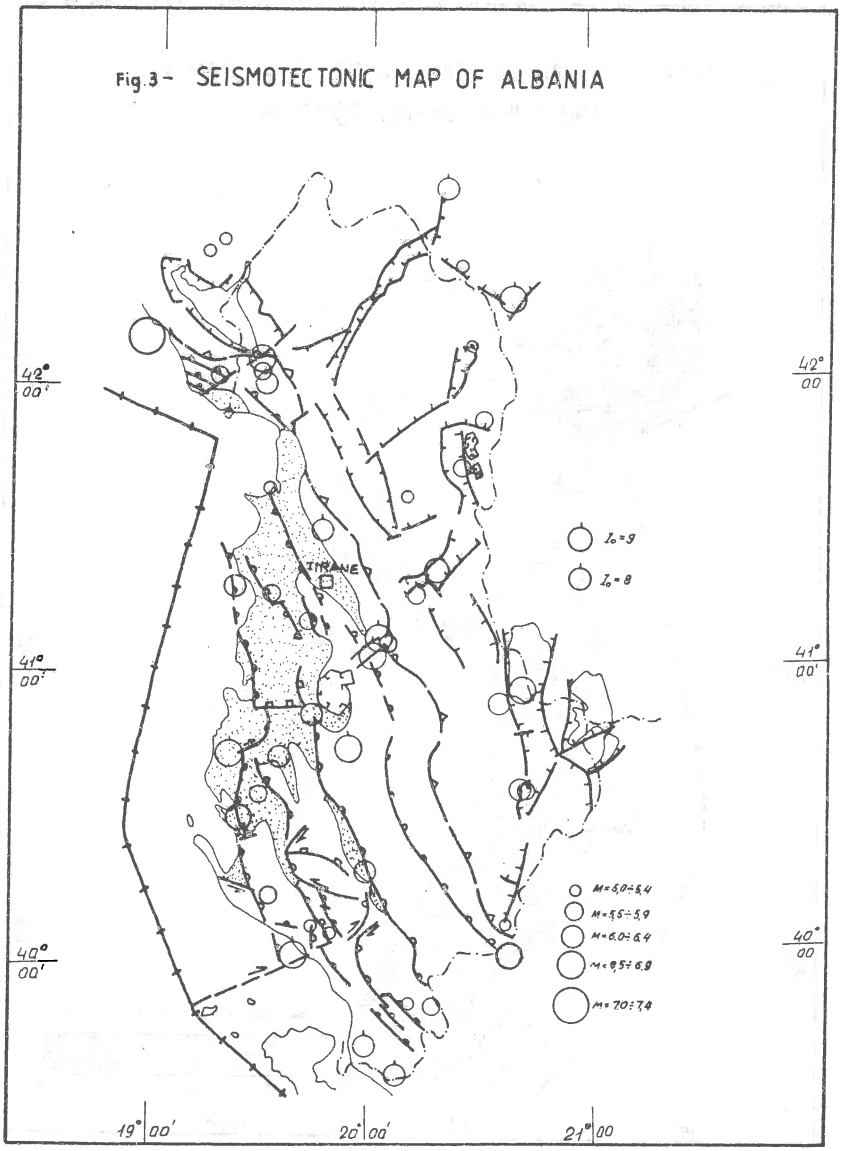

transversal, may be generated, hereafter, earthquakes with Mmax=6.5-6.9 and in south of Shkodra-Peja fault ones with Mmax= =5.0-5.4.

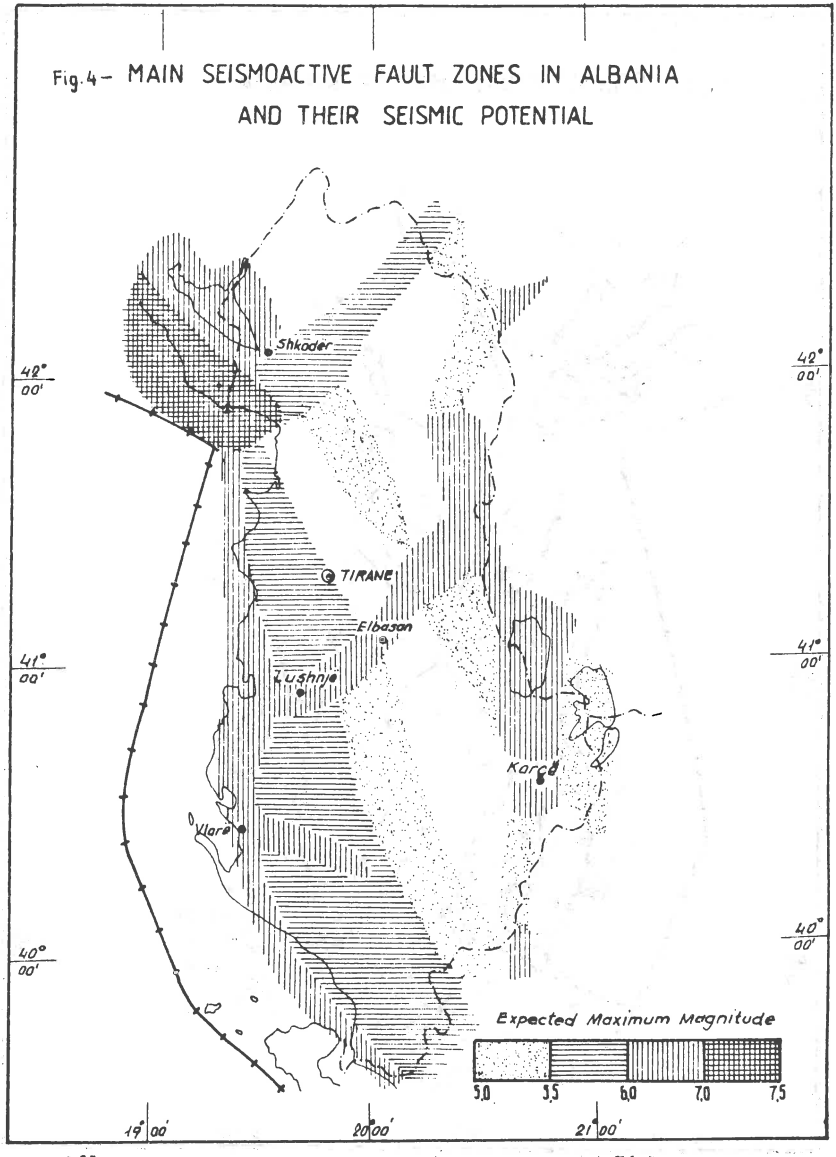

Korça-Ohri-Dibra seismoactive fault zone, this is the most seismoactive zone in the internal domain of tensional regime. It is a graben zone nearly of north extention and very well distinguished in the relief. Along this zone, only this century the following strong earthquakes are recorded: at Ohri Lake on Feb-

ruary 18, 1911, M=6.7; at Mokra (dep. of Pogradeci) on February 13, 1912, M=6.0; at Konica-Leskovik on December 22, 1919, M=6.1; at Peshkopia on March 30, 1921, M=5.8; at Korabi on December 7, 1922, M=5.7; in Korça on January 28, 1931, M=5.8; at Peshkopia on August 27, 1942, M=6.0 and at Korça in 1960 with M=6.4 (Sulstarova, Koçiaj, 1975 ; Sulstarova, Koçiaj, Aliaj, 1980).

Korça-Ohri-Dibra fault zone has an expected seismic potential of Mmax=6.0-6.9.

2.2 - Transversal seismoactve fault zones. The main transversal seismoactive fault zones are: 1. Shkodra-Peja, 2. Lushnja--Elbasani-Dibra, 3. Vlora-Tepelena, 4. Borshi-Kardhiqi.

Shkodra-Peja seismoactive fault zone is presented by a graben unit of NNE direction from Tropoja to Puka in the internal domain, and by strike-slips in the external one. Along this fault, during this century are recorded such earthquakes as: at Gjakova on September 3, 1922, M=5.0; at Trush (dep. of Shkodra) on August 27, 1948, M=5.5; at Iballë (dep. of Puka) on December 13, 1956, M==4.9; at Ulqin on November 3, 1968, M=5.5; the series of earthquakes occurred at Korthpulë (dep. of Puka) in November-December 1984, the strongest shock of which was the one M=4.0; the series of Nikaj-Mërturi (dep. of Tropoja) beginning in November 1985 until February 1986, the magnitude of the strongest shock was 4.4 (Sulstarova, Koçiaj, 1975 ; Sulstarova, 1986).

In the past centuries strong earthquakes had occurred at Peja, for ex. the one of February 11, 1662, Io=8 degrees and at Shkodra on July 3, 1885, Io=8 degrees.

Shkodra-Peja transversal fault zone is active in all its extention and its expected potential is Mmax=5.0-5.9 (fig. 4).

Lushnja-Elbasani-Dibra seismoactive fault zone is the zone of transversal faults of high seismic potential and is presented by a transversal fault zone that intersects the orogen of Albanides. During this century these strong earthquakes are recorded: at Elbasan on December 18, 1920, M=5.6; at Çermenikë on March 31, 1935 M=5.7; at Lushnja on September 1, 1959, M=6.2; and at Golloborda on November 30, 1967, M=6.6 (Sulstarova, Koçiaj, 1975 , Sulstarova, Koçiaj, Aliaj, 1980).

Lushnja-Elbasani-Dibra transversal seismoactive fault zone has an expected seismic potential of Mmax=6.0-6.9.

Vlora-Tepelena seismoactive fault zone is situated in the external domain of compressional regime and is presented like a flexure of WNW extention, northwards of which the Ionian chain plunge and develops the Pre-Adriatic depression. Along this fault the following earthquakes are recorded: at Tepelena on March 19, 1701 Io=9 and on November 26, 1920, M=6.4, Io=9, at Vlora on January 19, 1833, on October 12, 1851 and on January 2, 1866, Io=9 degrees (Sulstarova, Koçiaj, 1975).

The expected seismic potential of Vlora-Tepelena seismoactive fault zone is Mmax=6.0-6.9 (fig. 4).

Borshi-Kardhiqi seismoactive fault zone of NE extention operating as dextral strike-slip is situated in the external domain. Along this fault the following earthquakes are recorded: at Kuç--Zhulat on September 20, 1850, Io=8 degrees; at Shtëpëz (dep. of Gjirokastër) on February 22, 1963, M=5.2; the series of Ftera (dep. of Saranda) occurred during May-June 1966, the strongest shock of which was M=5.0; at Fushëbardhë (dep. of Gjirokastra) on March 26, 1988, M=4.5.

Borshi-Kardhiqi seismoactive fault zone may generate in the future earthquakes of Mmax=5.0-5.9.

CONCLUSIONS

Representing syntheticaly, only in one map (fig. 4), the seismoactive fault zones with the expected seismic potential we can point out the longitudinal and transversal seismoactive fault zones in Albania with different degrees of seismicity.

From the above summary results:

Firstly, in the external domain, the higher seismicity may occur at the fault zones behind the Adriatic collision, northwards Shkodra-Peja transversal (Mmax> 7.0) and southwards Shkodra-Peja transversal (Mmax=6.0-6.9); the seismicity gradually decreases from Mmax=6.0-6.9 to Mmax=5.0-5.9, behind the Adriatic collision. In the external domain these zones constitute a potential seismogenous belt, called the Ionian-Adriatic seismogenous belt.

Secondly, in the internal domain the higher seismicity may occur in Korça-Ohri-Dibra longitudinal fault zone, and in the fault zone of Shkodra depression (Mmax=6.0-6.9). The Mati-Librazhdi-Bilishti fault zone is a zone of average seismicity (Mmax= =5.0-5.4), the other part of the internal domain, except that of transversal seismoactive fault zones, has aweak seismicity.

Thirdly, Lushnja-Elbasani-Dibra and Vlora-Tepelena fault zones are distinguished, among the transversals, for the high seismicity (Mmax=6.0-6.9). The expected seismic potential of Shkodra-Peja and Borshi-Kardhiqi transversals is weaker than that of the two firsts (Mmax=5.0-5.9).

REFERENCES

1. Aliaj, Sh. (1982) - General features of neotectonic structure of Albania, Earthquake Risk Reduction in the Balkan Region, UNESCO, Athens.
2. Aliaj, Sh. (1987) - Shkëputjet sizmoaktive në Shqipëri, Bul. Shk. Gjeol., Nr. 2.
3. Mihajlovic, J. (1947) - La seismicité de la region de la côté sud de l'Adriatique (Stone-Ulqin).
4. Sorel, D. (1976) - Etude neotectonique dans l'arc égéen externe occidental: Les iles ioniennes de Kephallenia e Zakinthos et l'Elide Occidental, Orsay.
5. Sulstarova, E., Koçiaj, S. (1975) - Katalogu i tërmeteve të Shqipërisë, Akademia e Shkencave, Tiranë.
6. Sulstarova, E., Koçiaj, S. Aliaj, Sh. (1980) - Rjonizimi Sizmik i RPS të Shqipërisë, 8 Nëntori, Tiranë.
7. Sulstarova, E., Muço, B. (1983) - Fusha makrosizmike e tërmetit të 15 prillit 1979, Tërmeti i 15 prillit 1979, 8 Nëntori, Tiranë.
8. Sulstarova, E. (1986) - Mekanizmi i vatrës të tërmeteve dhe fusha e sforcimeve tektonike të sotme në Shqipëri, Disertacion për gradën "doktor i shkencave", Tiranë.

G. Sh. Shengelaia, E. P. Antonov, T. V. Shulaia

TOWARDS THE DETERMINATION OF THE OPTIMAL STRATEGY OF GRAVIMETRIC OBSERVATIONS AND RERUN LEVELLING IN SEISMIC ZONES.

While studying seismotectonic processes in seismic zones interest attaches to the use of the method of rerun levelling to identify anomalous variations of the velocities of the vertical movements of the Earth's surface, as the precursors of expected earthquakes.

In order that rerun levelling be more informative (in terms of the search for precursors) the seismic region must be sufficiently covered by the level-line system. The necessary number of profiles and their total extent can be determined in this case proceeding from the ratio of the seismic zone area (1) to the precursor zone area served by a levelling profile of a definite length. The value of the latter is determined by the product of the length of the levelling profile with respect to the double radius of the preparation zone defined by the magnitude of the expected earthquake. Assuming that the informative length of the rerun level-line does not exceed 2Rm, the necessary number of levelling profiles transversely crossing the seismic zone is determined by the ratio of the maximal linear extent of the fracture zone to the deformation zone diameter of the expected earthquake of a definite magnitude.

In this case the total length of levelling profiles proves to be independent of the magnitude of the predicted earthquakes and is equal to the linear extent of the seismic zone (Lp). If a system of levelling profiles is constructed in order to detect the precursors of earthquakes of a magnitude ranging from M_{min} to M_{max}, the total length of the levelling profiles, with account of their overlapping, proves to be equal to:

$$L_{\ell p} = L_p\left[1 + (M_{max} - M_{min})/\Delta M\,(1 - 10^{-b\Delta M})\right] \qquad (1)$$

The system of levelling profiles of the given extent and with the distance between these profiles not exceeding 2Rm provides the basis for detecting geodesic earthquake precursors of magnitudes from a given interval, with the probability of P=100%.

When $P_i \leq 1$ the minimal length of levelling profiles proves to be equal to:

$$L_{\ell p} = L_p\left(P_m + 0{,}56 \sum_{i=1}^{n-1} P_i\right) \qquad (2)$$

where P_m is the probability of detecting earthquake precursors with the maximal magnitude, $P_i \leq 1$ being the same for $M \in (M_{min}, M_{max})$.

Detection of earthquake precursors and the degree of their informativity depend on the distribution of rerun levellings in time. In the perfect version, rerun levelling with respect to separate profiles should facilitate the identification of the principal stages of deformations of the medium in the focal zone.

According to the investigations of Y.A. Meshcheryakov (2), three stages of the Earth's crust deformation are identifiable as the principal attribute of the earthquake cycle. These phases are α - slow secular movements, ρ - anomalous variations of the velocity of secular movements prior to the earthquake, and χ - quick movements immediately preceding the earthquake. For a complete description of the deformation processes in the stage of preparation and the realization of an earthquake it is necessary to add a fourth stage, ϑ - displacements as a result of earthquakes. From the given model (which incidentally agrees well with the dilatation-diffusion model) it follows that the distribution of rerun levelling in time should facilitate the identification and quantitative assessment of all the above-cited phases of the seismic process. Here, as before, it is important to minimize the scope of rerun levelling without materially decreasing its informativity.

Rerun levelling, with account of the above remarks, is effected according to an hierarchic principle conformably to the main stages of earthquake prediction. The time intervals between the cycles of rerun levelling are established according to the empirical relationship between time T of precursor occurrence and the magnitude of the expected earthquake.

For the interval of magnitudes from 4.5 to 7.0 the time between the cycles of levelling ranges from 0.1 to 5 years. From the obtained results it follows that the frequency of interrogating (rerun levelling) of separate profiles varies from 10 per year - for the profiles controlling the earthquakes in PFZ with M = 4.5 to once per 5 years for the profiles controlling the earthquakes in PFZ with M = 7. At detecting earthquake precursors along this or that profile the frequency of its interrogation increases according to the magnitude of the expected earthquake.

From the above consideration, let us discuss the search for earthquake precursors on the basis of rerun levelling in the seismic areas of the South-Georgian plateau. On the territory of the given region, over the 1974-1981 period a network of rerun levelling lines was set up with the total length of more than 500 km (fig.1). Two cycles of rerun levelling with the interval of 3 - 5 years along separate lines allowed for the first time to estimate the vertical movements of the Earth's crust in the given region (the map of velocities is given in fig.1). The graphs of velocities and velocity gradients along separate lines (fig.2,3) point to the presence of tectonically active fault structures, constituting the principal generators of seismic processes in the given region. It was assumed that carrying out a rerun levelling along the given lines, with periodicity from 3 to 5 years, would yield the necessary prognostic information about the processes of earthquake preparation in the given region. However, in the light of the foregoing, rerun levelling in the given network - even under optimal organization - ensures the detection of only 15% of the total number of possible earthquakes in the region with M (4.5; 7.0).

The table presents the percentage probability of detecting precursors of possible earthquakes of various magnitudes by the method of rerun levelling, along the existing profiles crossing five main fractures of the South-Georgian plateau. As seen from these results, of all possible earthquakes with $M \in (4.5;7.0)$, only earthquakes with M = 6.5 and M = 7.0 are sufficiently provided with prognostic levelling profiles. For earthquakes with $M \leq 6.0$, the provision with prognostic profiles of rerun levelling

is less than 50%.

Table

Name of faults	Extent over the region	Provision (in %) of the earthquake prediction by various lines of repun levelling					
		4.5	5	5.5	6.0	6.5	7.0
1. Kechut (Javakheti)	90	16	22	31	44	100	100
2. Abul-Samsar	45	23	33	47	57	100	100
3. South-Trialeti	120	10	15	21	29	55	100
4. Loki-Agdam	150	12	17	23	33	73	100
5. Sagamo Fault	30	23	33	47	58	100	100
Average over the region		13	20	26	42	86	100

Analogous calculations for the Caucasus as a whole show that provision of earthquake prediction with the profiles of repun levelling is as follows: for earthquakes with M = 6.0 - 32%; with M = 6.5 - 58%; and with M = 7.0 - 93%.

In some cases variations of the gravitational field elements reflect the tectonic processes occurring in the Earth's crust.

Taking the Caucasus area as an example, questions of calculating the effects of the gravitational field elements are discussed, depending on the recent vertical movements of the Earth's crust blocks, with account of their thickness, structure and density. The direct three-dimensional problem of gravimetry is solved for separate blocks by means of three-dimensional modelling in geological reduction with a view to calculating the effects of the first and the second derivatives of the gravitational potential. The difference of effects before and after the displacement of blocks is taken as the criterion for evaluating the time variation of the gravitational field elements.

Let us explain this with an example: Assume that we have two blocks: A and B. Block A is rising relatively to the daily surface, while block B is subsiding. To calculate the gravitational effects emerging here we used the package of programes developed by V.N. Strakhov and M.I. Lapina (3) for a particular form of a uniform polyhedron - a horizontal plate. Proceeding from the thickness and density of the sedimentary layer, the depths of the Conrad and Moho discontinuities, and from the values of recent mean annual vertical movements in the zones of separate blocks, and by solving the direct problem of gravimetry, the values of the mean annual variations of gravitational field elements at points covering the territory of observation within every 10 km, have been determined.

The calculation results showed that the maximal values of these elements correspond to the demarcation zones of separate

blocks of the Earth's crust, identified by averaging the velocity values of the vertical movements. (fig.4). The averaging was carried out independently for each section according to the map of the velocities of vertical movements of the European part of the USSR, M 1:2 500 000 (publ. by MAGC, 1985).

In all probability the above results are due to alternating vertical movements of the Earth's crust blocks differing in thickness.

The pictures of distribution of Δg, V_{xz} and V_{yz} other elements, like the gravitational effects of recent vertical movements in seismopredictional areas, give a clear idea of the organization of high-precision gravimetric and variometric studies aimed at identifying displacements of blocks of the Earth's crust that are related to the probable stresses in the interior of the Earth: Such studies are of decisive importance in organizing research related to the problem of earthquake prediction.

The results of the solution of direct problem of gravimetry can prove a reliable help in selecting the site for high-precision gravimetric observations along profiles, or for variometric stationary observations. These results also define the requirements set to precise calculations of the gravitational field elements.

REFERENCES

1. Kasahara K. Mekhanika ochaga zemletryasenia. -M., 1985

2. Meshcheryakov U.A. Izuchenie sovremennikh vertikalnikh dvizhenii zemnoi kori i problemy prognoza zemletryasenii. Sb. "Sovremennie dvizhenia zemnoi kory" -M.: 1982, p. 46-62

3. Strakhov V.N.; Lapina M.I. Ob ekonomizatsii reshenii nekotorykh klassicheskikh pryamikh zadach gravimetrii magnitorazvedki. BKN.: Teoria i metodika interpretatsii gravimagnitnikh polei. Kiev, Naukova Dumka, 1981.

EMGE Geophysical Institute, USSR

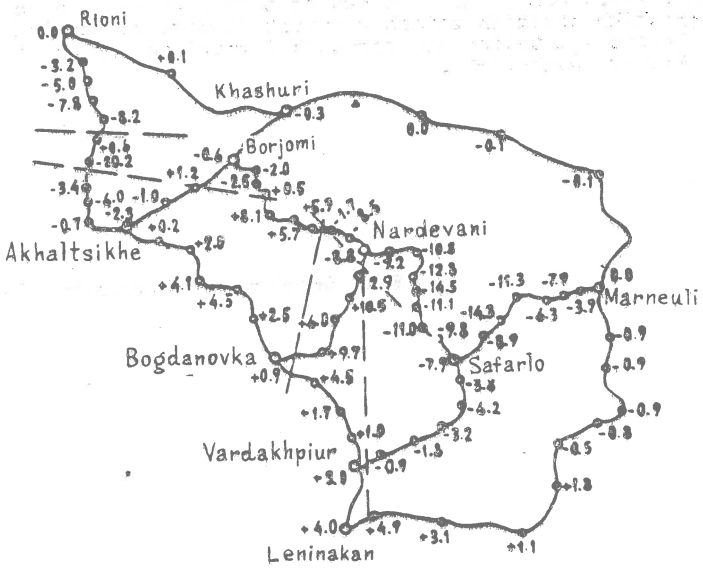
Rioni
Khashuri
Borjomi
Akhaltsikhe
Nardevani
Marneuli
Bogdanovka
Safarlo
Vardakhpiur
Leninakan

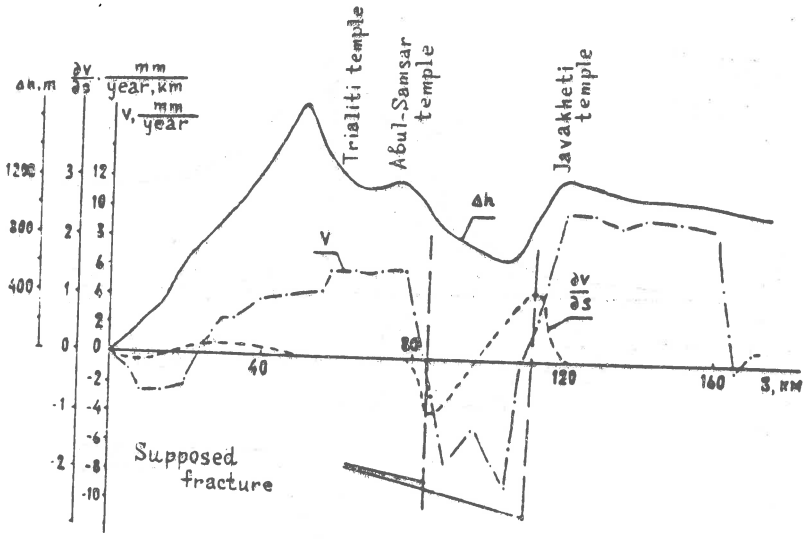
Δh, m
∂v/∂s · mm/year, km
V, mm/year
Trialiti temple
Abul-Samsar temple
Javakheti temple
Δh
V
∂v/∂s
1200
800
400
3
2
1
0
-1
-2
12
10
8
6
4
2
0
-2
-4
-6
-8
-10
40
80
120
160
S, km
Supposed fracture

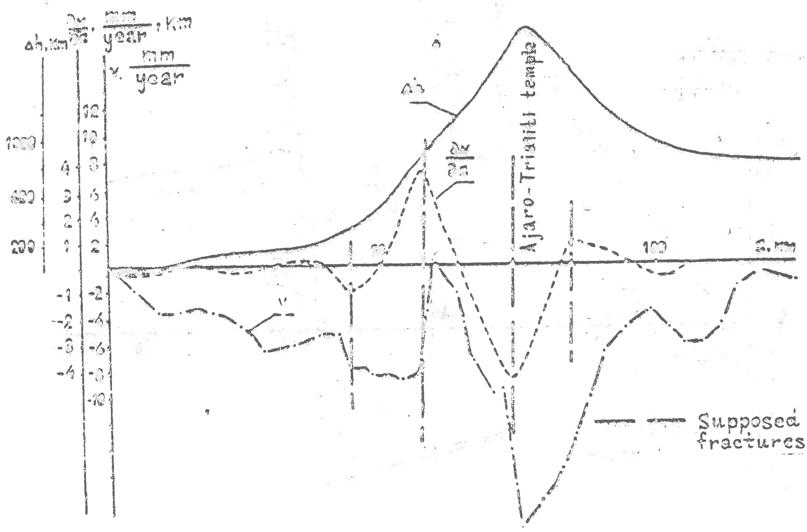

Δh, km
year
mm
year
Δh
Ajaro-Trialiti temple
100
Supposed fractures

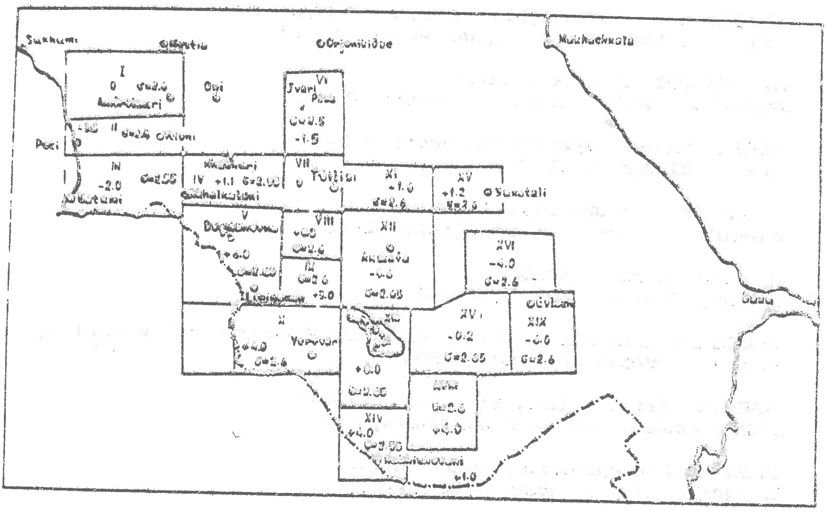
Sukhumi
Oni
Jvari Pass
Makhachkala
Poti
Tbilisi
I
VI
-1.5
VII
-2.0
IV +1.1
V
VIII
XII
XV
+1.2
XVI
-4.0
XIX
XIV
-0.2
+1.0

LIST OF SEISMOLOGISTS, PARTICIPANTS IN ASSEMBLY

A TORIA El Mrabet, C.C.N.R.P.S.T.
Maroko, Rabat, C.N.R.P.S.T. - B.P. 1346

ADAMS Robin, Int. Seismological Centre
U.K., Newbury, Pipers Lane,Thatchan,RG134,NS

AICHELE Helmut, Seismological Central Observatory
FRG, Erlangen, D-8520,Krankenhausstr 1

AKOPIAN C., Inst. Appl. Problem of Physics
USSR, Yerevan 14,375014,Nersesian st. 25

AL. KHOUBBI I., Geoph.Inst.
Bulgaria, Sofia, Akad. G.Bonchev 3

ALBINI Paola, Reparto Terremoti - CNR
Italy, Milano 90131,Via Ampere 56

ALIAY Sh., Seismological Center
Albania, Tirana, Seismological Center

ALSAKER Alfred, NORSAR
Norway, Kjeler, POB 51,N-2607

ARDELIANU Luminita, Centre of Earth Physics and Seismology
Romania, Bucharest, POBox MG-2

AREFIEV Sergei, Inst.Phys. of the Earth
USSR, Moskow 123810,B.Gruzinskaya 10

BABACKOVA Blagovesta, Geoph.Inst.
Bulgaria, Sofia, Acad.G.Bonchev 3

BABUSKA Vlodislav, Geophysikal Institute,CAS
CSSR, Praha, 141 31,Praha 4

BADAL Jose, Fisica Teorica Univ. de Zaragoza
Spain, Zaragoza 50009

BAER M., Inst. for Geophysics
Switzerland ,Zurich 8093

BARBANO Maria Serafina, Instituto di Science della Tere
Italy, Udine 33100,Viale Ungheria 43

BAUMBACH Michael, Zentralinst. fur Phys.der Erde
DDR, Potsdam 1561,Telegrafenberg 26

BELOBORODOV Vladimir, Comp.Center,Sibiria Branch Accad. Sci.
USSR, Novosibirsk

BEQUIGNON Jerome, E.M.S.C.
France, Strasbourg, F-67084 Strasbourg Cedex

BERARDI Raniero, Roma Viale Regina
Italy, Roma, Margherita 137 - 0019

BERCKHEMER H., Inst. Meteorologie u Geophysik
FRG, Frankfurt Main D-6000,Feldbergstr. 47

BODVARSSON Reynir, University of Uppsala
Sweden, Uppsala, S-75112, Box 556

BONIN Jean, CSEM
France, Strasbourg 5,rue R.Descartes F-67084

BONJER Klaus-Peter, Geophysical Institute
FRG, Karlsruhe, Hertz str. 16,D-75,Karlsruhe 21

BORMAN Peter, Zentralinst.fur Phys.der Erde
DDR, Potsdam 1561,Telegrafenberg A 26

BOTEV Emil, Geoph.Inst.
Bulgaria, Sofia, Akad.G.Bonchev 3

BRUCK Mark, Inst.Phys.of the Earth
USSR, Moskva 123810,B.Gruzinskaja 10

BRUSSA TOI Barbara, Inst.di Geodesia e Geofisica
Italy, Trieste, Via Dell'Universita 7-I-34100

BUFORN Elisa, Geophys.Universidao
Spain, Madrid, Fac.C.F.Univ.Complutense 28040

BULOCHNICOV
USSR

BURTON Paul, British Geological Survey
U.K., Edinburg, West Mains Road EH93LA

CARA Michel, Institut de Physiqoe du Globe
France, Strasbourg 5,Rue R.Descartes 67084,Cedex

CHRISTOSKOV Ludmil, Geophysical Institute
Bulgaria, Sofia, Akad.G.Bonchev 3

CONSOLE Rodolfo, Inst.Nazionale di Geofisika
Italy, Roma 00161,Via di Villa Ricotti 42

CORCHETE V., Dep. de Fisica Teorica,Univ.de Zaragoza
Spain, Zaragoza 50009

DARBYSHIRE Jack, Eigionea,Cadnant Rd
U.K., Gwynedd, LL 59 SE,Menai Bridge,Anglesey

DE BECKER Martine, Royal Obserwatory of Belgium
Belgium, Bruxells, 3 avenue Circulaire, 1180

DE CROOK Theo, KNMI
Neitherland ,De Bilt, POBox 201,3730 AE

DENEVA Daniela, Geoph.Inst.
Bulgaria, Sofia, Akad.G.Bonchev 3

DIMITRIU P.
Greece, Thessaloniki, Egnatia 311

DIMITROV Borislav, Geoph.Inst.
Bulgaria, Sofia, Acad.G.Bonchev 3

DINEVA Savka, Geoph.Inst.
Bulgaria, Sofia, Acad.G.Bonchev 3

DOBREV Chavdar, Geoph.Inst.

Bulgaria, Sofia, Acad.G.Bonchev 3

DOMANSKI Boguslaw, Inst. of Geoph. Pol.Ac.Sci.
Poland, Warszawa, Pasteura 3

DONKOVA Konstantina, Geoph. Inst.
Bulgaria, Sofia, Acad.G.Bonchev 3

DOST Bernard, Inst. of Earth Sciences
Netherlands ,Utrecht, P.O.Box 80021,3508 TA

DOTSEV Nikolay, Geoph. Inst.,BAS
Bulgaria, Sofia, Akad.G.Bonchev 3

DRAKATOS G., Seism.Inst.
Greece, Athens, GR118 10,NOA,Seism.Inst.,POB 20048

DRIEWEL J., Zentralanstat fur Meteor.&Geoph.
Austria, Vienna, A-1180,Hohe Warte 38

DUDA Severin, Geophys. Inst. Hamburg University
FRG, Hamburg 13,D-2000,Bundesstr. 55

DUMITRASCU Aleksandru, Nat.Inst.Sci.& Techn. Creation
Romania, Bucharest, BD. Pacii 220,79622

ELENKOV Sasho, Geoph.Inst.
Bulgaria, Sofia, Acad.G.Bonchev 3

FARRUGIA Pauline, Department of Physics,Univ. of Malta
Malta, Msida

FERRARI G., S.G.A
Italy, Bologna 40136,Via Bellombra,24/2

FIOSOBOVA Irina, Inst.Phys.of the Earth
USSR, Moskva 123810, B.Gruzinskaja 10

GABISONEJA G.
USSR

GADOMSKA Bozanna, Inst. of Geoph. Pol.Ac.Sci.
Poland, Warszawa 00-973,Pasteura 3,P.O.Box 155

GARCIA M., Inst. fuer Geophysik
Switzerland , Zurich, ETH-Hoenggerberg CH-8093

GASAKOV Arif, Geology Institute
USSR, Baku 370001,Efima Saratovsa 9

GEODAKYAN Edward,
USSR, Moscow, GSP-1,Molodezhnaya 3

GEORGIEV Cvetan, Geoph.Inst.
Bulgaria, Sofia, Acad.G.Bonchev 3

GHARIB Aly Ahmed, Helwan Inst.of Astr.&Geoph.
Egypt, Helwan Cairo, Institute of Astr. and Geoph.

GLAHN Andreas, Geophysicalische Institut
FRG, Karlsruhe 21,Hertzstr. 16,75

GLAVCHEVA Rumiana, Geoph.Inst.
Bulgaria, Sofia, Acad.G.Bonchev 3

GLOWSKA Ewa, Inst. of Geoph. Pol.Ac.Sci.
Poland, Warszawa 02-093,Pasteura 3

GOSPODINOV Dragomir, Geoph.Inst.
Bulgaria, Sofia, Acad.G.Bonchev 3

GRUNTHAL Gottfrid, Zentralinst.fur Phys.der Erde
DDR, Potsdam 1561,Telegrafenberg 26

GUTDEUTCH Rudolf, Inst.fur Geoph.,Univ. of Vienna
Austria, Vienna, A-1090,Wachringerstr. 17

GUTERH Barbara, Inst. of Geoph. Pol.Ac.Sci.
Poland, Warszawa 00-973,Pasteura 3

HADJIGENCHEV Svetoslav, Geoph.Inst.
Bulgaria, Sofia, Acad.G.Bonchev 3

HARADJA Octav, Inst. of Earth Phys.& Seism.
Romania, Buchurest, P.O.B. MG-2

HJORTENBERG Eric, Geodetic Institute
Denmark, Charlottenlund, Gamlehave Alee 22,DK 2920

HOJMETOV G.
USSR

HOUTGAST Gerhard, Royal Netherlands Meteorological Inst.
Neitherland , De Bilt, POBox 201 3730

HURTIG Eckart, Zentralinst.fur Phys.der Erde
DDR, Potsdam 1561,Telegrafenberg 26

JANEZ Lapajane, Seismological Survey
Yugoslavia, Ljubljana, Kersnikova 3

JANKOWSKA Agata, Observatory of Geoph.Pol.Ac.Sc
Poland, Warszawa 02-093,Pasteura 3

JMENEZ Encatnacion, Institut de Physique du Globe
France, Strasbourg 5,Rue R.Descartes 67084,Cadex

KACHAROV Georgy, Geoph.Inst.
Bulgaria, Sofia, Acad.G.Bonchev 3

KALMETIEVA
USSR

KALOGERAS C., Seism.Inst.
Greece, Athens, GR118 10,NOA,Seism.Inst.,POB 20048

KANDLER Manfred, Austrian Archeol.Inst.,Univ. Vienna
Austria, Vienna

KARNIK Vit, Geoph. Inst.
CSSR, Praha 14131,Bochni II

KEBEASY Rashad, Nat.Res.Inst.Astr.&Geoph.
Egypt, Helwan, Helwan Observatory

KEBEDE ALAMNEH Fekadu, Seism.Dept Uppsala University
Sweden, Uppsala, BOX 12019,S-750 12

KERAMOVA [illegible]a, Geology Survey
USSR, Baku [illegible]001,Efima Saratovsa 9

KHROMETSKAJA Elena, Inst.Phys.of the Earth
USSR, Moskva, 123810, B.Gruzinskaja 10

KIJKO Andrzej, Inst.of Seismology,Poland
Finland Helsinki, Et.Hesperiankatu 4,SF-00100

KIREEV Igor, Inst. Phys.of the Earth
USSR, Moscow 123810, B.Gruzinskaja 10

KITANOV P., Geoph.Inst.
Bulgaria, Sofia, Acad. G.Bonchev 3

KONDORSKAJA Nadja, Inst.Phys.of the Earth
USSR, Moskva 123810, B.Gruzinskaja 10

KORHONEN Heikki, Inst. of Seismology,Univ. of Helsinki
Finland, Helsinki, Et Hasperian 4 SF-00100

KOSTUK O., Geoph. Inst.,Seism.Observatory
USSR, Lvov 290011,Jaroslavenko 27

KOWALLE Georg, Zentralinst.fur Phys.der Erde
DDR, Potsdam 1561,Telegrafenberg 26

KOZAK Jan, Geoph.Inst.
CSSR, Praha 14131,Bocni II/1401

KRADOLFER U., Inst. of Geoph.
Switzerland , Zuerich

KUMPEL Hans-Joachim, Inst.of Geophys. Univ.of Kiel
FRG, Kiel, D-2300,Leibnizstr. 15

KVAMME Leif, NORSAR
Norway, Kjeller, POBox 51, n-2007

LANGER H., Inst. of Geoph., Univ. of Stutgart
FRG, Stutgart, D-7000,Richard Wagnerstr 44

LEVI Emil, Geoph.Inst.
Bulgaria, Sofia, Akad.G.Bonchev 3

LOKAJICHEK T., Geoph.Inst.
CSSR, Praha 14131, Bocni II/1401

LUOSTO Urmas, Institute of Seismology
Finland, Helsinki, SF-001000,Et.Hesperiankatu 4

MANTLIK F., Geoph.Inst.
CSSR, Praha 14131, Bocni II/1401

MAO Weijian, Inst.de Geodesia e Geofisica
Italy, Trieste, Via dell'Universita 7-I-34100

MARTINELLI G., Servizio Informativo e Statistica
Italy, Bologna 40100,Viale Silvani,4/3

MARTINEZ-GUEVARA J.
Spain, Murcia, E-30008,Marques Velez 9-5B

MARZA Vasile, Center for Earth Phys.& Seism.

Romania, Bucharest 28, POBox:28-19,RO-75200

MASLINKOVA Svetla, Geoph.Inst.
Bulgaria, Sofia, Acad.G.Bonchev 3

MAYER-ROSA Dieter, Institut of Geophysiks
Switzerland , Zurih, ETH,Honggerberg,CH-8093

MCGREGOR David, Internationale Seism. Centre
U.K., Newbury, Pip.Lane,Thatham,Berks,R6134NS

MEZCUA J., Inst. Geogrfico Nacional
Spain, Madrid

MICHAJLOV Dimitar, Geoph.Inst.
Bulgaria, Sofia, Acad.G.Bonchev 3

MIHALACHE Georgeta, Nat.Inst.Sci.& Techn.Creation
Romania, Bucharest, BD. Pacii 220,79622

MKHITARIAN L., Inst. of Geoph.&Earth. Engeneering
USSR, Leninakan

MOLOTKOV Sergei, Inst.Phys.of the Earth
USSR, Moskow 123810,B.Gruzinskaya 10

MONOZ Peter, Seism.Obs. of GGRI,HAS
Hungary, Budapest, Meredek 18,H-1112

MORELLI Carlo, Miniere e Geoph. Appl. Univ of Trieste
Italy, Trieste 1,Piazzale Europa - 34127

MUELLER Stephan, Institute of Geophysics
Switzerland , Zurich, ETH-Honggerberg,CH-8093

MUSSON R., British Geological Survey
U.K., Edinburg, EH93LA

NIEWAIDOMSKI Janusz, Inst.of Geoph.
Poland, Warszawa 00-973,Pasteura 3

NIKOLAEV Aleksey, Inst. of Phys. of the Eart
USSR, Moscow 123810,B.Gruzinskaja 10

NIKOLOVA Svetla, Geoph.Inst.
Bulgaria, Sofia, Akad.G.Bonchev 3

NIKONOV Andrej, Inst.Phys.of the Earth
USSR, Moskow 123810,B.Gruzinskaya 10

NOVOTNY Oldrich, Inst. of Geoph.,Charles Univ.
CSSR, Praha 2,Ke Kariovu 3,121 16

OANCEA Victoria, Center of Earth Phys.& Seism.
Romania, Bucharest, P.O.B. MG-2

OLIVERA Carmen, Servei Geologic de Catalunya
Spain, Barcelona, Diputacio 92,08015

ONCESCU Corneliu, Center of Earth Phys.& Seism.
Romania, Bucharest, P.O.B. MG-2,R-76900

PACHOVA S., Geoph.Inst.
Bulgaria, Sofia, Acad. G.Bonchev 3

PANAJOTOV Nikolaj, Geoph.Inst.
Bulgaria, Sofia, Acad.G.Bonchev 3

PANTELEEVA T., Dep. of Seism.,Inst.Geoph.
USSR, Simferopol

PAPANDOPULO G., Inst. Phys. of The Earth
USSR, Moscow 123810,B.Gruzinskaya 10

PAPAZAHOS B., Geoph.Lab.Univ.of Thesaloniki
Greece, Thesaloniki GR54006,Univ.Geoph.Lab.

PAPOULIA Joanna, Earthquake Plan.&Prot.Organis.
Greece, Athens, Mesogion,226,155 61-Cholargos

PAYO Gonzalo, Instituto Geografico Nacional
Spain, Toledo, Observatorio Geofisico,Apdo 46

PEARCE RG, Dept.of Geology University College
U.K., Cardiff, CFIIXC, POBox 78

PERCHUC Edward, Inst. of Geoph. Pol.Ac.Sci.
Poland, Warszawa 00-973,Pasteura 3,P.O.Box 155

PERSSON Astrid
Sweeden, Stockholm, Dep 260, FOA

PETKOV Ivan, Ass. Earth Physics
Bulgaria, Sofia

PETROV Ljuben, Geoph.Inst.
Bulgaria, Sofia, Acad.G.Bonchev 3

PIRUSIAN C., Lab of Microzonation,Inst. of Geophys.
USSR, Yerevan 375019,Bagramian st. 23

PLESINGER Alex, Geoph.Inst.
CSSR, Praha 14131,Bocni II/1401

PLOMEROVA Vatoslava, Geophysikal Institute,CAS
CSSR, Praha 14131,Bocni II/1401

POSTPISCHIL D., Inst. Topografia
Italy, Bologna 40136,Vidle Rosorgikeuto 2

PROCHAZKOVA Dana, Geoph. Inst.,CAS
CSSR, Praha 4, Bocni II,14131

PURCARU G., Inst. of Met.Geophysics
FRG, Frankfurt Main 6,Feldbergstr. 47

PUSTOVITENKO B., Inst of Geoph.
USSR, Simferopol

RABINOWITZ Nitzan, Inst. for Petroleum Res.&Geoph
Israel, Holon, Box 2286,58122

RACCICHINI Sertgo, Observatory Geofysiko Macerata
Italy, Macerata 52100,V. Independenza

RADU Cornelius, Centre of Earth Phys.& Seism.
Romania,, Bucharest, P.O.B. MG-2

RANGELOV Bojko, Geoph.Inst.
Bulgaria, Sofia, Akad.G.Bonchev 3

RAUTIAN T., Compl. Seism. Expedition
USSR, Garm 735450

REBEZ Alesandro, Osservatorio Geofisico Spermentale
Italy, Trieste, POBox 2011

REISNER G., Inst.Phys.of the Earth
USSR, Moscow 123810,B.Gruzinskaya 10

ROCA Antoni, Servei Geologic de Catalunya
Spain, Barcelona, Diputacio 92,08015

ROZLUSKI Cezary
Poland

SAARI Jouni, Imatran Voima Oy,Civ.Eng.Dep
Finland, Vantaa, P.O.Box 112,01600

SAMARDJIEVA Elena, Geoph.Inst.
Bulgaria, Sofia, Acad.G.Bonchev 3

SAURA-RAMOS S.
Spain, Murica 30001,Plaza Fuensanta, 2-15B

SCHENK Vladimir, Geoph.Inst.,CAS
CSSR, Praha 4, Bocni II,14131

SCHENKOVA Zdenka, Geoph.Inst.,CAS
CSSR, Praha 4, Bocni II,14131

SCHMIDT Manfred, Zentralinst.fur Phys.der Erde
DDR, Jena 6900,Burgweg 11

SCHMIDT Peter, Bibl.der Bergakademie
DDR, Freiberg, Schlussfauh 47,9200

SCHNEIDER M., Zentralinst.fur Phys.der Erde
DDR, Potsdam 1561,Telegrafenberg 26

SCHULZE Albrecht, Zentralinst.fur Phys.der Erde
DDR, Potsdam 1561,Telegrafenberg 26

SEIDL Diter, Seism. Zentralobservatorium
FRG, Erlangen, Krankenhaus str. 1-3,852

SEIDUZOVA Saida, Lab.of Geol.&Geophys.
USSR, Tashkent 33,Suleimanova str., 700 017

SERCI Angel, KINEMETRICS SA
Switzerland , Lausanne 3,rue de la Vigie,1003

SHAROV N., Geol.Inst.
USSR, Apatity 184200,Fersman str. 14

SHENGELAIA G., EMSE Geoph. Inst.
USSR, Tbilisi

SHIMSHONI Michael, The Weizman Inst.of Science
Israel, Rehovod, Dept. of Appl.Math.Weizm.Inst.

SIMEONOVA Stela, Geoph.Inst.

Bulgaria, Sofia, Acad.G.Bonchev 3

SLAVINA Lidija, Inst.Phys. of the Earth
USSR, Moscow 123810, B.Gruzinskaja 10

SLEJKO Dario, Osserv.Geofisico Sperimentale
Italy, Trieste, P.O.Box 2011, 34016

SOBOLEV G., Inst. of Oceanology
USSR, Moscow 117218,Krasikova 23

SOKEROVA Darina, Geoph.Inst.
Bulgaria, Sofia, Acad.G.Bonchev 3

SOLAKOV Dimcho, Geoph.Inst.
Bulgaria, Sofia, Acad.G.Bonchev 3

SOLOVYOV Sergey, Inst.Phys. of the Earth
USSR, Moscow, 123810,B.Gruzinskaya 10

SOUSA Maria Luisa, Cabinete de Proteccao Nuclear
Portugal, Lisboa 1000,Av. Republica 45, 6

SPANOCHE Eleonora, Inst. Geregiesi Gerbizrea
Romania, Bucharest

SPASOV Edelvais, Geoph.Inst.
Bulgaria, Sofia, Acad.G.Bonchev 3

STANKIEVICZ Tadeusz, Inst. of Geoph. Pol.Ac.Sci.
Poland, Warszawa, Inst. of Geoph. Pol.Ac.Sci.

STAVRAKAKIS Georgios, Seism. Inst.
Greece, Athens GR118 10 NOA,Seism.Inst.,P.O.B. 20048

STOJANOV Toshko, Geoph.Inst.
Bulgaria, Sofia, Acad.G.Bonchev 3

STUCHI Massimiliano, Reparto Terremoti - CNR
Italy, Milano 20131,Via Ampere 56

SULTANKHODJAEV Abdumubdy, Seism. Lab. Uzbek SSR,Ac. Sci.
USSR, Tashkent 700128, Khurshid str. 3

SUSAGNA Teresa, Servei Geologic de Catalunya
Spain, Barcelona, Diputacio 92,08015

SZEIDOUITZ Guozo, Geod. and Geoph.Res.Inst.,HAS
Hungary, Budapest, Meredek 18,H-1112

TARVAINEN Matti, Inst.of Seismology
Finland, Helsinki, Et.Hesperiankatu 4,SF-00100

TEISSEYRE Krzysztof, Inst. Of Geoph. Pol.Ac.Sci.
Poland, Warszawa 00-973,P.O.Box 155,Pasteura 3

THEODOLIDIS N., Inst.Eng.Seism.&Earth.Engineering
Greece, Thessaloniki

TOTH Laszlo, GGRI,Dept.Seism.,HAS
Hungary, Budapest, Meredek 18,1112

TRAMPRET Jeannot, Institut de Physique du Globe
France, Strasbourg 5,Rue R.Descartes 67084,Cedex

TRIFU Cezar-Ioan, Center of Earth Phys.&Seism.
Romania, Bucharest, P.O.B.MG-2,Bucharest-Magurele

UCHRENBACHER R., Inst. fur Geophysik
FRG, Kiel 2300,Olshausenstr. 40

UDIAS Augustin, Catedra de Geofisica
Spain, Madrid, Fac.C.F.Univ.Complutense,28040

VACCARI Franco, Inst.di Geodesia e Geofisica
Italy, Trieste, Via Universita 7 - I-34100

VANEK Jiri, Geoph.Inst,CAS
CSSR, Praha 4, 14131, Bocni II

VASAPOLLO N., Servizio Informativo e Statistica
Italy, Bologna 40121,Via Dei Millk 21

VASILIEV V., Inst. Phys. of the Earth
USSR, Moscow 123810,B.Gruzinskaja 10

VELICHKOVA Silvia, Geoph.Inst.
Bulgaria, Sofia, Acad.G.Bonchev 3

VOGEL A., Inst. fur Geoph.,Freie Univ.
FRG, Berlin 33,Rheinbabenallee 49

VOGT J.
France, Strasbourg F-67000,Rue du Docter Woehrlin

WANIEK Ludvik, Geoph. Inst.
CSSR, Praha 4 14131, Sparilov

WEIGELT E., Inst fur Met. und Geophys.
FRG, Frankfurt Main 6000,Feldbergstr. 47

WESTERHAUS M., Inst fur Geophysik
FRG, Kiel 2300,Olshausenstr. 40

YATMAN A., Earthquake Res. Inst.
Turkey, Ankara

YLINIEMI Jukka, Geoph. Observ.
Finland, Oulu 90570 Oulu

YUNGA Sergey, Inst.of Phys. of the Earth
USSR, Moscow 123810, B. Grusinskaja 10

ZAHAROVA A., Inst.Phys.of the Earth
USSR, Moscow 123810, B.Gruzinskaya 10

ZIMAKOV L.
USSR

ZONNO Gaetano, Inst. per la Geofisica
Italy, Milano, Via Ampere 56 - 20131

ZSIROS Tibor, GGRI,Dept.Seism.,HAS
Hungary, Budapest, Meredec 18,1112

НАРОДЕН ДВОРЕЦ НА КУЛТУРАТА
"ПЕЧАТНО-РАЗМНОЖИТЕЛЕН ЦЕНТЪР"